NEUROTOX '88

Molecular Basis of Drug & Pesticide Action

Editor:

G.G. LUNT

EXCERPTA MEDICA

International
Congress Series

89 2 22 0 682

Price: ₤.2/0.75.

NEUROTOX '88
Molecular Basis of Drug
& Pesticide Action

NEUROTOX '88

Molecular Basis of Drug & Pesticide Action

Proceedings of Neurotox '88, Molecular Basis of Drug & Pesticide Action, University of Nottingham, England, 10–15 April 1988

Editor:

G.G. Lunt
School of Biological Sciences, Biochemistry Department, University of Bath, Bath BA2 7AY, England

1988

Excerpta Medica, Amsterdam · New York · Oxford

Preface

Neurotox '88 was the third in a series of meetings organised under the auspices of The Society of Chemical Industry. Since the first meeting in 1979 in York, Neurotox has grown in stature and has acquired a truly international reputation. Neurotox '88 set out to achieve a blend of historical perspective and the best of current research coupled with speculative predictions of future developments. Natural neurotoxins received much attention and it was clear that nature has provided us with a vast reservoir of molecules that can serve as both tools for the biological scientist and as signposts for the synthetic chemist. The chemist and the biologist were also drawn closer together in the new fields of molecular recognition and molecular modelling. Here we saw the beginnings of a comprehensive quantitative description of the interactions of neurotoxicants with their target molecules.

Looking to the future molecular neurobiology seems ready to move to centre-stage and to provide a new impetus in our fight against the spectre that haunts the entire pesticide industry – resistance.

This volume is comprised of the invited papers that constituted the Neurotox '88 meeting. I hope that in addition to serving as a valuable synthesis of data it will also help to recapture the spirit of international friendship and vigorous enthusiasm for neuroscience that characterised Neurotox '88.

G.G. Lunt
Bath, England
June 1988

Prologue

It is a pleasure and an honour to be invited to present the prologue at this Neurotox '88 meeting. It is a particular pleasure for me to be part of this meeting as I was an officer in the Pesticides Group of the Society of Chemical Industry when the first meeting, which laid the foundations for Neurotox, was being discussed. This one day meeting took place at Belgrave Square, London, in October 1976 and was entitled *Neurophysiological Action of Pesticides*. It was, in fact, arranged by the Physicochemical and Biophysical Panel of the Pesticides Group. Many people associated with that initial meeting are still associated with Neurotox and have been instrumental in bringing it from a local one day meeting to a week long International Symposium. We are indebted to them for their continuing efforts in search of important, timely subjects, and I am sure you will agree with me that they have been successful in this.

This year Neurotox '88 has a very broad base encompassing both drug and pesticide action with an emphasis on the molecular aspects of each of these. The fact that interaction with the nervous system can be discussed in molecular terms is impressive and reflects the great developments that have taken place in recent years. We have moved relatively quickly from whole organism studies, via physiology and biochemistry, to molecular biology and the detailed understanding of some aspects of the nervous system. However, great advances remain to be made both at the molecular level and in relating this detail to the behaviour of organised biological structures. The knowledge gained will be relevant to many studies remote from the original objectives and these interdisciplinary developments must be encouraged. Relationships might develop with psychology bringing insight to the processes of thought, perception, learning and memory, while another avenue may lead to developments in computing and mathematics.

My own knowledge and background in this area is limited to the Agrochemical Industry's interests, specifically the study of insect control. Thus I hope that participants at the Conference will bear with me as my remarks will view the subject of Neurotox from this perspective.

Interest in the nervous system goes back several thousand years and in Aristotle's time it was known that certain fish can communicate a numbing sensation to people who touch them. Many eminent scientists studied the nervous system as part of Natural Philosophy and the 17th, 18th and 19th centuries are quite rich with comments about such studies.

Golding Bird, in his book *Elements of Natural Philosophy* published in 1839, discusses organic electricity and describes some of the experiments of Hunter, Galvani and Faraday, amongst others. The concept of an electrical fluid was looked upon as the basis of all the functions of life in these early times. The positive and negative aspects of electricity were recognised and organic systems were classified in these categories. Pfaff and Ahrens reported that "women are not unfrequently negative, especially during pregnancy". Many of the observations, in these early

times, were by natural philosophers pursuing interests rather than careers. They often worked alone employing logic and reasoning based mainly upon macroscopic observations, although from the late 17th century light microscopy developed giving a further degree of insight.

The first molecular studies did not occur until the 20th century and we can take the modern era to begin around 1930. Not only did the structure and function of the nervous system become clearer, but also important molecular events associated with it began to be defined. Many classical pieces of research emerged with studies of invertebrate systems complementing those of the vertebrate systems. For example, the Nobel prizewinning work of Hodgkin and Huxley, in 1952, defined the kinetic details of changes in ionic permeabilities. It is interesting to observe that only a year later Watson and Crick were publishing their work on DNA in *Nature*. A considerable number of recent studies of the nervous system find their foundations in these two pieces of prizewinning research.

A further feature of this century has been the change in the characteristics of a researcher. No longer are they independent Natural Philosophers pursuing interesting phenomena in a hobby-like manner, but rather they are highly qualified scientists pursuing careers in specific disciplines This does not mean that the interest has diminished, but rather that the societal structure of research has changed. Partially because it is recognised that the products of research can have commercial as well as intellectual value. It may be, however, that there has been an associated transition to results production which has replaced some of the logic and reasoning of the earlier philosophers. Data has become a preeminent feature and perhaps we would all benefit from spending a little more time on logic and reasoning. It might allow us to be more critical and selective regarding the necessary experimentation. Another change in recent years has been the move to larger research groups although usually of the same, or a closed related, discipline. This, together with the potential commercial aspects, means that both management and economic skills become features of present day research. It is unlikely that the natural philosophers of old considered such questions as:

How long will it take?
How much will it cost?
Who should do it and who will benefit from it?
Can the various aspects be tackled and managed successfully?
What is the value of the output?

And of at least equal importance:

What will the people involved do when the present tasks are completed?

Naturally these questions are relevant to all research, not just studies of the nervous system.

I would like to speculate about a few of these statements to see if we can determine some pointers for the future. It would be too ambitious to call these forecasts, however, they may provide a basis for discussion.

Let us consider the commitment of resources and the research output. I will take the number of publications as a measure of output. This is somewhat unsatisfactory as quality and quantity are not distinguished, but it may serve to highlight some

points. A search of several databases and a rather arbitrary, but consistent, averaging process yielded the following data.

Worldwide Publications on the Nervous System

Year	1970	1975	1980	1985	2005
Number	5000	8000	13000	19000	55000 ± 10000
Cost *	$100M	$160M	$260M	$380M	$1100M ± $200M

* Assuming $20000 total investment per publication. This does not allow for increasing research costs, in real terms, with time. Thus the earlier figures should probably be lower.

Thus in 1985 about 4 times the number of publications were generated over 1970. I will assume that the direct operating and infrastructure costs of a researcher are $15000 p.a.; averaged over academic, industrial and government workers in different countries. It is also assumed that, on average, between 1 and 2 research-years are required to produce a publication. I have taken $20000 as the 'rounded' figure for the investment per publication. This allows the investment in nervous system research worldwide to be estimated. The assumption is made that the number of people trained in this area per year is roughly half the number of publications. On this basis we now have 4 times the number being trained relative to 1970 and this could rise by a factor of about 3 between 1985 and 2005. In 2005 we could be generating about 27500 ± 5000 scientists familiar with research in the nervous system. Naturally this crude assessment can be criticised on several counts: the investment is arbitrary; multiple authorship of papers is increasing; the skills involved are becoming more diverse and only one author may be a nervous system researcher.

If we put the criticisms to one side and consider the trends we can speculate that the next 20 years will produce as much research on the nervous system as the last 85 years. In the year 2005 this research will cost over $1 billion, worldwide, at 1985 rates. As research costs increase faster than inflation the real costs are likely to be substantially greater than this. Particularly as some countries' contributions remain to be measured because much of their growth in research of this nature has yet to occur. or is not recorded fully at present; China and the USSR are significant in this regard.

If value is to be obtained from this investment, substantial management issues must be addressed, not only managing the resources, but also the data and information and, not least, the science itself.

These data, if correct, raise significant questions.

(i) Is this growth curve sustainable? In common with other resource utilisation processes it will be a logistic (S-shaped) curve; but what is the appropriate plateau level? Many individuals trained in neuroscience will continue in the same skill area for a considerable time and some will train further Ph.D.s. As a career expectancy is 30 years the total neuroscientist population could become quite large.

(ii) As the subject area becomes less attractive what will these skilled people do?

(iii) If we had control of the worldwide investment what research priorities would we set?

(iv) Can such a priority order be agreed and who should address this?

(v) What is the benefit from pursuing this research and how does it measure up against other opportunities remote from neuroscience?

(vi) How will the research be funded in the future and can sufficient commitments of resources be made over long time periods? As I speculate that the research costs in 2005 will be over $1 billion (1985 rate) and this research might be 2.5% of the business generated, then we are going to generate $40 billion (1985 rate) worth of new proceeds in 2005 related to the nervous system. Do we believe this? I use the figure 2.5% of proceeds as we are only considering research not development.

(vii) Who will benefit from the research? I believe that the insect control business derived from this research will only be a small fraction of the speculative proceeds. It may be that the pharmaceutical industry and health care fields will exploit the research more extensively.

(viii) In an area of increasing sophistication in techniques, and increasing costs, how will the cooperation and communication amongst different groups of different disciplines be optimised?

(ix) How do we avoid spending increasing amounts of money to generate additional data which provide little additional information?

We cannot give very high credibility to the numerical values discussed here but the implications of the trends are dramatic and the questions raised warrant attention. It seems reasonable for a nation to choose which options it wishes to pursue and then it must tackle them effectively. This requires Government, Academia and Industry working in close collaboration. Such a process might be criticised as it could tend to minimise intellectual freedom and the speculative research that many in academia wish to protect. Some protection should be possible, but only in the support of excellence. The dilemma is how to give individuals the chance to exhibit excellence.

After all a nation has limited resources and many calls upon these resources, thus choices must be made. Governments recognise that the future wealth of their country is, in part, related to the creativity and innovation of its trained skilled people. As larger amounts of investment are required by research, often with long commitment times, the analysis of options and decisions about choices are critical. Just as critical is the manner of implementation; it is of little value if the analysis and decisions are correct but the implementation is so poor that the objectives are not achieved. The U.K. seems particularly prone to poor implementation. The types of demarcations inherent to the Research Council system would not be tolerated in other spheres of activity. In my opinion, the SERC Initiative on Invertebrate Neurosciences was an example of good analysis and poor implementation, and I have first hand experience of the bureaucracy involved. Attempting to obtain optimal value across the MRC-SERC interface is quite a challenge. It appears that there are neither 'receptors' nor 'channels' involved at this interface and the sooner we achieve permeability the better.

Some of the issues I have touched upon may be important to you and others may not, however, the Conference we are attending is laying out current research and assisting in formulating views on what we might do next. Thus the questions I have posed are relevant and how we address them is as important as the technical data that will be presented.

A fundamental question to answer is: "is the nervous system an attractive area for study intellectually and commercially?" Individuals must answer on behalf of their own intellectual ambition; as an industrial participant I think that for insect control it continues to a be an attractive target; I guess that the pharmaceutical industry also finds several aspects of neuroscience attractive.

I would like to address some aspects of the scientific future in my closing remarks.

From an agrochemical viewpoint the history is that 80% or more of the $5.5 billion insecticide market involves chemicals which interfere with invertebrate nervous systems. Commercially attractive alternatives are few and biotechnology has not yet impacted in a product sense, although expectations remain high.

Can new chemicals and/or new targets relating to the nervous system of insects improve upon those currently available? Probably yes, as far as the key questions are concerned.

(i) Will they work?

We know that materials interfering with the nervous system can produce commercial pesticides. They perform well and the industry has consistently supplied products which perform better than earlier generations. Thus in 40 years we have reduced dosages from several kilograms per hectare to about 10 grams per hectare and I anticipate that at least one order of magnitude in improvement remains for chemicals.

(ii) Will they be safe?

The industry will continue to meet the challenges of increasing legislation and constraints. The future products will be safer in toxicological terms and environmentally more acceptable provided our knowledge on selectivity, persistence and placement continues to improve. I expect this to be the case.

(iii) Will they be cost effective?

They will have to be otherwise they will not be a commercial success. The trend in increasing molecular complexity will demand higher manufacturing costs but these should be offset by the lower doses. Thus the user (the farmer) should find the products attractive. Improvements in environmental acceptabilities should make the next generation of products more attractive to the public and to the registration authorities.

An unknown in the cost effectiveness of future products that act via the insect nervous system is the influence of insect resistance. This is an area requiring research attention.

In the longer term as biotechnological developments make greater impact it is possible that neuropeptides could become important in insect control. Their complexity may preclude conventional manufacture, however, the possibility of using

the crop plant as the 'manufacturing' and 'delivery' system could be a reality in the next 20 years. Thus the role of neuroscience in insect control could be prominent for many years to come. A broader range of skills will be demanded by this research than those applied historically and we will see moves to newer technologies in Agrochemicals. The importance of computing and molecular design will be prominent as well as bioanalytical techniques and molecular biology.

In the next 20 years certain parts of this research, currently at the edge of credibility, will move to centre stage and generate great excitement. If I am allowed to pick three areas, they will be:

(1) modelling of the nervous system and the interplay of cognitive psychology and computing;
(2) the production of functioning artificial neurones;
(3) the ab initio design of chemicals which will function as predicted both in the isolated nervous system and on whole organisms.

The challenge is for younger scientists to move the 'centre of gravity' of the subjects studied from the classical base to a new base that sits comfortably with molecular biology, psychobiology and computing. Eventually the new 'neurobiologists' will be providing essential inputs to the development of Robotics and Artificial Intelligence. At that time the participants in 'Neurophenomena 2000' may look back at Neurotox '88 with nostalgia.

I hope that you all find the Conference stimulating, informative and enjoyable and I thank the Organisers of Neurotox '88 for giving me this platform. I also thank you for being so tolerant in listening to me so patiently at what is, primarily, one of the social events in Neurotox '88.

Neil R. McFarlane

Acknowledgements

Contents

SECTION I NATURAL PRODUCTS

xviii

Natural products

CHAPTER 1

The natural pyrethrins: a chemist's view

L. CROMBIE

Department of Chemistry, The University of Nottingham,
Nottingham NG7 2RD, U.K.

The natural pyrethrins mixture is the most valuable of the botanical insecticides [1-5] and despite many decades of use it remains an important article of commerce. The mixture consists of six compounds (Fig. 1) and a typical composition is pyrethrin I 38%, pyrethrin II 35%, cinerin I 7%, cinerin II 12%, jasmolin I 4% and jasmolin II 4%. This group of compounds has formed the natural template from which the new generation of synthetic pyrethroids (e.g. see Fig. 2), so important today, has been built. Apart from being good insect-kill agents, the natural pyrethrins have that important paralytic effect on flying insects known as 'knock-down' and they have repellency effects also. Their comparative instability makes them unsuitable as field insecticides, but it has the advantage of hindering the development of insecticide resistance.

The source of the pyrethrins is the flower head (or more specifically the achenes) of *Chrysanthemum cinerariaefolium* (Compositae) and one or two closely related species. *C. cinerariaefolium* appears to have originated in Persia and the Middle East and it has been grown commercially in Europe in Dalmatia, as well as in Japan. Commercial quantities are grown today in Africa (especially Kenya), and South America. Extracts containing about 25% pyrethrins content are usually prepared in the growing areas and exported after decolorisation to remove carotenoids which cause staining. Pyrethrum flowers are harvested at the half-open stage and as this means picking over the crop repeatedly in a selective manner, it is a process more suited to economically priced hand-labour than to mechanical harvesting.

Over the years the chemistry of the pyrethrins has been of continuing interest to me and since this is the year in which I retire from the Sir Jesse Boot Chair of
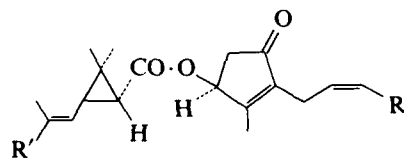
FIG 1 The six natural pyrethrin (pyrethrum flowers (*Chrysanthemum cinerariaefolium*)) insecticides. Pyrethrin I, $R = CH = CH_2$, $R' = Me$; pyrethrin II, $R = CH = CH_2$, $R' = CO_2Me$; cinerin I, $R = Me$, $R' = Me$; cinerin II, $R = Me$, $R' = CO_2Me$; jasmolin I, $R = Et$, $R' = Me$; jasmolin II, $R = Et$, $R' = CO_2Me$.

4
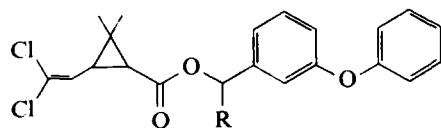
R = H   Permethrin
R = CN   Cypermethrin
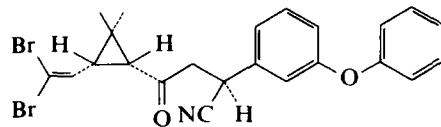
(1R)-cis-   (α-s)

Deltamethrin

FIG 2   Modern synthetic pyrethroids.
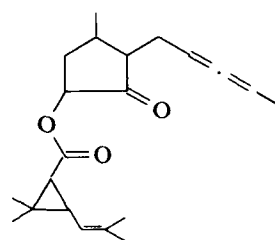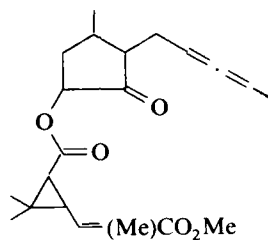
Pyrethrin I   Pyrethrin II

Staudinger and Ruzicka 1924 (1910–1916)

FIG 3   Early formulae for pyrethrins.
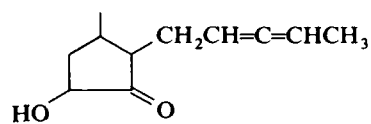
Staudinge and   La Forge
  Ruzicka (1924)
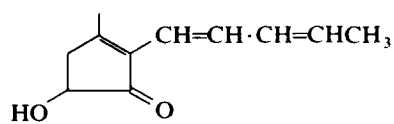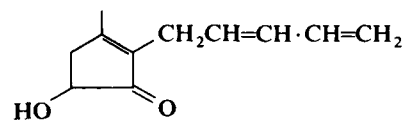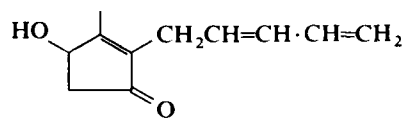
Woodward   La Forge and Soloway
(Gillam and West)   (1947)

FIG 4   Early formulae for pyrethrolone.
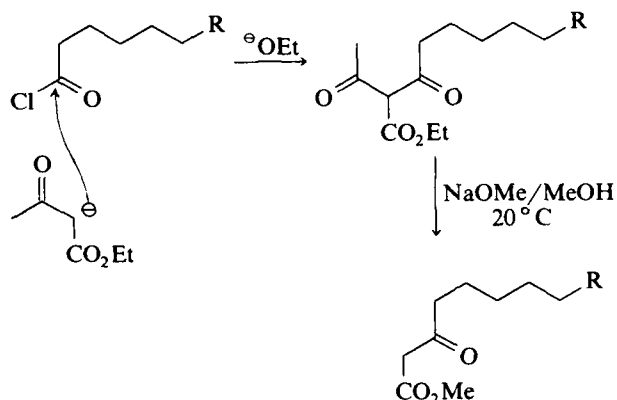
FIG 5 Synthesis of γ-substituted acetoacetates.

Organic Chemistry in Nottingham (though not, I hastily add, from chemistry), I thought I might be allowed to take a more personal view of my subject. I first ventured into pyrethrum chemistry in 1946 as a Ph.D. student under Professor (then Dr.) Stanley H. Harper at Kings College University of London and my two companions in research were Michael Elliott and Hugh W.B. Reed. Sadly, Stanley Harper died last August and I would like to pay a special tribute to him as a scientist of the highest integrity. Without him and his foresight it seems unlikely to me that there would have been much of a British contribution to the chemistry of pyrethrins and pyrethroids. We three research students would have worked on other topics and developments might have occurred elsewhere.

At the time I began research the field of pyrethrins chemistry was dominated by a massive contribution from Staudinger and Ruzicka carried out in Switzerland between 1910 and 1916, though not published in *Helvetica* until 1924 [6]. I don't think this work has ever had the recognition it deserved: it is an incredibly brilliant achievement made at a time when chemical techniques were not adequately developed to cope with mixtures of closely related, unstable, non-crystalline compounds.
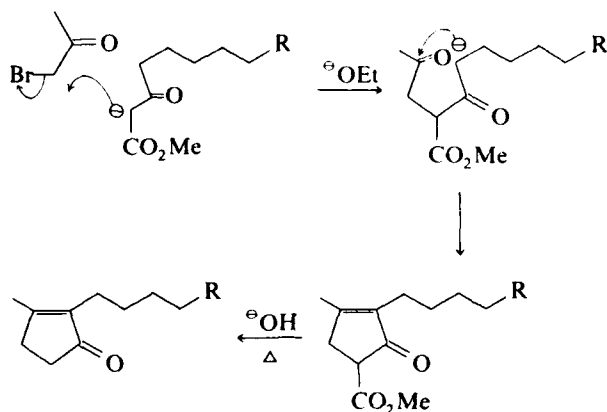
FIG 6 Synthesis of rethrones.

That full purification was not possible, that only two compounds were recognized (Fig. 3), and that the structure of the ketol portions needed substantial revision and the stereochemistry needed development, should in no way obscure the enormous leap they had made. Prior to their work other investigators had made little progress.

Our major competing group in the 1940s was that of LaForge and his colleagues at the U.S. Department of Agriculture. In their hands, along with contributions from others, the structure of pyrethrolone underwent various revisions [7] until it reached that accepted today (the 1947 structure) (Fig. 4). It was the LaForge group too that eventually recognized the existence of the cinerins [8] though stereochemical information was lacking for both pyrethrins and cinerins.

Our early synthetic approach to the pyrethrins resolved around a cyclopentenone synthesis used earlier by Hundsdiecker [9]. γ-Substituted acetoacetates were prepared as in Fig. 5 and then converted into cyclopentenones (or rethrones) (Fig. 6). Stanley Harper along with his colleague Dr. Ishbel Campbell had already improved Ruzicka's synthesis of chrysanthemic acid, the cyclopropane acid fragment of the rethrins I, and had optically resolved the ($\pm$)-cis- and ($\pm$)-trans- forms [10,11]. Treatment of the synthetic rethrones dihydrocinerone and tetrahydropyrethrone with N-bromosuccinimide, followed by reaction of the allylic bromide with silver ($\pm$)-trans- chrysanthemate gave the first totally synthetic rethrins, dihydrocinerin I and tetrahydropyrethrin I (Fig. 7): the ($\pm$)-cis-isomers were similarly prepared. This work was reported by Crombie, Elliott, Harper and Reed in Nature in 1948 [12] and the compounds were each prepared as a pair of ($\pm$)-diastereoisomers.

You must remember the conditions under which we worked in those post-war days. Our laboratories at Kings College London were exactly as they had been at the turn of the century. Fume cupboards were either not provided or were ventilated by lighting a gas-flare in the extraction outlet. Bromacetone (cf. Fig. 6), a potent
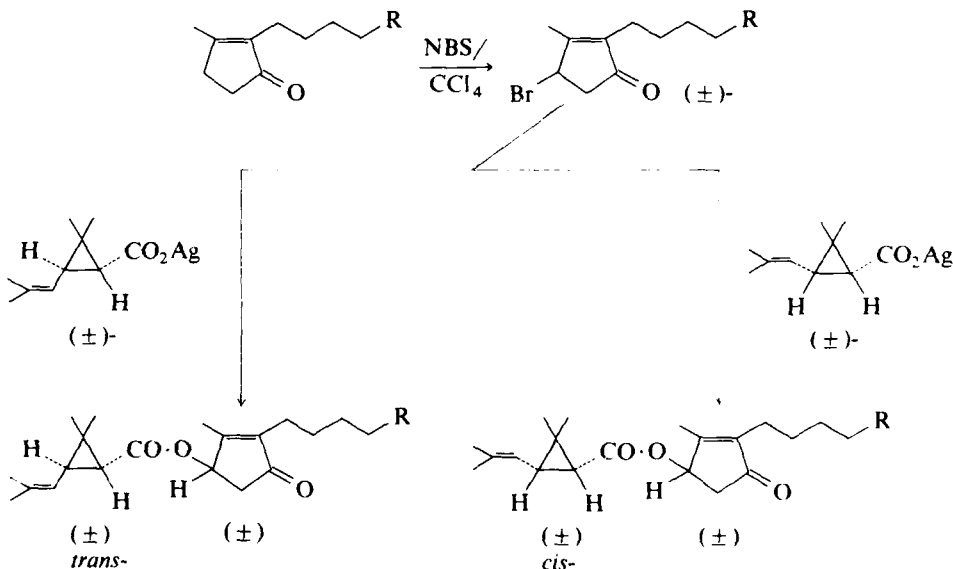
FIG 7 The first synthesis of rethrins. Dihydrocinerin I, R = H; tetrahydropyrethrin I, R = Me.
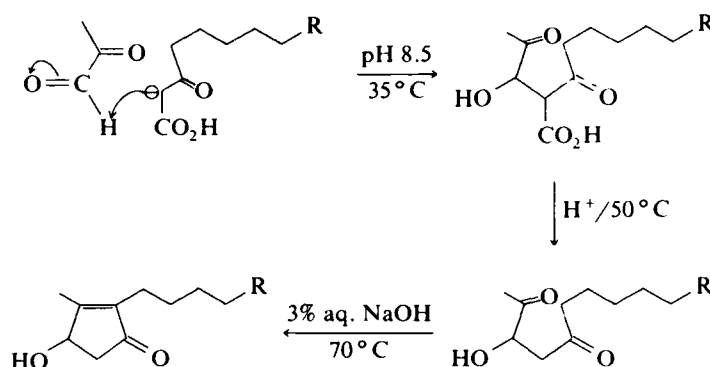
FIG 8 Synthesis of rethrolones.

lachrymator, was made by us on quite a large scale and was weighed out on a scale pan-balance in the open laboratory: our tears would splash copiously on the old gnarled wooden bench. It was a laboratory of corks and soda-glassware: a Pyrex flask with a ground glass joint was a great luxury. Plastic or rubber tubing, always short, was bought with our own money at Woolworths around the corner in the Strand. But it was a very happy and stimulating atmosphere.

At about this time LaForge and his colleagues [13] improved a reaction originally studied by Henze and Stohr in which the anion of a substituted acetoacetate was used in an aldol rather than a displacement sense (Fig. 8), the reaction giving a cyclopentenolone (or rethrolone). This was an important advance as the N-bromo-succinimide method was unsuitable for making bromorethrones having unsaturated side-chains and such unsaturation was necessary for good insecticidal activity in the finished rethrin. LaForges' work eventually led to the non-natural insecticide allethrin, sold as a complex mixture of stereoisomers.

Hugh Reed went off to I.C.I. in 1948 and Michael Elliott joined Rothamsted in 1949, whilst I continued with Stanley Harper as a post-doctoral fellow before going off to Imperial College as a lecturer in 1950. The side-chains of the pyrethrins involved problems in geometrical isomerism and surprisingly little was known about cis- and trans- [or (Z) and (E)] olefins and how you made them. I looked at various

(z)-Cinerone   (z)-Cinerolone
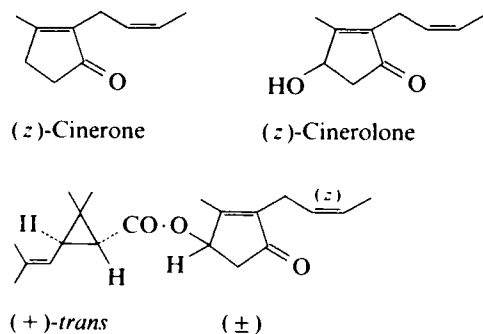
(+)-trans   (±)

Cinerin I

FIG 9 Synthetic cinerin I and relatives.
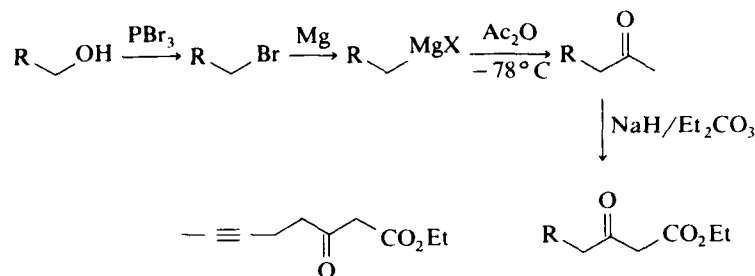
FIG 10   Alternative synthesis of γ-substituted acetoacetates.

ways of making cis- and trans-hex-4-enoic acids, and monitoring the stereochemistry, and this led in 1949 to the synthesis of the first natural pyrethrin, cinerin I, as a pair of diasteroisomers, along with cinerone and cinerolone [14] (Fig. 9). The unnatural trans-(E)-compounds were made at the same time and we developed other methods for making the necessary γ-substituted acetoacetate intermediates (e.g. Fig. 10) [151].

One of the tasks I undertook in connection with rethrin syntheses was making the complete set of isomeric heptenoic acids (Fig. 11) [16] and this brought me into contact with leaf alcohol which I made synthetically and showed was cis [17]. Leaf alcohol is widespread in nature and much later in my career its biosynthetic origins became of interest to me. With the heptenoic acids available I thought it would be as well to clear up what dihydropyrethrone, a hydrogenation product obtained from pyrethrone, was, as some confusion over the nature of the pyrethrolone side chain still persisted in the literature. First I made jasmone in cis- and trans- forms [18]. Jasmone is an expensive perfumery material found in the extract of jasmine flowers and I was able to show that the natural material was cis- with an odour much superior to the trans- (or dihydrojasmone sold as a substitute). cis-Jasmone was equated with dihydropyrethrone.
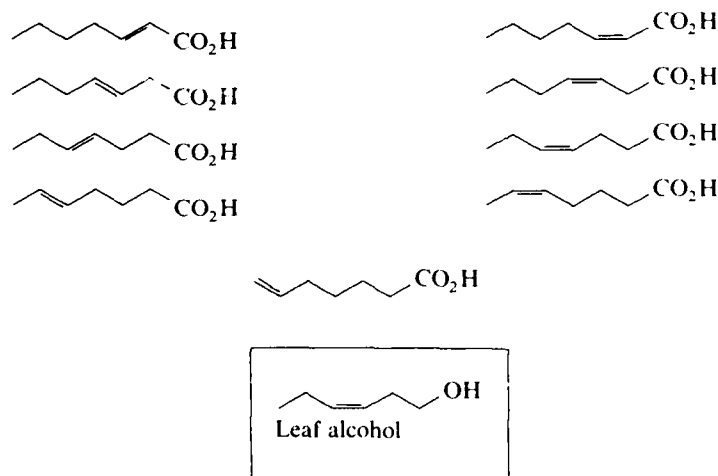
FIG 11   The isomeric heptenoic acids.

(*z*)-Jasmone   (*z*)-Jasmolone

(+)-*trans*   (±)
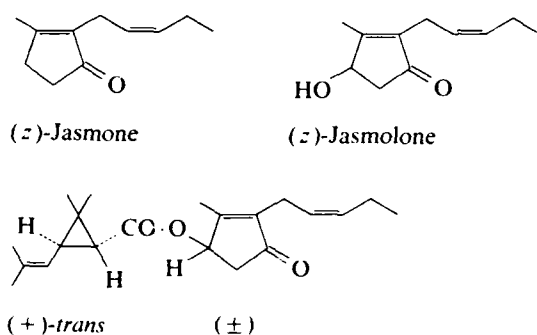
Jasmolin 1

FIG 12 Synthetic jasmolin 1 and relatives.

As in the case of the cinerins we also made jasmolin I [15] (Fig. 12) though at the time we had no idea that it was a natural product. Many years later my former research student Peter Godin, then at the Tropical Products Institute, visited me and told me that he and his colleagues had been studying pyrethrum extract by gas-liquid chromatography and had found a new pyrethrin which he thought could be jasmolin I [19]. I had our original synthetic specimen, and a few minutes GLC work proved this to be correct.

Pyrethrolone itself was a more difficult synthetic proposition. Pyrethrolone with a *trans*- or (*E*) side chain was easier than the natural *cis* and I was able to make the necessary *trans*- diene precursors in a number of ways and this led to the synthesis of (*E*)- pyrethrin I [20] (Fig. 13). For *cis*-(*Z*)-pyrethrolone, vinyl acetylene was our starting material and we had to make this rather laboriously ourselves (Fig. 14). It was converted to a γ-substituted en-yne acetoacetate and thence by pyruvaldehyde condensation into an en-yne rethrolone (Fig. 15). Careful catalytic partial hydrogenation gave (*Z*)-pyrethrolone and (*Z*)-pyrethrin I and its successful accomplishment is a tribute to the skill of Frank Newmann. Conjugated en-ynes are rather more stable than the exposed and sensitive terminal *cis*-diene system so selective partial hydrogenation, followed by purification, was left until the final synthetic stage.

(*E*)-Pyrethrone   (*E*)-Pyrethrolone

(+)-*trans*   (±)
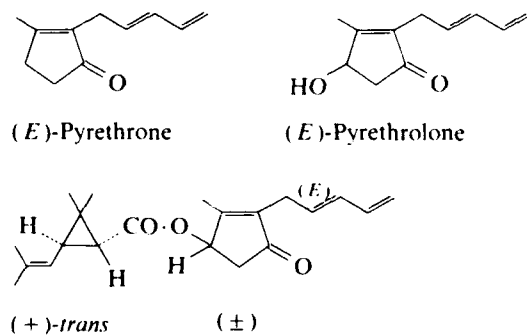
(*E*)-Pyrethrin I

FIG 13 Synthetic (*E*)-pyrethrin I and relatives.
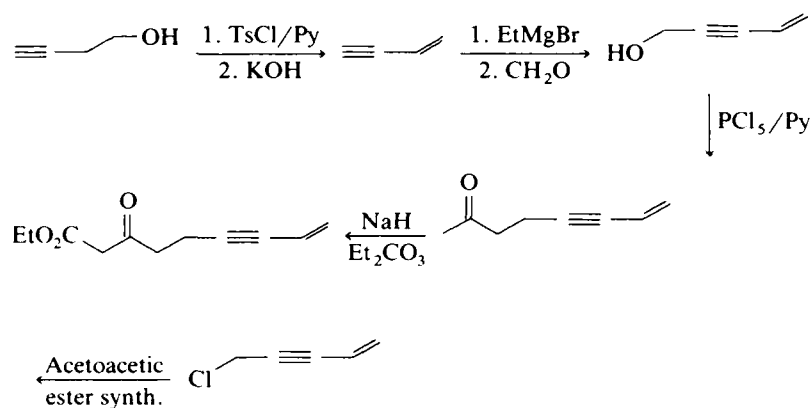
FIG 14   Intermediates for the synthesis of (Z)-pyrethrins.

For me, that completed one chapter in pyrethrins research. However, later we took up the subject of rethrolone synthesis again, exploiting the salt-free Wittig reaction to create double bonds which were essentially *cis*- and employing a common intermediate (Fig. 16) [23]. Carboxylation using methyl magnesium carbonates was also a considerable improvement over the use of diethyl carbonate followed by hydrolysis. For reasons of history we also made the rethrolone having an allene side-chain such as Ruzicka had originally postulated (Fig. 17) [23]. A quick route to cinerone and jasmone (Fig. 18) [24] was also devised but because the Wittig reaction is reversed, the allylic phosphonium yield is somewhat stabilized in the pyrethrone case giving poor *cis*-selectivity and the *trans*-material has to be removed by a Diels-Alder reaction.

Our comparisons with natural pyrethrolone were aided by Michael Elliott's finding [25] that it formed a crystalline hydrate that could be highly purified and, in collaboration with his group, we studied reactions of natural pyrethrolone including its interesting dehydrodimerization (Fig. 19) [26]. We also joined forces to publish definitive ^{1}H nuclear magnetic resonance (NMR) spectra for the pyrethrins and their components [27] and, because of their instability and the purification difficul-

(*z*)-Pyrethrolone

(+)-*trans*   (±)
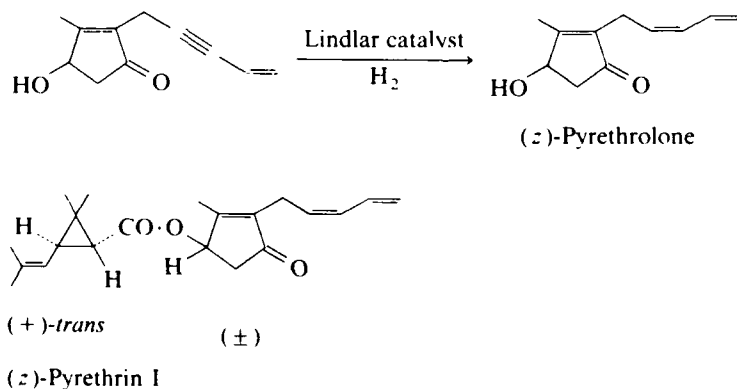
(*z*)-Pyrethrin I

FIG 15   Synthesis of (Z)-pyrethrin I.
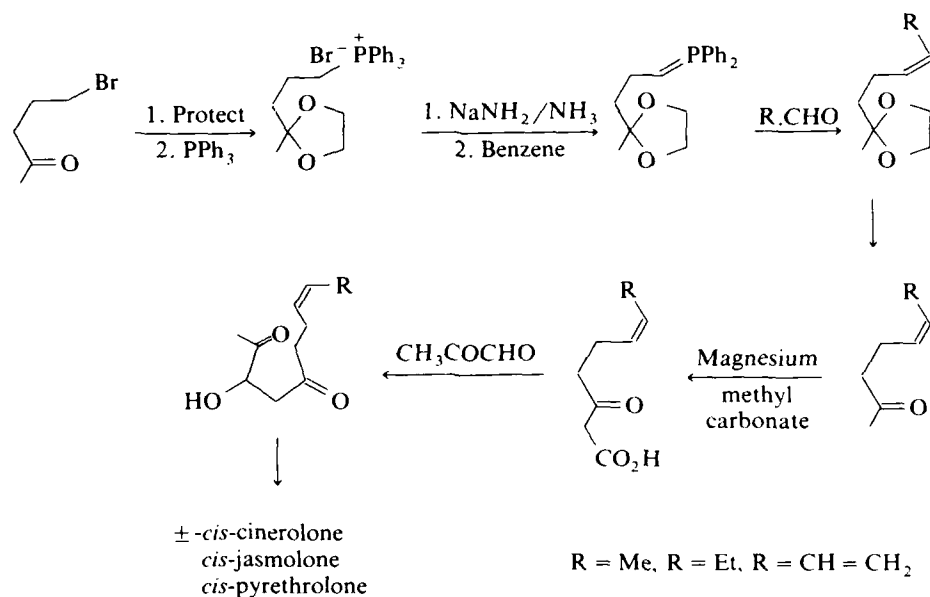
FIG 16 Alternative synthetic approach to the pyrethrolones.

ties, these have proved a useful reference set for other researchers. Later my group extended the data to ^{13}C NMR [28] and to mass spectra [29].

Whilst a research student, I found that if you reflux (±)-cis-chrysanthemic acid with aqueous sulphuric acid, a beautiful crystalline lactone is obtained. I formulated
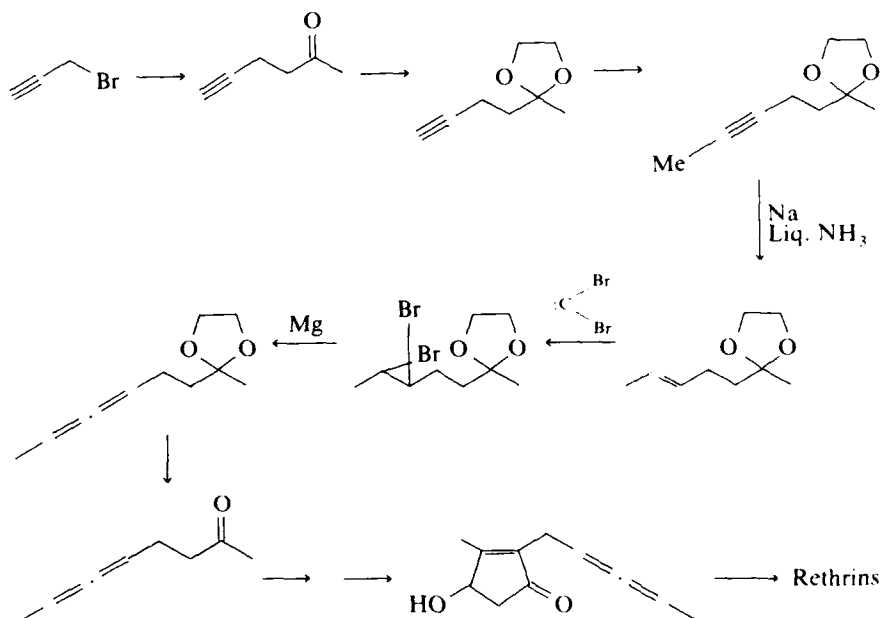
FIG 17 Synthesis of Ruzicka's allenic formula for pyrethrolone.

12
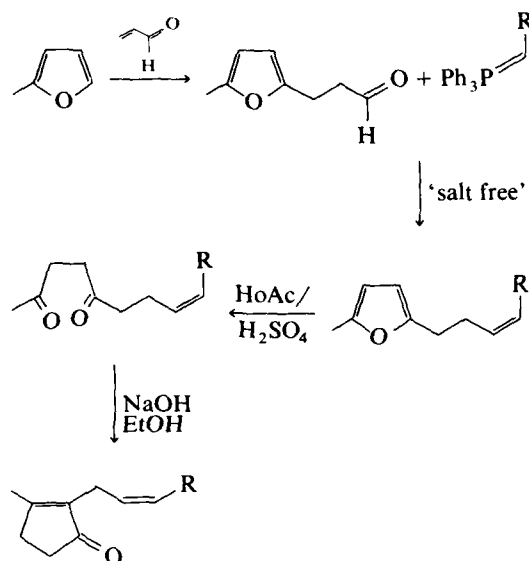
FIG 18 A short route to rethrones. Cinerone, 32–35% yield (~12% *trans*-); jasmone 32–35% yield (~12% *trans*); pyrethrone 32–35% yield (~60% *trans*-) removed by *p*-benzoquinone.

it as a six-membered lactone (see Fig. 20) [30]. I was surprised when a little later it was reported [31] that pyrolyses of either (±)-*cis*- or (±)-*trans*- chrysanthemic acid gave a lactone called pyrocin which was accorded the same structure. On re-investigation we found that pyrocin was in fact a five-membered lactone with the cyclopropane ring ruptured [30], and this had important consequences. Making pyrocins from optically active *cis*- and *trans*- chrysanthemic acids, I discovered that (+)-*trans* and (−)-*cis*- gave one and the same pyrocin [32] (Fig. 21). The reaction retains chiral centre B so this is the same in both acids: in other terms, they have an epimeric relationship at centre A. Further, by degradation and a series of correlations we could relate (−)-pyrocin to a glyceraldehyde standard, thereby determining for the first time the absolute configuration of the chrysanthemic acids. The epimeric nature of the A centre in (+)-*trans*- and (−)-*cis*- chrysanthemic acid was then confirmed as follows [33] (Fig. 21). Each acid was subjected to Arndt-Eistert synthesis thereby achieving one carbon chain extension of the carboxyl pendant. Pyrolysis of the two homo-acids gave two new five-membered lactones in which the A centre is retained but the B is destroyed. This process gave two enantiomeric lactones. This early stereochemical work was important because only the (+)-*trans*- and (+)-*cis*- esters of chrysanthemic acid give highly insecticidally active esters [34].
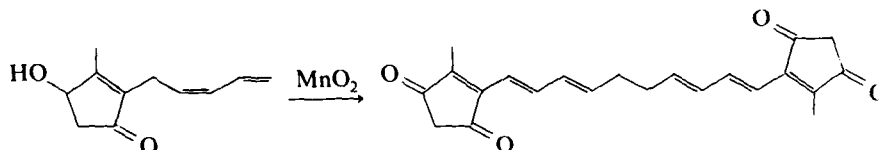
FIG 19 Oxidative dehydrodimerisation of pyrethrolone.
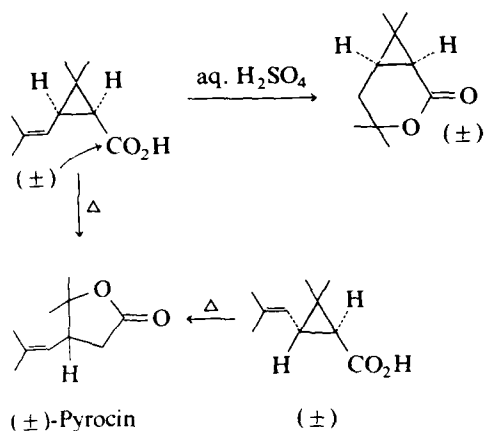
FIG 20   Pyrocin and *cis*-chrysanthemolactone.

showing that the absolute stereochemistry at the carboxyl-bearing centre of the acid is critical.

Extension of the diazoacetic ester synthesis used to make the chrysanthemic acids, employing 2,5-dimethylsorbic ester as the second component, gave on hydrol-
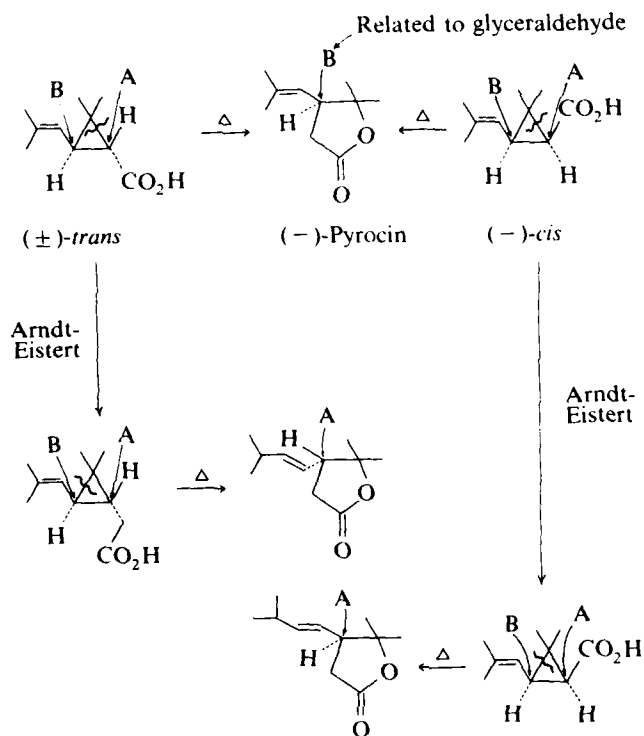
FIG 21   The absolute configuration of the chrysanthemic acids.

ysis chrysanthemum dicarboxylic acid which was separated into (±)-*cis*- and (±)-*trans*- forms (Fig. 22). [35]. Partial hydrolysis of (+)-dimethyl chrysanthemum decarboxylate gave pyrethric acid which was esterified to give a model rethrin II (Fig. 22). The (*E*)-geometry of the cyclopropane side chain was established by ¹H NMR shielding data [33].

Diazoacetic ester was, I suppose, a bit hazardous to handle in that old Kings College laboratory but Hugh Reed made a total of 1.69 kg and I have memories of him distilling a large batch under water pump vacuum with the apparatus set up on the floor, bunsen roaring beneath the flask heated in an oil bath. We were not always as fortunate. I had a diazomethane explosion, and later Ken Sleep, who worked on the chrysanthemum dicarboxylic acid problem, had a nasty bang on distilling diazoacetonitrile. It was so violent that his glass apparatus disappeared and his hair was filled with powdered glass, but he suffered little personal damage. I have memories of a reagent bottle containing ether on a shelf nearby issuing a fine jet of ether from a tiny hole where it had been cleanly punctured with a fine sliver of glass.

For many years the absolute configuration of the natural rethrin ketols was uncertain and I resolved to clear the matter up (and confirm at the same time all our other stereochemical conclusions) by X-ray crystallography using a suitable heavy atom derivative. It proved exceedingly difficult to obtain a suitable crystal but after many attempts we succeeded in the case of the 6-bromo-2,4-dinitrophenylhydrazone
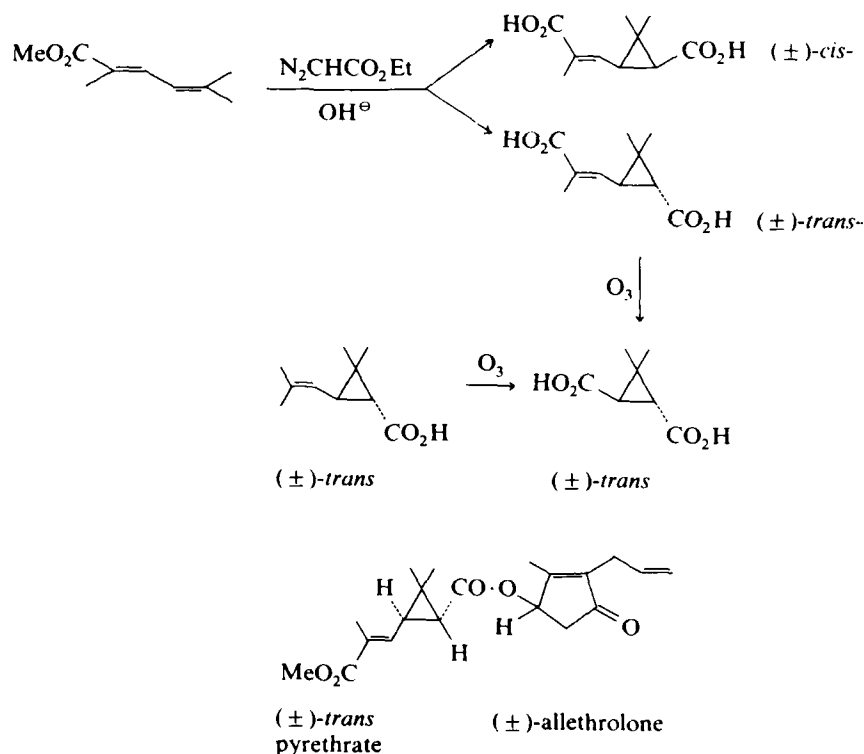
FIG 22 Synthesis of chrysanthemum dicarboxylic acid and a rethrin II.

15
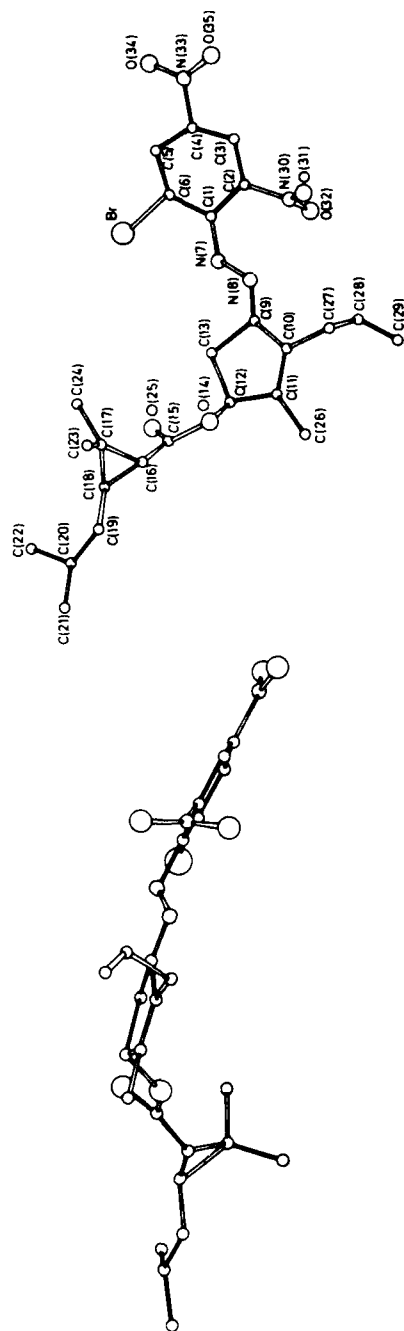
FIG 23   X-Ray structure of (+)-allylrethronyl-(+)-*trans* chrysanthemate-6-bromo-2,4-dinitrophenylhydrazone (two views).
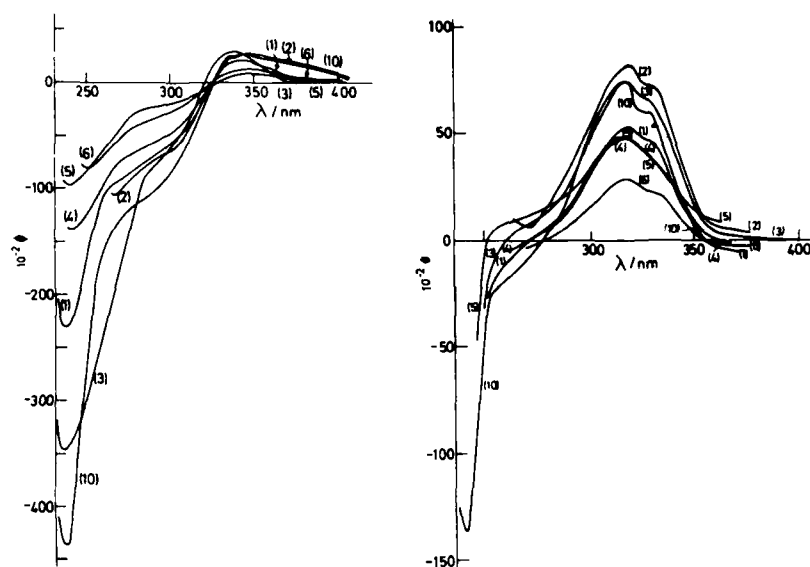
FIG 24   Optical rotatory dispersion and circular dichroism curves for rethrins (1–6 are the natural pyrethrins and 10 is (+)-allylrethronyl-(+)-trans-chrysanthemate).

of (+)-allethronyl (+)-trans-chrysanthemic acid (Fig. 23) [36,37]. Using this as our reference, we were then able to relate the ketol stereochemistry at C-4 by circular dichroism and optical rotatory dispersion curves (Fig. 24) [37].

After studies relating to methods for selectively breaking each of the carbon-carbon linkages of the cyclopropane ring in chrysanthemic acid, which permits the formation of important terpene skeletons (Fig. 25) [38], we studied the pyrolysis of chrysanthemum mono- and di-carboxylic acids [39], a matter of significance in connection with early biosynthetic results. We also showed how chrysanthemic and pyrethric acids can be easily radiolabelled via reconstructive synthesis using degradation followed by a Wittig reaction (Fig. 26) [40]. Foreign side chains can be easily inserted by this method, which proved valuable in structure-activity studies.

Unfortunately positive and informative results on chrysanthemic acid biosynthesis are still sparse, though the problem appears to be similar to that of biosynthetic
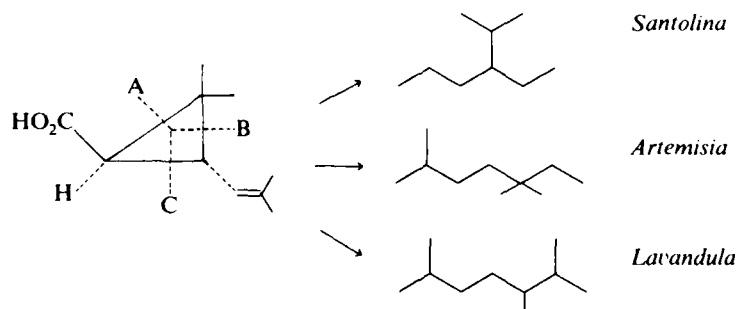
FIG 25   Cyclopropane scissions of chrysanthemic acid.
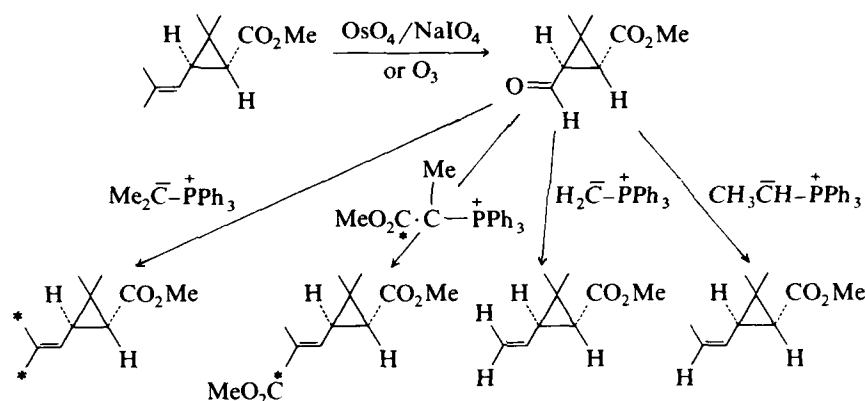
FIG 26   Synthesis of labelled chrysanthemic acid and analogues.

formation of presqualene alcohol and prephytoene alcohol (Fig. 27) [41]. Fig. 28 shows a suggested pathway [42] for chrysanthemyl alcohol formation. Oxidation then leads to chrysanthemic acid, then to pyrethric acid with the methyl of the ester being methionine derived [43,44,46]: there is however evidence of uneven labelling between the two isoprene units when mevalonate is used as a precursor [45].

Pyrethrins occur in the achenes of *C. cinerariaefolium*, structures which contain linoleic and linolenic acid. Many years ago LaForge [47] showed that pyrethrolone esters of these fatty acids occur in the achenes so there is circumstantial evidence to suggest that the rethrolones might be of fatty acid derivation. We might hypothesize (Fig. 29) that either the front or rearward part of linolenic acid could provide the carbon frame of a rethrolone and that these could be distinguished by employing suitable $[2-^{14}C]$- and $[10-^{14}C]$-labelled precursors. In the event, administration of $[2-^{14}C]$linoleate and $[10-^{14}C]$oleate (precursors that one would expect plant enzymes

Chrysanthemyl alcohol

Presqualene alcohol

Prephytoene alcohol
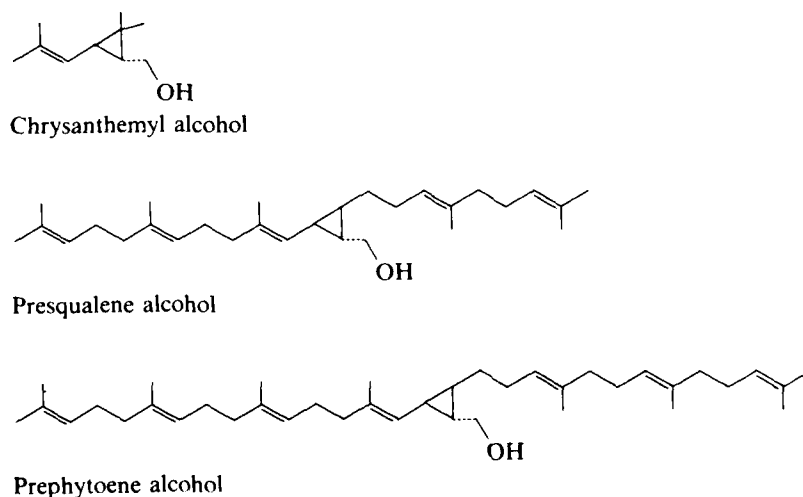
FIG 27   Chrysanthemyl alcohol and important natural analogues.

18

Chrysanthemic Acid
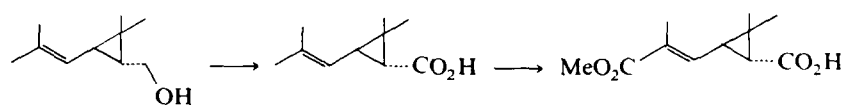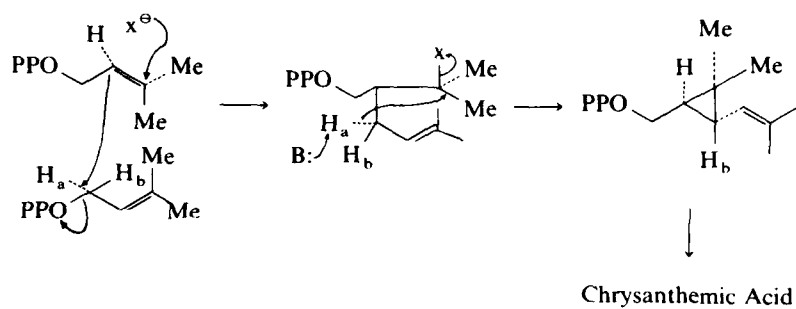
FIG 28 Pathways to chrysanthemic acids.
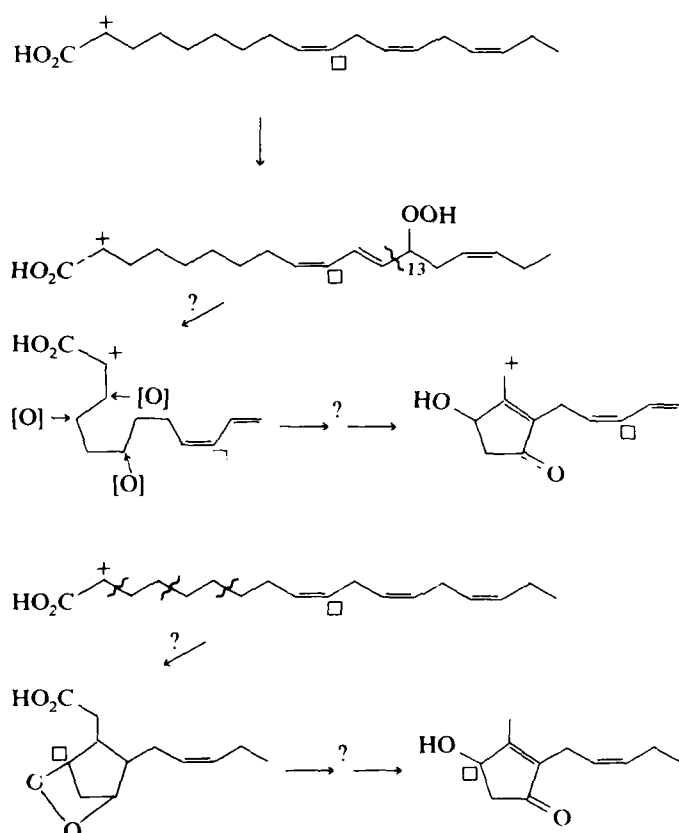
FIG 29 Hypothetical derivations of rethrolones.

FIG 30 Linolenic acid transformations (products from flax seed enzyme preparation).

to dehydrogenate to linolenate) failed to make the required distinction [48]. Instead, much degradation to acetate occurred, followed by re-incorporation of the latter with much label scrambling: the labelled acetate also entered the chrysanthemic

FIG 31 The allene-epoxide biosynthetic route.

20

FIG. 32   The colnelenic pathway: chain fracture of linolenic acid.

acid part of the molecules. Crude achene homogenate was used in this work and more detailed biochemical study of the system will be needed to make further progress. Nevertheless other avenues have opened.

Zimmerman [49] has shown that when linolenic acid is treated with a crude enzyme preparation from flax seed an α-ketol, a γ-ketol and 12-oxophytodienoic acid (12-oxoPDA) are formed (Fig. 30). The latter undergoes biochemical hydrogenation and a series of β-oxidations, forming cis-jasmonic acid. We have studied these reactions using deuterium labelled linoleic and linolenic acid and have shown that all three compounds, the α- and the γ-ketol and 12-oxoPDA originate from the linolenic 13-hydroperoxide via an epoxycation which loses a proton to form an allene epoxide (Fig. 31) [50,51,53]. The mechanism is related to the carbon chain fracture processes which we have shown leads to colnelenic acid and smaller fragments of considerable importance to food and perfumery chemistry (Fig. 32) [52,53].
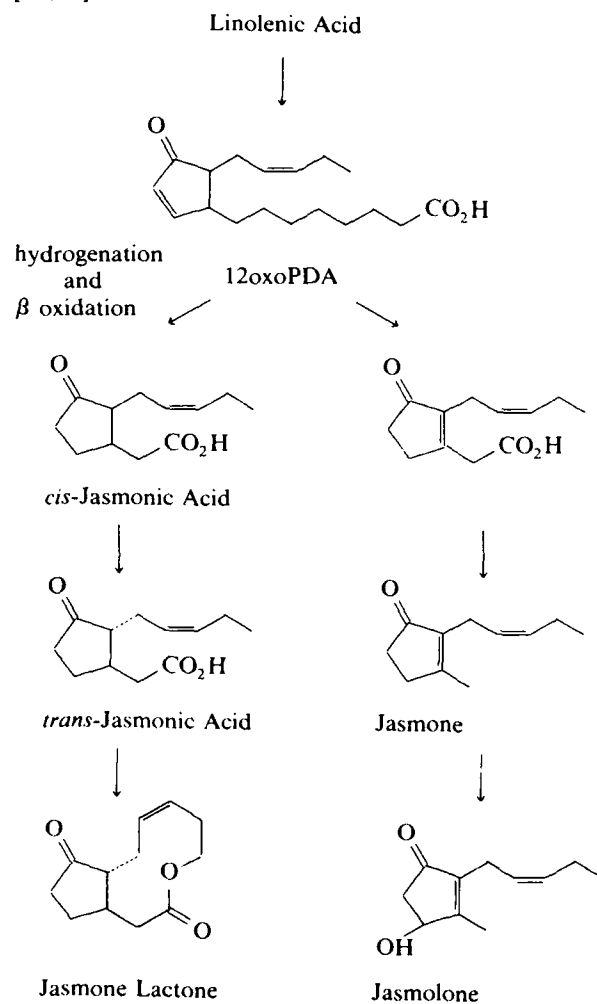
FIG 33 Suggested route to jasmonoids and jasmolone.

We believe that 12-oxoPDA and the jasmonic acid pathway give important grounds for developing a biogenetic theory of rethrolone formation. Extract of jasmine flowers contains jasmonic acid, jasmone lactone and jasmone (Fig. 33) [54]. *trans*-(Z)-Jasmonic acid can arise by epimerisation of the *cis*-(Z), the β-oxidation product of 12-oxoPDA [55]. Jasmone lactone is a product of β-oxidation of the unsaturated side chain. If instead of reduction of the ring double bond of 12-oxoPDA, there is migration to the thermodynamically stable tetrasubstituted position α- to the ketone, the resulting vinylogous β-keto acid will decarboxylate easily giving jasmone. There is already evidence in the literature [56] that rethrones can be oxidized microbiologically to rethrolones and such a process would afford jasmolone. A possible route to cinerone with loss of a terminal carbon atom is via ω-oxidation and an ultimate decarboxylation, and a similar oxidation/dehydration is one possibility for formation of the diene side chain of pyrethrolone. Such hypotheses clearly increase the desirability of finding more amenable biological systems for studying pyrethrins biosynthesis directly: there is much to do in this area.

The market for synthetic pyrethroids emanating from the Rothamsted/BTG patents is between 900 and £1,000 million per annum. Even for those merely interested in monetary wealth generation rather than science there are important lessons in the pyrethrins story and its implications. If basic exploration work—the value of which industry does not necessarily recognize initially—does not go on in universities, both industry and government will find themselves with dried up wells of ideas. Often on shoestring budgets, and under adverse conditions, the wells have to be dug and filled with water, and this is an important contribution the university sector has to make to the economy.

References

1 Gnadinger, C.B. (1936–1945) Pyrethrum Flowers, 2nd Edn. and Supplement. McLaughlin Gormley King Co., Minneapolis, Minnesota.
2 Nelson, R.H. (Ed.) (1945–1972) Pyrethrum Flowers, 3rd Edn., McLaughlin Gormley King Co., Minneapolis, Minnesota.
3 Jacobson, M. and Crosby, D.G. (Eds.) (1971) Naturally Occurring Insecticides. Dekker, New York.
4 Casida, J.E. (Ed.) (1973) Pyrethrum, The Natural Insecticide. Academic Press, New York and London.
5 Leahey, J.P. (Ed.) (1985), The Pyrethroid Insectides, Taylor and Francis, London and Philadelphia.
6 Staudinger, H. and Ruzicka, L. (1924) Isolation and constitution of the active portion of Dalmatian insect powder. Helv. Chim. Acta. 7, 177–201, and the ten papers which immediately follow (to page 458).
7 For a contemporary review see Harper, S.H., (1948) Annual Reports of the Chemical Society 45, 162.
8 LaForge, F.B. and Barthel, W.F. (1944) Heterogenous nature of pyrethrolone. J. Org. Chem. 9, 242–249. See also idem, ibid. (1945) 10, 106–113, 114–120.
9 Hunsdiecker, H. (1947) On the preparation of γ-diketones. The cyclopentenone ring-closure of γ-diketones of the type $CH_3COCH_2CH_2COCH_3$. Chem. Ber. 75, 460–468.
10 Campbell, I.G.M. and Harper, S.H. (1945) Synthesis of chrysanthemum monocarboxylic acid, J. Chem. Soc., 283–286.
11 Campbell, I.G.M. and Harper, S.H. (1957) Optical resolution of the chrysanthemic acids, J. Sci. Food Agric. 3, 189–192.

12 Crombie, L., Elliott, M., Harper, S.H. and Reed, H.W.B. (1948) Total synthesis of some pyrethrins. Nature (London) 162, 222.

13 Schechter, M.S., Green, N., and LaForge, F.B. (1949) Cinerolone and the synthesis of related cyclopentenolones. J. Am. Chem. Soc. 71, 3165–3173.

14 Crombie, L., and Harper, S.H. (1950) Synthesis of cinerone, cinerolone and cinerin I. Nature (London) 164, 534; J. Chem. Soc., 1152–1160.

15 Crombie, L., Harper, S.H., Stedman, R.E. and Thompson, D. (1951) New syntheses of the cinerolones. J. Chem. Soc., 2445–2449.

16 Crombie, L. (1949) Olefinic acids and their relation to the synthesis of pyrethrins. Ph.D. Thesis, University of London, and unpublished work.

17 Crombie, L. and Harper, S.H. (1950) Leaf alcohol and the stereochemistry of the cis- and the trans-n-hex-3-en-1-ols and -n-pent-3-en-1-ols. J. Chem. Soc., 873–877.

18 Crombie, L. and Harper, S.H. (1952) Stereochemistry of jasmone and identity of dihydro-pyrethrone. J. Chem. Soc., 869–875.

19 Godin, P.J., Sleeman, R.J., Snarey, M. and Thain, E.M. (1966) The jasmolins, new insectidally active constituents of Chrysanthemum cinerariaefolium vis. J. Chem. Soc., 332–334.

20 Crombie, L., Harper, S.H. and Thompson, D.J. (1957) Synthesis of trans-pyrethrone, trans-pyrethrolone and a pyrethrin I. J. Chem. Soc., 2906–2915.

21 Crombie, L., Harper, S.H., Newman, F.C., Thompson, D., and Smith, R.J.D.S. (1956) Intermediates for the synthesis of cis-pyrethrolone. J. Chem. Soc., 126–135.

22 Crombie, L., Harper, S.H. and Newman, F.C. (1954) Synthesis of cis-pyrethrolone and pyrethrin I. Introduction of the cis-penta-2,4-dienyl system by selective hydrogenation. J. Chem. Soc., 3963–3971.

23 Crombie, L., Hemesley, P. and Pattenden G. (1969) Synthesis of ketols of the natural pyrethrins. J. Chem. Soc. (C), 24.

24 Crombie, L., Hemesley, P., and Pattenden, G. (1969) Synthesis of cis-jasmone and other cis-rethrones, J. Chem. Soc. (C), 1024–1027.

25 Elliott, M. (1964) Purification of (+)-pyrethrolone as the monohydrate, and the nature of pyrethrolone C. J. Chem. Soc., 5225–5228.

26 Crombie, L., Ellis, J.A., Gould, R., Pattenden, G., Elliott, M., Janes, N.F. and Jeffs, K.A. (1971) Oxidative dimerisation of natural rethrolones and related compounds with manganese dioxide. J. Chem. Soc. (C), 9–13.

27 Bramwell, A.F., Crombie, L., Hemesley, P., Pattenden, G., Elliott, M. and Janes, N.F. (1969) Nuclear magnetic resonance spectra of the natural pyrethrins and related compounds. Tetrahedron 25, 1727–1741.

28 Crombie, L., Pattenden, G. and Simmonds, D.J. (1975) Carbon-13 nuclear magnetic resonance spectra of the natural pyrethrins and related compounds. J. Chem. Soc., Perkin Trans. 1, 1500–1502.

29 Pattenden, G., Crombie, L. and Hemesley, P. (1973) The mass spectra of pyrethrins and related compounds. Org. Mass Spectrom. 7, 719–735.

30 Crombie, L., Harper, S.H. and Thompson, R.A. (1951) Lactonistion of the chrysanthemic acids. J. Sci. Food Agric. 9, 421–428.

31 Matsui, M. (1950) Pyrocin (a new insecticide). Botyu Kagaku 15, 1–20.

32 Crombie, L., and Harper, S.H. (1954) The configuration of the chrysanthemic acids. J. Chem. Soc., 470.

33 Crombie, L., Crossley, J. and Mitchard, D.A. (1963) Synthesis, absolute configuration and ring fission of cis- and trans-homocaronic acids. Their configurative relation to natural terpenes. J. Chem. Soc., 4957–4967.

34 Elliott, M., Needham, P.H. and Potter, C. (1964) Relative toxicity of sters from optical and geometrical isomers of chrysanthemic, pyrethric and related acids and optical isomers of cinerolone and allethrolone. J. Sci. Food Agric. 20, 561–565.

35 Crombie, L., Harper, S.H. and Sleep, K.C. (1957) Total synthesis of (±)-cis- and -trans-chrysanthemum dicarboxylic acid, (±)-cis- and -trans-pyrethric acid and rethrins II. J. Chem. Soc., 2743–2754.

24

36 Begley, M.J., Crombie, L., Simmonds, D.J. and Whiting, D.A. (1972) Absolute configuration of the pyrethrins. Configuration and structure of (+)-allethronyl (+)-*trans*-chrysanthemate 6-bromo-2,4-dinitropenylhydrazone by X-ray methods. J. Chem. Soc. Chem. Commun., 1276–1277.

37 Begley, M.J., Crombie, L., Simmonds, D.J. and Whiting, D.A. (1974) X-ray analysis of synthetic (4S)-2-(prop-2'-enyl)rethronyl (1R) (3R)-chrysanthemate 6-bromo-2,4-dinitrophenylhydrazone and, (3R)chiroptical correlation with the six natural pyrethrin esters. J. Chem. Soc., Perkin Trans. 1, 1230–1235.

Crombie, L., Firth, P.A., Houghton, R.P., Whiting, D.A. and Woods, D.K. (1972) Cyclopropane cleavage of chrysanthemic acid relatives to santolinyl, artemisyl and lavandulyl structures: acid-catalysed and biosynthetic experiments. J. Chem. Soc., Perkin Trans. 1, 642–652.

39 Crombie, L., Doherty, C.F., Pattenden, G. and Woods, D.K. (1971) The acid thermal decomposition products of natural chrysanthemum dicarboxylic acid. J. Chem. Soc. (C), 2739–2743.

Crombie, L., Doherty, C.F. and Pattenden, G. (1970) Syntheses of ^{14}C-labelled (+)-*trans*-chrysanthemum mono- and di-carboxylic acids, and of related compounds. J. Chem. Soc. (C), 1074–1080.

41 Campbell, R.V.H., Crombie, L., Findley, D.A.R., King, R.W., Pattenden, G. and Whiting, D.A. (1975) Syntheses of presqualene alcohol, prephytoene alcohol and structurally related compounds. J. Chem. Soc., Perkin Trans. 1,897–913.

42 Coates, R.M. (1976) Prog. Org. Nat. Products 33, 73–230.

43 Abou Donia, S.A., Doherty, C.F. and Pattenden, G. (1973) Biosynthesis of chrysanthemum dicarboxylic acid, and the origin of the pyrethrin II's. Tetrahedron Lett., 3477.

44 Pattenden, G., Popplestone, C.R. and Storer, R. (1975) Investigation of the role of chrysanthemyl, lavandulyl and artemisyl alcohols in the biosynthesis of chrysanthemic acid. J. Chem. Soc. Chem. Commun., 290–291.

45 Pattenden, G. and Storer, R. (1973) Studies on the biosynthesis of chrysanthemum monocarboxylic acid. Tetrahedron Lett., 3473–3476.

46 Crowley, M.P., Godin, P.J., Inglis, H.S., Snarey, M. and Thain, E.M. (1962) The biosynthesis of the pyrethrins. Biochim. Biophys. Acta 60, 312–319.

47 Acree Jr., F. and LaForge, F.B. (1937) Identification of the fatty acids combined with pyrethrolone. J. Org. Chem. 2, 308.

48 Crombie, L. and Holloway, S.J. (1985) Biosynthesis of the pyrethrins. Unsaturated fatty acids and the origins of the rethrolone fragments. J. Chem. Soc., Perkin Trans. 1, 1393–1400.

49 Vick, B.A. and Zimmerman D.C. (1987) Oxidative systems for modification of fatty acids. the lipoxygenase pathway. In: The Biochemistry of Plants (Stumpf, P.K. and Conn, E.E., eds), Academic Press, 1987.

50 Crombie, L., and Morgan, D.O. (1988) The conversion of linoleic (13S)-hydroperoxide into (13R)-hydroxy-12-oxo-octadec-(9Z)-enoic acid and 9-hydroxy-12-oxo-octadec-(10E)-enoic acid by flax enzyme. Isotopic evidence for an allene-epoxide intermediate. J. Chem. Soc. Chem. Commun. 556.

51 Crombie, L., and Morgan, D.O., (1988) Formation of acyclic α- and γ-ketols and 12-oxophytodienoic acid from linolenic acid 13-hydroperoxide by flax enzyme preparation. Evidence for a single enzyme leading to a common allene epoxide intermediate. J. Chem. Soc., Chem. Commun. 558.

52 Crombie, L., Morgan, D.O. and Smith, E.H. (1987) The enzymic formation of colneleic acid, a divinyl ether fatty acid: experiments with [(9S)-^{18}O$_2$]-hydroperoxyoctadec-(10E), (12Z)-dienoic acid. J. Chem. Soc. Chem. Comm. 502–503.

53 Crombie, L., and Morgan, D.O. (1987) Experiments with [9,10,12,13-^{2}H$_4$]-linoleic acid on the formation of 9-[nona-(1'E), (3'Z)-dienyloxyl-non-(8E)-enoic (colneleic) acid and (13R)-hydroxy-12-oxo-octadec-(9Z)-enoic acid by plant enzymes. J. Chem. Soc. Chem. Commun., 503–504.

54 Demole, E., Willhalm, B., and Stoll, M. (1984) Properties and Structure of the ketolactone $C_{12}H_{16}O_3$ from Jasmine (Jasminium gradiflorum L) essence. Helv. Chim. Acta 47, 1152.

55 Vick, B.A. and Zimmerman, D.C. (1984) Biosynthesis of Jasmonic acid by several plant species. Plant Physiol. 75, 458–461.

56 LeMahieu, R.A., Tabenkin, B., Berger, J. and Kierstead, R.W. (1970) Microbiological oxidation of allethrone. J. Org. Chem. 35, 1687–1688.

CHAPTER 2

Effects of kinins and related peptides on synaptic transmission in the insect CNS

BERNARD HUE [1] AND TOM PIEK [2]

[1] Department of Neurophysiology, UA CNRS 611, Medical Faculty, University of Angers, 49045 Angers Cedex, France and [2] Department of Pharmacology, University of Amsterdam, Meibergdreef 15, 1105 AZ Amsterdam, The Netherlands

Introduction

The venoms of bees, wasps and ants, all belonging to the insect order of Hymenoptera, show a diversity of combinations of chemical weapons against a variety of enemies or prey [1]. In three taxonomically related groups, i.e., the social wasps, the scoliid wasps and the ants, a characteristic group of polypeptide toxins has been found [1–3], the action of which on vertebrate smooth muscle, as well as the chemical structure is closely related to that of bradykinin. These bradykinin-like peptides have been called kinins by Jacques and Schachter [4].

Because scoliid wasps use their venom to paralyse beetle larvae by stinging them in the nerve ganglia [5], we have studied the action of the venom of the wasp *Megascolia flavifrons*, and one of the kinins present in the venom, on cholinergic synaptic transmission and axonal excitability in the sixth abdominal (A6) ganglion of the cockroach, *Periplaneta americana*.

Materials and methods

Experiments were done using a preparation of the desheathed A6 ganglion of the cockroach, connected to the cercal nerve XI and to the connective, or one of its identified isolated giant axons (GI2, according to the nomenclature of Harris and Smith [6]) between ganglion six and five (Fig. 1). For recording electrical activity a double mannitol-gap or a single-fibre oil-gap method was used [7]. Subthreshold composite excitatory postsynaptic potentials (EPSPs) were evoked by electrical stimulations applied to the ipsilateral cercal nerve XI via Ag/AgCl hook electrodes. Continuous recording of the postsynaptic resting potential was accompanied by recording of EPSPs, and action potentials. The latter potentials were evoked by passing short square pulses of depolarizing current through the axonal membrane using a balanced Wheatstone bridge included in the recording circuit. Direct depolarization of cholinergic postsynaptic membranes of the giant interneuron was achieved by means of ionophoretic injection of acetylcholine or carbamylcholine

28

FIG 1   Photomicrograph of cobalt sulphide staining of cercal nerves (n. X and n. XI) and giant interneuron 2 in the sixth abdominal ganglion of the cockroach. Note that the general pattern of tracts and distribution of nerve endings correspond with the dendritic tree of the giant interneuron. Dendritic processes of the giant interneuron neurite on the contralateral half of the ganglion are indicated by arrows. Arrows with dark point indicate collateral branches. Sometimes they pass through the midline of the ganglion indicated with dashed line [11]. Neuropharmacological tests of this study were performed on cholinergic synapses located between n. XI and giant interneuron 2.

within the neuropile of the A6 ganglion. The EPSPs were recorded as the averages of ten sweeps. The desheathed A6 ganglion was superfused or perfused as has been described earlier [8].

Wasps, *Megascolia flavifrons* were collected in France, and their venom and its fractions obtained by HPLC, were prepared [2,8,9]. Thr^6bradykinin (Thr^6BK) was synthesized by Bachem (Bubendorf, Switzerland). Bradykinin was obtained from Sigma Chemical Co.

Results

Effects of the venom and the Thr^6BK containing fraction
Superfusion of the desheathed A6 ganglion with an extract of 40 venom reservoirs of *Megascolia flavifrons* females per ml caused a slow and irreversible block of synaptic transmission, followed by a delayed and irreversible depolarization of the giant neuron [8]. Intraganglionic injection of a single μl or less of the venom causes
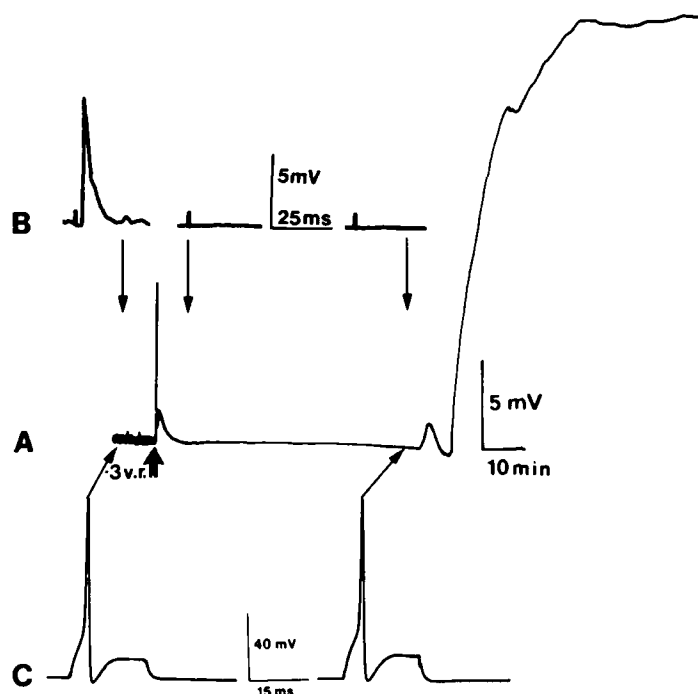
FIG 2   Effects of intraganglionic perfusion of the Thr^{6}BK containing HPLC-fraction of the venom of *M. flavifrons*, at a concentration equivalent to 0.3 venom reservoir (v.r.) per ml. A: effects on the resting membrane potential (thick arrow indicates the moment of perfusion). B: effects on EPSPs (averages of 10 sweeps). Note that in the control the background of unitary potentials has been reduced to a noisy baseline, due to the averaging, and that this noise disappears after perfusion with the venom fraction. C: action potentials. Arrows in B and C indicate correspondence in time with the record in A.

a direct block of synaptic transmission also followed by a delayed depolarization of the neuron after about one hour.

Intraganglionic perfusion with a Thr^{6}BK containing HPLC-fraction, equivalent to 0.3 venom reservoir per ml, caused an immediate and transient depolarization of the giant interneuron and a permanent block of synaptic transmission. This was followed after about one hour by an instability of the neuronal membrane, and a subsequent depolarization (Fig. 2). During the first hour, i.e., before the membrane became depolarized, the action potentials remained unaffected. This is in agreement with earlier findings [8] from current-clamp experiments performed on a portion of axonal membrane of an isolated giant axon of the cockroach, where the venom did not induce any change in resting potential, postpolarization or spike amplitude. Hence, it could be concluded that the venom did not contain blocking agents, channel modifiers or inactivation inhibitors for either the electrically excitable sodium channel or potassium channel [8].

It can be concluded that this fraction shows an effect comparable to that of the whole venom. Since this fraction contains Thr^{6}BK, we have tested both the effects of synthetic bradykinin and synthetic Thr^{6}BK.
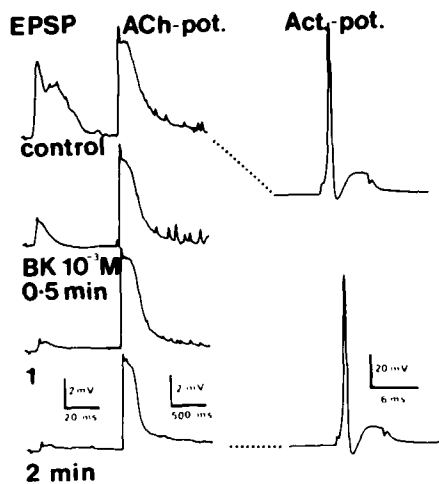
FIG 3 Effects of intraganglionic perfusion of 10^{-3} M bradykinin (Arg-Pro-Pro-Gly-Phe-Ser-Pro-Phe-Arg) on EPSPs and alternatively ionophoretically evoked acetylcholine potentials as well as on action potentials, recorded from the A6 ganglion. Note the fast decrease in EPSP amplitude, without a concurrent effect on the ACh potential and on the action potential.

Effects of bradykinin

Intraganglionic perfusion, at a relatively high concentration of bradykinin (10^{-3} M), caused a block of synaptic transmission from the stimulated cercal nerve to the giant interneuron within a minute. However, microionophoretically evoked acetylcholine potentials were not affected before 5 min (Fig. 3), indicating that the initial block of transmission could be a presynaptic effect.

Effect of Thr⁶BK

Intraganglionic perfusion of Thr^6BK at the high concentration of 10^{-3} M causes an immediate and permanent block of transmission, sometimes with a concurrent transient depolarization of the membrane of the neuron. In none of the experiments was a delayed depolarization seen.

At a ten-times lower concentration (10^{-4} M), perfusion during 5–6 min with Thr^6BK, this kinin frequently gave rise to an initial increase in EPSP amplitude (Fig. 4A). Then, in the absence of further perfusion the amplitude of the EPSPs gradually decreased in a period of 2–3 h. However, ionophoretically applied carbamylcholine could evoke a carbamylcholine potential that did not change in amplitude during the last hour of observation (Fig. 4A). In a different experiment, not shown in the figure, carbamylcholine potentials were also not affected by perfusion with Thr^6BK during the first hour.

When during the progressive decrease in EPSP amplitude, induced by a preceding perfusion with Thr^6BK, the stimulus voltage was increased, the EPSP amplitude could be restored temporarily, in the beginning even to a spiking level, but finally after one to several hours, stimulation with maximal voltage and pulse duration did not increase the amplitude. Obviously this peptide causes a slow decrease in EPSP amplitude (composite EPSPs as well as unitary EPSPs, Fig. 4A, B) with a very slow
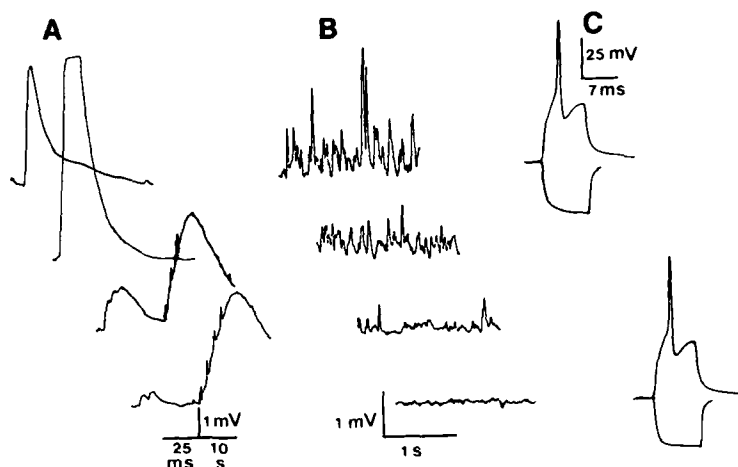
FIG 4 Effects of intraganglionic perfusion of 10^{-4} M Thr⁶BK, during 15 min, on EPSP and ionophoretic induced carbamylcholine potentials (A), on unitary EPSPs (B) and on action potentials (evoked by depolarizing square pulse current) and membrane conductance (measured as hyperpolarizing square pulse current) (C). Note that the lowest two records of A show the EPSP at the left and the ionophoretic carbamylcholine potential at the right (both have different x-axes, as indicated). The upper traces represent the control values, the traces on the second line, after 10 min (during perfusion), the third and bottom lines represent the situations after two and three hours, respectively.

time course, often preceded by a period of enhanced transmitter release during presynaptic stimulation. Recently, using the same preparation, quite similar results were obtained with external application of 10^{-4} M hemicholinium-3, which is generally accepted as a blocker of ACh synthesis, probably by preventing the access of choline to presynaptic terminals [10]. A comparable slow decrease in amplitude is seen at observation of the 'spontaneous' unitary potentials (Fig. 4B).

The perfusion of Thr⁶BK had no effect on either the action potential (Fig. 4C, active membrane response to the depolarizing pulse), or the membrane conductance measured as a hyperpolarizing pulse (Fig. 4C).

It can be concluded that the Thr⁶BK blocks synaptic transmission at a presynaptic site, probably causing depletion of transmitter availability.

Using a double mannitol-gap preparation, microperfusion of the A6 ganglion with Thr⁶BK neither depolarized axons present in the connective between the 6th and the 5th abdominal ganglion, nor those present in the cercal nerve. This indicates that the supposed presynaptic action of Thr⁶BK is not induced by depolarization of terminal axons. However, also in the double mannitol-gap preparation, microperfusion with Thr⁶BK (5×10^{-5} to 10^{-4} M) causes a decrease in EPSP amplitude (Fig. 5A). At the lowest concentration (5×10^{-5} M) a more or less stable situation was present for about 20 min. During that period of time a train of 1 Hz pulses triggered in the dendritic area an initial composite EPSP, followed by EPSPs of progressively decreasing amplitude (Fig. 5B). After 5–10 pulses a plateau amplitude was reached, of course showing the normal variation in amplitude of the individual potentials. The average (plateau) amplitude depends on the stimulus frequency. The higher the frequency, the lower the plateau (Fig. 5C). In control experiments (not illustrated
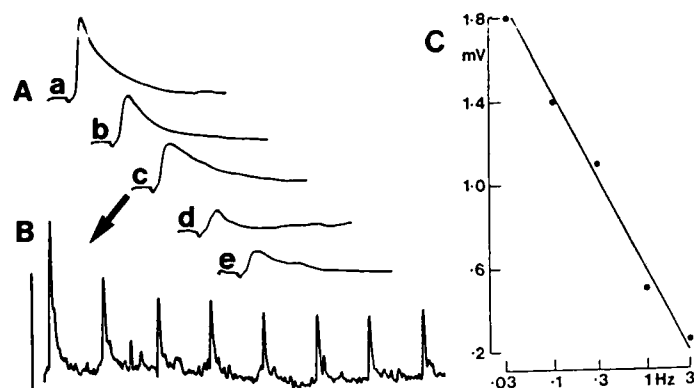
FIG 5 Effects of Thr^{6}BK on composite EPSPs recorded from a mannitol-gap preparation. (Aa): control; (b): after perfusion of the A6 ganglion with 5×10^{-5} M during 5 min. Note the stable level of EPSP amplitude after 20 min (Ac). (Ad, e): two responses 10 min after perfusion at 10^{-4} M during 2 min. B: progressive decrease in amplitude at 1 Hz stimulation to a plateau of EPSPs during the stable situation corresponding to (Ac). C: relationship of the stimulus frequency and the plateau amplitude during the stable situation corresponding to (Ac).

here) this phenomenon only occurs at a high stimulus frequency (> 5 Hz), but not in the frequency range of 0.03–3 Hz.

Discussion

The two kinins examined in this study cause a slowly decreasing synaptic output, which takes place after a relatively short period of perfusion with the kinins. The effect seems not to be restricted to the nicotinic transmission between cercal input and giant interneuronal output, since all axonal output in the connectives becomes silent after a couple of hours. The kinins have no dramatic effect on potentials evoked by microionophoretically applied acetylcholine or carbamylcholine, indicating that the effect of these peptides on the synaptic transmission is not a postsynaptic block. Moreover, the most active kinin (Thr^{6}BK) did not affect the conductance of the postsynaptic membrane, and also did not change the excitability of the giant axon.

It can be concluded that these kinins block the uptake or synthesis of the transmitter substance, or its transport or storage. The stimulus dependent decrease in EPSP amplitude during a pulse train of low frequency strongly suggests a depletion of readily releasable transmitter during low frequency release, and it is possible that after a couple of hours, the complete block of synaptic transmission is due to complete depletion of transmitter. The fact that the readily releasable store is partly replenished between pulse trains, suggests that kinins may affect the transport system rather than the storage of transmitter.

This hypothesis is supported by the similarity between the results obtained with Thr^{6}BK and with hemicholinium-3. In both cases the block of transmission is preceded by a period of enhanced transmitter release, and in both cases the EPSP amplitude becomes stimulus frequency dependent.

Thr^6BK does not show all characteristics of the venom or even of its Thr^6BK containing fraction. The dramatic action of the venom and a number of its fractions may be induced by interaction of two or more toxins. Further research on the activity and chemical characterization of subfractions is underway. At the moment it is evident that kinins or kinin-like peptides may play an important role in the long term paralysis due to stings of the wasps into the insect CNS.

Summary

The effects, on synaptic cholinergic transmission in the sixth abdominal ganglion of the cockroach, *Periplaneta americana*, of the venom of the wasp *Megascolia flavifrons* and one of its fractions are compared with those of bradykinin and Thr^6bradykinin. The venom and the Thr^6bradykinin containing fraction cause block of synaptic transmission from cercal nerve XI to an identified giant interneuron, and delayed depolarization of the neuron. The kinins induce a presynaptic block of transmission possibly by depletion of the transmitter substance.

Acknowledgements

References

1 Piek, T. (1982) Venoms of the Hymenoptera. Biochemical, Pharmacological and Behavioural Aspects. Academic Press, London, pp. 1–570.
2 Yasuhara, T., Mantel, P., Nakajima, T. and Piek, T. (1987) Two kinins isolated from an extract of the venom reservoirs of the solitary wasp *Megascolia flavifrons*. Toxin 25, 527–535.
3 Piek, T., Schmidt, J.O., de Jong, J.M. and Mantel, P. (1988) Kinins in ant venoms—A comparison with venoms of related Hymenoptera. Comp. Biochem. Physiol. in press.
4 Jacques, R. and Schachter, M. (1954) The presence of histamine, 5-hydroxytryptamine and a potent slow contracting substance in wasp venom. Br. J. Pharmacol. 9, 53–57.
5 Piek, T., Buitenhuis, A., Simonthomas, R.T., Ufkes, J.G.R. and Mantel, P. (1983) Smooth muscle contracting compounds in the venom of *Megascolia flavifrons* (Hym: Scoliidae) with notes on the stinging behaviour. Comp. Biochem. Physiol. 75C, 145–152.
6 Harris, C.L. and Smyth, T. (1971) Structural details of cockroach giant axons revealed by injection dye. Comp. Biochem. Physiol. 40, 295–304.
7 Callec, J.J., Sattelle, D.B., Hue, B. and Pelhate, M. (1980) Central synaptic actions of pharmacological agents in insects: oil-gap and mannitol-gap studies. In: Insect Neurobiology and Pesticide Action (Soc. Chem. Industry, ed.), London, pp. 93–100.
8 Piek, T., Hue, B., Mony, L., Nakajima, T., Pelhate, M. and Yasuhara, T. (1987) Block of synaptic transmission in insect CNS by toxins from the venom of the wasp *Megascolia flavifrons* (Fab.). Comp. Biochem. Physiol. 87C, 287–295.
9 Piek, T., Hue, B., Pelhate, M. and Mony, L. (1987) The venom of the wasp *Campsomeris sexmaculata* (F.) blocks synaptic transmission in insect CNS. Comp. Biochem. Physiol. 87C, 283–286.
10 MacIntosh, F.C. (1961) Effect of HC-3 on acetylcholine turnover. Fed. Proc. 20, 562–568.
11 Hue, B. and Callec, J.J. (1988) Electrophysiology and pharmacology of synaptic transmission in the central Nervous System of the cockroach. In: Cockroach as Models for Neurobiology: Applications in Biomedical Research (Huber, Y. et al., eds.), in press.

CHAPTER 3

On the site of action
of the insect selective neurotoxin AaIT

ELIAHU ZLOTKIN [1], LENA FISHMAN [1] AND DALIA GORDON [2]

[1] The Institute of Life Sciences, The Department of Zoology, The Hebrew University, Jerusalem 91904, Israel and [2] Department of Pharmacology, SJ-30, University of Washington, Seattle, WA 98195, U.S.A.

AaIT; a venom-derived neurotoxin

Venom is defined as a mixture of substances which are produced in specialized glandular tissues in the body of the venomous animal and introduced by the aid of a stinging or piercing apparatus into the body of its prey or opponent in order to paralyse and/or kill it. The vast majority of the venomous animals (such as snakes, many spiders, venomous snails and various coelenterates) are slow, and even static predators which feed on freshly killed prey which are mobile and relatively vigorous animals. Such a drastic difference in the locomotory capacity of the venomous predator when compared to its potential prey demands special adaptations for prey encounter. They include first, behavioural adaptations in the form of ambush hunting tactics and second, the development of the venomous apparatus for the quick immobilization of the prey at the earliest moment after encounter.

The fast paralysis induced by venoms is attributed to the neuroactive constituents of venom, the so-called neurotoxins and is due to a direct effect on the excitable-nervous and neuromuscular target tissues which control locomotion, and the neurotoxins are characterized by a high binding affinity for given sites in these tissues [1]. The various neurotoxins so far obtained from various animal venoms are commonly classified according to their effects and sites of action in nervous systems. They are thus defined as ion channel toxins which modify ion conductance; presynaptic toxins which affect neurotransmitter release; and postsynaptic toxins which interfere with the binding and the resulting expression of neurotransmitters [2,3]. A very common characteristic of the various biologically active venom constituents, including neurotoxins, is their protein-polypeptide nature. This chemical characteristic has a double significance. First, polypeptides through their high diversity of covalent structures and the resulting spatial arrangements, may have a highly diverse array of functional specificities such as site directed and selective neurotoxicity (see below). Second, polypeptides are the structures most readily amenable to adaptive modifications through the genetic machinery.

Scorpions demonstrate all the above mentioned characteristics of venomous animals. They are slow, practically blind, nocturnal ambush hunters. They sense
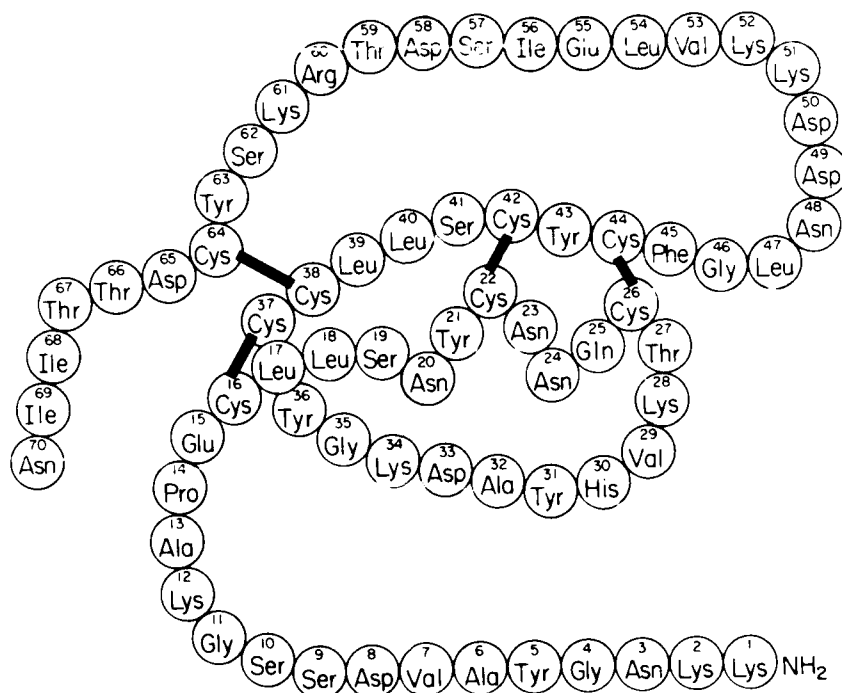
FIG 1   Schematic diagram of the complete covalent structure of the AaIT (according to Darbon et al. [11]).

their relatively fast prey through ground vibrations from only short distances, hardly exceeding their own body length [1,4]. The stinging activity of scorpions in nature is mainly directed to arthropods and especially soft-bodied insects which serve as their food.

The immediate spastic knock-down paralysis of insects [5] by venoms derived from Buthinae scorpions is mainly attributed to certain venom constituents, the so-called excitatory insect toxins [6] such as AmIT, LqqIT$_1$, BjIT$_1$, isolated from the venoms of the scorpion *Androctonus mauretanicus, Leiurus quinquestriatus quinquestriatus* and *Buthotus judaicus*, respectively [7–9]. These toxins are represented by the extensively studied insect toxin purified from the venom of the North African scorpion *Androctonus australis Hector* [10] and designated as AaIT.

The AaIT is a typical venom-derived neurotoxin with the following characteristics:

(a) It is a single chain polypeptide composed of 70 amino acids (M_r 8000) and cross linked by four disulfide bridges [11] (Fig. 1).

(b) It causes a fast paralysis due to a general stimulation and contracture of the insect's skeletal musculature, due to the induction of a repetitive firing of the motor nerves [12].

(c) The toxin binds with a high affinity (K_d = 1.2–2 nM) and low capacity 1.2–2 pmol/mg protein to a single class of non-interacting binding sites located on the insect neuronal membrane [13] (Fig. 5A).

The AaIT and the above excitatory toxins, however, possess an additional feature, which is their selective and exclusive action to insects. Such selectivity was

assessed through assays of paralysis and lethality of the whole animal, electrophysiological studies with various nerve-muscle preparations and binding assays with the radioiodinated toxin [6]. It has been shown that AaIT doesn't affect crustaceans, arachnids and mammals and doesn't specifically bind to their neuronal preparations as well as to non-innervated insect tissues [13–15].

The aspect concerning the site of action of AaIT is treated on two separate levels: (a) on the supracellular-morphological level, which is concerned with the sites of accessibility of the insect nervous system to the toxin; (b) the subcellular-molecular level, which is concerned mainly with the nature of the receptor.

Accessibility of the nervous system

Venoms, in general, possess cytolytic polypeptides which are capable of penetrating, modifying and disrupting biological membranes due to their amphipathic (detergent-like) or enzymatic properties [16,17]. These substances, however, are devoid of the pharmacological specificity of the neurotoxins since they interact with every tissue. On the other hand, the neurotoxins, relatively large polar molecules which interact with specific surface receptors, are devoid of tissue penetrability. The aspect of penetrability is emphasized by the fact that the nervous systems are surrounded by enveloping layers of protective tissues (see below). With this background it was decided to study the binding of the AaIT in situ to authentic nerves from various regions of the insect nervous system and detect the morphological site of accessibility to the AaIT in conditions resembling a natural scorpion sting through injec on into the body cavity.

In our study the nervous tissues of *Periplaneta americana* were treated with the radioiodinated toxin ([^{125}I]AaIT) and its occurrence in the nervous system was followed by light microscopy (LM) autoradiography. Details of methodology are presented in the legends of Figs. 2–4. The various experiments can be subdivided into incubation and injection assays. In incubation assays dissected nervous tissue with associated enveloping layers including mechanically desheathed pieces of the ventral nerve cord were detached, and various peripheral outbranchings of motor nerves were incubated in the *Periplaneta* ringer with [^{125}I]AaIT in the absence of (total binding) or presence (nonspecific binding) of a high concentration (1 μM) of the native AaIT.

The data presented in Fig. 2 indicate that the toxin possesses specific binding sites in both the central as well as peripheral sections of the insect's nervous system. The data presented in Fig. 3 point to the fact that actually the nervous system of *Periplaneta americana* injected with a dose capable of inducing motor disturbances is impermeable to the toxin. As shown (Fig. 3) the phenomenon of toxin impermeability occurs in the central nervous system (Fig. 3A,B), thick peripheral branches (Fig. 3C) and thin terminal peripheral branches (Fig. 4D). In our preliminary studies the claimed permeability of peripheral nerves to the toxin shown by incubation assays [6] should be attributed to the anatomical damage caused by the dissection. The data presented in Fig. 3 raise the question what is the origin of the above motor disturbances. An answer to this question is given in Fig. 4 which demonstrates binding of the toxin to the terminal branches of motor nerves at a close proximity to the skeletal muscles.

38
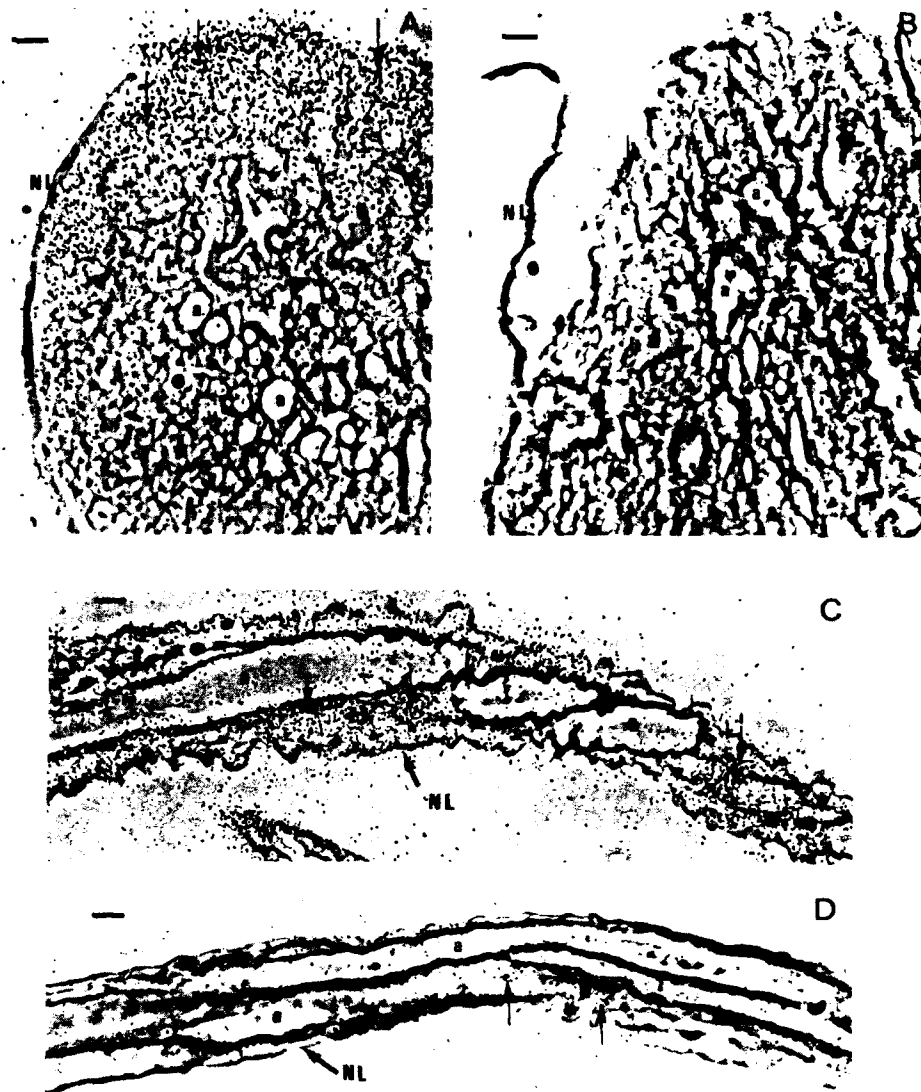
FIG 2   Autoradiography of [^{125}I]AaIT in the nervous tissue of *P. americana*. The dissected nerves were incubated in the *Periplaneta* ringer 5 mg/ml BSA (550 mosM pH 7.2) with 5 nM of the radioiodinated toxin ([^{125}I]AaIT) in the absence (A. C) or presence (B, D) of the native AaIT (1 µM) for 50 min at room temperature followed by three successive rinsings (45 s each) by the cold Ringer which included 5 mg/ml BSA. The tissues were fixed in 4% glutaraldehyde in 0.1 M cacodylate buffer, pH 7.4 (which contained 1 drop per 10 ml of H_2O_2) for 120 min, post-fixed in 1% OsO_4 and embedded in SPURR. Unstained sections of 3 µm were treated with nuclear track emulsion NTB2 (Kodak, USA) for 7–9 days and examined and photographed using a phase-contrast microscope (Zeiss Universal). A and B present sections of desheathed connectives and C and D peripheral nerves of similar dimensions which include few axons. The sparse occurrence of photographic grains in the presence of the cold toxin (B and D) strongly contrast their massive occurrence around the axons in A and C. thus clearly indicating a specific binding. a, axons; NL, neural sheath; arrows point to the photographic grains. Bars = 10 µm.
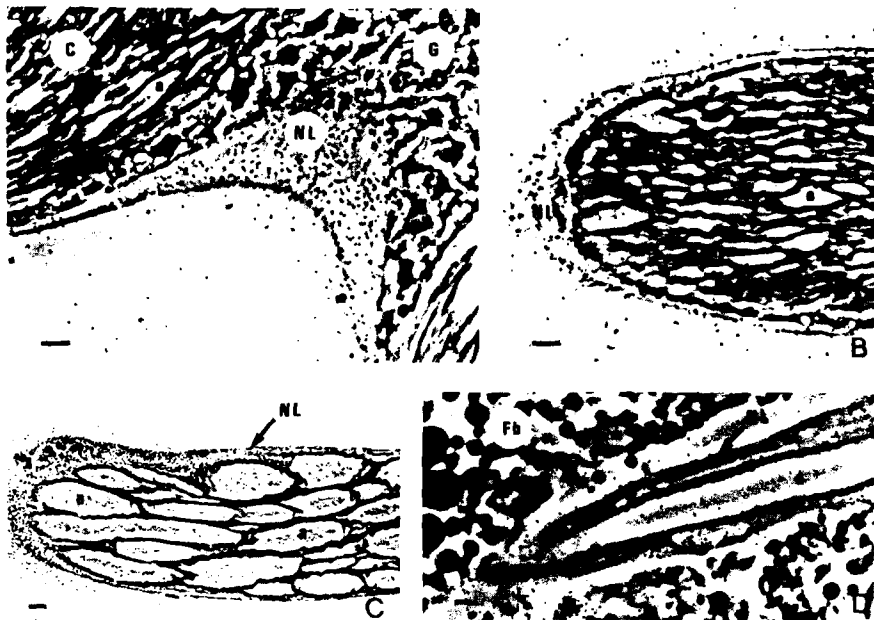
FIG 3 Autoradiography of the nervous tissue of *P. americana* injected by [^{125}I]AaIT. Female adult cockroaches were injected through the intersegmental membrane at ventral side of the second abdominal segment with a dose of 20 ng of the [^{125}I]AaIT per 100 mg of body weight. 1–2 Minutes following injection animals which had demonstrated symptoms of paralysis (sluggish and uncoordinated movements of the legs) were imediately fixed by perfusion with about 20–30 ml of fixative (3% gluteraldehyde, 1% formaldehyde, 5% sucrose in 0.1 M cacodylate buffer, pH 7.4), followed by an additional hour of fixation of the dorsally cut exposed insect, followed by dissection of the neuronal and muscle tissues and further fixation in the cold for 24 h. Postfixation was performed in 1% OsO$_4$ and embedded in SPURR. Autoradiography as indicated in the legend to Fig. 2. A: a section in a joint region of a connective and ganglion. B: a tangential-diagonal section of a connective. C: a tangential-diagonal section in a thick peripheral nerve. D: a longitudinal section in a peripheral nerve which appears to be composed of few axons. In all these preparations no photographic grains were noticed on axonal membranes. The toxin was shown to accumulate on the enveloping neurolemma, which appears to serve as a kind of diffusion barrier. a, axon; c, connective; G, ganglion; Fb, fat body; NL, neural sheath. Bars = 10 µm.

The above findings (Fig. 4) are supported by two separate pieces of information: (1) Walther et al. [12] while studying the effect of AaIT on a locust extensor tibiae nerve-muscle preparation have shown that the cutting of the terminal side branches of the motor nerve was accompanied by a progressive reduction of the rate of the toxin-induced spontaneous activity recorded from the main trunk of the motor nerve, thus indicating that the peripheral branches of motor axons are the most likely site of primary attack of the toxin. (2) Histological studies [18–20] consider the neuroglial elements as the basis of the permeability barrier in the insect CNS. They form the outer glial layer, the perineurium, which appears to be present around all insect nervous systems, except the very small peripheral nerves where it disappears, leaving only the unmodified glial cells to ensheath the neurons. Such
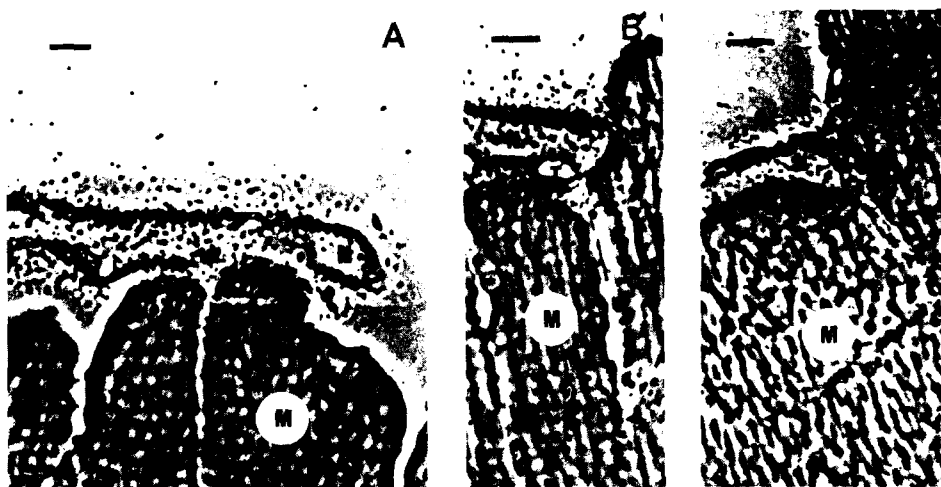
FIG 4 Autoradiography of terminal branches of motor nerves at their close proximity to muscles in *P. americana* injected by [^{125}I]AaIT. For technical details see legend to Fig. 3. A, B and C correspond to three separate examples. The neuronal membrane is marked by the dense layer of the photographic grains. Notice the clear distinction between the nerve and adjacent muscle which is sparsely and non-specifically (data not shown) marked by the toxin. M, muscle; N, nerve. Bars = 10 μm.

structures may serve as selective barriers that govern the accessibility of the nervous system to neurotoxins and demand further clarification by cytochemical EM techniques.

Nature of the receptor

When dealing with the pharmacological identity of the AaIT receptor the following evidence suggests that the toxin interacts with the insect neuronal sodium channel.

(1) AaIT possesses binding constants and pharmacological characteristics typical of the so-called β-scorpion toxins affecting vertebrates and which are well known markers of sodium channels in vertebrate systems. In contrast to the scorpion venom α-toxins the action of AaIT and β-toxins is independent of the membrane potential and they do not interact cooperatively with veratridine [13,21,22].

(2) It was recently shown [23] that the β-toxin VII from the South American scorpion *Tityus serrulatus* (Ts. VII) is highly toxic both forfly larvae (inducing the contraction paralysis typical for excitatory insect toxins) and the mouse. It was shown that the radioiodinated TsVII and AaIT bind to the same sites on housefly head synaptosomes. The AaIT, however, was unable to displace the TsVII from its binding sites on rat brain synaptosomes.

(3) It was shown that AaIT and saxitoxin (STX, a well known universal blocker of sodium channels) share the same number of binding sites in locust synaptosomal membrane vesicles (Fig. 5) and fly head neuronal preparations [24].

(4) Voltage clamp studies with an isolated single insect nerve fiber supply direct evidence, indicating that the AaIT specifically affects sodium conductance (in a
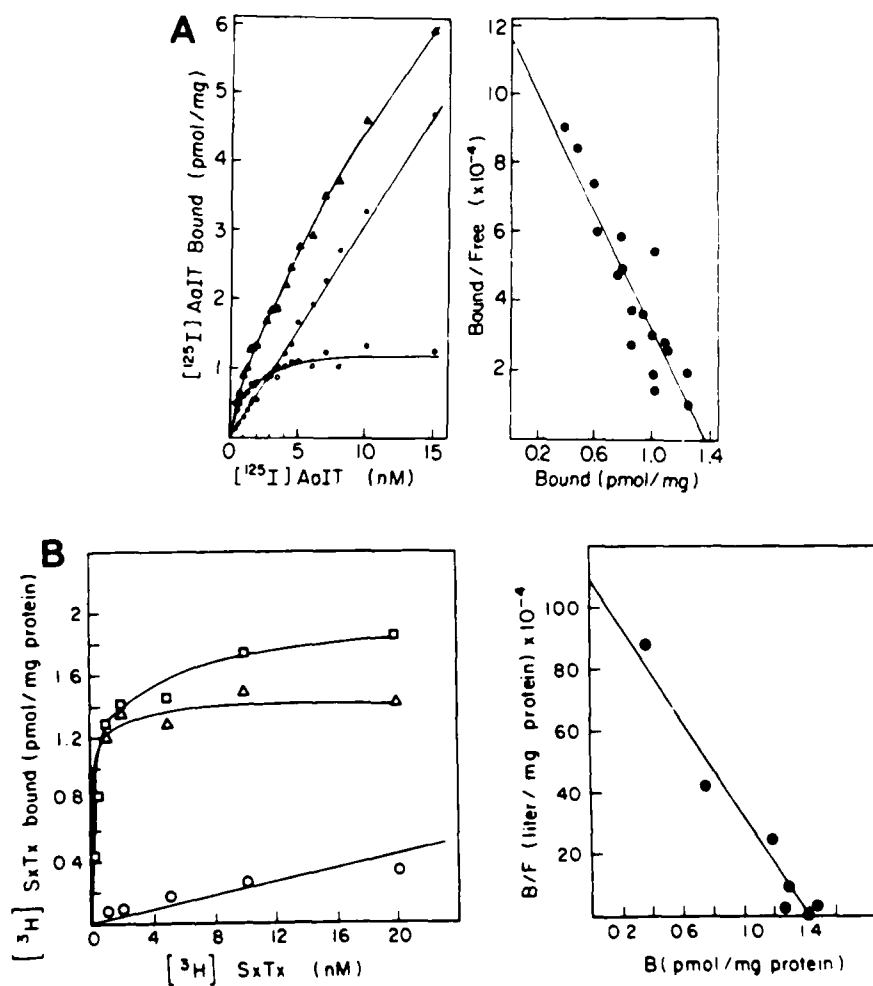
FIG 5 The binding capacity of locust synaptosomal membrane vesicles to [^{125}I]AaIT (A) and [^{3}H]STX (B) determined by saturation equilibrium assays with the respective Scatchard analyses (on the the right). A: [^{125}I]AaIT binding at 20 °C for 30 min with 40 μg protein in the reaction mixture. ▲, total binding; ●, nonspecific binding (in the presence of 1 μM of unlabelled AaIT); ○, specific binding. The calculated K_d equals 1.19 nM and the maximal capacity is equal to 1.37 pmol/mg of membrane protein. B: [^{3}H]STX binding at 2°C for 15 min with 75 μg of membrane protein in the reaction mixture. □ Total binding; ○, nonspecific binding; △, specific binding. The calculated K_d equals 0.138 nM and the maximum capacity is equal to 1.43 pmol/mg of membrane. Taken from Gordon et al. [13](A) and [24](B).

STX sensitive manner) and that there was no effect on potassium conductance (Fig. 6A). The effect of AaIT differs from that of the mammalian toxin MTII derived from the same venom. In contrast to MTII the AaIT: (a) possesses an irreversible effect; (b) acts at about one order of magnitude lower concentration; (c) induces a repetitive firing instead of action potential prolongation (Fig. 6Ba, b); (d) Increases
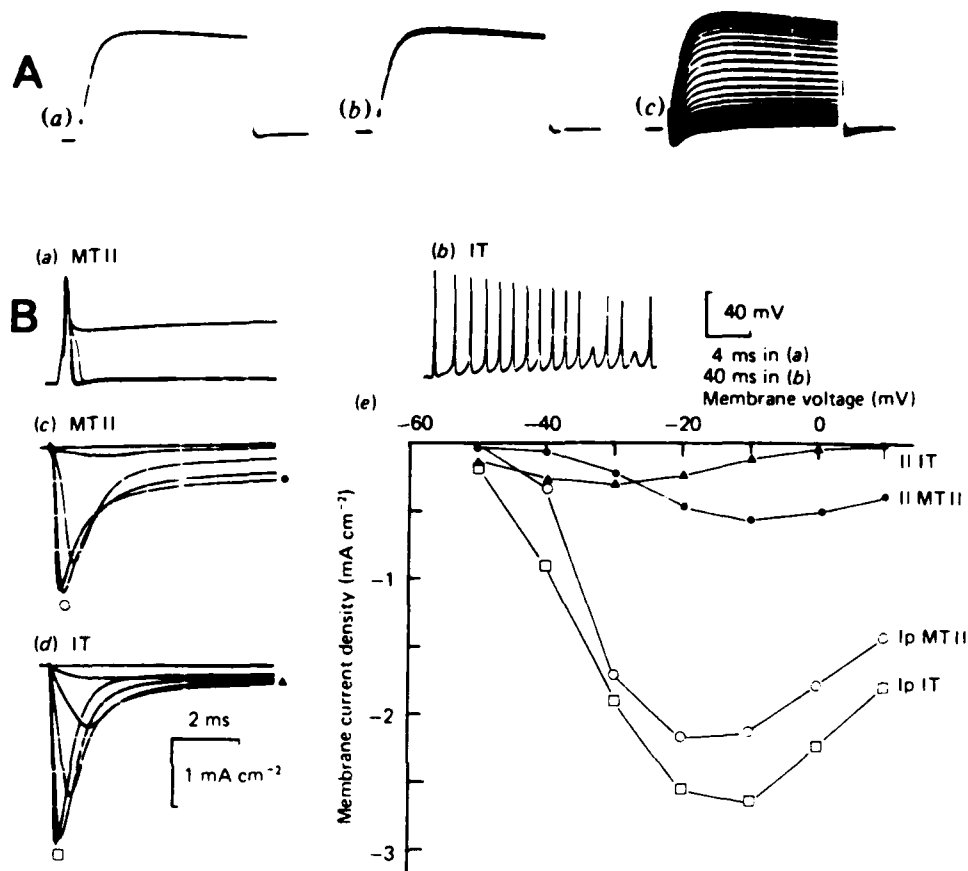
FIG 6 The effect of AaIT on action potentials and ionic currents recorded from the isolated axon of the cockroach CNS in voltage clamp conditions. A: the effect on K$^+$ current, I_k associated with a voltage step from $E_h = -60$ mV to $E_m = +40$ mV in a preparation pretreated with STX 2×10^{-7} M. (a) Control. (b) continuous recording of I_k during 10 min of superfusion with AaIT (3.3 μM). The I_k was in practice unaffected. (c) Superimposed records during the progressive action of 2×10^{-4} M 4-AP completely suppressing the I_k in less than 3 min. (From Pelhate and Zlotkin [26].) B: the effects of AaIT (IT) and the *A. australis* mammal toxin II (MTII). (a, b) Current clamp experiments: (a) 3.5 μM of AaMT2; (b) 1.3 μM of AaIT. (c, d) Voltage-clamp experiments. The preparation was pre-treated with 4-aminopyridine, thus suppressing the potassium currents (c) and sodium current (d) following the treatment by 3.5 and 1.3 M of MTII and AaIT, respectively, corresponding to 10 pulses from $E_h = -60$ mV to $E_m = 10$ mV in 10 mV steps. (e) Current-voltage relations of the data obtained in (c) and (d). IP, Na$^+$ peak current; II, sodium late steady-state current (From Pelhate and Zlotkin [25]).

sodium peak current (Fig. 6Bd, e) and (e) lowers Na$^+$ current turnoff in a voltage dependent manner. The combination of the two latter effects may explain the repetitive firing induced by the AaIT ([25,26] and Fig. 6B).

To summarize it appears that the insect sodium channel is the site of action of AaIT thus indicating that it possesses a certain structural peculiarity (which serves
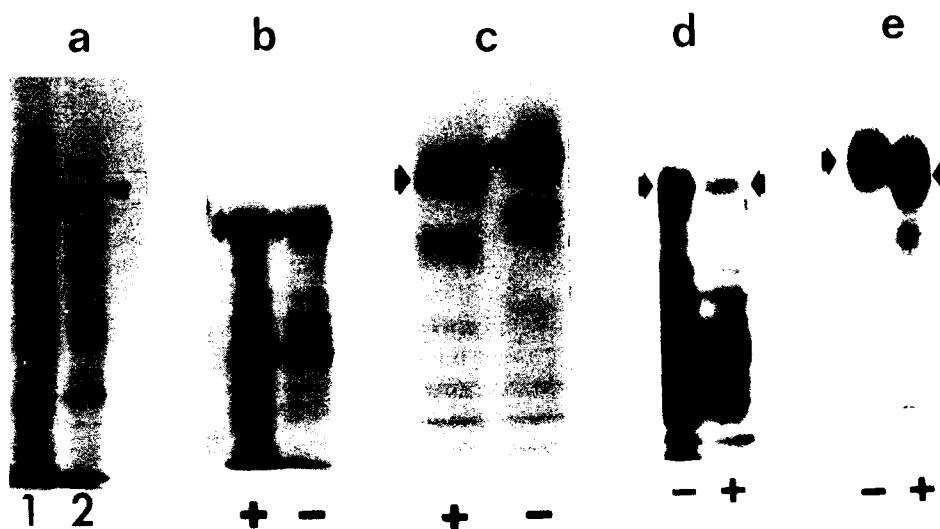
FIG 7 Identification and characterization of the locust sodium channel by immunoprecipi-
tation with anti-SP19 antibodies. Neuronal membrane preparations with Na$^+$ channel capac-
ity equivalent to 10 fmol of [^{3}H]saxitoxin receptor from the central nervous system of
Schistocerca americana (a, b, d) or rat brain (c, e) were solubilized, immunoprecipitated,
phosphorylated by the catalytic subunit of cAMP dependent protein kinase and [^{32}P]ATP
and resolved by SDS–PAGE with (b$^+$, c$^+$) or without (b$^+$, c$^+$) reduction of disulfide bonds
with 5 mM βME and visualized by autoradiography. Lanes a represent locust neuronal
preparation which was preincubated in absence (a1) or presence (a2) of the synthetic peptide
(1 μM) SP19. The peptide, as shown, has blocked the specific antibodies and thus prevented
the occurrence of the channel α-subunit (a2). Lanes d and e demonstrate the effect of
neuraminidase treatment on the apparent M_r of the locust CNS (d) and rat brain (e) sodium
channel subunits. Following solubilization, immunoprecipitation and phosphorylation sodium
channel protein were incubated with (d$^+$, e$^+$) or without (d$^-$, e$^-$) 0.5 units of neuraminidase
in 50 mM Tris-HCl, pH 5.5, containing the above mixture (see text) of proteolytic inhibitors,
for 16 h at 4°C, followed by reduction of disulfide bonds and SDS–PAGE separation.

as the recognition site for the AaIT) of a critical functional significance (as indicated
by the toxic potency of AaIT).

With this background the locust sodium channel was recently characterized
through the development of two seperate tools for its identification and visualiza-
tion respectively. The identification of the locust sodium channel was achieved with
the aid of antibodies raised against a synthetic peptide (SP19-KTEEQKK-
YYNA[norleucine]KKLGSKK) corresponding to a highly conserved predicted
intracellular region of the sodium channel α-subunit and which was recently shown
to recognize α-subunits from rat (Fig. 7c, e) and eel brain, rat skeletal muscle, rat
heart and eel electroplax [27]. The attempt to use these antibodies for the isolation
of an insect channel was strongly supported by recent information concerning the
amino acid sequence of a putative sodium channel gene in *Drosophila*. The deduced
amino acid sequence possessed a very close similarity and virtually identical
organization to the vertebrate sodium channel protein including the occurrence of
the above conserved region corresponding to the SP19 synthetic peptide [28]. The

visualization of the locust channel was performed by radiophosphorylation using the catalytic subunit of cAMP dependent protein kinase and [^{32}P]ATP followed by SDS–PAGE autoradiography.

The experimental procedure included the following steps: (1) preparation of the P$_2$ membranes [29] from freshly dissected CNS of Schistocerca americana in the presence of protease inhibitors (50 μg/ml PMSF; 1 mM iodoacetamide and 1 mM pepstatin in 0.25 M sucrose, 10 mM EDTA, 10 mM EGTA, 50 mM potassium phosphate, pH 7.4); (2) solubilization of membranes in portions equivalent to 100 fmol of sodium channels, as assessed by STX binding [24], in the above medium containing 5% Triton X-100, incubation for 30 min at 4°C and sedimentation of the residual membranes at 8000 × g for 15 min; (3) immunoprecipitation of the sodium channels. The supernatants of step 2 were incubated with antibodies for 16 h at 4°C, and the antigen-antibody complexes were isolated by adsorption to protein A-Sepharose; (4) phosphorylation of the immunoprecipitated sodium channels (500 ng of the catalytic subunit of cAMP dependent protein kinase and 10 μCi [^{32}P]ATP for 1 min at 36°C according to Schmidt et al. [30]); (5) SDS–PAGE of the immunoprecipitated samples, stacking gel 3%, running gel 3–10% acrylamide according to [30]; (6) visualization of the radiolabeled bands by autoradiography; (7) in order to test a possible sialylation of the locust channel the solubilized, immunoprecipitated, phosphorylated channel preparations were incubated with neuraminidase and analysed by SDS–PAGE after reduction of disulfide bonds (Fig. 7d, e).

The data are presented in Fig. 7 and they indicate:

(1) The antibodies raised against the SP19 peptide recognize sodium channel of insect. The specificity of the immunoprecipitation is demonstrated in Fig. 7a showing that the synthetic peptide corresponding to the conserved sequence of an α-subunit, completely blocks the immunoprecipitation of the 280 kDa phosphorylated protein of the locust channel α-subunit. The same phenomenon was observed with the rat brain sodium channel preparation (data not shown).

(2) The molecular weight of the locust channel α-subunit corresponds to about 280 kDa (data not shown). This is in accordance with the molecular dimensions of all the sodium channel α-subunits so far characterized from rat brain, heart, skeletal muscle, eel brain and electroplax which cover a range of 230–290 kDa [27].

(3) The locust channel α-subunit serves as a substrate of phosphorylation by cAMP-dependent protein kinase thus resembling the α-subunits from rat and eel brain, rat heart and eel electroplax [27]. It has been shown [31] that stimulation by 8-Br-cAMP of endogenous phosphorylation of sodium channels in intact synaptosomes of rat brain, decreased the initial rate of veratridine stimulated ^{22}Na influx into synaptsomes suggesting the cAMP dependent phosphorylation may influence Na$^+$ channel gating and conductance. The regulatory role of phosphorylation in the function of ionic channels was previously demonstrated in the mammalian heart calcium and molluscan sensory nerve potassium channels [32,33].

(4) In contrast to the rat brain sodium channel α-subunits which are disulfide linked to β$_2$-subunits [36] (Fig. 7c), the locust sodium channel seems to be devoid of such linkage to a small subunit (Fig. 7b), thus resembling the rat heart and eel electroplax [27]. It is noteworthy that the β$_2$-subunit can be removed from the purified rat brain sodium channel without loss of functional activity [34].

(5) As shown in Fig. 7d and in contrast to the α-subunits of rat brain (Fig. 7e), eel brain and eel electroplax [27] the neuraminidase treatment of the α-subunit of the

locust channel does not reduce its apparent M_r, indicating that it is devoid of sialic acid. This is consistent with previous work showing that insect glycoproteins generally do not have complex carbohydrate chains or sialic acid [35].

Our present results provide the first identification of the α-subunit polypeptide of sodium channel from insect nervous system. On the basis of the present and previous data [27,36] it may be concluded that sodium channels have similar, but not identical α-subunits in all excitable tissues. When taking into consideration that AaIT interacts with the insect sodium channels (see above) it is noteworthy that this toxin is one of the few substances which is able to distinguish between a neuronal membrane of an insect and that of a mammal. It has been recently shown [37] that AaIT was ineffective when injected either intravenously or intraventricularly into mice in doses 4–5 orders of magnitude higher than the effective doses of the so-called scorpion venom mammal toxin. This may indicate a certain functionally significant, structural difference between the insect and the mammal sodium channels.

The present data concerning the characterization of the locust sodium channel provide a methodological approach for the further study of the interaction of AaIT with the insect sodium channel.

Concluding remarks

(1) AaIT, an insect-selective neurotoxic polypeptide (M_r 8000) derived from scorpion venom, interacts with specific, high affinity binding sites on neuronal membranes located in the various regions of the central as well as peripheral nervous system of an insect.

(2) When confronted with an intact and anatomically protected nervous system the toxin, in practice, has no access to the vast majority of the above regions of the insect nervous tissue.

(3) In a natural sting the only sites in the insect nervous system which are accessible to the toxin are the peripheral terminal branches of the motor nerves located at a close proximity to the skeletal muscles.

(4) A series of voltage clamp studies coupled with binding assays strongly suggest that the insect excitable sodium channels serve as the receptor and primary target for the action of AaIT.

(5) The locust sodium channel was characterized by antibodies raised against a synthetic peptide corresponding to a highly conserved predicted intracellular region of the sodium channel α-subunit and it has been shown that the locust channel α-subunit (a) has a molecular weight of about 280 kDa; (b) serves as a substrate of phosphorylation by cAMP-dependent protein kinase; (c) is devoid of a disulfide linkage to a small subunit, and (d) is devoid of sialic acid.

The present data supply the basis and approach for a further study of the interaction of the AaIT with the insect sodium channel.

Acknowledgement

References

1 Zlotkin, E. (1987) Pharmacology of survival: insect selective neurotoxins derived from scorpion venom. Endeavour 11, 168–174.
2 Eaker, D. and Wadstrom, T. (eds.) (1980) Natural Toxins, Pergamon Press, Oxford, 1980.
3 Hucho, F. and Ovchinnikov, Y.A. (eds.) (1983) Toxins as Tools in Neurochemistry. de Gruyter, Berlin, 1983.
4 Brownell, P.H. (1984) Prey detection by the sand scorpion. Sci. Amer. 251, 94–105.
5 Zlotkin, E., Fraenkel, T., Miranda, F. and Lissitzky, S. (1971) The effect of scorpion venom on blowfly larvae; a new method for the evaluation of scorpion venom potency. Toxicon 9, 1–8.
6 Zlotkin, E. (1986) The interaction of insect-selective neurotoxins from scorpion venoms with insect neuronal membranes. In: Neuropharmacology and Pesticide Action (M.G. Ford, G.G. Lunt, R.C. Reay and P.N.R. Usherwood, Eds.), pp. 352–383. Ellis Horwood, Chichester.
7 Zlotkin, E., Teitelbaum, Z., Rochat, H. and Miranda, F. (1979) The insect toxin from the venom of the scorpion *Androctonus mauretanicus*: Purification, characterization and specifity. Insect Biochem. 9, 347–354.
8 Zlotkin, E., Kadouri, D., Gordon, D., Pelhate, M., Martin, M.F., and Rochat, H. (1985) An excitatory and depressant insect toxin from scorpion venom—both affect sodium conductance and possess a common binding site. Arch. Biochem. Biophys. 240, 877–887.
9 Lester, D., Lazarovici, P., Pelhate, M. and Zlotkin, E. (1982) Two insect toxins from the venom of the scorpion *Buthotus judaicus*: Purification, characterization and action. Biochim. Biophys. Acta 701, 370–381.
10 Zlotkin, E., Rochat, H. Kupeyan, C. Miranda, F. and Lissitzky, S. (1971) Purification and properties of the insect toxin from the venom of the scorpion *Androctonus australis* Hector. Biochimie (Paris) 53, 1073–1078.
11 Darbon, H., Zlotkin, E., Kopeyyan, C., Van Rietschoten, J. and Rochat, H. (1982) Covalent structure of the insect toxin of the North African scorpion *Androctonus australis* Hector. Int. J. Peptide Res. 20, 320–330.
12 Walther, C., Zlotkin, E. and Rathmayer, W. (1976) Action of different toxins from the scorpion *Androctonus australis* on a locust nerve-muscle preparation. J. Insect Physiol. 22, 1187–1194.
13 Gordon, D., Jover, E., Couraud, F. and Zlotkin, E. (1984) The binding of the insect selective neurotoxin (AaIT) from scorpion venom to locust synaptosomal membranes. Biochim. Biophys. Acta 778, 349–358.
14 Rathmayer, W., Ruhland, M., Tintpulver, M., Walther, Ch. and Zlotkin, E. (1978) The effect of toxins derived from the venom of the scorpion *Androctonus australis* Hector on neuromuscular transmission In: Toxins: Animal, Plant and Microbial (P. Rosenberg, ed.), pp. 629–637. Oxford, Pergamon Press.
15 Teitelbaum, Z., Lazarovici, P. and Zlotkin, E. (1979) Selective binding of the scorpion venom insect toxin to insect nervous tissue. Insect Biochem. 9, 343–346.
16 Piek, T. (ed.) (1986) Venoms of the Hymenoptera. Academic Press.
17 Tu, A.T. (ed.) (1984) Handbook of Natural Toxins, Vol. 2: Insect Poisons, Allergens and Other Invertebrate Venoms. Marcel Dekker, New York.
18 Lane, N.J. (1985) Structure of components of the nervous system In: Comprehensive Insect Physiology Biochemistry and Pharmacology (G.A. Kerkut and L.I. Gilbert, eds.), pp. 1–49. Pergamon, Oxford.
19 Lane, N.J. and Treherne, J.E. (1973) The ultrastructural organization of peripheral nerves in two insect species (*Periplaneta americana* and *Schistocerca gregaria*). Tissue Cell. 5, 703–714.
20 Treherne, J.E. (1985) Blood-brain barrier. In: Comprehensive Insect Physiology Biochemistry and Pharmacology (G.A. Kerkut and L.I. Gilberg, eds.), pp. 115–137. Pergamon, Oxford.

21 Jover, E., Couraud, F. and Rochat, H. (1980) Two types of scorpion neurotoxins characterized by their binding to two separate receptor sites on rat brain synaptosomes. Biochem. Biophys. Res. Commun. 95, 1607–1614.

22 Bablito, J., Jover, E. and Couraud, F. (1986) Activation of the voltage sensitive sodium channel by a β-scorpion toxin in rat brain nerve-ending particles. J. Neurochem. 46, 1763–1770.

23 De Lima, M.E., Martin,M.F., Diniz, C.R. and Rochat, H. (1986) *Tityus serrulatus* toxin VII bears pharmacological properties of both β-toxin and insect toxin from scorpion venoms. Biochem. Biophys. Res. Commun. 139, 296–302.

24 Gordon, D., Zlotkin, E. and Catterall, W.A. (1985) The binding of an insect-selective neurotoxin and saxitixin to insect neuronal membranes. Biochim. Biophys. Acta 821, 130–136.

25 Pelhate, M. and Zlotkin, E. (1981) Voltage dependent slowing of the turn off of Na^+ current in the cockroach giant axon induced by the scorpion venom 'insect toxin'. J. Physiol. (Lond.) 319, 30–31.

26 Pelhate, M., and Zlotkin, E. (1982) Actions of insect toxin and other toxins derived from the venom of the scorpion *Androctonus australis* in isolated giant axons of the cockroach (*Periplaneta americana*). J. Exp. Biol. 97, 67–77.

27 Gordon, D., Merrick, D., Wollner, D.A. and Catterall, W.A. (1988) Biochemical properties of sodium channels in a wide range of excitable tissues studied with site-directed antibodies. Biochemistry, In Press.

28 Salkoff, L., Butler, A., Wei A. Scavarda, N., Griffen, K., Ifune, C., Goodman, R. and Mandel, G. (1987) Genomic organization and deduced amino acid sequence of a putative sodium channel gene in *Drosophila*. Science 237, 744–749.

29 Gordon, D., Zlotkin, E. and Kanner, B. (1982) Functional membrane vesicles from the nervous system of insects. I. Sodium and chloride dependent aminobutyric acid transport. Biochim. Biophys. Acta 688, 229–236.

30 Schmidt, J., Rossie, S. and Catterall, W.A. (1985) A large intracellular pool of inactive Na channel α-subunits in developing rat brain. Proc. Natl. Acad. Sci. USA 82, 4847–4851.

31 Costa, M.R. and Catterall, W.A. (1984) Cyclic AMP-dependent phosphorylation of the α-subunit of the sodium channel in synaptic nerve ending particles. J. Biol. Chem. 259, 8210–8218.

32 Reuter, H. (1983) Calcium channel modulation by neurotransmitters, enzymes and drugs. Nature 301, 569–574.

33 Siegelbaum, S.A. and Tsien, R.W. (1983) Modulation of gated ion channels as a mode of transmitter action. Trends Neurosci. 6, 307–313.

34 Messner, D.J., Feller, D.J., Scheuer, T. and Catterall, W.A. (1986) Functional properties of rat brain sodium channels lacking the β1 or β2 subunit. J. Biol. Chem. 261, 14882–14890.

35 Hsieh, P. and Robbins, P.W. (1984) Regulation of asparagine-linked oligosaccharide processing. J. Biol. Chem. 259, 2375–2382.

36 Catterall, W.A. (1986) Molecular properties of voltage sensitive sodium channels. Ann. Rev. Biochem. 55, 953–985.

37 De Dianous, S., Hoarau, F. and Rochat, H. (1987) Reexamination of the specificity of the scorpion *Androctonus australis Hector* insect toxin towards arthropods, Toxicon 25, 411–417.

CHAPTER 4

Synaptic ion channel toxins from spider venoms

MICHAEL E. ADAMS

Division of Toxicology and Physiology, Department of Entomology,
University of California, Riverside, CA 92521, U.S.A.

Introduction

Neurotox '88 brought basic and applied science to bear on the problem of developing more rational pest control strategies. Adopting a 'rational approach' to insecticide development essentially means promoting some form of directed chemical synthesis based on prior knowledge. In considering the *modus operandi* of chemical companies to direct synthesis, two strategies are evident. One involves the optimization of existing toxophores through the design of analogues. A second approach, one that can make use of basic neurobiology, would result from the identification of novel points of attack within the insect system. Many of our existing insecticides point to chemical signalling mechanisms within insects as vulnerable points of attack.

The most successful of present day insecticides (as measured by worldwide sales) induce poisoning in insects through impairment of chemical signalling within the nervous system. This is accomplished by affecting parameters of transmitter release, turnover or receptor function. Thus, the cholinesterase inhibitors (organophosphates, carbamates) inhibit acetylcholine breakdown while the nereistoxin analogue cartap mimics acetylcholine. Avermectins and cyclodienes affect GABA-sensitive chloride channels, while the formamidines mimic octopamine. Transmitter release is affected more generally by ion channel poisons such as pyrethroids, which modify the open state of the sodium channel.

It is noteworthy that many insecticides derive from naturally occurring substances, and so it is perhaps appropriate that this conference devoted an entire session to natural products. What is the likelihood that basic studies of natural products and their actions on insect chemical signalling systems will lead to new classes of insecticides? One clear precedent was set by the development of methoprene and hydroprene, juvenile hormone analogues that have achieved a degree of commercial success as adulticides against fleas, cockroaches and mosquitoes [1]. While these compounds do not qualify as agricultural insecticides, they represent admirable examples of directed synthesis around a known endocrine signal which is critical to insect development.

Our understanding of critical mechanisms operating in the insect nervous system continues to grow through the use of natural toxins as pharmacological probes. Their high affinity and selectivity for functionally distinct classes of receptors and

ion channels makes them enormously useful for the classification and isolation of receptors and channels. Classification of nicotinic and muscarinic cholinergic receptors by α-bungarotoxin and atropine is a prime example of the utility of toxins. Progress in the classification and functional analysis of voltage-sensitive ion channels has likewise benefited from the use of scorpion toxins for sodium channel [2] and more recently, conotoxins [3] which distinguish between sodium channels in nerve and muscle and define new classes of calcium channels.

Two potential targets for newer insecticides may be voltage-sensitive calcium channels and excitatory neuromuscular transmission in insects. We have isolated a variety of toxins from spider venoms which affect these syn .ptic ion channels as well as others. Although these toxins hold little promise as insecticidal molecules themselves (excluding the option of genetically engineering insect pathogens), their use as receptor and channel probes should provide valuable information regarding the structural and functional aspects. This includes characterization of the critical steps in synaptic transmission, which involves the sequential activation of ion channels controlling transmitter release and the resulting postsynaptic responses.

This short review covers some of our biochemical and physiological analyses of orb weaver (Araneidae) and funnel web (Agelenidae) spider venoms. The orb weaver spiders combine silk wrapping and reversible paralysis by envenomation to incapacitate their prey. The paralytic actions of these venoms appear to be associated primarily with postsynaptic block of glutamate receptor channels. The funnel web spider, *Agelenopsis aperta* employs a more complex venom which is lethal. *Agelenopsis* venom, while containing polyamine toxins similar in structure and physiological action to the orb weaver toxins, also contains two types of presynaptic toxins affecting voltage-sensitive ion channels. In all, we have isolated and characterized three classes of venom toxins affecting insect neuromuscular transmission: postsynaptic antagonists, presynaptic activators and presynaptic antagonists. This paper provides a summary of their structural features and physiological actions.

Postsynaptic toxins

Orb weaver spider toxins

Until about five years ago, potent and selective antagonists of postjunctional receptors in insect skeletal muscle were unavailable. This state of affairs has changed quickly with the discovery of a new class of postsynaptic toxins from orb weaver spider venom toxins. Kawai and colleagues [4] first reported the neuromuscular blocking actions of Joro spider venom, and subsequently an account describing antagonism by semi-purified fractions on crustacean neuromuscular transmission has appeared [5]. Usherwood et al. [6,7] have demonstrated use-dependent, postsynaptic antagonism of locust neuromuscular transmission by orb weaver venom fractions on locust neuromuscular transmission. The identification of individual synaptic toxins and analyses of their physiological actions has followed at a rapid pace [8-11]. The following summarizes some of the work of myself and colleagues on postsynaptic toxins from orb weaver and funnel web spider venoms.

We find that venoms from orb weaver spiders (*Argiope aurantia, Araneus gemma* and *Neoscona arabesca*) induce reversible paralysis in a variety of insects, including representatives of the Orthoptera (*Periplaneta americana, Schistocerca nitens*),

1:20,000 Crude Venom
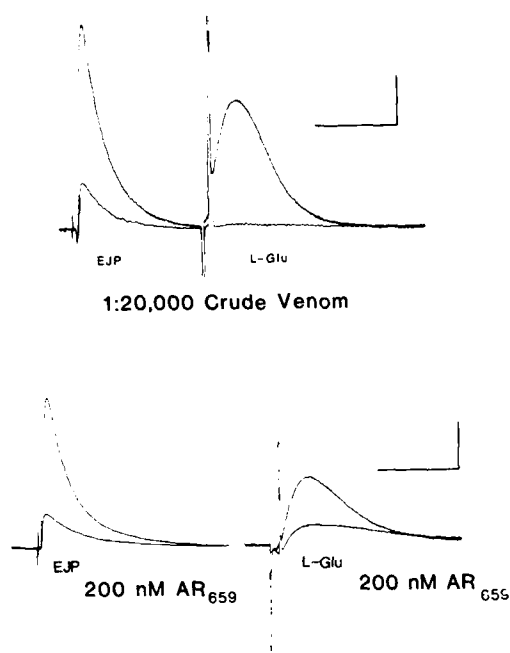
FIG 1   Bath perfusion of crude *A. aurantia* venom or purified AR_{659} suppresses neurally-evoked synaptic potentials (EJP) and iontophoretic glutamate potentials (L-Glu) in the pre-pupal house fly longitudinal ventrolateral muscle. Methods are described in Ref. 11. In both sets of data, larger amplitude waveforms represent pre-treatment controls, lower amplitudes are responses after 10 min of continuous perfusion with whole venom or AR_{659}. Top: saline perfusion with crude *Argiope* venom at $1:20,000$ dilution causes 80% reduction of the EJP and virtually abolishes the iontophoretic glutamate potential. Bottom: treatment with 200 nM AR_{659} reduces both the EJP and glutamate potential in a similar manner. Calibration bars: 5 mV, 100 ms.

Lepidoptera (*Heliothis virescens, Galleria mellonella, Spodoptera exigua*) and Diptera (*Musca domestica*) [11]. We have pursued a detailed analysis of argiope venom, which produces hours-long paralysis upon injection into house flies at saline dilutions of up to 1:5000. The paralytic effects of *Argiope* venom are correlated with suppression of EPSPs and iontophoretic glutamate potentials in larval longitudinal ventrolateral muscles of prepupal *Musca domestica* (Fig. 1). Synaptic block is stimulus-dependent and partially reversible. In fact, the degree of reversibility depends on structural aspects of each particular polyamine toxin (see below). Threshold dosages of whole *Argiope* venom producing neuromuscular block in the fly preparation are of the order of 1:50,000.

Fractionation of *Argiope* venom using reversed-phase high performance liquid chromatography (RPLC), yields multiple low-molecular-weight paralytic toxins (Fig. 2) which act in a manner similar to the crude venom. All of the larger peaks shown in Fig. 1 cause paralysis and suppress synaptic potentials in flies (Figs. 1, 3, 4). Details regarding the isolation and identification of three paralytic toxins from *Argiope* venom are described in a recent publication [11].
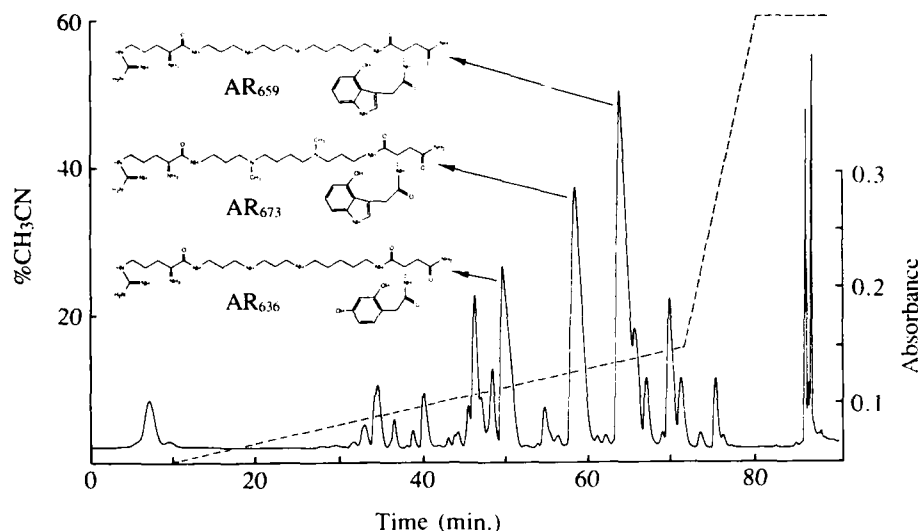
FIG 2 Reversed phase LC fractionation of *Argiope aurantia* venom. Gradient elution (dotted line) using acetonitrile (CH_3CN)/water in constant 1% trifluoroacetic acid reveals a series of polyamine-like synaptic toxins. The three large peaks are 'argiotoxins', the structures of which are indicated by arrows as AR_{636}, AR_{659} and AR_{673} [11]. LC conditions: Brownlee C_8 widepore column, 1 ml/min flow rate, absorbance measured at 280 nm.

Structure elucidation studies using a variety of chemical methods led to the assignment of structures for three 'argiotoxins' shown in Fig. 1. These toxins are designated according to molecular weight as AR_{636}, AR_{659} and AR_{673}. The structural motif common to the argiotoxins and to other orb weaver toxins thus far reported [8,9,12] consists of Arg-polyamine-Asn-aromatic acid, except for JSTX-3 [9] and Nephilatoxins 7 and 8 [12], which do not contain N-terminal arginine. The polyamine in AR_{636} and AR_{659} consists of 1,13-diamino-4,8-diazatridecane, whereas AR_{673} contains dimethylated spermine or 1,12-diamino-4,9-dimethyl-4,9-diazadodecane. Two families of toxins can be distinguished by characteristic UV chromophores. AR_{659} and AR_{673} contain 4-hydroxyindole-3-acetic acid, while AR_{636} contains 2,4-dihydroxyphenylacetic acid (see also Ref. 13). Synthetic AR_{636} and AR_{659} were prepared and shown to be chemically and biologically indistinguishable from the native compounds.

The argiotoxins are the main constituents of whole *Argiope* venom, occurring at concentrations of about 20 mM each. Since paralysis and neuromuscular block caused by individual argiotoxins is indistinguishable from that caused by crude venom, they are assumed to be the active principles. Concentrations necessary to achieve 50% suppression of the EPSP range from 0.2 μM for AR_{659} and AR_{636} to 0.45 μM for AR_{673} (Fig. 3). AR_{659} is the most active paralytic toxin in house fly injection assays, while AR_{636} and AR_{673} are 4-6 times less active.

The argiotoxins belong to a growing family of polyamine-like toxins identified from various Eurasian and North American orb weaver spiders. Over the past two years, at least 8 structures have appeared [8,9,11,12], all of which show a similar structural design. AR_{636} is identical to argiopine, which was isolated from a Russian
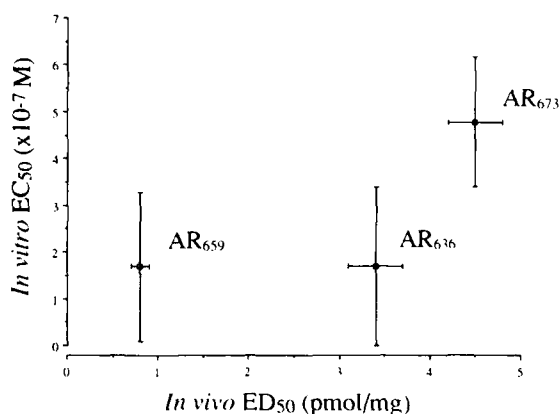
FIG 3   Biological activities of AR_{636}, AR_{659} and AR_{673} (adapted from Table 1, Ref. 11). ED_{50} values plotted on the abscissa represent dose of toxin (pmol/mg; ca. 15 mg per adult fly) required to paralyse 50% of injected adult house flies. Paralysis is defined as loss of righting response at 1 h post-injection. ED_{50} values and 95% confidence limits (bars) were obtained by probit analysis. EC_{50} values plotted on the ordinate represent the concentration of each toxin required to achieve 50% reduction in the neurally-evoked EPSP recorded in the pre-pupal fly neuromuscular preparation. EC_{50} values and 95% confidence limits (bars) were obtained from linear dose response curves by inverse prediction [21]. The in vivo paralytic activity of AR_{659} is some 4–6 times higher than either AR_{636} or AR_{673}. Interestingly, AR_{659} and AR_{636} are equipotent as in vitro neuromuscular antagonists, and are some 2–3 times more active than AR_{673}.

orb weaver spider, *Argiope lobata* [8] and similar if not identical toxins are reported to occur in *Argiope trifasciata* and *A. florida* [13].

We recently isolated several polyamine toxins from *Araneus gemma* (AN_{622}, AN_{758}) and *Neoscona arabesca* (NA_{659}, NA_{673}, NA_{687}). Most of the chemical and biological properties of these toxins are similar to the argiotoxins. However synaptic block by AN_{758} shows a striking degree of reversibility as compared to the argiotoxins (Fig. 4). A 10 minute saline wash following AN_{758} treatment results in 80–90% recovery of EPSP amplitude (Fig. 4), while reversal of block by AR_{659} is much slower. Further analysis is needed to compare the binding characteristics of these two types of polyamine toxins.

In a relatively brief period, low-molecular-weight antagonists with high potency and selectivity for insect postsynaptic receptor channels have been described. Unfortunately, the polyamine toxins do not appear to constitute bona fide competitive receptor antagonists of the α-bungarotoxin type, nor do they bind irreversibly in our hands, although such claims are made for *Nephila* toxins in crustacean neuromuscular preparations [5]. A further feature which must be disconcerting to synthetic chemists is the lack of topical or appreciable oral activity in insects. Synthesis of analogues ultimately may solve this problem. However, despite problems with practical utility of the native substances, they have opened up exciting new biological tools and possibly synthetic leads pertinent to studies of synaptic transmission and pest control in insects.

54

Time (min.)
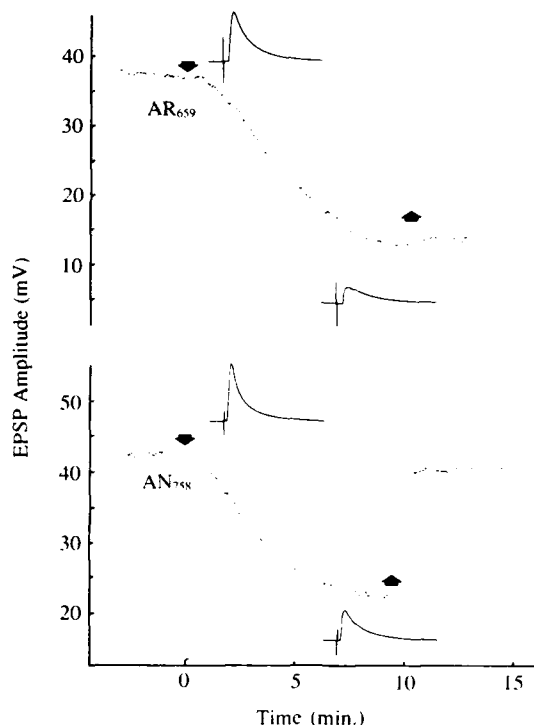
FIG 4 Trend analysis of neuromuscular block and recovery after treatment with two orb weaver toxins: AR_{659} from *Argiope aurantia* (upper ordinate) and AN_{758} from *Araneus gemma* (lower ordinate). EPSPs in pre-pupal fly longitudinal ventrolateral muscle are neurally-evoked at 0.4 Hz. EPSP amplitudes (in mV; ordinate) are plotted as a series of dots from left to right over the time (in min; abscissa). Pre-treatment amplitudes plotted prior to application of toxin at 0 time (downward arrow) are 38 mV for AR_{659} and 43 mV for AN_{758}. Pre-treatment waveform samples (average of 10) are shown in the upper left in each experiment and after 10 min of toxin perfusion at lower right. At the downward arrow, either 1 μM AR_{659} or 1 μM AN_{758} is added to the perfusion medium, causing a gradual reduction of EPSP amplitude over a 10-min interval. At the upward arrows, nerve stimulation is stopped and toxin is washed from the bath during a second 10-min interval. During the washing phase, no further stimuli are applied and trend analysis stops. Re-introduction of stimuli at the upward arrow shows that little recovery has occurred after treatment with AR_{659}, but that 80–90% recovery is achieved in the preparation treated with AN_{758}.

Funnel web spider 'α-agatoxins': a new type of polyamine-like postsynaptic antagonist Venom of the funnel web spider, *Agelenopsis aperta* contains a more complex mixture of toxins as compared with venoms of the orb weaver family. Three types of synaptic actions involving both pre- and postsynaptic ion channels have been defined. Postsynaptic antagonists affecting glutamate receptor channels or 'α-agatoxins' are polyamine-like substances which show chemical and biological properties similar to the argiotoxins. Four α-agatoxins have been isolated and identified according to molecular weight as AG_{488}, AG_{489}, AG_{504} and AG_{505}. Although structural studies of the α-agatoxins are still under way, several chemical features
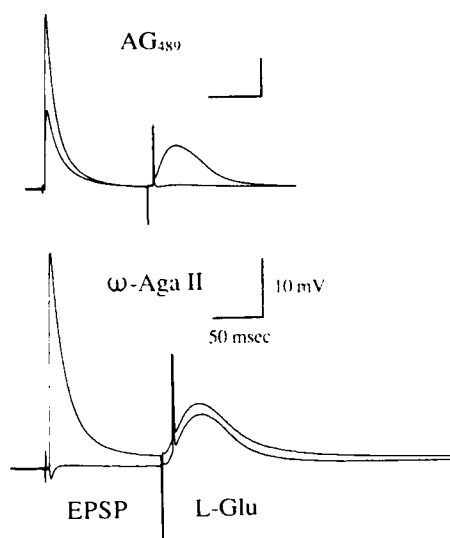
FIG 5 Effects of α- and ω-agatoxins from *Agelenopsis aperta* venom toxins on neuromuscular responses in the pre-pupal fly. Perfusion with the α-agatoxin, AG_{489} at 0.8 μM leads to 50% reduction of the evoked EPSP and virtually complete block of the iontophoretic glutamate potential over a 10-min interval. These effects are attributed to postsynaptic block of glutamate receptor channels. In contrast, treatment with the α-Aga II, a presynaptic blocker, suppresses the evoked EPSP but has no effect on the iontophoretic glutamate potential. Calibration bars: 10 mV, 50 ms.

are apparent. They are smaller than the orb weaver toxins and do not contain conventional amino acids. However, they do conform to the structural motif outlined above, containing a basic, polyamine moiety and exclusively indolic type chromophores. The α-agatoxins are present in crude *Agelenopsis* venom at concentrations ranging from 5–30 mM, which are comparable to those of the argiotoxins.

Injection of α-agatoxins into flies quickly induces a transient paralysis which is correlated with suppression of neuromuscular EPSPs and iontophoretic glutamate potentials (Fig. 5). Concentrations causing 50% block of evoked synaptic potentials are comparable to those of the argiotoxins. For example, AG_{488} and AG_{489} produce 50% block of evoked EPSPs at 0.8–1.0 μM. Postsynaptic block by the α-agatoxins, like the polyamine toxins from orb weaver spiders, depends on synaptic activation [15]. Substantial recovery from synaptic block, resembling that of AN_{758} (Fig. 4) also is observed after treatment with α-agatoxins. The potencies of α-agatoxins in paralytic assays using house fly adults is some 20–100 times lower than those of the argiotoxins, possibly due to enhanced degradation in vivo or to faster off time of binding to the receptor channel.

Presynaptic toxins

In contrast to orb weaver spider venom which causes reversible paralysis, venom of *Agelenopsis aperta* is lethal. Its toxicity correlates with irreversible presynaptic

actions of polypeptide toxins: the 'μ-agatoxins' and 'ω-agatoxins'. The μ-agatoxins induce repetitive firing and massive transmitter release in motor units, possibly through sodium channel activation as described for certain scorpion toxins [2,14]. The ω-agatoxins cause an opposite effect, namely suppression of transmitter release.

μ-Agatoxins: presynaptic excitatory toxins

Six excitatory μ-agatoxins (μ-Aga I-VI) have been characterized as homologous polypeptides of 36–37 amino acids with four disulfide bridges. The μ-agatoxins cause spastic paralysis in vivo, which is correlated with repetitive activity in motoneurons (Fig. 6). The concentrations of μ-agatoxins in whole *Agelenopsis* venom are approximately 1 mM, some ten-fold lower than those of the α-agatoxins. They are stable to boiling and resistant to proteolytic digestion.

Sub-micromolar concentrations of the μ-agatoxins induce both spontaneous and neurally-evoked repetitive activity in pre-pupal house fly motor units (Fig. 6). Repetitive activity caused by treatment with μ-agatoxins is abolished by tetrodotoxin, indicating the involvement of voltage sensitive sodium channels in toxin action. Although the exact origin of the repetitive activity has not been pinpointed, it probably arises in the terminal branches of the innervating nerves. Repetitive firing begins slowly and increases in intensity over a period of hours until activation of motor units is essentially constant.
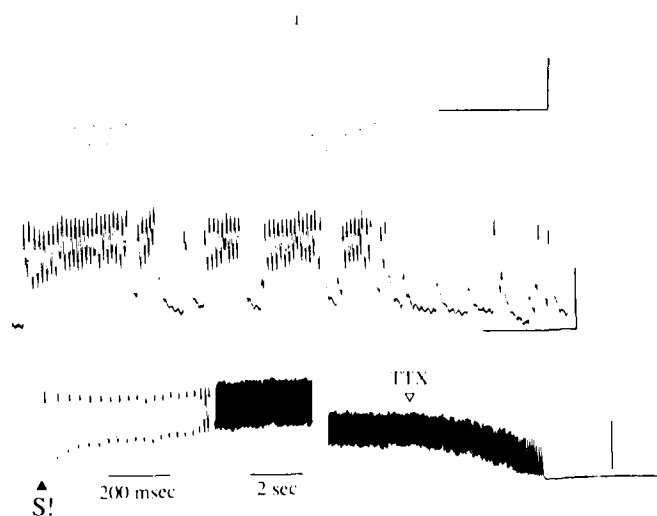
FIG 6 Repetitive activity in pre-pupal fly motor units caused by μ-agatoxins. Top trace: spontaneous EPSPs following treatment with μ-Aga I (0.2 μM). Both fast (single large amplitude event) and slow EPSPs (smaller amplitude events) are evident. Middle trace: spontaneous EPSPs following treatment with μ-Aga IV (0.1 μM). Lower trace: a single stimulus in the presence of μ-Aga I (0.2 μM) leads to a prolonged burst of EPSPs. Application of 50 nM tetrodotoxin (TTX; open arrow) blocks repetitive activity, indicating that voltage-sensitive sodium channels may be involved in the action of the μ-agatoxins. Note that a 30-s interval is removed at the break in the lower trace. Calibration bars: upper: 10 mV, 20 ms; middle: 20 mV, 500 ms; lower: 20 mV, 200 ms, 2 s.

Co-injection experiments indicate that the μ-agatoxins enhance paralysis in house flies caused by the α-agatoxins. This effect may relate to synaptic activation by the μ-agatoxins, which is a prerequisite for synaptic block by the α-agatoxins [15].

ω-Agatoxins: presynaptic inhibitory toxins

Agelenopsis venom contains a third variety of polypeptide toxin which causes irreversible block of neurally evoked EPSPs at nanomolar concentrations. Three of these 'ω-agatoxins' have been isolated and are currently being characterized. Synaptic block by the ω-agatoxins does not correlate with suppression of iontophoretic glutamate potentials (Fig. 5), suggesting that postsynaptic receptor channels are not involved. Interestingly, the ω-agatoxins cause a marked reduction in the quantal content of synaptic potentials, possibly by reducing presynaptic calcium currents. A detailed account of the mechanisms underlying ω-agatoxin action will appear elsewhere (Bindokas and Adams, in preparation).

The ω-agatoxins are polypeptides ranging from about 7000 to 15,000 Da and, like the μ-agatoxins, appear to contain multiple disulfide bridges. Their abundance in crude *Agelenopsis* venom is in the range of 10-100 μM.

Conclusions

There is little doubt that spider venoms contain a multitude of interesting substances affecting insect synaptic transmission. Our survey of only a few venoms shows that several types of synaptic ion channels are targeted by various paralytic toxins. Polyamine-like toxins common to both orb weaver and funnel web venoms produce a transient, flaccid paralysis in insects through antagonism of postsynaptic. glutamate-sensitive receptor channels. The slow reversibility of these toxins correlates with recovery of treated insects. The more complex venom of *Agelenopsis aperta* contains additional toxins which act presynaptically, the μ- and ω-agatoxins. The lethal action of *Agelenopsis* venom is correlated with the irreversible effects of these toxins on transmitter release.

Synaptic block by the orb weaver polyamine toxins is use-dependent and is enhanced by hyperpolarization [6,7,10], suggesting that they do not act as competitive antagonists of glutamate receptors. Indeed, argiopine (AR_{636}) is reported to antagonize cholinergic transmission in the frog [10], albeit at higher concentrations, indicating that the toxin binds to open cation channels rather than to the transmitter binding site. It therefore remains to be seen if this new class of polyamine toxins will possess sufficient specificity for studies of glutamate receptor channels. An encouraging sign is a recent autoradiographic study demonstrating the localized accumulation of ^{125}I-JSTX on crustacean muscle membranes [16], indicating the potential of using these toxins as histochemical and possible biochemical probes for postsynaptic receptor channels.

Agelenopsis venom exerts at least three types of effects on insect neuromuscular transmission: postsynaptic antagonism, presynaptic activation and presynaptic inhibition. Each of these actions appears to involve a different type of ion channel. Antagonism of glutamate-sensitive receptor channels by α-agatoxins involves use-dependent toxin binding which parallels that of the orb weaver toxins. It is intriguing that the spider co-injects the μ-agatoxins, leading to massive transmitter release as a result of repetitive activity. This might enhance the actions of the

58

α-agatoxins, which cause use-dependent block. Indeed, we now have evidence that co-injection of these two types of toxin into whole insects results in marked enhancement of paralysis [15].

The repetitive activity and spastic paralysis caused by the μ-agatoxins appears remarkably similar to the actions of excitatory scorpion toxins, which are known to act on voltage-sensitive sodium channels in nerve [14]. This suggestion is supported by the evidence that repetitive firing caused by μ-Aga I is abolished by treatment with tetrodotoxin. However, it is not yet possible to rule out the involvement of potassium channels in the physiological actions of one or more μ-agatoxins. It also remains to be seen to what extent the μ-agatoxins are selective for insects, since such selectivity is suggested for certain scorpion toxins [18].

The ω-agatoxins are a third class of ion channel toxin found in *Agelenopsis* venom. Preliminary results indicate that these toxins act on nerve terminals to irreversibly block transmitter release. The physiological actions of the ω-agatoxins resemble those of *Hololena* and *Plectruerys* toxins [19,20], although our evidence indicates that the *Agelenopsis* toxins possess a much wider spectrum of action across animal groups (Bindokas and Adams, in preparation). As of this writing, we have isolated three ω-agatoxins and are characterizing their chemical and biological properties. It appears likely that these toxins will be useful as high affinity, selective probes for voltage-sensitive calcium channels.

References

1 Menn, J.J. and Henrick, C.A. (1981) Rational and biorational design of pesticides. Phil. Trans. R. Soc. Lond. B 295, 57–71.

2 Catterall, W.A. (1984) The molecular basis of neuronal excitability. Science 223, 653–661.

3 Olivera, B.M., Gray, W.R., Zeikus, R., McIntosh, J.M., Varga, J., Rivier, J., de Santos, V. and Cruz, L.J. (1985) Peptide neurotoxins from fish-hunting cone snails. Science 230, 1338–1343.

4 Kawai, N., Niwa, A. and Abe, T. (1982) Spider venom contains specific receptor blocker of glutaminergic synapses. Brain Res. 247, 169–171.

5 Miwa, A., Kawai, N., Saito, M., Pan-Hou, H. and Yoshioka, M. (1987) Effect of a spider toxin (JSTX) on excitatory postsynaptic current at neuromuscular synapse of spiny lobster. J. Neurophysiol. 58, 319–326.

6 Usherwood, P.N.R., Duce, I.R. and Boden, P. (1984) Slowly-reversible block of glutamate receptor-channels by venoms of the spiders, *Argiope trifasciata* and *Araneus gemma*. J. Physiol. (Paris) 79, 241–245.

7 Bateman, A., Boden, P., Dell, A., Duce, I.R., Quicke, D.L.J. and Usherwood, P.N.R. (1985) Postsynaptic block of a glutamatergic synapse by low molecular weight fractions of spider venom. Brain Res. 339, 237–244.

8 Grishin, E.V., Volkova, T.M., Arseniev, A.S., Reshetova, O.S., Onoprienko, V.V., Magazanic, L.G., Antonov, S.M. and Fedorova, I.M. (1986) Structure-functional characterization of argiopine- an ion channel blocker from the venom of spider, *Argiope lobata*. Bioorg. Khim. 12, 110–112 (In Russian).

9 Aramaki, Y., Yasuhira, T., Higashijima, T., Yoshioka, M., Miwa, A., Kawai, N. and Nakajima, T. (1986) Chemical characterization of spider toxin, JSTX and NSTX. Proc. Japan Acad. 62B, 359–362.

10 Magazanik, L.G.,Antonov, S.M., Fedorova, I.M., Vokova, T.M. and Grishin, E.V. (1987) Argiopin—a naturally occurring blocker of glutamate-sensitive synaptic channels. In: Receptors and Ion Channels (Y.A. Ovchinnikov and F. Hucho, eds.) pp. 305–312. de Gruyter, New York.

11 Adams, M.E., Carney, R.L., Enderlin, F.E., Fu, E.T., Jarema, M.A., Li, J.P., Miller, C.A., Schooley, D.A., Shapiro, M.J. and Venema, V.J. (1987) Structures and biological activities of three synaptic antagonists from orb weaver spider venom. Biochem. Biophys. Res. Commun., 148, 678–683.

12 Toki, T., Yasuhara, T., Aramaki, Y., Kawai, N. and Nakajima, T. (1988) A new type of spider toxin, Nephilatoxin, in the venom of the Joro spider, *Nephila clavata*. Biomed. Res. 9, 75–79.

13 Budd, T., Clinton, P., Dell, A., Duce, I.R., Johnson, S.J., Quicke, D.L.J., Taylor, G.W., Usherwood, P.N.R. and Usoh, G. (1988) Isolation and characterization of glutamate receptor antagonists from venoms of orb-web spiders. Brain Res. 448, 30–39.

14 Zlotkin, E., Kadouri, D., Gordon, D., Pelhate, M., Martin, M.F. and Rochat, H. (1985) An excitatory and a depressant insect toxin from scorpion venom both affect sodium conductance and possess a common binding site. Arch. Biochem. Biophys. 240, 877–887.

15 Adams, M.E., Herold, E.E. and Venema, V.J. (1988) Two classes of channel-specific toxins from funnel web spider venom. J. Comp. Physiol. in press.

16 Shimazaki, K., Hagiwara, K., Hirata, Y., Nakajima, T. and Kawai, N. (1988) An autoradiographic study of binding of iodinated spider toxin to lobster muscle. Neurosci. Lett. 84, 173–177.

17 Papponc, P.A. and Cahalan, M.D. (1987) *Pandinus imperator* scorpion venom blocks voltage-gated potassium channels in nerve fibers. J. Neurosci. 7, 3300–3305.

18 Zlotkin, E. (1983) Insect selective toxins derived from scorpion venoms: an approach to insect neuropharmacology. Insect Biochem. 13, 219–232.

19 Bowers, C.W., Phillips, H.S., Lee, P., Jan, Y.N. and Jan, L.Y. (1987) Identification and purification of an irreversible presynaptic neurotoxin from the venom of the spider, *Hololena curta*. Proc. Natl. Acad. Sci. U.S.A. 84, 3506–3510.

20 Branton, W.D., Kolton, L., Jan, Y.N. and Jan, L.Y. (1987) Neurotoxins from *Plectreurys* spider venom are potent presynaptic blockers in *Drosophila*. J. Neurosci. 7, 4195–4200.

21 Zar, J.H. (1984) Biostatistical Analysis, 2nd edition. Prentice-Hall, Englewood Cliffs, NJ.

CHAPTER 5

Polyamine like toxins—
a new class of pesticides?

T. Piek [1], R.H. Fokkens [3], H. Karst [1], C. Kruk [3], A. Lind [1], J. van Marle [2],
T. Nakajima [4], N.M.M. Nibbering [3], H. Shinozaki [5], W. Spanjer [1]
and Y.C. Tong [6]

Departments of [1] Pharmacology, [2] Electron Microscopy, Meibergdreef 15, 1105 AZ,
Amsterdam, [3] Organic Chemistry, Nieuwe Achtergracht 129, 1018 WS Amsterdam,
The Netherlands; [4] Faculty of Pharmaceutical Sciences, [5] the Tokyo Metropolitan
Institute of Medical Science, Bunkyo-ku, Tokyo 113, Japan; [6] Dow Chemical Research
Co., Walnut Creek, CA, U.S.A.

Introduction

Evolutionary development of natural toxins which are active against insects has
taken place, particularly in plants and arthropods; in the latter both for offensive
and defensive purposes. Owing to the limited amounts of venoms which are
available in arthropods, our knowledge of them is much less than that of plant
toxins. The modern study of arthropod venoms with insecticidal action was initiated
in the fifties, and only in the seventies did papers appear on spider, scorpion and
wasp venoms with neurotoxic effects [1].

In the beginning of the eighties it became evident that venoms of some species of
spiders and solitary wasps contain a number of active components. Recent work by
Kawai and coworkers [2,3] has provided evidence that a component of the venom of
the Joro spider (Nephila clavata), called Joro spider toxin or JSTX, irreversibly
suppresses the glutamatergic excitatory postsynaptic potentials (EPSPs) of a skeletal
nerve-muscle preparation of the lobster. The results by Bateman et al. [4] suggest
that the venom of spiders belonging to the genera Argiope and Araneus contain
heat-stable toxins of low molecular weight, inducing transmission failure in the
insect nerve-muscle preparation, possibly by open ion channel block of the
glutamatergic channel. Although these toxins were originally characterized as poly-
peptides [4,5], it became evident that the low-molecular-weight spider toxins may be
composed of peptide as well as of polyamine moieties. In 1986 Volkova et al. [6]
reported that the venom of Argiope lobata contains a peptide-polyamine structure
called argiopine (Fig. 1). The toxic principle for the venom glands of the Nephila
spiders consists of 2,4-dihydroxyphenylacetyl-asparaginyl-cadaverine, elongated with
a variable polyamine and amino acid chain as, for example, arginyl-putreanine in
the toxin from the venom of N. maculata [7,8]. The present paper describes the
effects of two spider toxins called NSTX-3 and JSTX-3 (Fig. 1) from the venom of

62

NH$_2$
|
C=O
|
CH$_2$
|
HO—[benzene ring]—OH CH$_2$CNHCHCHNH(CH$_2$)$_5$NH(CH$_2$)$_3$NH(CH$_2$)$_3$NHCCH(CH$_2$)$_3$NHCNH$_2$
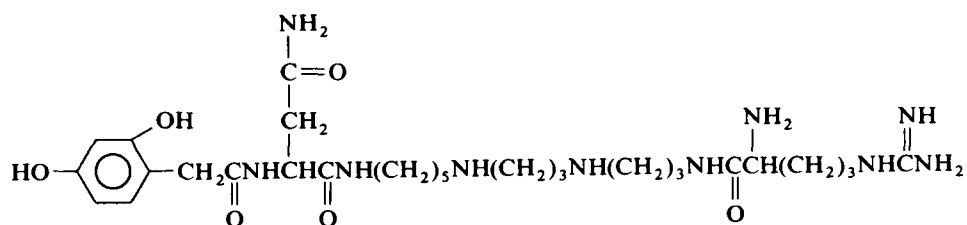
argiopine
(Argiope lobata)
Volkova et al., 1986 [6]

NH$_2$
|
C=O
|
CH$_2$
|
HO—[benzene ring]—OH CH$_2$CNHCHCHNH(CH$_2$)$_5$NHC(CH$_2$)$_2$NH(CH$_2$)$_4$NHCCH(CH$_2$)$_3$NHCNH$_2$
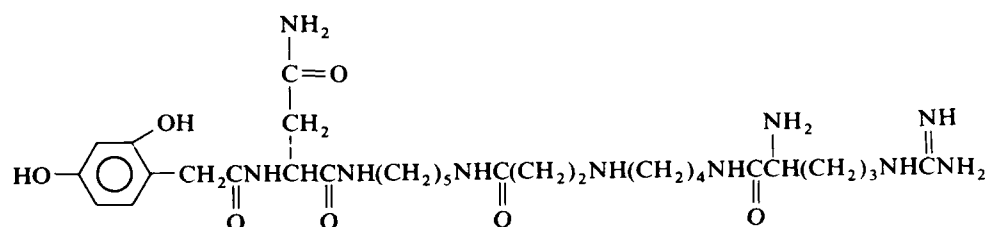
NSTX-3
(Nephila maculata)
Aramaki et al., 1987 [7]

NH
|
C=O
|
CH$_2$
|
HO—[benzene ring]—OH CH$_2$CNHCHCHNH(CH$_2$)$_5$NHC(CH$_2$)$_2$NH(CH$_2$)$_4$NH(CH$_2$)$_3$NH$_2$
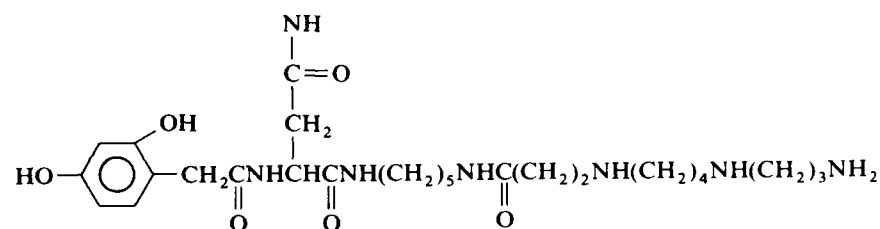
JSTX-3
(N. clavata)
Aramaki et al., 1987 [17]

C$_3$H$_7$
|
C=O
|
NH
|
HO—[benzene ring]—CH$_2$CHCNH(CH$_2$)$_4$NH(CH$_2$)$_3$NH(CH$_2$)$_3$NH$_2$

δ-PTX
(Philanthus triangulum)

C$_5$H$_{11}$
|
[benzene ring]—CHCHNH(CH$_2$)$_4$N[piperidine ring]
|
OH
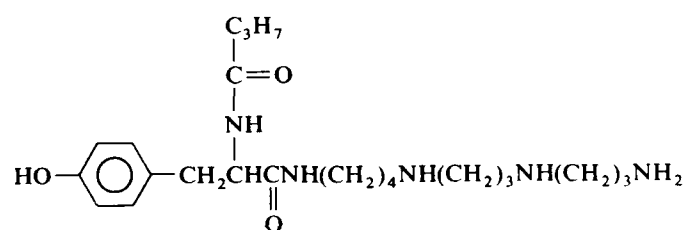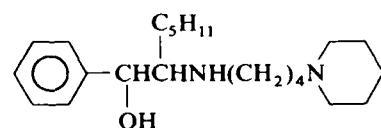
MLV-5860
Shinozaki & Ishida, 1986 [13]

Fig. 1. For legend see opposite page.

N. maculata and *N. clavata* respectively, on glutamatergic synaptic transmission in insects.

In the sixties, studies were started to investigate the paralysing venom of the solitary wasp *Philanthus triangulum*. The initial results showed effects on the skeletal neuromuscular transmission of insects. The excitatory transmission is affected in two different ways: by a presynaptic inhibition of the reuptake of glutamate [9], and by a postsynpatic block of open ion channels of the glutamatergic receptor–ionophore complex [10,11]. The venom of *P. triangulum* contains two polyamine antagonists for the glutamatergic transmission [12].

The present paper describes the chemical structure of the most active of the philanthotoxins: δ-philanthotoxin (δ-PTX), in this study applied as the synthetic toxin (δ-PTX-S$_1$), and its action on synaptic transmission of insects.

Besides the above mentioned two groups of polyamine-containing natural toxins (the spider toxins and the philanthotoxins) a family of synthetic channel blockers for glutamatergic transmission has been described by Shinozaki and Ishida [13]. The most active substance is 5-methyl-1-phenyl-2(3-piperidinopropylamine)-hexane-1-ol or MLV-5860.

This paper describes the effects of MLV-5860 and an analogue MLV-6976 (see Fig. 1) on synaptic transmission of insects.

Materials and methods

δ-Philanthotoxin was prepared as described by Piek and Spanjer [14]. Electron Impact (EI) and Field Desorption (FD) mass spectra were obtained with a Varian MAT-711 mass spectrometer and Fast Atom Bombardment (FAB) mass spectra were recorded with a VG Micromass ZAB-2HF double focusing instrument [15]. They showed unambiguously that the molecular weight of δ-PTX was 435 Da, while accurate mass measurements under EI conditions at a resolution of 12,000 (10% valley definition) established that the molecule of δ-PTX had the elemental composition of $C_{23}H_{41}N_5O_3$. ^1H and ^{13}C nuclear magnetic resonance (NMR) spectra (1D and 2D) were recorded for a solution of δ-PTX in CD_3OD on Bruker AM500 and WM250 spectrometers. Collision induced dissociation MS experiments [16] and NMR solvent-suppression techniques and double resonance experiments were applied for the chemical characterization of δ-PTX. The synthetic toxin (δ-PTX-S$_1$) was supplied by Dr Y.C. Tong.

C_4H_9

⟨O⟩—CHCHNH(CH₂)₃N⟨ ⟩

O——C=O
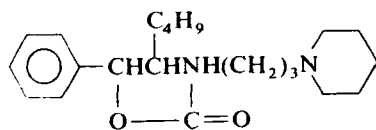
MLV-6976
Masaki & Shinozaki, 1986 [29]

FIG 1 Survey of a number of polyamine-like toxins, which inhibit the glutamatergic transmission. Argiopine is the first described spider toxin. δ-philanthotoxin (δ-PTX) is originally described here. The effects of these toxins, except argiopine, on the neuromuscular transmission of the locust skeletal muscle are described in this paper.

Toxic principles from the venom of the spider *Nephila clavata* and *N. maculata* (JSTX and NSTX) were chemically characterized [7,17], and synthesized [18,19]. The synthesis of the glutamate inhibitors MLV-5860 and -6976 has also been described [10].

The electrophysiological techniques were standard, electron-microscope (EM) experiments were carried out with isolated retractor unguis muscles of the hindleg of the locust *Schistocerca gregaria* F. [9]. EM autoradiographs were prepared using the flat substrate method [21,22]. The amount of [^{3}H]glutamate accumulated in glia and axon terminals is expressed as density, i.e. the number of silver grains per square μm [23]. Five toxins (δ-PTX-S$_1$, NSTX-3, JSTX-3, MLV 5860 and MLV 6976) were tested for effects on transmission with electrophysiological techniques, and for effects on high affinity uptake using EM autoradiography.

Results

Structural elucidation of δ-philanthotoxin (δ-PTX)

By a joint application of chromatographic methods, mass spectrometry (MS) and NMR, the structure of δ-PTX was established as depicted in Fig. 1. Detailed information about the spectroscopic results will be published elsewhere. NMR and mass spectra of both the natural δ-PTX and the synthetic toxin, called δ-PTX-S$_1$, are identical. The polyamine chain is thermospermine.

Effects of δ-PTX-S$_1$ on intact honeybee workers and locusts

δ-PTX-S$_1$ causes a reversible paralysis of honeybee workers, the natural prey of the wasp *Philanthus triangulum*. The paralysis takes place immediately after intrathoracic injection of the toxin. Fig. 2 shows the dose–effect relationship, representing the 50% recovery against the dose on a log scale. The bees were injected with
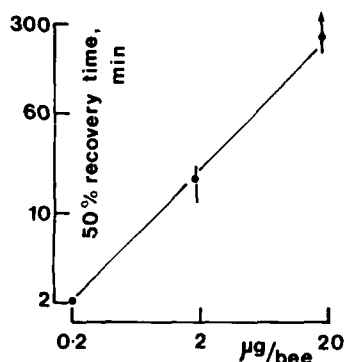
FIG 2 Dose–effect relationship, representing the 50% recovery of honeybee workers, injected intrathoracically with δ-PTX-S$_1$ against the dose on log scale. Eight bees were injected, and the average recovery time was calculated. At the highest dose one of the eight bees did not recover (arrow). The latter point has been calculated from 7 recovery times, ignoring the last bee. At concentrations higher than 20 μg per bee, the bees did not recover.
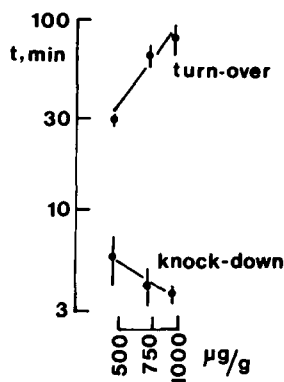
FIG 3 Dose–effect curves of the knock-down and recovery (turn-over) times of locust (*Locusta migratoria*) fifth instar larvae injected intrathoracically with δ-PTX-S$_1$.

7 μl saline containing respectively 20 μg, 2 μg, and 0.2 μg of the toxin per bee ($n = 8$). At higher doses some of the bees did not recover. At 40 μg or more the paralysis turned out to be irreversible for all bees. However, it is not certain if this irreversibility is due to a secondary effect. Bees paralysed for more than 400 min never recovered. The ED$_{50}$ (at 60 min) is about 5.2 μg.

Comparison of the effects of the natural and the synthetic toxin is problematic, since the former is no longer available in quantities necessary for such experiments. However, a partly purified preparation of δ-PTX, of which an equivalent of a single venom reservoir was injected into each of 10 bees, resulted in an immediate paralysis with a recovery time of about 25 min [14]. The yield of δ-PTX is about 1 μg per wasp [12]. Therefore, 1 μg δ-PTX may cause a a paralysis with a recovery time (ED$_{50}$) of 25 min. Fig. 2 indicates that a recovery time of 25 min corresponds to 2.3 μg δ-PTX-S$_1$ per bee. Hence, δ-PTX-S$_1$ seems to be about half as effective as the natural toxin. For an explanation, see the Discussion.

Locusta migratoria is less sensitive to δ-PTX-S$_1$ than honeybee workers. Intrathoracic injection of 750 μg/g caused a knock-down in 4.0 ± 1.0 (S.E.M., $n = 3$) min. Recovery from a flaccid paralysis, resulting in a turnover, occurred in 65 ± 8 (S.E.M., $n = 3$) min. Fig. 3 shows the dose–effect curves of the knock-down and the recovery at three different doses of toxin. Higher concentrations caused long lasting paralysis of variable duration, which was however, always reversible. In view of the results presented in Figs. 2 and 3, and the fact that the weight of 10 honeybees is always very close to 1 g, locusts may be at least 10-times less sensitive to the toxin than honeybee workers.

Effects of polyamine toxins on the reuptake of glutamate

The glutamate uptake in the locust neuromuscular junction is inhibited by δ-philanthotoxin [9]. From the analysis of EM autoradiographs of toxin-treated muscles (see for example Fig. 4) it appeared that δ-PTX at a concentration of 26 μg/ml caused a significant reduction of the [^{3}H]glutamate uptake in glia and axon terminals. In both cases the radioactivity is reduced to about 15% ($P < 0.003$) [9].

TABLE 1   Grain densities (expressed as the amounts of developed silver grains per μm^2; average values $\pm$ S.E.M.) over both terminal axons (TA) and their surrounding glial cells (Gl) of retractor unguis muscles incubated with 10 μM δ-PTX-S$_1$, compared with control

		TA	Gl
Control	1	20.3	52.1
	2	15.4	54.9
	3	16.1	35.7
	4	13.0	39.3
	5	17.3	47.8
		16.4 ± 1.2	46.0 ± 3.7
δ-PTX-S$_1$	1	9.2	17.8
	2	5.2	14.8
	3	4.3	13.2
	4	12.0	25.7
		7.7 ± 1.8	17.9 ± 2.8

For each muscle at least 12 synapses were analysed. No correction has been made for background, which was below 0.2 ± 0.002 (mean $\pm$ S.E.M., $n = 3$) silver grains per 100 μm^2. The reduction of the glutamate uptake obtained with δ-PTX-S$_1$ at a concentration of 54 μg/ml is about 50% for the terminal axons and about 60% for the glial cells.

This presynaptic high affinity glutamate uptake has a K_m of approximately 15 μM in both glial cells and terminal axons [24]. This value was in agreement with biochemical estimation of the kinetics of presynaptic high affinity uptake systems in the insect glutamatergic neuromuscular junction and mammalian glutamatergic central nervous system.

Effects of δ-PTX-S$_1$ on glutamate uptake

In the present study we repeated the experiments with δ-PTX, described above, using the synthetic δ-PTX-S$_1$. Since in honeybees the latter toxin is less (ca. 50%) effective than the natural toxin (see also Discussion) we used twice the amount of synthetic toxin, i.e. 54 μg/ml (= 10 μM) δ-PTX-S$_1$. Table 1 shows the average grain densities above both terminal axons and their surrounding glial cells in control and toxin treated retractor unguis muscles of *S. gregaria*. The reduction of the glutamate uptake obtained with δ-PTX-S$_1$ at a concentration of 54 μg/ml is about 50% for the terminal axons and about 60% for the glial cells.

A current investigation of the activity of analogues of δ-PTX indicates that small changes in the structure of this toxin completely abolish the ability to inhibit the glutamate uptake in some cases, while the blocking activity to the postsynaptic ion channel is still present. In order to see if the spider toxins and the MLVs may have an effect on the uptake system, we have applied the latter toxins at a relatively high concentration.

Effects of spider toxins on glutamate uptake

Fig. 4 shows cross sections of the locust muscles at the level of the neuromuscular junction. Silver grains are present above the axon terminal as well as above the glial cells. The density of silver grains above sections from the toxin (NSTX-3) treated muscle is higher than that of the control muscle sections. Table 2 shows the average
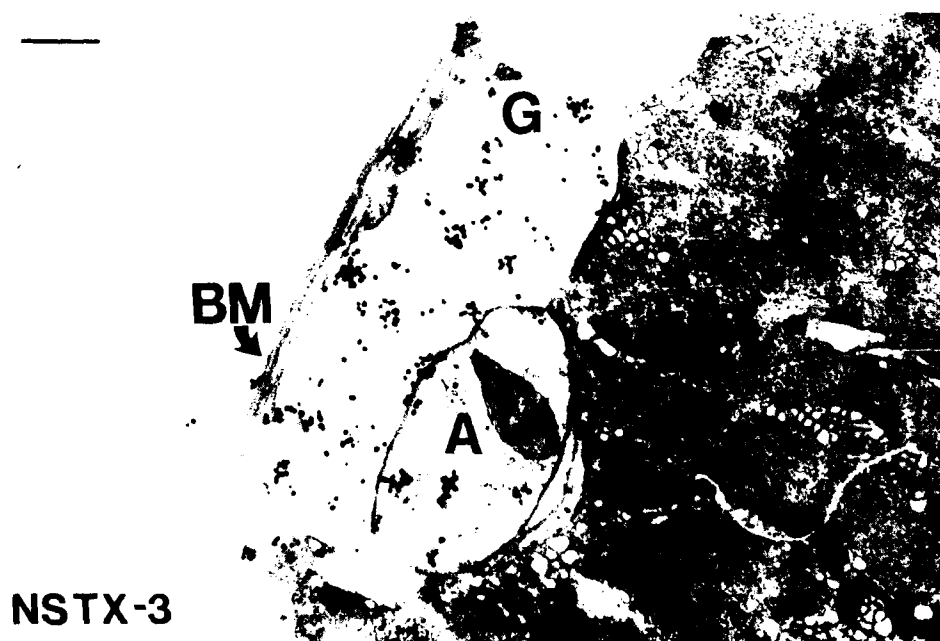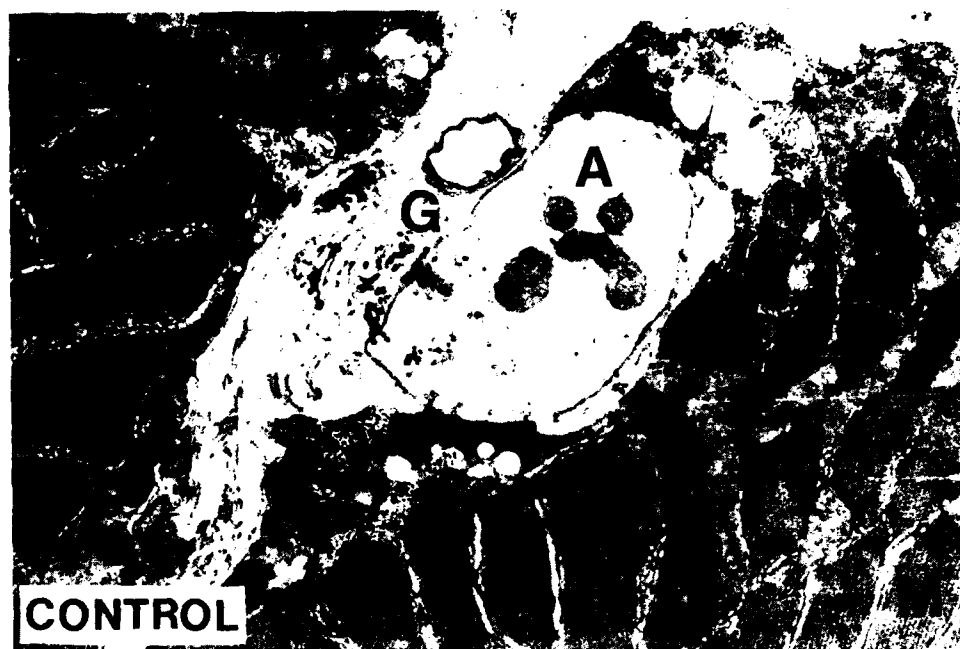
FIG 4 Electron microscope autoradiographs of [³H]glutamate-labelled synapses in an isolated locust muscle. Top: control; bottom: treated with 100 μM NSTX-3. Silver grains are present above the axon terminal (A), glial cells (G) and subsynaptic reticulum (SSR). M, muscle fibre; BM, basal membrane. Scale bar = 0.5 μm.

TABLE 2 Grain densities over terminal axons and their surrounding glial cells of retractor unguis muscles incubated with NSTX-3 or JSTX-3, at a concentration of 100 μM

		TA	Gl
Control	1	5.7	24.1
	2	10.6	36.8
	3	8.1	21.9
	4	8.0	36.4
		8.1 ± 1.0	29.8 ± 4.0
NSTX-3	1	18.2	52.5
	2	17.5	32.3
	3	23.5	55.7
	4	11.5	41.5
		17.7 ± 2.5	45.5 ± 5.3
JSTX-3	1	14.9	46.6
	2	19.1	43.3
	3	14.1	46.1
	4	13.0	51.3
		15.3 ± 1.3	46.8 ± 1.7

For abbreviations see Table 1.

grain densities above both axon terminals and glial cells in control and toxin treated muscles. At a concentration of 100 μM both NSTX-3 and JSTX-3 significantly increase the grain densities above axons (about 100%) and glia (about 55%).

Effects of the MLV toxins on glutamate uptake
Table 3 shows the average grain densities above terminal axons and glial cells of control muscles and muscles incubated with 400 μM MLV-5860 or MLV-6976. At this relatively high concentration, the glutamate uptake was not affected significantly, neither by MLV-5860 nor by MLV-6976.

Effects of δ-PTX-S$_l$ on postsynaptic and glutamate potentials

The toxin δ-PTX isolated from the venom of *P. triangulum* blocks the excitatory transmission of the locust muscle postsynaptically. This toxin depresses both the iontophoretic glutamate potential and the excitatory junctional currents of a glutamate receptor, in an activation-dependent way [10,11].

Comparable to the above described effects of the natural toxin, the synthetic δ-PTX-S$_1$ depresses the amplitude of excitatory junctional potentials in a dose-dependent way. Moreover, this block of transmission is activation-dependent. The higher the frequency of stimulation, the more sensitive will be the transmission process for the toxin. At a concentration of 10^{-6} M, the amplitude of excitatory postsynaptic potentials of a metathoracic retractor unguis muscle fibre of the locust *Shistocerca gregaria*, evoked at a frequency of 20 Hz, is reduced to about 15% of the control value. The resting membrane potential remains stable for at least 30 min.

Glutamate potentials were also blocked by δ-PTX-S$_1$. In order to study this phenomenon without the concurrent desensitization, which also curtails the gluta-

TABLE 3 Grain densities above terminal axons and their surrounding glial cells of retractor
unguis muscles incubated with MLV-5860 and MLV-6976, at a concentration of 200 μM

		TA	Gl
Control	1	13.0	48.1
	2	8.5	15.7
	3	12.6	67.2
	4	7.1	23.0
		10.3 ± 1.5	38.5 ± 11.8
MLV-5860	1	8.7	42.7
	2	6.9	21.4
	3	3.4	21.1
		6.3 ± 1.6	28.4 ± 7.2
MLV-6976	1	8.2	44.5
	2	4.7	44.6
	3	6.2	32.6
		6.4 ± 1.0	40.6 ± 4.0

For abbreviations see Table 1.

mate potentials, in a number of experiments the nerve muscle preparations were
pretreated with 2×10^{-6} M concanavalin A (Con A), which blocks desensitization
resulting in an increase of the decay time of the glutamate potential (Fig. 5A).
Figures 5B and C indicate the reversible effect of the toxin on a glutamate potential,
evoked by an iontophoretically applied glutamate pulse of 3 nC. These potentials
were recorded in a fibre of the metathoracic retractor unguis muscle of *S. gregaria*.
It is obvious that the potentials are curtailed, resulting in a decrease in time constant
of the decay (Fig. 5E), a shift of the top of the potentials to the left, and a
concurrent decrease of amplitude (Fig. 5B, C).

Effects of spider toxins on glutamate potentials

Both spider toxins block glutamate potentials to a steady state plateau, the level of
which depends on the concentration and frequency of stimulation used. Fig. 6
(A–D) shows the effect of 1.5×10^{-8} M NSTX-3, in a Con A pretreated muscle
fibre. The glutamate potentials are curtailed (Fig. 6B), resulting in a decrease in the
decay time constant (Fig. 6D). Without pretreatment by Con A such a decrease in
decay time constant is difficult to observe, since the control decay time constant is
mostly close to the time constant of the membrane (Fig. 6E). The decrease in decay
time constant may indicate a stimulus-dependent channel block by the toxin.

The block is quickly reversible with a time course which is higher than after
treatment with δ-PTX (cf. Figs. 5D and 6A). Moreover, the recovery takes place
asymmetrically with the block (cf. Fig. 6B and C). During the recovery the
amplitudes of the potentials are lifted after the original peak, indicating a stimulus-
induced unblocking of the ion channels.

Without pretreatment reversibility is very slow (Fig. 7) for both toxins. Only
when the block was caused by NSTX-3, pretreatment with Con A, causes a much
faster time course of reversibility. In the Con A pretreated muscle NSTX-3 is 2–3
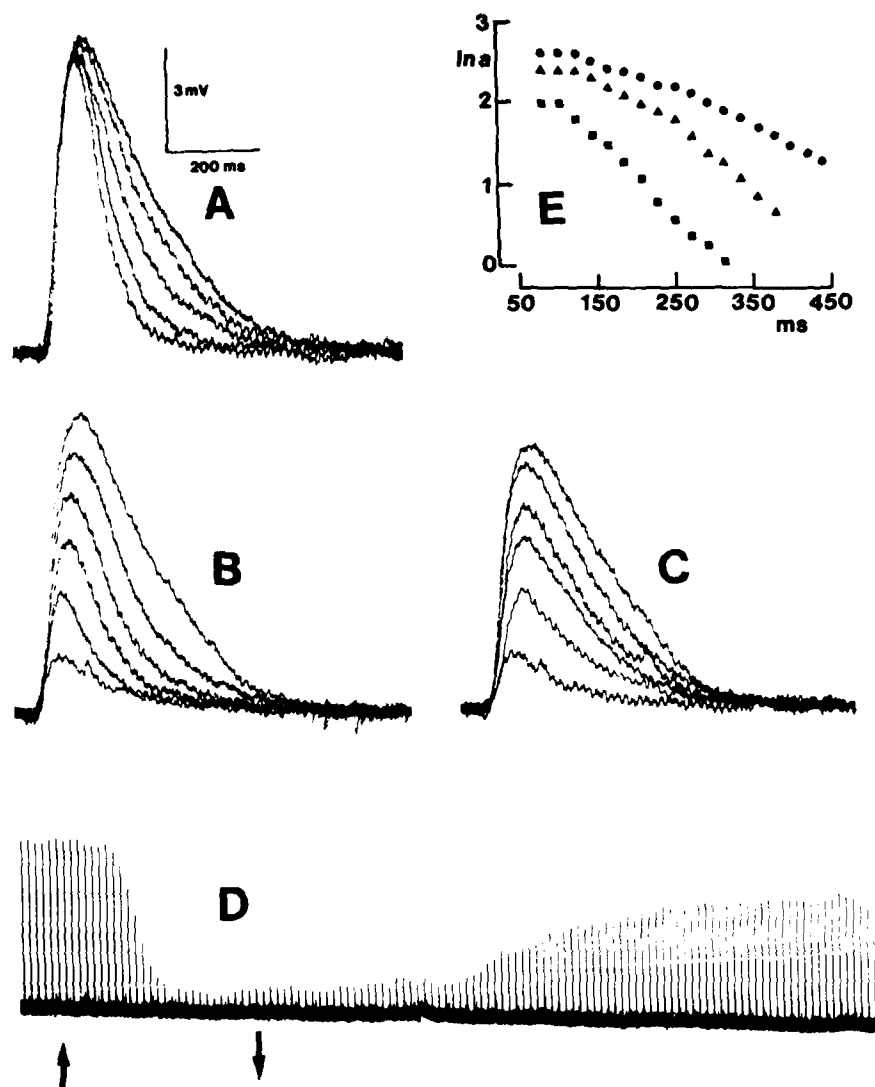
FIG 5 Effects of δ-PTX-S₁ on glutamate potentials iontophoretically evoked by 3 nC pulses, in fibres of the retractor unguis muscle of *Schistocerca gregaria*, pretreated with 2×10^{-6} M concanavalin A. Owing to inhibition of desensitization Con A causes a slow-down of the repolarization (A). Once this situation has been caused irreversibly by Con A, δ-PTX-S₁ at a concentration of 1.8×10^{-7} M caused a curtailing of the potentials (B). resulting in an increase of the decay time constant (E). The restoration of glutamate potentials during wash (C) was slower than the block (D). Arrows indicate the period at which the toxin was present in the bathing saline. ●, ▲, ■ correspond to the upper three traces of B.
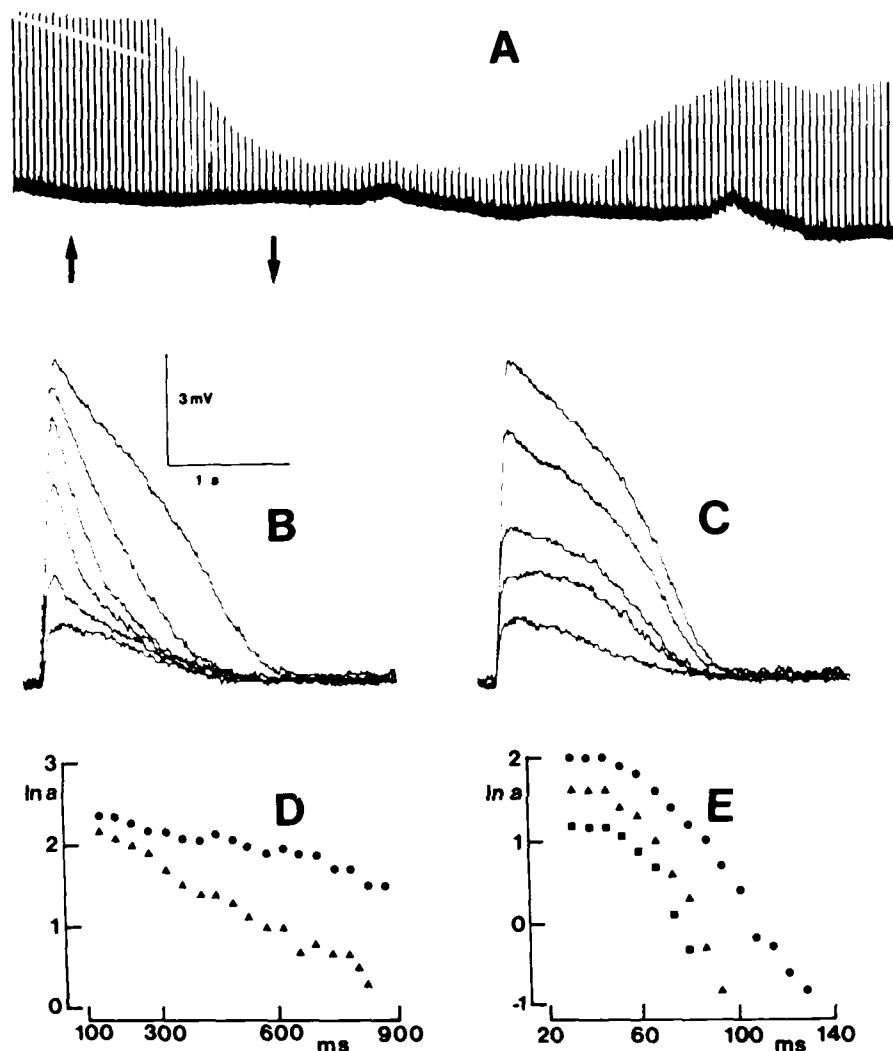
FIG 6 Effects of NSTX-3 on glutamate potentials. A–D: potentials from muscle fibres pretreated with 2×10^{-6} M Con A. Arrows in A indicate the presence of 1.5×10^{-8} M of the toxin in the bathing saline. Note the slow block (A) compared with δ-PTX, and the asymmetrical recovery (C). Curtailing of the potentials (B) resulted in an increase in decay time constant (D). E shows the decay of the potentials in a preparation not pretreated with Con A. ●, ▲, in D correspond to the upper two traces in B; ●, ▲, ■ in E correspond to the upper three traces in C.

times more active as a blocker, and its reversibility is enhanced. This is in contrast with δ-PTX and δ-PTX-S₁, whose action is not affected by Con A. In experiments with JSTX-3 pretreatment with Con A has only a small effect. The Con A pretreated preparation seems to be more sensitive to the JSTX-3 and the time course of reversibility is only slightly increased (Fig. 7).
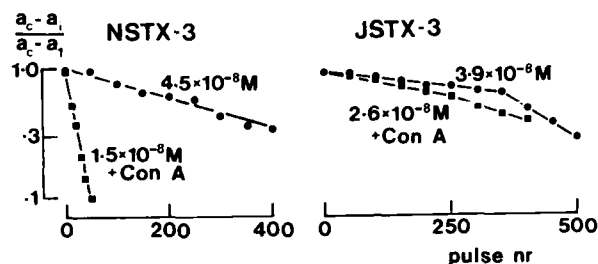
FIG 7 Exponential decay of the block of glutamate potentials, caused by spider toxins, during wash. The amplitude of each response (a_i) has been subtracted from the control amplitude (a_c), and the difference $(a_c - a_i)$ has been normalized to the difference for the first pulse in the train of recovery $(a_c - a_1)$. The value of $(a_c - a_i)$ over $(a_c - a_1)$ is plotted against the pulse member. Note the very slow reversibility of both toxins in the absence of Con A, and the remarkable faster time course of recovery from NSTX-3 blockage, when the muscle is pretreated with Con A.

Effects of MLVs on glutamate potentials

At a concentration of 1.3×10^{-6} M, MLV-5860 causes the glutamate potentials to decrease reversibly in amplitude to a steady state level of about 50 percent (Fig. 8B and C). Twice that concentration causes a steady state level of about 10 percent (Fig. 8A). MLV-6976 is less active, and neither toxin curtails glutamate potentials, not even in the Con A pretreated muscle fibres.

Discussion

This paper describes the structure of a toxin isolated from the venom of the wasp *Philanthus triangulum*, the δ-philanthotoxin (δ-PTX). The toxin reveals structural similarities with the recently described spider toxins and with the synthetic MLVs.

The synthetic δ-PTX (δ-PTX-S_1) is probably about half as active as the natural product. This could be explained by assuming that the natural product is just one of the two optical isomers present in the synthetic one, and by assuming that only the naturally occurring isomer is active.

In this paper five different toxins have been compared in their action on glutamate potentials evoked iontophoretically in locust muscle fibres, and in their action on the presynaptic reuptake of glutamate by nerve terminals and their surrounding glial cells. Three toxins, NSTX-3, JSTX-3 and δ-PTX-S_1 are synthetic toxins identical to toxins present in arthropod venoms. They are polyamines containing one or more amino acid residues. The MLVs are completely synthetic products.

Pan-Hou et al. [25] argued that all spider toxins contained a 2,4-dihydroxyphenylacetylasparagine residue, and that this common moiety may be the essential requirement for the toxins to express their biological activity on the glutamate receptors in rat brain synaptic membranes. Even 2,4-dihydroxyphenylacetic acid inhibited glutamate binding in rat synaptosomes [26]. For the glutamatergic receptor ion-channel complex present in insect skeletal muscle, this moiety may be less
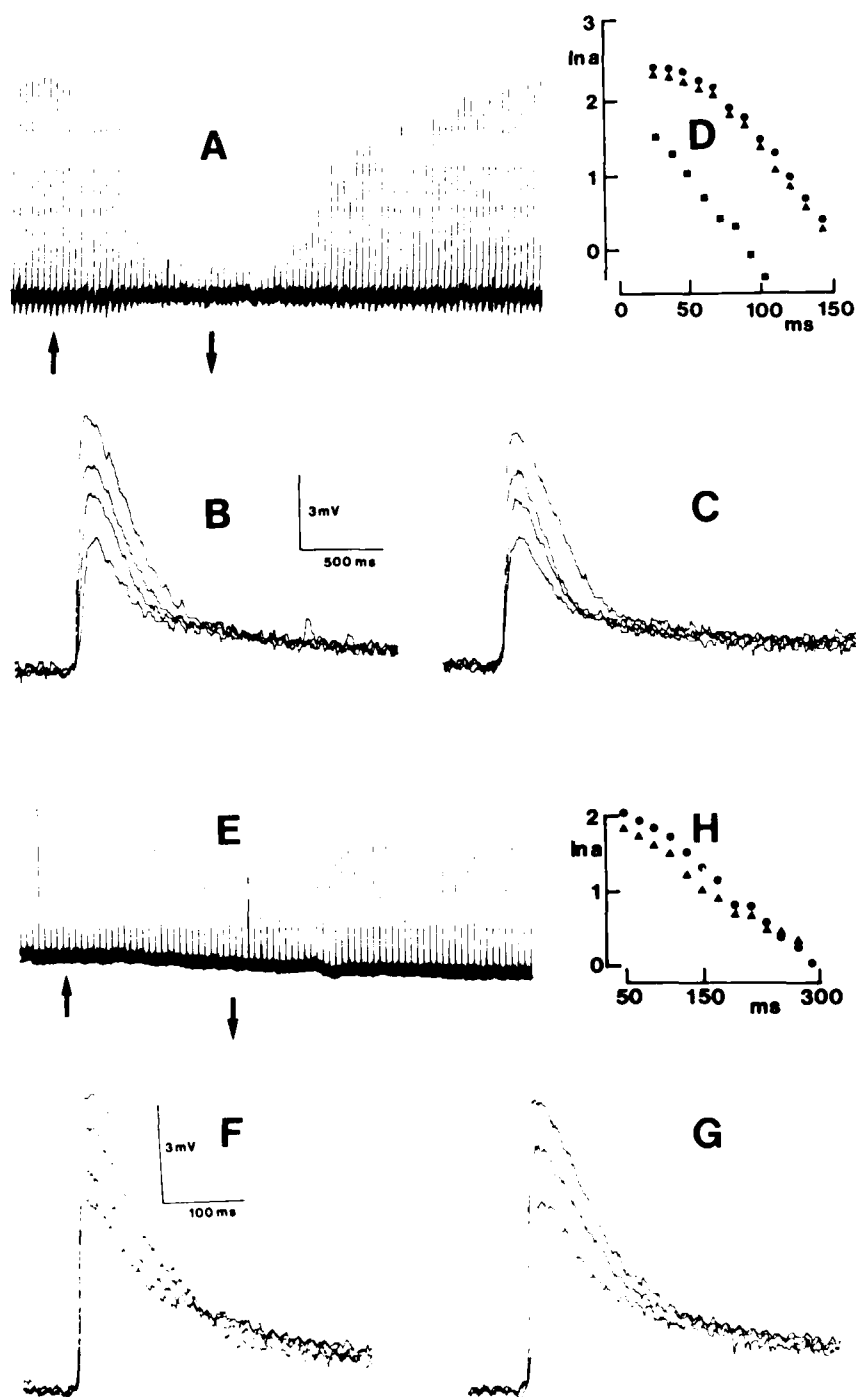
FIG 8 Effects of MLV-5860, 2.7×10^{-6} M (A) and 1.3×10^{-6} M (B–D) and of MLV-6976, 5.2×10^{-5} M (E–H) on glutamate potentials of locust muscle fibres pretreated with 2×10^{-6} M Con A. Exponential decay time constants of control and of toxin-treated muscles are comparable (D and H). Arrows in A and E indicate the presence of the toxins in the bathing saline. ●, ▲, ■ present the decay time course at 1, 2 and 3 min after administration of the toxin.

important since it does not occur in δ-PTX and the MLVs. The high activity of the spider toxins and their slow reversibility seem to be related to the length of their polyamine chain. JSTX-3 is not only intermediate in chain length between NSTX-3 and δ-PTX, but also in relative activity and in susceptibility for Con A. In locust muscle fibres, not pretreated with Con A, both spider toxins induce a slowly reversible block of synaptic transmission. The reversibility of the effect of these toxins is still a matter of controversy. In the insect muscle the venoms of *Argiope trifasciata* and *Araneus gemma* induce a slowly reversible block of the glutamate receptor-channel complex [27]. In the lobster muscle purified Joro-spider toxin induces an irreversible block, however, on storage in the freezer partly purified JSTX converted from an irreversible to a reversible blocker [28].

The inhibitory effect on the high affinity uptake of glutamate by nerve terminals and glial cells, seen with δ-PTX, is absent with the MLVs. The spider toxins, on the contrary, cause an increased glutamate uptake instead of inhibition. Small changes in structure of δ-PTX, which in some cases do not affect its channel blocking activity, result in a loss of all presynaptic activity (unpublished results). This may indicate that the presynaptic effect is more specific than the postsynaptic effect, and that considering their partial dissociation, both effects are not based on one and the same principle.

The effects on reuptake are only seen using relatively high concentrations of the toxins. An explanation for this phenomenon may be that reuptake inhibition is very sensitive to the stimulus frequency. This is a well-known and perhaps comparable phenomenon in the cholinergic system, where reuptake is replaced by enzymatic degradation. In both cases an almost complete inhibition of the enzymatic degradation or the high affinity reuptake respectively has little or no effect during low frequency stimulation, but has a dramatic effect during high frequency stimulation. Since EM autoradiographical techniques are difficult to combine with high frequency stimulation and therefore resemble low frequency stimulation conditions, relatively high concentrations of toxins must be added in order to observe a moderate effect. This does not rule out the possibility that under physiological circumstances much lower concentration may cause a substantial presynaptic effect.

The above results may lead to the use of a new class of polyamine-like toxins for the study of glutamatergic transmission, both post- and presynaptically and the toxins may be used as a model for the development of a new class of pesticides.

Acknowledgements

References

1 Piek, T. (1981) Arthropod venoms as tools for the study of neuromuscular transmission. Comp. Biochem. Physiol. 68C, 75–84.
2 Kawai, N., Niwa, A. and Abe, T. (1982) Spider venom contains specific receptor blocker of glutamanergic synapses. Brain Res. 247, 169–171.
3 Abe, T., Kawai, N. and Miwa, A. (1983) Effects of a spider toxin on the glutamatergic synapse of lobster muscle. J. Physiol. (Lond.) 399, 243–252.

4 Bateman, A., Boden, P., Dell, A., Duce. I.R., Quicke, D.L.J. and Usherwood, P.N.R. (1985) Postsynaptic block of a glutamatergic synapse by low molecular weight fractions of spider venom. Brain Res. 339, 237–244.

5 Usherwood, P.N.R. and Duce, I.R. (1985) Antagonism of glutamate receptor channel complexes by spider venom polypeptides. Neurotoxicology 6, 239–250.

6 Volkova, T.M., Grishin, E.V., Arseniev, A.S., Reshetova, O.S. and Onoprienko, V.V. (1986) Structural characteristics of Argiopine-blocker of glutamate channels from the venom of spider *Argiope lobata*. Proc. 6th Europ;. Soc. Neurochem. Meet., p. 189.

7 Aramaki, Y., Yasuhara, T., Higashijima, T., Miwa, A., Kawai, N. and Nakajima, T. (1987) Chemical characterization of spider toxin, NSTX. Biomed.Res. 8, 167–173.

8 Nakajima, T. and Kawai, N. (1987) Spider toxins, NSTX and JSTX, in the venoms of *Nephila maculata* and *Nephila clavata*. Abstr. Asia-Pac, Congr. Anim., Plant Microb. Toxins, Singapore, p. 0059.

9 Van Marle, J., Piek, T., Lind, A. and Van Weeren-Kramer, J. (1983) Inhibition of the glutamate uptake in the excitatory neuromuscular synapse of the locust by delta-philanthotoxin; a component of the venom of the solitary wasp *Philanthus triangulum*. A high resolution autoradiographic study. Comp. Biochem. Physiol. 79C, 213–215.

10 Clark, R.B., Donaldson, P.L., Gration, K.A.F., Lambert, J.J., Piek, T., Ramsey, R., Spanjer, W. and Usherwood, P.N.R. (1982) Block of locust muscle glutamate receptors by δ-philanthotoxin occurs after receptor activations. Brain Res. 241, 105–114.

11 Piek, T. (1982) Delta-philanthotoxin, a semi-irreversible blocker of ion-channels. Comp. Biochem. Physiol. 72C, 311–315.

12 Piek, T. and Spanjer, W. (1986) Chemistry and pharmacology of solitary wasp venoms. In: Venoms of the Hymenoptera (T. Piek, ed.) pp. 161–307. Academic Press, London.

13 Shinozaki, H. and Ishida, M. (1986) A new potent channel blocker: Effects on glutamate responses at the crayfish neuromuscular junction. Brain Res. 372, 260–268.

14 Piek, T. and Spanjer, W. (1978) Effects of chemical characterization of some paralysing venoms of solitary wasps. In: Pesticide and Venom Neurotoxicity (D.L. Shankland et al., eds.). Plenum Press, New York.

15 Nibbering, N.M.M. (1982) Survey of ionization methods with emphasis on liquid chromatography-mass spectrometry. J. Chromatogr. 251, 93–104.

16 McLafferty, F.W. (1981) Tandem mass spectrometry. Science 214, 280–287.

17 Aramaki, Y., Yasuhara, T., Shimazaki, K., Kawai, N. and Nakajima, T. (1987) Chemical structure of Joro spider toxin (JSTX) Biomed. Res. 8, 241–245.

18 Hashimoto, Y., Endo, Y., Shudo, K., Aramaki, Y., Kawai, N. and Nakajima, T. (1987) Synthesis of spider toxin (JSTX-3) and its analogs. Tetrahedron Lett. 28, 3511–3514.

19 Teshima, T., Wakamiya, T., Aramaki, Y., Nakajima, T., Kawai, N. and Shiba,T. (1987) Synthesis of a new neurotoxin NSTX-3 of Papua New Guinean spider. Tetrahedron Lett. 28, 3509–3510.

20 Masaki, M., Morito, N., Hashimoto, K. and Shinozaki, H. (1985) Synthesis of new glutamate inhibitors. J. Pharmac. Dyn. 8, S 173.

21 Kopriwa, B.M. (1973) A reliable standardized method for ultrastructural microscopic radiography. Histochemie 37, 1–17.

22 Van Marle, J., Piek, T., Lind, A. and Van Weeren-K amer, J. (1983) Localization of a Na⁺-dependent uptake system for glutamate in excitatory neuromuscular junctions of the locust *Schistocerca gregaria*. Comp. Biochem., Physiol. 74C, 191–194.

23 Van Marle, J., Piek, T., Lammertse, T., Lind, A. and Van Weeren-Kramer, J (1985) Selectivity of the uptake of glutamate and GABA in two morphologically distinct insect neuromuscular synapses. Brain Res. 348, 107–111.

24 Van Marle, J., Piek, T. and Veldsema-Currie, R.D. (1986) Presynaptic, high-affinity glutamate uptake in excitatory neuromuscular junctions of the retractor unguis muscle of the locust: determination of the K_m value using high resolution autoradiography. Exp. Brain Res. 62, 25–28.

76

25 Pan-Hou, H., Suda, Y., Sumi, M., Yoshioka, M. and Kawai, N. (1987) Inhibitory effect of 2,4-dihydroxyphenylacetylasparagine, a common moeity of spider toxin, on glutamate binding to rat brain synaptic membranes. Neurosci. Lett. 81, 199–203.
26 Pan-Hou, H. and Suda, Y. (1987) Molecular action mechanism of spider toxin on glutamate receptor: role of 2,4-dihydroxyphenylacetic acid in toxin molecule. Brain Res. 418, 198–200.
27 Usherwood, P.N.R., Duce, I.R. and Boden, P. (1984) Slowly-reversible block of glutamate receptor-channels by venoms of the spiders *Argiope trifasciata* and *Araneus gemma*. J. Physiol. (Paris) 79, 241–245.
28 Miwa, A., Kawai, N., Saito, M., Pan-Hou, H. and Yoshioka, M. (1987) Effect of a spider toxin (JSTX) on excitatory postsynaptic current at neuromuscular synapse of spiny lobster. J. Neurophysiol. 58, 319–325.
29 Masaki, M. and Shinozaki, H. (1986) A new class of potent centrally acting muscle relaxants: pharmacology of oxazolidinones in rat decerebrate rigidity. Br. J. Pharmacol. 89, 219–228.

CHAPTER 6

Animal toxins of low molecular mass

T. Nakajima[1], T. Yasuhara[1] and N. Kawai[2]

[1] Department of Analytical Chemistry, Faculty of Pharmaceutical Sciences, University of Tokyo, Bunkyo-ku, Tokyo, 113, Japan and [2] Department of Neurophysiology, Tokyo Metropolitan Institute for Neurosciences, Musashidai, Fuchu, 183 Japan

Introduction

Non-mammals utilize many kinds of materials as venoms, toxins or repellents for protecting them from the predators, or as a tool for preying on their victims. The chemical nature of venomous components covers a wide array of compounds such as hydrocarbon-like terpenes, steroids, fatty acids etc., or nitrogenous compounds like alkaloids, amines, amino acids, peptides and proteins including enzymes. Some such venomous components are known to be analogous or homologous in mammalian species where they act as hormones, autocoids or transmitters. Thus the venoms often affect cells and tissues by modulating the normal functions of cellular membranes. Some novel toxic components of low molecular mass have been characterized from non-mammals in the Far East.

Novel cardiac steroids in the snake

The snake belonging to the genus *Rhabdophis* has a pair of special glands, nuchdosal glands, along the neck. The material in these glands was reported to cause severe injury when splashed into eyes by careless handling of the snake or by beating the snake's neck with a club. The glandular materials were analysed chemically and were found to contain novel cardiac steroids (Fig. 1). It is well known that bufonid toads contain cardiac steroids in the prominent parotid gland located behind the eyes. The cardiac steroids in the snake are different from those in toads, and occur in a non-conjugated form in the glands and are characteristically tetrahydroxylated constituents i.e. 3, 5, 11, 14; 3, 7, 11, 14 or 3, 5, 14, 16, respectively. A trihydroxylated cardiac steroid, gamabufotalin is also present. Some snake cardiac steroids are as potent as ouabain in the positive inotropic action on the guinea pig papillary muscle.

Novel cytotrophic peptides in wasp venom

The social wasps commonly contain two series of hydrophobic peptide families in addition to waspkinin as the main venom peptides. One group is the histamine-re-

78
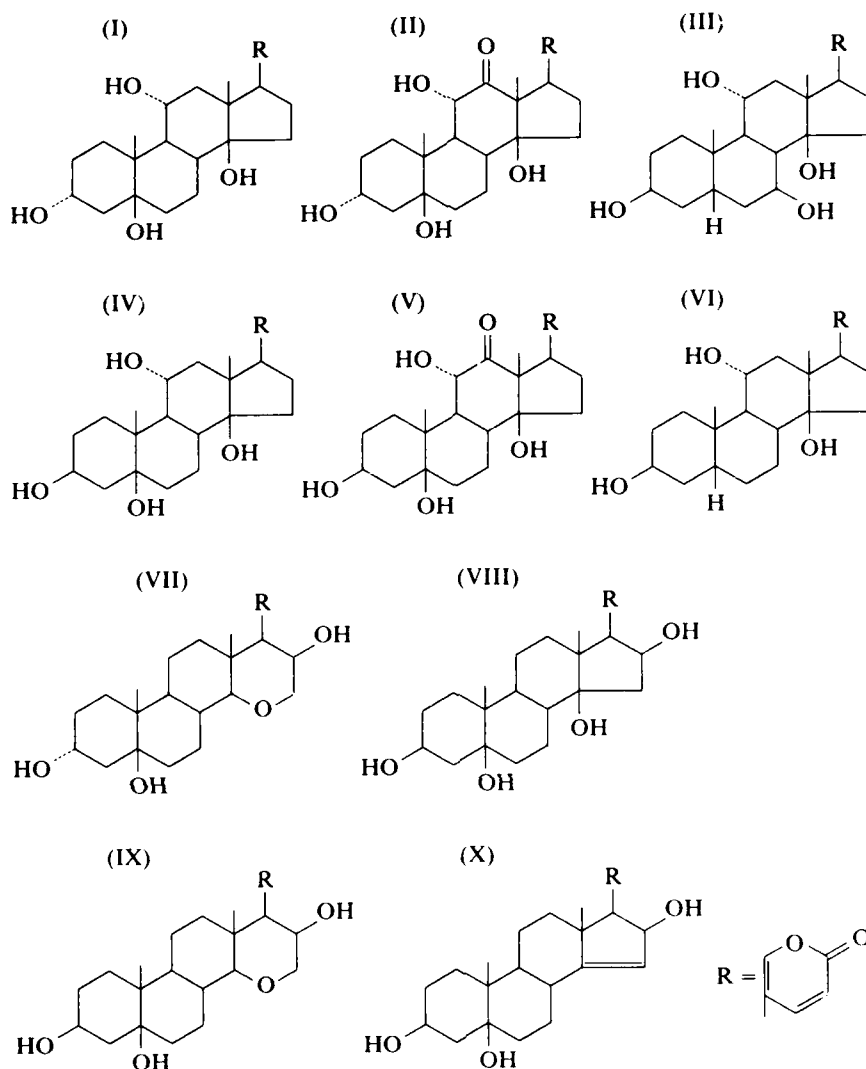
FIG 1   Cardiac stroids in the nuchodosal glands of the snake. *Rhabdophis tigrinus*.

leasing peptides, called mastoparans, and the others are vespid chemotactic peptides. Both families of peptides are composed of hydrophobic amino acids and basic amino acids (Table 1). Among these peptides, mastoparan shows a variety of biological actions in addition to mast cell degranulation and histamine release. Mastoparan acts on adrenal chromaffin cells and on platelets to release catecholamines and serotonin respectively, and also releases prolactin from pituitary cells. It was also reported that mastoparan bound to calmodulin in the presence of Ca^{2+} with very high affinity and inhibited calmodulin-sensitive enzymes such as phosphodiesterase. Mastoparan activates membrane-bound phospholipase A_2. Recently mastoparan was found to be a direct activator of GTP-binding protein without any

TABLE 1 Hydrophobic peptide families in wasp venom

Species	Amino Acid Sequence	Nomenclature
Paravespula lewisii	Ile-Asn-Leu-Lys-Ala-Leu-Ala-Ala-Leu-Ala-Lys-Lys-Ile-Leu-NH$_2$	mastoparan
Vespa mandarinia	Ile-Asn-Leu-Lys-Ala-Ile-Ala-Ala-Leu-Ala-Lys-Lys-Leu-Leu-NH$_2$	mastoparan-M
Vespa tropica	Ile-Asn-Leu-Lys-Ala-Ile-Ala-Ala-Phe-Ala-Lys-Lys-Leu-Leu-NH$_2$	mastoparan-T
Vespa orientalis	Ile-Asn-Leu-Lys-Ala-Ile-Ala-Ala-Leu-Val-Lys-Lys-Ala-Leu-NH$_2$	mastoparan-II
Vespa crabro	Ile-Asn-Leu-Lys-Ala-Leu-Ala-Val-Ala-Lys-Lys-Ile-Leu-NH$_2$	mastoparan-C
Vespa xanthoptera	Ile-Asn-Trp-Lys-Gly-Ile-Ala-Ala-Met-Ala-Lys-Lys-Leu-Leu-NH$_2$	mastoparan-X
Vespa analis	Ile-Lys-Trp-Lys-Ala-Ile-Leu-Asp-Ala-Val-Lys-Lys-Val-Ile-NH$_2$	mastoparan-A
Polistes jadwigae	Val-Asp-Trp-Lys-Lys-Ile-Gly-Gln-His-Ile-Leu-Ser-Val-Leu-NH$_2$	polistes mastoparan
Vespa tropica	Phe-Leu-Pro-Ile-Leu-Gly-Lys-Ile-Leu-Gly-Gly-Leu-Leu-NH$_2$	Ves-CP-T
Vespa mandarinia	Phe-Leu-Pro-Ile-Ile-Gly-Lys-Leu-Leu-Ser-Gly-Leu-Leu-NH$_2$	Ves-CP-M
Vespa analis	Phe-Leu-Pro-Met-Ile-Ala-Lys-Leu-Leu-Gly-Gly-Leu-Leu-NH$_2$	Ves-CP-A
Vespa xanthoptera	Phe-Leu-Pro-Ile-Ile-Ala-Lys-Leu-Leu-Gly-Gly-Leu-Leu-NH$_2$	Ves-CP-X
Vespa crabro	Phe-Leu-Pro-Leu-Ile-Leu-Arg-Lys-Ile-Val-Thr-Ala-Leu-NH$_2$	crabrolin
Vespa orientalis	Phe-Leu-Pro-Leu-Ile-Leu-Gly-Lys-Lys-Val-Lys-Gly-Leu-Leu-NH$_2$	HR-II
Paravespula lewisii	Phe-Leu-Pro-Leu-Ile-Ala-Lys-Leu-Val-Ser-Gly-Leu-Leu-NH$_2$	Ves-CP-L
Ropalidia sp.	Ile-Val-Pro-Phe-Leu-Gly-Pro-Leu-Leu-Gly-Leu-Leu-Thr-NH$_2$	Icaria-CP

$CH_2CONHCHCONHCHCONH(CH_2)_5NHCO(CH_2)_2NH(CH_2)_4NHCO(CH_2)_4NH(CH_2)_4NH_2$

Nephilatoxin-7

$CH_2CONHCHCONH(CH_2)_5NHCO(CH_2)_2NH(CH_2)_4NH(CH_2)_3NH_2$

Nephilatoxin-8

$CH_2CONHCHCONH(CH_2)_5NHCOCHNHCOCH(CH_2)_3NHCNH_2$

Nephilatoxin-9

$CH_2CONHCHCONH(CH_2)_5NHCO(CH_2)_2NH(CH_2)_4NH(CH_2)_3NH_2$

JSTX-3

$CH_2CONHCHCONH(CH_2)_5NHCO(CH_2)_2NH(CH_2)_4NHCOCH(CH_2)_3NHCNH_2$

NSTX-3
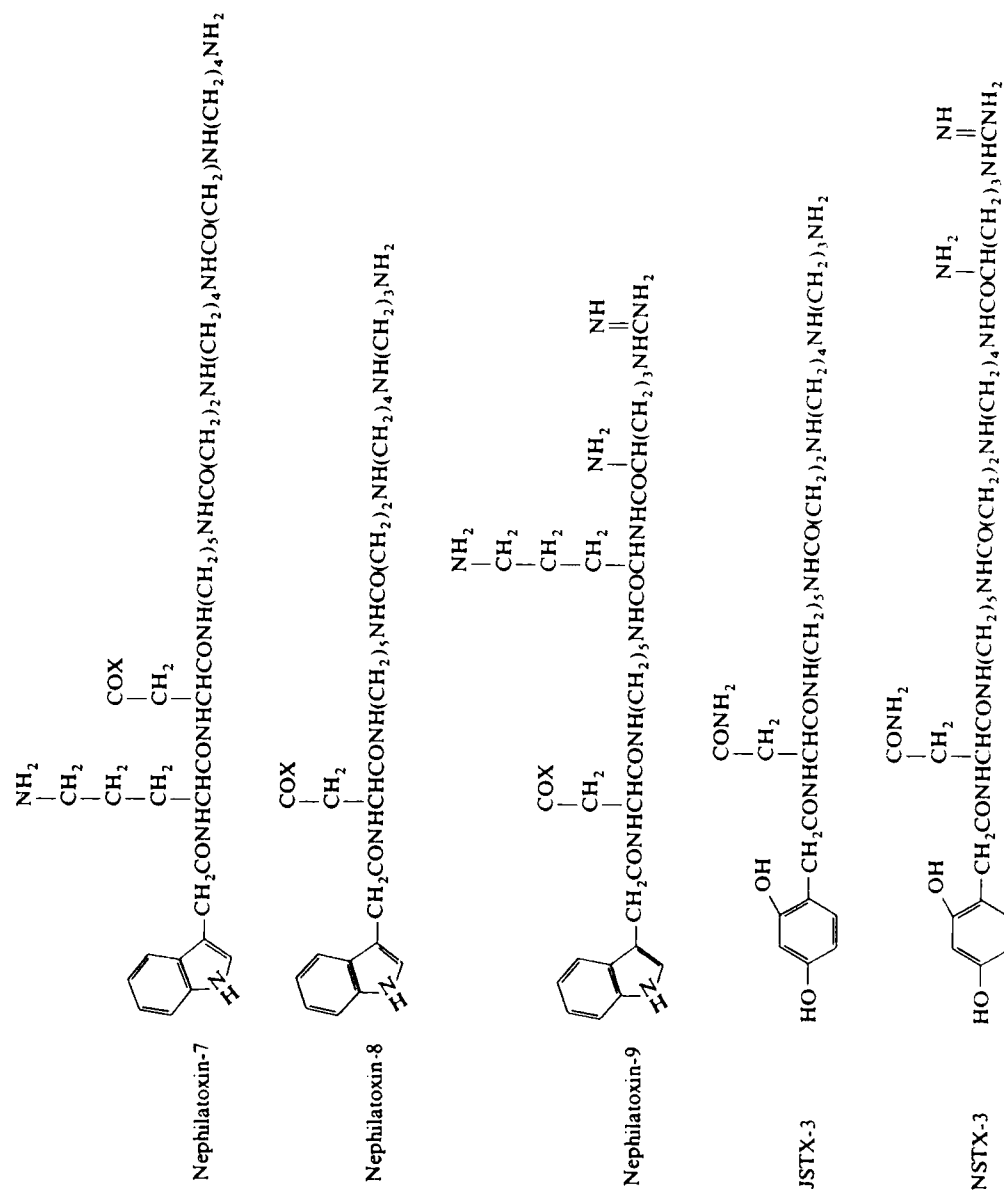
FIG 2 Chemical structures of some spider toxin isolated from the spider belonging to the genus *Nephila*

receptor activation. Vespid chemotactic peptide is a tridecapeptide amide which causes chemotaxis for polymorphonuclear leucocytes and macrophages. A transient elevation of intracellular Ca^{2+} and generation of active oxygen have been observed in neutrophils when the cells are treated with the peptides. Unlike mastoparan, the peptide does not affect a GTP-binding protein but interacts directly with the FMLP receptor in the neutrophils.

Novel neurotoxins in the spider, genus *Nephila*

Spider toxin obtained from the venom of the spider belonging to the genus *Nephila* has been recognized as a new neurotoxin which suppresses irreversibly the excitatory postsynaptic potential and the glutamate potential in the lobster neuromuscular junction with a high degree of specificity. The toxic principles from the venom of *Nephila clavata* (JSTX) and from *Nephila maculata* (NSTX) were found to be composed of many kinds of structurally similar compounds. Some of these toxins were identified chemically and have a common structural core composed of a

POLYCATIONIC CHAIN
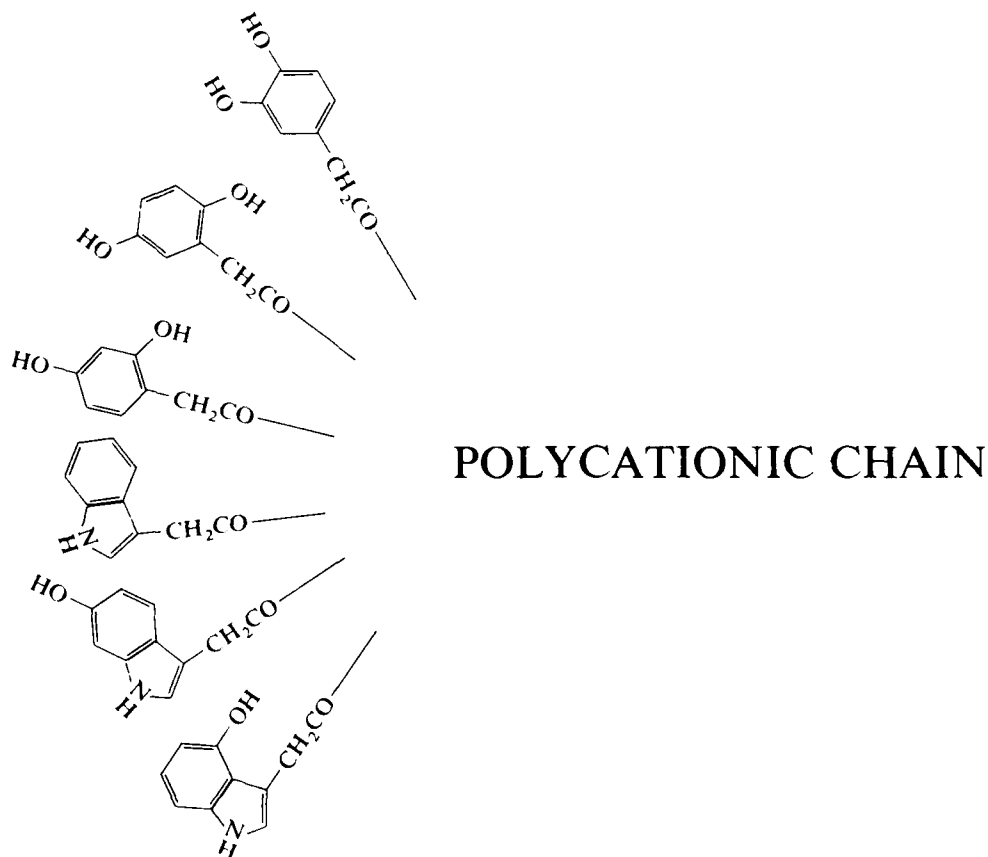
FIG 3 General structures showing glutamate blocking action on the lobster leg.

2,4-dihydroxyphenylacetyl-asparaginyl-cadverinoethylamino-derivative. In addition to these types of neurotoxin, a different series of toxins (Nephilatoxins) which possesses an indoleacetic acid moiety instead of 2,4-dihydroxyphenylacetyl moiety, has also been found in the venom of *Nephila clavata*. Some of these structures are illustrated in Fig. 2.

Two toxins (JSTX-3, NSTX-3) and the related compounds were chemically synthesized and the structure–activity relationships were investigated. The polycationic part lacking the 2,4-dihydroxyphenylacetyl moiety did not show neurotoxic activity, whereas the common moiety, 2,4-dihydroxyphenylacetyl asparaginyl cadaverin and 2,4-dihydroxyphenylacetyl asparaginyl spermine suppressed the excitatory postsynaptic potentials in a similar manner to natural spider toxin (JSTX-3). While the effect of JSTX was irreversible, the synthetic toxins were irreversible. Combined results obtained from the other synthetic materials lead us to the tentative conclusion that compounds which show neurotoxic activity all have the common structure as shown in Fig. 3. Using synthetic analogues we are currently carrying out conformational analysis and we are investigating the details of structure–activity relationships and the possible mechanism of the toxin as a glutamate receptor blocker.

References

1 Akizawa, T., Yasuhara, T., Kano, R. and Nakajima, T. (1985) Biomed. Res. 6, 437–441.
2 Nakajima, T. (1986) In: Venoms of Hymenoptera (T. Piek, ed.) pp. 309–327 Academic Press, London.
3 Malencik, D.A. and Anderson, S.R. (1983) Biochem. Biophys. Res. Commun. 114, 50–56.
4 Argiolas, A. and Pisano, J.J. (1983) J. Biol. Chem. 258, 13697–13702.
5 Higashijima, T., Uzu, S., Nakajima, T. and Ross, E.M. (1988) J. Biol. Chem. 263, 6491–6494.
6 Koike, M., Yasuhara, T., Nakajima, T., Higashijima, T., Miyazawa, T., Kitada, C., Fujino, M. and Tsukamoto, Y. (1987) Peptide Chemistry, 63–68.
7 Kawai, N., Niwa, A. and Abe, T. (1982) Brain Res. 3, 353–355.
8 Aramaki, Y., Yasuhara, T., Higashijima, T., Yoshioka, M., Miwa, A., Kawai, N. and Nakajima, T. (1986) Proc. Japan Acad., Ser. B. 62, 359–362.
9 Toki, T., Yasuhara, T., Aramaki, Y., Kawai, N. and Nakajima, T. (1988) Biomed. Res., 9, 75–79.
10 Shudo, K., Endo, Y., Hashimoto, Y., Aramaki, Y., Nakajima, T. and Kawai, N. (1987) Neorosci. Res. 5, 82–85.

CHAPTER 7

Purification of an inhibitor of brain synaptic membrane glutamate binding sites from the venom of the spider *Araneus gemma*

Elias K. Michaelis, Vinh Thai, Sumita Gosh, Sherrell L. Early
and Charles Decedue

*Department of Biochemistry and Pharmacology and the Center for Biomedical
Research, University of Kansas, Lawrence, KS 66046, U.S.A.*

Introduction

L-Glutamic acid is the most widespread excitatory neurotransmitter in the mammalian central nervous system [1]. An important goal in current neurobiological investigations is to identify and isolate selective inhibitors that may be used to probe the receptors for the excitatory amino acid neurotransmitters L-glutamic acid and L-aspartic acid. There is substantial evidence that L-glutamate is the excitatory neurotransmitter at insect neuromuscular junctions [2], therefore, logical sources of an L-glutamate antagonist are the venoms from wasps and arachnids which prey on insects.

Inhibitory effects of venoms from *Nephila clavata* and *Araneus ventricosus* on glutamate-activated synapses at neuromuscular junctions in invertebrates and in vertebrate central nervous system neurons were reported first by Kawai and colleagues [3–7]. These initial reports were soon followed by repeated demonstrations that the venoms of other orb-weaving spider species such as *Argiope trifasciata* and *Araneus gemma* also contained inhibitors of insect muscle glutamate receptors [8,9] and of vertebrate glutamate-sensitive excitatory transmission [10].

In our studies, we sought to determine whether spider venoms contain components that interact directly with glutamate receptor-associated macromolecules and to identify these venom components. The approach that we have followed is to measure venom-induced inhibition of L-glutamate binding to synaptic membranes isolated from rat brain neurons. L-Glutamate binding sites in isolated plasma membranes from the synaptic region of brain neurons are thought to represent the recognition sites of physiologic receptors with which L-glutamic acid interacts to bring about neuronal excitation (e.g. Refs. 11–14). Therefore measurement of the interaction of the venoms with these glutamate-binding sites may be a very general approach to detect venom effects on L-glutamate receptors.

Venom interaction with plasma membranes in a manner that alters the supramolecular structure of the membranes could affect indirectly L-[^{3}H]glutamate binding

to the recognition macromolecules embedded in these membranes. In addition, the presence of free amino acids, such as L-glutamic or L-aspartic acid, in venom extracts may have a strong 'inhibitory' effect on L-glutamate binding to its recognition sites in synaptic membranes. In order to address the first issue, i.e., a venom effect on membrane structure that indirectly alters glutamate binding activity, we performed all our studies using two preparations to measure L-glutamate interaction with putative receptor sites: glutamate binding to synaptic membranes and glutamate binding to a purified glutamate-binding protein [15]. This glutamate-binding protein has been isolated from synaptic plasma membranes and retains ligand binding characteristics similar to some of the glutamate binding sites in synaptic membranes [16–18]. In order to explore the second potential confounding effect of venom constituents on glutamate binding sites, i.e., the presence of free amino acids that may compete with L-[^{3}H]glutamate binding, we undertook chemical analyses of the one spider venom that had the highest inhibitory activity against L-glutamate binding to synaptic membranes and the isolated binding protein [19].

Spider venom inhibition of L-glutamate binding

The venoms from three spider species were found to inhibit L-[^{3}H]glutamate binding to rat brain synaptic membranes and to the isolated glutamate-binding protein [15]. These venoms were obtained by a milking procedure from the venom glands of *Araneus gemma, Neoscona arabesca*, and *Argiope aurantia*. Venom from *Araneus gemma* had the highest inhibitory activity per unit volume and also caused the most rapid inhibition of L-glutamate binding to the purified protein. The venom from *Argiope aurantia* had the weakest inhibition per unit volume and exhibited relatively slow kinetics of inhibition of L-glutamate binding to the isolated binding protein. Nearly identical effects were observed also by measuring L-glutamate binding to synaptic membranes. Finally, we showed that inhibition of glutamate binding to synaptic membranes by both the venom from *Araneus gemma* and *Neoscona arabesca* were completely reversible following washing and dilution, but that such reversal to baseline binding activity required 150–210 min.

The observations made with regard to reversibility of venom inhibition of L-glutamate binding fit well with physiological observations of slow recovery of glutamate-induced responses in insect muscle following wash-out of *Araneus gemma* venom [8]. However, results obtained from either ligand binding studies or physiological measurements of responses to L-glutamate and related analogs may not be that easy to analyse and interpret if the venom constituents include high concentrations of L-glutamic or L-aspartic acid. These amino acids would, of course, cause rapid and reversible inhibition of L-[^{3}H]glutamate binding in ligand binding studies and they may produce receptor desensitization in physiological studies. Desensitization in physiological glutamate receptor responses has recently been described as part of the action of *Araneus gemma* venom on central nervous system neurons [20].

Amino acids, biogenic amines and proteins in *Araneus gemma* venom

The suspicion that some of the spider venoms may contain high concentrations of free amino acids was confirmed by our studies of the composition of the venom

from *Araneus gemma* [19]. Different batches of the milked venom from this spider species had free glutamate concentrations ranging between 180 and 425 mM (average 273 mM). The fact that this free glutamate in the venom was the L-enantiomer of glutamate was documented by titrating the L-glutamate-specific transport activity in synaptic membranes and demonstrating that the estimated concentration of free glutamate in venom matched within 10% or less the effects of authentic L-glutamic acid added to these transport assays.

Few other free amino acids were detected in the venom (aspartic acid, serine and cysteine) and their concentrations were equal to or less than 1.3 mM [19]. In addition, very low concentrations of free biogenic amines and catechols were detected (0.04-0.9 nM). Four catecholamines and metabolites were identified: epinephrine, epinine, dopamine and 3,4-dihydroxyphenylacetic acid. Finally, the venom from *Araneus gemma* has one other constituent besides glutamate at very high concentrations, that is, proteins or peptides. The estimated concentration of proteins varies between 200 and 400 mg/ml in different batches of the venom.

The studies on the chemical characterization of the venom from *Araneus gemma* were undertaken as part of our effort to identify the inhibitor or inhibitors of glutamate receptors which are present in this venom. We considered it very important to know the constituents of the venom prior to initiation of the purification and identification of the receptor inhibitors. It is important to understand the possible contribution of these substances to the physiological actions of the venom and also to select the most appropriate procedures for further purification of the inhibitory substances.

Progress in purification of inhibitors of L-glutamate receptors

The observation that large quantities of apparently free glutamate were present in the milked venom was indicative that, at least to some extent, the inhibition of glutamate binding to synaptic membranes and the purified glutamate binding protein was due to competition of non-radioactive glutamate with L-[^{3}H]glutamate for binding to those sites. Our most recent efforts have been centred on the identification of the venom components, other than free L-glutamate, which may inhibit the binding or activation of receptors by L-glutamate. Using an intact neuronal tissue preparation, the caudate nucleus of the anesthetized rat, we were able to show that whereas L-glutamate applied by pressure ejection causes a rapid rise in the extracellular K$^+$ concentration measured by ion-selective electrodes [21], the application of milked *Araneus gemma* venom not only did not produce such K$^+$ flux, but, it also inhibited the effects of L-glutamic acid on both field potentials and K$^+$ efflux [22]. These observations indicated that despite the presence of free L-glutamate in the milked venom, some other component must also be present which prevents the activation of glutamate receptors by this amino acid. In order to identify this inhibitor of glutamate receptors we have followed the approach described below.

The milked venom samples have been subjected to reverse phase high performance liquid chromatography (HPLC) on Ultrasphere C18 columns using an acetic acid-ammonium phosphate-acetonitrile gradient. A one minute collection period was used to obtain fractions eluted from the HPLC and these fractions were tested for their inhibition of glutamate binding to purified binding protein and to synaptic

membranes. Two peaks of inhibition of glutamate binding have been detected by both procedures, one centred between fractions 2 and 5 and the other between fractions 9 and 12. The elution pattern was monitored at 278 nm and only fractions 9-12 corresponded to a peak of eluted material detectable at this wavelength. The fractions 2-5 were lyophilized, resuspended, and analysed by high performance thin layer chromatography (HPTLC) according to the procedures described by Early and Michaelis [19]. They were found to contain large quantities of glutamate with no detectable other amino acids or proteins. Fractions 8-12 have been analysed in a similar fashion and were found to contain small amounts of glutamate together with other unidentified constituents which react with chlorine-benzidine reagent [23] to give blue spots in HPTLC plates. A particularly consistent spot is one that has an R_f of 0.44-0.47.

The pooled fractions 8-15 were subjected to ion exchange chromatography on Dowex-1, acetate form. All of the detectable glutamate on HPTLC plates is removed by this ion exchange chromatography step, and the material that migrates on HPTLC with an R_f of 0.44 is eluted in the initial wash with H_2O. This material exhibits good inhibitory activity towards glutamate binding, causing greater than 80% inhibition at dilutions of the lyophilized material approximately equal to those of the HPLC fractions 8-12. We have lyophilized this material, rechromatographed it through Dowex-50 cation exchange columns and have found that the substance with R_f 0.44 is is retained by the Dowex-50 and can be eluted by either 0.1 M ammonium hydroxide or potassium hydroxide. The material that migrates in HPTLC plates with an $R_f = 0.44$ stained by the Sakaguchi reagent which indicates the presence of an arginine residue. This substance retains its inhibitory activity against glutamate binding to synaptic membranes, producing inhibition of 73-80% when diluted to the same relative volume as the original pooled fractions from the HPLC.

The material eluted from the Dowex-50 columns was neutralized, lyophilized, and subjected to reverse phase HPLC analysis on Ultrasphere C18 columns using an acetonitrile: water : triethylammonium formate gradient. Most of the eluted material was in two closely eluting peaks at ~ 3 min. This fraction was resuspended in water following lyophilization and rechromatographed on the same HPLC column with a slowly developing acetonitrile gradient. Two major peaks were resolved, but only one of these peaks inhibited L-glutamate binding to synaptic membranes and the purified protein. There was no detectable free L-glutamate in this peak with inhibitory activity as was ascertained by HPTLC and nuclear magnetic resonance techniques. We have performed UV spectral analyses of this fraction and have identified three absorbance peaks. The largest peak is at 198 nm, followed by one at 224 nm and finally a small peak at 275 nm. The other HPLC fractions did not have any distinct absorbance peaks. Examination of the fractions obtained from the HPLC by means of sodium dodecyl sulfate polyacrylamide gel electrophoresis did not reveal any proteins in the range of molecular weights between 3 and 43 kDa.

Conclusions

The observations described above are indicative of the presence of small molecular weight, basic components in the venom of *Araneus gemma* which inhibit L-[³H]glutamic acid binding to synaptic plasma membranes and to the purified

glutamate-binding protein. These active substances can be separated from free L-[^{3}H]glutamic acid by sequential HPLC and ion exchange chromatography procedures. Although we have not achieved complete chemical identification of the compounds that inhibit L-glutamate binding to glutamate receptor sites on central nervous system neurons, we have preliminary indications that this substance contains an arginine residue and a chromophoric group that may be similar to either tyrosine or tryptophan.

Investigators from several laboratories have reported on the chemical analysis and identification of the glutamate receptor inhibitor in the venoms of *Argiope lobata* [24], *Nephila maculata* and *Nephila clavata* [25], and *Argiope aurantia* [26]. The structure of these active venom components consists of a polyamine linked to an asparagine whose NH$_2$ group is in amide linkage with either 2,4-dihydroxyphenylacetic acid or 4-hydroxyindole-3-acetic acid. Some of these active compounds also contain a terminal arginine. The dihydroxyphenylacetic acid or the hydroxyindoleacetic acid are the chromophoric species in these molecules. It is possible that the material we have isolated has a similar chemical structure to those reported for other venom glutamate receptor inhibitors, but we have not yet established the structural characteristics of the venom compounds that we have isolated.

Summary

The procedures used to isolate components of *Araneus gemma* venom that interact directly with glutamate receptor ligand recognition sites are described in this paper. Chemical analysis of this venom was indicative of very high concentrations of free L-glutamate. Chromatographic procedures were developed to separate an inhibitor of glutamate recognition sites of both synaptic plasma membranes and a purified glutamate binding protein. The inhibitory fraction contained a chromophore with maximum absorbance at 275 nm, secondary amine structure and an arginine residue. Exact chemical characterization of this material has not yet been obtained.

Acknowledgements

References

1 Curtis, D.R. and Johnston, G.A.R. (1974) Amino acid transmitters in the mammalian central nervous system. Ergeb. Physiol. 69, 97–188.
2 Usherwood, P.N.R. (1981) Glutamate synapses and receptors on insect muscle. In: Glutamate as a Neurotransmitter (G. Dichiara and G.L. Gessa, eds.) p. 183. Raven Press, New York.

3 Kawai, N., Niwa, A. and Abe, T. (1982) Spider venom contains specific receptor blocker of glutaminergic synapses. Brain Res. 24, 169–171.

4 Kawai, N., Niwa, A. and Abe, T. (1982) Effect of a spider toxin on glutaminergic synapses in the mammalian brain. Brain Res. 3, 353–355.

5 Kawai, N., Niwa, A. and Abe, T. (1983) Specific antagonism of the glutamate receptor by an extract from the venom of the spider Araneus ventricosus. Toxicon 21, 438–440.

6 Kawai, N., Niwa, A., Saito, M., Pan-Hou, H.S. and Yoshioka, M. (1984) Spider toxin (JSTS) on the glutamate synapse. J. Physiol. (Paris) 79, 228–231.

7 Abe, T., Kawai, N. and Niwa, A. (1983) Effects of a spider toxin on the glutaminergic synapse of lobster muscle. J. Physiol (Lond.) 339, 243–252.

8 Usherwood, P.N.R., Duce, I.R. and Boden, P. (1984) Slowly reversible block of glutamate receptor-channels by venoms of the spiders, Argiope trifasciata and Araneus gemma. J. Physiol. (Paris) 79, 241–245.

9 Bateman, A., Boden, P., Dell, A., Duce, I.R., Quicke, D.L.J. and Usherwood, P.N.R. (1985) Postsynaptic block of a glutaminergic synapse by low molecular weight fraction of spider venom. Brain Res. 339, 237–244.

10 Jackson, H., Urnes, M., Gray, W.R. and Parks, T.N. (1987) Effects of spider venoms on transmission mediated by non-N-methyl-D-aspartate receptors in the avian cochlear nucleus. In: Excitatory Amino Acid Transmission (T.P. Hick, D. Lodge and H. McLennan, eds.), pp. 51–54. Alan R. Liss, New York.

11 Foster, A.C. and Roberts, P.J. (1978) High affinity L-[^{3}H]glutamate binding to post-synaptic receptor sites on rat cerebellar membranes. J. Neurochem. 31, 1467–1477.

12 Michaelis, E.K., Michaelis, M.L., Grubbs, R.D. and Kuonen, D.R. (1981) Molecular characteristics of glutamate receptors in the mammalian brain. Mol. Cell. Biochem. 38, 163–179.

13 Foster, A.C., Mena, E.E., Fagg, G.E. and Cotman, C.W. (1981) Glutamate and aspartate binding sites are enriched in synaptic junctions isolated from rat brain. J. Neurosci. 1, 620–625.

14 Fagg, G.E. and Foster, A.C. (1984) Acidic amino acid binding sites in mammalian neuronal membranes: their characteristics and relationship to synaptic receptors. Brain Res. Rev. 7, 103–164.

15 Michaelis, E.K., Galton, N. and Early, S.L. (1984) Spider venoms inhibit L-glutamate binding to brain synaptic membrane receptors. Proc. Natl. Acad. Sci. U.S.A. 81, 5571–5574.

16 Michaelis, E.K. (1975) Partial purification and characterization of a glutamate-binding membrane glycoprotein from rat brain. Biochem. Biophys. Res. Commun. 65, 1004–1012.

17 Michaelis, E.K., Michaelis, M.L., Stormann, T.M., Chittenden, W.L. and Grubbs, R.D. (1983) Purification and molecular characterization of the brain synaptic membrane glutamate-binding protein. J. Neurochem. 40, 1742–1753.

18 Chen, J.-W., Cunningham, M.D., Galton, N. and Michaelis, E.K. (1988) Immune labeling and purification of a 71-kDa glutamate-binding protein from brain synaptic membranes. J. Biol. Chem. 263, 417–426.

19 Early, S.L. and Michaelis, E.K. (1987) Presence of proteins and glutamate as major constituents of the venom of the spider Araneus gemma. Toxicon 25, 433–442.

20 Vyklicky, L., Jr., Krusek, J., Vyklicky, L. and Vyskocil, F. (1986) Spider venom of Araneus opens and desensitizes glutamate channels in chick spinal cord neurones. Neurosci. Lett. 68, 227–231.

21 Nagy, G., Moghaddam, B. and Adams, R.H. (1985) Simultaneous monitoring of voltammetric and ion selective electrodes in mammalian brains. Neurosci. Lett. 55, 151–155.

22 Early, S.L. (1984) Characterization of the venom from the spider Araneus gemma: Search for a glutamate antagonist. Ph.D Dissertation, University of Kansas.

23 Bischel, M.D. and Austin, J.H. (1963) A modified benzidine method for the chromatographic detection of sphingolipids and acid polysaccharides. Biochim. Biophys. Acta 70 598–600.

24 Grishin, E.V., Volkova, T.M., Arseniev, A.S., Reshetova, O.S., Onoprienko, V.V., Mag-
azanic, L.G., Antonov, S.M. and Fedorova, I.M. (1986) Structure-functional characteriza-
tion of argiopine – an ion channel blocker from the venom of spider *Argiope Lobata*.
Bioorgan. Chem. 12, 1121–1124.

25 Aramaki, Y., Yasuhara, T., Higashijima, T., Yoshioka, M., Miwa, A., Kawai, N. and
Nakajima, T. (1986) Chemical characterization of spider toxin, JSTX and NSTX. Proc.
Jpn. Acad. 62, 359–362.

26 Adams, M.E., Carney, R.L., Enderlin, F.E., Fu, E.T., Jarema, M.A., Li, J.P., Miller, C.A.,
Schooley, D.A., Shapiro, M.J. and Venema, V.J. (1987) Structures and Biological activities
of three synaptic antagonists from orb weaver spider venom. Biochem. Biophys. Res.
Commun. 148, 678–683.

91

CHAPTER 8

Novel excitatory amino acid related compounds of natural origin

H. SHINOZAKI AND M. ISHIDA

The Tokyo Metropolitan Institute of Medical Science, 3-18-22, Honkomagome, Bunkyo-ku, Tokyo 113, Japan

Introduction

In the history of neuroscience research, naturally occurring substances have played an important role as valuable pharmacological tools. The potentially valuable excitatory amino acids, such as kainic acid [1–3], ibotenic acid [4], quisqualic acid [3,5] and domoic acid [6], are natural products related structurally to glutamate, and share with them both neuroexcitatory and neurotoxic properties [7]. A neurotoxic amino acid, β-N-oxalyl-L-α,β-diaminopropionate (β-ODAP), found in seeds of *Lathyrus sativus* [8], and willardiine [9] are also known as potent excitants, and some compounds isolated from venoms have been spotlighted as an inhibitor of excitatory amino acids [10,11]. In the course of our neuropharmacological studies on excitatory amino acids, theanine, matrine and tuberostemonine, which were all naturally occurring substances, were found to be useful as pharmacological tools in the field of neuroscience [12–14]. In addition to these compounds, we recently found profoundly interesting actions of two novel amino acids of natural origin [15,16]. One of them is acromelic acid and the other is stizolobic acid (Fig. 1).

Acromelic acid A and B were isolated in 1983 from the Japanese poisonous mushroom, *Clitocybe acromelalga*, by Shirahama and his colleagues [17]. The erroneous ingestion of the poisonous mushroom causes a sharp pain and a marked reddish edema (erythromelalgia) in the hand and foot about a week later, which continue for about a month. The mechanism of its toxic action is not yet known although its neurological symptoms are of great interest. Shirahama and his colleagues succeeded in the isolation of acromelic acid A and B from the mushroom, and designed a method for the chemical synthesis of acromelic acid to confirm its proposed chemical structure [17,18]. Acromelic acid is one of the biologically active kainoids which possess a constitutional moiety of kainic acid. Kainoids possess four characteristic neuropharmacological properties; (1) a depolarizing action on the mammalian central neurones and invertebrate muscles, (2) potentiation of the glutamate response in invertebrates and vertebrates, (3) inhibitory action on the response to quisqualate in invertebrates and (4) neuronal death. Kainic acid is not

92

HOOC—[N(H)=O ring]—CH₂COOH / COOH structure
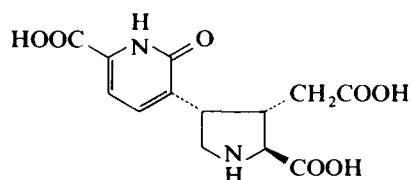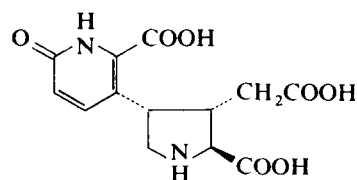
Acromelic acid A

Acromelic acid B
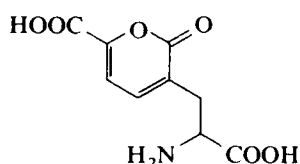
Stizolobinic acid
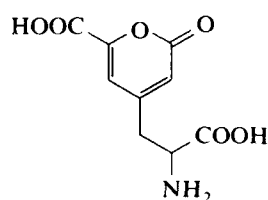
Stizolobic acid

FIG 1 Chemical structure of acromelic acid A and B, stizolobic acid and stizolobinic acid.

particularly active on the invertebrate muscle as a depolarizant [2,6], in spite of the fact that it causes a marked depolarization of mammalian central neurones [1]. In the light of the neuroexcitatory properties of kainic acid and domoic acid, it is of great interest to examine neuropharmacological actions of a new kainoid, acromelic acid, in invertebrates and vertebrates.

Another compound, stizolobic acid, was found in 1959 together with stizolobinic acid in the sap exuded from the cut surface of the epicotyl tips of etiolated seedlings of *Stizolobium hassjoo* [19]. When Shirahama and his colleagues determined the chemical structure of acromelic acid A and B, they referred to the structure of stizolobinic acid and stizolobic acid [17]. There is a structural similarity between acromelic acid and stizolobinic acid (see Fig. 1), which prompted us to examine possible actions of stizolobic acid and stizolobinic acid on the glutamatergic system in invertebrates and vertebrates. In our previous study [16], stizolobic acid depressed the response to quisqute in a competitive manner at the crayfish neuromuscular junction without affecti.g the resting membrane potential and responses to GABA and kainoids. At present highly specific antagonists for quisqualate-type receptors are not yet available, although antagonists for NMDA-type receptors have been considerably well documented [20-22].

Methods

Crayfish neuromuscular junction

The opener muscle of the dactyl in the walking leg of the crayfish (*Cambarus clarkii*) was used to examine the action of test compounds. The muscle was perfused with fresh physiological saline at a fixed flow rate of 3 ml/min in a 0.3 ml bath with

the dactyl and the carpopodite fixed. The solution used was a modified van Harreveld's solution containing (in mM) NaCl 195, $CaCl_2$ 18, KCl 5.4, Tris-maleate buffer (pH 7.4) 10, and glucose 11. A nerve bundle containing excitatory axons to this muscle was exposed and stimulated with a suction electrode. Potential changes produced by nerve stimulation and by application of excitatory amino acids and test compounds were recorded either intracellularly from the muscle fibre with a 3 M KCl-filled microelectrode or extracellularly from the neuromuscular junction with a 2 M NaCl-filled microelectrode. In some experiments the membrane potential of the muscle fibre was clamped with two intracellular microelectrodes to measure the currents induced by iontophoretic application of agonists in the absence and presence of test compounds. In order to measure the membrane input resistance of the muscle fibre, two intracellular microelectrodes were inserted separately into the middle of a muscle fibre less than 50 μm apart, one for recording and the other for passing hyperpolarizing pulse current. Experiments were made at a bath temperature of about 22°C.

Newborn rat spinal cord

The spinal cords of 1–5 days old Wistar rats were used for the experiments, and the methods were similar to those previously described [23]. Under ether anesthesia, the spinal cord below the thoracic part was isolated, hemisected sagittally and placed in a 0.3 ml bath perfused with artificial cerebrospinal fluid (mM: NaCl 138.6, KCl 3.35, $CaCl_2$ 1.26, $MgCl_2$ 1.15, $NaHCO_3$ 20.9, NaH_2PO_4 0.58, glucose 10.0) which was oxygenated with a gas mixture of 95% O_2 and 5% CO_2. Tetrodotoxin (TTX) was added at all times to the perfusing solution at a concentration of 0.5 μM to block spontaneous depolarization and indirect drug effects. In some cases, $MgCl_2$ was replaced with NaCl to examine whether the action was dependent on Mg^{2+} concentrations. Perfusion rate was 5 ml/min, and the bath temperature was kept at 27°C. The potential changes generated in the motoneurones were recorded extracellularly from the L3–L5 ventral root with a glass capillary, whose inner diameter fitted tightly with the recorded ventral roots. Glutamate agonists and test compounds were applied to the preparation by brief-pulse injection into the perfusion system at a constant duration (10 s) as described previously by Otsuka and Yanagisawa [24].

Rat cortical neurones

Albino rats (Wistar strain, 250–350 g) were anaesthetized by intraperitoneal injection of urethane-chloralose (urethane 750 mg/kg and α-chloralose 50 mg/kg). A small hole about 3 mm in diameter was drilled in the middle of the rat parietal bone, and through it a seven-barrel glass micropipette with a tip diameter of about 4 μm was inserted into the cerebral cortex (less than 2.0 mm in depth from the surface). Iontophoretic ejection was effected by an apparatus incorporating automatic balancing at the electrode tip. Action potentials of single neurones were recorded by means of the centre barrel (2 M NaCl) of seven-barrel micropipettes and were monitored on an oscilloscope and either photographed, or electronically counted with a frequency counter and displayed on a pen recorder trace. The outer barrels of the seven-barrel micropipette contained aqueous solutions of test compounds.

Results

Acromelic acid

Crayfish neuromuscular junction

Depolarizing action of acromelic acid   Two isomers of acromelic acid (acromelic acid A and B) were isolated from the mushroom, *Clitocybe acromelalga* [17]. From the structural similarity of acromelic to kainic acid (acromelic acid is one of the kainoids), it is possible to predict some neuropharmacological actions of acromelic acid. When acromelic acid A was added to the perfusing fluid, it caused a depolarization of the crayfish opener muscle fibre in a concentration dependent manner at much lower concentrations than kainic acid or domoic acid (Fig. 2). The membrane input resistance was slightly increased by acromelic acid A (less than 10%), depending on amplitudes of the depolarization of the muscle membrane. There was no significant qualitative difference in their actions between both isomers, and their depolarizing potency seemed to be almost equal at the crayfish neuromuscular junction. In the present paper, only acromelic acid A was used on account of the limited availability of acromelic acid B.

A single- or double-barrelled micropipette was critically adjusted to a glutamate sensitive spot on the crayfish opener muscle, and glutamate and acromelic acid was iontophoretically applied by a negative pulse current. Brief iontophoretic application of acromelic acid produced a depolarization which lasted longer than the glutamate-induced potentials, and the decay time constant of its decay phase was more than 2-times larger than that of the glutamate potential [15]. This large depolarization was in contrast to responses to kainic acid or domoic acid, which
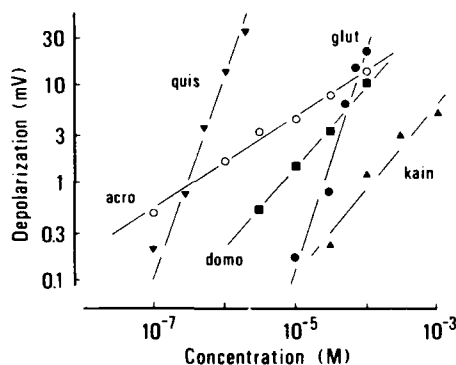
FIG 2   Concentration–depolarization relationships of excitatory amino acids at the crayfish neuromuscular junction. Responses to test compounds were recorded intracellularly. Test compounds were added to the bathing solution for a period of 2 min under the same experimental conditions, and the peak amplitude of the depolarization was plotted against their concentrations on a log-log scale. The depolarizing activity of N-methyl-D-aspartate (NMDA) was also examined, but NMDA did not cause any depolarization at all even in a concentration of 1 mM. Each plot represents the mean value of the peak amplitude ($n = 3$–10). Ordinate, depolarization (mV). Abscissa, concentration (M). acro, acromelic acid (o); quis, quisqualic acid (▼); domo, domoic acid (■); glut, glutamic acid (●); kain, kainic acid (▲).

were not able to produce a fast and large depolarization even when their large amounts were iontophoretically applied at the crayfish neuromuscular junction [6]. When a prolonged pulse current of acromelic acid was applied, the depolarization did not decline during the continued application of this amino acid as far as tested, in strong contrast to the glutamate response, which declined during its continued application due to development of desensitization of the receptors. The acromelate-sensitive area was circumscribed and seemed to be almost identical to the gluta-mate-sensitive area.

Potentiation of the glutamate response Potentiation of the glutamate response is a characteristic of the kainoid actions at the crayfish neuromuscular junction. When both glutamate and kainoid, such as acromelate or domoate, were simultaneously added to the bathing solution, marked potentiation of their responses was observed (Fig. 3A). The potentiation of the glutamate response was observed at extremely low concentrations of acromelic acid, well below those causing a depolarization. Acromelate was about 100-times as potent as kainic acid, and was about 10-times more potent than domoic acid on a molar basis, when the potency was compared in terms of their threshold concentration to induce the potentiation of the glutamate response. On the other hand, the amplitude of excitatory junctional potentials (EJPs) was reduced by acromelic acid in a dose-dependent manner similar to kainic acid, reducing it to about 85% of the control level at a concentration of 0.01 mM.

Depression of the quisqualate response Some kainoids augment the response to bath-applied glutamate [2], but depress the quisqualate response at the crayfish neuromuscular junction [25], in spite of the fact that quisqualate acts on the common receptor to glutamate at this junction [5]. As mentioned above, acromelate is one of the kainoids, therefore, it is expected that acromelate also depresses the response to quisqualate. When acromelate was added to the perfusing solution,

A

B

				10 mV
control	acromelate	acromelate	domoate	1 min
	0.1 µM	1 µM	1 µM	
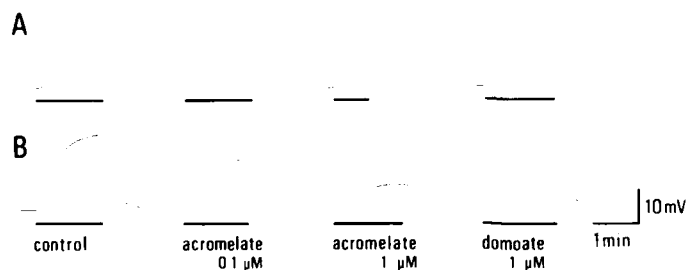
FIG 3 Opposite actions of acromelic acid on the responses to bath-applied glutamate and quisqualate at the crayfish neuromuscular junction. A: potentiation of the glutamate response induced by acromelic acid. Glutamate was added to the bathing solution at a concentration of 50 µM in the absence and presence of acromelic acid or domoic acid for a period indicated by bars. When acromelic acid was added to the perfusing fluid at a concentration of 1 µM in combination with glutamate, contraction of the crayfish opener muscle was sometimes observed with a large depolarization of the muscle membrane. B: depression of the quisqua-late response by acromelic acid. Quisqualate (1 µM) was added to the bathing solution for a period indicated with or without acromelate (0.1 or 1 µM) or domoate (1 µM). Acromelate 0.1 µM was almost equi-potent to domoate 1 µM in reducing the quisqualate response.
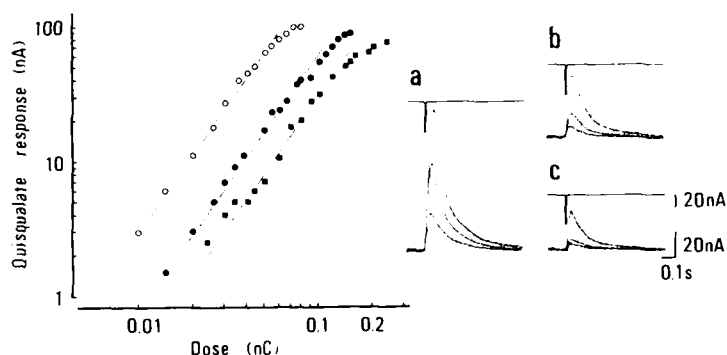
FIG 4 Competitive inhibition of responses to quisqualate by acromelic acid at the crayfish neuromuscular junction. In the voltage-clamped muscle fibre, the currents induced by iontophoretically applied quisqualate were measured in the absence and presence of various concentrations of acromelic acid. The amplitude of the quisqualate-induced current was plotted against the amounts of applied currents on a log-log scale. o, control; ●, 1 μM acromelic acid; ■, 3 μM acromelic acid. Superimposed traces on the right side were the quisqualate-induced current and the monitored injection current: a, control; b, 1 μM acromelic acid; c, 3 μM acromelic acid.

acromelate markedly depressed the depolarization induced by iontophoretically or bath-applied quisqualate in a dose-dependent manner at extremely low concentrations (Fig. 3B). The threshold concentration to depress the quisqualate response was much less than 0.1 μM, which was much lower than that of kainate or domoate. The synaptic current induced by iontophoretically applied quisqualate was determined in the voltage-clamped muscle fibre. The dose–response curve for quisqualate was shifted in parallel to the higher concentration side in the presence of acromelate, suggesting a competitive antagonism (Fig. 4). These results show that acromelic acid possesses an inhibitory action on quisqualate responses as well as EJPs, together with a marked depolarizing activity at the crayfish neuromuscular junction.

Mammalian central neurones

Depolarizing responses in the rat spinal cord   Acromelic acid caused a depolarizing response of newborn rat spinal cord ventral roots in a concentration-dependent manner. Although GABA caused a slight depolarizing response in this preparation, which was blocked by 20 μM picrotoxin, the acromelate-induced depolarizing response was not affected by picrotoxin. Kainate, domoate and acromelate were repeatedly added to the perfusing solution in various concentrations at a fixed interval and a constant duration (10 s), in order to compare their potency in terms of amplitudes of depolarizing responses to them. Acromelate demonstrated the most potent activity in the TTX-containing solution and the order of the depolarizing activity was as follows: acromelate > domoate > kainate (Fig. 5). A puzzling problem is a difference of the time course of responses to kainate and acromelate. The decay rate of the response to acromelate was much larger than that of kainate. Although the amplitude of the kainate response increased in a concentration dependent manner, its decay rate apparently differed from that of acromelate.

As mentioned above, acromelate depressed the response to quisqualate at the crayfish neuromuscular junction. On the other hand, in the newborn rat spinal cord,
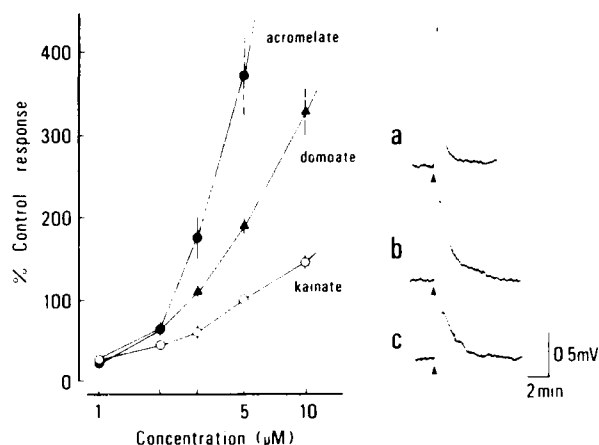
FIG 5 Excitatory action of kainoids in the newborn rat spinal cord. The figure on the left side represents dose-response curves for acromelate (●), domoate (▲) and kainate (○). Responses from individual preparations have been normalized, so that results are expressed as a percentage of the control depolarization to 5 μM kainate. The traces on the right represent records of depolarizing response induced by acromelic acid (a), domoic acid (b) and kainic acid (c) at a concentration of 3 μM, which were extracellularly derived from the newborn rat spinal cord ventral root in the Mg^{2+}-free, TTX-containing (500 nM) solution.

acromelate did not affect the depolarizing response to quisqualate at all. Since acromelate is one of the kainoids, as a matter of course, acromelate is expected to bind to the kainate receptor. At present, highly specific antagonists for kainate- and quisqualate-type receptors are not yet available, therefore, responses to kainate and quisqualate could not be differentiated pharmacologically or electrophysiologically. Neither Mg^{2+} (1.15 mM) nor APV (2-amino-5-phosphonovaleric acid, 50 μM) affected the acromelate-induced depolarization. These experimental observations strongly suggest that acromelate preferably binds to a receptor other than NMDA-type receptors.

Spike discharges in the adult rat cortical neurones Glutamate and acromelate were iontophoretically applied to the rat cortical neurone using a multi-barrel microelectrode. Acromelic acid easily induced spike discharges from rat cortical neurones. Spike discharges induced by acromelate lasted for a long period of time after the cessation of the iontophoretic ejection, similar to those induced by kainate. When acromelate was applied in addition to iontophoretic administration of other excitatory amino acids, acromelate did not affect responses to other excitatory amino acids. The frequency of spike discharges induced by acromelate was decreased by iontophoretic application of kynurenate, but the spike discharges were resistant to iontophoretic APV.

Stizolobic acid

Crayfish neuromuscular junction

Depression of responses to glutamate and quisqualate When stizolobic acid or stizolobinic acid was added to the bathing solution at various concentrations (0.1 1
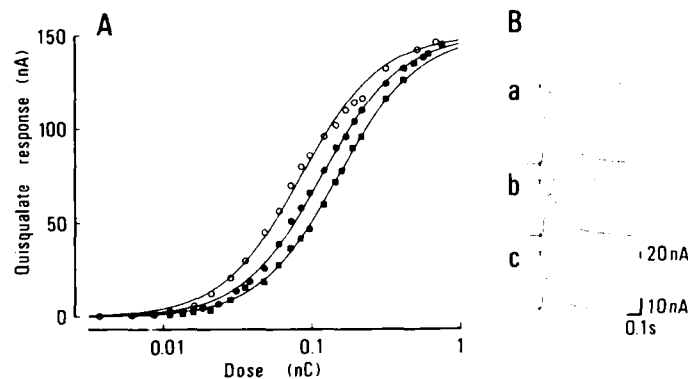
FIG 6 A: dose–response curves for quisqualate in the presence and absence of stizolobic acid at the crayfish neuromuscular junction. Ordinate, amplitudes of synaptic currents induced by quisqualate in the voltage-clamped muscle. Abscissa, logarithmic amounts of iontophoretic quisqualate. The continuous curves were drawn by the method of least-squares according to the equation: $y = Y_{max}/[1 + K_a(1 + I^m/K_b)/A^n]$, where A is agonist concentration; I, inhibitor concentration; K_a and K_b, equilibrium constant; Y_{max}, maximal response; m and n, the number of antagonist and agonist molecules, respectively, assuming $K_a = 0.0187$, $K_b = 0.0056$, $n = 1.62$, $m = 0.69$, and $Y_{max} = 149.6$. ○, control; ●, stizolobic acid 0.3 mM; ■, stizolobic acid 1 mM. B: Currents induced by iontophoretically applied quisqualate and the monitored injection current. a, control; b, stizolobic acid 0.3 mM; c, stizolobic acid 1 mM.

mM), neither amino acid caused any depolarization of the muscle fibre in the concentration range used. The membrane input resistance of the muscle fibre, inhibitory junctional potentials and GABA actions were not affected by them. In the presence of these amino acids, amplitudes of EJPs and responses to quisqualate or glutamate were reduced in a concentration-dependent manner, and recovery from the drug action was very rapid after washing the preparation. Stizolobinic acid seemed to be about 5-times less potent than stizolobic acid. The action of stizolobic acid in a concentration of 1 mM was almost equivalent to that of 0.2 mM stizolobic acid.

A quantum analysis of extracellularly recorded EJPs demonstrated that the average unit size was markedly reduced from 0.24 mV to 0.14 mV by the addition of 0.5 mM stizolobic acid, while the quantum content was slightly affected. The decay time constant of the tail of extracellular EJPs was slightly decreased from 0.67 ± 0.01 ($n = 94$) to 0.56 ± 0.01 ms ($n = 97$).

The synaptic current induced by iontophoretically applied quisqualate was determined in the voltage-clamped muscle fibre. The dose–response curve for quisqualate shifted in parallel to the higher dose side in the presence of stizolobic acid, suggesting that stizolobic acid reduced the response to quisqualate in a competitive manner (Fig. 6). If stizolobic acid would bind to only the quisqualate-type receptor as a competitive antagonist, stizolobic acid should not demonstrate a use-dependent action. In the experiment shown in Fig. 7, when stizolobic acid was added to the perfusing solution, the amplitude of glutamate potentials, evoked every 5 s, was decreased to a steady state level of about 35% of their control value relatively rapidly. After a wash in the normal (stizolobic acid free) solution the response was restored to its control level very rapidly. After confirming the response
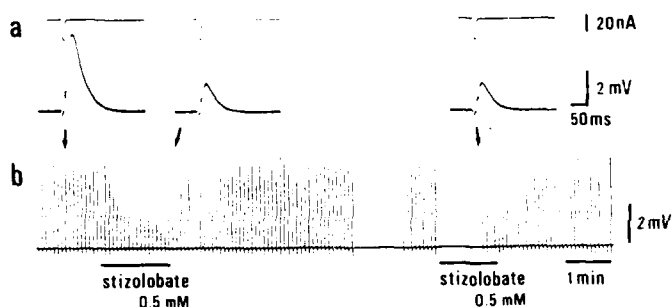
FIG 7 Depression of glutamate-induced potentials caused by stizolobic acid. a: monitored ejection currents and glutamate-induced currents corresponding to the record in b indicated by arrows. b: records by an AC amplifier. Glutamate was applied by iontophoresis in pulses at intervals of 5 s. Stizolobic acid (0.5 mM) was bath-applied as indicated by bottom lines. Stizolobic acid relatively rapidly reduced the amplitude of repetitive glutamate-induced potentials. The resting membrane potential was not affected by stizolobic acid. After response had recovered, the responses were found to be sufficiently stable and stizolobic acid was re-introduced but glutamate pulses were discontinued for 1 min. The first response after resuming the iontophoretic pulse of glutamate was reduced to a similar level to that in the control, suggesting that the action was not use-dependent. c: record by a DC amplifier.

to be sufficiently stable, solution containing stizolobic acid (0.5 mM) was reintroduced, but the iontophoretic pulses of glutamate were discontinued until the muscle fibre had been exposed to stizolobic acid for 1 min. The amplitude for the first glutamate potential after resuming the iontophoretic pulses was already reduced to about 35% of the control, indicating that the action of stizolobic acid was not use-dependent.

In order to examine the specificity of stizolobic acid to quisqualate-type receptors, actions of stizolobic acid on responses to kainoids were examined. At the
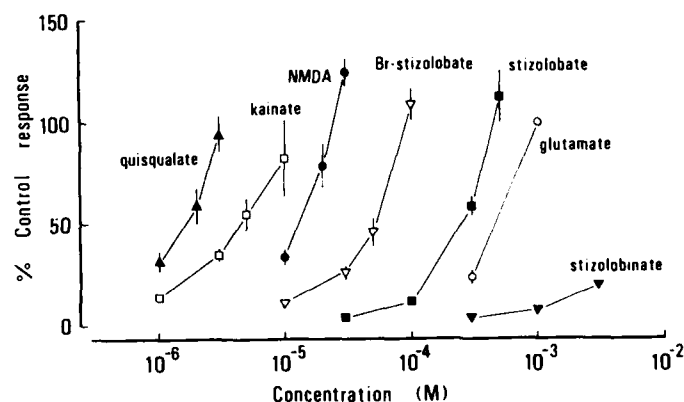
FIG 8 Concentration–depolarization relationships of excitatory amino acids in the newborn rat spinal cord. The responses to excitatory amino acids were recorded from the ventral root extracellularly in the Mg^{2+}-free, TTX-containing (500 nM) solution. Responses from individual preparations have been normalized, so that results are expressed as a percentage of the control depolarization to 1 mM glutamate. Vertical bars represent S.E.M. $(n \geqslant 3)$. Br-stizolobate: 3-bromo-stizolobic acid.

crayfish neuromuscular junction acromelic acid is one of the most potent kainoids and possesses common pharmacological properties to kainoids [15]. NMDA does not cause any depolarization at all at the crayfish neuromuscular junction, and its antagonists, such as APV and kynurenate, do not affect the depolarization induced by glutamate and quisqualate, namely, there is no evidence of existence of the NMDA-type receptor on crayfish muscle fibres. Therefore, we could not examine the action of stizolobic acid on the NMDA-type receptor on the crayfish muscle. Stizolobic acid slightly augmented the sub-maximal response to acromelic acid rather than reduced it, in spite of the fact that stizolobic acid significantly reduced responses to glutamate and quisqualate.

Excitatory actions in the rat spinal cord

In spite of the fact that stizolobic acid depresses responses to quisqualate in a competitive manner at the crayfish neuromuscular junction, it causes a depolarizing response of the isolated newborn rat spinal cord, without affecting responses to quisqualate, kainate, glutamate and NMDA. Thus stizolobic acid highlights major differences between the mammalian central nervous system and the crayfish neuromuscular junction. In the isolated newborn rat spinal cord preparation, the potency of stizolobic acid to cause depolarization was considerably less than that of kainoids or quisqualate, but was almost similar to that of L-glutamate. Some derivatives of stizolobic acid also demonstrated the depolarizing response in this preparation. 3-Bromo-stizolobic acid (2-amino-2-(3-bromo-6-carboxy-2-oxo-2H-pyran-4-yl)propanoic acid) was one of the most potent excitants among these derivatives, being about 5-times more potent than stizolobic acid. On the other hand, stizolobinic acid was much less potent than stizolobic acid. There was no significant qualitative difference in actions between stizolobic acid and 3-bromo-stizolobic acid in the rat spinal cord.

The NMDA-induced depolarization is decreased by the existence of Mg^{2+} and some compounds, such as APV, APH, CPP and MK-801 in the mammalian central nervous system [20–22,26]. When the bathing solution was changed from Mg^{2+}-free saline to a Mg^{2+}-containing (1.15 mM) one, responses to quisqualate, kainate and stizolobic acid were not affected at all, but the amplitude of NMDA responses was significantly reduced and the response to glutamate was slightly reduced. Kynurenate (1 mM) depressed all responses to these excitatory amino acids. In addition, only the NMDA response was reduced by the addition of APV (20 μM) or MK-801 (1 μM), in spite of the fact that responses to other excitatory amino acids including stizolobic acid were not affected by APV or MK-801, suggesting that stizolobic acid and 3-bromo-stizolobic acid acted on a receptor other than the NMDA-preferred receptor.

Spike discharges of single cortical neurones in rats

Most neurones that responded to glutamate were also excited by the iontophoretic administration of stizolobic acid. When the potencies were compared in terms of the frequency of spike discharges produced by iontophoretic currents of the same strength, stizolobic acid seemed to be more potent than glutamate. When large amounts of stizolobic acid were applied, the amplitude of the spikes gradually decreased and then the discharges were abolished, presumably by excessive depolarization or receptor desensitization. At this stage, further application of other excitatory amino acids did not cause any spike discharges. The cessation of

discharges evoked by application of stizolobic acid was much more delayed than by glutamate. When glutamate, quisqualate or kainate was applied together with stizolobic acid by brief pulses of iontophoretic currents, the frequency of responses to these excitatory amino acids was not affected by stizolobic acid, but constant additional spike discharges were observed by stizolobic acid. When responses to stizolobic acid, quisqualate, kainate, and NMDA were induced in the presence of iontophoretically applied APV, responses to stizolobic acid were not affected like those to kainate and quisqualate but only the response to NMDA was significantly reduced. Spike discharges induced by stizolobic acid were decreased by iontophoretic application of kynurenate.

Discussion

In the present paper we introduce interesting neuropharmacological actions of two novel compounds of natural origin, acromelic acid and stizolobic acid. They are related structurally to excitatory amino acids. From the structural similarity of acromelic acid to kainic acid, acromelic acid is expected to bind to the kainate receptor. However, there are some differences in pharmacological actions between acromelic acid and kainic acid. When they were systemically administered to the rat, the difference in behavioural signs became striking. The most pronounced behavioural changes after the injection of kainic acid were strong immobility ('catatonia'), increased incidence of 'wet-dog-shakes' (WDS), and long-lasting generalized tonic-clonic convulsions [27,28]. Components of the syndrome were evoked in a dose-dependent manner with low doses inducing WDS only and progressively higher doses being associated with an increasing incidence of WDS together with convulsions and brain damage. On the other hand, incidence of WDS was not observed in any doses of acromelate. The lethal dose of acromelic acid in rats and mice was considerably lower than that of kainic acid. In a sub-lethal dose, acromelic acid caused a marked long-lasting extension of the hindlimb of the rat, which was quite different from the rigidity or convulsions induced by kainate, and sometimes caused generalized clonic convulsions. The extension of the hindlimb was followed by a flaccid paralysis of skeletal muscles of the hindlimb for about two hours. Most rats receiving acromelate at an intravenous dose of 5 mg died from convulsions within about 30 minutes, but surviving rats on the next day of the injection demonstrated the severe extension of the hindlimb, which was markedly reinforced by sensory stimuli and lasted for more than 1 month without a further administration of acromelic acid.

Kainic acid is less effective in depolarizing the crayfish muscle fibre than glutamate and quisqualate, on the other hand, acromelate causes a large depolarization of the crayfish muscle irrespective of whether applied iontophoretically or by bath application. Acromelic acid causes depolarizing responses in both vertebrates and invertebrates, and is the most potent excitant among the kainoids. Therefore, acromelic acid is available for the stimulation of the kainate receptor, but at the crayfish neuromuscular junction acromelic acid markedly potentiates the glutamate responses at extremely low concentrations, in spite of the fact that it reduces the quisqualate response in a dose-dependent and competitive manner. These actions are common to the kainoids [2,15,25]. Stizolobic acid does not depress but slightly augments the acromelate-induced depolarization of the crayfish muscle fibre, while

it depresses the response to quisqualate and glutamate in a competitive manner. Therefore, we were interested in the interaction between kainoids and quisqualate. In contrast to the action of kainoids, stizolobic acid did not potentiate the glutamate response but depressed it at the crayfish neuromuscular junction. Stizolobic acid was proved to be a competitive antagonist of the quisqualate-type receptor at the crayfish neuromuscular junction and did not cause any depolarization of the crayfish opener muscle fibre even when high concentrations of stizolobic acid were applied [16]. Stizolobic acid, therefore, seems to be a selective quisqualate antagonist at the crayfish neuromuscular junction. On the other hand, stizolobic acid causes a significant depolarization in the rat central neurones in contrast to the crayfish neuromuscular junction. In the preliminary study on the receptor binding of stizolobic acid in the frog spinal neurones, stizolobic acid inhibited the binding of [^{3}H]kainate to the receptor, suggesting that stizolobic acid binds to the kainate-type receptor in the frog spinal cord (Maruyama, personal communication). The interaction between kainoids and quisqualate was also observed in the fish retina [29]. Therefore, it is possible to consider that stizolobic acid may be a weak kainate agonist.

The present study demonstrated that a derivative of stizolobic acid, 3-bromo-stizolobic acid, possessed a potent depolarizing activity in the isolated rat spinal cord, being about 5-times more potent than stizolobic acid. However, at the crayfish neuromuscular junction, derivatives with halogens in the 3-positions of stizolobic acid, including 3-bromo-stizolobic acid, were of almost equal potency to stizolobic acid in reducing responses to glutamate and quisqualate. Although there is an apparent contradictory action between the mammalian central nervous system and the crayfish neuromuscular junction, there are some possibilities as regards the mode of action worthy to be considered, including the receptor subtype and the above possibility that stizolobic acid may be a weak kainate agonist. Since there are some differences in action between stizolobic acid and kainoids, for example, potentiation of the glutamate response by kainate and not by stizolobic acid, as a matter of course, the possibility that stizolobic acid binds to a novel receptor subtype for excitatory amino acids cannot be definitely ruled out.

These new materials may provide useful information about elucidating the pharmacology of the glutamatergic system in invertebrates and vertebrates, and moreover, will provide a very useful tool for neuroscience research in addition to established excitatory amino acids.

Summary

The actions of two novel amino acids of natural origin, acromelic acid and stizolobic acid, are presented in order to encourage the utilization of these new and potentially valuable compounds. Acromelic acid is one of the most potent kainoids, and causes a marked depolarization in vertebrates and invertebrates. At the crayfish neuromuscular junction, the potency of acromelate to cause depolarization was about 100-times as potent as that of kainate. Iontophoretic application of acrome-late produced a marked depolarization at the crayfish neuromuscular junction unlike other kainoids, such as domoate and kainate, which did not produce such a large depolarization even when their large amounts were iontophoretically applied at this junction. In addition to the marked depolarizing action, acromelate markedly

potentiated the responses to glutamate at extremely low concentrations at the crayfish neuromuscular junction, in spite of the fact that it reduced the quisqualate response in a dose dependent manner. In the mammalian central nervous system, acromelate is one of the most potent agonists of excitatory amino acids, and acromelate is much more potent than kainate.

Stizolobic acid reduced responses to quisqualate and glutamate in a competitive manner at the crayfish neuromuscular junction without affecting the resting membrane potential, the membrane input resistance and the responses to GABA and kainoids. The blocking action on the response to quisqualate and glutamate was not use-dependent. The amplitude of excitatory junctional potentials (EJPs) was also reduced by stizolobic acid in a concentration dependent manner. On the other hand, stizolobic acid caused a marked depolarization in the newborn rat spinal cord ventral roots and the adult rat cortical neurones. The depolarizing action of stizolobic acid was not affected by Mg^{2+} or N-methyl-D-aspartate (NMDA) receptor antagonists, suggesting that stizolobic acid binds to a receptor distinct from the NMDA-preferred receptor in the rat.

References

1 Shinozaki, H. and Konishi, S. (1970) Actions of several anthelmintics and insecticides on rat cortical neurones. Brain Res. 24, 368–371.
2 Shinozaki, H. and Shibuya, I. (1974) Potentiation of glutamate induced depolarization by kainic acid in the crayfish opener muscle. Neuropharmacology 13, 1057–1065.
3 Shinozaki, H. (1978) Discovery of novel actions of kainic acid and related compounds. In: Kainic Acid as a Tool in Neurobiology (E.G. McGeer, J.M. Olney and P.L. McGeer, eds.) pp. 17–35 Raven Press, New York.
4 Johnstone, G.A.R., Curtis, D.R., De Groat, W.C. and Duggan, A.W. (1968) Central actions of ibotenic acid and muscimol. Biochem. Pharmacol. 17, 2488–2489.
5 Shinozaki, H. and Shibuya, I. (1974) A new potent excitant, quisqualic acid: effects on crayfish neuromuscular junction. Neuropharmacology 13, 665–672.
6 Shinozaki, H. and Shibuya, I. (1976) Effects of kainic acid analogues on crayfish opener muscle. Neuropharmacology 15, 145–147.
7 McGeer, E.G. Olney, J.W. and McGeer, P.L. (1978) Kainic Acid as a Tool in Neurobiology. Raven Press, New York.
8 Rao, S.L.N., Adiga, P.R. and Sarma, P.S. (1964) The isolation and characterization of β-N-oxalyl-L-α,β-diaminopropionic acid: A neurotoxin from the seeds of Lathyrus sativus. Biochemistry 3, 432–436.
9 Evans, R.H., Jones, A.W. and Watkins, J.C. (1981) Willardiine: a potent quisqualate-like excitant. J. Physiol. (Lond.), 308, 71–72P.
10 Kawai, N., Niwa, A. and Abe, T. (1982) Spider venom contains specific receptor blocker of glutaminergic synapses. Brain Res. 247, 169–171.
11 Clark, R.B., Donaldson, P.L., Gration, K.A.F., Lambert, J.J., Piek, T., Ramsey, R., Spanjer, W. and Usherwood, P.N.R. (1982) Block of locust muscle glutamate receptor by δ-philanthotoxin occurs after receptor activations. Brain Res. 241, 105–114.

12 Shinozaki, H. and Ishida, M. (1978) Theanine as a glutamate antagonist at a crayfish neuromuscular junction. Brain Res. 151, 215–219.

13 Ishida, M. and Shinozaki, H. (1984) Glutamate inhibitory action of matrine at the crayfish neuromuscular junction. Br. J. Pharmacol. 82, 523–531.

14 Shinozaki, H. and Ishida, M. (1985) Inhibitory actions of tuberostemonine on the excitatory transmission at the crayfish neuromuscular junction. Brain Res. 334, 33–40.

15 Shinozaki, H. Ishida, M. and Okamoto, T. (1986) Acromelic acid, a novel excitatory amino acid from a poisonous mushroom: effects on the crayfish neuromuscular junction. Brain Res. 399, 395–398.

16 Shinozaki, H. and Ishida, M. (1988) Stizolobic acid, a competitive antagonist of the quisqualate-type receptor at the crayfish neuromuscular junction. Brain Res. 451, 353–356.

17 Konno, K., Shirahama, H. and Matsumoto, T. (1983) Isolation and structure of acromelic acid A and B. New kainoids of Clitocybe acromelalga. Tetrahedron Lett. 24, 939–942.

18 Konno, K., Hashimoto, K., Ohfune, Y., Shirahama, H. and Matsumoto, T. (1986) Synthesis of acromelic acid A, a toxic principle of Clitocybe acromelalga. Tetrahedron Lett. 27, 607–610.

19 Hattori, S. and Komamine, A. (1959) Stizolobic acid: a new amino acid in Stizolobium hassjoo. Nature (Lond.) 183, 1116–1117.

20 Cotman, C.W. and Iversen, L.L. (1987) Excitatory amino acids in the brain—focus on NMDA receptors. Trends Neurosci. 10, 263–265.

21 Watkins, J.C. and Olverman, H.J. (1987) Agonists and antagonists for excitatory amino acid receptors. Trends Neurosci. 10, 265–272.

22 Kemp, J.A., Foster, A.C. and Wong, E.H.F. (1987) Non-competitive antagonists of excitatory amino acid receptors. Trends Neurosci. 10, 294–298.

23 Otsuka, M. and Konishi, S. (1974) Electrophysiology of mammalian spinal cord in vitro. Nature (Lond.) 252, 733–734.

24 Otsuka, M. and Yanagisawa, M. (1980) The effects of Substance P and baclofen on motoneurones of isolated spinal cord of the new-born rat. J. Exp. Biol. 89, 201–214.

25 Shinozaki, H. and Ishida, M. (1976) Inhibition of quisqualate responses by domoic or kainic acid in crayfish opener muscle. Brain Res. 109, 435–439.

26 Davies, J. and Watkins, J.C. (1977) Effects of magnesium ions on the responses of spinal neurones to excitatory amino acids and acetylcholine. Brain Res. 130, 364–368.

27 Fuller, T.A. and Olney, J.W. (1979) Effects of morphine or naloxon on kainic acid neurotoxicity. Life Sci. 24, 1793–1798.

28 Collins, R.C., McLean, M. and Olney, J. (1980) Cerebral metabolic response to systemic kainic acid: ^{14}C-deoxyglucose studies. Life Sci. 27, 855–862.

29 Ishida, A.T. and Neyton, J. (1985) Quisqualate and L-glutamate inhibit retinal horizontal-cell responses to kainate. Proc. Natl. Acad. Sci. U.S.A. 82, 1837–1741.

CHAPTER 9

Acromelic acids A and B, very potent excitatory amino acids from a poisonous mushroom

H. SHIRAHAMA, K. KONNO, K. HASHIMOTO AND T. MATSUMOTO

Department of Chemistry, Faculty of Science, Hokkaido University, Sapporo 060, Japan

Historically, muscarine was isolated from the toadstool *Amanita muscaria* and it has played a very important role in pharmacology and physiology. Since then, a number of biologically active substances have been obtained from various mushrooms. The mushroom has been one of the great sources of significant compounds. Twenty-five years ago, we isolated an antitumor sesquiterpene, illudin S (lampterol, lunamycin) from *Lampteromyces japonicus*, determined its structure and synthesized it totally [1–4]. Illudin S was shown to be biosynthetically derived from humulene and a hundred sesquiterpenes belonging biogenetically to the same class as illudin have been found in mushrooms at many laboratories [5]. We named
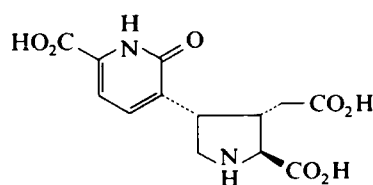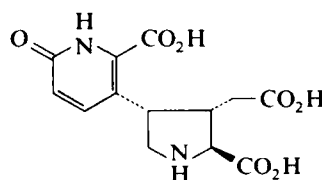
acromelic acid A (1) acromelic acid B (2)
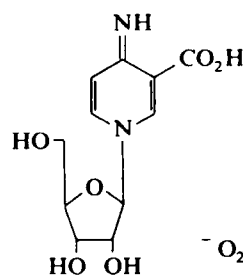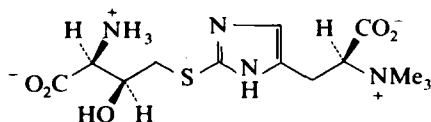
clitidine clithioneine 4-aminoquinolinic acid
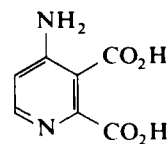
them cyclohumulanoids [6] and converted humulene chemically into more than ten of them through a biosynthetic-like pathway [7]. During this work we applied molecular mechanics calculations (MMC) to solve the biosynthesis stereochemically and the deduced assumptions were confirmed by chemical syntheses [6,8]. Our development of cyclohumulanoid chemistry stimulated the use of MMC in the field of natural products chemistry and facilitated the achievement of a new chemistry of cyclization of medium-size cycloalkenes [9].

Recently we have found new compounds, acromelic acids, in a Japanese toadstool. Dokusasako (*Clitocybe acromelalga*) is known to contain potent slow poisons. Accidental ingestion of the toadstool causes a sharp and serious pain and a marked reddish edema in the hand and foot after several days which continues for about a month. The symptoms are unique and similar to acromelalgia and erythromelalgia. Fractionation of the toxins was carried out by monitoring the lethal effect in mice. It led to the isolation of five new compounds (see page 105); clitidine, a toxic nucleoside [10]; clithioneine, an unusual nontoxic betaine [11]; 4-aminoquinolinic acid, a weak neuroexcitant [12]; acromelic acids A and B, powerful neuroexcitatory amino acids [13]. We report here the isolation, characterization, synthesis and biological activity of acromelic acids A and B.

Isolation

The water extract of fresh fruiting bodies was treated with acetone to give precipitates, which were then dialysed against water. The dialysate was chromatographed on charcoal with stepwise elution of EtOH and water. The fraction eluted by 2.5–5% aq EtOH was subjected sequentially to anion-exchange resin (Amberlite IR-45) and paper electrophoresis (pH 4.6) to give a material with high toxicity. Cellulose TLC using nBuOH/AcOH/H$_2$O (4 : 1 : 5) as the solvent system separated acromelic acid A (R_f 0.41) and B (R_f 0.28). Each acid was finally purified by cellulose TLC and paper electrophoresis. Amounts of pure acids A and B were about 110 μg and 40 μg, respectively, from a total of 16.2 kg of fruiting bodies. Both compounds showed a yellow coloration with the ninhydrin test and behaved as strong acids on ion-exchange chromatography and paper electrophoresis (Fig. 1).

Structure

Due to the scarcity of the samples, spectral data were limited. For example, no ^{13}C-NMR signals could be observed even after 35912 transients (25.0 MHz), and all attempts to measure the mass spectrum (FD-MS, SIMS) were unsuccessful. Thus, the data obtained were only those of ^{1}H-NMR (360 MHz), UV and CD spectra. The formulas 1 and 2, however, could be inferred from the data by comparison with those of related compounds.

The ^{1}H-NMR spectra of both 1 and 2 consisted of the signals of two aromatic protons, three methine and two methylene groups. The sequence of the methine and methylene groups was consistent with the presence of a partial structure (A) in both compounds by the decoupling experiments (Fig. 2). The terminal methine proton was thought to be an α-proton of an amino acid [14] judging from the chemical shift values (4.13 in 1 and 4.16 in 2). On the other hand, one of the methylenes was

fruiting bodies (16.2 kg)
|
water extract
|
add acetone
|
precipitate   supernatant
|
dialysis
|
dialized fr.   non-dialized fr.
|
charcoal
|
2.5–5%   EtOH (7 g)   10% EtOH (5 g)   30% EtOH (4 g)

Amberlite IR-45
(HCO_2^- form)

clithioneine [11]   clitidine [10]

10–20% HCO_2H (1 g)

PEP (pH 4.6)

+9 cm   (52 mg)

cellulose TLC
($nBuOH/HCO_2H/H_2O = 6/1/2$)

Rf 0.41 (9 mg)   Rf 0.28 (6 mg)

cellulose TLC
($nBuOH/AcOH/H_2O = 4/1/5$)

PEP (pH 4.6)

4-aminoquinolinic acid [12]

Rf 0.35 (2 mg)

PEP (pH 4.6)

acromelic acid A (ca. 110 μg)   acromelic acid B (ca. 40 μg)

ninhydrin-test: yellow   ninhydrin-test: yellow

PEP = paper electrophoresis

FIG 1   See text.

indicated to be α to a carbonyl group because of its chemical shifts (2.01, 2.54 in 1 and 2.23 in 2) and a high J value between geminal protons (16.5 Hz). These analyses led to a partial structure (B) possessing a glutamic acid moiety, which was

TABLE 1
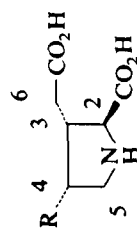
	H$_2$	H$_3$	H$_4$	H$_5$	H$_{5'}$	H$_6$	H$_{6'}$
Acromelic acid A	4.13, d (8.1)	3.12, dddd (5.4 7.1 8.1 10.8)	3.82, q (7.1)	3.73, dd (7.1 12.0)	3.76, dd (7.1 12.0)	2.01, dd (10.8 16.5)	2.54, dd (5.4 16.5)
Domoic acid	3.98, d (8.2)	3.05, dddd (5.8 7.6 8.2 9.1)	3.83, q (7.6)	3.49, dd (7.6 12.3)	3.70, dd (7.6 12.3)	2.50, dd (9.1 16.8)	2.75, dd (5.8 16.8)
Acromelic acid B *	4.16, d (3.6)	3.15, ddd (3.6 7.2 7.7)	4.47, dt (7.2 11.7)	3.67, t (11.7)	3.78, dd (7.2 11.7)	2.23, d (7.7)	
Kainic acid	4.12, d (3.6)	3.10, dddd (3.6 6.3 7.2 8.3)	3.03, dt (7.2 11.7)	3.45, t (11.7)	3.65, dd (7.2 11.7)	2.40, dd (8.3 16.6)	2.49, dd (6.3 16.6)

* Data are variable depending on concentration of sample.
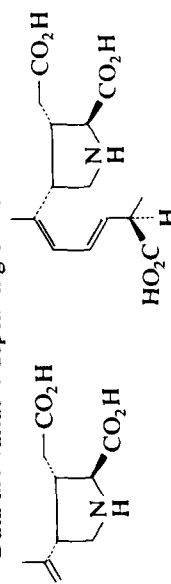
kainic acid (3)

domoic acid (4)

A ■—CH₂—CH—CH—CH₂—■ ... CH—■ ... ■

$■-CH_2-CH-CH-CH_2-■$

A

B

C

D
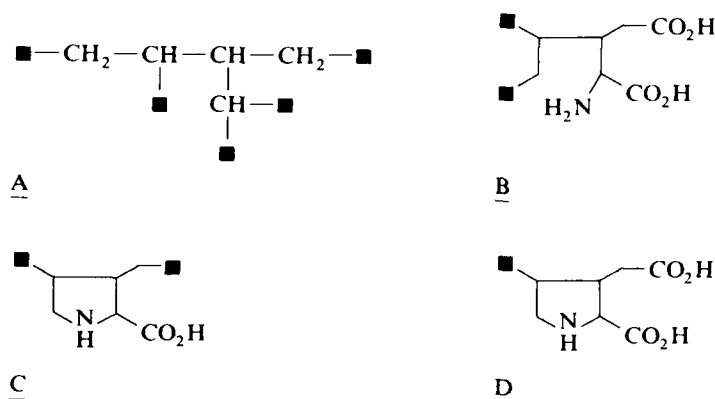
FIG 2 See text.

in accord with the strongly acidic nature of 1 and 2 on chromatography. Another partial structure (C) including a proline moiety was suggested from the fact that both 1 and 2 showed a yellow coloration with the ninhydrin test and the chemical shifts of the other methylene (3.73, 3.76 in 1 and 3.67, 3.78 in 2) were assignable to a methylene α to an ammonium nitrogen. Taking all this evidence into consideration, a structure of 4-substituted 2-carboxy-3-carboxymethyl pyrrolidine (D) was inferred for both 1 and 2. Indeed, as shown in Table 1, the ^{1}H-NMR spectral data (360 MHz) of 1 and 2 closely resembled those of domoic acid 4 [15,16] and kainic acid 3 [17] respectively, except for the signals of C-4 protons.

The structure of the aromatic portion was deduced by UV and NMR analyses. The UV spectra of both compounds exhibited two pH-independent maxima at around 240 and 310 nm, characteristic of 2-pyridone, in particular of 2-pyridone-6-carboxylic acid derivatives [18]. Moreover, in the ^{1}H-NMR spectrum, coupling constants of 9 and 7 Hz are known to be indicative of $J_{3,4}$ and $J_{4,5}$, respectively, in 2-pyridone-6-carboxylic acid derivatives [19]. Therefore, 3- and 5-substituted 2-pyridone-carboxylic acids were suggested as the structure of the aromatic portion of 1 and 2, respectively.

TABLE 2

5 R = Me
6 R = ...

	^{1}H-NMR			λ_{max}		
	δ_4	$\delta_{5(3)}$	$J_{4\text{-}5(3)}$	pH 2	pH 7	pH 12
Acromelic acid A	7.54	6.98	7.2	240, 313	242, 317	241, 312
5	7.62	6.96	7.0	241, 306	242, 310	245, 307
6	7.66	7.08	7.0	239, 311	241, 315	244, 311
Acromelic acid B	7.63	6.68	9.3	231, 308	227, 300	241, 311
7	7.69	6.68	9.0	239, 310	235, 302	242, 313

110

isoprene unit   glutamic acid   kainic acid, domoic acid
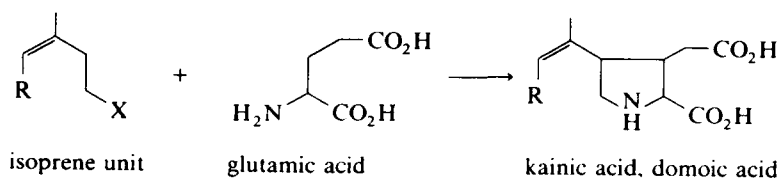
Scheme 1.

In order to verify the above argument, appropriate model compounds such as 5, 6 and 7 were prepared and their spectral data were compared with those of 1 and 2. As shown in Table 2, the ^{1}H-NMR and UV data of the aromatic portion of the natural products were almost identical to those of corresponding model compounds, supporting the deduced structures.

The conclusion that the pyrrolidine and pyridone thus far deduced were linked directly at C-4 of the former to the 3- or 5-position of the latter was reached as described below. A biosynthetic consideration suggested the directly linked formulas 1 and 2. For biosynthesis of kainic acid and domoic acid, condensation of an isoprene unit with glutamic acid followed by cyclization to form a pyrrolidine ring as shown in Scheme 1 is most likely. Consequently, it was supposed that the pyrrolidine moiety of 1 and 2 arose from glutamic acid. For the origin of the aromatic portion, DOPA was suggested, since the fission of a catechol ring and subsequent recyclization to a pyrone ring have been established biosynthetically in the case of stizolobinic acid (scheme 2) [20,21]. Accordingly the extradiol cleavage (Scheme 3, path a) followed by cyclization with ammonia would give pyridone amino acid which then condenses with glutamic acid to afford 1 along with deamination and decarboxylation. In a similar way, the intradiol cleavage (path b) would lead to 2.

^{1}H-NMR analyses gave support for the formulas 1 and 2. In both compounds the doublet signals assigned to H$_4$ of pyridone (7.54 in 1 and 7.63 in 2) appeared to a lower height and were broader than the other pyridone proton (6.98 in 1 and 6.68 in 2), indicating a small long-range coupling between the C-4 proton of pyridone and H$_4$ of pyrrolidine. In fact, in the case of model compounds 5 and 7, clear long-range couplings were observed.

Conformational analyses further supported the above argument. As the main conformation, 1' and 2' shown in Fig. 3 were deduced from J values and inspection of molecular models, anomalous down-field shifts of pyrrolidine H$_4$ peaks (3.82 in 1 and 4.47 in 2) were well rationalized from these models, since in 1' and 2', the

dopa   stizolobinic acid

Scheme 2.

acromelic acid A 1'
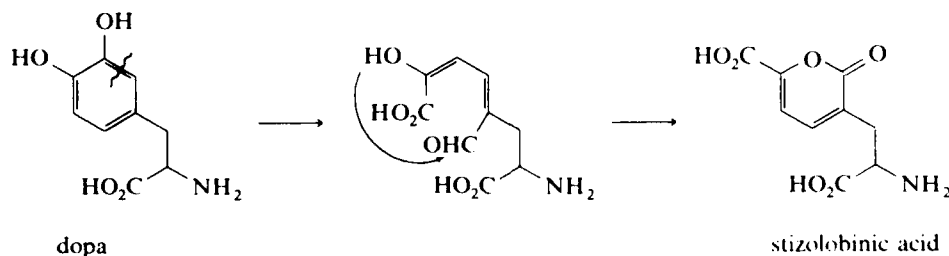
acromelic acid B 2'
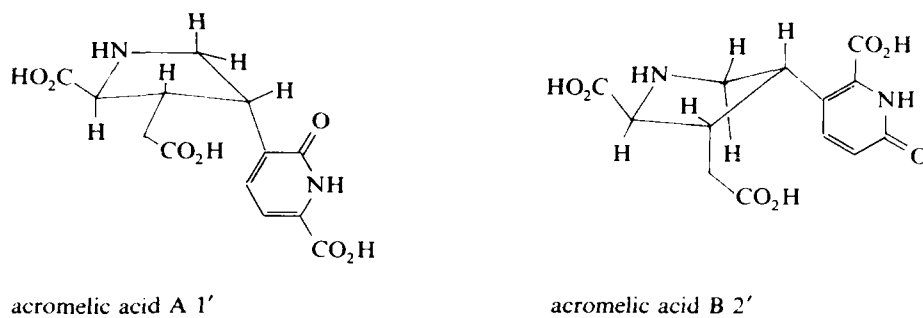
FIG 3   See text.

carbonyl and carboxyl groups respectively, can approach close to H_4, giving the anisotropy effect. This implies a direct linkage of the pyrrolidine and pyridone rings.

The relative stereochemistry of three asymmetric centers on the pyrrolidine ring in both 1 and 2 was indicated to be the same as kainic acid 3 and domoic acid 4 respectively, 2-3 *trans* and 3-4 *cis*, since the corresponding *J* values of the ring protons of 1 and 2 were almost the same as 4 and 3 respectively, as shown in Table 1.

Furthermore, the 2,3-*trans* structure was suggested by the chemical shifts of α-protons. In the kainoids so far investigated, when the 2,3-substituents (carboxyl

kainic acid (3)

allo-kainic acid
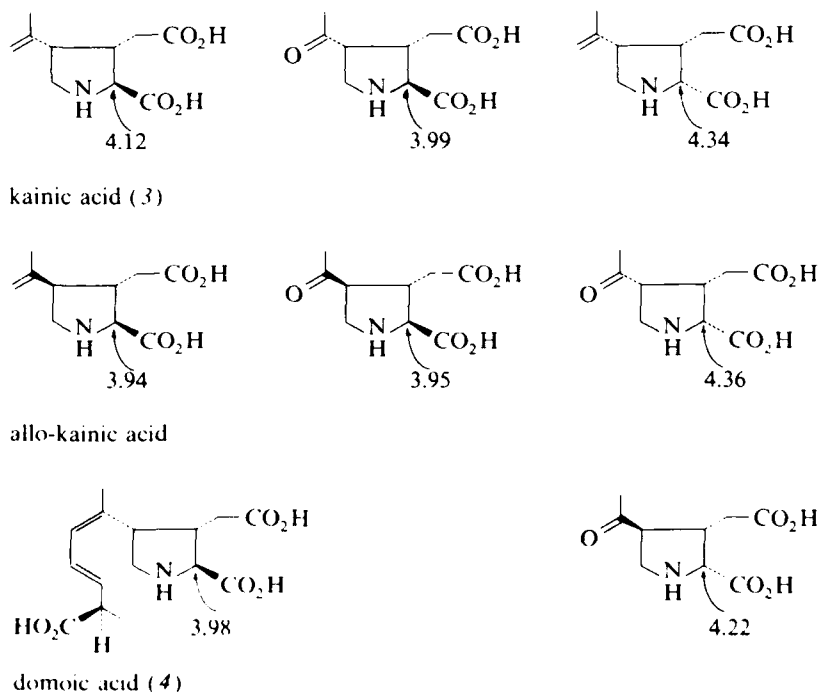
domoic acid (4)

FIG 4   Chemical shifts of α-protons in kainoids. All these kainoids except for kainic acid and domoic acid were prepared from kainic acid by the known method [22].

acromelic acid A (1)

Scheme 3.

114

acromelic acid A (**1**)

acromelic acid B (**2**)
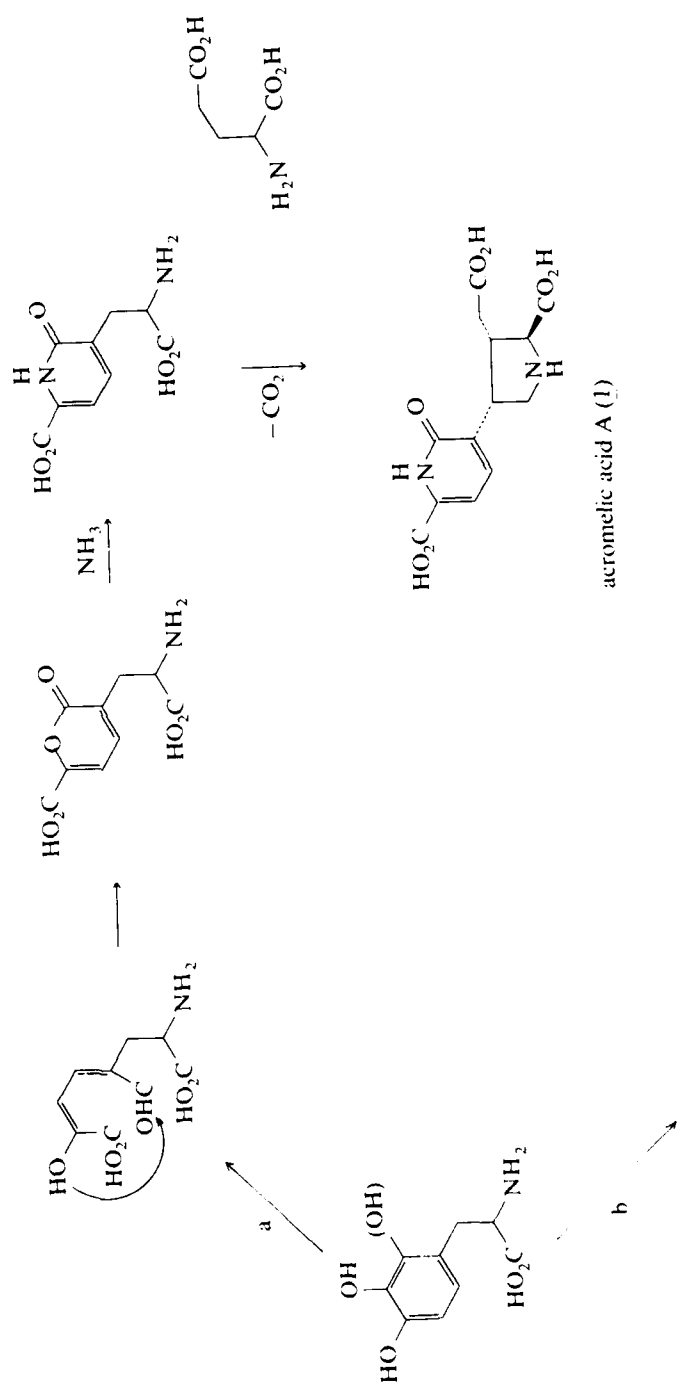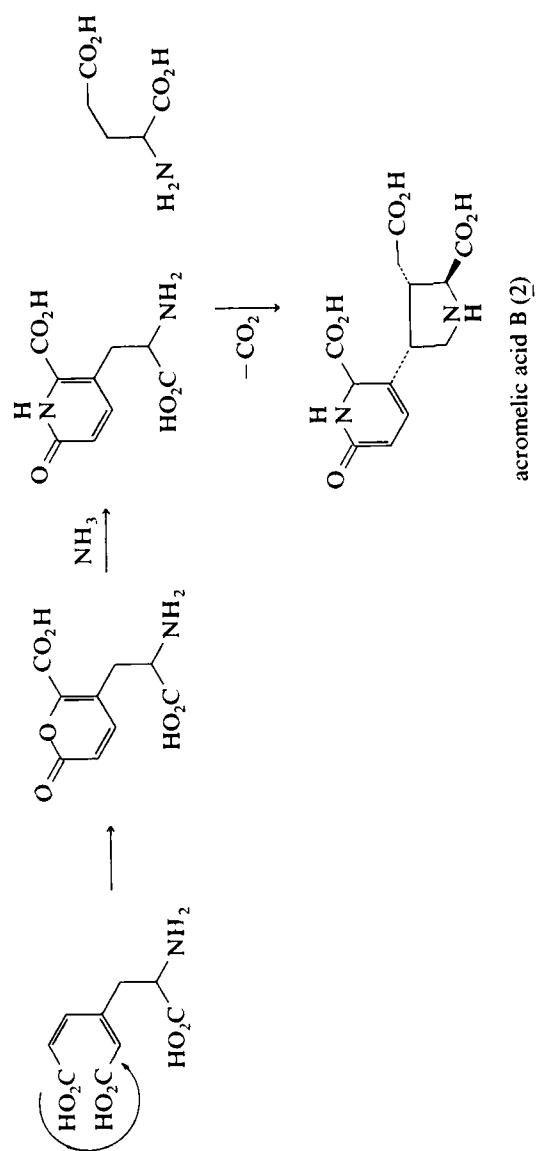
kainic acid (**3**)
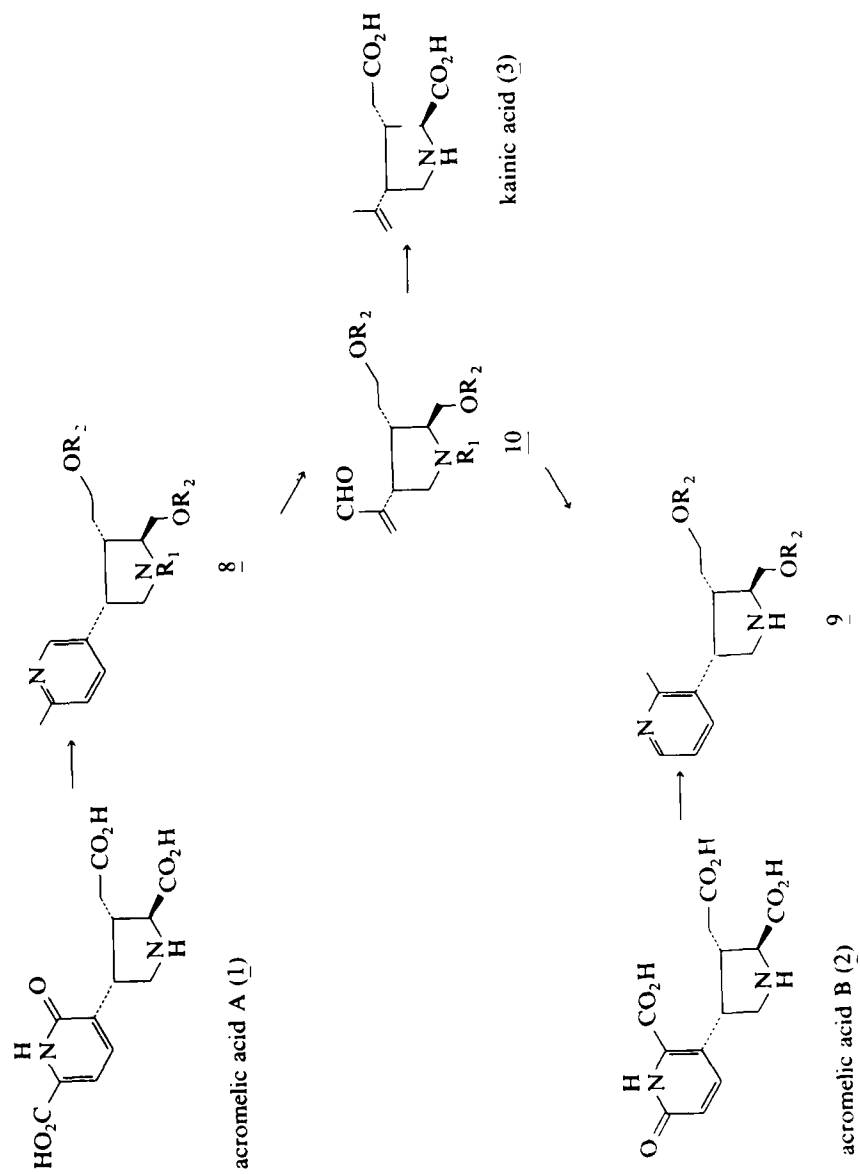
Scheme 4.

and carboxymethyl) are *trans* oriented, the signals of the α-proton appear at higher field than 4.2 ppm. On the other hand, in the *cis*-compounds, they appear at lower than 4.2 ppm, irrespective of the substituent at C-4. These data are shown in Fig. 4. The chemical shift values of the α-protons of 1 and 2 (4.13 and 4.16) were consistent with this empirical rule. Thus, acromelic acids A and B are best expressed by 1 and 2 respectively, except for absolute configuration.

Syntheses

Acromelic acids A 1 and B 2 were synthesized in order to corroborate the proposed structures and to provide samples for the biological assays.

The synthetic plan is outlined in Scheme 4. We chose L-α-kainic acid 3, which is commercially available in an optically pure form, as the starting material because it has stereochemistry identical to that of the target molecules. The key intermediates methylpyridines 8 and 9 would lead to 1 and 2, respectively, through the sequential oxidation of a methyl group to carboxylic acid and pyridine to pyridone. The α,β-unsaturated aldehyde 10 can be a precursor of the key intermediates 8 and 9 since it is convertible to the pyridines. Allylic oxidation of kainic acid should then afford the aldehyde 10.

The imino and carboxyl groups were successively protected in the conventional way ((1) Boc-ON (2) CH_2N_2) to afford dimethyl *N*-Boc-kainate in quantitative yield. In order to avoid the racemization at the α-position [16], the ester groups were reduced to alcohols ($LiAlH_4$), and then protected by silyl groups (TBDMSCl) to provide 11 in 70% yield. The use of selenium dioxide for the allylic oxidation of 11 afforded an undesired alcohol 13 instead of the desired material 12, as main product (Scheme 5). So the stepwise procedure that involved epoxidation and subsequent

1) $mCPBA/CH_2Cl_2$
2) Lithium tetramethylpiperidide/Et_2O
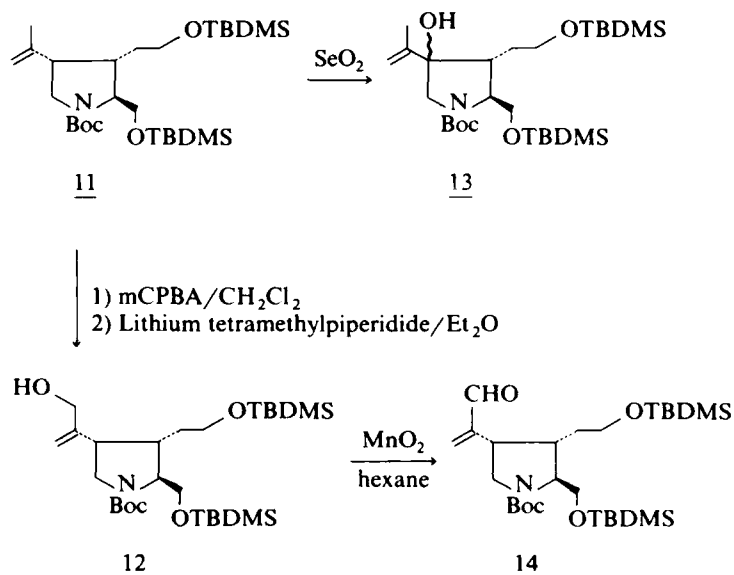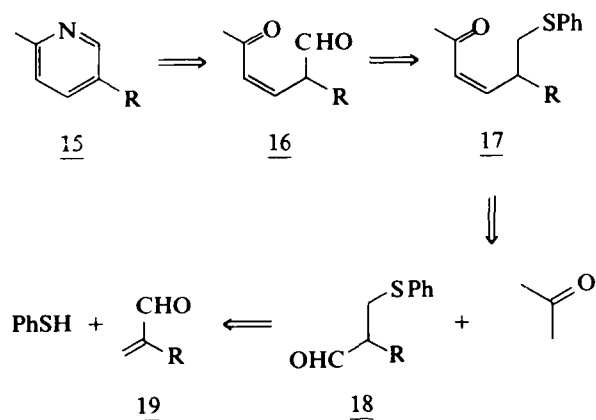
Scheme 5.

Scheme 6.

isomerization of the epoxide to allylic alcohol was examined. Epoxidation of 11 with mCPBA gave a corresponding epoxide in 97% yield, which was exposed to various reagents under various conditions. The best result was obtained by using LiTMP (4 equiv) in ether (0°C, 1 h → rt, 1 h), by which allylic alcohol 12 was obtained in
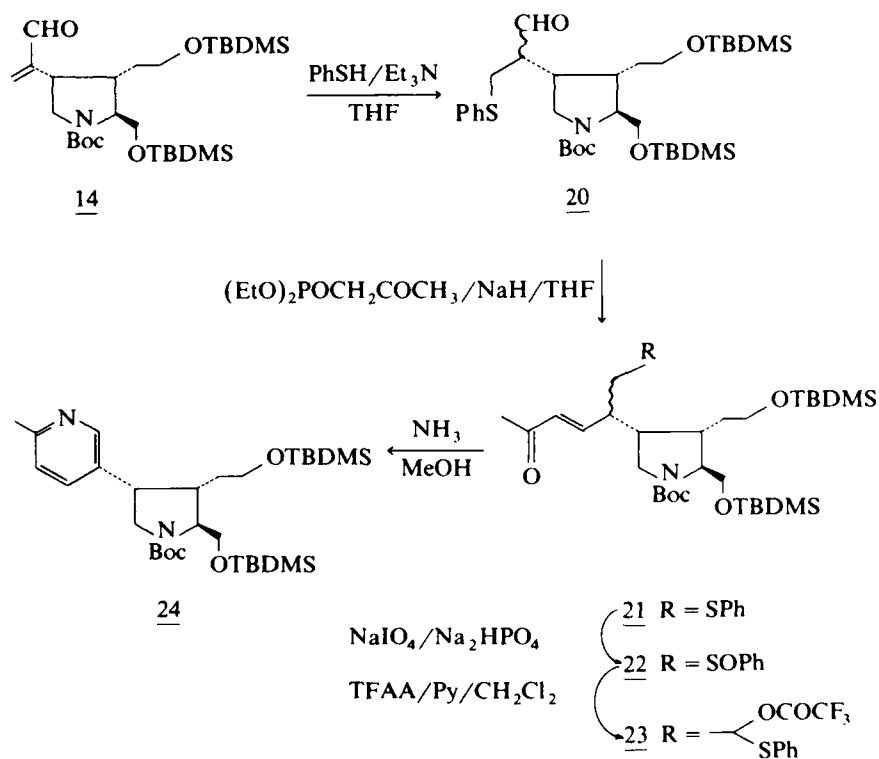
Scheme 7.

60% yield. Protective groups other than TBDMS (Me, MOM, MEM and Bzl) resulted in decrease of the yield. No epimerization of C-4 on the pyrrolidine ring was demonstrated by the conversion of 12 back to 11 ((1) TsCl, LiCl-MeLi (2) Zn). Further oxidation of 12 with MnO$_2$ produced aldehyde 14 in 86% yield.

Construction of the pyridine ring is the most crucial stage of this synthesis. After numerous model studies, we found a mild and efficient method of pyridine synthesis starting from α,β-unsaturated carbonyl compound [23]. Cyclization of unsaturated 1,5-dicarbonyl compound with a variety of ammonia sources is a facile process for pyridine ring formation [24]. However, difficulties encountered in preparation of the unsaturated 1,5-dicarbonyl system made it of limited use in synthesis. In our method the problem was solved by the use of the Pummerer reaction. As shown in Scheme 6, ketosulfide 17 can be regarded as a synthetic equivalent of ketoaldehyde

24

1) SeO$_2$/Py

2) CH$_2$N$_2$
3) n-Bu4NF/THF
4) PDC/DMF
5) CH$_2$N$_2$

25

mCPBA
CH$_2$Cl$_2$

26

TFAA
DMF

1) KOH/EtOH
2) TFA

acromelic acid A

1

27
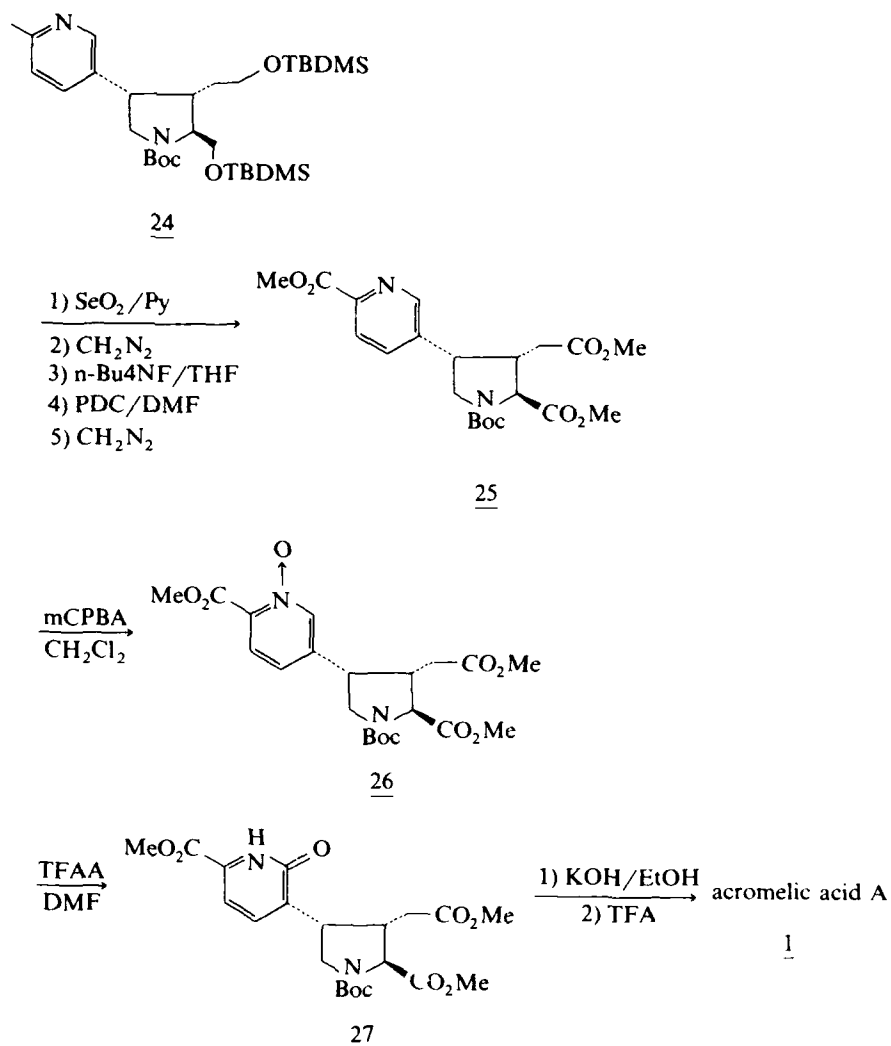
Scheme 8.

16, since the phenylthiomethyl group is convertible to an aldehyde by the Pummerer reaction. The ketosulfide 17 is readily accessible because the reaction sequence 19 → 18 → 17 is a feasible and conventional process.

Treatment of 14 with thiophenol afforded adduct 20 as a mixture of diastereoisomers in 93% yield, which was then converted to ketone 21 by the Horner-Emmons reaction. For oxidation of sulfide 21 into sulfoxide 22, Na_2HPO_4 was added to buffer the reaction mixture, otherwise the silyl protecting groups were partially removed. The Pummerer reaction of 22 proceeded smoothly under mild and neutral conditions (TFAA/Py, 0°C, 1 h) to furnish a rearranged product 23 in quantitative yield. The Pummerer product 23 was rather unstable, so that it was immediately cyclized by methanolic ammonia, in the same reaction vessel, to afford key intermediate 24 in good yield (Scheme 7).

The stage was set to complete the synthesis. Oxidation of methyl group in 24 by SeO_2 [25] gave the corresponding carboxylic acid, which was immediately esterified with CH_2N_2 and then desilylated with nBu_4NF. Treatment of the resulting diol successively with PDC/DMF and CH_2N_2 afforded triester 25 in 20% overall yield, which in turn was converted to N-oxide 26 by mCPBA in 77% yield.

The conversion of pyridine N-oxide into 2-pyridone in acetic anhydride is a well-known procedure developed by E. Ochiai and colleagues [26]. However, application of this procedure to picolinic acid derivatives resulted in low yield [27]. In addition, the conditions seemed to be too harsh for our compound. After some model studies, we found a better procedure with which the reaction proceeded rapidly but was mild enough, namely, by using trifluoroacetic anhydride instead of acetic anhydride in dimethylformamide at room temperature [28]. Exposure of N-oxide 26 to our modified condition gave pyridone 27 in good yield. Finally, acromelic acid A 1 was obtained from pyridone 27 by removal of the protective groups in a conventional manner (Scheme 8).

For the synthesis of acromelic acid B 2, methylpyridine 28 is the key intermediate. Again it can be prepared by our newly developed pyridine synthesis with only slight modification. In this case, the ketosulfide 30 is a precursor for pyridine 28 (Scheme 9). This can be obtained by 1,6-conjugate addition of thiophenol to $\alpha,\beta,\gamma,\delta$-unsaturated aldehyde 31. Two-carbon extension and subsequent Pummerer reaction would convert the sulfide 32 to the aldehyde 31 (Scheme 9).
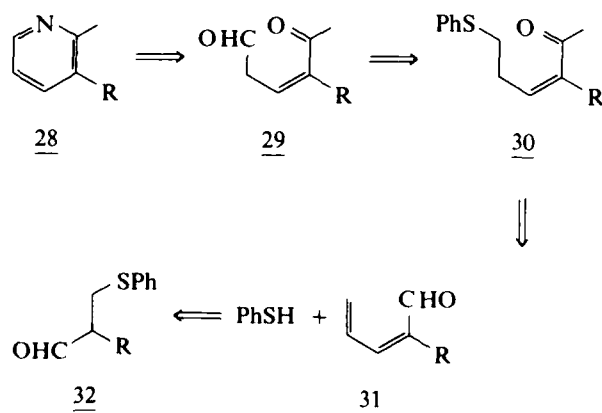
Scheme 9.

The sulfide 20 was subjected successively to the Horner-Emmons reaction and DIBAH reduction to afford allylic alcohol 33 as a mixture of diastereoisomers in high yield. The alcohol 33 was then converted to $\alpha,\beta,\gamma,\delta$-unsaturated aldehyde in

1) $(EtO)_2POCH_2CO_2Et$
   NaH/THF
2) DIBAH/PhCH$_3$

1) NaIO$_4$
   ─────────
   Na$_2$HPO$_4$
2) TFAA/Py
3) Na$_2$CO$_3$ aq.
4) MsCl/Et$_3$N/CH$_3$CN

34

1) PhSH
   ─────────
   Et$_3$N/DMF
2) MeLi/THF
3) PDC/DMF

35

1) NaIO$_4$
   ─────────
   Na$_2$HPO$_4$
2) TFAA/Py
3) NH$_3$ aq.

36

1) SeO$_2$/Py
   ─────────
2) CH$_2$N$_2$
3) pTsOH/MeOH
4) PDC/DMF
5) CH$_2$N$_2$

Scheme 10.

37
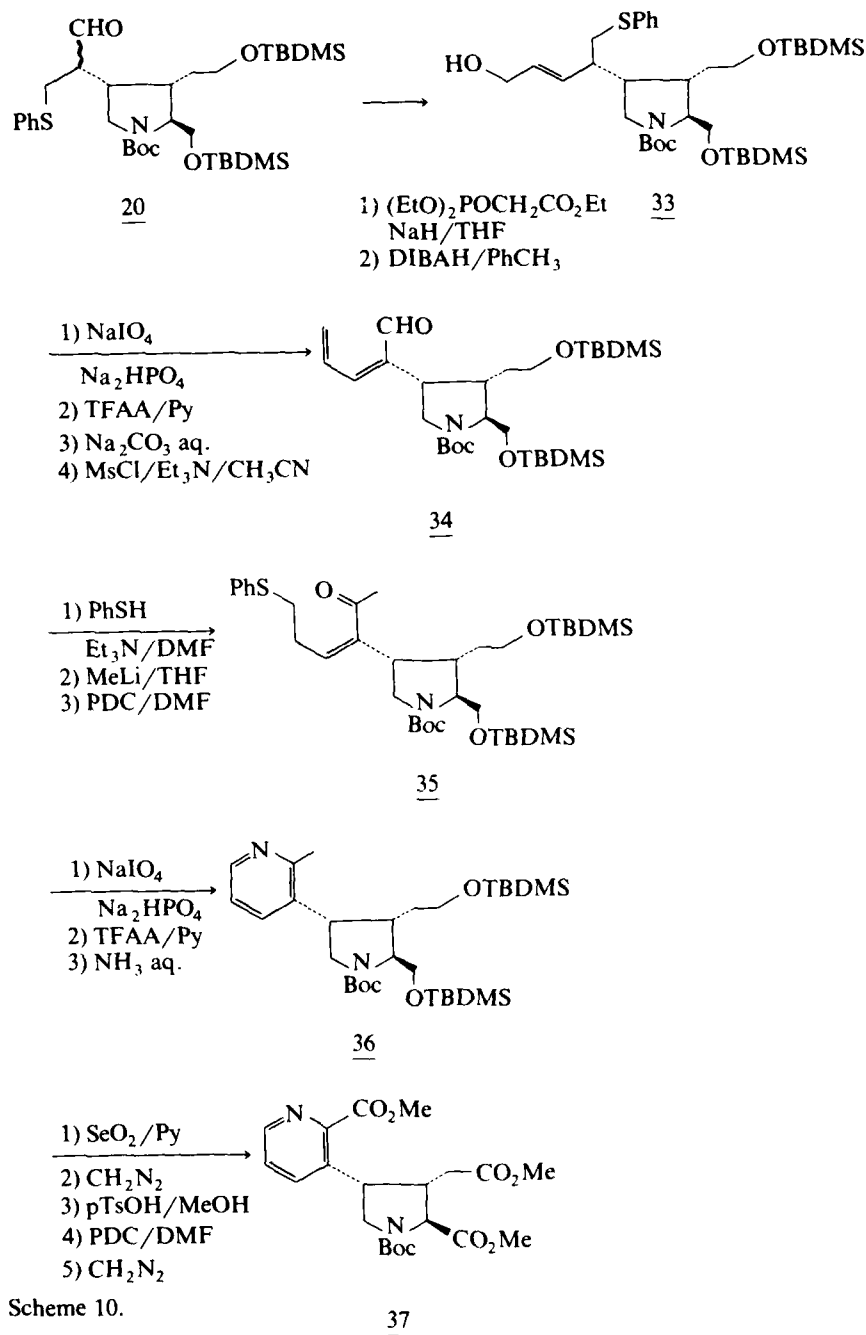
120

good yield by the Pummerer reaction and subsequent dehydration. Selective 1,6-conjugate addition of thiophenol to aldehyde 34 proceeded smoothly and the resulting adduct was successively treated with MeLi and PDC to yield ketone 35. In a similar manner to the conversion of 21 → 24, methylpyridine 36 was obtained from 35 in modest yield. Acromelic acid B 2 was synthesized from methylpyridine 36 through 37 and 38 in a similar manner to before (Scheme 10).

The synthetic materials were identical with natural products in all respects (^{1}H-NMR, UV and TLC, PEP mobilities), confirming the inferred structures of acromelic acids A 1 and B 2. The absolute configurations of both compounds were determined to be L, i.e. all three configurations were S, by the CD spectral comparison. Thus, the structures of acromelic acid A and B were established to be 1 and 2 respectively, including absolute configuration.

Two other synthetic studies on acromelic acid A have since been reported [29,30].

Neuroexcitatory properties

Examination of the action of acromelic acids at a crayfish neuromuscular junction revealed that both of the acids yielded the most potent depolarization among the compounds related to L-glutamic acid ever known. Acromelic acid A was 100 times more potent than kainic acid. The same action was also confirmed in rat central neurons. Thus, acromelic acids were found to be powerful neuroexcitants, and may be very useful tools in the field of neuroscience research [31].

In order to determine structure-activity relationships, several analogues of acromelic acid were prepared from intermediates obtained in the synthesis of 1 and
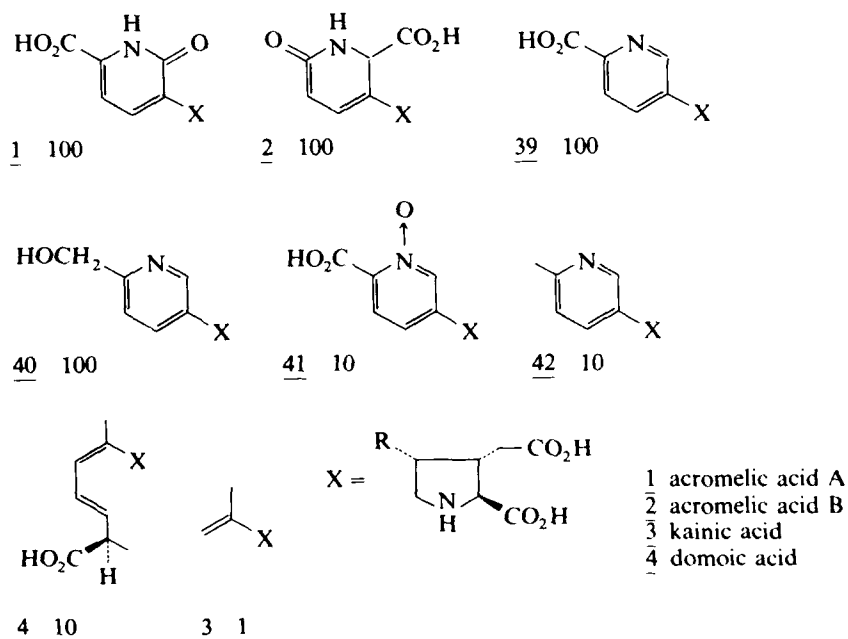
FIG 5   Relative strength of potentiation of excitatory responses to glutamate induced by acromelic acids A and B and their derivatives is roughly indicated.

their biological action was observed. Results are listed in Fig. 5. Substituents with π-electrons at C(4) of the pyrrolidine ring seem to enhance excitatory activity. A hydroxyl group on the carbon placed at C(6) of the pyridine nucleus, the opposite side of the pyrrolidine substituent, may also enhance activity. Further investigations are now being undertaken to differentiate between agonist and antagonist properties of the analogues.

References

1 Shirahama, H., Fukuoka, Y. and Matsumoto, T. (1962) Isolation and characterization of lunamycin, an antitumoric substance from *Lampteromyces japonicus*. Bull. Chem. Soc. Jpn. 35, 1048.

2 Matsumoto, T., Shirahama H., Ichihara, A., Fukuoka, Y., Takahashi, Y., Mori, Y. and Watanabe, M. (1965) Structure of lampterol (illudin S). Tetrahedron 21, 2671–2676.

3 Matsumoto, T., Shirahama, H., Ichihara, A., Shin, H., Kagawa, S., Sakan, F., Nishida, S. and Matsumoto, S. (1968) Total synthesis of d,l-illudin M. J. Am. Chem. Soc. 90, 3280.

4 Matsumoto, T., Shirahama, H., Ichihara, A., Shin, H., Kagawa, S., Sakan, F. and Miyano, K. (1971) Synthesis of illudin S. Tetrahedron Lett. 2049–2052.

5 Ayer, W.A. and Browne, L.M. (1981) Terpenoid metabolites of mushroom and related Basidiomycetes. Tetrahedron 37, 2199–2248.

6 Shirahama, H., Hayano, K., Kanemoto, Y., Misumi, S., Ohtsuka, T., Hashiba, N., Furusaki, A., Murata, S., Noyori, R. and Matsumoto, T. (1980) Conformationally selective transannular cyclization of humulene 9,10-epoxide. Synthesis of the two skeletally different cyclohumulanoids: dl-bicyclohumulenone and dl-africanol. Tetrahedron Lett. 21, 4835–4838.

7 Shirahama, H., Ohfune, Y., Misumi, S. and Matsumoto, T. (1978) Biogenetic like syntheses of illudoid sesquiterpenes. J. Synth. Org. Chem. Jpn. 36, 569–580.

8 Shirahama, H., Osawa, E. and Matsumoto, T. (1980) Conformational studies on humulene by means of empirical force field calculations. Role of stable conformers of humulene in biosynthetic and chemical reactions. J. Am. Chem. Soc. 102, 3208–3213.

9 Shirahama, H. (1986) Organic synthesis based on the physical organic chemistry. Kagaku to Kogyo 39, 106–109.

10 Konno, K., Hayano, K., Shirahama, H., Saito, H. and Matsumoto, T. (1982) Clitidine. A new toxic pyridine nucleoside from *Clitocybe acromelalga*. Tetrahedron 38, 3281–3284.

11 Konno, K., Shirahama, H. and Matsumoto, T. (1984) Clithioneine, an amino acid betaine from *Clitocybe acromelalga*. Phytochemistry 23, 1003–1006.

12 Hirayama, F., Konno, K., Shirahama, H. and Matsumoto, T. (1988) Studies on toxins of *Clitocybe acromelalga*. Ann. Meet. Chem. Soc. Jpn. Apr.: 4 IX B43.

13 Konno, K., Hashimoto, K., Ohfune, Y., Shirahama, H. and Matsumoto, T. (1988) Acromelic acids A and B. Potent neuroexcitatory amino acid isolated from *Clitocybe acromelaga*. J. Am. Chem. Soc. 100, 4807–4815.

14 Roberts, G.C.K. and Jardetzky, O. (1970) Nuclear magnetic resonance spectroscopy of amino acids, peptides, and proteins. Adv. Protein Chem. 24, 447–545.

15 Takemoto, T., Daigo, K., Kondo, Y. and Kondo, K. (1966) Studies on the constituents of *Chondria armata* VIII. On the structure of domoic acid. J. Pharm. Soc. Japan. 86, 874–877.

16 Ohfune, Y. and Tomita, M. (1982) Total synthesis of (–)-domoic acid. A revision of the original structure. J. Am. Chem. Soc. 104, 3511–3513.

17 McGeer, E.G., Olney, J.W. and McGeer, P.L. (1978) Kainic Acid as a Tool in Neurobiology, Raven Press, New York.

18 Rateb, L., Mina, G.A. and Soliman, G. (1968) Reactions of hydroxymethylene ketones. Part III. Synthesis of 1,2-dihydro-2-oxopyridine polycarboxylic acids. J. Chem. Soc. (c), 2140–2144.

122

19 Weber, H. (1976) Decker-oxidation 2-substituierter N-Alkylpyridiniumverbindungen, 5 Mitt. Die Decker-oxidation von Homarin. Arch. Pharm. 309, 664–669.
20 Saeki, Y., Nozaki, M. and Senoh, S. (1980) Cleavage of pyrogallol by non-heme iron-containing dioxygenases. J. Biol. Chem. 255, 8465–8471.
21 Musso, H. (1979) The pigments of fly agaric, *Amanita muscaria*. Tetrahedron 35, 2843–2853.
22 Nakamori, R. (1956) Studies on the active components of *Digenea simplex* Ag. and related compounds XXXI. Studies on the ozone oxidation products of kainic acid and its isomers. J. Pharm. Soc. Japan. 76, 275–300.
23 Konno, K., Hashimoto, K., Shirahama, H. and Matsumoto, T. A new pyridine synthesis starting from α,β-unsaturated carbonyl compounds, Tetrahedron Lett. 27, 3865–3868.
24 Klinsberg, E. (1960) The Chemistry of Heterocyclic Compounds. Vol. 14, Pyridine and its derivatives, Interscience, New York.
25 Jerchel, D., Bauer, E. and Hippchen, H. (1955) Die Oxydation von Alkylpyridinen mit Selendioxyd. Chem. Ber. 88, 156–163.
26 Ochiai, E. (1967) Aromatic Amine Oxides, Elsevier, Amsterdam.
27 Boekelheide, V. and Lehn, W.L. (1961) The rearrangement of substituted pyridine N-oxides with acetic anhydride. J. Org. Chem. 26, 428–430.
28 Konno, K., Hashimoto, K., Shirahama, H. and Matsumoto, T. (1986) Improved procedures for preparation of 2-pyridones and 2-hydroxymethylpyridines from pyridine N-oxides. Heterocycles 24, 2169–2172.
29 Takano, S., Iwabuchi, Y. and Ogasawara, K. (1987) A concise enantioselective synthesis of acromelic acid A. J. Am. Chem. Soc. 109, 5523–5524.
30 Baldwin, J.E. and Li, C.S. (1988) Enantiospecific synthesis of acromelic acid A via a cobalt-mediated cyclisation reaction. J. Chem. Soc. Chem. Commun. 261–263.
31 Shinozaki, H., Ishida, M. and Okamoto, T. (1986) Acromelic acid, a novel excitatory amino acid from a poisonous mushroom: effects on the crayfish neuromuscular junction. Brain Res. 399, 395–398.

Receptor sites for GABA and acetylcholine

CHAPTER 10

Trioxabicyclooctanes as probes for the convulsant site of the GABA-gated chloride channel in mammals and arthropods

JOHN E. CASIDA[1], RUSSELL A. NICHOLSON[2] AND CHRISTOPHER J. PALMER[1]

[1] *Pesticide Chemistry and Toxicology Laboratory, Department of Entomological Sciences, University of California, Berkeley,California 94720, U.S.A.;*
[2] *Wellcome Research Laboratories, Berkhamsted, Hertfordshire, U.K.*

Introduction

GABA receptor–chloride ionophore complex

γ-Aminobutyric acid (GABA) is the major inhibitory neurotransmitter in the vertebrate central nervous system (CNS) [1,2] and in the arthropod CNS and neuromuscular junction [3–5]. Activation of GABA receptors produces sedation and a decrease in motor activity while their inhibition provokes excitation and generalized seizures. The transmembrane portion of the GABA receptor ionophore complex functions as a chemically-gated chloride channel and is predominantly postsynaptic. This $GABA_A$ receptor contains the GABA recognition site and binding sites for benzodiazepines, barbiturates, anions and convulsants (Fig. 1) [1,2,6–8]. GABA-stimulated chloride flux is blocked by convulsants such as bicuculline, a highly-selective competitive antagonist, and picrotoxinin (PTX), a non-competitive antagonist. Chloride transport is enhanced by those benzodiazepines which are anxiolytic and by those barbiturates which function as anti-convulsants. The $GABA_A$ receptor consists of two α subunits and two β subunits, each of defined amino acid sequence and DNA coding, which are glycosylated and incorporated into the postsynaptic membrane [6]. The benzodiazepine binding site is on the α subunit and the GABA or muscimol binding site is on the β subunit, probably in the large N-terminal extracellular domains with extensive N-glycosylation [6]. The convulsant site is either at the mouth (extracellular opening) of the chloride channel [7] or at the anion binding site located in the channel lumen [9]. All of these sites are allosterically coupled so that a compound acting at one site affects binding of other compounds at their sites and binding at any site may disrupt the receptor's function [2,8].

GABAergic synapses and insecticide action

GABAergic neurotransmission is one of the most important and sensitive sites of insecticide action. PTX was used as an insecticide more than a century ago [10] and

GABA_A RECEPTOR IN POSTSYNAPTIC CELL MEMBRANE
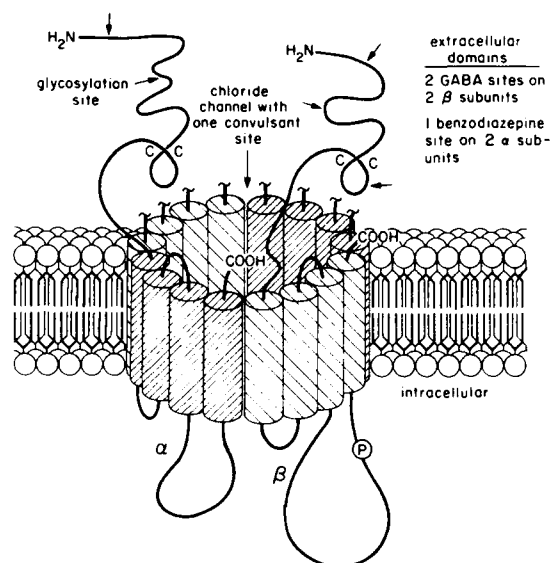
FIG 1 Schematic model for the topology of the GABA$_A$ receptor in the plasma membrane of the postsynaptic cell based on Barnard and coworkers [6]. Each subunit of the tetrameric structure $\alpha_2\beta_2$ consists of four membrane-spanning helices. Extracellular structures are shown for the presumed β-loop formed by a disulfide bond and for N-glycosylation sites. The intracellular site for cAMP-dependent serine phosphorylation on the β-subunit is also shown. A channel with a 5.6 Å bore lumen is formed by these 16 helices either in the extended relationship shown or preferably in a more compact arrangement with fewer helices actually making up the bore. This chloride channel is opened by the action of GABA and closed by competitive antagonists such as bicuculline. Benzodiazepines increase the frequency of channel opening and barbiturates prolong the channel open time. The GABA-gated chloride channel is blocked by convulsants such as picrotoxinin, trioxabicyclooctanes and polychloro-cycloalkanes acting at the mouth of the channel or at the anion binding site in the channel.

its action as a non-competitive GABA antagonist at the crayfish inhibitory neuro-muscular junction was elucidated in the mid-1960s [11]. Many PTX analogues have been examined as convulsants and candidate insecticides but without finding significantly more active compounds. Among other classes of chemicals the aver-mectins (including avermectin B$_{1a}$ and ivermectin), extremely potent insecticides/ acaricides/nematocides, are macrolide-like antibiotics isolated and shown in the late 1970s to act as agonists at GABA-mediated synapses and to increase chloride ion channel conductance [12]. The polychlorocycloalkanes (PCCAs) including lin-dane, the insecticidal bornane components of toxaphene, and the cyclodienes are a major group of insecticides developed mostly in the 1940s.

About 3×10^9 pounds of PCCAs have been used in the past 40 years. Their application is now restricted and only lindane, endosulfan, aldrin and chlordane are still used in amounts individually exceeding 1,000,000 pounds per year. The action of the PCCAs on GABAergic neurotransmission was elucidated in the early 1980s.

PTX   R = $\rangle$···}   lindane   toxaphene   polychloro-cyclodienes

[^{3}H]DHPTX R = ^{3}H ^{3}H$\rangle$···}   (Y-hexachloro-cyclohexane)   (octachlorobornane component 8-Cl-B)

2,6,7-trioxabicyclo[2.2.2]octanes (TBOs)

PO X = O phosphate   OB orthobenzoate (R$_I$ = Ph)

PS X = S phosphorothionate   OC orthocarboxylate (R$_I$ = aliphatic)
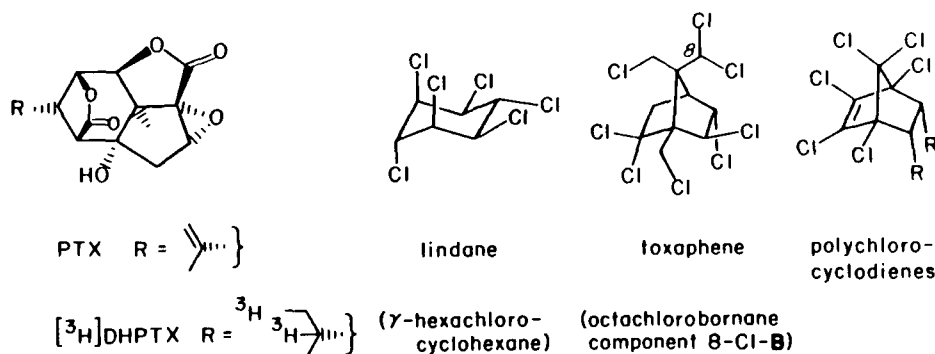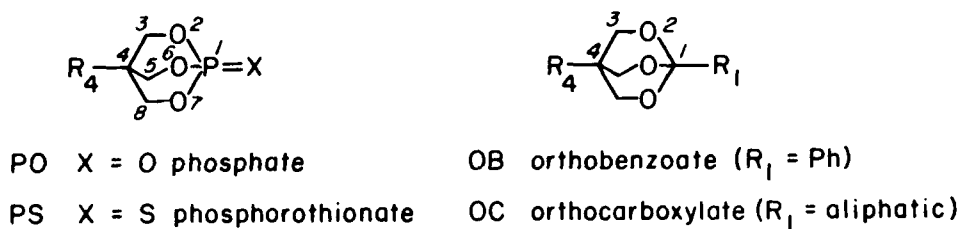
in part by comparing their neurotoxic mechanism to that of PtX and bicyclic cage convulsants discussed below.

Trioxabicyclooctanes as probes

2,6,7-Trioxabicyclo[2.2.2]octanes (TBOs) are relatively new probes for GABAergic neurotransmission in mammals [13–15] and some have significant levels of insecticidal activity [16,17].

The two TBOs most commonly used as probes are *t*-butylbicyclophosphorothionate (TBPS) and *t*-butylbicycloorthobenzoate (TBOB) [18]. shown below as isotopically-labelled compounds.

[^{35}S]TBPS   [^{3}H]TBOB
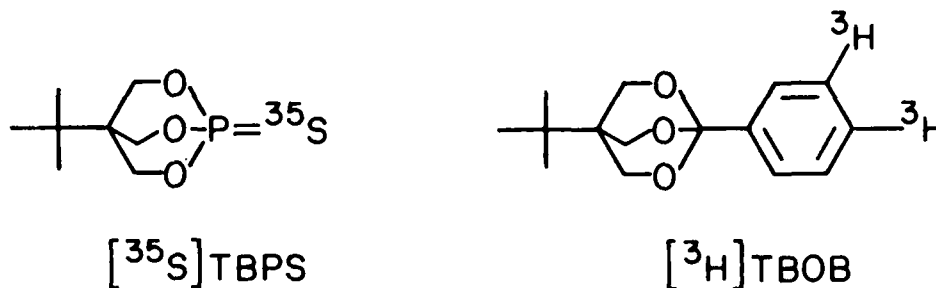
Analogues of TBOB with substituents in the 3-position of the bicyclic system or the *para* position of the phenyl group are referred to in this review by using prefixes for these substituents. Other TBOs are designated by trivial names derived from their substituents in the 4-position (i.e., Me methyl, Et ethyl, nPr n-propyl, iPr isopropyl, nBu n-butyl, sBu secondary butyl, tBu tertiary butyl, nPen n-pentyl, cHex cyclohexyl and cHept cycloheptyl) and the 1-substituent (i.e., PO, PS, OB or OC).

Neurophysiological studies

Vertebrates

The POs are highly toxic to mammals without inhibition of cholinesterase or disruption of the cholinergic system [13]. Convulsions induced in rats inhaling EtPO are associated with high amplitude spike discharges in their electroencephalograms which increase in frequency with the exposure time and poisoning signs and culminate in grand mal seizures [19]. Benzodiazepines and phenobarbital protect against poisoning by several POs and BOCs [13–15]. Cyclic GMP levels in rat cerebellum are elevated by EtPO and iPrPO at both convulsive and subconvulsive doses, and diazepam decreases the PO effect on both cyclic GMP and on toxicity. This PO-induced elevation in cyclic GMP levels may be an expression of an increased release of excitatory transmitters from neurons synapsing on the Purkinje cells [20]. With a series of 4-alkylPOs, their potencies as GABA antagonists assessed from the depression of depolarizing responses to GABA in the rat superior cervical ganglion and the frog spinal cord are correlated with their convulsant potency in intravenously (i.v.)-treated mice [21,22] (Fig. 2).
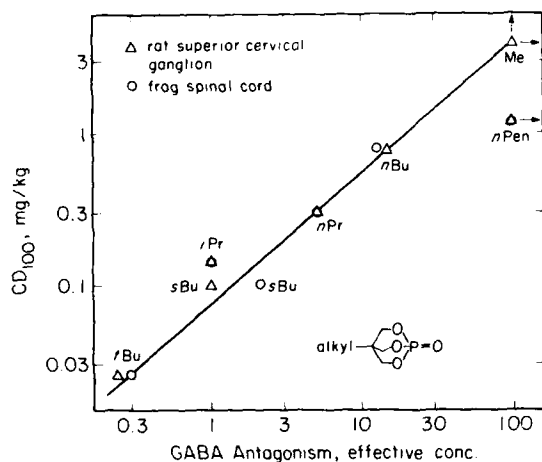
FIG 2   Correlation between potency of 4-alkylbicyclophosphates as inhibitors of GABA-induced depolarization in the rat superior cervical ganglion and the frog spinal cord and their convulsant potency in i.v.-treated mice. The effective concentration for GABA antagonism is relative to iPrPO as 1.0. CD_{100} is the convulsant dose for 100% of the mice (based on Refs. 21 and 22).
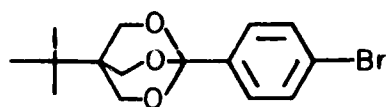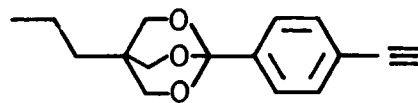
p-bromo-TBOB *p*-ethynyl-*n*PrOB

Arthropods

*t*BuPO, TBPS and PTX antagonize the GABA-induced relaxation of the crayfish neuromuscular junction [11] with IC_{50}s of 25, 140 and 830 μM, respectively [23]. GABA-mediated relaxation of the *Periplaneta americana* coxal depressor muscle is inhibited by 5 μM *p*-bromo-TBOB but not as quickly or completely as by 5 μM PTX [24]. Intoxication in *P. americana* and *Blabera craniifer* by *p*-ethynyl-*n*PrOB is closely associated with bursting activity in the CNS monitored in situ in the abdominal nerve cord with associated connectives [25]. This bursting activity originates predominantly in the 6th abdominal ganglion rather than in the nerve cord or the cercal nerves. The actions of *p*-ethynyl-*n*PrOB on the cockroach CNS are consistent with the expected block in GABA-mediated chloride channels [25].

Ivermectin-stimulated release of neurotransmitter from *P. americana* CNS synaptosomes (measured as release of radiolabel from nerve terminal loaded with [^{3}H]choline) is inhibited by various convulsants with IC_{50}s of about 300 nM for PTX, 200, 100, 30 and 10 nM for four PCCAs (bromocyclen, dieldrin, lindane and endosulfan, respectively), and 2 nM for a particularly potent TBOB analogue discussed later [26,72]. In contrast, TBPS even at 1000 nM does not inhibit neurotransmitter release from *P. americana* synaptosomes [27]. Although the TBOs appear to act as GABA antagonists in insects and other arthropods, these physiological findings and binding studies discussed later indicate that they may not all act at the same site or in the same manner.

Chloride conductance

The use of ^{36}chloride enables direct measurement of GABA-induced chloride uptake or efflux in tissue or membrane preparations.

Vertebrates

GABA-stimulated ^{36}chloride uptake is sensitive to inhibition by GABA$_A$ receptor antagonists using membrane vesicles or microsacs from rat cerebral cortex and mouse brain [28-34] or cultured cerebral neurons from chick embryo cerebrum [35,36]. The inhibitory potency of various convulsants for GABA-stimulated ^{36}chloride uptake in brain membrane preparations is generally correlated with their toxicity to rats and mice. This applies not only to the TBOs [34] but also to the PCCAs [29-34], PTX and tetramethylenedisulfotetramine (TETS) [34].

Arthropods

PTX inhibits GABA-stimulated ^{36}chloride uptake in crayfish abdominal muscle [37] and PTX and two PCCAs (lindane and heptachlor epoxide) are inhibitory in *P.*

TABLE 1 Binding characteristics and biological activities of five radioligands for the convulsant site of the GABA-gated chloride channel in mammalian brain

Parameters	PTX	Phosphorus esters		Orthobenzoates	
		nPrPO	TBPS	TBOB	p-Cyano-sBuOB
Radioligands [a]					
Isotope	^{3}H	^{3}H	^{35}S	^{3}H	^{3}H
B_{max}, pmol/mg protein	5	2	6	1.6	– [b]
K_d, nM	1000–2000	30000	17	61	– [b]
Specific binding, %	10	– [b]	67–77	80–90	– [b]
IC$_{50}$, [^{35}S]TBPS site, nM [c]	245	1100	62	49	5 [d]
LD$_{50}$, mg/kg					
Mouse IP [e]	4	0.38	0.053	1.3	0.56 [d]
Housefly topical [f]					
Alone	> 500 [d]	> 500 [d]	> 500	> 500	45 [d]
Piperonyl butoxide	> 500 [d]	> 500 [d]	> 500	23	1.1 [d]

[a] References are given in the text. The radioligand data are for [^{3}H]DHPTX and the IC$_{50}$ and LD$_{50}$ values are for PTX.
[b] Data not available.
[c] Refs. 24 and 47.
[d] Unpublished results.
[e] Refs. 18, 24 and 47. IP = intraperitoneal.
[f] Ref. 16. Temperature 25°C.

americana coxal muscle [38,39]. The effect of the TBOs on ^{36}chloride flux has apparently not been examined in arthropod systems.

Convulsant binding sites

PTX was the only significant probe for the action of non-competitive convulsants on the GABAergic system until the 1970s; [^{3}H]dihydropicrotoxinin ([^{3}H]DHPTX) was introduced in 1978 as the first radioligand for the convulsant binding site [40,41]. The TBOs provided improved radioligands with [^{3}H]nPrPO recognized in 1982 [42], [^{35}S]TBPS in 1983 [43,44], [^{3}H]TBOB in 1985 [45] and [^{3}H]p-cyano-sBuOB in 1988 [46]. It is obvious from the low dissociation constants (K_ds) and high percentages of specific binding in mammalian brain preparations that [^{35}S]TBPS
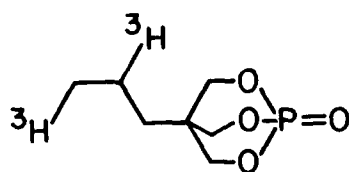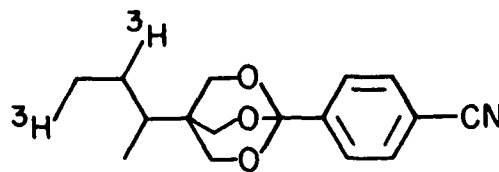
[^{3}H]nPrPO   [^{3}H]p-cyano-sBuOB

and [^{3}H]TBOB are preferred over [^{3}H]DHPTX and [^{3}H]nPrPO (Table 1). Current commercial radioligands for the convulsant site are [^{35}S]TBPS (NEN Research Products) and [^{3}H]TBOB (Amersham Corporation); [^{3}H]DHPTX (NEN Research Products) was discontinued as a commercial radioligand in 1984. The most toxic of these compounds to mice is TBPS and to houseflies is p-cyano-sBuOB, which is also the most potent at the mammalian binding site.

Vertebrates

[^{35}S]TBPS can be used in a simple and rapid radioligand binding assay for the convulsant receptor and modulatory sites of the GABA-gated chloride channel [43,44]. The potencies of various cage convulsants in inhibiting [^{35}S]TBPS binding are generally correlated with their potencies in inhibiting GABA-stimulated ^{36}chloride flux [29–34], giving apparently different lines for the TBOs and other cage convulsants compared with the lipophilic PCCAs (Fig. 3). The convulsants are several-fold relatively more potent in the [^{35}S]TBPS assay than in the ^{36}chloride flux system possibly because the modulating effect of GABA is absent in the [^{35}S]TBPS investigations but is necessarily present in the ^{36}chloride assays [34].

The possible relationship between receptor site potency and toxicity, first considered with PTX, POs and TETS for [^{3}H]DHPTX binding [40,41], was established with the TBOs in general for [^{35}S]TBPS binding [24,43]. The potencies of convulsants in the [^{35}S]TBPS assay are closely correlated with their mammalian toxicities as established with the TBOs [24,43], PCCAs [48] and other GABA$_A$ receptor antagonists [24,43,48]. A series of correlations between potencies as GABA antagonists with convulsions, inhibitions of TBPS binding with inhibitions of chloride flux, inhibitions of chloride flux with toxicities, and inhibitions of TBPS binding with toxicities strongly indicate that the GABA-gated chloride channel is the target site involved in toxicant action (Table 2).

Mice and rats poisoned with PCCAs and a potent OB show inhibition of the [^{35}S]TBPS binding site in brain correlated with the poisoning symptoms (Table 3).
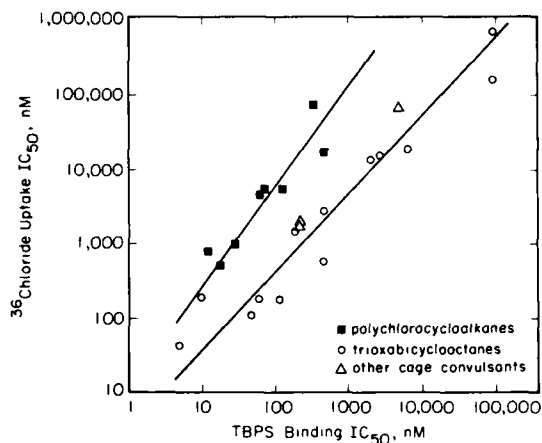
FIG 3 Correlation between potency of trioxabicyclooctanes, polychlorocycloalkanes and other cage convulsants as inhibitors of [^{35}S]TBPS binding in human and mouse brain membranes and as inhibitors of GABA-stimulated ^{36}chloride uptake in membrane vesicles from rat cerebral cortex (based on Ref. 34).

TABLE 2 Correlations between potency of cage convulsants as GABA antagonists, as inhibitors of chloride flux and TBPS binding, and as convulsants and toxicants

Correlation		Compounds		Fig. [a]
Relationship [a]	Coeff.	Type	No.	
GABA antagonism with convulsions	0.97 [b]	POs	5	2
TBPS binding with chloride flux	0.94	PCCAs	8	3
	0.96	Others	16	3
Chloride flux with toxicity	0.90	A [c]	15	4
	0.92	B [c]	8	4
TBPS binding with toxicity	0.77	A [c]	60	5
	0.96	B [c]	15	5

[a] Assay systems are defined in Figs. 2–5.

[b] Correlation coefficient based on 10 data sets for two assay systems. Two other compounds were of little or no activity.

[c] Type A: OBs, OCs with large 1-substituents, PTX and PCCAs. Type B: POs, PSs, OCs with small 1-substituents and TETS.

Detection of in vivo inhibition from in vitro assays (i.e., ex vivo studies) is not possibly with present techniques for PTX, TBPS, TBOB, TETS and several other convulsants possibly due to their more rapid dissociation from the binding site during receptor preparation involving repeated washes to remove endogenous GABA [47–49].

[^{35}S]TBPS binds to sites which are allosterically coupled to separate (but interacting) GABA, benzodiazepine, barbiturate, and chloride ion recognition sites [43]. Scatchard analyses indicate that the convulsants PTX [44], TBOB [45,50] and four PCCAs (lindane, endrin, 12-ketoendrin and the 8-Cl-B component of toxaphene) [48,51,52] interact competitively with TBPS at the same, or at a closely-coupled site. GABA inhibits [^{35}S]TBPS binding non-competitively [43,53]; this inhibition is reversed by the amidine steroid R5135 and other GABA$_A$ receptor blockers [43,54]. Basic neuroproteins such as GABA-modulin from brain synaptosomes modulate the GABA receptor-ionophore complex and are non-competitive inhibitors of [^{35}S]TBPS binding [55]. Some benzodiazepines and barbiturates also strongly interact with the [^{35}S]TBPS binding site [43,54,56]. Avermectin B$_{1a}$ and ivermectin inhibit [^{35}S]TBPS binding with IC$_{50}$s of 400 nM [57] and 60 nM [58], respectively, but in other studies avermectin B$_{1a}$ at low concentration stimulates [^{35}S]TBPS binding [59,60].

TABLE 3 Ex vivo inhibition of [^{35}S]TBPS binding site in brains of mice and rats with mild symptoms or convulsions following administration of polychlorocycloalkanes or a bi-cycloorthobenzoate

Compound	Species	% Inhibition		Ref.
		Mild symptoms	Convulsions	
Dieldrin	rat	33	78	48
PCCAs	mouse	32 ± 3 [a]	62 ± 4 [a]	47
3-Cyano-p-ethynyl-TBOB	mouse	35	70	49

[a] S.E. values (n = 13)

TABLE 4   Characteristics of [^{35}S]TBPS specific binding to human and rat brain receptor preparations [58]

Characteristic	Human	Rat
K_d, nM	61	66
B_{max}, pmol/mg protein	7	6
Specific binding, % of total	89	90
Association rate, $t_{1/2}$ in min	10	5
IC$_{50}$s of inhibitors, nM		
TBOs		
TBPS	32	28
TBOB	51	24
PCCAs		
Heptachlorobornane **B**	26	32
12-Ketoendrin	44	36
α-Endosulfan	7 [a]	11 [a]
Lindane	960	1000
Others		
Muscimol	306	259
GABA	2400	1400
PTX	418	551
Anisatin	305	138
Ivermectin	57	61

[a] Value corrected from original reference.

The vertebrate brain [^{35}S]TBPS receptor varies surprisingly little in its binding parameters between human, cow, rat, chicken and fish indicating that the GABA$_A$ receptor is evolutionarily conserved [58]. The principal difference between species is that α-endosulfan is 2.4- to 5-fold more potent in inhibiting [^{35}S]TBPS binding in mammalian brain than in chick or fish brain [58]. The almost identical characteristics of [^{35}S]TBPS specific binding to human and rat receptor preparations (Table 4) [58] are particularly interesting. Endrin-resistant mosquitofish, which also tolerate PTX and TBPS, have as one factor in the resistance mechanism a modified binding site in brain with reduced binding affinity for [^{35}S]TBPS [1].

Arthropods

An understanding of the comparative properties of the mammalian and arthropod convulsant receptors may help in the development of selective insecticides. If these receptors are very similar or identical, then data for the mammalian [^{35}S]TBPS binding site should be predictive of the toxicity not only to mammals but also to insects. The most appropriate insect data for this comparison are for houseflies pretreated with piperonyl butoxide, since this synergist blocks oxidative detoxification and therefore emphasizes differences at the neuroreceptor. Correlation coefficients for potency at the mammalian brain TBPS site and toxicity to houseflies (for all compounds with discrete data) vary with the substituents [1,24]. They are relatively good for the OBs [$r = 0.84$ ($n = 8$) for *para*-substituted TBOBs, $r = 0.64$ ($n = 9$) for p-chloro-OBs varying in the 4-substituents, and $r = 0.68$ ($n = 34$) for all the OBs] but are very poor for the OCs [$r = 0.07$ ($n = 16$)]. There are many additional compounds, not included in these correlations, that are potent inhibitors at the TBPS site but are inactive on houseflies. It appears that the structural features

TABLE 5 Four radioligands for the convulsant site in arthropods

Characteristics	$[^3\text{H}]$DHPTX		$[^3\text{H}]n$PrPO	$[^{35}\text{S}]$TBPS				$[^3\text{H}]p$-Cyano-s-BuOB
	Crayfish muscle	Cockroach CNS	Housefly [a]	Crayfish muscle	Housefly [a]		Cockroach CNS	Cockroach CNS
K_d, μM	1.1	0.8	0.004	0.03	0.05	0.2	0.02	0.003 [b]
B_{max}, pmol/mg protein	6.5	1.4	0.03	0.1	0.25	2.3	0.2	0.1
Specific binding, %	10–20	11	89	55	40	70–75	50–70	84
Inhibitors [c]								
PTX	+	+	−	+	+	+	nt	+
POs, PSs	nt	+	+	+	+	+	nt	±
PCCAs	nt	+	−	+	+	+	nt	+
OBs	nt	nt	−	nt	nt	+	nt	+
GABA effect	none	nt	none	none	none	stim.	inhib.	inhib.
References	62	63, 64	65, 66	67	67	68,69	70	46

[a] Membranes from head used for Refs. 65–67 and thoraces plus abdomens for Refs. 68 and 69.
[b] Level at which specific binding is essentially saturated.
[c] Sensitive to inhibition (+), insensitive to inhibition (−) or not tested (nt).

conferring fit at the housefly receptor are considerably different than those for the mammalian site(s).

The nature and properties of the arthropod convulsant receptors (Table 5) are not as well understood as those for mammals (Tables 1 and 4). [^{3}H]DHPTX was first used to study crayfish muscle [62] and then the cockroach CNS with particular reference to chlorinated insecticides [63,64] but this radioligand is unsatisfactory due to low specific binding, as with mammals. Cyclodiene-resistant strains of German cockroaches also tolerate PTX and their brain binding site has a lower binding capacity for [^{3}H]DHPTX than that from a susceptible strain [64]. The scope of this modified target site resistance in limiting insecticide action remains to be defined.

Results with housefly preparations differ considerably with [^{3}H]nPrPO [65,66] and [^{35}S]TBPS [67–69] as the radioligands. The most potent inhibitor among 10 POs examined with[^{3}H]nPrPO as the radioligand is the compound itself and there is no more than a trend in relating receptor potency of POs to their injected toxicity in piperonyl butoxide-pretreated houseflies; other GABA$_A$ receptor antagonists active in mammals are inactive in these fly preparations [65,66]. The [^{35}S]TBPS receptor in houseflies is the most extensively studied insect preparation [67–69]. The receptor potency of 4 PSs parallels their injected toxicity but this correlation does not extend to 9 POs. Cyclodienes of low toxicity are poor inhibitors of [^{35}S]TBPS binding relative to those of high toxicity. In contrast to mammals, PTX and heptachlor epoxide are non-competitive inhibitors of [^{35}S]TBPS binding in housefly preparations. The stereospecificity of the hexachlorocyclohexane isomers with γ more toxic than α, β or δ is reproduced in their potency at the fly and roach receptors [63,69]. This stereospecificity also extends to isomers of the chlorocyclohexane attractants trimedlure and siglure with their potency at the housefly receptor paralleling their attractancy for the male Mediterranean fruit fly but not their toxicity to houseflies [69]. These overall findings with chlorocyclohexanes indicate that the GABA receptor–ionophore complex may be involved in both toxicant and attractant action and that receptor potency does not always confer insecticidal activity [69].

A recent attempt to optimize a radioligand for the insect receptor used a potent insecticide, p-cyano-sBuOB (Table 1), and the cockroach CNS. p-Cyano-sBuOB itself is a better inhibitor than another OB, PTX and two PCCAs [46]. In an overall consideration of the arthropod systems examined (Table 5), GABA inhibits in two and stimulates in another but is usually without effect. No combination of radioligand and insect nerve preparation examined to date adequately predicts insecticidal activity.

Structure–activity relationships

The influence on biological activity of modifications at the 4-position of TBOs differs greatly from that of comparable changes at the 1-position. Effective 4-substituents are C_3 to C_6 alkyl or phenyl with tBu at or near the optimum. This observation applies to the POs, PSs, OBs and OCs. It also holds for the [^{35}S]TBPS receptor of mammalian brain and for toxicity to mice and houseflies. The convulsant receptor appears in each case to include a binding site that accommodates tBu or a similar substituent.

TABLE 6 Discontinuous structure–activity relationships and two types of action of 4-*t*-butyltrioxabicyclooctanes as inhibitors of [^{35}S]TBPS binding in mammalian brain membranes and as toxicants for mice and houseflies [16,18,24,71]

X substituent of *t*BuC(CH$_2$O)$_3$X	Receptor IC$_{50}$, nM	LD$_{50}$, mg/kg [a]			Type of action
		Mouse	Housefly	Housefly/ mouse	
P=S (TBPS)	62	0.053	> 500	> 9434	B
P=O	170	0.036	> 500 [b]	> 13889	B
CC≡CH	480	0.43	90	209	B
CH	7200	9.5	> 500	> 53	B
CMe	23000	6.0	> 500	83	B
CEt	100000	145	> 500	> 3	B
C*i*Pr	> 10000 (0%)	> 500	> 500	– [c]	– [c]
C*n*Pr	1150	13	425	33	A
C*n*Bu	118	1.4	55	39	A
C*n*Pen	27	6.6	33	5	A
C*c*Hex	970	25	3.5	0.14	A
C*c*Hept	1285	92	2.0	0.02	A
CPh (TBOB)	49	1.3	23	18	A
CPh-*p*-CN	5	0.06	0.23	4	A

[a] IP for mice and topical with the synergist piperonyl butoxide for houseflies. Temperature 25°C.
[b] Unpublished result.
[c] Inactive in all assays.

Two different relationships are evident from results for compounds with various 1-substituents, e.g. as illustrated with the 4-*t*Bu series in Table 6. First, there is a discontinuous structure–activity relationship for inhibition of TBPS binding and mouse toxicity. The active compounds have small (PSs, POs and some OCs) or large (OBs and some OCs) 1-moieties whereas compounds with 1-substituents of intermediate size (CEt, C*i*Pr) have little or no activity. Second, the 1-substituent has a marked influence on the selective toxicity, i.e., the LD$_{50}$ ratio for housefly/mouse. Compounds with small 1-substituents are selectively toxic to mice whereas those with large 1-substituents are less selective for mice or even become selectively toxic to houseflies. The greatest selectivity is conferred by the 1-*c*Hex and 1-*c*Hept substituents. The data in Table 6 further illustrate that the TBPS assay with mammalian brain predicts mouse toxicity better than housefly toxicity.

Two apparent types of action

Several observations with mammals and one with insects led to the subdivision of the cage convulsants into two types (A and B), possibly differing in their sites or types of action at the GABA-gated chloride channel [71]. Initially, the discontinuous structure–activity relationships of the TBOs suggested this subdivision [18] (Table 6). Studies relating potency at the TBPS site and toxicity gave poor correlations for all the TBOs but with increasing improvement in the correlation coefficients on first separating the OCs from the OBs [24] and then dividing the OCs with large 1-substituents from those with small 1-substituents [71]. It then became apparent
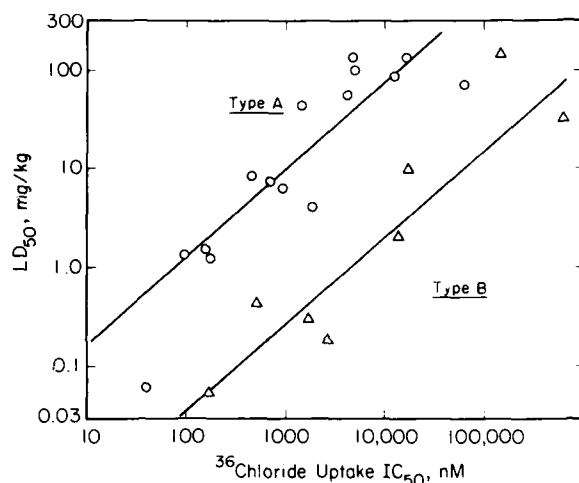
FIG 4 Correlation between potency of types **A** and **B** convulsants in inhibiting GABA-stimulated ^{36}chloride uptake by membrane vesicles from rat cerebral cortex and their toxicity to IP-treated mice. Type **A** convulsants are the bicycloorthobenzoates, bicycloorthocarboxylates with large 1-substituents, polychlorocycloalkanes and picrotoxinin. Type **B** convulsants are the bicyclophosphorus esters, bicycloorthocarboxylates with small 1-substituents and tetramethylenedisulfotetramine (based on Ref. 71).

that the OCs with large 1-substituents fall in with the OBs and, perhaps surprisingly, also with PTX and the PCCAs, collectively designated as type **A** action [71]. This left the OCs with small 1-substituents which behaved the same way as the POs, PSs and TETS, designated as type **B** action. The type **A** compounds are generally larger or more extended and include the OBs (such as TBOB), the OCs with large 1-substituents (nPr, nBu, nPen, cHex and cHept), PTX and the PCCAs. The type **B**s are generally smaller molecules and include the PSs (such as TBPS), POs, OCs with small 1-substituents (H, Me, Et and ethynyl) and TETS [71].

Type **A** convulsants are generally 300- to 500-fold better inhibitors of the TBPS site and 30- to 50-fold more potent at the chloride channel than those of type **B**, when the comparisons are based on compounds with similar mouse LD_{50} values (Figs. 4 and 5). More rapid detoxification of compounds of type **A** than of type **B** action might contribute to this difference, but this hypothesis is not supported by available synergism [24] and metabolism [72,73] studies. The two types of action are not evident in the TBPS or chloride flux assays alone but only when the potency in the in vitro assays is related to the mammalian toxicity. As noted above, the binding sites of [^{35}S]TBPS, [^{3}H]TBOB, PTX and 4 PCCAs in brain membranes are not differentiated by Scatchard plots or other types of competitive displacement studies. There is also a similar distribution of binding sites in brain for [^{35}S]TBPS and [^{3}H]TBOB [17]. Compounds of types **A** and **B** may interact with a single convulsant site but differ in the degree to which receptor binding leads to a block in GABA-mediated neurotransmission. Alternatively, they may act at sites differing in their localization within the CNS, significance in the overall poisoning process, or inhibitor specificity. The types **A** and **B** categories may also be applicable to insecticidal activity and the insect nervous system. Interestingly, on topical applica-
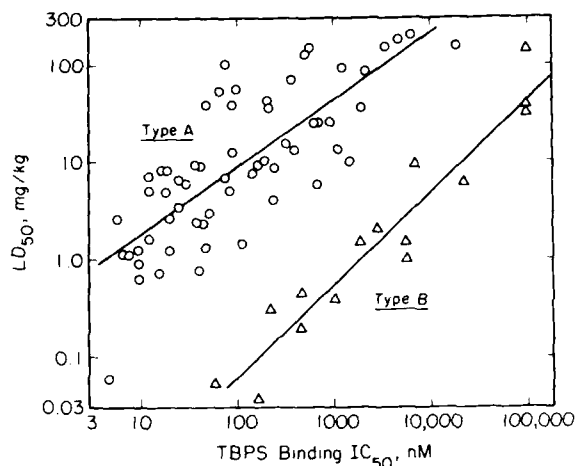
FIG 5 Correlation between potency of types A and B convulsants as inhibitors of [^{35}S]TBPS binding in human and mouse brain membranes and their toxicity to IP-treated mice. Convulsants falling into the types A and B categories are defined in the legend to Fig. 4 (based on Ref. 71).

tion compounds of type A action are generally much more potent insecticides than those of type B action [71] (Table 6). The molecular mechanism(s) that differentiates types A and B actions in mammalian brain is therefore also likely to be present in the insect nervous system.

Potency relationships

The TBOs are a relatively recent class of synthetic organic toxicants and candidate insecticides. They are remarkable in their combination of structural simplicity and neurotoxic potency. The most toxic TBOs to mice are p-cyano-TBOB, TBPS and the corresponding phosphate and phosphite [18,24].

The most insecticidal TBO in topical tests with houseflies is p-ethynyl-TBOB which is equal in potency to [1R,cis]permethrin at 25°C and [1R,cis,αS)]cypermethrin at 35°C (and much more potent than [1RS,cis,trans]permethrin or [1RS,cis,trans,αRS]cypermethrin) [74]. It is also very toxic to P. americana.
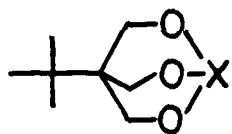
X = P, P = O, P = S

X = CPh-p-CN

mouse IP LD$_{50}$s 0.04-0.06 mg/kg
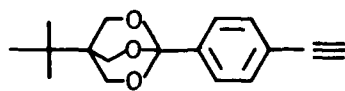
topical housefly and
American cockroach $LD_{50}s$

p-ethynyl-TBOB

0.06-0.6 mg/kg alone
0.01-0.4 mg/kg with piperonyl butoxide

in vitro $IC_{50}s$

CN
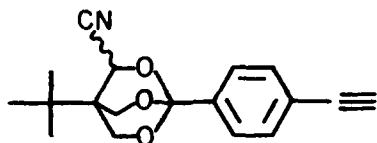
3-cyano-p-ethynyl-TBOB

0.25 nM at $[^{35}S]$TBPS receptor [49]
2 nM for ivermectin-stimulated
    neurotransmitter release [26]
25 nM for GABA-dependent
^{36}chloride flux [49]

The most potent TBO in in vitro assays for the GABA-gated chloride channel is
($\pm$)-3-cyano-p-ethynyl-TBOB [49].

It therefore appears that optimal TBOs acting at the GABA-gated chloride
channel in mammals and insects rival the potency of the most active neurotoxicants
and insecticides acting on sodium channels and the cholinergic system.

Summary

Bicycloorthocarboxylates $[R_4\text{-}C(CH_2O)_3C\text{-}R_1]$ and bicyclophosphorus esters $[R_4\text{-}C(CH_2O)_3P=X; X=O \text{ or } S]$ with selected R_4 and R_1 substituents (e.g., R_4 = *t*-butyl
and R_1 = substituted-phenyl) are potent convulsants and $GABA_A$ receptor
antagonists. These 2,6,7-trioxabicyclo[2.2.2]octanes antagonize non-competitively
the action of γ-aminobutyric acid (GABA) in the central nervous systems of
mammals and possibly of arthropods and at the arthropod neuromuscular junction.
$[^3H]t$-Butylbicyloorthobenzoate and $[^{35}S]t$-butylbicyclophosphorothionate ($[^{35}S]$-
TBPS) are useful radioligands in binding assays to probe the convulsant site(s) and
coupled receptors of the GABA-gated chloride channel in vertebrate brain mem-
branes. Many of these trioxabicyclooctanes act at the brain convulsant receptor in
vitro at 0.1 to 10 nM and in vivo at 0.1 to 1 mg/kg. Their potency in inhibiting the
$[^{35}S]$TBPS binding site is closely correlated with their activity in blocking GABA-
stimulated chloride flux in brain vesicles and with their mammalian toxicity.
Orthobenzoates (R_1 = substituted-phenyl) and orthocarboxylates with large 1-sub-
stituents (R_1 = *n*-propyl or larger alkyl substituent) appear to act in brain mem-
branes at the same site and in a similar manner to picrotoxinin and the polychloro-
cycloalkane insecticides (type **A** action). In contrast, the phosphorus esters, ortho-
carboxylates with smaller 1-substituents (R_1 = hydrogen, methyl, ethyl or ethynyl)
and tetramethylenedisulfotetramine appear to act in a related but somewhat differ-
ent manner (type **B** action). Compounds with type **A** action are generally much

more potent insecticides than those with type **B** action. Binding studies with radiolabelled $GABA_A$ receptor antagonists and insect nerve preparations do not at present predict insecticidal activity well. 4-t-Butyl-1-(p-ethynylphenyl)-2,6,7-trioxabicyclo[2.2.2]octane is a remarkably potent insecticide and its 3-cyano analogue is the most potent known $GABA_A$ receptor antagonist in mammalian systems. The insecticidal potency a·d neuroactivity of these trioxabicyclooctanes rival those of the most effective organophosphorus compounds and pyrethroids. The sensitivity and toxicological significance of the convulsant site of the GABA-gated chloride channel therefore approaches that of voltage-dependent sodium channels and the cholinergic system.

Acknowledgements

References

1 Olsen, R.W. (1982) Drug interactions at the GABA receptor-ionophore complex. Ann. Rev. Pharmacol. Toxicol. 22, 245–277.

2 Bowery, N.G., Price, G.W., Hudson, A.L., Hill, D.R., Wilkin, G.P. and Turnbull, M.J. (1984) GABA receptor multiplicity. Visualization of different receptor types in the mammalian CNS. Neuropharmacology 23, 219–231.

3 Callec, J.J. (1985) Synaptic transmission in the central nervous system. In: Comprehensive Insect Physiology, Biochemistry, and Pharmacology, Vol. 5 (G.A. Kerkut, L.I. Gilbert, eds), Pergamon, New York, pp. 139–179.

4 Lummis, S.C.R., Pinnock, R.D. and Sattelle, D.B. (1987) GABA receptors of the insect central nervous system. In: Sites of Action for Neurotoxic Pesticides (R.M. Hollingworth, M.B. Green, Eds.), pp. 14–24. ACS Symposium Series 356, American Chemical Society, Washington, DC.

5 Miller, T.A. and Chalmers, A.E. (1987) Actions of GABA agonists and antagonists on invertebrate nerves and muscles. In: Sites of Action for Neurotoxic Pesticides (R.M. Hollingworth, M.B. Green, eds.) pp. 2–13. ACS Symposium Series 356, American Chemical Society, Washington, DC.

6 Schofield, P.R., Darlison, M.G., Fujita, N., Burt, D.R., Stephenson, F.A., Rodriguez, H., Rhee, L.M., Ramachandran, J., Reale, V., Glencorse, T.A., Seeburg, P.H. and Barnard, E.A. (1987) Sequence and functional expression of the $GABA_A$ receptor shows a ligand-gated receptor super-family. Nature, 328, 221–227.

7 Stephenson, F.A. (1987) Progress towards the understanding of the $GABA_A$ receptor structure. J. Receptor Res. 7, 43–54.

8 Casida, J.E. (1987) Insecticides acting as $GABA_A$ receptor antagonists. In: Pesticide Science and Biotechnology (R. Greenhalgh, T.R. Roberts, eds.), pp. 75–80. Blackwell, Oxford.

9 Havoundjian, H., Paul, S.M. and Skolnick, P. (1986) The permeability of γ-aminobutyric acid-gated chloride channels is described by the binding of a 'cage' convulsant, t-butylbicyclophosphoro[^{35}S]thionate. Proc. Natl. Acad. Sci. U.S.A. 83, 9241–9244.

10 Bentley, R. and Trimen, H. (1875) *Anamirta paniculata*, in Medicinal Plants. Being Descriptions with Original Figures of the Principal Plants Employed in Medicine and an Account on Their Properties and Uses; J.&A. Churchill, London; Part 2, Item 14, 5 pp.

11 Takeuchi, A. and Takeuchi, N. (1969) A study of the action of picrotoxin on the inhibitory neuromuscular junction of the crayfish. J. Physiol. 205, 377–391.

12 Wright, D.J. (1986) Biological activity and mode of action of avermectins. In: Neuropharmacology and Pesticide Action (M.G. Ford, G.G. Lunt, R.C. Reay, P.N.R. Usherwood, eds.), pp. 174–202. Ellis Horwood, Chichester.

13 Bellet, E.M. and Casida, J.E. (1973) Bicyclic phosphorus esters: high toxicity without cholinesterase inhibition. Science 182, 1135–1136.

14 Casida, J.E., Eto, M., Moscioni, A.D., Engel, J.L., Milbrath, D.S. and Verkade, J.G. (1976) Structure-toxicity relationships of 2,6,7-trioxabicyclo[2.2.2]octanes and related compounds. Toxicol. Appl. Pharmacol. 36, 261–279.

15 Casida, J.E. and Palmer, C.J. (1988) 2,6,7-Trioxabicyclo[2.2.2]octanes: chemistry, toxicology and action at the GABA-gated chloride channel. In: Chloride Channels and Their Modulation by Neurotransmitters and Drugs (G. Biggio, E. Costa, eds.), Raven, New York; in press.

16 Palmer, C.J. and Casida, J.E. (1985) 1,4-Disubstituted 2,6,7-trioxabicyclo[2.2.2]octanes: a new class of insecticides. J. Agric. Food Chem. 33, 976–980.

17 Palmer, C.J. and Casida, J.E. (1987) Bicycloorthocarboxylates. Potent insecticides acting at the GABA-regulated chloride ionophore. In: Sites of Action for Neurotoxic Pesticides (R.M. Hollingworth, M.G. Green, eds.) pp. 71–82. ACS Symposium Series 356, American Chemical Society, Washington, DC.

18 Milbrath, D.S., Engel, J.L., Verkade, J.G. and Casida, J.E. (1979) Structure-toxicity relationships of 1-substituted-4-alkyl-2,6,7-trioxabicyclo[2.2.2]octanes. Toxicol. Appl. Pharmacol 47, 287–293.

19 Petajan, J.H., Voorhees, K.J., Packham, S.C., Baldwin, R.C., Einhorn, I.N., Grunnet, M.L., Dinger, B.G. and Birky, M.M. (1975) Extreme toxicity from combustion products of a fire-retarded polyurethane foam. Science 187, 742–744.

20 Mattsson, H., Brandt, K. and Heilbronn, E. (1977) Bicyclic phosphorus esters increase the cyclic GMP level in rat cerebellum. Nature 268, 52–53.

21 Bowery, N.G., Collins, J.F. and Hill, R.G. (1976) Bicyclic phosphorus esters that are potent convulsants and GABA antagonists. Nature 261, 601–603.

22 Bowery, N.G., Collins, J.F., Hill, R.G. and Pearson, S. (1977) *t*-Butyl bicyclophosphate: a convulsant and GABA antagonist more potent than bicuculline. Br. J. Pharmacol. 60, 275–276P.

23 Gammon, D. and Casida, J.E. (1983) Pyrethroids of the most potent class antagonize GABA action at the crayfish neuromuscular junction. Neurosci. Lett. 40, 163–168.

24 Casida, J.E., Palmer, C.J. and Cole, L.M. (1985) Biocycloorthocarboxylate convulsants. Potent $GABA_A$ receptor antagonists. Mol. Pharmacol. 28, 246–253.

25 Casida, J.E., Ouldlamghitnia, H. and Pichon, Y. (1988) Excitation of the cockroach central nervous system by 1-(4-ethynylphenyl)-4-*n*-propyl-2,6,7-trioxabicyclo[2.2.2]octane. Pest. Biochem. Physiol. in press.

26 Nicholson, R.A., Robinson, P.S., Palmer, C.J. and Casida, J.E. (1988) Ivermectin-stimulated release of neurotransmitter in the insect central nervous system: modulation by external chloride and inhibition by a novel trioxabicyclooctane and two polychlorocycloalkane insecticides. Pestic. Sci. in press.

27 Nicholson, R.A., Baines, P. and Robinson, P.S. (1987) Insect synaptosomes in superfusion. A technique to investigate the actions of ion channel directed neurotoxicants by monitoring their effects on transmitter release. In: Sites of Action for Neurotoxic Pesticides (R.M. Hollingworth, M.B. Green, eds.), pp. 262–272. ACS Symposium Series 356, American Chemical Society, Washington, DC.

28 Allan, A.M. and Harris, R.A. (1986) γ-Aminobutyric acid agonists and antagonists alter chloride flux across brain membranes. Mol. Pharmacol. 29, 497–505.

142

29 Bloomquist, J.R. and Soderlund, D.M. (1985) Neurotoxic insecticides inhibit GABA-dependent chloride uptake by mouse brain vesicles. Biochem. Biophys. Res. Commun. 133, 37–43.

30 Bloomquist, J.R., Adams, P.M. and Soderlund, D.M. (1986) Inhibition of γ-aminobutyric acid-stimulated chloride flux in mouse brain vesicles by polychlorocycloalkane and pyrethroid insecticides. Neurotoxicology 7, 11–20.

31 Bloomquist, J.R., Adams, P.M., Soderlund, D.M. (1987) Neurotoxic insecticides as antagonists of the $GABA_A$ receptor function. In: Sites of Action for Neurotoxic Pesticides (R.M. Hollingworth, M.B. Green, eds.), pp. 97–106. ACS Symposium Series 356, American Chemical Society, Washington DC.

32 Gant, D.B., Eldefrawi, M.E., Eldefrawi, A.T. (1987) Cyclodiene insecticides inhibit $GABA_A$ receptor-regulated chloride transport. Toxicol. Appl. Pharmacol. 88, 313–321.

33 Eldefrawi, M.E., Gant, D.B., Abalis, I.M. and Eldefrawi, A.T. (1987) Interactions of insecticides with GABA-operated and voltage-dependent chloride channels. In: Sites of Action for Neurotoxic Pesticides (R.M. Hollingworth, M.B. Green, eds.) pp. 107–121. ACS Symposium Series 356, American Chemical Society, Washington, DC.

34 Obata, T., Yamamura, H.I., Malatynska, E., Ikeda, M., Laird, H., Palmer, C.J. and Casida, J.E. (1988) Modulation of γ-aminobutyric acid-stimulated chloride influx by bicycloorthocarboxylates, bicyclophosphorus esters, polychlorocycloalkanes and other cage convulsants. J. Pharmacol. Exp. Ther. 244, 802–806.

35 Thampy, K.G. and Barnes, E.M., Jr. (1984) γ-Aminobutyric acid-gated chloride channels in cultured cerebral neurons. J. Biol. Chem. 259, 1753–1757.

36 Tehrani, M.H.J., Vaidyanathaswamy, R., Verkade, J.G. and Barnes, E.M., Jr. (1986) Interaction of t-butylbicyclophosphorothionate with γ-aminobutyric acid-gated chloride channels in cultured cerebral neurons. J. Neurochem. 46, 1542–1548.

37 Ticku, M.K. and Olsen, R.W. (1977) γ-Aminobutyric acid-stimulated chloride permeability in crayfish muscle. Biochim. Biophys. Acta 464, 519–529.

38 Ghiasuddin, S.M. and Matsumura, F. (1982) Inhibition of gamma-aminobutyric acid (GABA)induced chloride uptake by gamma-BHC and heptachlor epoxide. Comp. Biochem. Physiol. 73C, 141–144.

39 Matsumura, F. and Ghiasuddin, S.M. (1983) Evidence for similarities between cyclodiene type insecticides and picrotoxinin in their action mechanisms. J. Environ. Sci. Health B18, 1–14.

40 Ticku, M.K., Ban, M. and Olsen, R.W. (1978) Binding of [^{3}H]α-dihydropicrotoxinin, a γ-aminobutyric acid synaptic antagonist, to rat brain membranes. Mol. Pharmacol. 14, 391–402.

41 Leeb-Lundberg, F. and Olsen, R.W. (1980) Picrotoxinin binding as a probe of the GABA postsynaptic membrane receptor-ionophore complex. In: Psychopharmacology and Biochemistry of Neurotransmitter Receptors (H.I. Yamamura, R.W. Olsen, E. Usdin, eds.), pp. 593–606. Elsevier North Holland, New York.

42 Ozoe, Y., Mochida, K. and Eto, M. (1982) Binding of toxic bicyclic phosphates to rat brain synaptic membrane fractions. Agr. Biol. Chem. 46, 2521–2526.

43 Squires, R.F., Casida, J.E., Richardson, M. and Saederup, E. (1983) [^{35}S]t-Butylbicyclophosphorothionate binds with high affinity to brain-specific sites coupled to γ-aminobutyric acid-A and ion recognition sites. Mol. Pharmacol. 23, 326–336.

44 Lawrence, L.J. and Casida, J.E. (1983) Stereospecific action of pyrethroid insecticides on the γ-aminobutyric acid receptor-ionophore complex. Science 221, 1399–1401.

45 Lawrence, L.J., Palmer, C.J., Gee, K.W., Wang, X., Yamamura, H.I. and Casida, J.E. (1985) t-[^{3}H]Butylbicycloorthobenzoate: new radioligand probe for the γ-aminobutyric acid-regulated chloride ionophore. J. Neurochem. 45, 798–804.

46 Nicholson, R.A., Palmer, C.J. and Casida, J.E. (1988) 4-s-[^{3}H]Butyl-1-(4-cyanophenyl)2,6,7-trioxabicyclo[2.2.2]octane: specific binding in the American cockroach central nervous system. Pestic. Sci. in press.

47 Cole, L.M. and Casida, J.E. (1986) Polychlorocycloalkane insecticide-induced convulsions in mice in relation to disruption of the GABA-regulated chloride ionophore. Life Sci. 39, 1855–1862.

48 Lawrence, L.J. and Casida, J.E. (1984) Interactions of lindane, toxaphene and cyclodienes with brain-specific t-butylbicyclophosphorothionate receptor. Life Sci. 35, 171–178.

49 Palmer, C.J., Cole, L.M. and Casida, J.E. (1988) ($\pm$)-4-t-Butyl-3-cyano-1-(4-ethynylphenyl)-2,6,7-trioxabicyclo[2.2.2]octane: synthesis of a remarkably potent GABA$_A$ receptor antagonist. J. Med. Chem. 31, 1064–1066.

50 Fishman, B.E. and Gianutsos, G. (1987) Differential effects of gamma-hexachlorocyclohexane (lindane) on pharmacologically-induced seizures. Arch. Toxicol. 59, 397–401.

51 Casida, J.E. and Lawrence, L.J. (1985) Structure-activity correlations for interactions of bicyclophosphorus esters and some polychlorocycloalkane and pyrethroid insecticides with the brain-specific t-butylbicyclophosphorothionate receptor. Environm. Health Perspect. 61, 123–132.

52 Abalis, I.M., Eldefrawi, M.E. and Eldefrawi, A.T. (1985) High-affinity stereospecific binding of cyclodiene insecticides and γ-hexachlorocyclohexane to γ-aminobutyric acid receptors of rat brain. Pestic. Biochem. Physiol. 24, 95–102.

53 Seifert, J. and Casida, J.E. (1985) Regulation of [^{35}S]t-butylbicyclophosphorothionate binding sites in rat brain by GABA, pyrethroid and barbiturate. Eur. J. Pharmacol. 115, 191–198.

54 Squires, R.F. and Saederup, E. (1987) GABA$_A$ receptor blockers reverse the inhibitory effect of GABA on brain-specific [^{35}S]TBPS binding. Brain Res. 414, 357–364.

55 Seifert, J. and Casida, J.E. (1986) Basic neuroproteins modulate TBPS recognition site. Eur. J. Pharmacol. 122, 157–158.

56 Supavilai, P. and Karobath, M. (1984) [^{35}S]t-Butylbicyclophosphorothionate binding sites are constituents of the γ-aminobutyric acid benzodiazepine receptor complex. J. Neurosci. 4, 1193–1200.

57 Abalis, I.M., Eldefrawi, A.T. and Eldefrawi, M.E. (1986) Actions of avermectin B$_{1a}$ on the γ-aminobutyric acid$_A$ receptor and chloride channels in rat brain. J. Biochem. Toxicol. 1, 69–82.

58 Cole, L.M., Lawrence, L.J. and Casida, J.E. (1984) Similar properties of [^{35}S]t-butylbicyclophosphorothionate receptor and coupled components of the GABA receptorionophore complex in brains of human, cow, rat, chicken and fish. Life Sci. 35, 1755–1762.

59 Drexler, G. and Sieghart, W. (1984) [^{35}S]$tert$.-Butylbicyclophosphorothionate and avermectin bind to different sites associated with the γ-aminobutyric acid-benzodiazepine receptor complex. Neurosci. Lett. 50, 273–277.

60 Olsen, R.W. and Snowman, A.M. (1985) Avermectin B$_{1a}$ modulation of γ-aminobutyric acid/benzodiazepine receptor binding in mammalian brain. J. Neurochem. 44, 1074–1082.

61 Bonner, J.C. and Yarbrough, J.D. (1987) Alteration of the t-butylbicyclophosphorothionate binding site as a mechanism of vertebrate cyclodiene insecticide resistance. Pestic. Biochem. Physiol. 29, 260–265.

62 Olsen, R.W., Ticku, M.K. and Miller, T. (1978) Dihydropicrotoxinin binding to crayfish muscle sites possibly related to γ-aminobutyric acid receptor-ionophores. Mol. Pharmacol. 14, 381–390.

63 Tanaka, K., Scott, J.G. and Matsumura, F. (1984) Picrotoxinin receptor in the central nervous system of the american cockroach: its role in the action of cyclodiene-type insecticides. Pestic. Biochem. Physiol. 22, 117–127.

64 Kadous, A.A., Ghiasuddin, S.M., Matsumura, F., Scott, J.G. and Tanaka, K. (1983) Difference in the picrotoxinin receptor between the cyclodiene-resistant and susceptible strains of the German cockroach. Pestic. Biochem. Physiol. 19, 157–166.

65 Ozoe, Y., Eto, M., Mochida, K. and Nakamura, T. (1986) Characterization of high affinity binding of [^{3}H]propyl bicyclic phosphate to house fly head extracts. Pestic. Biochem. Physiol. 26, 263–274.

144

66 Ozoe, Y. (1987) Bicyclic phosphorus esters. Insecticidal properties and binding sites in the housefly. In: sites of Action for Neurotoxic Pesticides (R.M. Hollingworth, M.G. Green, eds.), pp. 83–96. ACN Symposium Series 356, American Chemical Society, Washington, DC.

67 Szamraj, O.I., Miller, T. and Olsen, R.W. (1986) Cage convulsant [^{35}S]TBPS binding to GABA receptor-chloride channel complex in invertebrate tissues. Society for Neuroscience Abstracts, 16th; No. 180.7, p. 656.

68 Cohen, E. and Casida, J.E. (1986) Effects of insecticides and GABAergic agents of a house fly [^{35}S]t-butylbicyclophosphorothionate binding site. Pestic. Biochem. Physiol. 25, 63–72.

69 Cohen, E. and Casida, J.E. (1985) Chlorocyclohexane insecticides and male medfly attractants: similar stereospecificity for neuroactivity and interactions with a housefly [^{35}S]t-butylbicyclophosphorothionate binding site. Life Sci. 36, 1837–1842.

70 Lummis, S.C.R. and Sattelle, D.B. (1986) Binding sites for [^{3}H]GABA, [^{3}H]flunitrazepam and [^{35}S]TBPS in insect CNS. Neurochem. Int. 9, 287–293.

71 Palmer, C.J. and Casida, J.E. (1988) Two types of cage convulsant action at the GABA-gated chloride channel. Toxicol. Lett. in press.

72 Milbrath, D.S., Eto, M. and Casida, J.E. (1978) Distribution and metabolic fate in mammals of the potent convulsant and GABA antagonist t-butylbicyclophosphate and its methyl analog. Toxicol. Appl. Pharmacol. 46, 411–420.

73 Scott, J.G., Palmer, C.J. and Casida, J.E. (1987) Oxidative metabolism of the GABA$_A$ receptor antagonist t-butylbicycloortho[^{3}H]benzoate. Xenobiotica 17, 1085–1093.

74 Palmer, C.J. and Casida, J.E. (1988) 1-(4-Ethynylphenyl)-2,6,7-trioxabicyclo[2.2.2]-octanes: a new order of potency for insecticides acting at the GABA-gated chloride channel. J. Agric. Food Chem. in press.

CHAPTER 11

Molecular pharmacology of GABA and GABA synaptic mechanisms

P. Krogsgaard-Larsen, L. Nielsen, E. Falch, L. Brehm and F.S. Jørgensen

PharmaBiotec, Department of Chemistry BC, The Royal Danish School of Pharmacy, 2 Universitetsparken, DK-2100 Copenhagen, Denmark

GABA, a complex molecule with multiple functions

The neutral amino acid, 4-aminobutyric acid (GABA), is an inhibitory neurotransmitter which plays an important role in the control of neuronal activity in the mammalian central nervous system (CNS). GABA is involved in the central [1,2] and peripheral [3] regulation of many physiological mechanisms, and GABA dysfunctions may play an important role in certain neurological and psychiatric disorders [2,4,5]. These aspects focus attention on the various processes and mechanisms associated with GABA-mediated neurotransmission as potential targets for clinically useful drugs [6].

The development on a rational basis of compounds with specific effects on different GABA synaptic mechanisms requires information about the mechanisms of interaction of the GABA molecule with the recognition sites concerned. A considerable degree of conformational flexibility is a trait of the molecule of GABA (Fig. 1). Although the molecule of GABA is achiral, the enantiotopic hydrogen atoms at each carbon atom of the GABA backbone become mutually distinct upon the interaction of GABA with the chiral macromolecules concerned with the function of GABA in synaptic transmission. Furthermore, molecular orbital calculations have disclosed a relatively high degree of delocalization of the positive as well
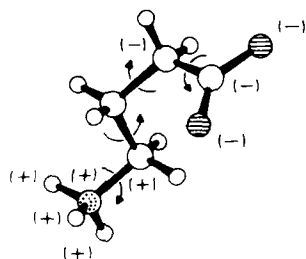
GABA

FIG 1   The conformation of GABA in the crystalline state [7]. The approximate charge delocalization and conformational mobility of the molecule is indicated.

as the negative charges of GABA [8]. Synthesis and structure–activity studies of GABA analogues, in which the conformational and electronic parameters have been systematically modified, and model compounds containing chiral centres with established absolute stereochemistry have shed light on the molecular pharmacology of the GABA synaptic mechanisms. As a result of such studies a variety of compounds with specific actions at different sites of GABA-operated synapses are now available [2,6,9,10].

Structural requirements of GABA-operated synaptic mechanisms

$GABA_A$ and $GABA_B$ receptors

The GABA receptors are divided into two main classes [1,11]: (1) $GABA_A$ receptors, at which a number of cyclic GABA analogues, notably THIP, are selective agonists and which are blocked by bicuculline methochloride (BMC); and (2) BMC-insensitive GABA receptors including $GABA_B$ receptors, at which (R)-baclofen is a selective agonist and phaclofen a weak but selective antagonist [12] (Fig 2). Both classes of GABA receptors probably are heterogeneous [1,2].

$GABA_A$ receptors include postsynaptic (axosomatic or axodend·i ic) as well as presynpatic (axo-axonic) receptors. The postsynaptic $GABA_A$ receptor, which actually is a receptor complex comprising a number of subsynaptic receptors (Fig. 3A), regulates the passage of chloride ions. Similarly, presynaptic $GABA_A$ receptors are coupled to a chloride ion channel (Fig. 3B). The sensitivity of $GABA_A$ autoreceptors, which may play a role in the physiological regulation of GABA release, to $GABA_A$ agonists and antagonists appears to be very similar to that of the postsynaptic $GABA_A$ receptors [1]. However, in contrast to postsynaptic $GABA_A$
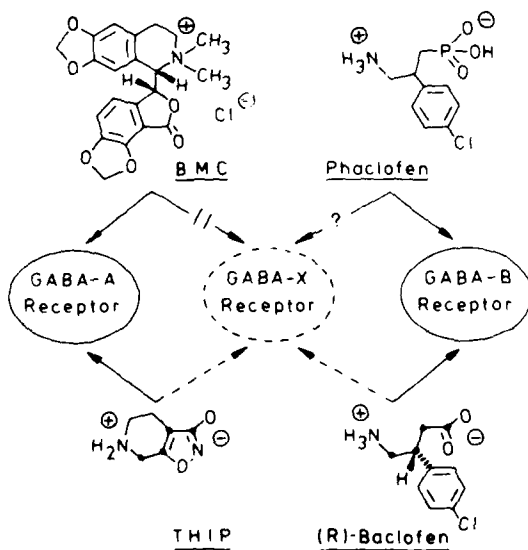
FIG 2 A schematic illustration of GABA receptor subtypes indicating sites of action of some agonists and antagonists.
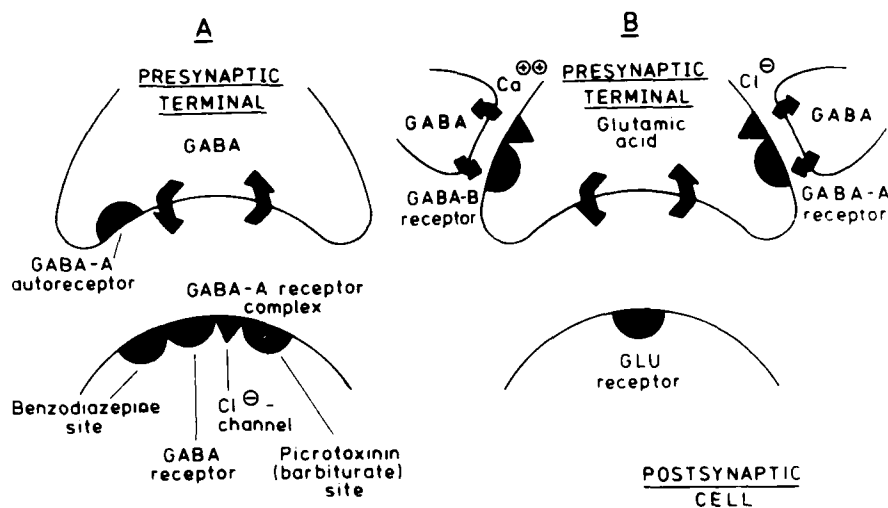
FIG 3 Schematic illustrations of an axo-somatic GABA synapse (A) and a glutamic acid-operated axosomatic synapse containing presynaptic GABA$_A$ and GABA$_B$ receptors (B).

receptors, autoreceptors do not seem to be coupled to benzodiazepine (BZD) sites [13] (Fig. 3A).

Very strict structural constraints are imposed on agonists at GABA$_A$ receptors [2,6], as exemplified in Fig. 4. Whereas THIP is a potent GABA$_A$ agonist, the

THIP   Thio-THIP   ● N
                                         ⊜ O
                                         ⦵ S

GABA- A Agonism
  (Rel. potency)   _ _ _ (—)   —

Inhibition of
  GABA - A Receptor
  Binding (IC$_{50}$, μM) 0.13   4.2
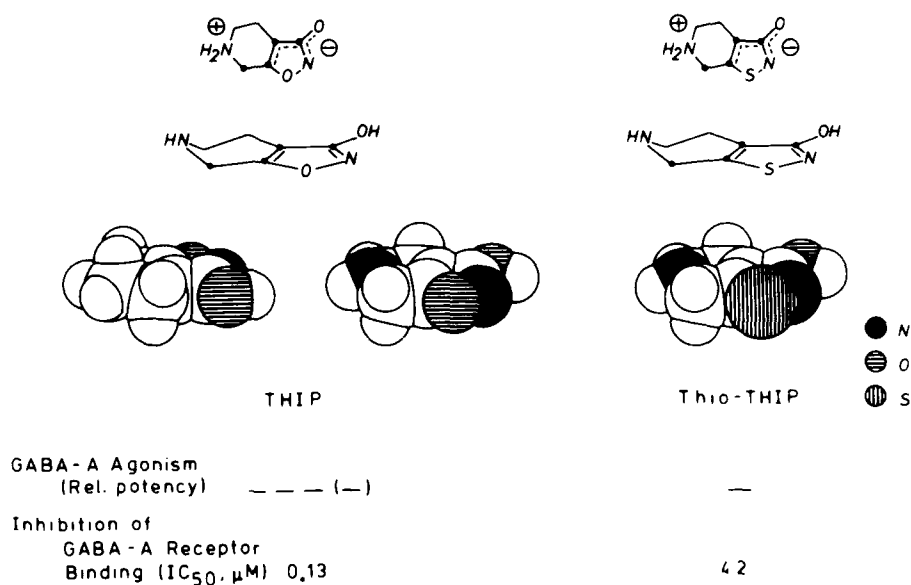
FIG 4 A comparison of the low-energy conformations of the GABA$_A$ agonists THIP and thio-THIP [15] and their in vivo and in vitro effects [14].

closely related analogue, thio-THIP, is only a very weak BMC-sensitive neuronal depressant, and it is more than 300-times weaker than THIP as an inhibitor of $GABA_A$ receptor binding [14]. Steric effects of the sulphur atom, which is somewhat more bulky than oxygen, and/or slightly different degrees of delocalizations of the negative charges of THIP and thio-THIP may be factors of importance for this quite dramatic loss of $GABA_A$ agonist activity in thio-THIP.

Within the group of central BMC-insensitive GABA receptors the $GABA_B$ receptors have been extensively studied [1,3,11]. Although little is known about the physiological role of $GABA_B$ receptors, they seem to regulate the release of certain neurotransmitters including glutamic acid as exemplified in Fig. 3B. Although accumulating evidence suggests that $GABA_B$ receptors are located presynaptically and that they affect neurotransmitter release via regulation of a calcium ion channel [1,11], postsynaptically located $GABA_B$ receptors linked to potassium channels may exist [11,16]. Neurochemical data have been interpreted in terms of the presence of $GABA_B$ autoreceptors [17].

The clinical effects of the $GABA_B$ agonist baclofen in spasticity and the therapeutic prospects of $GABA_B$ antagonists in certain types of psychiatric diseases have focused much pharmacological and therapeutic interest on $GABA_B$ receptors [1]. In recent years a variety of baclofen analogues and a number of $GABA_B$ agonists and antagonists structurally unrelated to baclofen have been developed [2] (see Table 1).

$GABA_X$ receptors (?)

Accumulating evidence derived from neurochemical and pharmacological studies suggests that GABA-operated receptors different from $GABA_A$ and $GABA_B$ receptor subtypes, tentatively named $GABA_X$ receptors (Fig. 2), may exist in the mammalian CNS. Binding studies using radioactive GABA and (R)-baclofen have revealed the existence of a population of BMC-insensitive GABA receptors that are not activated by (R)-baclofen [18]. These results of binding studies seem to be consistent with the evidence for two BMC-insensitive actions of GABA in rat hippocampal slices, only one of which is shared by baclofen [19].

Different structural classes of $GABA_A$ agonists show very different stimulatory effects on the binding of BZDs in vitro [2], as exemplified in Fig. 5. Whereas GABA and some $GABA_A$ agonists such as muscimol and the (S)-isomer of dihydro-muscimol (DHM) (Table 1) effectively enhance BZD binding under different experimental conditions, the $GABA_A$ agonists THIP and, in particular, P4S are much less efficacious. The new $GABA_A$ agonist, 4-PIOL, does not significantly affect BZD binding [20], showing a profile in this test system very similar to that of BMC. Interestingly, THIP seems to increase the receptor affinity of the BZDs in a BMC-sensitive manner, but to decrease the number of BZD receptor sites via a BMC-insensitive mechanism [21]. This latter effect of THIP may be mediated by a novel GABA receptor ($GABA_X$), and detailed studies on $GABA_A$ agonist–BZD interactions using THIP, P4S and 4-PIOL as tools may shed new light on these aspects of considerable pharmacological interest. Studies along these lines are in progress.

Behavioural pharmacological data on THIP and baclofen support the view that GABA receptors different from $GABA_A$ and $GABA_B$ receptors exist (Fig. 2). THIP and baclofen induce similar, although not identical, EEG abnormalities in animals,
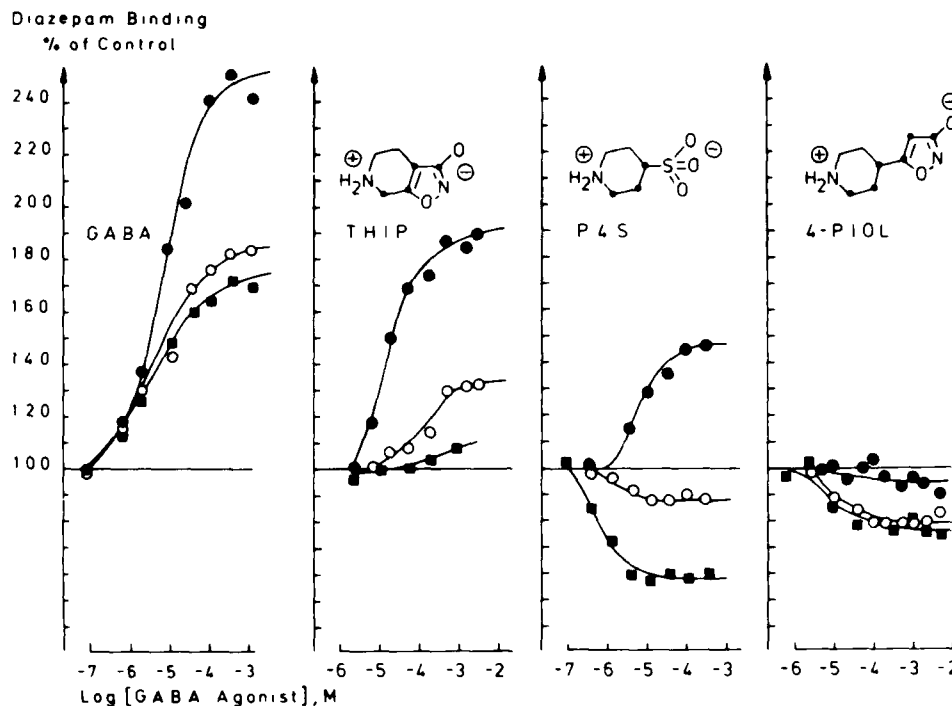
FIG 5   Effects of GABA and the $GABA_A$ agonists THIP, P4S, and 4-PIOL on the binding of radioactive diazepam at $0\,°C$ and in the absence of chloride (■) or at $30\,°C$ in the presence (●) or absence (○) of 150 mM sodium chloride.

and neither effect could be reversed by bicuculline [23]. Furthermore, THIP-induced analgesia [24] as well as the effects of THIP on sexual behaviour in the male rat [25] are insensitive to bicuculline.

GABA uptake mechanisms

It is generally accepted that the GABA uptake mechanisms (Fig. 3) are concerned with the termination of the GABA neurotransmission process, but the precise mechanism of action, including the time course and capacity of these mechanisms in vivo are not fully understood [2,26,27]. Inhibition of GABA uptake may represent a flexible way of stimulating GABA-mediated neurotransmission, but it is not possible at present to single out with certainty the transport mechanism(s) most susceptible to pharmacological intervention. The most logical and realistic strategies for pharmacological interventions in these systems with the purpose of stimulating GABA neurotransmission do, however, seem to be:

(1) effective blockade of both neuronal and glial GABA uptake in order to enhance the inhibitory effect of synaptically released GABA or

(2) selective blockade of glial GABA uptake in order to increase the amount of GABA taken up by the neuronal carrier with subsequent elevation of the GABA concentration in nerve terminals.

150
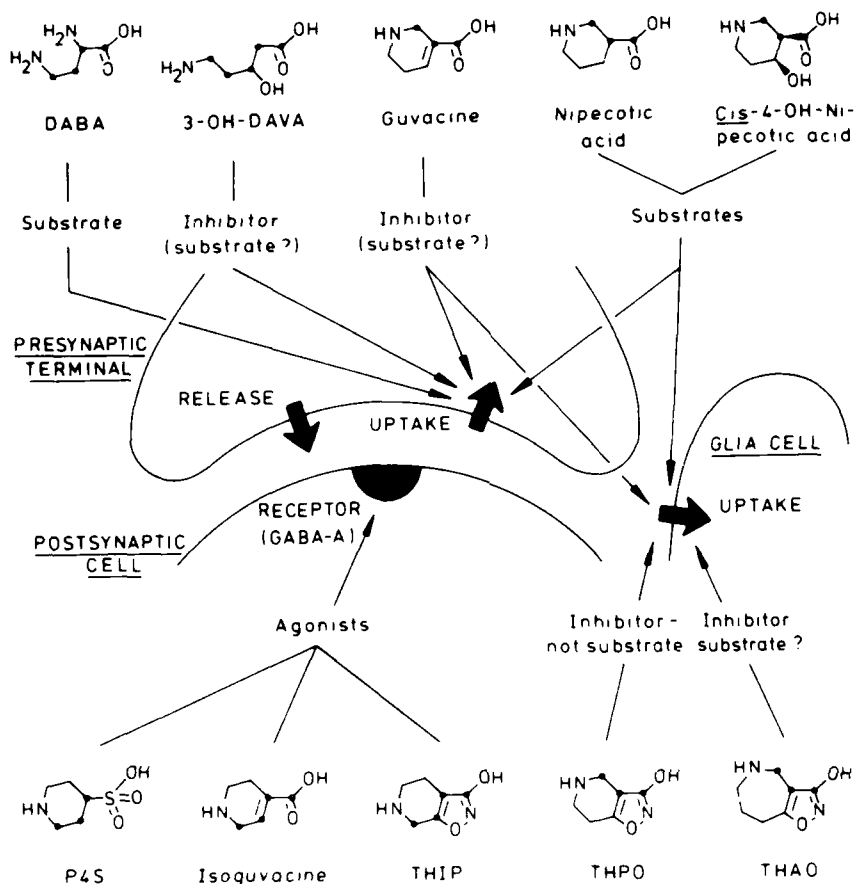
FIG 6 A schematic illustration of an axo-somatic GABA-operated synapse showing the sites of action of a number of GABA$_A$ agonists and GABA uptake inhibitors.
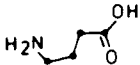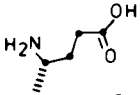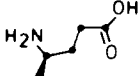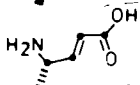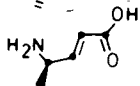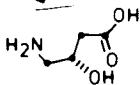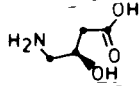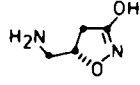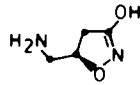
As illustrated in Fig. 6, it has been established that neuronal and glial GABA uptake mechanisms have dissimilar inhibitor/substrate specificities, which are distinctly different from the agonist specificities of the GABA$_A$ receptors [2,27].

Whereas substrates/inhibitors of neuronal GABA uptake appear to be convulsants or proconvulsants, compounds acting as selective inhibitors for the glial uptake system, such as THPO, have anticonvulsant effects [27].

Comparative stereostructure-activity studies

The different structural requirements of GABA synaptic mechanisms as illustrated in Fig. 6 have been supported by comparative stereostructure-activity studies as exemplified in Table 1. The degree of stereoselectivity of chiral GABA analogues is a function of the absolute configuration as well as the conformational flexibility of the molecules. Thus, the selectivity of the GABA synaptic recognition sites with respect to the enantiomers of 4-Me-GABA is much less pronounced than that

TABLE 1 Structure and effects in vitro on GABA synaptic mechanisms of GABA and some chiral GABA analogues

Compound	Structure (S)-Isomer (R)-Isomer	Inhibition of (IC$_{50}$ μM)			
		GABA receptor binding		GABA uptake	
		GABA$_A$	GABA$_B$	Neuronal	Glial
GABA		0.03	0.03	15	35
4-Me-GABA		5	25	750	1000
4-Me-GABA		5	100	200	100
4-Me-t-ACA		4	>100	>5000	>5000
4-Me-t-ACA		>100	>100	160	500
3-OH-GABA		0.4	2.5	130	300
3-OH-GABA		1	0.4	400	800
DHM		0.004	13	>5000	>5000
DHM		0.3	5	800	2000

observed for the enantiomers of the less flexible analogue, 4-Me-t-ACA. In this latter GABA analogue the GABA$_A$ receptor and GABA uptake affinities reside exclusively in the (S)- and (R)-isomers, respectively, and neither isomer affects GABA$_B$ receptor sites. Similarly, the (S)- and (R)-isomers of the conformationally flexible analogue 3-OH-GABA show a lower degree of stereoselectivity as GABA$_A$ agonists and GABA uptake inhibitors than that exhibited by the enantiomers of the less flexible cyclic bioisostere, DHM [28]. As exemplified by the in vitro pharmacological data for the enantiomers of 3-OH-GABA and DHM in Table 1, the GABA$_A$ and GABA$_B$ receptor sites exhibit opposite stereoselectivity, the (S)- and (R)-forms of these compounds being most tightly bound by GABA$_A$ and GABA$_B$ sites, respectively [29]. The (S)-isomer of DHM obviously is capable of mimicking almost perfectly the active conformation of GABA with respect to GABA$_A$ receptors [28]. Interestingly, the (R)-forms of 3-OH-GABA (Table 1) and baclofen (Fig. 2), which
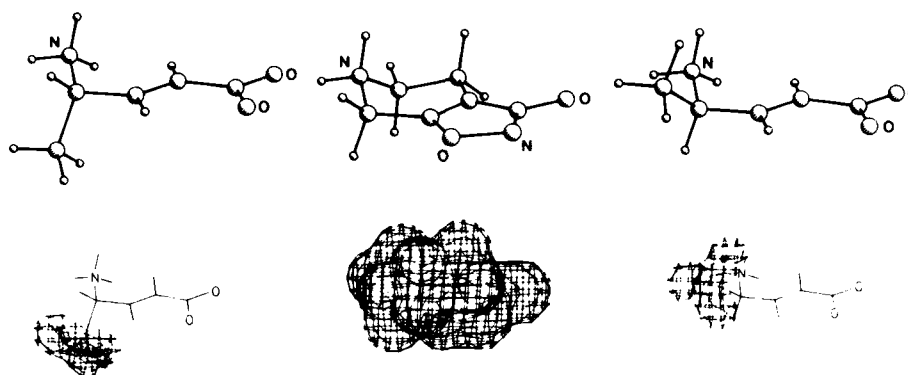
FIG 7   Three-dimensional representations of the GABA$_A$ agonist (S)-4-Me-t-ACA and the GABA uptake inhibitor (R)-4-Me-t-ACA in conformations fitted to a preferred conformation of the conformationally restricted GABA$_A$ agonist THIP. The extra volumes of the (S)- and (R)-forms of 4-Me-t-ACA relative to THIP and isoguvacine are indicated.

are the most active isomers with respect to GABA$_B$ receptor sites, actually have opposite stereochemical orientations of the hydroxy and 4-chlorophenyl groups, respectively. This observation strongly suggests that the polar hydroxy group of (R)-3-OH-GABA interacts with a structural element of the GABA$_B$ receptor site different from that which binds the lipophilic aromatic group of (R)-baclofen.

Molecular pharmacology of GABA

The relationship between the degree of stereoselectivity and conformational mobility of chiral GABA analogues described in the previous section can be rationalized. All of the model compounds used in these studies are analogues of GABA, in which chirality and/or conformational restrictions have been introduced by incorporating additional structural elements. Normally, such structural elements will cause steric hindrance for interaction with the synaptic recognition sites, and whereas the flexible chiral molecules may find it relatively easy to relieve the strain caused by the additional groups having the unfavourable orientations, the more rigid molecules may be unable to avoid such unfavourable effects. The different pharmacological profiles of the (S)- and (R)-isomers of 4-Me-t-ACA (Table 1) indicate that the GABA$_A$ receptors are capable of accommodating the methyl group of the (S)-form, but not that of the (R)-form, whereas the opposite applies to the GABA uptake sites (Fig. 7). These structure–activity relationships may also, or alternatively, reflect the fact that GABA adopts different conformations during its interaction with these synaptic mechanisms.

The potent GABA$_A$ agonist THIP (Figs. 2 and 7) is a conformationally restricted, almost rigid, analogue of GABA, and it is reasonable to conclude that this GABA bioisostere essentially reflects the active conformation of GABA at GABA$_A$ receptors. This conformation of GABA obviously is rather planar and partially folded. The conformational rigidity of THIP suggests that the ability of GABA$_A$ agonists to adopt different conformational modes is not essential to their postsynaptic actions.
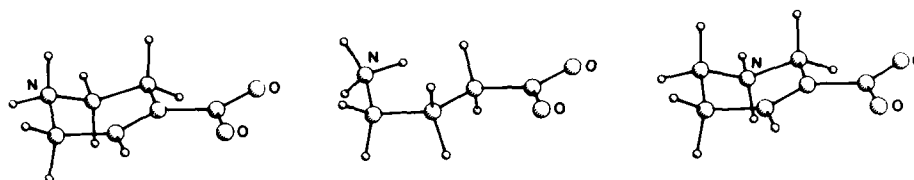
FIG 8 Three-dimensional representation of GABA, depicted in its proposed GABA$_A$ receptor-active conformation, and of the GABA$_A$ agonist isoguvacine and the GABA uptake inhibitor guvacine.

The potency and specificity of isoguvacine as a GABA$_A$ agonist [2] indicates that the GABA$_A$ receptor-active conformation of GABA, as expressed by THIP, is easily accessible to isoguvacine (Fig. 8). It is, on the other hand, surprising that nipecotic acid and related cyclic amino acids, which are not GABA analogues in the strict sense of the word, bind tightly to the GABA uptake systems and act as substrates for these transport carriers [27] (Fig. 6). Somehow these amino acids, as exemplified by guvacine in Fig. 8, must reflect the conformation(s) adopted by GABA during its binding to and transport by the GABA transport carriers. Since the glia-selective non-substrate inhibitor of GABA uptake, THPO, an almost rigid analogue of nipecotic acid and guvacine (Fig. 6), does not interact detectably with neuronal GABA uptake, the rotational freedom of the carboxylate groups of nipecotic acid and guvacine seems to be a factor of importance for their binding to and transport by the neuronal, but not the glial, GABA carrier.

In conclusion, these structure–activity studies support the view that GABA adopts different active conformations at GABA$_A$ receptors, the GABA uptake systems, and, perhaps, the GABA$_B$ receptors. Furthermore, the conformational flexibility of GABA appears to be important for some, but not all, of its synaptic functions.

Acknowledgements

References

1 Enna, S.J. (ed.) (1983) the GABA Receptors. Humana Press, Clifton, NJ.
2 Krogsgaard-Larsen, P., Hjeds, H., Falch, E., Jørgensen, F.S. and Nielsen, L. (1988) Recent advances in GABA agonists, antagonists and uptake inhibitors: structure-activity relationships and therapeutic potential. Adv. Drug Res. 17, 381–456.
3 Erdö, S.L. and Bowery, N.G. (eds.) (1986) GABAergic Mechanisms in Mammalian Periphery. Raven Press, New York.
4 DiChiara, G. and Gessa, G.L. (eds.) (1981) GABA and the Basal Ganglia. Raven Press, New York.
5 Nistico, G., Morselli, P.L., Lloyd, K.G., Fariello, R.G. and Engel, J. (eds.) (1986) Neurotransmitters, Seizures, and Epilepsy III. Raven Press, New York.

6 Krogsgaard-Larsen, P., Falch, E. and Hjeds, H. (1985) Heterocyclic analogues of GABA: chemistry, molecular pharmacology and therapeutic aspects. Prog. Med. Chem. 22, 67–120.

7 Tomita, K., Higashi, H. and Fujiwara, T. (1973) Crystal and molecular structure of ω-amino acids, ω-Amino sulfonic acids and their derivatives. IV. The crystal and molecular structure of 4-aminobutyric acid (GABA), a nervous inhibitory transmitter. Bull. Chem. Soc. 46, 2199–2204.

8 Steward, E.G., Borthwick, P.W., Clarke, G.R. and Warner, D. (1975) Agonism and antagonism of 4-aminobutyric acid. Nature (London) 256, 600–602.

9 Allan, R.D. and Johnston, G.A.R. (1983) Synthetic analogs for the study of GABA as a neurotransmitter. Med. Res. Rev. 3, 91–118.

10 Krogsgaard-Larsen, P. (1988) GABA synaptic mechanisms: stereochemical and conformational requirements. Med. Res. Rev. 8, 27–56.

11 Bowery, N.G. (ed.) (1984) Actions and Interactions of GABA and Benzodiazepines. Raven Press, New York.

12 Kerr, D.I.B., Ong, J., Prager, R.H., Gynther, B.D. and Curtis, D.R. (1987) Phaclofen: a peripheral and central baclofen antagonist. Brain Res. 405, 150–154.

13 Brennan, M.J.W. (1982) GABA autoreceptors are not coupled to benzodiazepine receptors in rat cerebral cortex. J. Neurochem. 38, 264–266.

14 Krogsgaard-Larsen, P., Mikkelsen, H., Jacobsen, P., Falch, E., Curtis, D.R., Peet, M.J. and Leah, J.D. (1983) 4,5,6,7-Tetrahydroisoxazolo[5,4-c]pyridin-3-ol and related analogues of THIP. Synthesis and biological activity. J. Med. Chem. 26, 895–900.

15 New, J.S. and Krogsgaard-Larsen, P. Unpublished.

16 Peet, M.J. and McLennan, H. (1986) Pre- and postsynaptic actions of baclofen: blockade of the late synaptically-evoked hyperpolarization of CA1 hippocampal neurons. Exp. Brain Res. 61, 567–574.

17 Anderson, R.A. and Mitchell, R. (1985) Evidence for $GABA_B$ autoreceptors in median eminence. Eur. J. Pharmacol. 118, 355–358.

18 Johnston, G.A.R. and Allan, R.D. (1984) GABA agonists. Neuropharmacology 23, 831–832.

19 Ault, B. and Nadler, J.V. (1983) Physiological evidence for two pharmacologically distinct, bicuculline-insensitive actions of GABA in the rat hippocampal slice. Soc. Neurosci. Abstr. 9, 411.

20 Byberg, J.R., Labouta, I.M., Falch, E., Hjeds, H., Krogsgaard-Larsen, P., Curtis, D.R. and Gynther, B.D. (1987) Synthesis and biological activity of a GABA-A agonist which has no effect on benzodiazepine binding and of structurally related glycine antagonists. Drug Des. Del. 1, 261–274.

21 Zarkovsky, A.M. (1987) Bicuculline-sensitive and insensitive effects of THIP on the binding of 3H-flunitrazepam. Neuropharmacology 26, 737–741.

22 Jensen, M.S. and Lambert, J.D.C. (1984) Modulation of the responses to the GABA-mimetics, THIP and piperidine-4-sulphonic acid, by agents which interact with benzodiazepine receptors. Neuropharmacology 23, 1441–1450.

23 Golden, G.T. and Fariello, R.G. (1984) Epileptogenic action of some direct GABA agonists: effects of manipulation of the GABA and glutamate systems. In : Neurotransmitters, Seizures, and Epilepsy II (R.G. Fariello, P.L. Morselli, K.G. Lloyd, L.F. Quesney, J. Engel, eds.), pp. 237–244. Raven Press, New York.

24 Kendall, D.A., Browner, M. and Enna, S.J. (1982) Comparison of the antinociceptive effect of GABA agonists: evidence for a cholinergic involvement. J. Pharmacol. Exp. Ther. 220, 482–487.

25 Agmo, A. and Paredes, R. (1985) GABAergic drugs and sexual behaviour in the male rat. Eur. J. Pharmacol. 112, 371–378.

26 Schousboe, A. (1981) Transport and metabolism of glutamate and GABA in neurons and glial cells. Int. Rev. Neurobiol. 22, 1–45.

27 Krogsgaard-Larsen, P., Falch, E., Larsson, O.M. and Schousboe, A. (1987) GABA uptake inhibitors: relevance to antiepilectic drug research. Epilepsy Res. 1, 77–93.

28 Krogsgaard-Larsen, P., Nielsen, L., Falch, E. and Curtis, D.R. (1985) GABA agonists. Resolution, absolute stereochemistry, and enantioselectivity of (S)-$(+)$- and (R)-$(-)$-dihydromuscimol. J. Med. Chem. 28, 1612–1617.

29 Falch, E., Hedegaard, A., Nielsen, L., Jensen, B.R., Hjeds, H. and Krogsgaard-Larsen, P. (1986) Comparative stereostructure-activity studies on $GABA_A$ and $GABA_B$ receptor sites and GABA uptake using rat brain membrane preparations. J. Neurochem. 47, 898–903.

CHAPTER 12

Structure–activity relationships of (+)anatoxin-a derivatives and enantiomers of nicotine on the peripheral and central nicotinic acetylcholine receptor subtypes

Y. Aracava [1,2], K.L. Swanson [1], R. Rozental [1,2] and E.X. Albuquerque [1,2]

[1] Department of Pharmacology and Experimental Therapeutics,
University of Maryland School of Medicine, 655 W. Baltimore St.,
Baltimore MD 21201, U.S.A.; and [2] Molecular Pharmacology Training Program,
Institute of Biophysics 'Carlos Chagas Filho', Federal University of Rio de Janeiro,
Ilha do Fundão, CEP 2194, RJ, Brazil

Introduction

The nicotinic acetylcholine receptor-ion channel complex (AChR) of vertebrate muscle and *Torpedo* electroplax has been subjected to numerous studies which have contributed to the understanding of its structure and function [1–3]. The potency of a nicotinic agonist in muscle is usually evaluated by the force of contracture induced by a given concentration of the agent. At the molecular level, the potency can be assessed by studying binding affinity, frequency of channel openings, duration of the open state of the channels and/or single channel conductance. It has been observed that single conductance is not influenced by the agonist's structure, since many agonists with varied potencies exhibit similar channel conductance values [4]. On the other hand, the duration of the channel open state and the frequency of channel activation showed great variations among agonists [5–7]. We have investigated the dynamics of ion channel activation initiated by agonist–receptor interaction, by studying structure–activity relationships involving both agonist potency and channel kinetics. Although considerable information may be gained about receptor sites based on structure–activity studies with antagonists, questions might be raised regarding the degree to which agonist and antagonist sites overlap. Therefore studies using agonists may be preferable. Among agonists, the least flexible molecules would be the most useful tools for describing the receptor binding sites, since the rigidity of molecules such as (+)anatoxin-a would limit the number of possible conformations.

In early 1975, Carmichael and Carmichael and collaborators [8,9] described the pharmacology and the toxicology of the toxin produced by the blue-green algae from freshwater *Anabaena flos-aquae*. The toxic principle named anatoxin-a (Fig. 1)

158

(S)-(-)-Nicotine   (R)-(+)-Nicotine

(+)Anatoxin-a   N,N Dimethylanatoxin   N-methylanatoxinol
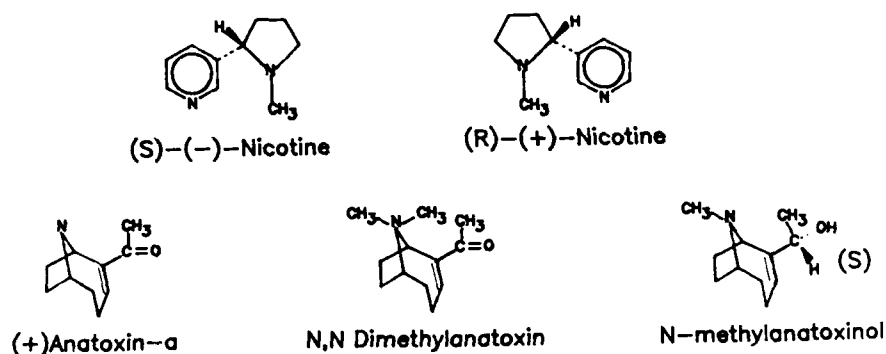
FIG 1   Stereochemistry of nicotinic agonists and antagonists. The two naturally occurring compounds, (+)anatoxin-a and (−)nicotine, are the more potent agonists. All of these compounds except anatoxin demonstrate antagonist properties.

was identified as a potent nicotinic agonist with potency much higher than that of the natural transmitter [7,10]. This toxin is a secondary amine with the nitrogen in a bicyclic ring system and the toxin has a conjugated enone, both of which confer some rigidity to the molecule. The natural toxin is the (+) isomer and it has also been obtained by partially synthetic means [11,12]. (−)Anatoxin-a was also synthesized in optically pure form [13]. Biochemical and electrophysiological analysis showed a high stereospecificity of the acetylcholine (ACh) recognition site at the nicotinic ACh receptor for the (+) isomer of anatoxin-a. Moreover, anatoxin-a has been shown to be highly specific for the nicotinic AChR compared to muscarinic cholinergic receptors in the brain [14]. Because of these pharmacological characteristics and owing to the molecular rigidity and small size (mol. wt. = 166) and its immunity to cholinesterase hydrolysis, (+)anatoxin-a serves as an excellent pharmacological probe for chemical manipulations. Therefore, analogues of (+)anatoxin-a have been synthesized with systematic modifications and assayed for agonist potency, channel activation kinetics and channel blocking properties using binding assays and electrophysiological analysis. The initial inspection of some of the related compounds has shown that the structural and geometric requirements postulated in the Beers and Reich model [15] do not suffice to explain their relative binding affinity and agonist potency. The high stereospecificity of an agonist such as that exhibited by (+)anatoxin-a at the muscle AChR means that at least three groups must be important.

Also, in this paper, we address the actions of nicotine enantiomers on the muscle AChRs. The actions of nicotine, naturally occurring as the (+) isomer, have been the object of numerous studies since its isolation from leaves of tobacco *Nicotiana tabacum* in 1828 and more specifically after the demonstration of its site of action on the autonomic ganglion in 1889 [16]. Although the comparative actions and toxicity of (+) and (−)nicotine have been studied for many decades, the results are still somewhat controversial in part because of the lack of detailed quantitative kinetic analysis. Another aspect of this controversy arose from the difficulty of obtaining highly purified optical isomers. Whereas (−)nicotine was obtained from natural sources, (+)nicotine was obtained either by resolution of a racemic mixture or by synthesis from optically pure (+)nornicotine obtained from *Duboisia hopwoodii*

[17]. In the present study, we analysed the actions of highly purified nicotine enantiomers (98% purity) of synthetic origin. Because nicotine enantiomers are much less stereospecific than anatoxin-a (indeed nicotine isomers are even equiactive according to some authors), two-point interaction may suffice for most of its action at the muscle or *Torpedo* ACh site. Single channel recordings of muscle AChR showed that both (+) and (−)nicotine actions include agonistic actions followed by AChR blockade via desensitization. Our data also disclosed other types of blockade which would include competitive blockade and noncompetitive antagonism via interactions with sites at the ion channel in different states.

Nicotinic receptors of the parasympathetic ganglia and central nervous system (CNS) receptors [17–19] have shown a greater degree of stereospecificity using nicotine stereoisomers as compared to the muscle endplate. Although previous studies have shown some similarity between brain and muscle AChR, pharmacologically, at the CNS, one can identify several binding sites [29–23]. One of them strongly interacts with α-bungarotoxin (BGT) and the other is a high affinity site probed by (−)nicotine. In the mammalian brain, the (−)nicotine site seems to be correlated to the ACh binding site whereas the functional significance of the α-BGT site remains controversial because this toxin often fails to block nicotinic stimulation [24]. (+)Anatoxin-a seems to compete for the high affinity (−)nicotine binding site whereas another toxin named methyllycaconitine, found in the seeds of the plant *Delphinium brownii*, is more effective at the α-BGT site [25]. Therefore, using (+)anatoxin-a and ACh as agonists, single channel recordings were performed on neurons cultured from the hippocampus and the medulla of the fetal rat brain. We have used (+)anatoxin-a to characterize the kinetics of the single channel currents activated at AChRs located in the CNS. Being a secondary amine and because of its high agonist potency and specificity for nicotinic AChR, this toxin is better suited than the natural transmitter or even (−)nicotine for the CNS studies [14,15].

Material and methods

Neuron culture

Hippocampal and brain stem medullary neurons were obtained in culture from Sprague–Dawley rat embryos using the methods described by Banker and Cowan [26,27]. Briefly, 16- to 18-day pregnant rats were killed by CO_2 narcosis and cervical dislocation and the forebrains and brain stems removed and maintained in cold physiological solution with the following composition (mM): NaCl 140, KCl 5.4, Na_2HPO_4 0.3?, KH_2PO_4 0.22, glucose 25 and N-2-hydroxyethylpiperazine-N'-2-ethanesulfonic acid (Hepes) 20, and pH of 7.3. The osmolarity was adjusted to 325 mosM with sucrose. Neurones were enzymatically dissociated from the hippocampus or portions of the medulla extending rostral to the obex and were cultured according to a procedure described elsewhere [28]. Mostly pyramidal cells were present in hippocampal cultures since granule cells were not yet present at the prenatal stage of the rats [27]. Cultures from the medulla contained neurons from the dorsal and ventral respiratory groups chiefly associated with inspiration and expiration, respectively, and included nucleus ambiguous and the nucleus tractus solitarius [29]. Neurons in the reticular formation of the medulla have been shown to respond to iontophoretic application of ACh [30]. The cells in the brain stem culture were either pyramidal, fusiform or spherical [31].

Single muscle fibres

Single fibres were enzymatically isolated from interosseal and lumbricalis muscles of the longest toe of hind legs from the frog *Rana pipiens*. The procedure for enzymatic dissociation of the single fibres was previously described [32]. The isolated fibres were kept in a dish containing frog Ringer's solution with 0.2–0.4 mg/ml bovine serum albumin and stored at 2–5°C prior to experiments. An adhesive mixture composed of parafilm (30%) and paraffin oil (70%) was used to immobilize the single muscle fibres on the bottom of the miniature recording chamber. Composition of the physiological bathing solution was (mM): NaCl 115; KCl 2.5; $CaCl_2$ 1.8; Hepes 3.0, and pH of 7.2. Tetrodotoxin (0.3 μM) was present in all solutions used to prevent muscle fibre contraction.

Single channel recordings and analysis

Single channel recordings were made using the patch clamp technique developed by Hamill et al. [33]. Micropipettes were pulled on two stages from borosilicate capillary glass (World Precision Instruments, Inc.) using a vertical electrode puller (Narishige Scientific Instruments Lab., Japan) and the tips of the pipettes were heat-polished using a microforge (also from Narishige). Further details are described elsewhere [33,34].

Recordings were obtained from the junctional and perijunctional region of the muscle fibre under cell-attached patch conditions using pipettes filled with solution containing ACh (0.4 μM) either alone (control) or combined with various concentrations of the drug being studied. To test the agonistic properties, patch pipettes were filled with different concentrations of the drug alone. A similar procedure was adopted for CNS recordings. All recordings were made at 10°C.

Single channel currents were recorded at various holding potentials with an LM-EPC-7 patch clamp system (List-Electronic, Darmstadt, West Germany). The data were filtered at 3 kHz with an 8-pole Bessel filter and stored on an FM magnetic tape recorder (Racal, 7.5 ips, DC-5 kHz). A PDP 11/40 and 11/24 minicomputers (Digital Equipment Corp.) or an IBM-AT microcomputer were used for data acquisition, detection and analysis of single channel currents digitized at 12.5 kHz and provided channel amplitude and open, burst and closed time histograms [7,35]. A channel was considered open when the current increased more than 80% of the mean estimated channel amplitude and the open time was defined as the duration of an open event (channel open times) terminated by a closing transition detected by a decrease in current amplitude to below 50% of the unitary channel amplitude. A burst was defined as either a single opening or a group of openings separated from adjacent openings by a given closed interval determined by the characteristics of the recorded currents. To have the best estimate of this interburst closed time delimiter, the histogram of all closed times was initially examined. Due to the characteristics of the channel activation, the total closed time distribution was composed of two distinct components. The fast phase, representing intraburst closures, was fitted to an exponential function and the τ_f obtained. A value of 10 times τ_f was used to discriminate consecutive bursts. Therefore, fast closed time histograms included only the short closures (intraburst gaps) with durations briefer than the chosen interburst off time delimiter. Bursts containing multiple simultaneous events, which usually constituted less than 5% of the total number of events, were excluded from calculations of open and burst durations.

Resting membrane potential was not routinely measured for each fibre used in patch-clamp recordings. However, the fibres used had a membrane potential ranging between -50 and -70 mV. Membrane potential was determined indirectly based on the conductance values obtained from the current amplitude–pipette potential relationship, no correction was made regarding reversal potential since its values usually were around -2 mV [36].

Results and discussion

Nicotine optical isomers

Agonist properties

The initial inspection of the effects of (+) and (−)nicotine (see structures in Fig. 1) on the muscle properties showed that both stereoisomers had a weak agonistic effect as measured by the membrane depolarization and muscle contracture. Under control conditions, the frog sartorius muscle usually had membrane potentials of -96 ± 2 mV. After an equilibration period of 60 min (control = 100%), a single concentration of a nicotine stereoisomer was added and kept in the bath by continuous superfusion for 60 min. Measurement of endplate potential at 5-min intervals during this period revealed depolarization; (+)nicotine was about 10-fold less effective than the (−) isomer. Equimolar concentrations (20 μM) of (−) and (+)nicotine produced maximal depolarizations of 30% and 10% from the resting potential, respectively. At 20 μM (−)nicotine and 200 μM (+)nicotine, i.e. roughly equipotent concentrations, the time necessary to reach maximum depolarization (30%) was about 10 min. Spontaneous repolarization occurred thereafter such that by 60 min of exposure to either stereoisomer, regardless of the concentration or the maximum depolarization reached, the membrane potential recovered to a similar level (90% of the control values). After a 1 h wash, recovery of membrane potential was nearly complete.

Agonistic potency of nicotine stereoisomers was assayed by measurement of contracture tension of the rectus abdominis muscle of the frog *Rana pipiens* (Fig. 2). The contracture potency of (−)nicotine was similar to that produced by carba-
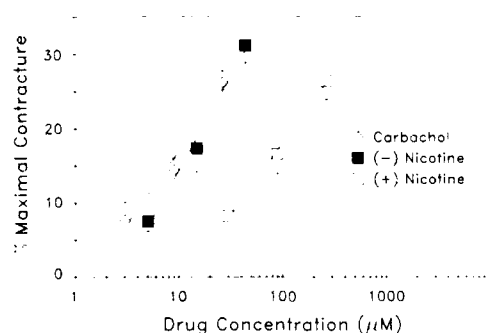
FIG 2 Potency assay of nicotine stereoisomers using rectus abdominis contracture. By direct comparison, the contracture potency of carbachol and the natural isomer (−)nicotine were similar. In contrast, synthetic (+)nicotine was 8-times less potent than (−)nicotine.

162
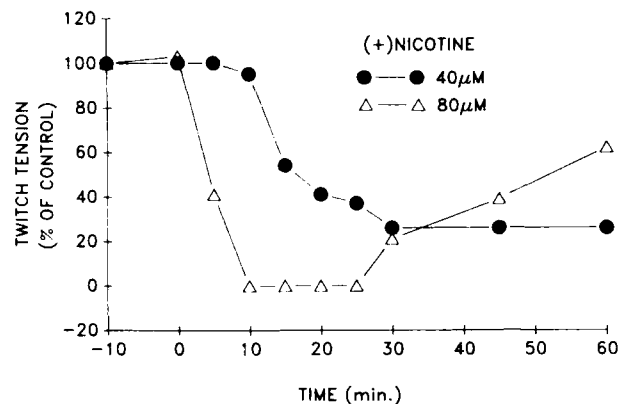
FIG 3 Inhibition of twitch by (+)nicotine. The sartorius muscle was stimulated indirectly via the sciatic nerve at a frequency of 0.2 Hz. The twitch tension (as % of control) was plotted as a function of time and recorded in the presence of 40 and 80 μM (+)nicotine. At 30 min, washing of the preparation with normal physiological solution was begun.

mylcholine; (+)nicotine, in contrast, was about 8-times less potent than (−)nicotine. The ED_{50} values obtained for the alkaloid and its synthetic (+) isomer (maximum contracture value determined with 100 mM KCl) were 23 μM and 130 μM, respectively, compared to the ED_{50} of 15 μM carbamylcholine. It is possible that the potency to produce contracture was reduced by the simultaneous blocking actions of both isomers.

Recordings of the indirectly elicited muscle twitches obtained at high doses of (+) and (−)nicotine showed blocking actions of both isomers. A slight, transient increase in resting tension followed by a clear blockade of the twitch tension was observed. Twitch tension was reduced in a concentration-dependent manner, the (−) isomer being more potent such that at 10 μM a significant blockade could be observed. In comparison, (+)nicotine exhibited a similar effect only at a dose of 40 μM (Fig. 3). Also, the establishment of the blockade was much slower in the presence of (+)nicotine. Regardless of the isomer used, this blockade only partially recovered upon extensive washing (Fig. 3).

Kinetics of currents activated by (+) and (−)nicotine

Patch clamp recordings of single channel currents are very useful to evaluate the kinetics of channel activation. In addition, due to the collagenase-protease treatment, our single fiber preparation had no cholinesterase activity and consisted only of the postsynaptic portions of the endplate, and therefore were very well suited to agonist assessment. Perijunctional AChRs were activated by various concentrations of either (+) or (−)nicotine present inside the patch pipettes. Single channel currents were recorded under the cell-attached patch configuration. Both (−)nicotine (1 and 25 μM) and (+)nicotine (10 and 50 μM) induced openings with increased fast flickerings during the open state of the channels as compared to ACh-activated currents (Fig. 4). It has been well documented that ACh (0.4 μM) activates square-wave currents with very few flickers (fast closures), the number of which is neither concentration nor voltage dependent (Fig. 4, see Refs. 7, 32, 37, 38).
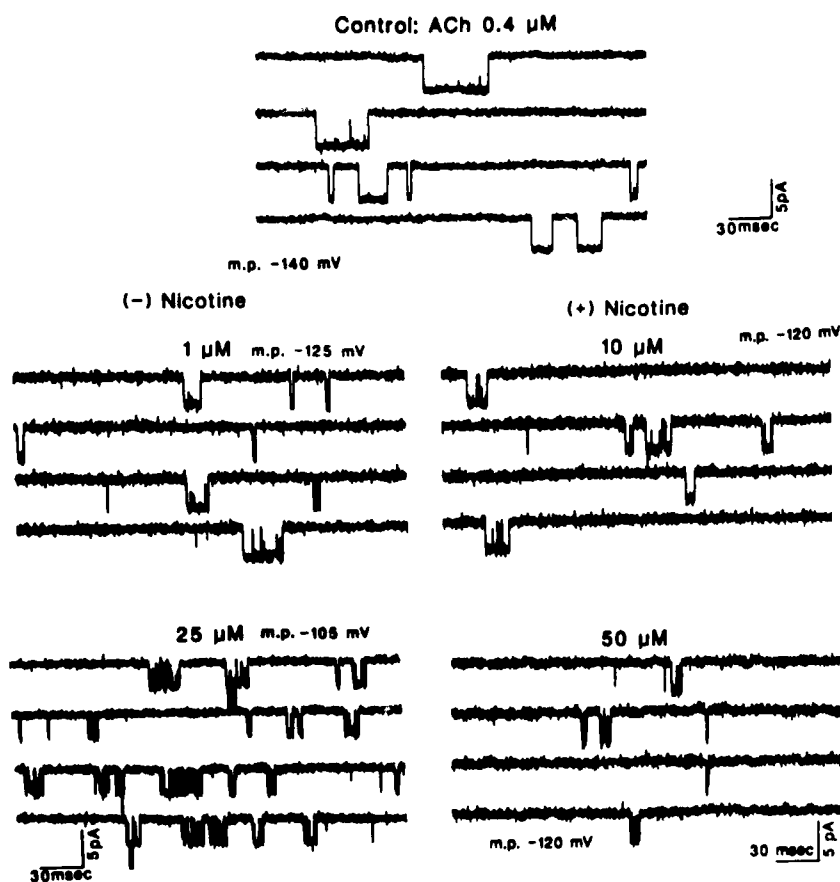
FIG 4 Single channel activation by ACh, (−)nicotine and (+)nicotine. AChRs were activated by agonist inside the patch pipette; recordings were made from cell attached patches.

Therefore, the presence of a few flickers during the open state resulted in a slightly longer burst duration (Fig. 4), giving a burst time/intraburst total open time ratio of 1.1–1.2. On the other hand, both nicotine isomers increased this ratio, and this increase was enhanced by hyperpolarization. Increasing concentrations of either nicotine isomer increased the number of openings per burst. However, as the frequency of bursts increased with the agonist concentration, the accuracy in the measurement of this parameter became poorer because the burst became progressively more difficult to discriminate. Although the number of intraburst closures was concentration- and voltage-dependent, the duration of these closures did not show a clear dependence on these two factors.

Analysis of the open and burst durations found that for (−)nicotine both kinetic parameters were significantly shorter compared to ACh-activated currents (Fig. 5). Open and burst times of the channels activated by 1 and 10 μM concentrations of (−)nicotine had similar values. As has been reported [32,39] and is shown in Fig. 5,

164
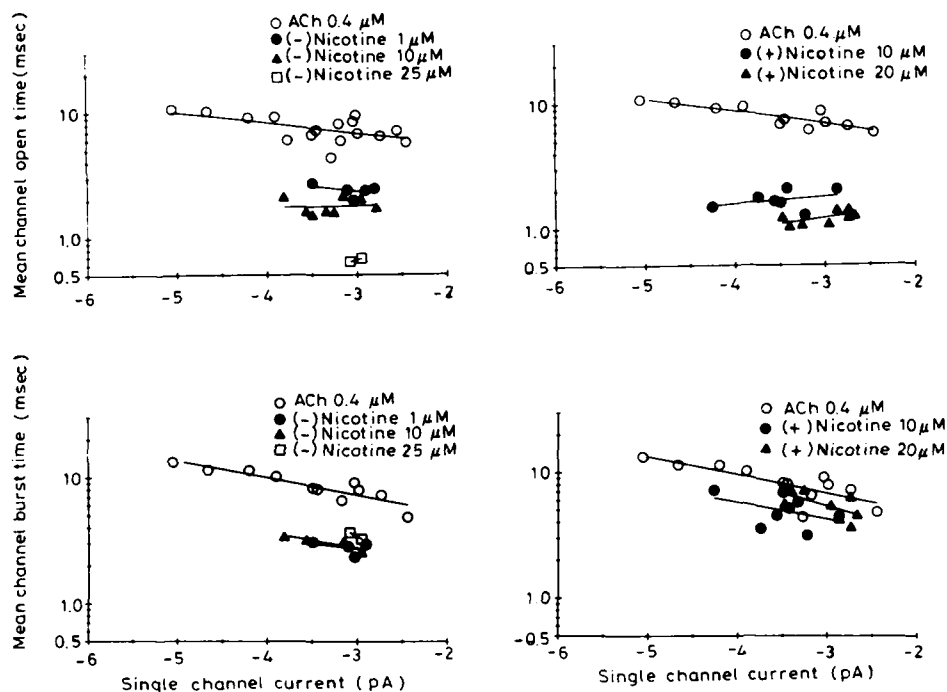
FIG 5   Kinetics of nicotinic activation of AChR. From 1 to 10 μM (−) or (+)nicotine, the durations of channel openings were similar, although in both cases shorter than those of ACh. Channel openings were separated by brief closures, whose durations (0.1 to 0.2 ms) did not have a clear voltage dependence. This decreases the open time/burst time ratio. There was a slight decrease in the open time between 1 and 10 μM (−)nicotine. For (+)nicotine the open time was even shorter at 10 to 20 μM.

the currents activated by ACh had longer open and burst times at more hyper-polarized potentials. Fig. 5 also shows that whereas nicotine-induced burst times maintained a similar voltage dependence to those disclosed by ACh-activated currents, the open times showed a lower sensitivity to voltage variations. Because (−)nicotine, at 25 μM or higher, significantly decreased the open times without changing the burst length (Fig. 5), this shortening occurred by virtue of a large increase in the number of the intraburst flickers. This alteration suggested a blockade of the open state in a manner predicted by the sequential model.

With (+)nicotine, higher concentrations (10–20 μM) were needed to unveil its agonist activity (Figs. 4 and 5). In this concentration range, blocking effects were clearly apparent such that the mean duration of the intraburst openings was progressively shortened with increasing concentrations of (+)nicotine (Fig. 5). Burst durations were only slightly shorter than ACh-induced bursts but did not show a clear dependence on (+)nicotine concentration. This pattern was, therefore, accompanied by a significant increase in the number of flickers in the burst. Similar to (−)nicotine, the duration of the fast intraburst closures was neither voltage- nor concentration-dependent. In conclusion, it seemed that both (−) and (+)nicotine produced blocking effects at concentrations used to test the agonist property.
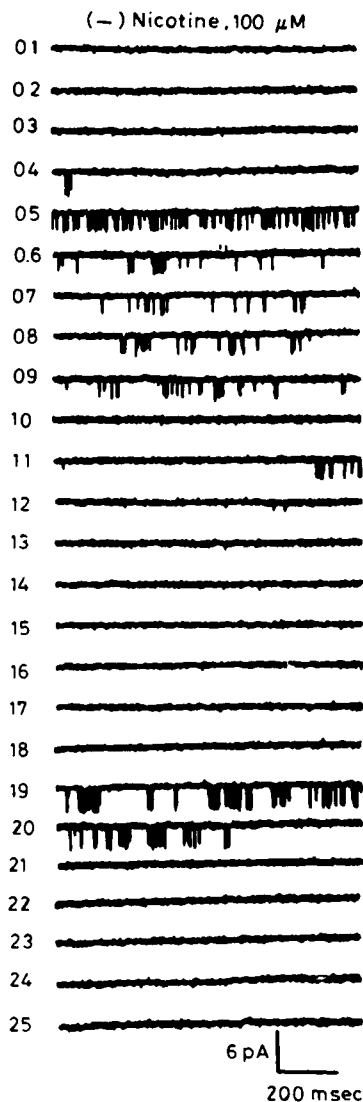
FIG 6   Desensitization. The clustered pattern of channel activity at high concentrations of
(−)nicotine was typical of desensitizing agonist concentrations. The single channel currents
are from a cell-attached patch at a holding membrane potential of − 140 mV.

In addition, high concentrations (> 100 μM) of both nicotine enantiomers
induced AChR desensitization. Long clusters of openings separated by long silent
periods (second to minute range) could be recorded (Fig. 6). The individual
openings within the clusters were very fast, such that they could not be adequately
detected by our recording system and the amplitude of the events seemed reduced.
This pattern was distinct from that observed for ACh and (+)anatoxin-a (see Fig.
11 and Ref. 40) that showed agonist and desensitizing actions at submicromolar and

low micromolar concentrations, respectively, whereas the channel blocking action of ACh only took place at a much higher range ($> 30 \ \mu$M). Therefore, in contrast to nicotine, with these potent agonists the duration and the amplitude of the events within the clusters were not significantly different from those recorded at low concentrations.

Effects of (+) and (−)nicotine and single channel currents activated in the presence of ACh

The probability of channel blockade was tested on the currents activated in the presence of a fixed concentration of ACh ($0.4 \ \mu$M) and a range of (+) or (−)nicotine concentrations. At 1 to 20 μM, the openings observed in the presence of either nicotine enantiomer had flickers during the open state of the channels (Fig. 7). The number of flickers increased with the concentration of either nicotine isomer. This effect was more prominent with (+)nicotine (Fig. 8). With the (+) isomer, the mean channel open times were shortened in a concentration- and voltage-dependent manner (Fig. 9). The shortening of the mean open times were more pronounced at more hyperpolarized potentials. Mean burst times were not significantly different from the control condition, i.e. ACh alone. The shortening of the mean open times occurred by virtue of an increasing amount of flickering. Therefore, a marked increase in the frequency of flickers was observed with increasing (+)nicotine concentration and with hyperpolarization of the membrane. This pattern was also observed when this isomer was tested alone inside the patch pipette in the agonist experiments (Fig. 4). It should be noted, however, that (+)nicotine produced these alterations at concentrations lower than those utilized to unveil its agonistic property.

Compared to the (+) isomer, (−)nicotine induced lesser flickering, because open times and burst times were both decreased with increasing (−)nicotine concentrations (Fig. 8). Voltage-dependence was not clearly discerned for open or burst times with (−)nicotine, a pattern also observed when this isomer was tested alone, i.e. without ACh (Figs. 4 and 5).

The results of single channel studies were interpreted according to the sequential channel blocking model previously used to describe the blocking actions of local anesthetics (QX222 [41]), anticholinesterase agents (neostigmine, pyridostigmine and edrophonium [40]), cholinesterase reactivators (2-PAM and HI-6 [36]):

$$2A + R \underset{k_{-1}}{\overset{k_1}{\rightleftharpoons}} A_2R \underset{k_{-2}}{\overset{k_2}{\rightleftharpoons}} A_2R^* \underset{D \ k_{-3}}{\overset{D \ k_3}{\rightleftharpoons}} A_2R^*D$$
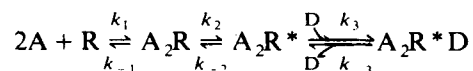
In this sequential set of reactions shown above, the AChR designated simply as R, interacts with two molecules of agonist (A) originating an intermediate, doubly agonist-bound closed conformation which in its turn shifted to the open channel state (A_2R^*). In this model, the open AChRs are subjected to blockade by either nicotine enantiomers, indicated by D, leading to the formation of a state with no conductance ($AChR^*D$).

With (+)nicotine, the mean open times were reduced in a voltage-dependent manner, i.e., the blocking effect was faster at hyperpolarized potentials, with a gradual reduction in the voltage pattern of the ACh-activated currents and even an inversion of the slope of the plots (Figs. 5 and 9). According to the model, this voltage-dependent profile of the blocking effect results from the contribution of the two rate constants, k_{-2} controlling the normal closure (i.e., in the absence of

Control : ACh 0.4 μM

ACh 0.4 μM − (+) Nicotine 20 μM

ACh 0.4 μM + (+) Nicotine 20 μM

m.p. −140 mV

5 pA

30 ms
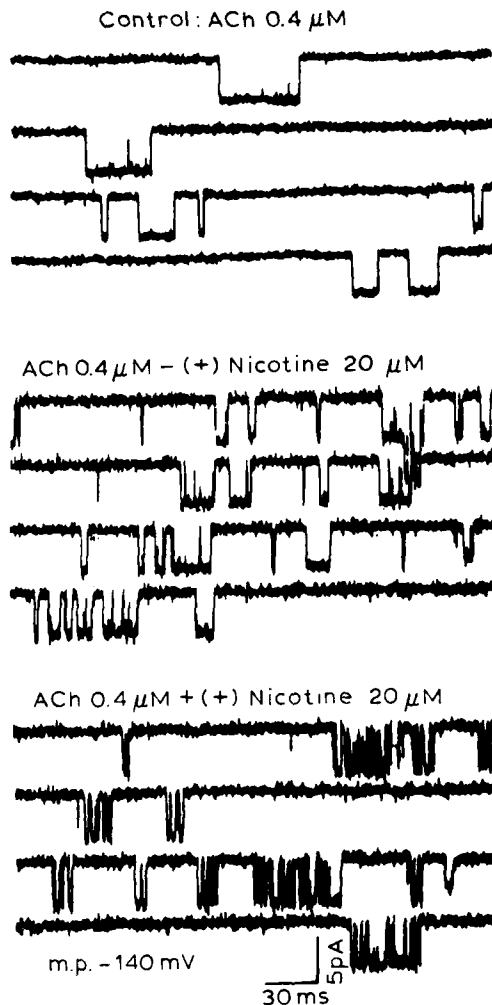
FIG 7 Samples of ACh-activated single channel currents recorded from frog interosseal muscle fibers. Top: ACh alone; middle: ACh plus 20 μM (−)nicotine in the patch pipette; bottom: ACh plus 20 μM (+)nicotine. Temperature: 10 °C.

blocker) and k_3 which governs the rate of the blocking reaction. These rate constants have opposing voltage-dependence. The contribution of k_3 to the open times is amplified by the drug concentration thus accelerating channel blockade and shortening of the open times at more hyperpolarized potentials. The analysis of the duration of the intraburst closures showed that they were neither voltage- nor concentration-dependent in contrast to many open channel blockers [36,42–44]. Also, the burst duration should theoretically be prolonged with concentration as the number of flickers increased with higher doses of the drug. However, this effect was not seen, and indeed, with (+)nicotine a slight shortening of the burst length was observed (Fig. 9). These findings suggested either a distinct mechanism from that
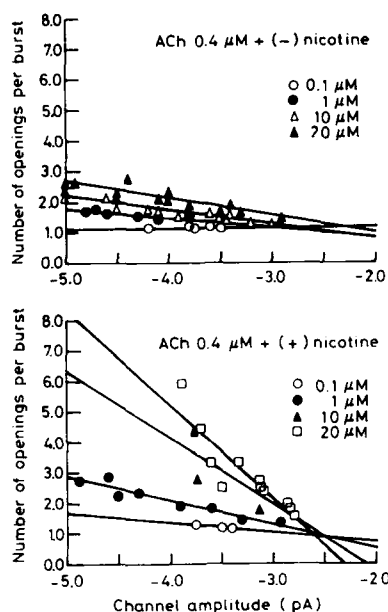
FIG 8   Number of openings per burst for ACh-activated single channel currents. Recordings were made from frog interosseal muscle fibers with ACh (0.4 μM) plus either ($-$) or ($+$)nicotine, at concentrations indicated (0.1–20 μM), in the patch pipette. Cell-attached patch, temperature 10°C.

predicted by the sequential model or a binding to a site outside of the electric field of the membrane.

Most of the channel alterations induced by ($-$)nicotine in the presence of ACh did not fit the predictions of the sequential model. The mean open times decreased with concentration but were not influenced by the transmembrane voltage (Fig. 9). In addition, mean burst times decreased with increasing ($-$)nicotine concentration to a value close to that obtained when ($-$)nicotine was used alone to test its agonist property (Figs. 4 and 5). Also, similar to ($-$)nicotine alone, the burst length maintained the same voltage-dependence of the ACh-activated currents. An alternative mechanism underlying these alterations may be a concomitant activation of the channels by both ACh and nicotine. This seemed especially true for ($-$)nicotine as this enantiomer produced significant agonistic activity at the same concentrations we used with ACh. The gradual decrease of the mean open times with ($-$)nicotine concentrations might have resulted from an increased contribution of ($-$)nicotine-induced currents to the total events recorded. A comparison of Figs. 5 and 9 showed that the mean open times of the currents activated in the presence of both ACh (0.4 μM) and ($-$)nicotine (20 μM) and their dependence upon the voltage, were not significantly different from those determined for the currents recorded in the presence of ($-$)nicotine alone. However, higher doses of ($-$)nicotine were not tested in the presence of ACh to ensure whether a further shortening of the mean open times would be observed. As mentioned earlier, with 25 μM ($-$)nicotine alone, the intraburst open times were clearly shortened without significant changes of the
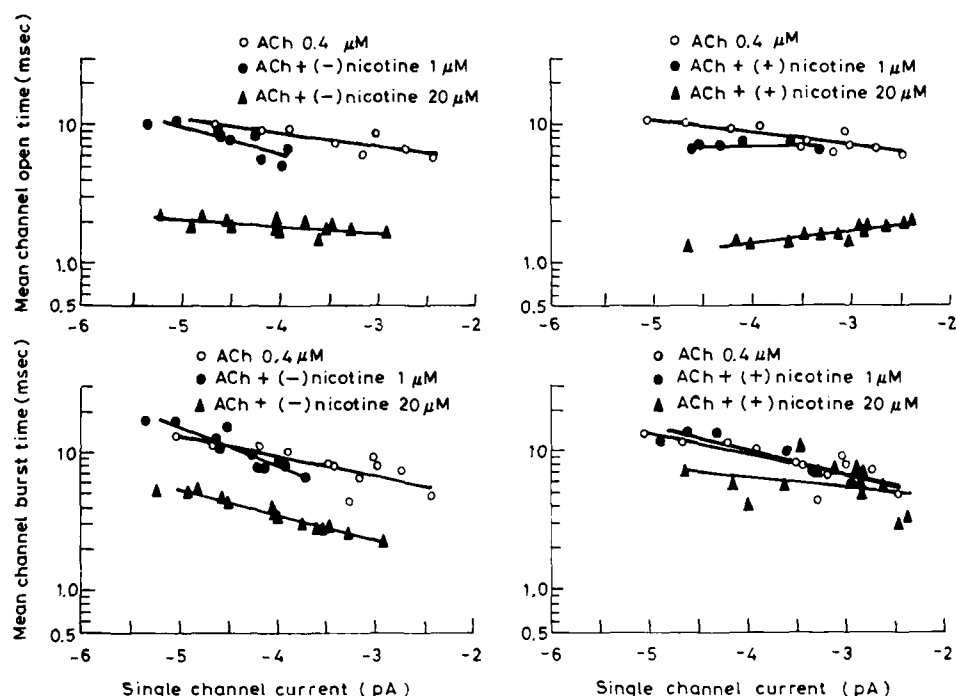
FIG 9 Kinetics of activation of AChR by a combination of ACh and nicotine. ACh (0.4 μm) was combined with 1 and 20 μM (−) and (+)nicotine in the patch pipette. Because ACh commonly causes isolated openings, it could have been possible to observe channel blockade by relatively low concentrations of nicotine where channels were predominantly activated by ACh. Increasing concentrations of nicotine produced a dose-dependent decrease in the open time of single channel currents. Burst times dropped from the control level to that observed with nicotine isomers alone.

burst duration, thus indicating occurrence of blockade of the open state of the channels. In the case of (+)nicotine, the agonist effect had a smaller contribution to the currents and the majority of the alterations resulted from the noncompetitive blockade of the open state of the channels activated by ACh. Indeed, most of the data could be fitted to the predictions of the sequential model described earlier.

Anatoxin-a stereoisomers and selected analogues

The agonist and antagonist properties of anatoxin-a stereoisomers and two geometric isomers (R)- and (S)-N-methylanatoxinols were studied on muscle contracture and on single channel currents activated at the perijunctional region of the frog skeletal muscle fibre. In addition, we present here the initial results obtained with the dimethyl derivative of (+)anatoxin-a on the single channel currents. The chemical structures of these analogues are shown in Fig. 1.

Agonist potency as determined from the muscle contracture

In the rectus abdominis contracture assay, (+)anatoxin-a was 110 times more potent than carbamylcholine. By comparison with ACh, after complete inhibition of

Binding to torpedo nicotinic receptors
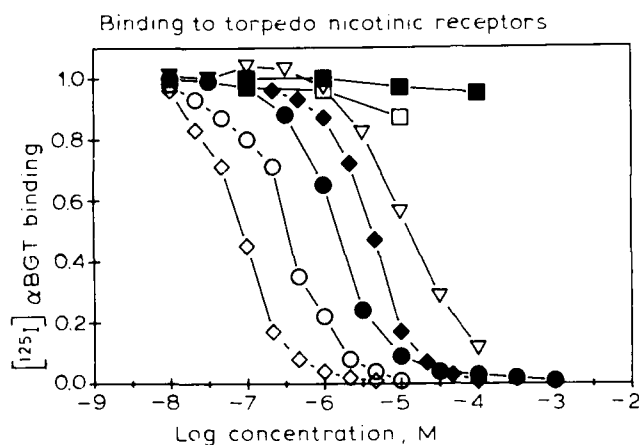
FIG 10 Inhibition of [^{125}I]α-bungarotoxin binding to *Torpedo* electropax receptors by (+)anatoxin-a (◇). ACh (○), carbamylcholine (●). (−)anatoxin-a (◆). *N*,*N*-dimethylanato-xin (▽). and (*S*)- and (*R*)-*N*-methylanatoxinols (□ and ■). respectively).

cholinesterase (ChE) with the irreversible anti-ChE agent diisopro-pylfluorophosphate. (+)anatoxin-a was 8-times more potent than the natural trans-mitter [7]. These data were in good agreement with assays performed in *Torpedo* electric organ membranes by measuring the inhibition of the binding of radioactive α-BGT, a specific probe for the agonist recognition site at the nicotinic AChR [7]. (+)Anatoxin-a was 3-fold more potent in inhibiting [^{125}I]α-BGT binding than ACh. thus indicating that the high agonistic potency of (+)anatoxin-a seemed to result from the its high affinity for the ACh recognition site at the AChR (Fig. 10).

In addition. we determined the stereospecificity of the ACh recognition site in relation to anatoxin-a enantiomers. (+)Anatoxin was more than 150-fold more potent than the (−) isomer [7]. Considering that the (−)anatoxin-a sample could be contaminated to some very small degree with (+)anatoxin-a. the difference could be even larger. This degree of stereospecificity is much higher than that shown by other enantiomeric pairs of nicotinic agonists. (−)Nicotine as we had shown in the previous section is only 8- to 10-times more potent than the (+) isomer (Fig. 2).

In the same rectus abdominis preparation. the contracture potency of (*S*) and (*R*) geometric isomers of *N*-methylanatoxinol was tested. These analogues have a methyl group attached to the nitrogen and a secondary alcohol substituting for the carbonyl group of (+)anatoxin-a. These structural alterations produced marked reduction in the ability of these isomers to act as nicotinic stimulants. These (*S*) and (*R*)-isomers were tested up to 170 μM and 250 μM. respectively. but neither of the *N*-methylanatoxinol isomers induced any contracture of the rectus abdominis muscle [44]. The absence of detectable muscle contracture was directly related to the lack of binding to the agonist recognition site as determined by the poor capability of both isomers to inhibit [^{125}I]α-BGT binding. The (*S*)-isomer inhibited [^{125}I]α-BGT slightly at 10 μM whereas the (*R*)-isomer even at 100 μM did not significantly affect this binding (Fig. 10).

In addition. it has been reported that strong nicotinic agonists greatly enhance the binding of probes such as [^{3}H]H$_{12}$HTX to sites at the AChR ion channel. These

sites are thought to be allosterically associated with the receptor gating process such that the binding of the agonist to its site removes some barriers thus increasing the rate of $[^3H]H_{12}HTX$ association [45,46]. The relative potencies of ACh, (+) and (−)anatoxin-a and the (S) and (R)-N-methylanatoxinols in stimulating $[^3H]H_{12}HTX$ binding were in close agreement with their potencies in inhibiting the binding of $[^{125}I]\alpha$-BGT to the agonist recognition site. Whereas (−)anatoxin-a and ACh markedly increased the $[^3H]H_{12}HTX$ binding, (−)anatoxin-a poorly stimulated and the N-methyl-anatoxinol analogues actually inhibited the interaction of this ion channel probe [7,44].

Kinetics of single channel currents activated by (+)anatoxin-a and analogues
Nicotinic AChR from the frog muscle endplate was activated by ACh and (+)anatoxin-a and its analogues. The agonists, at various concentrations, were placed inside the patch micropipette and the recordings obtained under cell-attached configuration.

(+)Anatoxin-a This toxin induced channel openings at nanomolar concentrations. The slope conductance of channels activated by (+)anatoxin-a was similar to that calculated for ACh, i.e. 30 pS, at 10°C. In comparison to ACh, the currents activated by (+)anatoxin-a showed more frequent interruption by short closures of the channels. These closures were neither concentration- nor voltage-dependent and were interpreted as resulting from the transition between the agonist-bound closed state and the open state. Due to the presence of these flickers, the mean of the open times for (+)anatoxin-a was one-half of the mean burst times whereas for ACh these two parameters differed only slightly. The duration of the bursts elicited by (+)anatoxin-a was significantly shorter than that activated by the neurotransmitter; for example, at −90 mV holding potential, the values found were 5 and 9 ms for (+)anatoxin-a and ACh, respectively [7].

In addition, at 10-fold higher concentrations, (+)anatoxin-a induced AChR desensitization like ACh and other strong agonists (Fig. 11 and see Fig. 14 in Ref. 40). After an initial period of simultaneous activation of many channels, typical clusters of channel openings [47,48] separated by long silent periods were recorded at high concentrations (1–3 μM) of (+)anatoxin-a. In the case of (+)anatoxin-a, because of the shorter open and burst duration the total cluster length was much shorter than those induced by desensitizing concentrations of ACh (Fig. 11 and Ref. 40). No significant change in the apparent single channel conductance was seen at desensitizing doses of (+)anatoxin-a. Binding assays have disclosed that although (+)anatoxin-a showed higher affinity than ACh for the agonist recognition site, the onset of desensitization induced by this toxin was slower than that produced by the neurotransmitter [7]. A similar difference was observed at lower concentrations of (+)anatoxin-a and ACh. The slower rate of desensitization caused by (+)anatoxin-a may partly contribute to the greater potency of (+)anatoxin-a over ACh seen in the measurement of contracture tension.

(S)- and (R)-N-methylanatoxinol Although contracture [44] and binding assays (Fig. 10) did not demonstrate significant agonist activity, (S)-N-methylanatoxinol (1–20 μM) activated low-frequency single channel currents. No channel activation, however, could be recorded with (R)-isomer up to 200 μM. In comparison to (+)anatoxin-a (0.02 μM) and ACh (0.3–0.4 μM), even at higher concentrations (100

(+) Anatoxin-a 3.2 μM

30ms | 5 pA
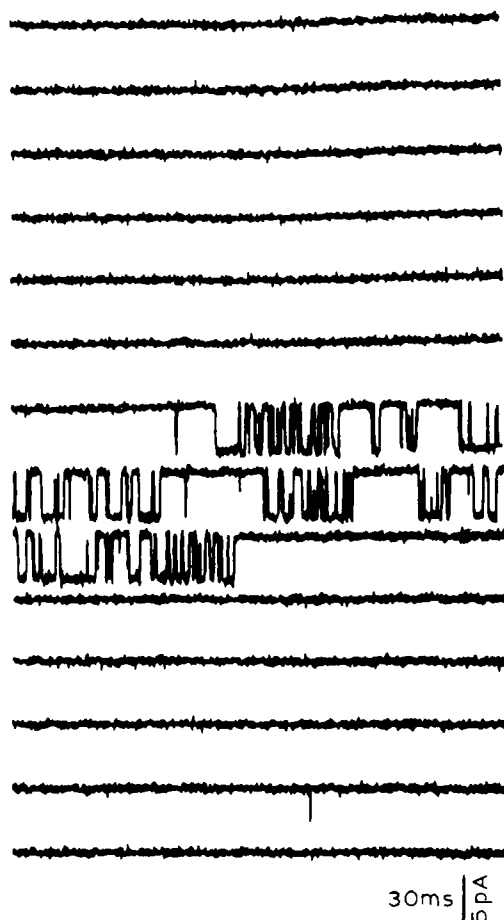
FIG 11 Desensitization of the AChR induced by (+)anatoxin-a (3.2 μM). Isolated bursts with openings of normal duration were separated by a long-lasting period without channel activity.

μM), the frequency of channel activation of (S)-N-methylanatoxinol was very low, with no multiple simultaneous openings. Recordings obtained with (S)-isomer at 1 to 10 μM concentrations consisted of bursts with 'flickers' similar to the those recorded with (+)anatoxin-a as nicotinic agonist (Fig. 12). At higher concentrations, (S)-N-methylanatoxinol induced alterations that suggested the occurrence of blockade of the open state of the channels. Because the frequency of openings was very low, this effect was further analysed on the channels activated by ACh (see below).

N,N-Dimethylanatoxin Although very preliminary, for qualitative comparison we present here the initial results obtained with another analogue of (+)anatoxin-a,
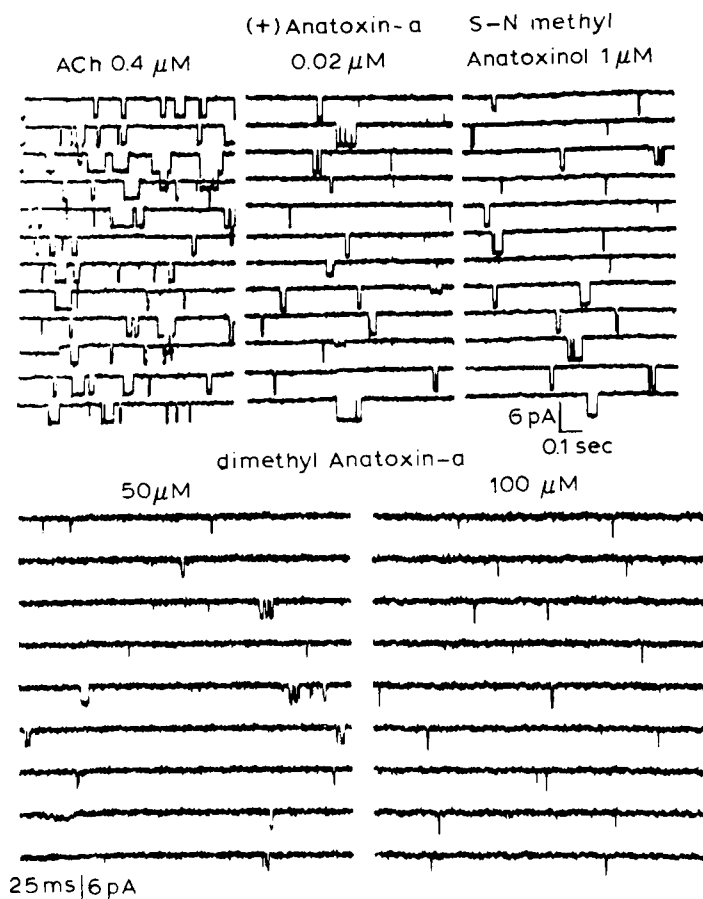
FIG 12   Samples of single channel currents activated by ACh. (+)anatoxin-a. (S)-N-methyl anatoxinol. and N,N-dimethylanatoxin. Holding potential: − 125 mV. Temperature: 10°C. Note the marked differences between concentrations of agonists that were required to elicit moderate frequency of bursts.

N,N-dimethylanatoxin. This analogue differs from (+)anatoxin-a only by two additional methyl groups which are attached to the nitrogen atom. This structural alteration led to a marked reduction in the muscle contracture potency of dimethyl-anatoxin [49]. This reduction was only partly due to the decrease in dimethylanato-xin affinity for the agonist recognition site as indicated by the [^{125}I]α-BGT competition assay carried out with Torpedo electroplax membranes (Fig. 10). At the single channel current level, in comparison to the original toxin, a 1000-fold higher concentration range (20–100 μM) was necessary to study the kinetic properties of the channels activated by this analogue. Similarly to (S)-N-methylanatoxinol. currents activated by dimethylanatoxin showed increased number of flickers (Fig. 12). The frequency of flickering increased with dimethylanatoxin concentration and was accompanied by a decrease in the mean open and burst times. an effect similar to that observed with anatoxinol isomers. As we pointed out before, some of these

alterations were suggestive of blockade of the open state of the channels. Because of low-frequency channel activation induced by dimethylanatoxin we decided to further analyse the blocking mechanism using ACh as the nicotinic agonist (see below).

Structure–agonist potency relationship   In an attempt to correlate the structural alterations with the marked reduction in the agonist potency observed with the two geometric isomers, (R)- and (S)-N-methylanatoxinol, the role of both the additional methyl groups at the amine group and the reduction of the ketone moiety present in anatoxin-a to a secondary alcohol should be considered. Beers and Reich's model [15] postulates for the interactions of ACh and other nicotinic agonists with their recognition sites on the AChR, that there are two main points separated from each other by a distance of 0.59 nm: an electrostatic interaction occurs involving the amine moiety and a hydrogen bond where the agonist carbonyl group functions as an acceptor.

The alcohol group should be a worse acceptor of H-bonds than either the carbonyl of (+)anatoxin-a or the ester group of carbamylcholine. In addition, the reduction of the ketone function led to the loss of the conjugated enone system present in (+)anatoxin-a structure providing free rotation of the alcohol moiety. Significant and comparable reductions of the agonist potency and lethality had also been observed when the enone system was lost by the saturation of the double bond of (+)anatoxin-a to form dihydroanatoxin [11]. Free rotation might remove the optimum distance between the positively charged nitrogen head and the hydrogen bond postulated for AChR activation, as encountered in (+)anatoxin-a and ACh molecules. Indeed, binding assays showed that both (R)- and (S)-isomers had higher affinity for muscarinic than for nicotinic receptors and that both analogues had higher affinity for muscarinic receptors than did (+)anatoxin-a [44]. These findings suggested a change in the orientation of the hydrogen bond and in the distance between the two functional groups to become closer to the 0.44 nm postulated for muscarinic stimulation [15,44]. Another cause for decrease in the affinity for the agonist recognition site could result from the loss in the planarity of the acetoxy group present in the ACh molecule by the reduction of the carbonyl group, thought to be critical for the expression of agonist potency [50].

In reference to the cationic head, the first inspection led us to discard an important role of the N-methylation or the non-quaternary nature of the amine group in the reduction of the agonist potency of the N-methylanatoxinol isomers. In the ACh molecule and many other strong nicotinic agonists the nitrogen is part of a quaternary ammonium group with a permanent positive charge [1,6]. In the case of (+)anatoxin-a and the N-methylanatoxinol isomers, although secondary and tertiary amines, respectively, they should be mostly protonated at the physiological pH of solutions used. Furthermore, the nicotinic agonism seems to be directly related to the depth of bulky groups in the direction perpendicular to the plane of the carbonyl group. A steric bulk around the cationic head appears to be important to achieve channel activation [1]. However, the initial results with dimethylanatoxin indicated that the functional and steric features delineated in Beers and Reich's model are insufficient to predict the potency of the nicotinic agonists. The dimethyl-anatoxin molecule contains the same (+)anatoxin-a carbonyl group and enone system but the amine moiety in this analogue is a quaternary ammonium resulting from the double N-methylation. Greater reduction in the agonist potency, compared

to N-methylanatoxinol isomers, observed with the dimethyl analogue suggested that not only the distance between the coulombic interaction and the H-bond, but the directionality and perhaps more subtle differences such as solvation, hydrophobicity, etc. are important features in the activation of AChR.

Blocking action of (R)- and (S)-N-methylanatoxinol on the ACh-activated channel currents

Binding assays performed on *Torpedo* electroplax membranes showed that (+)anatoxin-a did not produce significant noncompetitive blockade of the AChR ion channel as indicated by the absence of inhibition of binding of [^{3}H]H$_{12}$HTX [7]. On the contrary, as mentioned above, (+)anatoxin-a increased the affinity of the H$_{12}$HTX for its binding site by an allosteric coupling with the agonist recognition site. Electrophysiologically, recordings of nerve-elicited endplate currents did not show alterations of the time constant of the decay, a parameter that reflects the kinetics of the activated ion channel [10]. Only the peak amplitudes were markedly depressed as a consequence of AChR desensitization. It has been reported that ACh at concentrations of 30 μM or higher produced channel blockade [48,51]. This concentration range of (+)anatoxin-a, however, was not tested.

(R)- and (S)-N-methylanatoxinol In contrast to (+)anatoxin-a, inhibition of the [^{3}H]H$_{12}$-HTX binding at *Torpedo* electroplax membranes indicated that both (R)- and (S)-isomers interacted significantly with noncompetitive sites at the AChR [44]. Four-times greater potency for inhibiting [^{3}H]H$_{12}$-HTX binding was observed with (R)- compared to (S)-isomer. Moreover, whereas the binding of (S)-isomer was not influenced by the presence of nicotinic agonists such as carbachol, the inhibitory potency of the (R)-isomer was increased over 4-fold in the presence of this agonist [44].

We analysed the blocking actions of both isomers on the single channel currents recorded using admixtures of ACh (0.4 μM) with (S)- (1–20 μM) or (R)-N-methylanatoxinol (5–200 μM). The single channel conductance was not altered by the inclusion of either analogue. However, both analogues caused definite changes in the open state of the channels.

In the presence of (S)-N-methylanatoxinol, single opening events were divided by numerous flickers yielding bursting-like activity (Fig. 13). The effects of both isomers were analysed according to the sequential model presented earlier. The durations of intraburst openings were distributed according to a single exponential, at all concentrations or transmembrane potentials tested, indicating a single open state of the channels. The mean open times were shortened in a concentration- and voltage-dependent manner (Fig. 14A). The linearity of the relationship (within a small voltage range) between the reciprocal of the channel open times and the blocker concentration predicted by the sequential model and described according to the equation $1/\tau_{open} = k_{-2} + [D] \times k_3$ was observed with (S)-isomer (Fig. 14B). The slope of that relationship is the blocking rate k_3, and it in turn was exponentially dependent on the holding potentials (Fig. 14C). The magnitude and opposing voltage dependence of k_3 was responsible for the influence of the holding potentials on the blockade of the open state of the channels. Therefore, with increasing concentrations, the steep voltage dependence observed under control condition was gradually lost and the sign of the slope was even reversed at higher concentrations of (S)-isomer, as the rate of blocking (k_3) made increasingly greater contributions
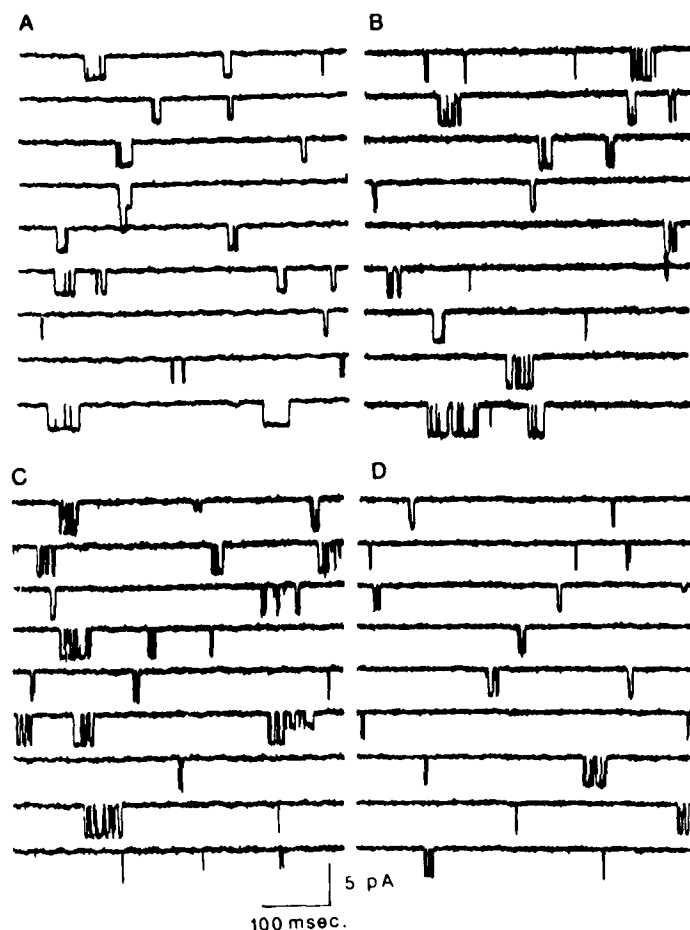
FIG 13 Samples of single channel currents activated by ACh in the presence of various concentrations of the (S)-N-methylanatoxinol. Holding potential -120 mV. Note that the channels are activated in bursts composed of many openings, i.e., the channels appeared to undergo many transitions between the open and short, blocked states. A: ACh 0.4 μM plus (S)-N-methylanatoxinol 1.25 μM. B: ACh 0.4 μM plus (S)-N-methylanatoxinol 6.25 μM. C: ACh 0.4 μM plus (S)-N-methylanatoxinol 12.5 μM. D: ACh 0.4 μM plus (S)-N-methyl-anatoxinol 25 μM.

to the shortening of mean channel open time (Fig. 14). Also, in the same figure one can see the steep voltage dependence of the forward rate constant (k_{+}) of the blocking reaction induced by (S)-N-methylanatoxinol.

Comparatively, the (R)-isomer induced longer bursts than the (S)-isomer with more prolonged intraburst closures which according to the model corresponded to the blocked state [44]. Though progressive shortening of the open times was observed from 6.25 to 200 μM concentrations of (R)-N-methylanatoxinol, in contrast to the (S)-isomer, the analysis of (R)-isomer actions indicated no clear linear relationship between the mean channel open time and its concentration. As
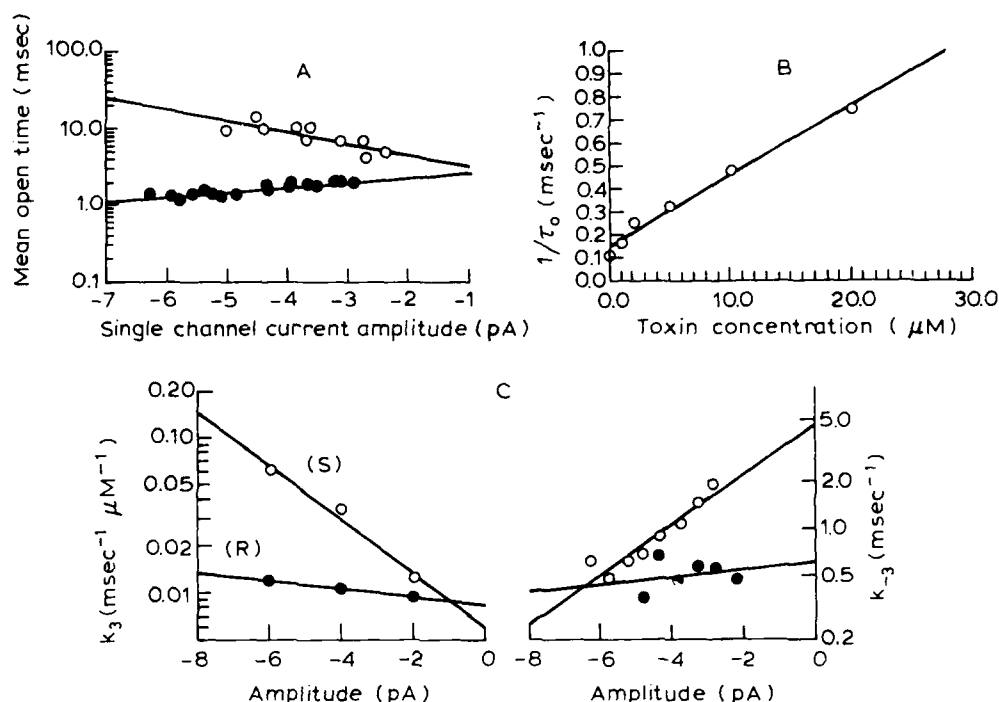
FIG 14 A: semilogarithmic plot of mean channel open times versus amplitude of the single channel currents activated in the presence of ACh (0.4 μM) either alone (○) or together with (S)-N-methylanatoxinol (10 μM, ●). Note that under control conditions, the open time durations increased with the amplitude and therefore with hyperpolarization. In the presence of ACh and (S)-N-methylanatoxinol, this voltage dependence is gradually lost with increasing concentrations of the toxin, the sign of the slope is inverted at concentrations of 10 μM and above. B: relationship of the reciprocal of the mean channel open times $(1/\tau_o)$ to toxin concentration. A linear relationship was seen up to 20 μM concentrations of (S)-N-methylanatoxinol. C: blocking (k_3) and unblocking (k_{-3}) rates for (S)- and (R)-N-methylanatoxinols (○ and ●, respectively), demonstrating a greater voltage dependence of the more polar S isomer.

seen in Fig. 14C, k_3 for (R)-N-methylanatoxinol showed very weak voltage dependence.

The more quantitative analysis of the closed times for both isomers disclosed two distinct components, the short-lasting population being associated with the channel blocked state. According to the sequential model for open channel blockade, the reciprocal of mean blocked times corresponds to the rate for unblocking (k_{-3}). The k_{-3} values for the (S)-isomer were voltage-dependent such that greater stability of blockade occurred at more hyperpolarized potentials. In comparison to the (S)-isomer, the (R)-isomer induced longer channel closures due to a lower unblocking rate. Furthermore, for the (R)-isomer these values were not significantly altered by the changes of the transmembrane holding potentials (Fig. C).

In addition, with increasing concentrations of the blocker, the sequential model predicts an increase in the number of openings per burst with no changes of the

total open time per burst. However, this premise was not supported with either analogue as the total open time per burst was decreased despite the increase in the number of openings per burst. This was particularly evident in the case of blockade induced by high concentrations of the (R)-isomer. This departure from the sequential model suggests the existence of alternate mechanism(s) such that transition of the blocked AChR towards its resting state occurs without passing through the open state.

Structure-channel blockade relationship   (+)Anatoxin-a did not produce significant noncompetitive blockade of the AChR ion channel. In contrast, both (S)- and (R)-methylanatoxinol and dimethylanatoxin demonstrated ion channel blocking activity. Both k_3 and k_{-3} for (S)-isomer were greater and voltage-dependent such that in the single channel recordings we could discern faster intraburst closures that were stabilized at more hyperpolarized potentials. The rate of unblocking by the (S)-isomer was comparable to that reported for slowly dissociating blockers such as scopolamine [43] and slower than for the rapidly reversible blockers pyridostigmine [52], physostigmine [34], neostigmine and edrophonium [40]. In contrast to the above mentioned blockers, both the blocking and unblocking rates for the (R)-isomer were voltage insensitive. The values of k_{-3} for the (R)-isomer were smaller those that of the (S)-isomer but apparently faster than those of quasi-irreversible (very slowly reversible) blockers such as atropine [43], bupivacaine [37] and cocaine [53].

The greater polarity of the (S)-isomer could contribute to a greater rate of binding as a noncompetitive antagonist via long range coulombic forces of attraction. The rate of blocking of (S)- would appear to be greater than that of (R)-methylanatoxinol as a result of its greater voltage sensitivity (Fig. 14C). However, (S) exhibited a faster dissociation (unblocking) rate, as this isomer induced shorter intraburst closures compared to the (R)-isomer. In the case of physiologically synchronized channel activity which occurs during neuromuscular transmission, the magnitude and the voltage dependence of these rate constants could alter the kinetics of the EPC decay. As indicated by the k_3 and k_{-3} values for (S)-isomer, the blockade is weaker and less stable at depolarizing potentials. Therefore, the depolarization that results during synaptic transmission would have a greater influence in diminishing the blocking potency of the (S)-isomer. This is confirmed by the low potency of antagonism of $H_{12}HTX$ binding measured in *Torpedo* homogenized membranes (near 0 mV) [44]. (R)-isomer, on the other hand, due to the lower voltage dependence of its blocking and unblocking rate constants, showed higher potency in inhibiting $H_{12}HTX$ binding. Indeed, though weak, the depression of muscle twitch response was only observed with the (R)-isomer.

(+)Anatoxin-a on the central AChR

The identification of AChR in central nervous system and the analysis of the agonist properties of ACh and (+)anatoxin-a were carried out in neurons cultured from the hippocampus and the medullary portion of the brain stem regions of fetal rats [28]. In contrast to the rather homogeneous and high density distribution of glutamate [54] and GABA-activated receptors [55] on the soma membrane, the activity of AChR was more likely to occur in the area close to the base of the apical
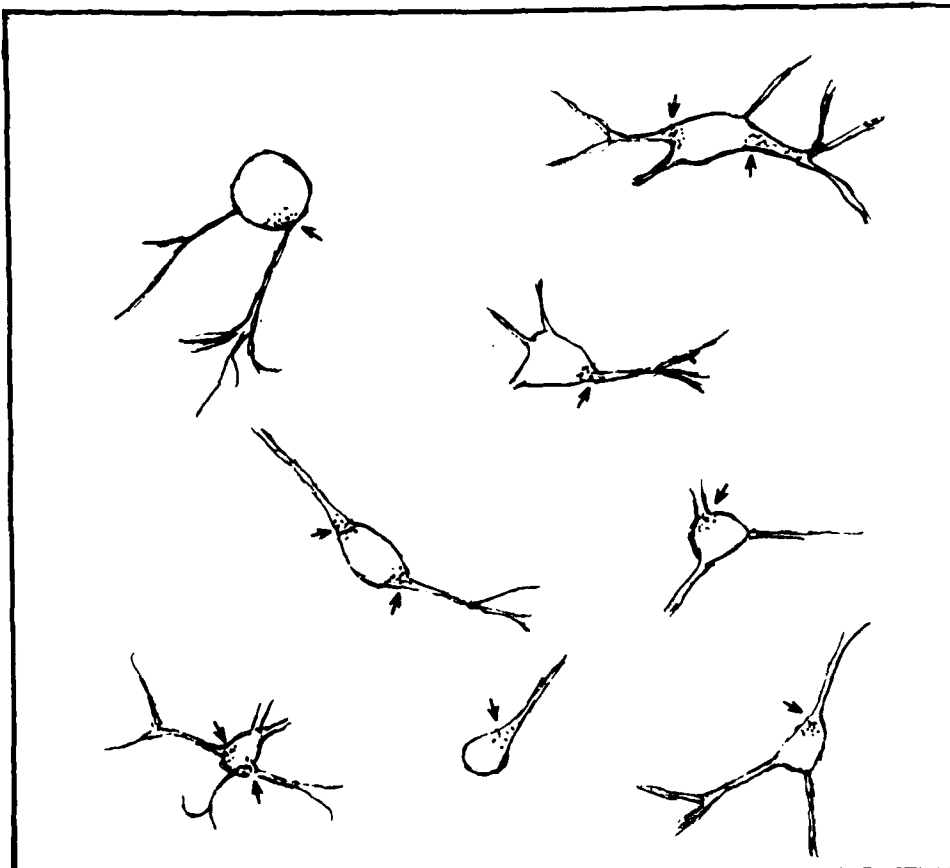
FIG 15   Hippocampal neurons cultured for 15 days. Hippocampal cultures contained mostly pyramidal cells, because granule cells are not present at the prenatal stage of these animals. The cells in the brain stem culture were either pyramidal, fusiform or spherical. We found that AChR activity was likely to occur near the axon hillock (indicated by arrows). Thus, most of our patch clamp recordings were obtained from this region.

dendrite or the axon hillock (Fig. 15). Most of the recordings were obtained from these areas of the pyramidal cell-like neurons.

Compared to the periphery, 5- to 10-times higher concentrations (1–5 μM) of both ACh and (+)anatoxin-a were necessary to activate central AChRs. Fig. 16 shows typical currents recorded using these agonists. Although muscle AChRs usually show some desensitization with clustering of channel activation at this concentration range (Fig. 11 and Refs. 40, 56), this pattern was not observed at the CNS. Instead, randomly occurring single channel events with occasional stepwise multiple activation due to simultaneous opening of two or more channels were recorded.

ACh 1 µM   (+) Anatoxin-a 1 µM
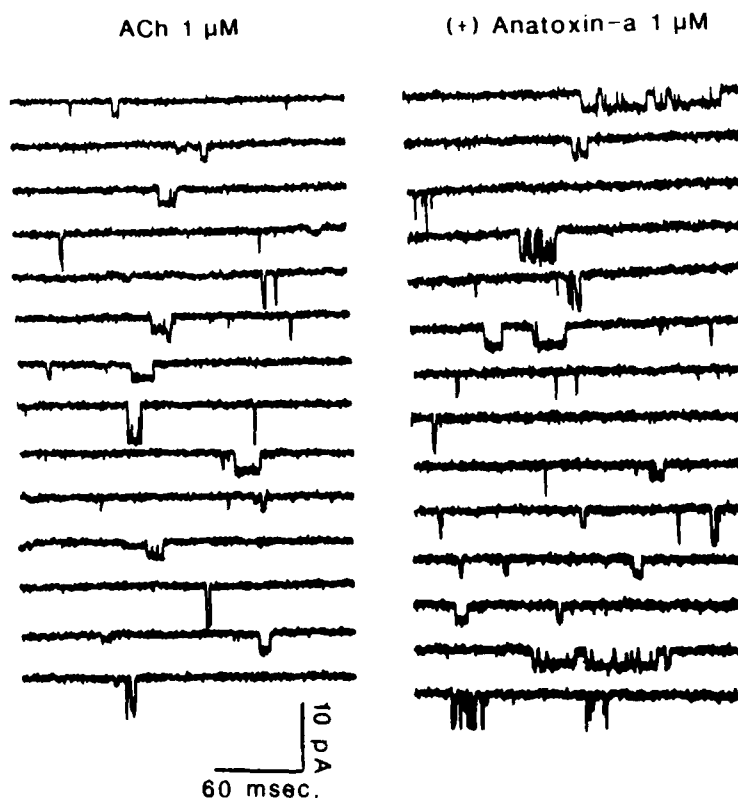
FIG 16   Samples of single channel currents activated by ACh and (+)anatoxin-a in central neurons. Multiple conductance states, typical of immature tissue, are apparent.

As has been reported in culture preparations for nicotinic [37] and other receptors such as glutamate receptors [57] and in preparations of chronically denervated muscle fibres [38], in some patches multiple conductance states could be discerned (Fig. 16). A similar pattern of conductance distribution was observed in cultured myoballs [37]. The predominant population of nicotinic receptors found on cultured brain stem neurons had a single channel conductance of 20 pS at 10°C [28]. A 10°C elevation of temperature increased the conductance by a factor of 1.3 to 1.5, in agreement with the Q_{10} values reported previously for muscle AChR [37].

For the kinetic analysis, 20 pS currents recorded at 10°C were used. Briefly, for qualitative comparison, the higher-conductance channels seemed to have faster closing kinetics, yielding shorter open-channel duration. ACh-activated currents showed only a few interruptions during the open state of the channels (Fig. 16). Similarly to the muscle AChR, (+)anatoxin-a induced channel openings that contained increased number of short interruptions (Fig. 16) which generated a double exponential distribution of the closed times. The fast component corresponded to the fast intraburst closures. The τ obtained from the fit of its distribution to an exponential function was determined to be 0.2 ms, and was shorter than that reported for currents activated by (+)anatoxin-a at the muscle endplate [7].

This implied that the opening rate was greater for the CNS AChR channels because these fast closures were interpreted as channel transitions between the doubly liganded closed conformation and the open state.

Both open and burst times could be fitted to a single exponential function with a τ of 1.7 and 2.7 ms, respectively for channel currents with amplitude of 1.6 pA. Because, in comparison to ACh, (+)anatoxin-a induced bursts with an increased number of brief closures and the individual openings within a burst were shorter, the burst duration was shorter than those elicited by the neurotransmitter. The number of openings per burst ranged between 1.2 and 1.6 and was neither voltage- nor concentration-dependent. This value was close to that found for muscle AChRs which together with the shorter closed interval indicated that the dissociation rate of (+)anatoxin-a from the CNS receptor site may be increased relative to the muscle AChR. This may partly account for low activation and absence of clear desensitization at the micromolar range used.

In conclusion, it seems that functionally the central AChRs share a great degree of homology with embryonic AChRs encountered in cultured myoballs [37] or denervated adult muscle fibre [38]. In addition, the similarity of the ion channels of the central and muscle AChRs determined from $H_{12}HTX$ binding [58] suggested that (+)anatoxin-a and some of its analogues may be important pharmacological tools to characterize the subtypes of the CNS nicotinic AChR.

Acknowledgements

References

1 Spivak, C.E., and Albuquerque, E.X. (1982) Dynamic properties of the nicotinic acetylcholine receptor ionic channel complex: activation and blockade. In: Progress in Cholinergic Biology: Model Cholinergic Synapses (I. Hanin, A.M. Goldberg, eds.), pp. 323–357. Raven Press, New York.
2 Stroud, R.M. (1983) Acetylcholine receptor structure. Neurosci. Commen. 1, 124–138.
3 Changeux, J.-P., Devillers-Thiéry, A., and Chemouilli, P. (1984) Acetylcholine receptor: an allosteric protein. Science 225, 1335–1345.
4 Gardner, P., Ogden, D.C. and Colquhoun, D. (1984) Conductance of single ion channels opened by nicotinic agonists are indistinguishable. Nature (Lond.) 309, 160–162.
5 Auerbach, A., Del Castillo, J., Specht, P.C. and Titmus, M. (1983) Correlation of agonist structure with acetylcholine receptor kinetics: studies on the frog end-plate and on chick embryo muscle. J. Physiol. (Lond.) 343, 551–568.
6 Spivak, C.E., Waters, J., Witkop, B. and Albuquerque, E.X. (1983) Potencies and channel properties induced by semirigid agonists at frog nicotinic acetylcholine receptors. Mol. Pharmacol. 23, 337–343.
7 Swanson, K.L., Allen, C.N., Aronstam, R.S., Rapoport, H. and Albuquerque, E.X. (1986) Molecular mechanisms of the potent and stereospecific nicotinic receptor agonist (+)-Anatoxin-a. Mol. Pharmacol. 29, 250–257.

8 Carmichael, W.W., Biggs, D.F. and Gorham, P.R. (1975) Toxicology and Pharmacological action of Anabaena flos-aquae toxin. Science 187, 542–544.

9 Carmichael, W.W., Biggs, D.F., and Peterson, M.A. (1979) Pharmacology of anatoxin-a, produced by the freshwater cyanophyte *Anabaena flos-aquae* NRC-44-1. Toxicon 17, 229–236.

10 Spivak, C.E., Witkop, B. and Albuquerque, E.X. (1980) Anatoxin-a: A novel potent agonist at the nicotinic receptor. Mol. Pharmacol. 18, 384–394.

11 Bates, H.A. and Rapoport, H. (1979) Synthesis of anatoxin-a via intramolecular cyclization of iminium salts. J. Amer. Chem. Soc. 101, 1259–1265.

12 Swanson, K.L., Rapoport, H., Aronstam, R.S. and Albuquerque, E.X. (1988) Studies of nicotinic acetylcholine receptor function using synthetic (+) anatoxin-a and derivatives. In: Marine Toxins: Origin, Structure and Pharmacology (S. Hall, ed.). American Chemical Society.

13 Koskinen, A.M.P., and Rapoport, H. (1985) Synthetic, conformational and pharmacological studies of anatoxin-a, a potent acetylcholine agonist. J. Med. Chem. 28, 1301–1309.

14 Aronstam, R.S., and Witkop, B. (1981) Anatoxin-a interaction with cholinergic synaptic molecules. Proc. Natl. Acad. Sci. USA 78, 4639–4643.

15 Beers, W.H. and Reich, H. (1970) Structure and activity of acetylcholine. Nature (Lond.) 288, 917–922.

16 Palmer, T. (1985) Ganglionic stimulating and blocking agents. In: The Pharmacological Basis of Therapeutics (A. Goodman Gilman, L.S. Goodman, T.W. Rall, F. Murad, eds.), pp. 215–221. MacMillan Publ. Co., NY.

17 Barlow, R.B. and Hamilton, J.T. (1965) The stereospecificity of nicotine. Br. J. Pharmacol. 25, 206–212.

18 Romano, C. and Goldstein, A. (1980) Stereospecific nicotine receptors on rat brain membranes. Science 210, 647–649.

19 Ikushima, S., Muramatsu, I., Sakakibara, Y., Yokotani, K., and Fujiwara, M. (1982) The effects of D-nicotine and L-isomer on nicotinic receptors. J. Pharmacol. Exp. Therap. 222, 463–470.

20 Clarke, P.B.S., Schwartz, R.S., Paul, S.M., Pert, C.B., and Pert, A. (1985) Nicotinic binding in rat brain: autoradiography comparison of [^{3}H]acetylcholine, [^{3}H]nicotine, and [^{125}I]-α-bungarotoxin. J. Neurosci. 5, 1307–1315.

21 Marks, M.J., Stitzel, J.A., Romm, E., Wehner, J.M. and Collins, A.C. (1986) Nicotinic binding sites in rat and mouse brain: comparison of acetylcholine, nicotine and α-bungarotoxin. Mol. Pharmacol. 30, 427–436.

22 Wonnacott, S. (1986) α-Bungarotoxin binds to low-affinity nicotine binding sites in rat brain. J. Neurochem. 47, 1706–1712.

23 Wonnacott, S. (1987) Brain nicotine binding sites. Hum. Toxicol. 6, 343–353.

24 Clarke, P.B.S. (1987) Recent progress in identifying nicotinic cholinoceptors in mammalian brain. Trends Pharmacol. Sci. 8, 32–35.

25 Macallan, D.R.E., Lunt, G.G., Wonnacott, S., Swanson, K.L., Rapoport, H., and Albuquerque, E.X. (1988) Methyllycaconitine and (+)-anatoxin-a differentiate between nicotinic receptors in vertebrate and invertebrate nervous systems. FEBS Lett. 226, 357–363.

26 Banker, G.A., and Cowan, W.M. (1977) Rat hippocampal neurons in dispersed cell culture. Brain Res. 126, 397–425.

27 Banker, G.A., and Cowan, W.M. (1979) Further observations on hippocampal neurons in dispersed cell culture. J. Comp. Neurol. 187, 469–494.

28 Aracava, Y., Deshpande, S.S., Swanson, K.L., Rapoport, H., Wonnacott, S., Lunt, G. and Albuquerque, E.X. (1987) Nicotinic acetylcholine receptors in cultured neurons from the hippocampus and brain stem of the rat characterized by single channel recording. FEBS Lett. 222, 63–70.

29 Howard, B.R., and Tabatabai, M. (1975) Localization of the medullary respiratory neurons on rats by microelectrode recording. J. Appl. Physiol. 39, 812–817.

30 Bradley, P.B. and Lucy, A.P. (1983) Cholinoceptive properties of respiratory neurones in the rat medulla. Neuropharmacology 22, 853–858.

31 Dekin, M.S., Getting, P.A., and Johnson, S.M. (1987) In vitro characterization of neurons in the ventral part of the nucleus tractus solitarius. I. Identification of neuronal types and repetitive firing properties. J. Neurophysiol. 58, 195–214.

32 Allen, C.N., Akaike, A. and Albuquerque, E.X. (1984) The frog interosseal muscle fiber as a new model for patch clamp studies of chemosensitive- and voltage-sensitive ion channels: actions of acetylcholine and batrachotoxin. J. Physiol. (Paris) 79, 338–343.

33 Hamill, O.P., Marty, A., Neher, E., Sakmann, B. and Sigworth, F.J. (1981) Improved patch-clamp techniques for high resolution current recording from cells and cell free membrane patches. Pflügers Arch. 391, 85–100.

34 Shaw, K.-P., Aracava, Y., Akaike, A., Daly, J.W., Rickett, D.L. and Albuquerque, E.X. (1985) The reversible cholinesterase inhibitor physostigmine has channel-blocking and agonist effects on the acetylcholine receptor-ion channel complex. Mol. Pharmacol 28, 528–538.

35 Sachs, F., Neil, J. and Barkakati, N. (1982) The automated analysis of data from single ionic channels. Pflügers Arch. 395, 331–340.

36 Alkondon, M., Rao, K.S. and Albuquerque, E.X. (1988) Acetylcholinesterase reactivators modify the functional properties of the nicotinic acetylcholine receptor ion channel. J. Pharmacol. Exp. Ther. 245, 543–556.

37 Aracava, Y., Ikeda, S.R., Daly, J.W., Brookes, N. and Albuquerque, E.X. (1984) Interactions of bupivacaine with ionic channels of the nicotinic receptor: analysis of single channel currents. Mol. Pharmacol. 26, 304–313.

38 Allen, C.N. and Albuquerque, E.X. (1986) Characteristics of acetylcholine-activated channels of innervated and chronically denervated skeletal muscles. Exp. Neurol. 91, 532–545.

39 Neher, E. and Sakmann, B. (1976) Single-channel currents recorded from membrane of denervated frog muscle fibers. Nature 260, 799–802.

40 Aracava, Y., Deshpande, S.S., Rickett, D.L., Brossi, A., Schönenberger, B. and Albuquerque, E.X. (1987) Molecular basis of anticholinesterase actions on nicotinic and glutamatergic synapses. Ann. N.Y. Acad. Sci. 505, 226–255.

41 Neher, E. and Steinbach, J.H. (1978) Local anaesthetics transiently block currents hrough single acetylcholine-receptor channels. J. Physiol. (Lond.) 339, 663–678.

42 Adams, P.R. and Sakmann, B. (1978) Decamethonium both opens and blocks endplate channels. Proc. Natl. Acad. Sci. U.S.A. 75, 2994–2998.

43 Adler, M., Albuquerque, E.X., and Lebeda, F.J. (1978) Kinetic analysis of end plate currents altered by atropine and scopolamine. Mol. Pharmacol. 14, 514–529.

44 Swanson, K.L., Aracava, Y., Sardina, F.J., Rapoport, H., Aronstam, R.S., and Albuquerque, E.X. (1988) N-methylanatoxinol isomers: Derivatives of the agonist anatoxin-a are non-competitive antagonists at the nicotinic acetylcholine receptor. Mol. Pharmacol. in press.

45 Aronstam, R.S., Eldefrawi, A.T., Pessah, I.N., Daly,J.W., Albuquerque, E.X. and Eldefrawi, M.E. (1981) Regulation of [³H]perhydrohistrionicotoxin binding to Torpedo ocellata electroplax by effectors of the acetylcholine receptor. J. Biol. Chem. 22, 3128–3136.

46 Heidmann, T., Oswald, R.E., and Changeux, J.-P. (1983) Multiple sites of action for noncompetitive blockers on acetylcholine receptor rich membrane fragments from Torpedo marmorata. Biochemistry 22, 3112–3127.

47 Colquhoun, D. and Sakmann, B. (1985) Fast events in single-channel currents activated by acetylcholine and its analogues at the frog muscle endplate. J. Physiol. 369, 501–557.

48 Colquhoun, D. and Ogden, D.C. (1988) Activation of ion channels in the frog end-plate by high concentrations of acetylcholine. J. Physiol. 395, 131–159.

49 Swanson, K.L., Aronstam, R.S., Rapoport, H., Sardina, F.J. and Albuquerque, E.X. (1988) Structure-activity relationships of anatoxin analogs at the nicotinic acetylcholine receptor (AChR). Neurosci. Abst. 14 (in press).

184

50 Chothia, C. and Pauling, P. (1970) The conformation of cholinergic molecules at nicotinic nerve receptors. Proc. Natl. Acad. Sci. U.S.A. 65, 477–482.

51 Sine, S.M. and Steinbach, J.H. (1984) Agonists block currents through acetylcholine receptor channel. Biophys. J. 46, 277–283.

52 Akaike, A., Ikeda, S.R., Brookes, N., Pascuzzo, G.J., Rickett, D.L., and Albuquerque, E.X. (1984) The nature of the interactions of pyridostigmine with the nicotinic acetylcholine receptor-ionic channel complex. II. Patch-clamp studies. Mol. Pharmacol. 25, 102–112.

53 Swanson, K.L. and Albuquerque, E.X. (1988) Nicotinic acetylcholine receptor ion channel blockade by cocaine: the mechanism of synaptic action. J. Pharmacol. Exp. Ther. 243, 1202–1210.

54 Ramoa, A.S. and Albuquerque, E.X. (1988) Phencyclidine and some of its analogues have distinct effects on NMDA receptors of rat hippocampal neurons. FEBS Lett., in press.

55 Allen, C.N. and Albuquerque, E.X. (1987) Conductance properties of GABA-activated chloride currents recorded from cultured hippocampal neurons. Brain Res. 410, 159–163.

56 Sakmann, B., Patlak, J., and Neher, E. (1980) Single acetylcholine-activated channels show burst-kinetics in presence of desensitizing concentrations of agonist. Nature (Lond.) 286, 71–73.

57 Jahr, C.E. and Stevens, C.F. (1987) Glutamate activates multiple single channel conductances in hippocampal neurons. Nature (Lond.) 325, 522–525.

58 Rapier, C., Wonnacott, S., Lunt, G.G. and Albuquerque, E.X. (1987) The neurotoxin histrionicotoxin interacts with the putative ion channel of the nicotinic acetylcholine receptors in the central nervous system. FEBS Lett. 212, 292–296.

CHAPTER 13

The biochemical characterization of insect GABA receptors

GEORGE G. LUNT, MICHAEL C.S. BROWN, KAYE RILEY AND DIANE M. RUTHERFORD

Department of Biochemistry, University of Bath, Bath, BA2 7AY, U.K.

Introduction

GABA is the major inhibitory neurotransmitter in the nervous systems of both vertebrates and invertebrates. In vertebrates at least two classes of GABA receptors have been identified. $GABA_A$ receptors activate Cl^- channels and are typically blocked by bicuculline whereas $GABA_B$ receptors may inactivate Ca^{2+} channels or activate K^+ channels, may be coupled to adenylate cyclase via G-proteins and are blocked by baclofen [1]. The $GABA_A$ receptor of mammalian brain has been extensively characterized and it is known to be a multi-subunit protein comprised of at least two classes of subunit. The complex constitutes a GABA-gated Cl^- channel and has several modulatory binding sites at which compounds such as the benzodiazepines, picrotoxinin, the cage convulsants (see Chapter 10) and some barbiturates act. The application of molecular cloning techniques to the study of the $GABA_A$ receptor of mammalian brain has resulted in the cloning of two subunits and in a description of the likely arrangement of the receptor complex in the membrane [2]. Such studies have also established that the $GABA_A$ receptor is a member of the superfamily of direct ligand-gated receptors that contains nicotinic acetylcholine receptors and glycine receptors among its numbers [3]; it seems likely that glutamate receptors will also be seen to be members of this same family. The work leading up to this almost complete description of the mammalian $GABA_A$ receptor ha recently been comprehensively reviewed by Stephenson [4].

What of the insect GABA receptors? Until relatively recently we could say little about them other than to report the electrophysiological measurement of hyperpolarizing responses to GABA in some insect muscle fibres and neurones. There has, however, been a surge of interest in insect GABA receptors stimulated in part by the growing realization that some groups of insecticides may act at sites on the receptor. Thus the cyclodienes, the polychlorocycloalkanes, the avermectins and the trioxabicyclooctanes all interact in different ways with $GABA_A$ receptors in mammalian brain (see Casida et al., Chapter 10). The majority of such studies, however, have been done using mammalian brain preparations and it would clearly be advantageous to have well-characterized preparations of insect GABA receptors on which to do such studies. Our laboratory commenced a programme of research in 1984 in collaboration with Dr. Richard Olsen at UCLA in which we have attempted

to characterize the biochemical and some of the pharmacological properties of GABA receptors in insects. The bulk of the work reported here was done using the supraoesophageal ganglion of the locust, *Schistocerca gregaria*, as our starting material but in addition membrane preparations from fly (*Musca domestica*) heads were used in some of the earlier experiments.

The GABA/muscimol binding site

Our first studies concentrated on the binding of muscimol, a potent GABA agonist that was known to bind with high affinity to mammalian $GABA_A$ receptors.

We found specific high-affinity binding of [³H]muscimol to membrane preparations from both locust and fly [7] with the following binding parameters, K_d 10 nM (locust), 40 nM (fly); B_{max} 60 fmol/mg protein (locust), 20 fmol/mg protein (fly). The binding was independent of Na^+ but an additional non-saturating binding could be seen in locust when Na^+ (0.15 M) was included in the binding assay buffers. We suspect that this part of the binding may represent association with an uptake site rather than a receptor site. In a further series of experiments we examined the binding of [³H]GABA to the locust preparations. Saturable specific binding was seen, with a K_d of 30 nM and a B_{max} of 150 fmol/mg protein [8]. We do not have an explanation for the marked increase in the B_{max} compared with the level of muscimol binding to the same membrane preparations other than the possibility that the GABA may also bind to uptake sites.

The effects of some GABAergic drugs on the binding of muscimol and GABA are shown in Table 1.

These data suggested that the binding was to a receptor site rather than an uptake site. Thus nipecotic acid and 2,4-diaminobutyrate were ineffective at blocking binding and these compounds are both good specific inhibitors of GABA uptake in mammalian brain [9]. The lack of effect of bicuculline points to a significant difference in specificity between the locust and mammalian $GABA_A$ receptors. There has been confirmation of this both from binding experiments from other laboratories and from electrophysiological studies [10]. It is interesting to note, however, that in some insects bicuculline-sensitive GABA responses can be seen (see Epilogue, J.G. Hildebrand).

TABLE 1   Effects of GABAergic drugs on the binding of [³H]muscimol and [³H]GABA to locust ganglion membranes

Drug	IC_{50} (μM)	
	[³H]Muscimol	[³H]GABA
Muscimol	0.03	0.1
GABA	0.04	0.09
Isoguvacine	0.1	5.0
3-Aminopropane-sulphonate	0.3	n.t.
Nipecotic acid	n.e.	n.e.
Bicuculline	n.e.	n.e.
2,4-Diaminobutyrate	n.e.	n.e.
Baclofen	n.t.	n.e.

n.t., not tested; n.e., no effect at 100 μM.

As mentioned in the Introduction the mammalian $GABA_A$ receptor is characterized by a series of modulatory interactions between the several distinct binding sites on the complex. We investigated the effect of pentobarbital on the binding of both muscimol and GABA in the locust. We saw no effect on muscimol binding at pentobarbital concentrations up to 1 mM; however, in the case of GABA binding we observed enhancement of binding by between 20 and 35% in the presence of 1 mM pentobarbital [8]. This effect was seen only when the binding assays were carried out at 4°C and could not be detected at 25°C. The enhancement was completely abolished by 1 mM picrotoxinin, suggesting that, as in the mammalian $GABA_A$ receptor, the barbiturates may act at the picrotoxinin site and allosterically modulate the GABA binding site. Olsen has subsequently reported a similar enhancement of [^{3}H]muscimol binding in fly head by 1 mM pentobarbital [10]. Thus we could conclude at this stage that insect ganglia have a bicuculline-insensitive GABA receptor site that is functionally coupled to a barbiturate/picrotoxinin binding site.

The benzodiazepine binding site

In 1978 it was reported that specific benzodiazepine binding sites were present in a wide variety of vertebrate brains but that such sites were absent from the nervous system of several invertebrates [11]. The suggestion was made at that time that such binding sites were in evolutionary terms a feature of vertebrates and not of invertebrates. However, Abalis et al. [12] reported the presence of specific binding sites for flunitrazepam in a housefly thorax preparation and showed that the sites were modulated by GABA. At that time, however, Abalis et al. [12] could not detect specific binding of muscimol to the same tissue preparation. Matsumura also reported [^{3}H]diazepam binding to cockroach ganglia [13] but it was not clear whether the sites formed part of a GABA receptor complex.

We have previously shown that locust ganglia contain [^{3}H]flunitrazepam binding sites [14]. In our hands it proved necessary to add Ca^{2+} to the isolated ganglion membranes in order to measure reproducible benzodiazepine binding [15]. We found that a concentration of 4 mM Ca^{2+} gave optimum binding and under these conditions benzodiazepine binding was enhanced by about 100% over the variable levels seen in control membrane preparations. In a parallel series of experiments we were unable to see any effect of varying the Ca^{2+} concentration on [^{3}H]flunitrazepam binding to rat brain preparations, a finding in keeping with several reports on the binding properties of mammalian $GABA_A$ receptors. Thus the Ca^{2+} dependence of the locust site may be a reflection of yet another difference between the insect receptor and its mammalian counterpart. The locust site has a K_D of 47 nM, indicating a lower affinity than that reported for mammalian $GABA_A$ receptors, where values of 1-4 nM are usually seen. Analysis of the rate constants of the binding suggest that there may be heterogeneity of sites in the locust [15] and this was borne out when we carried out photoaffinity labelling of the locust receptor. In most studies on mammalian $GABA_A$ receptors a single major protein with an M_r of about 50000 is photoaffinity labelled with [^{3}H]flunitrazepam [4]. In the locust, however, we observed two major bands at 46000 and 60000 and two minor bands at 50000 and 54000. None of these bands, in terms of M_r, corresponds to any published band for mammalian $GABA_A$ receptors [15]. More recently we have

repeated these studies using the radiolabelled benzodiazepine [^{3}H]Ro 15-4513 and see only a single band labelled in the locust with an M_r of 59 000. The multiple labelling seen with [^{3}H]flunitrazepam may reflect possible heterogeneity of sites or could be an indicator of proteolytic breakdown of the labelled protein: at present we do not have sufficient data to speculate further on these possibilities.

The finding that the locust binding site can be photoaffinity labelled with both flunitrazepam and Ro 15-4513 suggests that the site may be analogous to the GABA$_A$ receptor site. In vertebrate tissues there are present benzodiazepine binding sites that are not coupled to GABA receptors; these so called 'peripheral' benzodiazepine receptors cannot be photoaffinity labelled and Ro 15-4513 does not bind to them. Further differences between the peripheral sites and the central sites (i.e. those that are part of a GABA$_A$ receptor complex) are seen in their pharmacological profile. Thus peripheral sites are sensitive to the compound Ro 5-4864 but not to clonazepam whereas the reverse is true for the central sites. When we examined the ability of benzodiazepines to inhibit [^{3}H]flunitrazepam binding to locust preparations we found that Ro 5-4864 was at least 100-times more effective than clonazepam. Furthermore the enantiomers Ro 11-5073 and Ro 11-5231 were equipotent in the locust whereas the rat brain GABA$_A$ receptor is 100-times more sensitive to the former than to the latter [15]. The sensitivity of [^{3}H]flunitrazepam binding in insects to Ro 5-4864 is confirmed by Lummis and Sattelle [16] in studies on cockroach ganglia.

Thus the insect benzodiazepine binding site shows on the one hand a pharmacological specificity reminiscent of mammalian peripheral benzodiazepine receptors (i.e. not GABA receptor linked) but on the other hand we see photoaffinity labelling of the insect site, a property shared with mammalian GABA$_A$ receptors.

We were also able to demonstrate that the locust benzodiazepine binding site can be allosterically modulated by both GABA and pentobarbital. The latter, at a concentration of 0.1 mM, gave a 20% enhancement of benzodiazepine binding [10]. GABA (10^{-4} M) and isoguvacine (10^{-4} M) both enhanced [^{3}H]flunitrazepam binding by about 100%. Additionally GABA (10^{-8} M) showed an enhancement of the photoaffinity labelling of the locust site with [^{3}H]flunitrazepam [15].

Thus we have good evidence that the locust benzodiazepine binding site is part of a protein complex that also carries sites for GABA (and the GABA agonist isoguvacine) and pentobarbital. The sites are functionally coupled in a manner analogous to that seen in the mammalian GABA$_A$ type of receptors.

Supporting evidence for the presence of a GABA$_A$ type of receptor on insect neurones comes from electrophysiological studies done by Beadle and colleagues on cultured insect neurones. Thus GABA-evoked responses from these cells are enhanced by both flunitrazepam and pentobarbital [17,18]. Both binding data from membrane preparations in vitro and results from electrophysiological recordings from neurones in vivo indicate that a complex multi-site GABA receptor is present on insect neurones and that its function can be modulated by ligands known to act on mammalian GABA$_A$ receptors.

The convulsant binding site

The convulsant binding site of the mammalian GABA$_A$ receptor has often proved to be the most sensitive part of the receptor complex with respect to retention of its

binding properties when isolated from the membrane [4]. It is generally considered that this site is located in or very close to the integral Cl^- channel of the receptor complex. The site has been probed with two ligands, picrotoxinin and the cage convulsant t-butylbicyclophosphorothionate (TBPS) (see Chapter 10). Matsumura's group used radiolabelled picrotoxinin ($[^3H]$dihydropicrotoxinin) to examine binding sites in cockroach ganglia and reported differences in the levels of binding between cyclodiene-resistant strains and normals [19,20]. Olsen and colleagues had previously reported specific binding of picrotoxinin to crayfish muscle preparations [21] and concluded that the binding was associated with GABA receptors. In general, however, picrotoxinin has proved to be an unsatisfactory ligand for binding studies; its affinity is relatively low and the non-specific binding is high; additionally the specific radioactivity of the ligand is rather low. The preferred ligand for monitoring the convulsant site is $[^{35}S]$TBPS. Cohen and Casida [22] reported the specific binding of this ligand to a preparation of housefly thorax and abdomen. The binding site had a K_d of 210 nM, a figure rather higher than the value of 18 nM reported for $[^{35}S]$TBPS binding to cockroach ganglia [16]. Olsen and colleagues have reported a K_d of 51 nM for the binding site in housefly head [23]. In most of these reports picrotoxinin is seen as a relatively weak inhibitor of TBPS binding and this may indicate yet another difference between mammalian GABA$_A$ receptors and the insect GABA receptor described here. Some quite different effects were seen when the action of GABA itself on TBPS binding was investigated. Cohen and Casida [22] in the housefly thorax/abdomen saw an enhancement of $[^{35}S]$TBPS binding of up to 40% by 10–100 μM GABA, whereas Lummis and Sattelle [16] reported a 40% decrease in binding by micromolar concentrations of GABA. Olsen and colleagues saw no effect of either GABA or muscimol (up to 1 mM) on TBPS binding to their fly head preparation [23]. Clearly it is difficult to make direct comparisons between such widely differing preparations as whole thorax and abdomen vs. isolated ganglia prepared from quite different species of insect. What can be confidently stated is that TBPS seems to bind to a site that, in some cases, can be modulated by GABA.

In our own laboratory we have investigated $[^{35}S]$TBPS binding to the locust ganglia membranes. We see specific binding but the binding behaviour is complex and indicative of positive cooperativity [24]. We have tentatively identified two classes of binding site having K_d values of 25 nM and 400 nM. Measurements of both association and dissociation rates confirm our suggestions of positive cooperativity of the binding sites [24]. Parallel experiments in which we have measured $[^{35}S]$TBPS binding to rat brain indicate a single homogeneous class of binding site with a K_d of 53 nM, a value that is in good agreement with published values for mammalian GABA$_A$ receptors. We are confident therefore that the assay procedures used are reliable and that the observed differences between locust ganglia and rat brain are not artefactual.

Table 2 shows the results from the series of experiments in which we have examined the effects of a variety of compounds on the binding of $[^{35}S]$TBPS to locust membranes. The only ligands which have shown inhibition of binding are the cage convulsants TBPS and isopropylbicyclophosphate (IBP). As may be seen from the table, all other ligands either result in increased levels of binding or have no effect. It is of interest that picrotoxinin had no effect in these experiments whereas in mammalian GABA$_A$ receptors it is an inhibitor of TBPS binding. Picrotoxinin certainly interacts with the locust receptor as witnessed by its inhibitory effect on the pentobarbital enhancement of GABA binding as described earlier [8]. These

TABLE 2   The effects of various ligands on the binding of [^{35}S]TBPS to locust ganglia membranes

Ligand	Effect (% enhancement (+) or inhibition (−))	EC$_{50}$ (μM)
TBPS	− 100	0.7
IBP	− 100	2.2
GABA	+ 145	2.5
Diazepam	+ 130	*
Clonazepam	+ 130	0.06
Ro 5-4864	+ 155	0.13
Pentobarbital	+ 150	0.02
Cypermethrin	+ 160	45
Permethrin	0	*
Dieldrin	+ 310	1.4
Lindane	+ 175	2.5
Picrotoxinin	0	*

EC$_{50}$, concentration of ligand that gives 50% enhancement (+) or inhibition (−) of TBPS binding; IBP, isopropylbicyclophosphate.
* Tested at a single concentration only, 10^{-4} M.

data are preliminary and clearly the locust TBPS binding site is far from being fully characterized. It is clear, however, that the site is coupled to sites at which GABA and benzodiazepines are acting and that these sites can allosterically modulate the cage convulsant binding site. We have observed that the binding of [^{35}S]TBPS to the locust preparations is enhanced by Cl$^-$ over the range 50–350 mM [24] and in this respect it resembles the analogous site on the mammalian GABA$_A$ receptor.

More recently we have started some experiments in which we have measured Cl$^-$ flux into membranous vesicles prepared from locust ganglia and also into whole ganglia. The influx of ^{36}Cl$^-$ is stimulated by GABA and by isoguvacine and is insensitive to bicuculline. This system offers the possibility of reassessment of the various binding data described above in a functional assay. We have also obtained preliminary results for an investigation into the possibility of solubilizing the receptor complex from locust ganglia membranes. Using procedures based on those described by Stephenson for mammalian GABA$_A$ receptors [4] we have treated locust membranes with the detergent CHAPS and with phospholipid mixtures. The indications are that benzodiazepine binding sites are solubilized and that GABA modulation of the binding occurs.

Conclusions

Work from our own laboratory and from those of several colleagues is strongly suggestive of the presence of a GABA receptor complex on insect neurones that has the same organizational features as the GABA$_A$ receptor of mammalian brain. That is, it appears to have a number of interacting binding sites that show mutual allosteric modulation and that are associated with a GABA mediated Cl channel. However, some significant differences between the insect receptor and mammalian

GABA$_A$ receptors can already be identified. The insect receptor described here is insensitive to bicuculline and seems less sensitive to picrotoxinin than GABA$_A$ receptors. The insect receptor does not fall neatly into the mammalian classification with respect to benzodiazepine binding properties, thus its pharmacological specificity resembles the mammalian peripheral sites but its susceptibility to photoaffinity labelling is shared with mammalian central sites. The elucidation of the detailed structural and functional organization of the insect GABA receptor will depend heavily on the application of the techniques of molecular biology. Clearly the insect GABA receptor is a member of the direct ligand-gated superfamily of receptors [3] and this relationship between insect and vertebrate genes has already been successfully exploited in the case of the nicotinic acetylcholine receptor from the locust [25]. The insect GABA receptor with its multiple interacting sites is clearly a vulnerable target for neurotoxicants and we can anticipate the definition of such sites in terms acceptable to the pesticide chemist in the relatively near future.

Acknowledgements

References

1 Bowery, N., Price, G.W., Hudson, A.L., Hill, D.R., Wiekin, G.P. and Turnbull, M.J. (1984) GABA receptor multiplicity – visualisation of difference receptor types in the mammalian CNS. Neuropharmacology 23, 219–231.
2 Schofield, P.R., Darlison, M.G., Fujita, N., Burt, D.R., Stephenson, F.A., Rodriguez, H., Rhee, L.M., Ramachandran, J., Real, V., Glencorse, T.A., Seeburg, P.H. and Barnard E.A. (1987) Sequence and functional expression of the GABA$_A$ receptors shows a ligand-gated receptor super-family. Nature 328, 221–227.
3 Grenningloh, G., Rienitz, A., Schmitt, B., Methfessel, C., Zensen, M., Beyreuther, K., Gundelfinger, E.D. and Betz, H. (1987) The strychnine-binding subunit o^f .he glycine receptor shows homology with nicotinic acetylcholine receptors. Nature 328, 215–220.
4 Stephenson, F.A. (1988) Understanding the GABA$_A$ receptor: a chemically-gated ion channel. Biochem. J. 249, 21–32.
5 Abalis, I.M., Eldefrawi, M.E. and Eldefrawi, A.T. (1985) High affinity stereospecific binding of cyclodiene insecticides and hexachlorocyclohexane to aminobutyric acid receptors in rat brain. Pest. Biochem. Pharmacol. 24, 95–102.
6 Matsumura, F. and Ghiasuddin, S.M. (1983) Evidence for similarities between cyclodiene type insecticides and picrotoxin in their action mechanisms. J. Environ. Sci. Health B18, 1–14.
7 Lunt, G.G., Robinson, T.N., Miller, T., Knowles, W.P. and Olsen, R.W. (1985) The identification of GABA receptor sites in insect ganglia. Neurochem Int. 7, 751–754.
8 Rutherford, D.M., Jeffrey, D., Lunt, G.G. and Weitzman, P.D.J. (1987) GABA binding to receptor sites in locust supraoesophageal ganglion. Neurosci. Lett. 79, 337–340.
9 Olsen, R.W. (1981) GABA-benzodiazepine-barbiturate receptor interactions. J. Neurochem. 37, 1–13.
10 Robinson, T.N. and Olsen, R.W. (1988) GABA in Comparative Invertebrate Neurochemistry (Lunt, G.G. and Olsen, R.W., eds.), pp. 90–123, Croom-Helm, Beckenham.

11 Nielsen, M., Braestrup, C. and Squires, R.F. (1978) Evidence for a late evolutionary appearance of brain-specific benzodiazepine receptors: an investigation of 18 vertebrate and 5 invertebrate species. Brain Res. 141, 342–346.

12 Abalis, I.M., Eldefrawi, M.E. and Eldefrawi, A.T. (1983) Biochemical identification of putative GABA-benzodiazepine receptors in housefly thorax muscles. Pest. Biochem. Physiol. 20, 39–48.

13 Tanaka, K., Scott, J.G. and Matsumura, F. (1984) Picrotoxin receptor in the central nervous system of the American cockroach: its role in the action of cyclodiene insecticides. Pest. Biochem. Physiol. 22, 117–127.

14 Robinson, T.M., Lunt, G.G., Battersby, M., Irving, S. and Olsen, R.W. (1985) Locust ganglia contain [^{3}H]flunitrazepam binding sites. Biochem. Soc. Trans. 13, 716–717.

15 Robinson, T.M., MacAllan, D., Lunt, G.G. and Battersby, M. (1986) γ-Amino-butyric acid receptor complex of insect CNS: characterisation of benzodiazepine binding site. J. Neurochem. 47, 1955–1962.

16 Lummis, S.C.R. and Sattelle, D.B. (1986) Binding sites for [^{3}H]GABA, [^{3}H]flunitrazepam and [^{35}S]TBPS in insect CNS. Neurochem. Int. 9, 287–293.

17 Beadle, D.J., Benson, J.A., Lees, G. and Neuman, R. (1986) Flunitrazepam and pentobarbital modulate GABA responses of insect neuronal somata. J. Physiol 371, 273p.

18 Lees, G., Neuman, R., Beadle, D.J. and Benson, J.A. (1985) Flunitrazepam enhances GABA and muscimol induced responses in freshly dissociated locust neuronal somata. Pest. Sci. 16, 534.

19 Tanaka, K., Scott, J.G. and Matsumura, F. (1984) Picrotoxinin receptor in the central nervous system of the American cockroach: its role in the action of cyclodiene-type insecticides. Pest. Biochem. Physiol. 22, 117–127.

20 Kadous, A.A., Ghiasuddin, S.M., Matsumura, F., Scott, J.G. and Tanaka, K. (1983) Difference in the picrotoxinin receptors between cyclodiene-resistant and susceptible strains of the German cockroach. Pest. Biochem. Physiol. 19, 157–166.

21 Olsen, R.W., Ticku, M.K. and Miller, T. (1978) Dihydropicrotoxinin binding to crayfish muscle sites possibly related to aminobutyric acid receptor-ionophores. Mol. Pharmacol. 14, 381–390

22 Cohen, E. and Casida, J.E. (1986) Effects of insecticides and GABAergic agents on a housefly [^{35}S]t-butylbicyclophosphorothionate binding site. Pest. Biochem. Physiol. 25, 63–72.

23 Szamraj, O.I., Miller, T. and Olsen, R.W. (1986) Cage convulsant [^{35}S]TBPS binding to GABA receptor-chloride channel complex in invertebrate tissues. Soc. Neurosci. Abstr 16, 656.

24 Brown, M.C.S., Lunt, G.G. and Stapleton, A. (1988) Further characterisation of the binding site for [^{35}S]TBPS in locust ganglia membranes. Comp. Biochem. Physiol., in press.

25 Marshall, J., Sattelle, D.B., David, J.A., Darlison, M.G., Lunt, G.G. and Barnard, E.A. (1988) Cloning and expression of the nicotinic acetylcholine receptor from the locust Schistocerca gregaria. Pest. Sci., in press.

CHAPTER 14

Transmitter receptors on insect neuronal somata: GABAergic and cholinergic pharmacology

JACK A. BENSON

R & D Plant Protection, Agricultural Division, CIBA-GEIGY Ltd.,
CH-4002 Basel, Switzerland

Introduction

This paper addresses two related questions of significance to insect neurophysiologists and pesticide chemists. To what extent can chemicals used to define receptor subtypes in the mammalian nervous system (classical diagnostic compounds) be relied on to characterize receptors and ion channels in insects? How similar is the pharmacology of insect receptor subtypes to that of mammalian subtypes in the same and different receptor families?

Important early discoveries in the field of transmitter receptor pharmacology were made using arthropod electrophysiological preparations, but often insect receptors have been regarded largely as variants insignificantly differing from their well-known mammalian counterparts. During the past two or three years, however, there has been an explosive increase in our knowledge of the amino acid sequences of the membrane proteins that constitute neurotransmitter receptors and neuronal and muscular voltage-dependent ion channels. The new insights provided by molecular biology should cause us to reconsider some of our preconceptions about the relationships between receptor types. Probably only a few of the reported variations in amino acid sequence result in differences in the physicochemical properties of recognition sites for the endogenous ligand or other specifically-acting substances with different sites of action. Despite this, the complexities revealed in receptor families suggest that the standard classificatory concept is too simple.

All the receptor and ion channel proteins so far sequenced can be divided, on the basis of sequence homology, into three superfamilies [1,2]:

(a) voltage-activated ion channel superfamily (e.g. Na^+ channel family; K^+ channel family);

(b) ligand binding-activated receptor/channel complex superfamily (e.g. nicotinic acetylcholine (ACh) receptor family; $GABA_A$ receptor family; glycine receptor family);

(c) G-protein-associated receptor superfamily (e.g. muscarinic ACh receptor family; rhodopsin family).

Based on degrees of sequence similarity, one gains the impression that there is often a *smaller difference* between members of different families within one *super-family* than was hitherto supposed on the basis of classical pharmacology. On the other hand, the sequences of the members (subtypes) of a particular *family* seem to *differ more* from one another than was realized, depending on the species and the part of the nervous system they come from. The apparently great variety of receptor and channel subtypes admits the possibility that some of the classical diagnostic agonists and antagonists might not be as uniform in their actions as hitherto assumed and that they might show variation in their activities among receptors and channels of differing anatomical and phylogenetic origins.

Methods and materials

The methods of cell preparation and drug application used for these experiments have been described in detail elsewhere [3] and can be summarized as follows. The three thoracic ganglia were dissected free from adult locusts (*Locusta migratoria*), desheathed and aspirated three or four times through a Pasteur pipette tip. The resulting suspension of dissociated neuronal somata was then left in a few drops of physiological saline in a petri dish for 2 to 4 h. This allowed the dendritic stumps to seal off and the cell bodies to adhere to the petri dish. The cell bodies used in these experiments were all 100 to 150 μm in diameter. The cells were then impaled and voltage-clamped by conventional single-electrode means (Axoclamp). The agonists were pressure applied using a Picospritzer (General Valve Corp.) in combination with patch electrodes pulled on a Mecanex electrode puller. The antagonists were applied via the continuous perfusion of the bath. The bicuculline free base was first dissolved in a few drops of 1 N HCl and then added to physiological saline which was checked for pH. All solutions of bicuculline and its salts were made up 30 min or less before the experiment. The drugs were obtained from Sigma and the composition of the physiological saline, in mM was: NaCl 180; $MgCl_2$ 15; $CaCl_2$ 10; KCl 10; HEPES 10; pH of 6.8.

The somata were voltage-clamped at -50 mV and pulses of GABA, ACh, nicotine, or muscarine were applied to the somal membrane. To obtain dose response data, the putative antagonists were bath-applied, beginning at low concentrations and, after a constant effect was achieved, in increasing doses, without an intervening washout. To obtain current-voltage (I-V) curves, the somata were clamped at different voltages via a series of 10 mV steps, held at each potential until the membrane current reached a constant level and then challenged with a pulse of agonist. The voltage-dependence of the antagonist action was determined from the percent blockade at different clamp potentials at ca. 50% blockade in comparison with the control.

Results and discussion

Insect neuronal somata in situ and also when isolated from the rest of the neural tissue are sensitive to both ACh and GABA [3–5]. The mechanically-separated somata of neurones from the thoracic ganglia of *Locusta* remain viable in vitro under voltage-clamp for several hours [3,6,7] and under these conditions they all
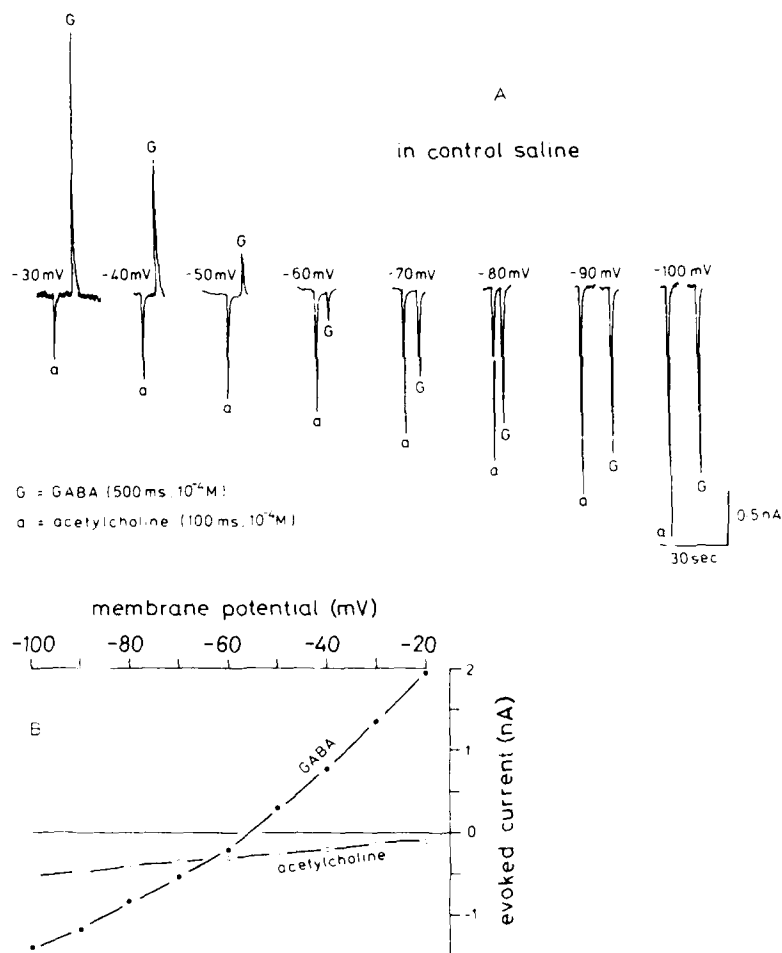
FIG 1 Membrane potential-dependence of ACh- and GABA-evoked currents. A: si gle electrode voltage-clamp current records from a neuronal soma clamped at potentials over the range - 30 to - 100 mV and exposed to pressure microapplications of 10 ⁻⁴ M ACh (a, 100 ms) and GABA (G, 500 ms). B: current-voltage (I-V) curves of the net evoked current from another soma exposed to pressure microapplications of 10 ⁻⁴ M ACh (open circles) and GABA (closed circles).

respond to pressure micro-application of GABA and ACh with readily distinguishable currents (Fig. 1A). GABA evokes a current that is outward at membrane potentials more positive than − 50 to − 65 mV where it reverses direction (Fig. 1A,B and Ref. 3). This current is carried by Cl⁻ ions [8]. ACh, on the other hand, elicits an inward current that decreases with membrane depolarization and has a projected reversal potential of 0 to 20 mV (Fig. 1 A,B and Ref. 9). The difference in dependence of these currents on membrane potential is illustrated by the I-V curves in Fig. 1B. The GABA-evoked current is typically outwardly rectifying. The

```
m = muscarine (1sec, 10⁻³M)
n = nicotine (100ms, 10⁻⁴M)
```
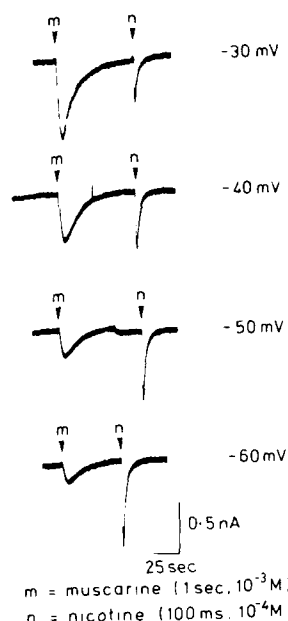
FIG 2   Membrane potential-dependence and kinetics of nicotine- and muscarine-evoked currents. Single electrode voltage-clamp current records from a neuronal soma clamped at potentials over the range -30 to -60 mV and exposed to pressure microapplications of 10^{-4} M nicotine (n, 100 ms) and 10^{-3} M muscarine (m, 1 s).

cholinergic curve is linear in the hyperpolarized range to potentials of about -30 mV. The predominant response to ACh, shown in Fig. 1A, masks a second current that is also activated by ACh. The two currents can be elicited individually by nicotine and muscarine (Fig. 2 and Refs. 6, 9). The nicotine-evoked current constitutes the overwhelmingly major component of the response to ACh [7,9] and consequently the properties of these two responses are very similar. Comparatively much higher doses of muscarine activate a current that has slower kinetics and which decreases with hyperpolarization over the range -30 mV to -60 mV (Fig. 2 and Ref. 9). The two components can be separated pharmacologically in the response to pulses of ACh [7].

The receptor subtype mediating the nicotine-evoked response has been designated ACh1 and that mediating the muscarine-evoked response ACh2 [9]. The ACh2 receptor has a pharmacological profile bearing many similarities to that of vertebrate muscarinic receptors [7,9] and might therefore perhaps be a member of the G-protein-associated receptor superfamily [10]. It need not concern us further here. Pharmacological profiles of the ACh1 and GABA receptors are given in Tables 1 and 2. These data have been arranged to illustrate the similarities and differences between the insect somal receptors and the corresponding mammalian subtypes, as well as the unexpected activity of certain diagnostic compounds. The latter are discussed in detail in the following paragraphs. The ACh1 receptor shares properties with both the neuromuscular and ganglionic nicotinic receptors of vertebrates (Table 1). The locust thoracic somal GABA receptor responds to agonists and

TABLE 1   Pharmacology of acetylcholine receptor subtypes

	Vertebrate		Locust
	nicotinic		soma
	neuromuscular	ganglionic	AChl
Nicotine	ag./blocker		agonist
Anabasine	agonist		ag./blocker
Decamethonium	ag./blocker	–	blocker *
Suberyldicholine	agonist	–	blocker *
1,1-Dimethyl-4-piperazinium	ag./blocker	agonist	ag./blocker
Lobeline	ag./blocker	agonist	ag./blocker
Tetramethylammonium	–	agonist	ag./blocker
α-Bungarotoxin	blocker	–	blocker
Gallamine	blocker	–	ag./blocker
D-tubocurarine	blocker	–	blocker
Mecamylamine	–	blocker	blocker
Hexamethonium	–	blocker	blocker
Chlorisondamine	–	blocker	blocker
Trimethephan camsylate	–	blocker	blocker
Tetraethylammonium	K^+ channel	blocker	blocker
Strychnine	glycine antagonist		blocker
Bicuculline	$GABA_A$ antagonist		blocker
Picrotoxin	GABA Cl^- channel blocker		blocker

In some cases, there is cross-reaction between neuromuscular and ganglionic receptors: the Table indicates the site of greater potency.

The compounds were tested at concentrations of up to 10^{-4} M.

A 'blocker' reduces the response to pulse-applied ACh in a dose-dependent manner. The mode of action may be any combination of ACh recognition site antagonism, 'allosteric' antagonism, channel block and desensitisation.

* These neuromuscular nicotinic agonists were also AChl agonists but only when ACh was present in the bathing saline [17].

TABLE 2   Pharmacology of GABA receptor-channel subtypes

	Vertebrate		Locust
	$GABA_A$	$GABA_B$	soma
Agonists			
muscimol	potent	very weak	potent
baclofen	inactive	potent	inactive
Antagonists			
picrotoxin	potent	inactive	potent
bicuculline	potent	inactive	inactive
pitrazepin	potent	inactive	inactive
Modulators			
(potentiators)			
benzodiazepine	potent	?	potent
barbiturate	potent	?	potent
Mechanism			
Cl^-	increase	no link	increase
K^+	no link	increase	no link

Locust data are from Refs. 3 and 8, and further experiments. Similar findings have been reported for cultured embryonic cockroach brain neurones [28].

A

control   wash following
            10^{-5}M TEA

$E_h = -50$mV

FIG 3 Characteristics of blockade by tetraethylammonium (TEA). A: single electrode voltage-clamp current records from a neuronal soma clamped at a holding potential (E_h) of -50 mV and exposed to periodic pressure microapplications of 10^{-4} M ACh (70 ms). The first panel shows the response in normal saline. The recording illustrated in the second panel was made during perfusion of the recording chamber with normal saline immediately following maximum blockade by saline containing 10^{-4} M tetraethylammonium (TEA). B: dose–response curve showing the dependence of the degree of blockade of the cholinergic response on the concentration of TEA in the superfusing saline. The response was evoked by 70 ms pressure pulses of 10^{-4} M ACh. C: the percentage reduction of the ACh-evoked current in TEA saline is plotted against the clamp potential at which the current was recorded. The degree of block was membrane potential-dependent. A, B and C are from different cells.

modulators similarly to the $GABA_A$ receptor but is insensitive to bicuculline (Table 2). Thus although the ACh1 and GABA receptors are not identical to any of the corresponding vertebrate subtypes, the many similarities show that they nevertheless belong to the nicotinic ACh receptor and $GABA_A$ receptor families respectively, and, together with the other subtypes in their families, they are both members of the ligand binding-activated receptor/channel complex superfamily.

Tetraethylammonium (TEA) has long been known to be both a selective blocker of certain K^+ channels and an agonist or antagonist at the nicotinic receptor [11] where it seems to act at both the ACh recognition site and the ion channel [12]. To invertebrate neurophysiologists, TEA is best known as a K^+ channel blocker acting at millimolar concentrations. When TEA is bath applied to an isolated locust neuronal soma (Fig. 3A), it blocks the ACh1 response reversibly with a threshold of about 3×10^{-7} M and an EC_{50} of $4.6 \pm 3.5 \times 10^{-5}$ (mean $\pm$ S.D., $n = 3$) (Fig. 3B) and the degree of blockade is highly dependent on the membrane potential (Fig. 3C). It is without effect on the GABA response at concentrations of up to 10^{-4} M. Thus, although TEA is well known as a K^+ channel blocker, it is effective at the ACh1 receptor/channel complex at concentrations on average 100-fold lower than its active extracellular concentration at most K^+ channels. The potential-dependence of the blockade suggests that it acts at the channel. Here we have a compound that is active as a blocker in two different superfamilies but with quite different potencies.

In contrast to TEA, strychnine shows equipotent cross-reactivity. This alkaloid is perhaps best known as a selective blocker of glycine-evoked responses [13] but it has also been reported to be active at cholinergic receptor/channel complexes [14]. Like the ACh1 receptor, the glycine receptor family belongs to the ligand binding-activated receptor/channel superfamily. Strychnine has proved to be extremely potent as a blocker of the ACh1 response (Fig. 4A,B), with a sub-nanomolar threshold and an EC_{50} of $2.3 \pm 0.5 \times 10^{-8}$ M (mean $\pm$ S.D., $n = 3$). The blockade is reversible and does not depend on membrane potential (Fig. 4C). A similar lack of potential-dependence has been reported for strychnine blockade of excitatory cholinergic responses in Aplysia neurones [15]. In this case, the active compound acts at different targets with similar potencies but both targets are members of the same superfamily. Interestingly, glycine potently inhibits α-bungarotoxin binding in the rat brain [16]. The relationship of the α-bungarotoxin binding proteins in vertebrate brain to functional nicotinic receptors is not entirely clear, but the ACh1 receptor is highly sensitive to α-bungarotoxin [9,17].

Picrotoxin (PTX) is a classical, non-competitive blocker of Cl^- current-mediated GABA responses, including $GABA_A$ responses and many arthropod GABAergic effects [18]. The GABA response of the locust thoracic neuronal somata, for example, is reduced to 30–50% by 10^{-7} M and completely blocked by 10^{-6} M PTX [3]. However, the ACh1 response in the same neurones is also sensitive to PTX (Fig. 5A). It is blocked by PTX with an activity threshold of approximately 3×10^{-7} M and an EC_{50} of $2.9 \pm 1.3 \times 10^{-5}$ M (mean $\pm$ S.D., $n = 4$) (Fig. 5B). The degree of blockade is not dependent on the membrane potential (Fig. 5C). This is another example of cross-reactivity within a superfamily, but in this case there is a marked difference in potency: PTX blocks the locust somal GABA response at a concentration about 100-fold lower than that required to block the ACh1 response.

Although PTX is universally considered to be a selective blocker of GABA-activated Cl^- channels, blockade of cholinergic responses by PTX has been reported

A

control

wash following
10^{-6}M strychnine

$$0.5\,nA$$

2 min

$E_h = -50\,mV$

log strychnine concentration (M)

C   membrane potential (mV)

3 × 10^{-8}M strychnine
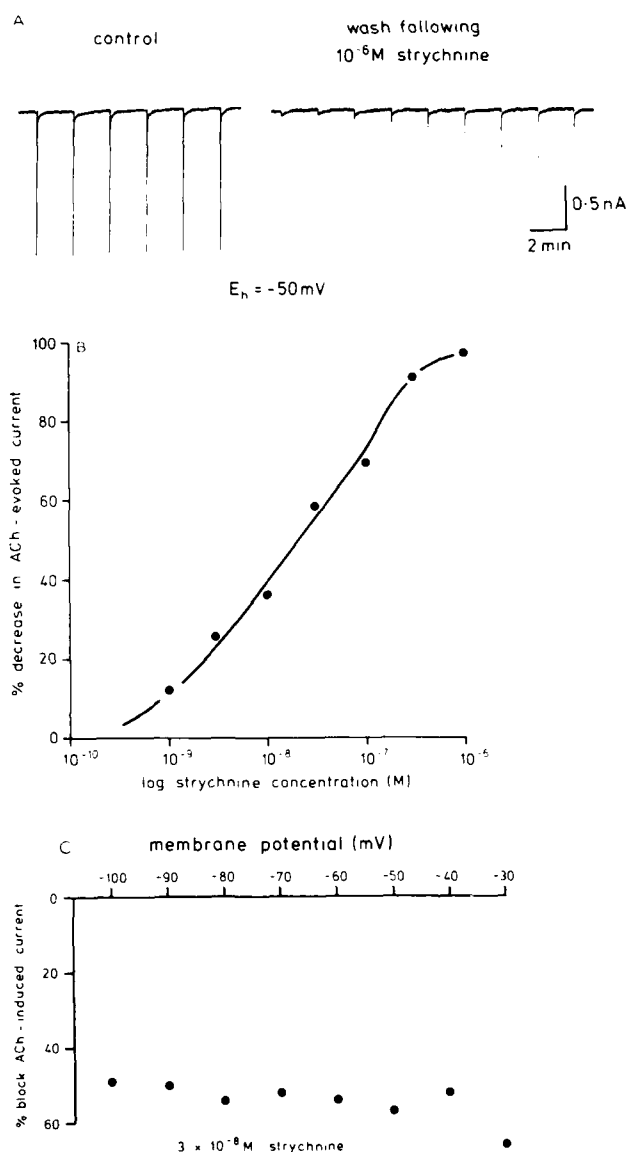
FIG 4   Characteristics of blockade by strychnine. A: single electrode voltage-clamp current records from a neuronal soma clamped at a holding potential (E_h) of − 50 mV and exposed to periodic pressure microapplications of 10^{-4} M acetylcholine (70 ms). The first panel shows the response in normal saline. The recording illustrated in the second panel was made during perfusion of the recording chamber with normal saline immediately following maximum blockade by saline containing 10^{-6} M strychnine. B: dose–response curve showing the dependence of the degree of blockade of the cholinergic response on the concentration of strychnine in the superfusing saline. The response was evoked by 70 ms pressure pulses of 10^{-4} M ACh. C: the percentage reduction of the acetylcholine-evoked current in strychnine saline is plotted against the clamp potential at which the current was recorded. The degree of block was independent of the membrane potential. A, B and C are from different cells.

A

control

wosh following
$10^{-4}M$ picrotoxin

$E_h = -50mV$

0·5nA

2 min

100 ┐ B

80

% decrease in ACh - evoked current

60

40

20

0

10^{-7} 10^{-6} 10^{-5} 10^{-4} 10^{-3}

log picrotoxin concentration (M)

C   membrane potential (mV)

-100 -90 -80 -70 -60 -50 -40 -30

0

20

40

60

% block ACh-induced current
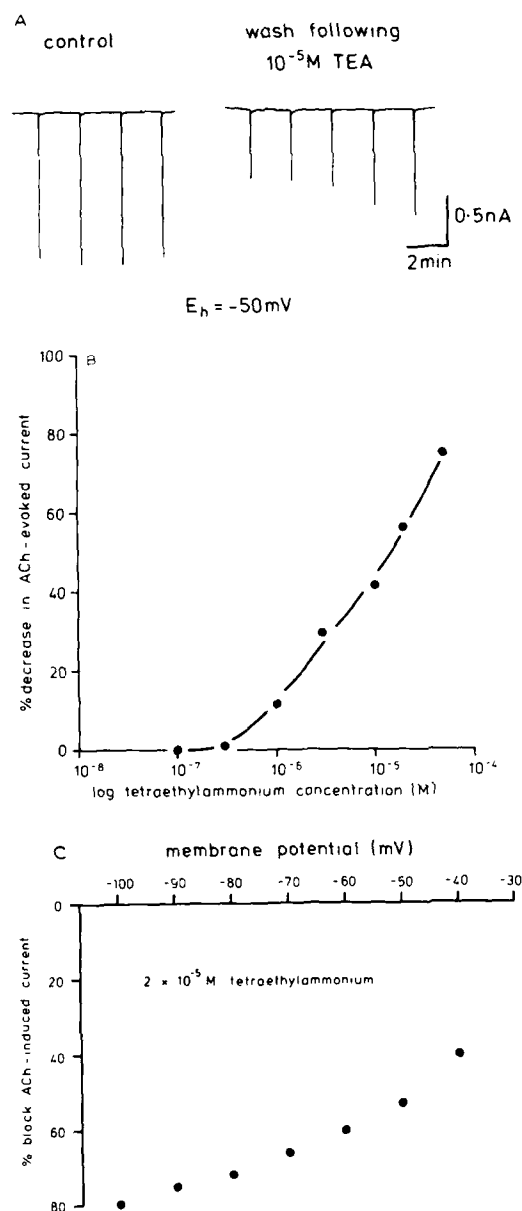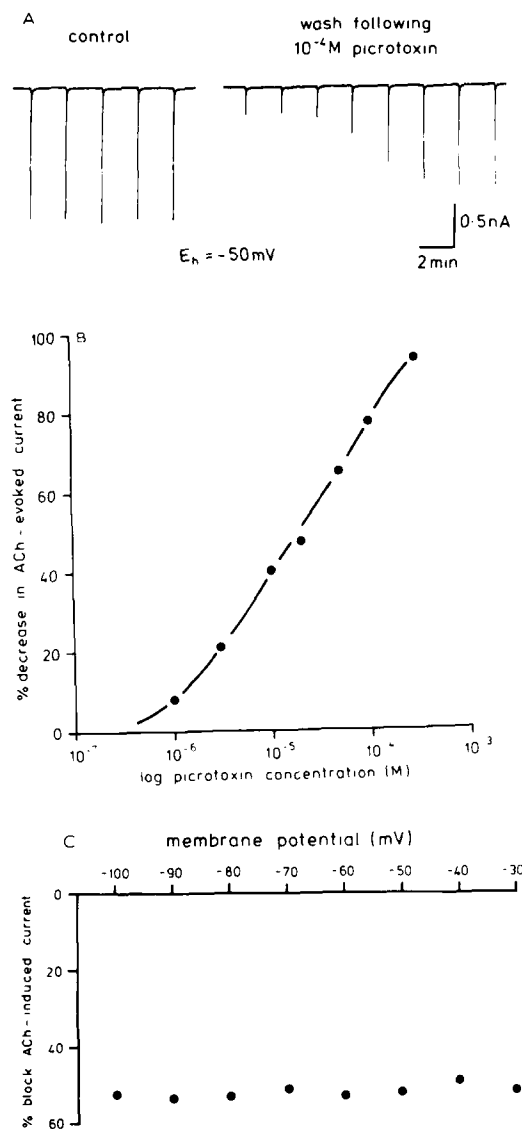
FIG 5 Characteristics of blockade by picrotoxin. A: single electrode voltage-clamp current records from a neuronal soma clamped at a holding potential (E_h) of − 50 mV and exposed to periodic pressure microapplications of 10^{-4} M acetylcholine (100 ms). The first panel shows the response in normal saline. The recording illustrated in the second panel was made during perfusion of the recording chamber with normal saline immediately following maximum blockade by saline containing 10^{-4} M picrotoxin. B: dose–response curve showing the dependence of the degree of blockade of the cholinergic response on the concentration of picrotoxin in the superfusing saline. The response was evoked by 100 ms pressure pulses of 10^{-4} M ACh. C: the percentage reduction of the ACh-evoked current in picrotoxin saline is plotted against the clamp potential at which the current was recorded. The degree of block was independent of the membrane potential. A, B and C are from different cells.

A control

wash following
10^{-4}M bicuculline methobromide

0·5nA

2min

$E_h = -50$mV

100 | B

% decrease in ACh - evoked current

80

acetyl-choline

GABA

60

40

20

0

10^{-7} 10^{-6} 10^{-5} 10^{-4} 10^{-3}

log bicuculline methiodide concentration (M)

C   membrane potential (mV)

-100   -90   -80   -70   -60   -50   -40   -30

% block ACh-induced current

0

20

40

60

4×10^{-6} M bicuculline methiodide
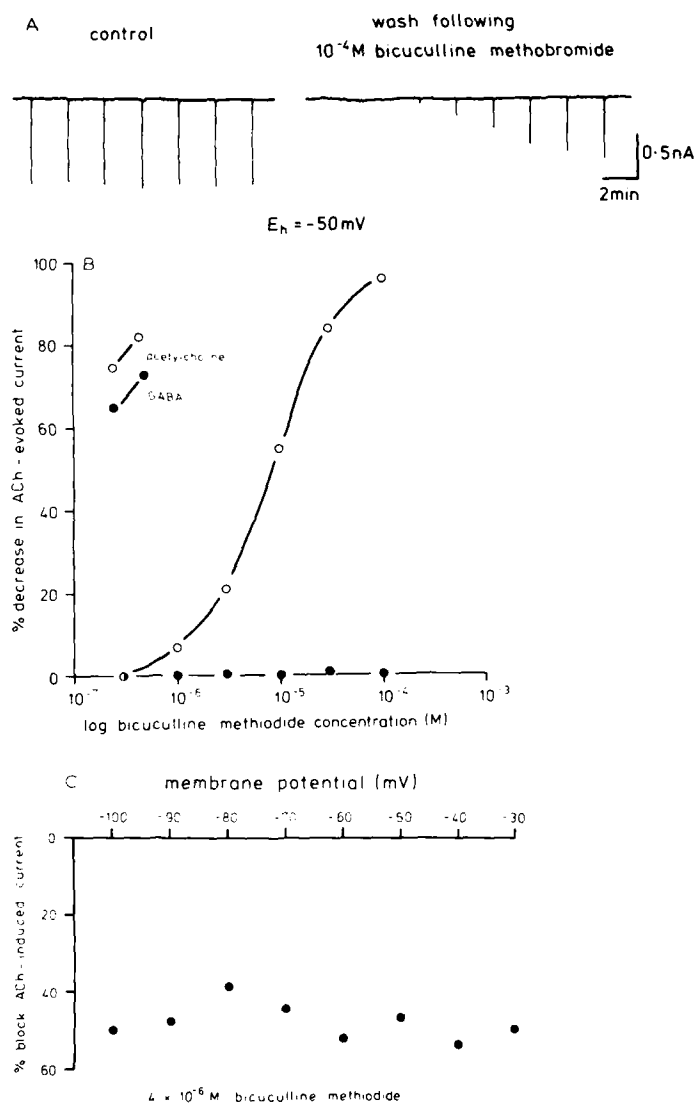
FIG 6   Characteristics of blockade by bicuculline salts. A: single electrode voltage-clamp current records from a neuronal soma clamped at a holding potential (E_h) of -50 mV and exposed to periodic pressure microapplications of 10^{-4} M ACh (100 ms). The first panel shows the response in normal saline. The recording illustrated in the second panel was made during perfusion of the recording chamber with normal saline immediately following maximum blockade by saline containing 10^{-4} M bicuculline methobromide. B: dose–response curves showing the dependence of the degree of blockade of the cholinergic (open circles) and GABAergic (closed circles) responses on the concentration of bicuculline methiodide in the superfusing saline. The responses were evoked by 500 ms pressure pulses of 10^{-4} M ACh and 100 ms pulses of 10^{-4} M GABA. C: the percentage reduction of the ACh-evoked current in bicuculline methiodide saline is plotted against the clamp potential at which the current was recorded. The degree of block was independent of the membrane potential. A, B and C are from different cells.

previously. Yarowsky and Carpenter found, using *Aplysia* neurones, that PTX blocks the responses to GABA and ACh mediated by Cl^- but not those mediated by Na^+ [19]. This led them to suggest that PTX acts as a blocker of transmitter-activated Cl^- channels generally. Similarly, PTX blocks the Cl^-- but not Na^+-mediated extra-junctional glutamate responses in insect muscle [20,21]. However, contrary to this hypothesis, the results reported above show that PTX can block a non-Cl^--mediated cholinergic response, and it has been demonstrated previously that the Cl^--mediated GABA response of crab stomatogastric neurones is insensitive to PTX while the glutamate and GABA-induced increases in K^+ conductance in the same cells are blocked by PTX [22]. Similarly, the Na^+-mediated cholinergic response of crab gastric mill muscle is blocked by PTX [23]. The effectiveness of PTX thus seems to be unrelated to the identity of the ion involved. A high degree of structural homology among the PTX-sensitive channels is a more likely hypothesis.

Bicuculline blockade of the response to GABA is a defining characteristic of the vertebrate $GABA_A$ receptor subtype. Part of the bicuculline molecule is similar in structure to GABA and bicuculline is thought to bind to the GABA recognition site as a competitive antagonist [24]. Bicuculline is, however, without effect on the locust thoracic somal GABA response at concentrations up to 10^{-4} M [3,8], despite the otherwise strong similarity between the locust somal GABA receptor and the vertebrate $GABA_A$ receptor subtype (Table 2). In contrast, bicuculline and its salts block the ACh1-mediated responses in the same neurones (Fig. 6A). For bicuculline free base, the activity threshold is approximately 3×10^{-7} M and the EC_{50} is $3.1 \pm 1.8 \times 10^{-5}$ M (mean $\pm$ S.D., $n = 6$). The values for the methiodide salt are

TABLE 3 Cross-reactivity of diagnostic compounds

Compound and Site of action	Superfamily		Comparative potency		Potential dependent		Probable mode of action	
	Same	Different	Weak	Potent	Yes	No	Non-competitive (e.g. channel blocker)	Competitive (receptor antagonist)
TEA		*						
K$^+$ channel			*		*		*	
ACh1 receptor				*	*		?	?
Strychnine	*							
Glycine receptor			*		–	–		*
ACh1 receptor			*			*		?
Picrotoxin	*							
Locust GABA receptor			*			*	*	
ACh1 receptor			*			*	?	
Bicuculline	*							
GABA$_A$ receptor			*		–	–		*
ACh1 receptor			*			*	mixed	

? indicates the more likely case, based on vertebrate studies, in the absence of direct evidence for the ACh1 receptor.
– indicates no data available.

204

similar (Fig. 6B) and the blockade shows no influence by the membrane potential (Fig. 6C). If the mode of action in all cases is the same, these results suggest a greater similarity of the bicuculline site of action between the AChl receptor and the $GABA_A$ receptor than between the latter and the locust somal GABA receptor. Blockade of an ACh-induced response in insect neurones by bicuculline has been reported previously [25] and Yarowsky and Carpenter found that bicuculline blocked a Cl^--mediated cholinergic response in mollusc neurones [19].

The results discussed above are summarized in Table 3. Some patterns can be tentatively discerned. Between superfamilies (e.g. actions of TEA), potency differs with target receptor. Gallamine also fits this pattern: at relatively high concentrations, it blocks some K^+ channels [26] and is a mixed agonist/antagonist at lower concentrations at the AChl receptor (Table 1). This difference in potency may reflect a difference in mode of action and/or comparatively large divergence in receptor/channel structure. Similar modes of action within a superfamily do not necessarily lead to similar potency. PTX is probably a channel blocker at both the GABA and AChl receptor/channel complexes. The observed similarity of action but difference in potency of PTX at these targets therefore most likely reflects the degree of homology at the target site. On the other hand, strychnine binds with remarkably high potency at both the vertebrate glycine and AChl receptors, probably reflecting a high degree of structural similarity at the binding site. The case of bicuculline is different again. There is evidence that bicuculline acts only partially competitively at the AChl receptor [6] and thus probably differs in its mode of action at the two target sites. This may account for the difference in potency in this case. However, in vitro ligand displacement binding studies will provide additional information on the precise mode of action of these compounds on the locust neurones and tests with further compounds will facilitate generalizations on the structural basis of cross-reactivity.

Conclusions

In answer to the first question posed at the beginning of this paper, it is unsafe to assume that a compound that is highly specific to a particular receptor or channel subtype in the vertebrates will exhibit the same specificity in the insects. The pharmacological variation observed among the receptor and channel subtypes is real and will produce not only false negatives but also unexpected cross-reactivity between receptors and channels from different families and even superfamilies [27].

A partial answer to the second question is that the locust thoracic somal GABA and AChl receptors recognizably belong to the same families as the vertebrate $GABA_A$ and nicotinic ACh receptors respectively, despite displaying unique features in the details of their pharmacology. Nevertheless, they appear to resemble receptor/channel complexes in other families more strongly than hitherto appreciated. The variety of pharmacologically distinct receptor subtypes is probably much greater than generally realized but future pharmacological studies should complement molecular genetic observations on receptor and channel relationships by showing to what extent sequence homology reflects functional homology. Ultimately, advances in molecular modelling should bring the pharmacological and molecular approaches together and possibly allow a rationalized classification of receptors and channels based on molecular phylogeny rather than purely on the relative effects of agonists and antagonists.

References

1 Schofield, P.R., Darlison, M.G., Fujita, N., Burt, D.R., Stephenson, F.A., Rodriguez, H., Rhee, L.M., Ramachandran, J., Reale, V., Glencorse, T.A., Seeburg, P.H. and Barnard. E.A. (1987) Sequence and functional expression of the GABA$_A$ receptor shows a ligand-gated receptor super-family. Nature (Lond.) 328, 221–227.

2 Grenningloh, G., Rienitz, A., Schmitt, B., Methfessel, C., Zensen, M., Beyreuther, K., Gundelfinger, E.D. and Betz, H. (1987) The strychnine-binding subunit of the glycine receptor shows homology with nicotinic acetylcholine receptors. Nature (Lond.) 328, 215–220.

3 Lees, G., Beadle, D.J., Neumann, R. and Benson, J.A. (1987) Responses to GABA by isolated insect neuronal somata: pharmacology and modulation by a benzodiazepine and a barbiturate. Brain Res. 401, 267–278.

4 Usherwood, P.N.R., Giles, D. and Suter, C. (1980) Studies of the pharmacology of insect neurones in vitro. In: Insect Neurobiology and Pesticide Action (Neurotox '79), pp. 115–128, Society of Chemical Industry, London.

5 Kerkut, G.A., Pitman, R.M. and Walker, R.J. (1969) Sensitivity of neurones of the insect central nervous system to iontophoretically applied acetylcholine or GABA. Nature (Lond.) 222, 1075–1076.

6 Benson, J.A. (1988) Bicuculline blocks the response to acetylcholine and nicotine but not to muscarine or GABA in isolated insect neuronal somata. Brain Res. 458, 65–71

7 Benson, J.A. (1988) Characterization of the acetylcholine responses recorded from isolated locust neuronal somata. (in preparation).

8 Neumann, R., Lees, G., Beadle, D.J. and Benson, J.A. (1987) Responses to GABA and other neurotransmitters in insect central neuronal somata in vitro. In: Sites of Action for Neurotoxic Pesticides (R.M. Hollingworth, M.B. Green, eds.), pp.25–43. American Chemical Society, Washington, DC.

9 Benson, J.A. and Neumann, R. (1987) Nicotine and muscarine evoke different responses in isolated, neuronal somata from locust thoracic ganglia. Neurosci. Abs. 13, 938.

10 Duggan, M.J. and Lunt, G.G. (1986) Second messengers linked to the muscarinic acetylcholine receptor in locust (Schistocerca gregaria) ganglia. In: Insect Neurochemistry and Neurophysiology (A.B. Borkovec and D.B. Gelman, eds.), pp. 251–254. Humana Press, Inc., Clifton.

11 Stanfield, P.R. (1983) Tetraethylammonium ions and the potassium permeability of excitable cells. Rev. Physiol. Biochem. Pharmacol. 1–67.

12 Adler, M., Oliveira, A.C., Albuquerque, E.X., Mansour, N.A. and Eldefrawi, A.T. (1979) Reaction of tetraethylammonium with the open and closed conformations of the acetylcholine receptor ionic channel complex. J. Gen. Physiol. 74, 129–152.

13 Curtis, D.R., Duggan, A.W. and Johnston, G.A.R. (1971) The specificity of strychnine as a glycine antagonist in the mammalian spinal cord. Exp. Brain Res. 12, 547–565.

14 Alving, B.O. (1961) The action of strychnine at cholinergic junctions. Arch. Int. Pharmacodyn. 131, 123–150.

15 Slater, N.T., Carpenter, D.O., Haas, H.L. and David, J.A. (1984) Blocking kinetics at excitatory acetylcholine responses on Aplysia neurons. Biophys. J. 45, 24–25.

16 Ono, J.K. and Salvaterra, P.M. (1981) Snake α-toxin effects on cholinergic and noncholinergic responses of Aplysia californica neurons. J. Neurosci. 1, 259–270.

17 Benson, J.A. (1988) Pharmacology of a locust thoracic ganglion somal nicotinic acetylcholine receptor. In: Nicotinic Receptors in CNS (F. Clementi, C. Gotti, E. Sher, eds.). Springer Verlag, Berlin. (in press).

18 Takeuchi, A. and Takeuchi, N. (1969) A study of the action of picrotoxin on the inhibitory neuromuscular junction of the crayfish. J. Physiol. (Lond.) 205, 377–391.

19 Yarowsky, P.J. and Carpenter, D.O. (1978) A comparison of similar ionic responses to γ-aminobutyric acid and acetylcholine. J. Neurophysiol. 41, 531–541

206

20 Usherwood, P.N.R. and Cull-Candy, S.G. (1975) Pharmacology of somatic nerve-muscle synapses. In: Insect Muscle (P.N.R. Usherwood, ed.), pp. 207–280. Academic Press, New York.

21 Cull-Candy, S.G. (1976) Two types of extra-junctional L-glutamate receptors in locust muscle fibres. J. Physiol. (Lond.) 255, 449-464.

22 Marder, E. and Paupardin-Tritsch, D. (1978) The pharmacological properties of some crustacean neuronal acetylcholine, γ-aminobutyric acid, and L-glutamate responses. J. Physiol. (Lond.) 280, 213–236.

23 Marder, E. and Paupardin-Tritsch, D. (1980) Picrotoxin block of a depolarizing ACh response. Brain Res. 181, 223–227.

24 Moehler, H. and Okada, T. (1977) GABA receptor binding with ³H(+)bicuculline-methiodide in rat CNS. Nature (Lond.) 267, 65–67.

25 Walker, R.J., Crossman, A.R., Woodruff, G.N. and Kerkut, G.A. (1971) The effect of bicuculline on the gamma-aminobutyric acid (GABA) receptors of neurones of Periplaneta americana and Helix aspersa. Brain Res. 33, 75–82.

26 Schauf, C.L. and Smith, K.J. (1981) Electrophysiological effects of gallamine triethiodide on mammalian and amphibian myelinated nerve fibres. J. Physiol. 312, 40-41P.

27 Eldefrawi, A.T. and Eldefrawi, M.E. (1987) Receptors for γ-aminobutyric acid and voltage-dependent chloride channels as targets for drugs and toxicants. FASEB J. 1, 262–271.

28 Shimahara, T., Pichon, Y., Lees, G., Beadle, C.A. and Beadle, D.J. (1987) Gamma-aminobutyric acid receptors on cultured cockroach brain neurones. J. Exp. Biol. 131, 231–244.

CHAPTER 15

Action of toxicants on GABA$_A$ and glutamate receptors

MOHYEE E. ELDEFRAWI AND AMIRA T. ELDEFRAWI

Department of Pharmacology and Experimental Therapeutics,
University of Maryland School of Medicine, Baltimore, MD 21201, U.S.A.

Introduction

The nervous system is controlled by many neurotransmitters and their receptor proteins, whose inhibition or modulation is deadly or incapacitating. Glutamate and its decarboxylated derivative γ-aminobutyric acid (GABA) are neurotransmitters, that mediate excitatory and inhibitory transmission, respectively, in the central nervous system (CNS) of vertebrates and invertebrates [1-3]. In addition, glutamate and GABA are the excitatory and inhibitory neurotransmitters, respectively, in invertebrate skeletal muscles [4,5]. Binding of these agonists to their respective receptors induces conformational changes in the proteins that result in opening of ion channels and flux of ions along their concentration gradients into and out of the cell. Agents that inhibit glutamatergic and/or potentiate GABAergic transmission depress neuronal activity and paralyse skeletal muscles of insects, while agents that inhibit GABAergic and/or potentiate glutamatergic transmission heighten nervous activity and induce seizures and/or convulsions. Accordingly, a combination of an inhibitor of glutamatergic and a potentiator of GABAergic transmission may be synergistic, while a combination of potentiators or inhibitors of both systems may be antagonistic.

Agonists and antagonists of both glutamate and GABA receptors are found in nature and are toxic to both vertebrates and invertebrates. Muscimol, found in the mushroom, *Amanita muscaria* is a potent GABA receptor agonist, while picrotoxinin, a plant alkaloid found in the shrub *Anamirta cocculus*, is a potent noncompetitive antagonist of GABA receptor [3]. Similarly, quisqualate, a natural amino acid found in seeds of *Quisqualis indica*, is a glutamate receptor agonist [6], while argiotoxin and jorotoxin from spider venoms, are noncompetitive antagonists of glutamate receptors [7,8]. Using the biochemical pharmacological techniques of radioligand binding and receptor regulated events, such as tracer ion fluxes, it is possible to detect interactions of numerous toxicants with both types of receptors and determine affinities and mechanisms of action.

208

GABA receptors

There are two types of GABA receptors in mammalian CNS [3]. The GABA$_A$ receptor is very senstive to muscimol but insensitive to baclofen, is inhibited by bicuculline (BIC) and picrotoxinin, and is potentiated by barbiturates and benzodiazepines (BZ), which stabilize a receptor conformation that has a higher affinity for GABA. This receptor is a GABA-gated Cl⁻ channel and is a tetramer made of two classes of subunit ($\alpha_2\beta_2$) [9]. The GABA$_B$ receptor is located mostly presynaptically, is relatively insensitive to muscimol and is sensitive to baclofen, is not inhibited by BIC or picrotoxinin and is not potentiated by BZ or barbiturates. GABA$_A$ receptors dominate postsynaptic inhibition in both vertebrate and invertebrate CNS. The insect GABA$_A$ receptors are insensitive to BIC, and GABA$_B$ receptors have not been identified in invertebrate CNS. GABA also plays a neuromodulatory role in vertebrate neural tissue [10] and this effect has not yet been detected in insect CNS. Our investigations over the last four years suggest that the GABA$_A$ receptor is a major target for a variety of toxicants, especially insecticides [11].

Action of polychlorocycloalkane insecticides on GABA$_A$ receptor

Cyclodiene insecticides are potent displacers of the specific binding of [³⁵S]t-butyl-bicylophosphorothionate (TBPS) to GABA$_A$ receptors in rat brain membranes with IC$_{50}$ values ranging from 30 nM for endrin and endosulfan I to 500 nM for aldrin [12,13]. Inhibition of [³⁵S]TBPS binding by endrin is competitive, suggesting that TBPS and cyclodienes bind to the same site in or close to the GABA$_A$ receptor's Cl⁻ channel. The GABA$_A$ receptor has higher affinities for the more toxic isomers of two pairs of cyclodienes (endrin, dieldrin and endosulfan I and II) (Fig. 1) as well as for the more toxic heptachlor epoxide than heptachlor. Since [³⁵S]TBPS is believed to bind to the picrotoxinin site on the GABA$_A$ receptor and act as a noncompetitive inhibitor, it was suggested that cyclodiene insecticides act also as noncompetitive blockers of GABA$_A$ receptors [12,13].

Direct evidence that cyclodiene insecticides inhibit GABA$_A$ receptor function was obtained by studying their effects on GABA-induced ³⁶Cl uptake into rat brain sealed membrane preparations (i.e. microsacs). The concentration-dependence and affinity of agonists as well as the effects of competitive and noncompetitive antagonists on this GABA-dependent ³⁶Cl uptake suggest that the assay is a good correlate of the physiological event regulated by the GABA$_A$ receptor, and is appropriate to use as a valid alternative to electrophysiological measurements or whole animal testing [14]. Cyclodiene insecticides inhibit this GABA-dependent ³⁶Cl⁻ influx with endosulfan I and endrin being more potent than their less toxic isomers endosulfan II and dieldrin, and the epoxides of heptachlor and aldrin were more potent than their less toxic parent compounds. There is excellent correlation ($r = 0.9$) between inhibition of [³⁵S]TBPS binding to rat brain membranes and inhibition of GABA-dependent ³⁶Cl flux by cyclodiene insecticides (Table 1).

The γ isomer of hexachlorocyclohexane (γ-BHC or lindane) affects binding of [³⁵S]TBPS and GABA-dependent ³⁶Cl⁻ flux into rat brain as do the cyclodienes (Table 1). Moreover, other non-toxic isomers (e.g. β-BHC) have little or no effect.
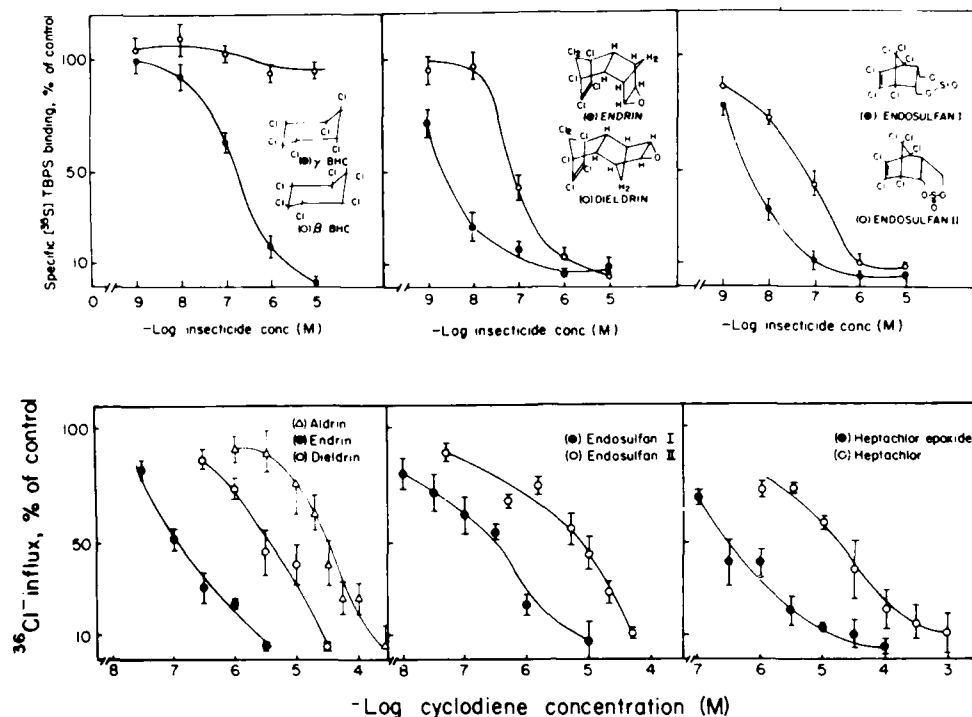
FIG 1 The effects of isomers of hexachlorocyclohexane (BHC) and cyclodiene insecticides on GABA$_A$ receptor. Top: inhibition of the specific binding of [^{35}S]TBPS (2 nM) to GABA$_A$ receptors of rat brain (from Ref. 24). Bottom: inhibition of ^{36}Cl$^-$ influx that is induced by 100 μM GABA and is inhibited by 100 μM bicuculline (from Ref. 14).

TABLE 1 Effect of GABAergic drugs on ^{36}Cl$^-$ influx into rat brain vesicles from Ref. 14

Chemical	IC$_{50}$ (μM)		Mammalian toxicity (LD$_{50}$, mg/kg)
	^{36}Cl$^-$ influx	[^{35}S]TBPS binding	
Drug			mice(i.p.)
(+)Bicuculline	3.07 ± 1.21		–
(−)Bicuculline	31.6 ± 7.6		–
Picrotoxinin	0.41 ± 0.13		3.0
TBPS	0.43 ± 0.05		1.1
Cyclodiene insecticides			rats(p.o.)
Endrin	0.19 ± 0.06	0.003	10
Dieldrin	3.27 ± 0.72	0.10	46
Endosulfan I	0.19 ± 0.07	0.003	18
Endosulfan II	8.09 ± 2.00	0.06	240
Heptachlor epoxide	0.45 ± 0.13	0.07	40
Heptachlor	22.90 ± 3.40	0.40	90

Thus, the stereospecificity of action on $GABA_A$ receptors is clearly manifested by these compounds. In collaboration with Dr. David Satelle (Cambridge, England), we found the action of lindane and endrin on insect ganglionic $GABA_A$ receptor to be as noncompetitive inhibitors, the same as their actions on mammalian brain $GABA_A$ receptor (unpublished data). An interesting finding is that lindane is more potent on a non-GABAergic voltage-dependent Cl^- channel than it is on the $GABA_A$ receptor, but even its non-toxic isomers affect this Cl^- channel [15]. Therefore, the mechanisms of toxicity of cyclodiene insecticides and lindane to mammals and insects is suggested to be mediated by their binding to an allosteric site on the $GABA_A$ receptor and inhibition of its function. This is manifested by seizures and convulsions in mammals and tremors and hyperexcitability in insects.

Action of pyrethroids on $GABA_A$ receptor

Pyrethroids modify the gating kinetics of voltage-dependent sodium channels in nerve cell membranes resulting in marked prolongation of channel open time, increasing depolarizing afterpotentials [16]. Thus, repetitive discharges are evoked in nerve fibers. However, pyrethroids have other actions as well which may explain why their symptoms of poisoning are of two types in mammals and insects [17]. The T syndrome, which is characterized by a rapid onset of tremors, and the CS syndrome, which is characterized by profuse salivation followed by spontaneous sinuous writhing (choreoathetosis) and clonic/tonic convulsions. Generally, pyrethroids that consist of a halogenated acid esterified with α-cyano-3-phenoxybenzyl alcohol (type II pyrethroids) produce the CS syndrome, while those that lack either or both moieties produce the T syndrome. In insects, type I pyrethroids generally produce restlessness, incoordination, prostration and paralysis, while type II pyrethroids produce incoordination, convulsions and intense hyperactivity [18].

Gammon et al. [19] drew attention to the possible involvement of $GABA_A$ receptor in the toxic action of pyrethroids, by showing that diazepam, which potentiates GABA function, delays the onset of toxicity symptoms in mice and cockroaches. The direct action of pyrethroids on $GABA_A$ receptor is shown by the inhibition of [^{35}S]TBPS binding to rat brain membranes by type II pyrethroids alone [20], or by inhibition of the GABA-induced $^{36}Cl^-$ influx (Fig. 2) by both types of pyrethroids, though type II pyrethroids are on the average 14-fold more potent than type I. Also, of eight cypermethrin isomers tested, only the toxic isomers *1R,cis,as* and *1R,trans,as* inhibit the GABA-dependent $^{36}Cl^-$ flux. The relative potencies of pyrethroids as inhibitors of $GABA_A$ receptor function do not correlate well with their mammalian toxicities (Table 2). However, their potencies on this receptor and stereospecificity argue for a specific action on the $GABA_A$ receptor which contributes to their toxicity. It also explains why type II pyrethroids have similar effects to picrotoxinin on the acoustic startle responses in rats [21], and potentiate the seizure inducing activity of pentylenetetrazole in mice [22]. Type II pyrethroids are also more potent inhibitors than type I of the binding of [^{3}H]Ro5-4864 (4'-chlorodiazepam) to rat brain, which is a specific probe for the peripheral benzodiazepine receptor, that is located in the outer membrane of mitochondria and is suggested to be an anion channel [23]. Lengthening the open time of the Na^+ channel by a pyrethroid results in increased transmitter release of both the inhibitory GABA and the excitatory glutamate and acetylcholine (ACh). The added
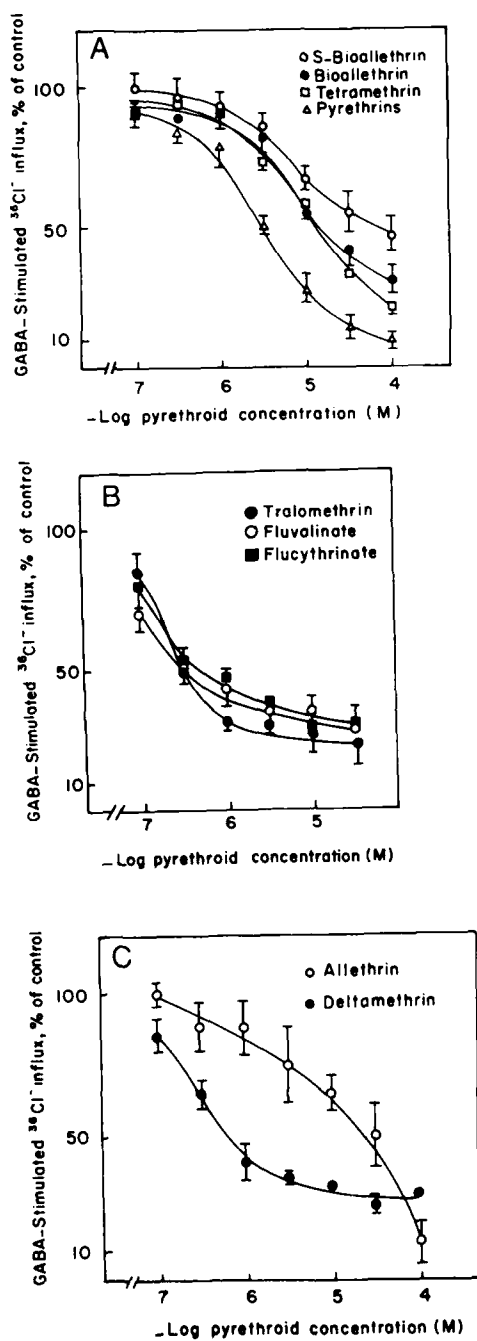
FIG 2   Inhibition of $^{36}Cl^-$ influx induced by 100 μM GABA into rat brain microsacs by (A) four type I pyrethroids, (B) three type II pyrethroids and (C) allethrin (type I) vs deltamethrin (type II). Symbols and bars are means ± S.D. of three experiments (from Ref. 44).

TABLE 2 Potencies of pyrethroids as inhibitors of GABA stimulated ^{36}Cl$^-$ influx, [^{3}H]Ro5-4864 binding to rat brain and their toxicities to mammals (from Refs. 45 and 46)

Pyrethroids	GABA-induced ^{36}Cl$^-$ uptake IC$_{50}$ (μM)	Binding of [^{3}H]Ro5-4864 IC$_{50}$ (μM)	LD$_{50}$ (oral-rat) (mg/kg)
Type I			
Allethrin	20 ±1.9	4 ±0.3	680
Bioallethrin	20 ±1.1	7 ±0.5	425
S-Bioallethrin	80 ±4.2	10 ±0.8	430
Permethrin	14 ±1.1	>10	2000
cis-Permethrin	10 ±0.7	>10	2000
trans-Permethrin	10 ±0.9	7 ±0.6	2000
Pyrethrins	3 ±0.2	1.2 ±0.1	750
Resmethrin	40 ±2.5	10 ±0.9	8000
Tetramethrin	15 ±0.9	3 ±0.2	5000
Type II			
Cyfluthrin	0.8±0.04	2 ±0.1	590
Cypermethrin	1.2±0.05	2 ±0.1	251
Deltamethrin	0.7±0.05	0.15±0.01	100
Fenvalerate	8.0±0.07	>10	451
Flucythrinate	0.4±0.03	1 ±0.1	81
Fluvalinate	0.3±0.02	>100	282
Tralomethrin	0.2±0.01	6 ±0.5	99

inhibitory effect of pyrethroids on GABA$_A$ receptor reduces the inhibitory input resulting in heightened excitation as would the inhibition of ACh receptor desensitization that is suggested to be produced by pyrethroids [24]. The high toxicity of type II pyrethroids, which are more potent inhibitors of GABA$_A$ receptor may be due in part to physiological synergy of action at two or at multiple sites.

Action of tremorgenic mycotoxins

Tremorgenic mycotoxins are secondary metabolities produced by fungi and are found contaminating a variety of agricultural commodities such as forages, corn and silage [25]. They cause a neurological syndrome in cattle known as 'staggers', whose clinical signs include muscle tremor, and uncoordinated movements of the forelegs which become more evident when the animals are disturbed. Though mortalities are low and the animals usually recover, affected animals become debilitated and may die from dehydration, drowning or limb injury. Most of these tremorgenic mycotoxins are derived from geranylgeraniol and tryptophan (Fig. 4). While four tremorgenic mycotoxins tested inhibit [^{35}S]TBPS binding to the rat brain GABA$_A$ receptor as well as the GABA-induced ^{36}Cl$^-$ flux, the nontremorgenic mycotoxin does not (Fig. 3). Inhibition of GABA$_A$ function may explain why the administration of 4 mg/kg (i.p.) aflatrem (a tremorgenic mycotoxin) in mice results in hyperactivity, hypersensitivity, tremors and convulsions [26]. The chemical structure of mycotoxins adds another dimension to the versatility of GABA$_A$ receptor inhibitors.

MYCOTOXINS

TREMORGENIC   NON-TREMORGENIC

Aflatrem   Paspalinine

Verruculotoxin

Paxilline   Verruculogen

(□) Aflatrem
(■) Paxilline
(○) Verruculogen
(●) Paspalinine
(△) Verruculotoxin

-Log Mycotoxin Concentration (M)

(□) Aflatrem
(■) Paxilline
(○) Verruculogen
(●) Paspalinine
(△) Verruculotoxin

-Log Mycotoxin Concentration (M)
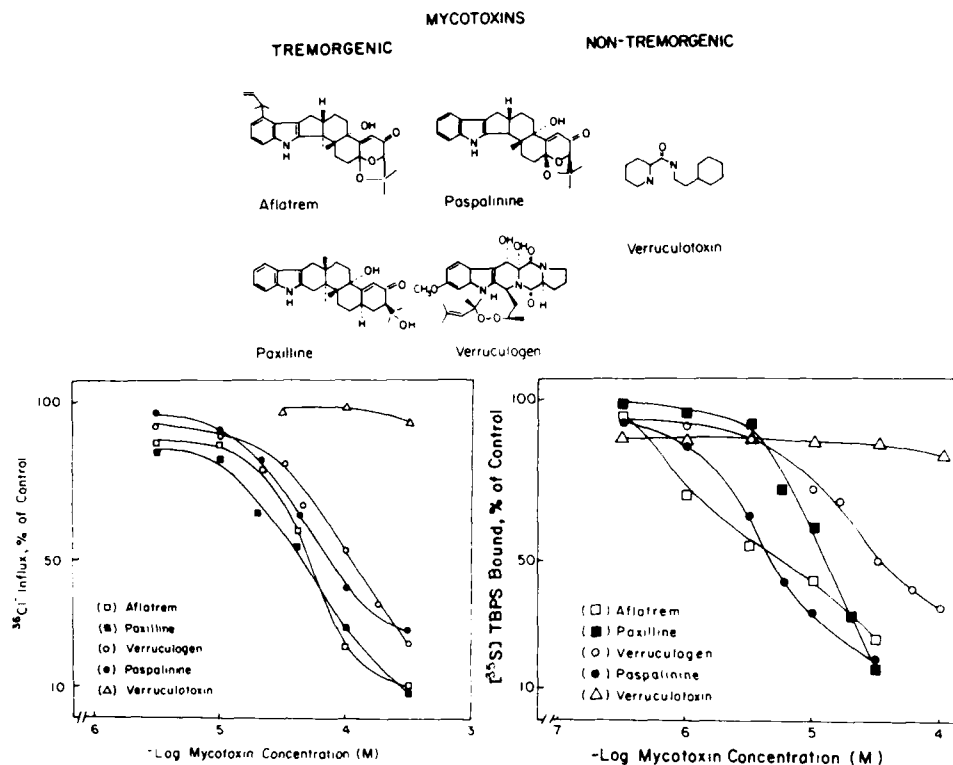
FIG 3   The effects of tremorgenic mycotoxins on $GABA_A$ receptor of rat brain. Top: chemical structures of one nontremorgenic (verruculotoxin) and four tremorgenic mycotoxins. Bottom left: inhibition of GABA-induced $^{36}Cl^-$ influx into rat brain microsacs. Microsacs were exposed to the indicated concentrations of mycotoxins for 15 min before the addition of 0.2 μCi $^{36}Cl^-$ and 100 μM GABA. Influx was halted after 4 s. Bottom right: inhibition of [^{35}S]TBPS (1 nM) binding to the same microsac preparation. Nonspecific binding was determined in the presence of 10 μM unlabelled TBPS (from Ref. 26).

(○) Leptophos
(●) Leptophos oxon
(△) EPN
(▲) TOCP

-LOG ORGANOPHOSPHATE CONCENTRATION (M)

(○) Leptophos
(●) Leptophos oxon
(△) EPN
(▲) TOCP

-LOG ORGANOPHOSPHATE CONCENTRATION (M)
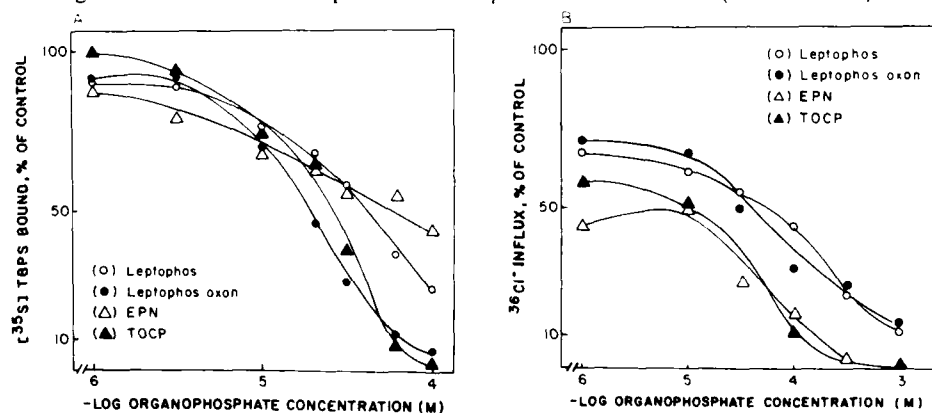
FIG 4   The dose-dependent inhibition of (A) GABA-induced $^{36}Cl^-$ influx and (B) [^{35}S]TBPS (1 nM) binding to rat brain by leptophos, leptophos oxon (○), EPN and TOCP. Values are means of three separate experiments; S.E.M. < 5% (from Ref. 32).

Action of organophosphates on $GABA_A$ receptor

Organophosphates (OP) constitute a large class of compounds that include industrial, insecticidal and clinical agents. Many are potent inhibitors of ACh esterase; whose toxicological and pharmacological effects are mediated primarily via its inhibition of ACh esterase and the resulting effects on cholinergic transmission. The bicyclophosphorothionates (e.g. TBPS) are poor inhibitors of ACh esterase but they are highly toxic and produce convulsions [27]. Their main target is the $GABA_A$ receptor as evidenced by (1) their rapid induction of seizures, (2) antagonism of
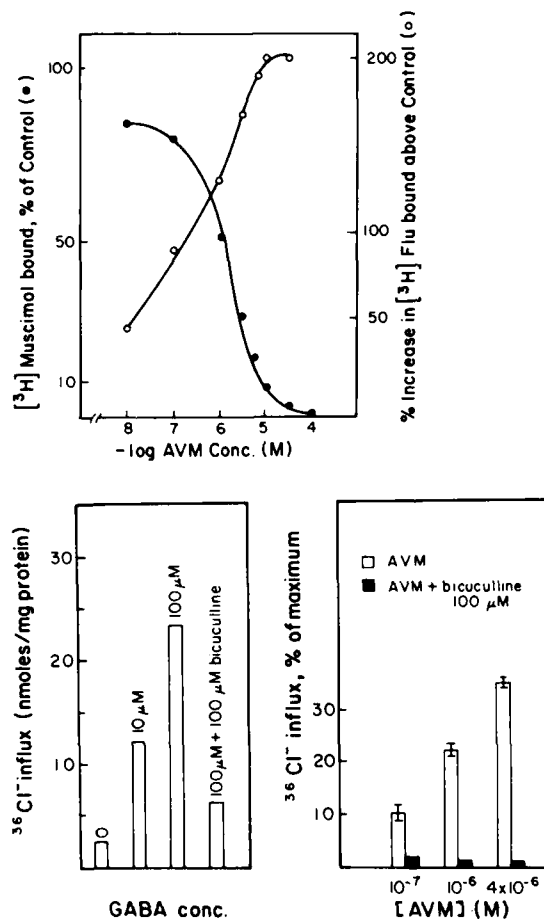
FIG 5 Action of AVM on $GABA_A$ receptor of rat brain. Top: the dose-dependent effect of AVM on the binding of 4 nM [^{3}H]muscimol (●) and 2 nM [^{3}H]Flu (o). Control binding of 4 nM [^{3}H]muscimol in the absence of AVM is 100%. In the case of [^{3}H]Flu binding. 0% is the control, and values above that resulting from AVM action are recorded as percentage increase. Bottom: influx of $^{36}Cl^-$ into microsacs which is activated by GABA or AVM. Left panel: activation by GABA is inhibited by bicuculline. Right panel: AVM activation is inhibited by bicuculline. Maximum $^{36}Cl^-$ influx is that obtained with 100 μM GABA. Each bar represents ± S.D. of three experiments (from Ref. 35).

their effects by GABA, (3) their inhibition of [^{3}H]dihydropicrotoxinin binding to rat brain, (4) their high affinity for GABA$_A$ receptor and (5) inhibition of GABA-dependent conductances and ^{36}Cl$^-$ flux [14,28,29]. Seizures and convulsions are among the major symptoms of acute intoxication by some OP anticholinesterases. Such neuronal manifestation may be precipitated by stimulated ACh transmission that results from inhibition of ACh esterase. However, OP-induced seizures and convulsions are suppressed by benzodiazepines [30], and intoxication with diisopropylfluorophosphate produces upregulation of GABA$_A$ receptors [31], which is a regulatory response expected of receptor inhibitors.

Although potent anticholinesterase OPs such as soman and sarin and the therapeutic echotiophate have no effect on GABA-induced ^{36}Cl$^-$ influx and [^{35}S]TBPS binding in rat brain preparations, the industrial tri-O-cresyl phosphate (TOCP), the flame retardant triphenylphosphate, and several insecticidal OPs including leptophos and EPN inhibit it (Fig. 5) [32]. It is interesting that some of the OPs that affect GABA$_A$ receptor function are also known to induce delayed neurotoxicity, but not all OPs that produce delayed neurotoxicity affect GABA$_A$ receptor [33]. The relatively high concentrations required, and the lack of correlation with toxicity, indicate that the GABA$_A$ receptor is not an important target in the toxicity of most OP anticholinesterases, though it may contribute to the toxicity of some.

Action of avermectin B$_{1a}$ on GABA$_A$ receptor

Avermectin B$_{1a}$ (AVM) is a macrocyclic lactone derived from *Streptomyces avermitilis* which has potent anthelmintic as well as insecticidal activities and affects GABA$_A$ receptor function [34,35]. AVM acts like GABA in several ways, such as potentiation of [^{3}H]flunitrazepam binding and inhibition of [^{3}H]muscimol and [^{35}S]TBPS binding (Fig. 5). AVM also induces ^{36}Cl$^-$ influx thus acting as an agonist, though to a lower degree than does GABA, and this is bicuculline-sensitive (Fig. 7). But in the presence of 100 μM GABA, AVM inhibits the GABA-induced ^{36}Cl$^-$ influx. Thus, although AVM may act primarily to open Cl$^-$ channels, it appears to act as partial agonist on GABA$_A$ receptors as has also been reported for insect muscle [3,6].

Glutamate receptors

There are at least three subtypes of glutamate receptors, which are classified according to their affinities for agonists and antagonists [1]. The quisqualate receptors is activated preferentially by quisqualate, is predominant in invertebrate skeletal muscle [2,3] and is inhibited noncompetitively by neurotoxins (e.g. argiotoxin and jorotoxin) [8]. The N-methyl-D-aspartate (NMDA) receptor is activated by NMDA and is selectively blocked by the anticonvulsant MK-801 ((+)-5-methyl-10,11-dihydro-5H-dibenzo(a,d)cyclohepten-5,10-imine maleate) and 2-APV (2-amino phosphonovalerate). This receptor plays important roles in memory and learning and its inhibition by MK-801 is therapeutic in ischemia-induced brain injury. So far, it has not been detected in insect tissues. The discovery and study of [^{3}H]MK-801 binding, for which the NMDA receptor has nM affinity [37], has

facilitated greatly the study of the NMDA receptor. The kainate receptor is activated preferentially by kainic and domoic acids and is much more sensitive to inhibition by γ-D-glutamylglycine [1]. It is the first 'subtype' of glutamate receptor to be purified [38]. Although [^{3}H]glutamate binding has been used to identify glutamate receptors in mammalian brain and insect muscle and brain [39], the artifacts in some binding studies and the presence of receptor subtypes complicate analyses of the data.

Effects of philanthotoxins and insecticides on glutamate receptors

The solitary digger wasp, *Philanthus triangulum F.,* which is a sphecid wasp that preys on honey bees, manufactures a venom which paralyses insects belonging to several orders [40], because it contains a toxin that is an allosteric inhibitor of insect muscle glutamate receptor [41]. We have purified the active neurotoxin from the wasp venom, identified its chemical structure and synthesized the pure toxin (Philanthotoxin-433) (PTX-433) [42]. It is a potent inhibitor of the neurally-evoked twitch contraction of locust skeletal muscle (Fig. 6). However, PTX-433 does not displace the binding of [^{3}H]glutamate to rat brain or insect muscles, which is to be expected since PTX appears to act as a noncompetitive blocker. We are currently investigating the effect of glutamate on the binding of [^{3}H]PTX to glutamate receptors and hope to use it as a label for the quisqualate receptor as [^{3}H]MK-801 is used for the NMDA receptor. Interestingly, PTX-433 also inhibits noncompetitively the glutamate-dependent binding of [^{3}H]MK-801 to rat brain (Fig. 7). The NMDA receptor which has high affinity for MK-801 (IC_{50} 7.7 nM) and phencyclidine (IC_{50} 143 nM) has a much lower affinity for PTX ($IC_{50} \simeq 39 \,\mu$M) and the Ca^{2+} channel antagonist diltiazem (IC_{50} 147 μM). PTX also inhibits binding of [^{3}H]perhydrohistrionicotoxin to the nicotinic ACh receptor of *Torpedo* electric organ with IC_{50} of $\simeq 10\,\mu$M. Since both the NMDA and nicotinic receptors have relatively non-selective cationic channels and their PTX binding sites appear to be in or near these channels, it suggests that PTX may be a nonselective cation channel blocker. The paralytic potency of PTX when injected in insects may be due to effects on multiple sites (i.e. inhibition of central nicotinic and peripheral glutamate receptors), that results in physiological synergy.

Several OP anticholinesterases, pyrethroids, and chlorinated hydrocarbons tested at 10 μM have no significant effect on the binding of [^{3}H]glutamate or the glutamate-dependent [^{3}H]MK-801 binding. However, at submicromolar concentrations several carbamate anticholinesterases increase the [^{3}H]MK-801 binding to brain significantly, suggesting that they may affect NMDA receptor function.

Concluding remarks

It is evident that toxicants interact with more than one vital molecular target, whether enzymes, receptors or ionic channels. It is usually difficult to establish which protein is the primary target of the toxic action and which are secondary ones. Several factors should be considered: 1. The effect on the target should account for the symptoms of poisoning. 2. The importance of the target molecule (e.g. acetylcholinesterase is more vital than butyrylcholinesterase). 3. The correlation
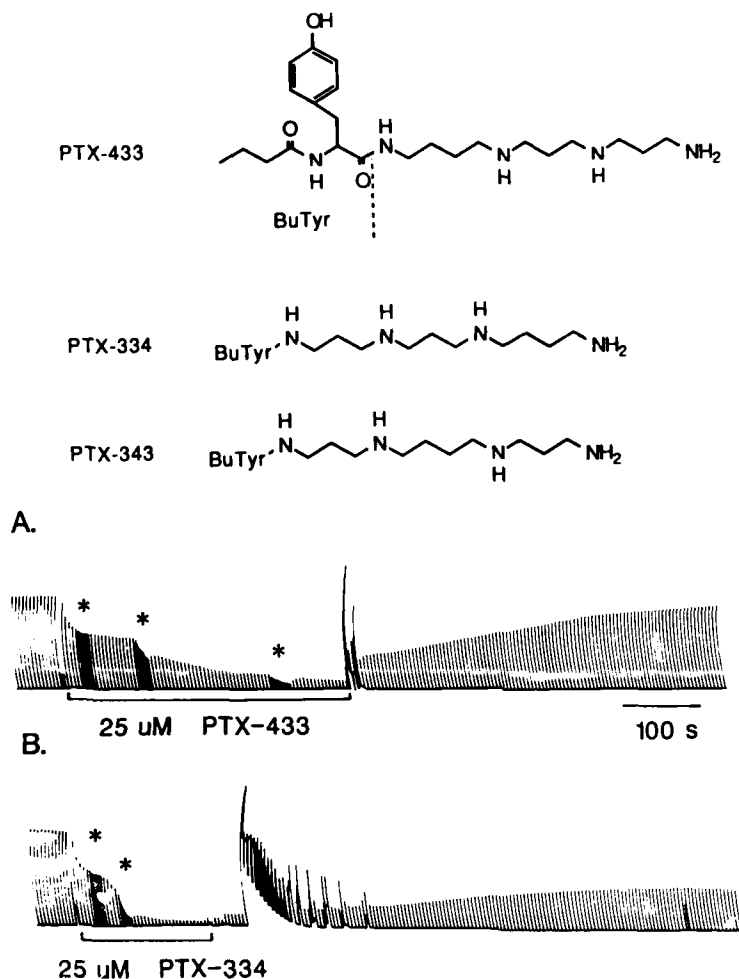
FIG 6   Philanthotoxins and their inhibition of insect leg neuromuscular transmission. The chemical structures of the natural philanthotoxin (PTX-433) and two synthesized isomers. The effects of PTX-433 (A) and PTX-433 (B) on the neurally-evoked twitch contraction of locust metathoracic retractor unguis muscle. (A) and (B) are data from different nerve-muscle preparations dissected from the same adult, female locust *Schistocerca gregaria* (from Ref. 42).

of potencies of series of chemicals with their toxicities, after corrections are made for penetration, bioactivation and/or metabolism and elimination. 4. The affinity that the target molecule has for the toxicant and the reversibility of the action (e.g. the irreversible inhibition of acetylcholinesterase by an OP vs its reversible inhibition of nicotinic receptor). 5. The percentage of the target protein molecules that needs to be inhibited to produce an effect (e.g. only 0.1% of Na^+ channels are required to be modified by a pyrethroid to produce repetitive discharges [43]). A toxicant may also act in vivo to produce excitation on more than one target, thereby producing physiological synergy.
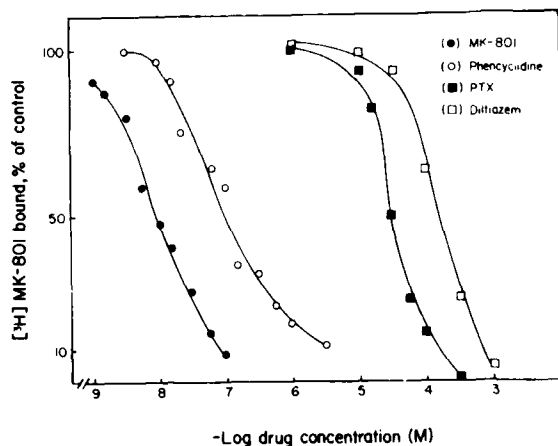
FIG 7 Inhibition of [^{3}H]MK-801 binding at 2 nM in presence of 10 μM glutamate to rat brain membranes by PTX-433, MK-801, phencyclidine and diltiazem. Each symbol is the mean of three experiments.

Glutamate Receptor   GABA Receptor
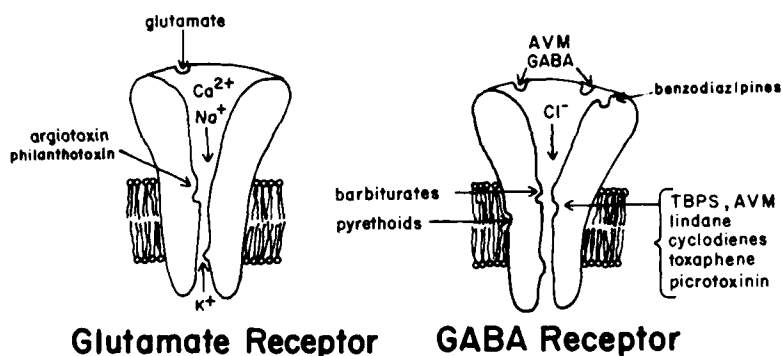
FIG 8 Diagram of the GABA$_A$ and glutamate receptors demonstrating the binding sites of drugs and toxicants.

Accordingly, it is suggested that GABA$_A$ and glutamate receptors are molecular targets for several types of insecticides and other toxicants (Fig. 8). The GABA$_A$ receptor is a primary target for cyclodienes and γ-BHC and possibly a secondary target for avermectin B$_{1a}$, tremorgenic mycotoxins, pyrethroids and a few OP anticholinesterases [44]. Glutamate receptors appear to be primary targets for *Philanthus* and spider toxins and possibly even certain carbamate insecticides.

Acknowledgements

References

1 Robinson, M.B. and Coyle, J.T. (1987) Glutamate and related acidic excitatory neurotransmitters: From basic science to clinical application. FASEB J. 1, 446–454.

2 Cotman, C.W. and Iversen, L.L. (1987) Excitatory amino acids in the brain: focus on NMDA receptors. TINS 10, 263–265.

3 Enna, S.J. (1983) The GABA Receptor. 341 pp. Humana Press Clifton, NJ.

4 Usherwood, P.N.R. (1981) Glutamate synapses and receptors on insect muscle. In: Glutamate as a Neurotransmitter (G. DiChiara, G.I. Gessa, eds.), pp. 183–193. Raven Press, New York.

5 Cull-Candy, S.G. (1980) Properties of postsynaptic channels activated by glutamate and GABA in locust muscle fibres. In: Neuropharmacology of insects, Ciba Found. Symp. 88, pp. 70–82. Pitman, London.

6 Watkins, J.C. and Evans, R.H. (1981) Excitatory amino acid transmitters. Ann. Rev. Pharmacol. 21, 165–204.

7 Usherwood, P.N.R. and Duce, I.R. (1985) Antagonism of glutamate receptor channel complexes by spider venom polypeptides. Neurotoxicology 5, 239–250.

8 Shudo, K., Endo, Y., Hashimoto, Y., Aramaki, Y., Nakijima, T. and Kawai, N. (1987) Newly synthesized analogues of the spider toxin block the crustacean glutamate receptor. Neurosci. Res. 5, 82–85.

9 Schofield, P.R., Darlinson, M.G., Fujita, N., Burt, D.R., Stephenson, F.A., Rodriguez, H., Rhee, L.M., Ramachandran, J., Reale, V., Glencourse, T., Seeburg, P.H. and Barnard, E.A. (1987) Sequence and functional expression of the $GABA_A$ receptor shows a ligand-gated receptor super-family. Nature (Lond.) 328, 221–227.

10 Karbon, E.W. and Enna, S.J. (1985) Characterization of the relationship between γ-aminobutyric acid B agonists and transmitter-coupled cyclic nucleotide-generating systems in rat brain. Mol. Pharmacol. 27, 53–59.

11 Eldefrawi, A.T. and Eldefrawi, M.E. (1987) Receptors for γ-aminobutyric acid and voltage-dependent chloride channels as targets for drugs and toxicants. FASEB J. 1, 262–271.

12 Abalis, I.M., Eldefrawi, M.E. and Eldefrawi, A.T. (1985) High affinity stereospecific binding of cyclodiene insecticides and γ-hexachlorocyclohexane to γ-aminobutyric acid receptors. Pest. Biochem. Physiol. 24, 95–102.

13 Lawrence, L.J. and Casida, J.E. (1984) Interactions of Lindane, Toxaphene and cyclodienes with brain-specific t-butylbicyclophosphorothionate receptor. Life Sci. 35, 171–178.

14 Gant, D., Eldefrawi, M.E. and Eldefrawi, A.T. (1987) Cyclodiene insecticides inhibit $GABA_A$ receptor-regulated chloride transport. Toxicol. Appl. Pharmacol. 88, 313–321.

15 Matsumoto, K., Eldefrawi, M.E. and Eldefrawi, A.T. (1985) Action of polychlorocycloalkane insecticides on a putative chloride channel and stereospecificity of the binding site. Tox. App. Pharmacol. (in press).

16 Narahashi T. (1985) Nerve membrane ionic channels as the primary target for pyrethroids. Neurotoxicology 6, 3–22.

17 Gray, A.T. (1985) Pyrethroids structure-toxicity relationships in mammals. Neurotoxicology 6, 127–138.

18 Gammon, D.W., Brown, M.A. and Casida, J.E. (1981) Two classes of pyrethroid action in the cockroaches. Pest. Biochem. Physiol. 15, 181–191.

19 Gammon, D.W., Lawrence, L.J. and Casida, J.E. (1982) Pyrethroid toxicologies: Protective effects of diazepam and phenobarbital in the mouse and the cockroach. Toxicol. Appl. Pharmacol. 66, 290–296.

20 Lawrence, L.J. and Casida, J.E. (1983) Stereospecific action of pyrethroids insectides on the γ-aminobutyric acid receptor-ionophore complex. Science 221, 1399–1401.

21 Sheets, L.P., Crofton, K.M. and Reiter, L.W. (1988) DDT and picrotoxin effects on the acoustic startle response (ASR) in preweanling rat resemble the effects of Type 1 and Type II pyrethroids. Soc. of Toxicology Abst. 8, 298.

22 Devaud, L.L., Szot, P. and Murray, T.F. (1986) PK11195 antagonism of pyrethroid-induced proconvulsant activity. Eur. J. Pharmacol. 120, 269–273.

23 Snyder, S.H., Verma, A. and Trifiletti, R.R. (1987) The peripheral-type benzodiazepine receptor: A protein of mitochondrial outer membranes utilizing porphyrins as endogenous ligands. FASEB J. 1, 282–288.

24 Sherby, S.M., Eldefrawi, A.T., Deshpande, S.S., Albuquerque, E.X. and Eldefrawi, M.E. (1986) Effects of pyrethroids on nicotinic acetylcholine receptor binding and function. Pestic. Biochem. Physiol. 26, 107–115.

25 Cole, R.J. (1981) In: Antinutrients and natural toxicants in Foods (R.L. Ory, ed.), pp. 17–33. Food and Nutrition Press, Wesport, CT.

26 Gant, D.B., Cole, R.J., Valdes, J.J., Eldefrawi, M.E. and Eldefrawi, A.T. (1987) Action of tremorgenic mycotoxins on GABA$_A$ receptors. Life Sci. 41, 2207–2214.

27 Bellet, E.M. and Casida, J.E. (1973) Bicyclic phophorus esters: High toxicity without cholinesterase inhibition. Science 182, 1135–1136.

28 Bowery, N.G., Collins, J.F. and Hill, R.G. (1976) Bicyclic phophorus esters that are potent convulsants and GABA antagonists. Nature (Lond.) 261, 601–603.

29 Squires, R.F., Casida, J.E., Richardson, M. and Saederup, E. (1983) [^{35}S]t-Butylbicyclophosphorothionate binds with high affinity to brain specific sites coupled to γ-aminobutyric acid -A and ion recognition sites. Mol. Pharmacol. 18, 315–318.

30 Lipp, J.A. (1973) Effect of benzodiazepine derivatives on soman-induced seizure activity and convulsions in the monkey. Arch. Int. Pharmacodyn. Ther. 202, 244–251.

31 Siram, S.P., Norris, J.L., Lim, D.K., Hoskins, B. and Ho, I.K. (1983) Effect of acute and chronic cholinesterase inhibition with diisopropylphosphate on muscarinic, dopamine and GABA receptors of the rat striatum. J. Neurochem. 40, 1414–1422.

32 Gant, D.B., Eldefrawi, M.E. and Eldefrawi, A.T. (1987) Action of organophosphates on GABA$_A$ receptor and voltage-dependent chloride channels. Fund. Appl. Toxicol. 9, 698–704.

33 Abou-Donia, M.B. (1981) Organophosphorus ester-induced delayed neurotoxicity Ann. Rev. Pharmacol. Toxicol. 21, 511–548.

34 Pong, S.S., Dehaven, R. and Wang, C.C. (1982) A comparative study of avermectin B$_{1a}$ and other modulators of the γ-aminobutyric acid receptor-chloride ion channel complex. J. Neurosci. 2, 966–971.

35 Abalis, I.M., Eldefrawi, A.T. and Eldefrawi, M.E. (1986) Actions of Avermectin B$_{1a}$ on the γ-aminobutyric acid$_A$ receptor and chloride channels in rat brain. J. Biochem. Toxicol. 1, 69–82.

36 Duce, I.R. and Scotto, RH. (1985) Actions of dihydroavermectin B$_{1a}$ on insect muscle. Br. J. Pharmacol. 19, 395–401.

37 Wong, E.H.F., Kemp, J.A., Priestley, T., Knight, A.R., Woodruff, G.N. and Iversen, L.L. (1983) The anticonvulsant MK-801 is a potent N-methyl-D-aspartate antagonist. Proc. Natl. Acad. Sci. U.S.A. 83, 7104–7108.

38 Hampson, D.R. and Wenthold, R.J. (1988) A kainic acid receptor from frog brain purified using domoic acid affinity chromatography. J. Biol. Chem. 263, 2500–2505.

39 Sherby, S.M., Eldefrawi, M.E. Wafford, K.A., Sattelle, D.B. and Eldefrawi, A.T. (1987) Pharmacology of putative glutamate receptors from insect skeletal muscles, insect central nervous system and rat brain. Comp. Biochem. Physiol. 87C, 99–106.

40 Rathmayer, W. (1962) Pralysis caused by the digger wasp Philanthus. Nature (Lond.) 196, 1148–1151.

41 Clark, R.B., Donaldson, P.L., Gration, K.A.F., Lambert, J.J., Piek, T., Ramsey, R., Spanjer, W. and Usherwood, P.N.R. (1982) Block of locust muscle glutamate receptors by δ-philanthotoxin occurs after receptor activation. Brain Res. 241, 105–114.

42 Eldefrawi, A.T., Eldefrawi, M.E., Konno, K., Mansour, N.A. Nakanishi, K., Oltz, E. and Usherwood, P.N.R. (1988) Identification and synthesis of a potent glutamate receptor antagonist in wasp venom. Proc. Natl. Acad. Sci. U.S.A. 85, 4910–4913.

43 Narahashi, T. (1985) Nerve membrane ionic channels as the primary target of pyrethroids. Neurotoxicology 6, 3–22.

44 Eldefrawi, A.T. and Eldefrawi, M.E. (1987) Receptors for γ-aminoLutyric and voltage-dependent chloride channels as targets foɪ drugs and toxicants. FASEB J. 1, 262–271.

45 Ramadan, A.A., Bakry, N.M., Marei, A, S.M., Eldefrawi, M.E. and Eldefrawi, A.T. (1988) Action of pyrethroids on $GABA_A$ receptor function. Pestic. Biochem. Physiol. in press.

46 Ramadan, A.A., Bakry, N.M., Marei, A.M., Aly, H.A., Eldefrawi, A.T. and Eldefrawi, M.E. (1988) Action of pyrethroids on the peripheral benzodiazepine receptor. Pestic. Biochem. Physiol. in press.

Second messenger systems

CHAPTER 16

Second messenger systems in insects: an introduction

PETER D. EVANS, LESLEY S. SWALES AND MATTHEW D. WHIM

AFRC Unit of Insect Neurophysiology and Pharmacology, Dept. of Zoology, University of Cambridge, Downing Street, Cambridge CB2 3EJ, U.K.

Second messenger systems are used to link the activation of membrane bound receptors by external stimuli, such as hormones, neurotransmitters and growth factors, to intracellular response mechanisms. Responses mediated by second messenger activation usually far outlast the period of receptor activation enabling a minimum amount of agonist to produce a long-lasting effect. In addition weak signals can be amplified many-fold by the use of a second messenger system, so that the system can be made very sensitive to small changes in the concentration of the agonist. Further, second messengers enable responses to be elicited in regions of a cell at a distance from the site of agonist receptor interactions. Since there are many steps in the second messenger mediated pathways between the binding of the agonist to a receptor and the actual response system, such systems are ideally suited to be modulated by other events, so that the responses may be amplified or inhibited depending perhaps on the arousal state of the insect.

In contrast to the diversity of signals used by cells for intercellular communication, the number of second messengers used for intracellular communication appears to be very small. Despite this the known messengers can control a large array of physiological and biochemical processes. Two major signalling pathways have been described in cells [1,2] and both can be seen to be present in insect cells. One pathway uses the cyclic nucleotide adenosine $3',5'$ cyclic monophosphate (cyclic AMP) as its second messenger whilst the second pathway uses a combination of second messengers including calcium ions, inositol trisphosphate (IP_3) and diacylglycerol (DG). The two latter compounds are derived by the enzymatic breakdown of a lipid precursor in the membrane. These two pathways have certain common features in their organization [1]. In both cases receptor activation by extracellular agonists leads to the activation of a specific class of guanosine triphosphate binding proteins (G proteins) [3] which transmit the information to an enzyme on the inner surface of the membrane. In the case of the cyclic AMP pathway the enzyme is adenylate cyclase that converts ATP into cyclic AMP and the enzyme is dually regulated by one G protein (G_s) that stimulates its activity and a second G protein (G_i) that inhibits its activity. In the case of the other pathway, the enzyme is phospholipase C or phosphoinositidase [2] which converts phosphatidylinositol 4,5-bisphosphate to inositol 1,4,5 trisphosphate (IP_3) and DG. Two

of the messengers produced then activate protein kinase enzymes that initiate the phosphorylation of specific proteins. Cyclic AMP activates a so-called A-kinase whilst DG, which stays in the membrane when produced, activates a so-called C-kinase. IP_3 on the other hand is released from the membrane into the cytoplasm where it acts on specific receptors on the endoplasmic reticulum to cause the release of Ca^{2+} from intracellular stores. In general the two main pathways outlined do not act in isolation but the cascade of products produced by their second messengers interact in a very complicated way, as do the products of the two limbs of the phosphoinositide cascade, to produce synergistic effects and to modulate the activities of the other pathways [2].

In insects a considerable amount of evidence exists for the receptor-activated increase in cyclic AMP levels by a wide range of agonists [4]. These include the biogenic amines, such as octopamine [5-7], dopamine [8-10] and serotonin [11] as well as a variety of peptides [12-14]. However, it should be noted that as in vertebrates not all receptors for a given agonist mediate their actions in this way. There are several examples in insects of multiple receptor subtypes for a given agonist that mediate their actions in different ways (see Ref. 4). Many studies on cyclic AMP mediated mechanisms in insects have just quantified the ability of the agonist to increase the levels of cyclic AMP in the tissue and shown that these effects can be potentiated in the presence of phosphodiesterase inhibitors. Several studies on the mode of action of octopamine have attempted to demonstrate that increasing cyclic AMP levels by mechanisms that bypass the receptor activation stage, such as application of phosphodiesterase inhibitors, the use of highly permeable phosphodiesterase resistant analogues of cyclic AMP and the direct activation of the catalytic subunit of adenylate cyclase by the diterpene compound forskolin, can all mimic receptor activation (e.g. Ref. 15). Direct evidence for the involvement of G proteins in the activation of insect adenylate cyclase is poor. It involves the fact that receptor activation of adenylate cyclase activity in tissue homogenates is GTP dependent [5,16] and that cholera toxin which is known to permanently activate G_s in many tissues by ADP-ribosylation can, after a delay, cause an elevation of cyclic AMP levels and a brilliant persistent glow of the firefly light organ [17]. Although adenylate cyclase appears to be dually regulated in many systems, no evidence for an action of an inhibitory G protein exists in insects. Studies on the properties of insect A-kinase are at present very limited [18-22].

Evidence for the existence of the second major pathway involving phosphatidylinositol metabolism in insect cells is, of course, very high since much of the pioneering work of Berridge and colleagues on this pathway has been conducted on the blowfly salivary gland where one class of serotonin receptor mediates its action by the activation of phosphoinositidase [2]. More recently evidence has been presented for the activation of this enzyme by muscarinic acetylcholine receptors in the locust nervous system [23] and by receptors for cardioacceleratory peptides in the heart of the tobacco hawkmoth, *Manduca sexta* [24].

In insects information concerning C-kinase activation by DG [25] produced by the second limb of the bifurcating phosphoinositidase activation pathway is very poor at present. However, recent evidence shows that the tumour-producing phorbol esters, which mimic the effects of endogenous DG to activate C-kinase, have specific high-affinity binding sites in locust nervous tissue [26]. In addition this binding is reduced by the C-kinase inhibitor polymyxin B. Further, micromolar concentrations of the phorbol esters activated C-kinase activity in subcellular preparations from

locust ganglia and also enhanced the high-affinity transport of choline and the release of acetylcholine by locust synaptosomes [26].

In many systems the activation of the enzyme guanylate cyclase that produces cyclic monophosphate (cyclic GMP) from guanosine triphosphate (GTP) appears to be linked to the agonist activation of the inositol-lipid pathway [2]. The resulting increased levels of cyclic GMP are thought to activate a G-kinase which phosphorylates proteins of as yet unknown function. At present evidence for such a pathway in insect cells is lacking. However, a direct receptor-mediated activation of guanylate cyclase activity has been demonstrated for eclosion hormone actions on the nervous system [27] and muscle targets [28] in moths.

Much interest has recently been aroused in the receptor-mediated activation of a second lipid metabolizing enzyme in cell membranes, called phospholipase A_2, which directly generates arachidonic acid and its numerous biologically active metabolites, such as the prostaglandins, the thromboxanes and the leukotrienes [29]. In the marine mollusc *Aplysia*, arachidonic acid metabolites have been suggested to act at second messengers for the action of the neuropeptide FMRFamide on sensory neurones [30]. At present no information is available on the role of this pathway in insect cells.

The regulation of cell growth by growth factors also appears to be mediated by second messenger systems [2]. The membrane bound receptors for insulin and epidermal growth factor (EGF) are transmembrane proteins that exhibit tyrosine kinase activity in their cytoplasmic domains. Recent work has shown that *Drosophila melanogaster* possesses a homologue of the mammalian insulin receptor, the *Drosophila* insulin receptor homologue (DIRH), which reacts with insulin but not with the related insulin-like growth factor, EGF or the insulin-like prothoracicotropic hormone purified from the silkworm [31]. The DIRH contains an α subunit that binds insulin and a β subunit that is phosphorylated on tyrosine in response to insulin in intact cells. In addition the *Drosophila* genome has been shown, by the use of vertebrate oncogenes as hybridization probes, to contain eleven different proto-oncogene homologues (see Ref. 32). Oncogenes are genes whose inappropriate function is linked to the incidence of cancer and their normal cellular counterparts are known as proto-oncogenes. Seven of the proto-oncogene homologues from *Drosophila* belong to the *src* oncogene family that all share the sequence coding for a tyrosine kinase domain. One of these, DER, is the *Drosophila* equivalent of C-*erb* B, the receptor for EGF. The complete nucleotide sequence of DER is known and it consists of a long extracellular sequence, a single transmembrane domain and a cytoplasmic region containing the tyrosine kinase sequence. The *Drosophila* genome also contains three homologues of the *ras* oncogene family which may code for a family of G proteins. It is very likely that the proto-oncogenes identified in *Drosophila* and expressed at different stages of embryogenesis will be shown to be involved in the control of cell growth and perhaps also differentiation in insect cells [32].

Recent information suggests that the functional significance of changes in the levels of second messengers in insect tissues must be considered in relation to a wide range of other factors including, compartmentation of the response within a tissue, age of the tissue, availability of substrate and physiological concentration range of the agonist.

In the extensor-tibiae muscle of the hindleg of the locust neurally evoked contractions are modulated by octopamine in a cyclic AMP dependent manner
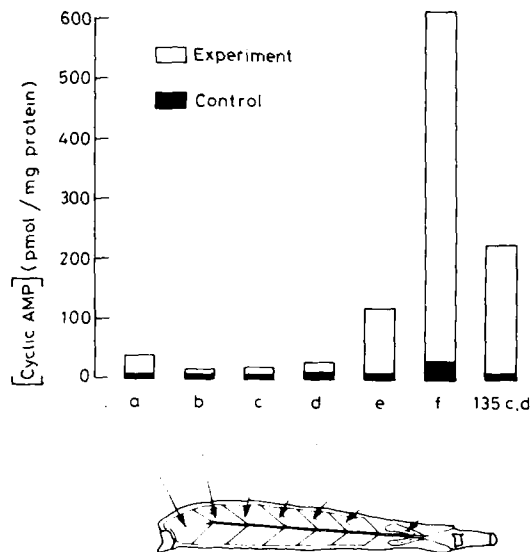
FIG 1 The effect of a 10 min exposure to 10^{-5} M DL-octopamine on cyclic AMP levels in different regions of the extensor-tibiae muscle of the locust hind leg. The results are expressed as pmol cyclic AMP mg^{-1} protein for each of the blocks of muscle fibres from a single muscle. Open bars show the levels in the experimental muscle and filled bars the levels in the contralateral control muscle. Both experimental and control muscles were preincubated for 10 min in 10^{-4} M isobutylmethylxanthine (IBMX). The experimental muscle was then incubated in octopamine plus IBMX for 10 min and the control for a further 10 min in IBMX. The diagram indicates the location of the blocks of muscle assayed (from Ref. 33).

[7,15]. However, the octopamine mediated increases in cyclic AMP levels differ in different parts of the muscle (see Fig. 1), the largest responses occurring in the distal part of the muscle which contains the highest proportion of slow and intermediate muscle fibre types [33]. This muscle also exhibits another example of compartmentation of cyclic AMP responses. The neuropeptide proctolin appears to produce its actions on the pacemaker muscle fibres generating a myogenic rhythm in one region of this muscle by a mechanism that involves an elevation of cyclic AMP levels [34]. These changes could not be detected biochemically but recently we have been able to show histochemically that proctolin induces a reaction product, indicating the presence of adenylate cyclase activity, in a limited number (3–6 per preparation) of exclusively slow muscle fibres in the medial region of the so-called fan region of this muscle. These are assumed to be the pacemaker fibres for the myogenic rhythm [35]. Neurally evoked contractions are also modulated by octopamine in another locust muscle, namely the dorsal longitudinal flight muscle [36], through a cyclic AMP dependent process (Whim and Evans, in preparation). However the octopamine mediated increases in cyclic AMP in the five motor units of this muscle vary differently with the age of the animal despite all being composed of exclusively fast muscle fibres. Fig. 2 shows their responses to a 10-min exposure to a pulse of 10⁻⁵ M DL-octopamine at different ages. One day after hatching all the motor units generate large increases in cyclic AMP levels in response to exposure to octopamine, but seven days after hatching the response has declined markedly in the more distal
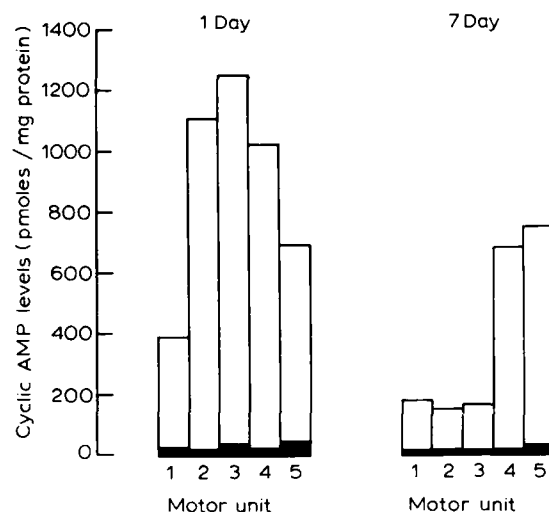
FIG 2   The effects of a 10 min exposure to 10^{-5} M DL-octopamine on cyclic AMP levels in the different motor units of the dorsal longitudinal muscle of the locust from an adult one day after moulting and 7 days after moulting. Experimental details are as in Fig. 1 (Whim and Evans, unpublished).

motor units (units 1, 2 and 3) whilst it is maintained in the more proximal units (units 4 and 5). The reason and physiological significance of this sequential decline in the effectiveness of octopamine in increasing cyclic AMP levels is not known but we speculate that it may be correlated with a change in the innervation pattern of the octopaminergic neurone to this muscle. It is unlikely to be related to differential changes in the protein content of the motor units since the absolute amount of cyclic AMP generated by each motor unit also changes in a similar pattern. The decline in the amounts of cyclic AMP generated by octopamine in this muscle within the first few days of adult life in the locust is accompanied by a decrease in the degree of the potentiation of neurally evoked tension in the muscle by octopamine. However, it is unlikely that the reduced levels of cyclic AMP generated by a given pulse of octopamine can completely explain the decline in the physiological response since the response of the muscle to cyclic AMP analogues, such as dibutyryl cyclic AMP, also declines at this time (Whim and Evans, in preparation). This suggests that changes are also occurring at some point beyond the level of the generation of cyclic AMP in the response cascade to the activation of the octopamine receptors.

Another example of an age-dependent receptor-mediated increase in a second messenger occurs in the nervous system of the moth, Manduca sexta. Here the increases in the cyclic GMP levels mediated by eclosion hormone depend critically on the age of the animal. The nerve cord becomes sensitive to eclosion hormone application, in behaviourial terms, for a very restricted period at the end of each moult cycle [27]. However, the ability of eclosion hormone to increase cyclic GMP levels precedes this behaviourial sensitivity by at least 9 hours in the pupal ecdysis. This suggests that an eclosion hormone-mediated increase in cyclic GMP levels is necessary, but not alone suffficient to produce a behaviourial response. Recent work

suggests that in this system it is the availability of a substrate phosphoprotein that regulates the sensitivity of the nervous system to eclosion hormone at the larval and pupal ecdysis but that at adult ecdysis other factors may also be involved in the regulation of sensitivity [37,38].

When assessing the significance of agonist-mediated changes in second messenger levels it is important to compare their dose-responsiveness with that of the observed physiological effects. When this is done for the changes in cyclic AMP levels induced by octopamine in the extensor-tibiae muscle of the locust, the physiologically observed modulatory effects appear to correlated well with the high-affinity component of the biphasic curve for the octopamine-induced increase in cyclic AMP levels in this muscle [7,39]. Both effects show thresholds in the range of 10^{-9} to 10^{-8} M and saturate between 10^{-6} and 5×10^{-6} M. This probably explains why a range of agonists such as clonidine, the formamidines and the phenylimidazolidine derivatives, which all show full physiological agonist activity, only produce relatively low increases in cyclic AMP levels in this muscle [39]. The lower affinity portion of the curve, between 10^{-5} and 10^{-3} M, for octopamine-mediated increases in cyclic AMP levels in this muscle does not correspond to any currently known physiological or biochemical process in the muscle.

To further understand the significance of the biphasic response curve for octopamine-mediated increases in cyclic AMP levels in the locust extensor-tibiae muscle we have used a histochemical technique [35,40,41] to localize the sites of adenylate cyclase activity in the muscle at a range of DL-octopamine concentrations from 10^{-8} M to 10^{-3} M. When intermediate type muscle fibres from the fan region of the muscle were incubated in low concentrations of DL-octopamine (10^{-8} to 10^{-7} M) adenylate cyclase reaction product is found preferentially in the sarcoplasmic reticulum component of the dyads (see Fig. 3A). Smaller amounts of reaction product occur in the sarcoplasmic reticulum, in the T-tubule and in association with the sarcolemmal membrane. At higher concentrations of DL-octopamine (between 10^{-5} M and 10^{-3} M) increasing amounts of dense reaction product are found associated with the T-tubule component of the dyads in the intermediate fibres (see Fig. 3B). Increased intensities of reaction product are also found in the sarcoplasmic reticulum and in association with the sarcolemma. The significance of this change in the distribution of the adenylate cyclase reaction product with increasing concentrations of octopamine is unclear. The technique is reported to localize the site of adenylate cyclase activity by precipitating the pyrophosphate released in the enzymatic reaction as insoluble lead phosphate close to its site of generation [40,41]. If this can also be taken to indicate the site of generation of cyclic AMP in the tissue, then it is easy to understand why reaction product accumulates beneath the sarcolemmal membrane. It also appears that the appearance of the intense reaction product in the T-tubules of the dyads corresponds with the low affinity component of the biphasic curve for octopamine-mediated cyclic AMP increases in this muscle. The physiological significance of this is not clear at present. However, it is hard to understand why at low octopamine concentrations the first appearance of reaction product occurs in the sarcoplasmic component of the dyads, a cellular compartment with no direct access to the octopamine in the extracellular fluid. Thus one is forced to speculate that either this is some artefact of pyrophosphate accumulation, or perhaps more interestingly, that octopamine receptors on the extracellular surface of the T-tubules, which have access to octopamine in the bathing medium, when stimulated can in some way initiate the activation of adenylate cyclase in the
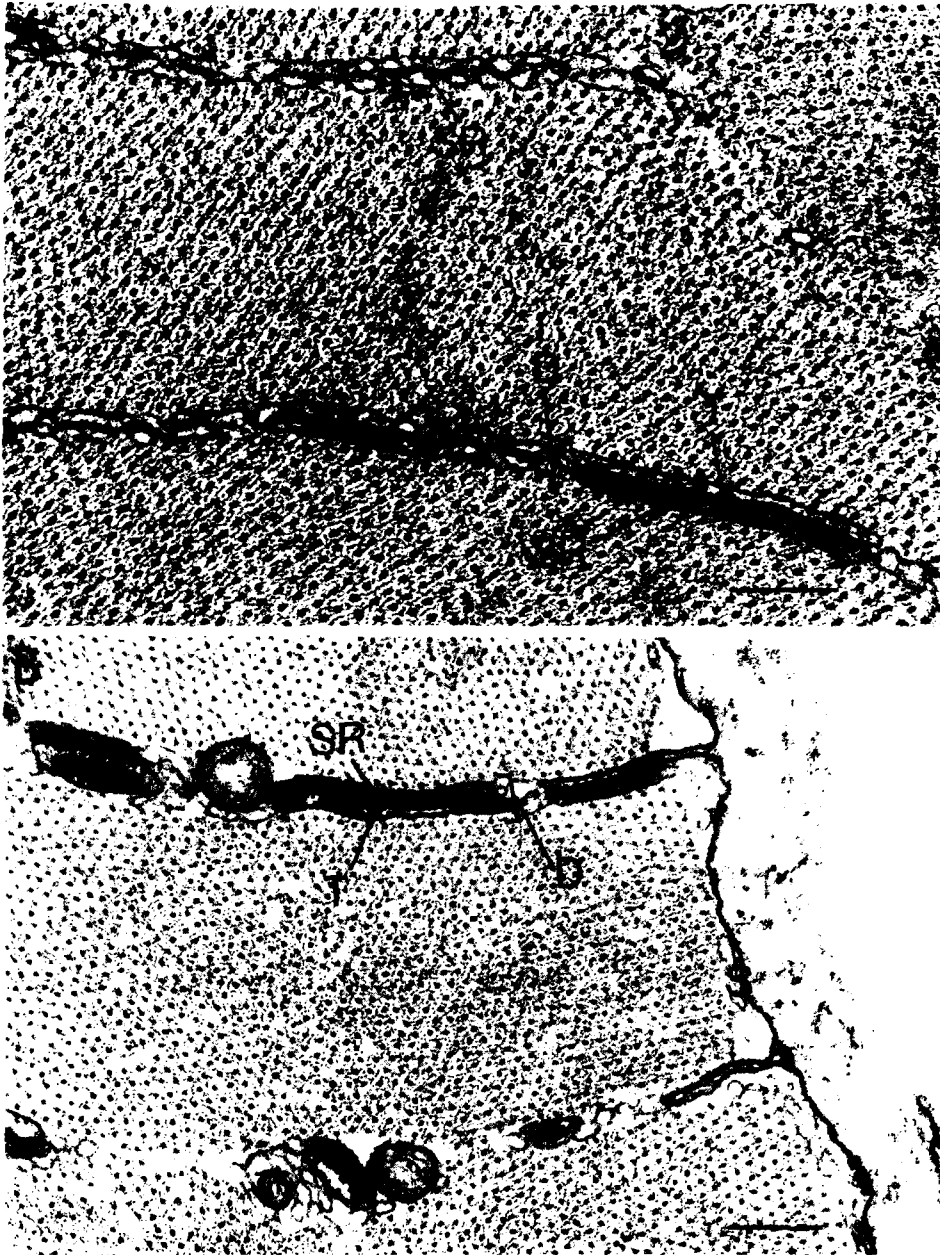
FIG 3 Histochemical localization of adenylate cyclase activity in intermediate muscle fibres from extensor-tibiae muscle of locust hindleg incubated for 60 min in DL-octopamine at different concentrations (see Refs. 41, 42 for methods). A: muscle incubated in presence of 10^{-7} M DL-octopamine shows most reaction product in sarcoplasmic reticulum (SR) component of dyads (D) and smaller amounts in the T-tubules (T) and in the non-dyad sarcoplasmic reticulum. B: muscle incubated in the presence of 10^{-3} M DL-octopamine shows intense reaction product in the T-tubule component of the dyad and heavy association with the sarcolemmal membrane (S). Scale bars = 0.25 μm (Swales and Evans, unpublished).
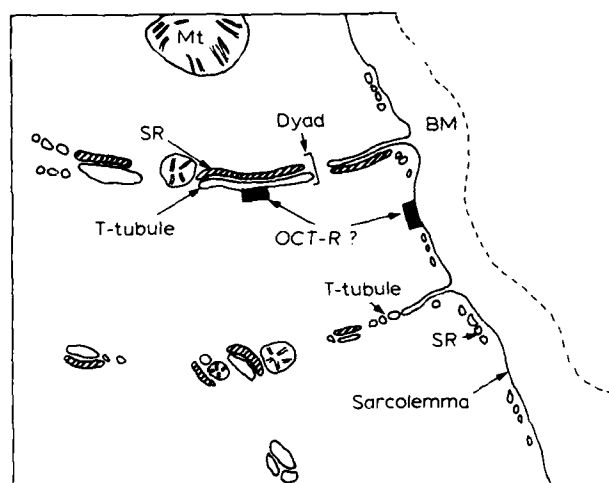
FIG 4 Diagram to show possible locations of octopamine receptors (OCT-R) responsible for the induction of adenylate cyclase histochemical reaction product in an intermediate muscle fibre from the extensor-tibiae muscle of the locust hindleg. The receptors on the sarcolemma have access to octopamine in the bathing medium and can account for the reaction product associated with the sarcolemma. The receptors on the T-tubules presumably account for the association of reaction product with the T-tubule membrane and its spill over into the T-tubules at higher octopamine concentrations. It seems likely that they may also in some way be responsible for the appearance of reaction product in the sarcoplasmic reticular component of the dyads at low octopamine concentrations. The text discusses possible mechanisms for this interaction.

sarcoplasmic reticulum component of the dyad (Fig. 4). There is much interest at present in the ideas that either IP_3 released from the T-tubules upon depolarization may act as a second messenger to stimulate the release of calcium from the stores in the sacroplasmic reticulum to initiate contraction in vertebrate skeletal muscle [42], or that mechanical cross-bridges between the T-tubules and the sarcoplasmic reticulum in the triads may mediate the same effect (see Ref. 43). Thus it is possible the octopamine-mediated activation of adenylate cyclase activity in the sarcoplasmic reticulum of insect muscle dyads may also be activated by parallel second messenger systems and/or parallel mechanical interactions.

References

1 Berridge, M.J. (1985) The molecular basis of communication within the cell. Scientific American 253, 124–134.
2 Berridge, M.J. (1987) Inositol trisphosphate and diacylglycerol: two interacting second messengers. Ann. Rev. Biochem. 56, 159–193.
3 Gilman, A.G. (1987) G proteins: transducers of receptor-generated signals. Ann. Rev. Biochem. 56, 615–649.
4 Evans, P.D. (1985) Biogenic amines and second messenger systems in insects. In: Approaches to New Leads for Insecticides (H.C. von Keyserlingk, A. Jäger, Ch. von Szczepanski, eds.), pp. 117–131. Springer-Verlag, Berlin.

5 Harmar, A.J. and Horn, A.S. (1977) Octopamine-sensitive adenylate cyclase in cockroach brain: Effects of agonists, antagonists and guanylyl nucleotides. Molec. Pharmacol. 13, 512–520.

6 Nathanson, J.A. (1979) Octapamine receptors, adenosine 3', 5'-monophosphate. and neural control of firefly flashing. Science 203, 65–68.

7 Evans, P.D. (1984) A modulatory octopaminergic neurone increases cyclic nucleotide levels in locust skeletal muscle. J. Physiol. (Lond.) 348, 307–324.

8 Bodnaryk, R.P. (1979) Basal, dopamine- and octopamine-stimulated adenylate cyclase activity in the brain of the moth, *Mamestra configurata*, during its metamorphosis. J. Neurochem. 33, 275–282.

9 Lafon-Cazal, M. and Bockaert, J. (1984) Pharmacological characterization of dopamine-sensitive adenylate cyclase in the salivary glands of *Locusta migratoria* L. Insect Biochem. 5, 541–545.

10 Hiripi, L. and Rozsa, K.S. (1984) Octopamine-and dopamine-sensitive adenylate cyclase in the brain of *Locusta migratoria* during its development. Cell Molec. Neurobiol. 4, 199–206.

11 Nathanson, J.A. and Greengard, P. (1974) Serotonin-sensitive adenylate cylase in neural tissue and its similarity to the serotonin receptor: a possible site of action of lysergic acid diethylamide. Proc. Natl. Acad. Sci. U.S.A. 71, 797–801.

12 Bodnaryk, R.P. (1983) Cyclic nucleotides. In: Endocrinology of Insects (R.G.H. Downer, H. Laufer, eds.), pp. 567–614. Alan R. Liss, New York.

13 Morgan, P.J. and Mordue, W. (1985) Cyclic AMP and locust diuretic action. Hormone induced changes in cAMP levels offers a novel method for detecting biological activity of uncharacterized peptide. Insect Biochem 15, 247–257.

14 Herault, J.-P., E and Proux, J.P. (1987) Cyclic AMP: the second messenger of an antidiuretic hormone from the glandular lobes of the migratory locust corpora cardiaca. J. Insect Physiol. 33, 487–491.

15 Evans, P.D. (1984) The role of cyclic nucleotides and calcium in the mediation of the modulatory effects of octopamine on locust skeletal muscle. J. Physiol. (Lond.) 348, 325–340.

16 Kilpatrick, A.T., Vaughan, P.F.T. and Donnellan, J.F. (1988) The effect of guanylnucleotides on the monoamine-sensitive adenylate cyclase of *Schistocerca gregaria* nervous tissue. Insect Biochem. 12, 393–397.

17 Nathanson, J.A. (1985) Choleratoxin, cyclic AMP, and the firefly flash. J. Cyclic Nucleotide Protein Phosphoryl. Res. 10, 157–166.

18 Kelly, L.E. (1981) The regulation of protein phosphorylation in synaptosomal fractions from *Drosophila* heads: the role of cyclic adenosine monophosphate and calcium/calmodulin. Comp. Biochem. Physiol. 69B, 61–67.

19 Hesse, J. and Marmé, D. (1985) A cAMP-binding phosphoprotein in *Drosophila* heads is very similar to the regulatory subunit of the mammalian type II cAMP-dependent protein kinase. Insect Biochem. 15, 835–844.

20 Combest, W.L. and Gilbert, L.I. (1986) Characterization of cyclic AMP-dependent protein kinase activity in the larval brain of *Manduca sexta*. Insect Biochem. 16, 597–605.

21 Combest, W. and Gilbert, L.I. (1986) Phosphorylation of endogenous substrates by the protein kinases of the larval brain of *Manduca sexta*. Insect Biochem. 16, 607–616.

22 Haro, A., Garcia, J.L., Olmo, N. and Municio, A.M. (1987) A natural non-protein low molecular weight cAMP-dependent protein kinase inhibitor from the incest *Ceratitis capitata*. Isolation and preliminary characterization. Insect Biochem. 17, 329–333.

23 Duggan, M.J. and Lunt, G.G. (1986) Second messengers linked to the muscarinic acetylcholine receptor in locust (*Schistocerca gregaria*) ganglia. In: Insect Neurochemistry and Neurophysiology (A.B. Borkovec, D.B. Gelman, eds.), pp. 251–254. Humana Press, Clifton, NJ.

24 Tublitz, N.J. and Trombley, P.Q. (1987) Peptide action on insect cardiac muscle is mediated by inositol trisphosphate (IP_3). Soc. Neurosci. Abstr. 13, 235.

234

25 Nishizuka, Y. (1986) Studies and perspectives of protein kinase C. Science 233, 305–312.

26 Knipper, M. and Breer, H. (1987) Protein kinase C in the nervous system of insects: effects of phorbol esters on cholinergic synapses. Neurochem. Int. 3, 323–328.

27 Morton, D.B. and Truman, J.W. (1985) Steroid regulation of the peptide-mediated increase in cyclic GMP in the nervous system of the hawkmoth, *Manduca sexta*. J. Comp. Physiol. 157, 423–432.

28 Schwartz, L.M. and Truman, J.W. (1984) Cyclic GMP may serve as a second messenger in peptide-induced muscle degeneration in an insect. Proc. Natl. Acad. Sci. U.S.A. 81, 6718–6722.

29 Axelrod, J., Burch, R.M. and Jelsema, C.L. (1988) Receptor-mediated activation of phospholipase A2 via GTP-binding proteins: arachidonic acid and its metabolites as second messengers. Trends Neurosci. 3, 117–123.

30 Piomelli D., Volterra A., Dale N., Siegelbaum S.A., Kandel E.R., Schwartz J.H. and Belmardetti, F. (1987) Lipoxygenase metabolites of arachidonic acid as second messengers for presynaptic inhibition of *Aplysia* sensory cells. Nature (Lond.) 328, 38–43.

31 Fernandez-Almonacid, R. and Rosen, O.M. (1987) Structure and ligand specificity of the *Drosophila melanogaster* insulin receptor. Mol. Cell Biol. 7, 2718–2727.

32 Shilo, B-Z. (1987) Proto-oncogenes in *Drosophila melanogaster*. Trends Genet. 3, 69–72.

33 Evans, P.D. (1985) Regional differences in responsiveness to octopamine within a locust skeletal muscle. J. Physiol (Lond.) 366, 331–341.

34 Evans, P.D. (1984) Studies on the mode of action of octopamine, 5-hydroxytryptamine and proctolin on a myogenic rhythm in the locust. J. Exp. Biol. 110, 231–251.

35 Swales, L.S. and Evans, P.D. (1988) Histochemical localization of octopamine- and proctolin-sensitive adenylate cyclase activity in a locust skeletal muscle. Histochemistry in press.

36 Whim, M.D. and Evans, P.D. (1988) Octopaminergic modulation of flight muscle in the locust. J. Exp. Biol. 134, 247–266.

37 Morton, D.B. and Truman, J.W. (1986) Substrate phosphoprotein availability regulates eclosion hormone sensitivity in an insect CNS. Nature 323, 264–267.

38 Morton, D.B. and Truman, J.W. (1988) The EGPs — the eclosion hormone and cyclic GMP regulated phosphoproteins. 1. Appearance and partial characterization in the CNS of Manduca sexta. J. Neurosci. 8, 1326–1337.

39 Evans, P.D. (1987) Phenyliminoimidazolidine derivatives activate both OCTOPAMINE1 and OCTOPAMINE2 receptor subtypes in locust skeletal muscle. J. Exp. Biol. 129, 239–250.

40 Howell, S.L. and Whitfield, M. (1977) Cytochemical localization of adenylate cyclase activity in rate islets of Langerhans. Histochem. Cytochem. 20, 873–879.

41 Cutler, L.S. (1983) Cytochemical methods for the localization of adenylate cyclase. A review and evaluation of the efficacy of the procedures. J. Histochem. Cytochem. 31, 85–93.

42 Vergara, J. and Asotra, K. (1987) The chemical transmission mechanism of excitation-contraction coupling in skeletal muscle. News Physiol. Sci. 2, 182–186.

43 Agnew, W.S. (1987) Dual roles for DHP receptors in excitation-contraction coupling? Nature 328, 297–298.

CHAPTER 17

Effects of pyrethroids on neural protein kinases and phosphatases of the squid optic lobe

FUMIO MATSUMURA [1] AND J. MARSHALL CLARK [2]

[1] Department of Environmental Toxicology and Toxic Substances Program, University of California, Davis, CA 95616, U.S.A. and [2] Department of Entomology, University of Massachusetts, Amherst, MA 01003, U.S.A.

Introduction

Pyrethroids are powerful insecticides [1] affecting normal functions of neurons [2]. Electrophysiological evidence indicates that they affect the gating kinetics of fast sodium channels in the nerve membrane [2,3]. However, there is evidence that some pyrethroids affect other ion channels [4–6]. Furthermore, from the total organism point of view pyrethroids cause such a variety of symptoms that it is difficult to ascribe all of them to a single cause [4,7–9]. Despite such complexity, to understand the underlying biochemical mechanisms of action one must start with a distinct physiological effect which occurs at low pyrethroid concentrations and at an early stage of poisoning. For this purpose, we have chosen the phenomenon of type II pyrethroid-induced enhancement of neurotransmitter release as the study subject. Earlier studies have shown that such a phenomenon is observable at very low concentrations of type II pyrethroids (e.g. 10^{-10} M) in synaptosomes from both rat brain [10] and squid optic lobes [11,12] involving both biogenic amines and cholinergic systems. The main characteristics of such a biochemial lesion are that first, tetrodotoxin at micromolar concentrations antagonizes only a part of such an effect; second, it requires an initial depolarizing treatment (e.g. veratridine) to express the pyrethroid effects (i.e. 'use dependent' effects); and third, it appears to represent at least in part, a fundamental alteration in the intrasynaptic process of neutrotransmitter release mechanisms, since similar effects of type II pyrethroids are observable even when the external Ca^{2+} is replaced by Ba^{2+}, and the transmitter release process is triggered by pentylenetetrazole (PTZ) to release Ca^{2+} from the internal storage sites (Brooks and Clark, unpublished data). Also, the same phenomenon is observed when A23187, a Ca^{2+} ionophore, is used as a depolarizing agent (Matsumura, unpublished data).

Meanwhile there has been recent progress in understanding the biochemical mechanisms of neurotransmitter releasing process, particularly along the line of depolarization-coupled phosphorylation activities involving intrasynaptosomal proteins [13–15]. In this project, we have examined synaptosomes from squid optic

lobes as an invertebrate model for this specific mode of action of type II pyrethroids. We found that they have a strong effect on protein phosphorylation, and we now report the results.

Materials and methods

All squid (*Loligo pealei*) used in this work were caught in June through August 1987 in Woods Hole, Massachusetts and kept alive until use (except those for Fig. 3 experiments which were from the 1985 season). The optic lobes were dissected out, washed briefly in isotonic, standard artificial seawater [11] and transferred to 1 M sucrose. The method to prepare synaptosomes was identical to the one used previously [11] following the original method of Pollard and Pappas [16]. Usually five squid were used per experiment (about 2 g wet weight of optic lobes). For initial homogenization a glass-glass homogenizer was used by applying 4 even strokes manually. After the initial centrifugation at 10,000 rpm at 4°C (12,100 × g Sorvall RCB with SS34 rotor) for 60 min, the floating synaptosomes were collected by aspiration, diluted 10-fold with standard artificial seawater and centrifuged at 15,000 × g at 4°C for 15 min. The pellet was resuspended in ice-cold artificial seawater (5 mg protein/ml approximately). In all cases fresh synaptosomes were kept at 0°C without freezing and used immediately, usually within five hours.

Phosphorylation of proteins in intact synaptosomes

The method used to phosphorylate synaptosomal proteins was essentially that o Dunkley et al. [15]. To an aliquot (usually 750 μl) of the above synaptosomal suspension in artificial seawater [^{32}P]phosphoric acid (New England Nuclear, Boston) in the same medium (usually 20 to 60 μl) was added so that the final level of radioactivity was 0.2 mCi/ml. The system was incubated for 30 min at 23°C. The labelled synaptosomes were chilled to 0°C, and 30 μl aliquots were transferred to small glass assay tubes. Deltamethrin (or any other solvent-soluble agents) was added with 0.5 μl ethanol to each tube, and the system incubated for 10 min at 23°C prior to the addition of the depolarizing agents. Control tubes received 0.5 μl ethanol only, but otherwise were treated similarly. The deltamethrin used was the active isomer (IR, *cis*).

Depolarization treatments of intact phosphorylated synaptosomes

To each tube containing the above ^{32}P-phosphorylated synaptosomal suspension a 30 μl aliquot of high K$^+$ artificial seawater [11] containing (mM): KCl 405, NaCl 0, CaCl$_2$ 0, MgCl$_2$ 45, glucose 9, sucrose 100 and Hepes 25 was added (final K$^+$ concentration = 207 mM) and incubated at 23°C for 0, 15, 30, 60 and 300 s. The reaction was stopped with 25 μl of 4 × SDS 'stopping solution' (0.25 M Tris-HCl pH 6.8, 8% sodium dodecylsulfate, 40% glycerol and 10% 2-mercaptoethanol) and immediately boiled for 2 min. Whenever veratridine was used as a depolarization agent, it was added with 0.5 μl of ethanol to each tube containing 30 μl of synaptosomal suspension to make the final concentration of 200 μM. Both pentylenetetrazole (PTZ) and 8-bromo-cAMP were added with 1.5 μl of distilled water to make 20 and 1 mM final concentrations, respectively. After incubation at 23°C, the reaction was stopped using 4 × SDS 'stopping solution' and boiled as before. In the cases where veratridine or PTZ was used as a depolarizing agent, high K$^+$ artificial

seawater (usually 30 μl) was added to each tube after boiling to adjust the total volume and concentration of SDS etc. equal to the high K^+ tubes.

Phosphorylation of membrane proteins from lysed synaptosomes

Phosphorylation of lysed synaptic proteins were carried out by using Schulman and Greengard's [18] method modified as follows: the synaptosomal preparation was subjected to osmotic shock by homogenizing synaptosomes after addition of 10 volumes of ice-cold distilled water. After 30 min at 0°C the suspension was centrifuged at 150,000 × g for 30 min. The precipitate was washed once in 15 ml of 5 mM Tris-HCl buffer at pH 7.0, and centrifuged. The final pellet was resuspended in the same buffer and stored at −20°C until use for up to 1 month. For phosphorylation assays, 0.1 ml of the above membrane preparation containing 1 mg/ml of protein was transferred to a test tube containing 0.4 ml of either basal or calcium-calmodulin kinase buffer. Their ion compositions were: 50 mM Tris-HCl, 5 mM $MgCl_2$, 0 mM $CaCl_2$ and 0.2 mM EGTA for the former and the same with 0.5 mM $CaCl_2$ and 100 units (1.1. μg) of bovine brain calmodulin (purchased from Boeringer Mannheim Co.) for the latter. In treated samples deltamethrin was added with 0.5 μl of ethanol (control received only ethanol) and the system was preincubated for 10 min. To initiate the reaction 1.5 pmol of $[\gamma^{-32}P]ATP$ (Amersham, starting specific activity of > 3000 Ci/mmol) was added to the tube at 24°C. After 30 s the reaction was stopped with 1 ml of 10% trichloroacetic acid. The methods for co-precipitation with 1 mg of bovine serum albumin, washing and measurement employed for ^{32}P-phosphoproteins were identical to those used by Doherty and Matsumura [19].

Electrophoresis, autoradiography and phosphoprotein analysis

SDS-polyacrylamide gel electrophoresis (SDS-PAGE) was developed according to the method of Laemmli [17]. Mini- and full-scale Protean II electrophoresis apparatus (Bio-Rad Lab., Richmond, CA) with 7 or 10% gels and 1.5 mm spacers were used. Other conditions used were identical to the ones supplied by the manufacturer. After staining and destaining with Coomassie blue R-250, the gels were sandwiched between two thin cellulose sheets, dried using a vacuum drier (Hoefer Scientific), and autoradiograms developed using X-ray films (Kodak X-OMAT AR) with an intensifying screen (Cronex Xtra Life, DuPont).

Effects of deltamethrin on purified cAMP-dependent protein kinase

Bovine heart cAMP-dependent protein kinase (PKA) was obtained from Sigma Chemical Co. (St. Louis, MO) in a form of lyophilized powder of the holoenzyme. The enzyme was dissolved in distilled water. To a glass test tube 87 μl of Tris-HCl 30 mM (pH = 7.4), 1 μl of 1 M $MgCl_2$ (final conc. 10 mM), 5 μl of PKA (2.5 μg protein) and 1 μl of 10^{-2} M disodium cAMP in distilled water (final conc. 10^{-4} M) were added and the system equilibrated at 23°C. To each tube deltamethrin (1 μl of ethanol) was added and the system was further incubated for 10 min at 23°C. After the addition of histone (200 μg in 100 μl of Tris-buffer) the system was warmed to 37°C. The reaction was initiated by the addition of approximately 0.1 μCi of $[\gamma^{-32}P]ATP$ (final conc. 2.5 μM sodium salt) and incubated for 10 min. The reaction was stopped with 100 μl of 20% trichloroacetic acid and briefly centrifuged to collect the precipitate. The subsequent 1 N KOH treatments, washing of the protein precipitates and liquid scintillation counting were similar to that employed by Doherty and Matsumura [19].

238

Results

To study the effects of depolarization on the phosphorylation activities in the intact squid synaptosomes, the same experimental approaches as the one used by Robinson and Dunkley [20] on the rat brain synaptosomes were adopted. The preloading step was carried out using $H_3{}^{32}PO_4$ and the depolarization process was initiated by introducing high K^+ external solution. The results shown in Fig. 1 clearly indicate that this depolarization treatment had the effect of increasing the level of overall protein phosphorylation, particularly on those proteins with high molecular weights. The level of phosphorylation under the experimental conditions was highest at the 15 s depolarization and gradually decreased thereafter over the next 5 min period. Addition of deltamethrin (0.1 μM) increased the level of protein phosphorylation throughout the depolarizing periods. To supplement the above qualitative studies the levels of labelling of total protein were determined by repeating the above experiment and precipitating the total protein using trichloroacetic acid [19]. The results shown in Table 1 indicate that the level of ^{32}P-labelling was always higher in the synaptosomes treated with 0.1 μM deltamethrin (pretreated for 10 min). A similar experiment was repeated using 200 μM veratridine (final concentration) as the depolarizing agent instead of high K^+. The results (Fig. 2) were similar to the previous ones. At the 30 s depolarization period the level of phosphorylation as assessed by the trichloroacetic acid precipitation method was 641 ± 76 and 915 ± 39
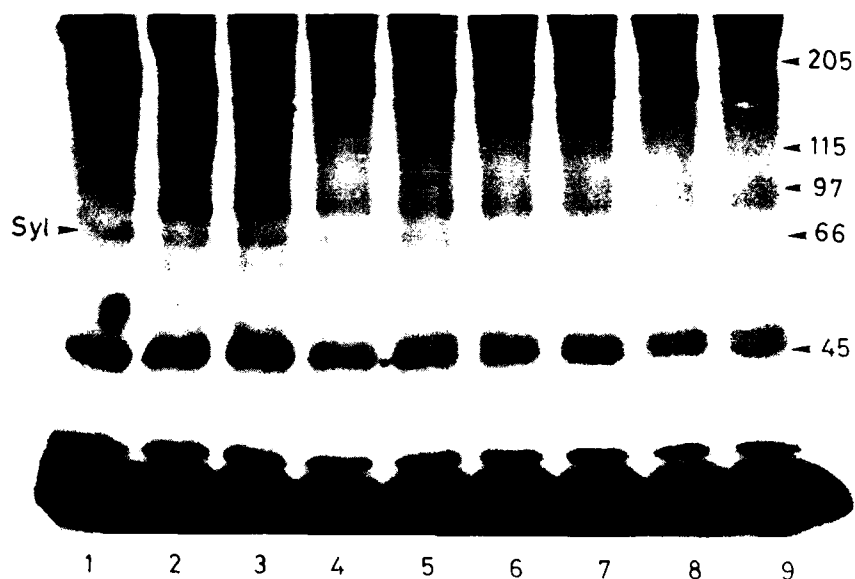
FIG 1 SDS–polyacrylamide gel electrophoresis/radioautogram of ^{32}P-phosphoproteins from control and deltamethrin treated intact synaptosomes from the squid optic lobe depolarized by excess external K^+. From left to right: (1) control undepolarized (i.e. loading only), (2) control depolarized for 15 s, (3) same in the synaptosomes pretreated with 10^{-7} M deltamethrin, (4) control after 30 s, (5) same as 4 but pre-treatment, (6) control depolarized for 60 s, (7) same as 6 but pre-treatment, (8) control depolarized for 30 s and (9) same as 8 but pre-treatment. The numbers shown on the right are the molecular weight markers expressed in kDa. Sy I indicates the location of synapsin I.

TABLE 1   Levels of ^{32}P-phosphorylation of total proteins from intact squid optic lobe synaptosomes depolarized by excess external K$^+$ in the presence and absence of 10^{-7} M deltamethrin

Length of depolarization (s)	Total ^{32}P-radioactivity (cpm) [a]	
	Control	Deltamethrin
0	2419 ± 469	–
15	2671 ± 213	3177 ± 315
30	2451 ± 53	3267 ± 249
60	2515 ± 664	2636 ± 408
300	1265 ± 23	1464 ± 81

[a] The results are expressed in cpm of ^{32}P bound per 150 μg synaptosomal proteins (mean ± S.D., 4 determinations).

cpm/150 μg protein for veratridine treated (lane 4) and veratridine plus deltamethrin treated (lane 5) synaptosomes (4 determinations each), respectively.

To determine the effective concentration of deltamethrin which affects the phosphorylation and/or dephosphorylation activities, various concentrations of this pesticide were tested on synaptosomes depolarized with 200 μM veratridine (Table 2). The results showed that under the present experimental conditions 10^{-13} M deltamethrin did not have any effect, but 10^{-11} M deltamethrin definitely elevated the level of veratridine-induced total phosphorylation ($P < 0.05$). Previously it has been shown that the threshold concentration of deltamethrin to cause a change in

Syl ►

◄ 205

◄ 115

◄ 97

◄ 66

◄ 45

1   2   3   4   5   6   7   8   9
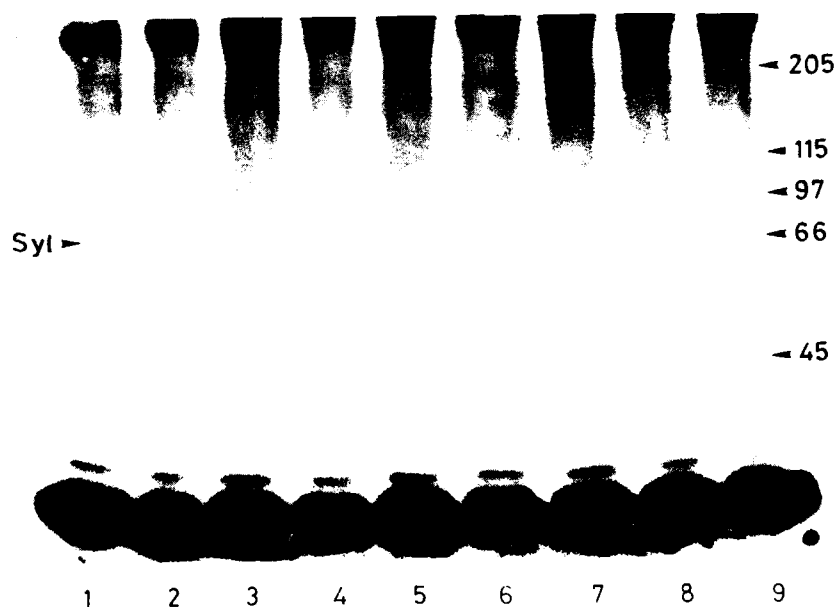
FIG 2   SDS-polyacrylamide gel electrophoresis/radioautogram of ^{32}P-phosphoproteins from intact synaptosomes depolarized by the addition of 200 μM veratridine. The sequence of the experiment was identical to the ones shown for Fig. 1 except for the use of veratridine in place of excess K$^+$ as a depolarization agent.

TABLE 2   Levels of phosphorylation of intact synaptosomal proteins affected by veratridine and various concentrations of deltamethrin [a]

Treatment	Deltamethrin concentration (M)	Post-depolarization period (s)	Levels of phosphorylation (cpm/150 μg protein) [b]
None (loading)	0	0	1281 ± 7
Veratridine treated (200 μM)			
Maximum labelling	0	15	2025 ± 36
Control (ethanol)	0	60	1554 ± 215
Deltamethrin	10^{-13}	60	1514 ± 15
	10^{-11}	60	2221 ± 259 *
	10^{-9}	60	1836 ± 295 *
	10^{-7}	60	1853 ± 39 *
	10^{-5}	60	1930 ± 465

[a] Experimental conditions are as shown in Table 1.
[b] Means are determined from 4 independent tests ± S.D. Means followed by asterisk are significantly different ($P < 0.05$) from the mean of 10^{-13} M deltamethrin treatment value which produced no effect.

[^{14}C]choline uptake in the squid optic lobe synaptosomes was of the order of 10^{-12} M [12] indicating similar levels of sensitivities between these two test results.

The above studies have established that deltamethrin has the property to elevate the levels of depolarization-coupled protein phosphorylation. To test the possibility that such an action of deltamethrin is at least partly caused by an increase in the internal free Ca^{2+} concentration we applied 50 mM pentylenetetrazole to the intact synaptosomes and thereby promoted Ca^{2+} influx and the release of calcium from internal sequestration sites [21]. We have found that PTZ indeed stimulates protein phosphorylation in the squid synaptosomes as in the case with the rat brain preparation [25,26], and that deltamethrin at 0.1 μM had the property of further increasing the levels of protein phosphorylation (data not shown). In the next approach we have directly measured the action of deltamethrin on lysed membranes

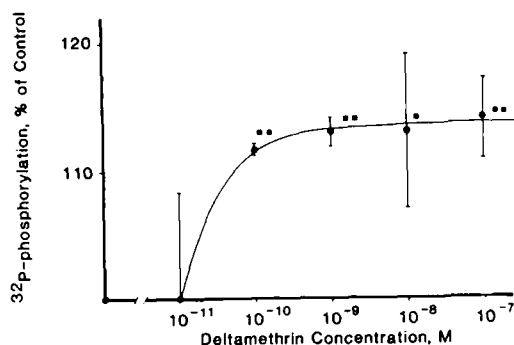FIG 3   Effect of varying the concentration of deltamethrin on the level of protein phosphorylation in the lysed synaptosomal membrane preparation [12]. Preincubation period with deltamethrin was 10 min at 23°C. The tests were carried out in calcium-calmodulin buffer. One and two square marks represent statistically significant differences from control at $P \leqslant 0.05$ and $\leqslant 0.01$, respectively.
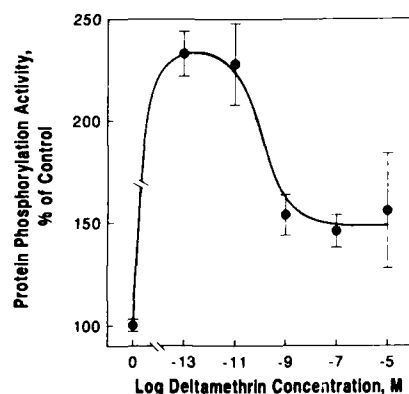
FIG 4   Effects of varying concentrations of deltamethrin on the level of phosphorylation of histone catalysed by a purified bovine heart cAMP-dependent protein kinase (holoenzyme).

(i.e. membranes from synaptosomes broken by osmotic shock) with regard to its effect on protein phosphorylation. In these experiments, lysed synaptosomal membranes were preincubated with deltamethrin for 10 min and the phosphorylation activities were assessed using $[\gamma\text{-}^{32}P]ATP$. The results (Fig. 3) indicate that deltamethrin has the property of increasing the level of protein phosphorylation even after the destruction of synaptosomal integrity. The threshold concentration of deltamethrin in this regard was of the order of 10^{-10} M.

Earlier it was noted that such a stimulatory action of deltamethrin was more pronounced when the test medium did not contain calcium and/or calmodulin [12]. The most prominent synaptosomal protein kinase which does not require either calcium or calmodulin is cAMP-dependent protein kinase (PKA) [13]. We have therefore tested the action of deltamethrin on purified PKA. The results clearly indicate a stimulatory action of this pesticide on PKA. Even at concentrations as low as 10^{-13} M deltamethrin greatly enhanced the protein kinase activity (Fig. 4). Similarly, treatment of labelled intact synaptosomes with 8-Br-cAMP, a membrane permeable cAMP analogue, also caused a rise in the overall levels of protein phosphorylation (data not shown).

Discussion

In the current study it has been shown that deltamethrin causes an increase in the level of depolarization-induced protein phosphorylation. Since it has been proposed that depolarization-coupled increases in protein phosphorylation in the presynaptic nerve terminals are intimately related to processes of neurotransmitter release [15,18,20,22], such effects of deltamethrin are likely to result in excess transmitter release. The effect of deltamethrin was still evident even after 300 s from the time of initial depolarization where in the case of control synaptosomes, the level of phosphorylation had already returned to the predepolarization level. One phosphoprotein of which the level of phosphorylation was clearly elevated was synapsin I (marked as Sy, I, Figs. 1 and 2, molecular weight approx. 83 kDa). Dephospho-synapsin I has been shown to be an active synaptic vesicle protein which inhibits

continuation of transmitter release [14,22]. Thus prolongation of the phosphorylation state of this protein is expected to deprive the synaptosome of its ability to stop the process of transmitter release over time. The fact that such a property of dephosphosynapsin I has been shown by using the giant synaptic process of the same squid species *Loligo pealei* [13] as studied here adds strong support to this hypothesis.

As to the cause for such an action of deltamethrin one of the likely possibilities is the increased influx of Na^+ and most likely of Ca^{2+} into the synaptosome. Pyrethroids are well known to interfere in the gating operations of the voltage sensitive sodium channel [2,23]. In fact in some systems the pyrethroid-induced changes in rates of transmitter release may be completely antagonized by tetrodotoxin [6,24] indicating the importance of the sodium channel effects. However, in other cases tetrodotoxin abolishes only a part of the pyethroid effect on neurotransmitter release [10–12,25]. As for Ca^{2+} there is no question about its effects on the process of depolarization-stimulated protein phosphorylation as well as depolarization-stimulated neurotransmitter releasing processes [14,15]. It has also been shown by Brooks and Clark [10] that deltamethrin causes an increase in the rat brain synaptosomal uptake of ^{45}Ca at the same concentration range ($\geqslant 10^{-11}$ M) as that which affects the [^{3}H]norepinephrine release from the synaptosome. The results of the PTZ experiment corroborate the above conclusion.

In addition to the above ion flux effects, deltamethrin also affects some intrasynaptosomal components to increase the level of protein phosphorylation. One of the likely candidates for the responsive target system is cAMP-dependent protein kinase, though there could be other potential candidate systems such as protein phosphatases and cAMP-independent protein kinases. In this model system which consists of only one enzyme system, protein phosphorylation activities were greatly enhanced by deltamethrin. Therefore a direct action of deltamethrin on this enzyme is certain. The most likely possibility is that deltamethrin acts on the PKA's regulatory subunit, which as a nondissociated form, normally inhibits the action of the catalytic subunit. Upon dissociation of these two units either as a result of cAMP or any other agents its phosphorylation activity is known to rise. However, more data will be needed to prove this point.

The observation that deltamethrin causes an increase in PKA activity brings up intriguing possibilities. PKA has been implicated in phosphorylation of K^+-channels which apparently results in either blockage of K^+ conductance in *Aplysia* sensory neurons [27] or its increase [28]. It has recently been reported by Leake et al. [4] that manipulation of intracellular concentration of cAMP PKA in the leech Retzius cell (R cell) modified S-bioallethrin-induced bursting activity. In these cells a rise in PKA, and, therefore phosphorylation of the K^+ channel protein, results in an increase in outward potassium current and probably an increased Ca^{2+} and Na^+ influx. Artificial increases in PKA resulted sometimes in preventing and sometimes exacerbating S-bioallethrin's action. The conclusion reached by these workers was that pyrethroids were possibly interfering with PKA. Certainly much more work would be needed before one could correlate these electrophysiological findings with the biochemical study described here. However, knowing the extreme sensitivity of PKA to deltamethrin and the importance of this enzyme in regulating not only some ion-channels but many other neural functions including transmitter release and intracellular Ca^{2+} homeostasis, our research results point to interesting future research avenues.

Acknowledgements

References

1 Elliott, M. (ed.) (1977) Synethetic pyrethroids. Am. Chem. Soc. Symp. Ser. No. 42. Washington, DC, 229 pp.
2 Narahashi, T. (1985) Nerve membrane ionic channels as the primary target of pyrethroids. Neurotoxicology 6, 3–22.
3 Vijverberg, H.P.M. and DeWeille, J.R. (1985) The interaction of pyrethroids with voltage dependent Na channels. Neurotoxicology 6, 23–24.
4 Leake, L.D., Dean, J.A. and Ford, M.G. (1986) Pyrethroid action and cellular activity in invertebrate neurons. In: Neuropharmacology and Pesticide Action (M.G. Ford, G.G. Lunt, R.C. Reay, P.N.R. Usherwood, eds.), pp. 244–266. Ellis Horwood Ltd., Chichester, England.
5 Cremer, J.E. (1983) The influence in mammals of the pyrethroid insecticides. In: Developments in the Science and Practice of Toxicology (A.W. Hayes, R.C. Schnell, T.S. Miya, eds.), pp. 61–72. Elsevier Sci. Pub., N.Y.
6 Berlin, J.R., Akera, T., Brody, T.M. and Matsumura, F. (1984) The inotropic effects of a synthetic pyrethroid decamethrin on isolated guinea pig atrial muscle. Eur. J. Pharmacol. 98, 313–322.
7 Gray, A.J. (1985) Pyrethroid structure-toxicity relationships in mammals. Neurotoxicology 6, 127–138.
8 Staatz, C.G., Bloom, A.S. and Lech, J.J. (1982) A pharmacological study of pyrethroid neurotoxicity in mice. Pestic. Biochem. Physiol. 17, 287–292.
9 Clark, J.M. and Matsumura, F. (1986) Membrane Receptors and Enzymes as Target of Insecticidal Action. Plenum Press, New York London, 256 pp.
10 Brooks, M.W. and Clark, J.M. (1987) Enhancement of norepinephrine release from rat brain synaptosomes by alpha cyano pyrethroids. Pestic. Biochem. Physiol. 28, 127–139.
11 Matsumura, F. (1987) Deltamethrin induced changes in synaptosomal transport of ^{3}H-epinephrine in the squid optic lobes. Comp. Biochem. Physiol. 87C, 31–35.
12 Matsumura, F. (1988) Deltamethrin induced changes in choline transport and phosphorylation activities in synaptosomes from the optic lobe of squid, Lologio pealei. Comp. Biochem. Physiol., in press.
13 Narin, A.C., Hemmings, H.C. and Greengard, P. (1985) Protein kinases in the brain. Annu. Rev. Biochem. 54, 931–976.
14 Browning, M.D., Huganir, R. and Greengard, P. (1985) Protein phosphorylation and neuronal function. J. Neurochem. 45, 11–23.
15 Dunkley, P.R., Baker, C.M. and Robinson, P.J. (1986) Depolarization-dependent protein phosphorylation in rat cortical synaptosomes: characterization of active protein kinases by phosphopeptide analysis of substrates. J. Neurochem. 46, 1692–1703.
16 Pollard, H.B. and Pappas, G.D. (1979) Veratridine-activated release of adenosine-5-triphosphate from synaptosomes: evidence for calcium dependence and blockade by tetrodotoxin. Biochem. Biophys. Res. Commun. 88, 1315–1321.
17 Laemmli, U.K. (1970) Cleavage of structural proteins during the assembly of the head of bacteriophage T4. Nature 227, 680–685.

244

18 Schulman, H. and Greengard, P. (1978) Stimulation of brain membrane protein phosphorylation by calcium and endogenous heat-stable protein. Nature 271, 478–479.

19 Doherty, J.D. and Matsumura, F. (1974) A highly ion-sensitive ATP-phosphorylation system in lobster nerve. Biochem. Biophys. Res. Commun. 57, 987–992.

20 Robinson, P.J. and Dunkley, P.R. (1985) Depolarization-dependent protein phosphorylation and dephosphorylation in rat cortical synaptosomes is modulated by calcium. J. Neurochem. 44, 338–348.

21 Onozuka, M., Imai, S. and Ozono, S. (1987) Movement of penlylenetetrazole in synapsin I phosphorylation associated with calcium influx in synaptosomes from rat cerebral cortex. Biochem. Pharmacol. 36, 1407–1415.

22 Krueger, B.K., Forn, J. and Greengard, P. (1977) Depolarization-induced phosphorylation of specific proteins, mediated by calcium ion influx, in rat brain synaptosomes. J. Biol. Chem. 252, 2764–2773.

23 Narahashi, T. (1986) Mechanisms of action of pyrethroids on sodium and calcium channel gating. In: Neuropharmacology and Pesticide Action (M.G. Ford, G.G. Lunt, R.C. Reay, P.N.R. Usherwood, eds.) pp. 36–50. Ellis Horwood Ltd., Chichester, England.

24 Nicholson, R.A., Wilson, R.G., Potter, C. and Black, H. (1983) Pyrethroid and DDT-evoked release of GABA from the nervous system in vitro. In: Pesticide Chemistry Vol. 3. Mode of Action, Metabolism, Toxicology (J. Miyamoto, P.C. Kearney, eds.). Pergamon Press, New York.

25 Brooks, M.W. (1986) Investigations of the actions of Type I and Type II pyrethroids on norepinephrine uptake and release by rat brain synaptosomes. M.S. Thesis. University of Massachusetts, Amherst, MA.

26 Clark, J.M. (1988) Neurotoxicity of pyrethroids: single or multiple mechanisms of action? Environm. Toxicol. Chem. (in press).

27 Shuster, M.J., Camardo, J.S., Siegelbaum, S.A. and Kandel, E.R. (1985) Cyclic AMP-dependent protein kinase closes the serotonin-sensitive K^+ channels of *Aplysia* sensory neurones in cell-free membrane patches. Nature 313, 392–395.

28 Green, D.J. and Gillette, R. (1983) Patch and voltage-clamp analysis of cyclic AMP-stimulated inward current underlying neuron bursting. Nature 306, 784–785.

CHAPTER 18

Coupling of muscarinic receptors to second messenger systems in locust ganglia

MICHAEL J. DUGGAN * AND GEORGE G. LUNT

Department of Biochemistry, University of Bath, Bath, U.K.

Introduction

The presence of putative muscarinic acetylcholine receptors (mAChR) in insect tissues was first demonstrated by Dudai and Ben-Barak [1]. They used the radio-labelled muscarinic antagonist quinuclidinylbenzilate ([^{3}H]QNB) to characterize a binding site in a membrane preparation from the heads of *Drosophila melanogaster*. This technique has been used for several other preparations from insect tissue (for review see Ref. 2) including dissected supraoesophageal ganglia from the desert locust *Schistocerca gregaria* [3]. In these initial studies the pharmacology of the insect [^{3}H]QNB binding site was shown to be similar, but not identical, to that of the better characterized mAChR of mammalian tissues.

Further evidence of similarity between the insect and vertebrate mAChR came when in 1984 Lummis et al. [4] used target size analysis of irradiated membranes from *Periplaneta americana* to estimate the size of the mAChR as 77 600 Da and Venter et al. [5] used an irreversible radioligand ([^{3}H]propylbenzilylcholine mustard, [^{3}H]PrBCM) followed by SDS–PAGE to estimate the size of the mAChR from *Drosophila melanogaster* as 80 000 Da. Both these molecular weights are within the range found for mAChR in vertebrate tissues. Venter et al. [5] further identified this binding site as a mAChR similar to that found in vertebrates by showing that six monoclonal antibodies raised against the mAChR purified from rat brain could immunoprecipitate [^{3}H]PrBCM labelled protein from solubilized membranes from *Drosophila melanogaster*. These data suggest that the mAChR from insects is homologous to that found in the vertebrates which has been considerably better characterized.

The history of research on vertebrate mAChR extends back to the work of Dale [6] who, in 1914, demonstrated the effect of muscarine on the frog heart. More recently the use of radiolabelled ligands such as [^{3}H]QNB allowed the characterization of the receptor (for review see Ref. 7). In early experiments antagonists such as atropine gave binding isotherms which were adequately described by a single population of binding sites; the binding characteristics of agonists, however, were

---

* Present address: MRC Molecular Neurobiology Unit, University of Cambridge Medical School, Cambridge, U.K.

complex and analysis indicated that there were three different subtypes or substrates of the mAChR which are at least partially interconvertible by chemical modifying reagents, metal ions and GTP [7]. Compounds have since been found that are antagonists yet also differentiate between subtypes/substrates of the receptor. The first of these was pirenzepine [8] which was used to differentiate two subclasses known as M_1 and M_2, although use of other compounds has since showed that the situation is rather more complex. In particular AF-DX 116, a pirenzepine derivative [9,10] and hexahydrosiladifenidol [11] have been used to define a pharmacological classification of three different subtypes of mAChR [12].

The increasing complexity of the field has been resolved, in part, by the use of the molecular genetic approach to derive the amino acid sequences of at least four different mAChRs [13,14]. The protein sequences resemble, in basic structure, those known for rhodopsin and the adrenergic receptors, which, like the mAChR and many others appear to exert their physiological effect by mobilizing GTP-binding proteins which allosterically modulate the activities of enzymes or ion channels found in the cell membrane (see Evans, this volume). The current explanation for the multiplicity of mAChR subclasses is that different subtypes interact preferentially with different members of the large family of GTP-binding proteins (G-proteins) to produce different responses in the cell.

While the number of recorded responses to mAChR stimulation is large and includes both increases and decreases in potassium currents, an increase in a sodium current, an increase in a chloride current and a decrease in a calcium current [15], the mAChR has been shown to be directly linked to just three second messenger systems. These are:

1. The increased metabolic turnover of the phosphoinositides, initially by a hydrolysis of phosphatidylinositol bisphosphate to form diacylglycerol and inositol trisphosphate [16].
2. A decrease in the level of cyclic-3',5'-adenosine monophosphate (cAMP), by an inhibition of adenylate cyclase [17].
3. The opening of a potassium-selective ion channel [15].

The first two systems which lead to the generation of intracellular second messengers capable of diffusing for some distance through the cell may have many effects, principally through the phosphorylation/dephosphorylation of proteins. This is especially true of the mobilization of inositol phosphates and production of diacylglycerol, a system of many ramifications.

Although both of these second messenger systems have been shown to exist in insects neither has previously been shown to be controlled by a mAChR in insect tissues. Some of the important early experiments on the role of phosphoinositide metabolites as second messengers were carried out in an insect system, the blowfly salivary gland, where the response was evoked by 5-hydroxytryptamine [18].

A neuronal adenylate cyclase has been shown in many insect species. It was first discovered by Nathanson and Greengard [19] in the cockroach and its existence has since been confirmed by many workers (for review see Ref. 20), who have been concerned mainly with the stimulation of adenylate cyclase by octopamine. This effect was shown in supraoesophageal ganglia from *Schistocerca gregaria* by Morton [21] who found that several putative monoamine neurotransmitters stimulated adenylate cyclase activity.

The studies reported here investigate first, the heterogeneity of the mAChR pharmacology, and second, the effect that muscarinic cholinergic ligands have on

phosphatidylinositol turnover and the level of cyclic AMP in preparations from supraoesophageal ganglion from *Schistocerca gregaria*.

Materials and methods

[³H]QNB binding experiments

The materials and methods used were essentially those of Aguilar and Lunt [3]. briefly, a P_2 membrane pellet from supraoesphageal ganglia of *Schistocerca gregaria* was incubated with [³H]QNB for 1 h in the presence or absence of other ligands and then the bound radiolabel separated from the free ligand by filtration through Whatman GF/B filters. Non-specific binding was defined as that determined in the presence of 0.1 mM atropine sulphate.

Measurement of phosphatidylinositol turnover

Phosphatidylinositol turnover was followed by measuring the incorporation of [³H]myoinositol into the lipid fraction.

Supraoesophageal ganglia were removed from the freshly decapitated heads of adult locusts (*Schistocerca gregaria*). The optic lobes and any connective tissue were removed and the ganglia cut in half before being placed into 5 ml gassed (O_2 : CO_2, 95 : 5) phosphate buffered saline pH 6.8 containing (in mM): NaCl 150, KCl 10, $CaCl_2$ 2, $MgCl_2$ 5, $NaHCO_3$ 8, KH_2PO_4 6, glucose 10. The ganglia (ten per sample) were allowed to equilibrate with the buffer for 1 h at room temperature. The saline was then changed to 2 ml of fresh gassed saline and 2 μCi of [³H]inositol (10–20 Ci mmol⁻¹, supplied by Amersham International PLC) were added in the presence or absence of 1 mM carbachol and other cholinergic drugs. After 1 h at room temperature the incubation was stopped by centrifuging the tubes to pellet the ganglia and decanting the supernatant, 5 ml of chloroform : methanol (2 : 1; v/v) were added and the ganglia rapidly homogenized (10 s, Ultraturrax). The lipids were extracted by a further homogenization (5 strokes, Jencons ground glass/glass homogenizer) and washed with 0.2 volumes of 0.1 M $MgCl_2$ after the method of Folch et al. [22].

The lipid samples were divided, 4/5 was taken, dried and dissolved in scintillant for liquid scintillation counting and the remainder ashed and assayed for phosphate content by the method of Bartlett [23].

Measurement of cAMP production

Supraoesophageal ganglia were dissected from freshly decapitated locust heads and immediately frozen with liquid nitrogen before storing at −80°C. Adenylate cyclase activity was assayed in homogenates of these ganglia. Ten ganglia were homogenized with a glass/glass homogenizer in 0.5 ml of 50 mM Tris-buffered saline (pH 7.5) containing $MgCl_2$, 6 mM; NaCl, 90 mM; EDTA, 0.8 mM and theophylline, 8 mM. The homogenate was passed through nylon mesh to remove large tissue fragments and the volume made up to 2 ml.

The assay was carried out in the same buffer as that used for the homogenization, with the addition of ATP (1 mM) and GTP (0.1 mM) and cholinergic ligands. A total volume of 0.5 ml was used for each assay tube including 0.05 ml of tissue homogenate. The reaction was started by the addition of the ATP and GTP and stopped by placing the tubes in boiling water for 5 min. Protein was precipitated by
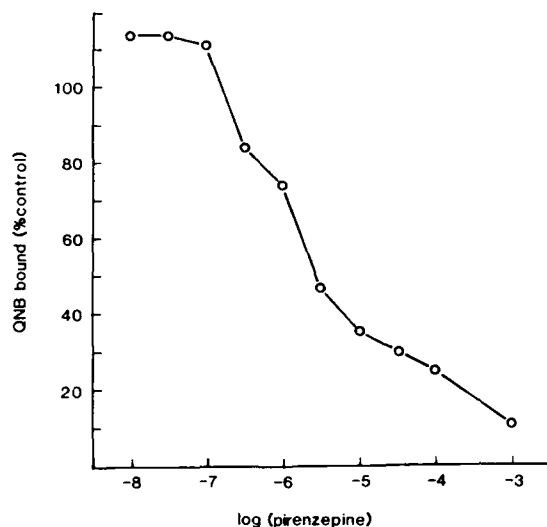
FIG 1 Inhibition of [^{3}H]QNB binding by pirenzepine. This is a representative experiment, one of four. The specific binding of 1 nM [^{3}H]QNB is expressed as a percentage of the specific binding in the absence of any competing ligand. All points are the results of triplicate determinations, the S.D. was always less than 7%.

centrifugation and the cAMP concentrations determined in a competition assay with [^{3}H]cAMP (Amersham International PLC) for a cAMP-binding protein (BDH Ltd) as described by Brown et al. [24].

Results and discussion

[^{3}H]QNB binding studies

Inhibition by selective antagonists
[^{3}H]QNB (1 nM) was incubated with locust ganglionic membranes in the presence of varying concentrations of pirenzepine, AF-DX 116 and hexahydrosiladifenidol. Although the specific binding of [^{3}H]QNB could be completely inhibited by high concentrations of these compounds the concentration dependence curves were flattened (see Fig. 1) and the Hill plots of the data, for concentrations giving 5–95% inhibition of the control specific binding, gave slopes < 1 (see Table 1).

Hill numbers < 1 indicate a possible heterogeneity of the binding sites. The proportions and affinities of these sites for pirenzepine were estimated using the 'by hand' program of Humrich and Richardson [25]. The results are given in Table 2; this analysis gave the best fit to the sites for a two site model and was significantly better than a one site model ($P < 0.01$).

Inhibition by agonists
[^{3}H]QNB (4 nM) was incubated with locust ganglionic membranes in the presence of varying concentrations of oxotremorine, in the presence or absence of GTP (0.1

TABLE 1 The effects of muscarinic antagonists on muscarinic receptor binding in the locust

Ligand	K_i (μM)	N_H
Pirenzepine	1.9 ± 1.1	0.50 ± 0.04
Hexahydrosiladifenidol	0.24 ± 0.12	0.65 ± 0.18
AF-DX 116	52 ± 34	0.63 ± 0.21

Inhibition constants (K_i) and Hill Numbers (N_H) for the inhibition of [^{3}H]QNB binding by selective muscarinic antagonists. Each value is the mean for three separate experiments and is given ±1 S.D.

TABLE 2 Parameters for pirenzepine inhibition of [^{3}H]QNB binding in the locust

	K_i	Proportion of sites (%)
Site 1	0.15×10^{-6} M	55
Site 2	7.5×10^{-6} M	60

Best fit ($P < 0.01$) two-site model for pirenzepine inhibition of [^{3}H]QNB binding to locust P_2 fraction.
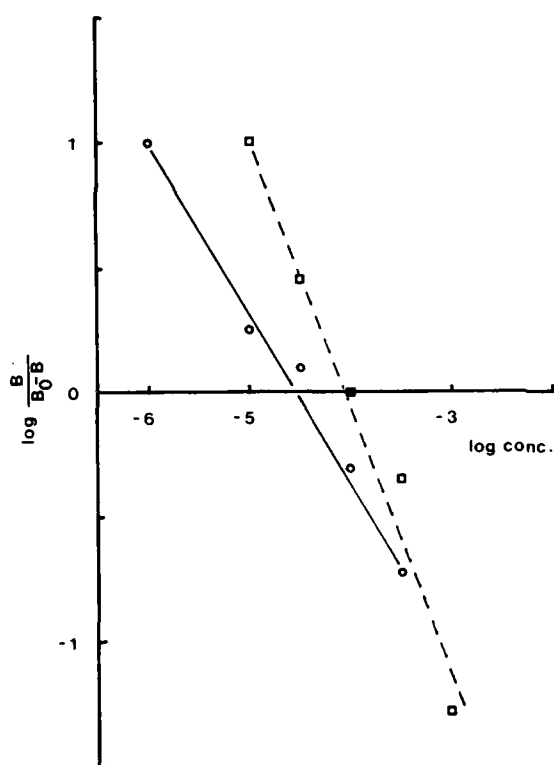

FIG 2 Hill plot of the inhibition of [^{3}H]QNB by oxotremorine, recalculated from Whyte and Lunt [31]. Data recalculated from the figure of Whyte and Lunt [31]; inhibition of the binding of 4 nM [^{3}H]QNB to locust ganglionic membranes in the presence (□——□) and absence (o——o) of 100 μM GTP.

mM). The GTP had no significant effect on the control [^{3}H]QNB binding but did affect the dose dependent inhibition of [^{3}H]QNB binding by oxotremorine (see Fig. 2), both decreasing the apparent affinity and increasing the slope of the Hill plot. This result is consistent with those found for the vertebrate brain mAChR where the presence of GTP results in the apparent conversion of a subpopulation of sites with a high affinity for agonists to low agonist affinity [7].

Incorporation of [^{3}H]inositol into phospholipids

The incorporation of [^{3}H]inositol into phospholipids was linear up to 1 h and thin-layer chromatography of the extracted lipids showed that it was limited to phosphatidylinositol (PI). Table 3 shows that carbachol (1 mM) increased the specific activity of the phospholipids, an effect which was reversed by the specific antagonist atropine and the subtype selective antagonist pirenzepine at a concentration at which it should be selective for the high affinity site, as determined by binding studies (Table 1).

Since this work began there have been other reports on the phosphoinositide metabolism of insect nervous tissue. Working on a preparation from the metathoracic ganglion of *Schistocerca gregaria* Trimmer and Berridge [26] showed that [^{3}H]QNB was incorporated into the inositol phosphates which are associated with second messenger function. They were however unable to show any effect on the concentrations of these compounds by a range of neurotransmitters and their analogues, including carbachol. Atropine, a muscarinic antagonist, reduced the production of inositol phosphates and this was taken as evidence for muscarinic regulation; the mechanism of atropine's action was presumed to be by competition with endogenous acetylcholine.

Ross and Brady [27] followed the incorporation of ^{32}P into the phospholipids of the nerve cord from the cricket *Acheta domesticus*. They found that in the presence of either acetylcholine or the anticholinesterase insecticide dichlorvos the activity of most of the phospholipid was increased. The interpretation of their data is difficult because they measured only the total activity in each class of phospholipid, rather than the specific activity, so that it cannot be known whether the increases are due to increased specific activity, caused by enhanced turnover, or different absolute amounts of phospholipid.

TABLE 3   Cholinergic modulation of PI turnover in locust ganglia

Ligand	Specific incorporation of [^{3}H]inositol (% of control)	n
None	100 ± 16	8
Carbachol (10^{-3} M)	164 ± 22	6
Carbachol (10^{-3} M) + Atropine (5 × 10^{-5} M)	91 ± 21	4
Carbachol (10^{-3} M) + Pirenzepine (5 × 10^{-6} M)	105 ± 25	2

n = no. of determinations. Results are expressed as mean ± S.D. of the % activity of the control, i.e. no additions.
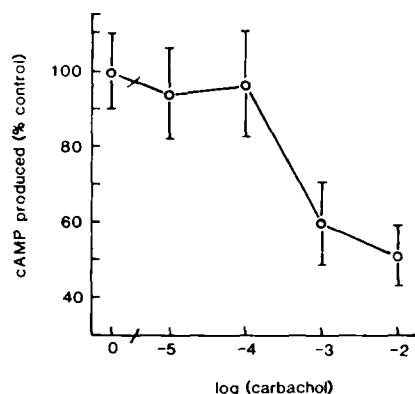
FIG 3 Effect of carbachol on the production of cAMP. Homogenates incubated in the presence of 90 mM NaCl were assayed for cAMP production in the presence of a range of carbachol concentrations. cAMP production is expressed as a percentage of that found in the absence of carbachol. Error bars are one S.D.

cAMP Levels

cAMP production was linear with time for 10 min. The value for the cAMP produced during the first 5 min can be used to calculate an apparent adenylate cyclase activity for the ganglionic homogenate of 205 ± 17 pmol cAMP $\cdot$ min^{-1} $\cdot$ mg protein^{-1}, which agrees closely with the value determined by Morton [21] for the same tissue. The cAMP level was reduced by carbachol in the presence but not the absence of 90 mM NaCl; this effect was dose dependent (Fig. 3) and reversible by atropine (Table 4).

Thus it has been demonstrated that the locust central nervous system has an Na$^+$-dependent carbachol-induced down-regulation of adenylate cyclase analogous to that seen in rat brain [17] and this sodium dependence explains the failure of previous workers to detect cholinergic regulation [28].

This study has shown that the mAChR defined previously by [^{3}H]QNB binding studies has both a pharmacology and a functional control of second messenger systems similar to that which has been seen in the vertebrate. To discover whether or not the third directly linked effector known in the vertebrates, the G-protein gated K$^+$ channel, is present in insects will require an electrophysiological survey.

To date there are no well established, published, electrophysiological responses to mAChR stimulation in the insect CNS; in the peripheral nervous system however

TABLE 4 Cholinergic modulation of adenylate cyclase activity in locust ganglia

Ligand	cAMP production (% of control)
None	100
Carbachol (10^{-3} M)	51 ± 8
Carbachol (10^{-3} M) + Atropine (5×10^{-5} M)	85 ± 4

Results are expressed as a % of cAMP production in the absence of carbachol and are presented as mean $\pm$ S.D. for four experiments.

252

the observation of Fulton [29] indicates that the mAChR may be capable of an excitatory role presynaptic to a neuromuscular junction in the locust.

Breer and Knipper [30] have provided evidence for an inhibitory role for the mAChR with the observation that mAChRs are involved in the regulation of ACh release in preparations of synaptosomes from locust ganglia; muscarinic agonists in this preparation reduce the depolarization-evoked release and antagonists increase release.

It may be that no electrophysiological responses have been observed because the mAChR acts in a neuromodulatory role, by enhancing or reducing the responses evoked by other neurotransmitters, in which case the addition of muscarinic antagonists in parallel with agonists for other systems may lead to some interesting discoveries.

Acknowledgement

References

1 Dudai, Y. and Ben-Barak, J. (1977) Muscarinic receptor in *Drosophila melanogaster* demonstrated by binding of [^{3}H]QNB. FEBS Lett. 81, 134–136.

2 Sattelle, D.B. (1985) Acetylcholine receptors. In: Comprehensive Insect Physiology Biochemistry and Pharmacology, Vol. 2 (G.A. Kerkut, L.I. Gilbert, eds.) pp. 395–434. Pergamon Press, Oxford.

3 Aguilar, J.S. and Lunt, G.G. (1984) Cholinergic binding sites with muscarinic properties on membranes from the supraoesophageal ganglion of the locust (*Schistocerca gregaria*). Neurochem. Int. 6, 501–507.

4 Lummis, S.C.R., Sattelle, D.B. and Ellory, J.C. (1984) Molecular weight estimations of insect cholinergic receptors by radiation inactivation analysis. Neurosci. Lett. 44, 7–12.

5 Venter, J.C., Eddy, B., Hall, L.M. and Fraser, C.M. (1984) Monoclonal antibodies detect the conservation of muscarinic cholinergic receptor structure from *Drosophila* to human brain and detect possible structural homology with α_1-adrenergic receptors. Proc. Natl. Acad. Sci. U.S.A. 81, 272–276.

6 Dale, H.H. (1914) The action of certain esters and ethers of choline, and their relation to muscarine. J. Pharmacol. Exp. Ther. 6, 147–190.

7 Hoss, W. and Ellis, J. (1985) Muscarinic receptor subtypes in the central nervous system. Int. Rev. Neurobiol. 26, 151–199.

8 Hammer, R., Berrie, C.P., Birdsall, N.J.M., Burgen, A.S.V. and Hulme, E.C. (1980) Pirenzepine distinguishes between different subclasses of muscarinic receptors. Nature 283, 90–92.

9 Giachitti, A., Micheletti, R. and Montagna, E. (1986) Cardioselective profile of AF DX-116—a muscarine M_2 receptor antagonist. Life Sci. 38, 1663–1672.

10 Hammer, R., Giraldo, E., Sehiari, G.B., Monferini, E. and Ladinsky, H. (1986) Binding profile of a novel cardioselective muscarine receptor antagonist, AF DX-116, to membranes of peripheral tissues and brain in the rat. Life Sci. 38, 1653–1662.

11 Lambrecht, G., Moser, U., Wess, J., Riotte, J., Fuder, H., Kilbinger, H., Muller, H., Linoh, H., Tacke, R., Zilch, H. and Mutscher, E. (1986) Hexahydrosiladifenidol: a selective antagonist at muscarinic M_2 receptor subtypes. Trends Pharmacol. Sci. Suppl. 91.

12 Birdsall, N.J.M., Curtis, C.A.M., Eveleigh, P., Hulme, E.C., Pedder, K., Poyner, D., Stockton, J.M. and Wheatley, M. (1987) Muscarinic receptor subclasses. In: Cellular and Molecular Basis of Cholinergic Function (M.J. Dowdall, J.N. Hawthorne, eds.). Ellis Horwood, Chichester.

13 Kubo, T., Fukuda, K., Mikami, A., Maeda, A., Takahashi, H., Mishima, M., Haga, T., Kaga, K., Ichiyama, A., Kangawa, K., Kojima, M., Matsuo, H., Hirose, T. and Numa, S. (1986) Cloning, sequencing and expression of complementary DNA encoding the muscarinic acetylcholine receptor. Nature 323, 411-416.

14 Peralta, E.G., Winslow, J.W., Ashkenazi, A., Smith, D.H., Ramachandran, J. and Capon, D.J. (1988) Structural basis of muscarinic acetylcholine receptor subtype diversity. Trends Pharmacol. Sci. Suppl., 6-11.

15 Christie, M.J. and North, R.A. (1988) Control of ion conductances by muscarinic receptors. Trends Pharmacol. Sci. Suppl., 30-34.

16 Fisher, S.K. (1986) Inositol lipids and signal transduction at CNS muscarinic receptors. Trends Pharmacol. Sci. Suppl., 61-65.

17 Olianas, M.C., Onali, P., Neff, N.H. and Costa, E. (1983) Adenylate cyclase activity of synaptic membranes from rat striatum. Mol. Pharmacol. 23, 393-398.

18 Berridge, M.J., Buchan, P.B. and Heslop, J.P. (1984) Relationship of polyphosphoinositide metabolism to the hormonal activation of the insect salivary gland by 5-hydroxytryptamine. Mol. Cell. Endocrinol. 36, 37-42.

19 Nathanson, J.A. and Greengard, P. (1973) Octopamine sensitive adenylate cyclase: evidence for biological role of octopamine in nervous tissue. Science 150, 303-310.

20 Smith, W.A. and Combest, W.L. (1985) Role of cyclic nucleotides in hormone action. In: Comprehensive Insect Physiology, Biochemistry and Pharmacology Vol. 8 (G.A. Kertcut, L.I. Gilbert, eds.) Pergamon Press, Oxford.

21 Morton, D.B. (1984) Pharmacology of the octopamine-stimulated adenylate cyclase of the locust and tick CNS. Comp. Biochem. Physiol. 78C, 153-158.

22 Folch, J., Lees, M. and Sloane Stanley, G.H. (1957) A simple method for the isolation and purification of total lipids from animal tissues. J. Biol. Chem. 226, 497-509.

23 Bartlett, G.R. (1959) Phosphorus assay in column chromatography. J. Biol. Chem. 234, 466-468.

24 Brown, B.L., Albano, J.D.M., Ekins, R.P. and Sgherzi, A.M. (1971) A simple and sensitive saturation assay method for the measurement of adenosine-3',5'-monophosphate. Biochem. J. 121, 561-562.

25 Richardson, A. and Hunrich, A. (1984) A microcomputer program for the analysis of radioligand binding curves and other dose-dependent data. Trends Pharmacol. Sci. 5, 47-49.

26 Trimmer, B.A. and Berridge, M.J. (1985) Inositol phosphates in the insect nervous system. Insect Biochem. 15, 811-815.

27 Ross, D.C. and Brady, U.E. (1986) Dichlorous and acetylcholine increase ^{32}P-labelling of phospholipids in cricket central nerve cords. Comp. Biochem. Physiol. 83C, 33-36.

28 Suter, C. (1986) Does cAMP mediate the action of octopamine on insect neurones? Comp. Biochem. Physiol. 84C, 189-193.

29 Fulton, B.P. (1982) Presynaptic acetylcholine receptors at the excitatory amino acid synapse in locust muscle. Neuroscience 7, 2117-2124.

30 Breer, H. and Knipper, M. (1984) Characterisation of acetylcholine release from insect synaptosomes. Insect Biochem. 14, 337-344.

31 Whyte, J and Lunt, G.G. (1986) The influence of guanine nucleotides on muscarinic receptor binding in the locust supraoesophageal ganglion. Biochem. Soc. Trans. 14, 690-691.

CHAPTER 19

Octopamine- and dopamine-sensitive receptors and cyclic AMP production in insects

ROGER G.H. DOWNER

Department of Biology, University of Waterloo, Waterloo, Ontario, Canada N2L 3G1

Introduction

Cyclic AMP, which is produced within the cell in response to extracellular hormonal signals, functions to mediate the specific physiological reactions of cells to particular hormones. The sequence of biochemical events by which the cyclic AMP transmembrane signalling system operates is shown in Fig. 1. According to this sequence, the hormone or other effector binds to a specific receptor protein located on the outer surface of the cell membrane and the hormone–receptor interaction leads to activation of the catalytic subunit of a membrane bound adenylate cyclase complex. The activated adenylate cyclase catalyses the conversion of ATP to cyclic AMP which, in turn, activates one of a family of cyclic AMP-dependent protein kinases. The protein kinase catalyses phosphorylation of a specific protein which, in phosphorylated form, assumes an altered state of biological activity and, thereby, effects a particular physiological response. The response is terminated by the actions of phosphodiesterase, which hydrolyses cyclic AMP, and by phosphoprotein phos-
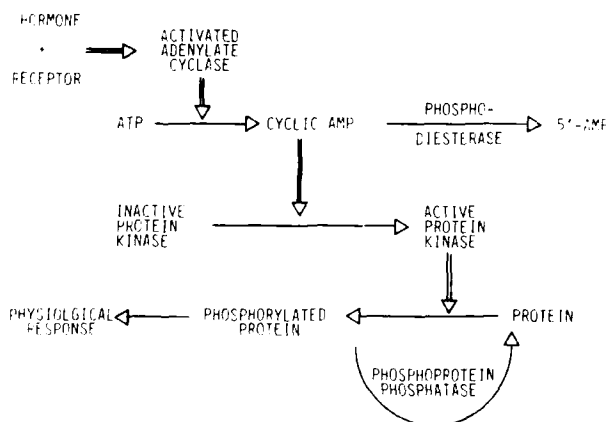

FIG 1 Sequence of events associated with cyclic AMP-mediation of hormonally induced physiological response.

phatase, which restores the phosphorylated protein to the nonphosphorylated, inactive state.

The various components of the sequence have been studied intensively in vertebrate tissues [1] and have been reported in insects [2,3]. The present account describes current understanding of octopamine- and dopamine-sensitive adenylate cyclase in insect tissues and considers the potential of this system as a target for insecticide development.

Adenylate cyclase

The proposed mechanism by which the hormonal signal is transduced across the cell membrane to alter the rate of cyclic AMP synthesis is derived principally from studies on vertebrate systems including mutant cell lines [4–6]. The results of these studies are illustrated in Fig. 2 and indicate at least three major types of protein associated with the adenylate cyclase complex. The signal, in the form of the endogenous ligand (L), binds to a specific receptor protein (R) located on the outer surface of the cell membrane. A guanyl nucleotide binding protein (G) serves as a link between the L–R complex and the third protein component of the system, a catalytic subunit (C) which catalyses the synthesis of cyclic AMP. The G-protein is an $\alpha\beta\gamma$ heterotrimer with the α-subunit containing a GTP-binding site and having GTPase activity. According to the proposed scheme for hormone-induced activation of adenylate cyclase, the binding of L to H promotes GTP binding to the α-subunit of G-protein. The α-GTP subunit dissociates from the $\beta\gamma$ complex and, by an unknown mechanism, activates C. The GTPase associated with α hydrolyses GTP and the resulting α-GDP reassociates with $\beta\gamma$ to reconstitute non-activated G-protein.

The adenylate cyclase system of insects has not been studied as extensively as that of vertebrates; however, the data that are available suggest that the mechanism of hormone-induced activation of adenylate cyclase is similar in all eukaryotic organisms (Fig. 3). Thus, magnesium and guanylnucleotide, which are required for activation of the G protein in the vertebrate system, are essential for activation of adenylate cyclase in insects [3,7]. Furthermore, as in vertebrates, the GTP-effect is dose-dependent and the non-hydrolysable analogue of GTP, 5-guanylylimidodiphosphate (Gpp(NH)p) enhances cyclic AMP production by about 20-fold [7]. The insect enzyme complex resembles that of the vertebrate system also in response to fluoride ions, forskolin and calmodulin [7].

A forskolin-insensitive adenylate cyclase has been reported in a cell line derived from spruce bud worm, *Chloristoneura fumiferana* [8]. The enzyme complex is activated by octopamine ($K_a = 50$ μM), guanyl nucleotides and sodium fluoride but forskolin does not activate, or potentiate the octopamine-mediated stimulation of enzyme activity. An adenylate cyclase that is insensitive to forskolin has been described in mammalian sperm and, because the enzyme is also insensitive to activation by sodium fluoride, Gpp(NH)p and hormones, the effect has been attributed to lack of a functional stimulatory G-protein [9–11]. However, the forskolin-insensitive enzyme from the spruce bud worm cell line is octopamine-sensitive and appears to have a functional regulatory G-protein; thus, it may differ from a normal, receptor-coupled adenylate cyclase only in lacking the forskolin receptor (S).
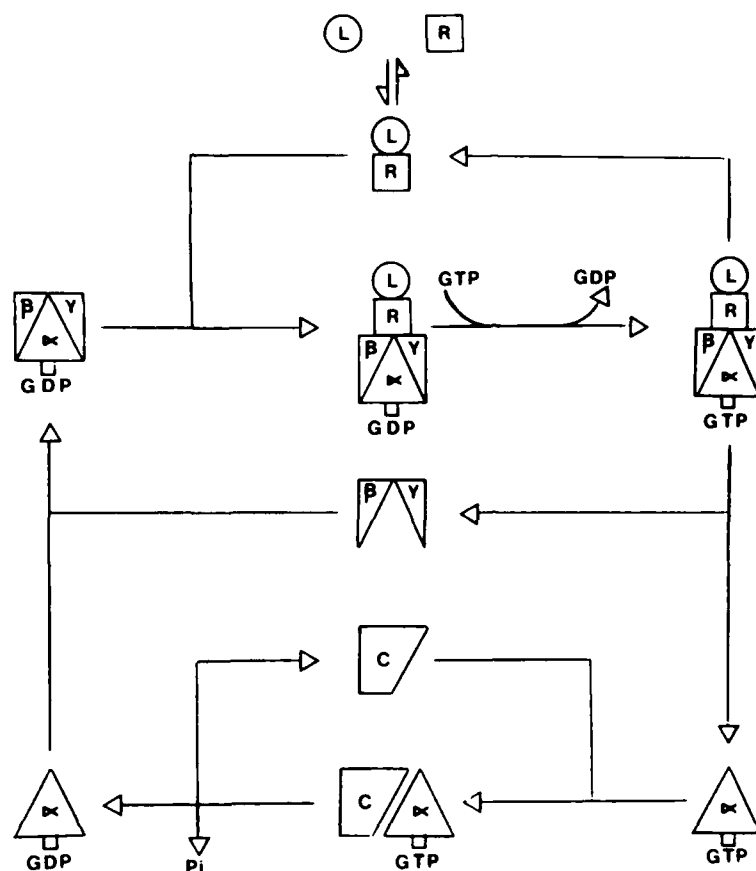
FIG 2 Proposed sequence of interactions involving the components of the adenylate cyclase complex during transduction of a stimulatory hormonal signal. Key: L. ligand; R. receptor; α, β, γ, subunits of stimulatory G-protein.

The adenylate cyclase complex that has been described for vertebrate systems is regulated also by an inhibitory guanyl nucleotide-binding G-protein [11]. The inhibitory G-protein is also an $\alpha\beta\gamma$ heterotrimer and dissociates into α- and $\beta\gamma$-subunits upon activation by GTP; however, the α-subunits of the stimulatory and inhibitory G-proteins differ in molecular weights. Ligand-mediated inhibition of adenylate cyclase activity has not yet been conclusively demonstrated in insects and, although Mn^{2+}-stimulation of adenylate cyclase is inhibited by Gpp(NH)p in wild type and rutabaga mutant *Drosophila* [12], there is no evidence to suggest that an inhibitory G-protein is present. The endotoxin of *Bordetella pertussis*, which inhibits the inhibitory G-protein [13], enhances agonist-mediated cyclic AMP production in vertebrate systems but has no effect on basal or octopamine-mediated cyclic AMP production in the spruce bud worm cell line [14]. These results suggest that the cell line lacks an inhibitory G-protein or that the inhibitory G-protein is insensitive to *pertussis* toxin. It is not known if this is a common property of the insect adenylate cyclase complex or if it is peculiar to the cell line.
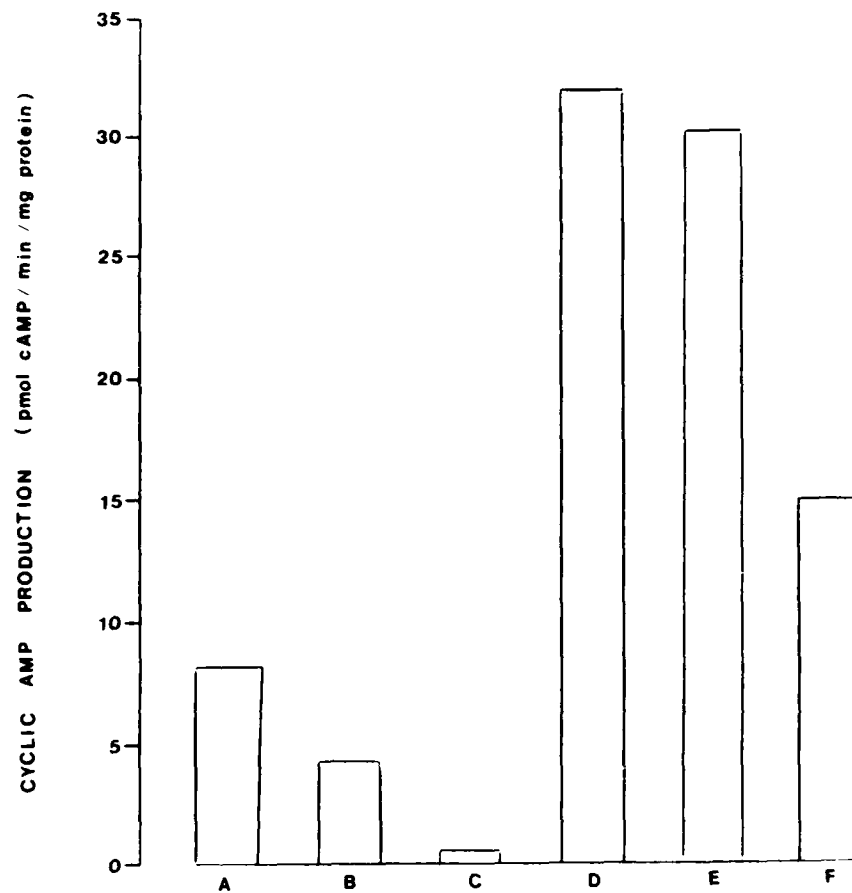
FIG 3 Factors influencing cyclic AMP production in haemocyte membrane preparation of *Periplaneta americana* (from Ref. 7). A, +GTP, +Mg^{2+}; B, +GTP, -Mg^{2+}; C, -GTP, +Mg^{2+}; D, +forskolin; E, +sodium fluoride; F, +calmodulin.

Inhibition of octopamine-mediated stimulation of adenylate cyclase by taurine and the taurine analogue guanidinoethane-sulphonic acid has been demonstrated in cockroach haemocytes [15]. However, taurine appears to exert this effect by competitive inhibition of the octopamine-stimulatory receptor site rather than through a separate inhibitory receptor. Taurine also inhibits the release of octopamine from the central nervous system [16] and, as haemolymph taurine levels increase rapidly in response to excitation, may serve as an important endogenous modulator of aminergic function in insects.

Pharmacology of octopamine-sensitive adenylate cyclase

Octopamine-sensitive adenylate cyclase activity has been described in neural and non-neural tissues from several insect species including brain and nerve cord

[17–20], corpus cardiacum [21,22], fat body [23] and haemocytes [7,24] of *Periplaneta americana*, brain [25], corpus cardiacum [26], lateral oviduct [27] and flight muscle [28] of *Locusta migratoria*, brain of *Schistocerca gregaria* [29], brain and optic lobes of *Mammestra configurata* [30–32], haemocytes of *Malacosoma disstria* [33], cultured cells of *Choristoneura fumiferana* [8], light organ of *Photinus pyralis* [34–36] and heads of *Drosophila* [37]. These studies have contributed much useful information on the pharmacological nature of the octopamine-receptor and indicate stereospecificity for the D(−) isomer and receptor preference for phenylethylamine derivatives with a hydroxylated β-carbon on the side chain and the single phenolic hydroxyl located in the *para* position. In addition, several adrenergic agonists [7,38], derivatives of formamidine [19,36,39,40], derivatives of phenyliminoimidazolidines [35] and substituted imidazothiozones [41] have been implicated as full or partial agonists of octopamine receptors. A preliminary classification of octopamine receptors in the locust extensor tibiae neuromuscular preparation recognizes three receptor classes on the basis of receptor response to a variety of potential agonists and antagonists [38]. According to the proposed classification, octopamine 1 receptors are more sensitive to clonidine than naphazoline and the converse applies to octopamine 2 receptors; octopamine 2 receptors can be further subdivided into octopamine 2A and octopamine 2B classes on the basis of the former having greater sensitivity to naphazoline than tolazoline whereas the latter are more sensitive to tolazoline than clonidine. According to these agonist criteria, the octopamine receptors that are coupled to adenylate cyclase in the American cockroach conform most closely to the octopamine 2A receptor class [42,43]. Consideration of additional classification criteria based upon interaction of octopamine receptors in the locust extensor tibiae preparation with potential antagonists, indicate that the proposed scheme is not absolute [42]. This is not surprising given differences in experimental procedures employed by different investigators, the possibility of inter-specific and inter-tissue variation and the fact that the classification is based upon drugs that have been developed for use with specific vertebrate receptors. The effects of some antagonists on octopamine-mediated elevation of cyclic AMP production in several insect tissues are summarized in Table 1. These data indicate that the most effective antagonists of octopamine-sensitive adenylate cyclase (S) are the α-adrenergic antagonist phentolamine and the anti-serotonergic/anti-

TABLE 1 Effects of some antagonists on octopamine-mediated elevations of adenylate cyclase activity

Antagonist	*Periplaneta americana*				*Locusta migratoria*	
	CC [22] [a]	NC [20]	B [43]	H [7]	Lat Ov [27]	Flt Mus [28]
Cyproheptadine	2	1	1	2	3	2
Mianserin	2	1	1	1	2	1
Phentolamine	2	1	1	2	1	1
Propranolol	3	3	–	3	–	–

Scale of antagonism: 1 indicates K_i or $IC_{50} \leq 0.1$ μM; 2 indicates K_i or $IC_{50} \leq 10.0$ μM; 3 indicates K_i or $IC_{50} \leq 1.0$ mM; 4 indicates no antagonism; –indicates not tested. CC, corpus cardiacum; NC, nerve cord; B, brain; H, haemocytes; Lat Ov, lateral oviduct; Flt Mus, flight muscles.
[a] References.

histaminergic/anti-α_2-adrenergic compound, mianserin. Cyproheptadine, which also has anti-serotonergic and anti-histaminergic properties, is a potent antagonist in most preparations, with the brain and nerve cord showing 10-times greater sensitivity than the corpus cardiacum and other peripheral tissues. Although the data are not yet sufficient to enable a definitive pharmacological characterization of octopamine-sensitive receptor(s) coupled to adenylate cyclase, it is evident that the receptor(s) is(are) pharmacologically distinct from any receptor class described previously in vertebrate systems.

Preliminary studies using [^{3}H]octopamine as a ligand indicate specific binding of octopamine to membrane preparations of *Drosophila* heads [44,45] and firefly light organ [46]. However, these reports suffer somewhat from the large tissue requirements of the assay and do not indicate if the binding site is coupled to adenylate cyclase. Mianserin, the most potent inhibitor of octopamine-mediated responses, has also been used as a radiolabelled ligand to investigate binding to putative octopamine receptors in the cockroach nerve cord [47]. These studies reveal a high affinity binding site ($K_d = 39.6$ nM and $B_{max} = 0.8$ fmol μg^{-1}) and a low-affinity binding site ($K_d = 648.9$ nM and $B_{max} = 5.9$ fmol μg^{-1}). A slope of 0.6 was determined from a Hill plot, thereby suggesting negative cooperativity between the binding sites. The demonstration that Gpp(NH)p eliminates the high affinity binding site as indicated by Scatchard analysis, together with similarities in the relative effectiveness of antagonists to inhibit octopamine-mediated production of cyclic AMP and compete with [^{3}H]mianserin for binding sites, suggests that a mianserin-binding site is coupled to the stimulatory G-protein of an adenylate cyclase complex [47]. The possible conversion of high-affinity binding sites to a low-affinity state in the presence of Gpp(NH)p may be similar to the conversion of D_2 receptors from high to low affinity states in the presence of NaCl and guanyl nucleotides [48].

Pharmacology of dopamine-sensitive adenylate cyclase

Dopamine-sensitive adenylate cyclase has been identified in the nervous tissue of several insects [17,18,30,31,49-51] and it is probable that some of the dopamine-mediated processes that have been described in peripheral tissues [28,52-58] are also expressed through the mediation of cyclic AMP. The dopamine receptor that is coupled with adenylate cyclase has not been studied extensively in insects and detailed information on the pharmacological nature of the receptor is restricted to a few studies on the cockroach [42]. These studies rely on drugs that have been developed to distinguish between the two major classes of dopamine receptor in vertebrates; namely, the D_1 receptor which is positively coupled to adenylate cyclase and the D_2 receptor which is either negatively coupled to the enzyme complex or is cyclase independent [59]. Some of the dopamine agonists used to characterize the insect receptor are illustrated in Fig. 4.

ADTN and epinine activate D_1 receptors in vertebrates and the fact that these compounds also enhance cyclic AMP production in cockroach brain, suggests the presence of a D_1 receptor in this tissue [60]. However, SKF 38393, which is also a strong D_1 agonist in vertebrates, has no effect on cyclic AMP production in the cockroach brain, whereas the potent vertebrate D_2 agonist, LY 171555, stimulates cyclic AMP production [60]. Thus, the studies with potential agonists indicate that
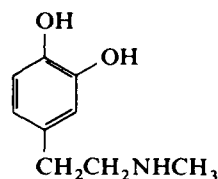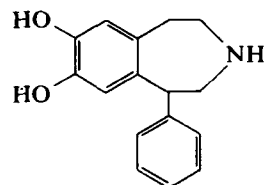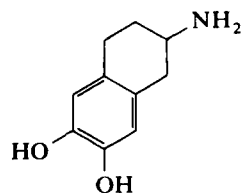
FIG 4   Structures of some dopamine agonists.

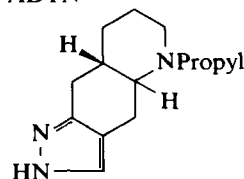the dopamine receptor in insect brain is pharmacologically distinct from those that have been characterized in vertebrate tissues and, therefore, comprise a new class of dopamine receptor. This conclusion is substantiated by studies with various antagonists of vertebrate dopamine receptors. The greatest inhibition of dopamine-mediated enhancement of cyclic AMP production in cockroach brain was observed with pifluthixol, cis-flupenthixol and (+)-butaclamol which, in vertebrates, are antagonists of both D_1 and D_2 receptors. However, marked inhibition was observed also with the selective D_1 antagonists SCH 23390 and SKF 83566, the D_2 antagonist spiperone and the anti-serotonergic/anti-histaminergic compound, cyproheptadine [60]. Scatchard analysis of saturation data from binding studies using [^{3}H]pifluthixol as a ligand of dopamine receptors in the insect brain indicate a single binding site with a K_d of 0.35 nM and a B_{max} of 1.4 pmol mg^{-1} [61]. However, the biphasic nature of the dose–response curve for dopamine-mediated production of cyclic AMP [30,62] may indicate negative cooperativity between two or more receptor types; a conclusion that is supported by the nonlinear nature of an Eadie-Hofstee plot of the same data [62].

Implications for insecticide discovery

Octopamine and dopamine are intimately involved in the mediation of several important physiological processes in insects [63,64], therefore, perturbation of octopaminergic or dopaminergic function is likely to affect insects adversely. The receptors on target cells to which the monoamines bind represent an obvious potential site of attack and there are strong indications that this approach may lead to the development of new classes of insecticides to which there is no endogenous resistance within pest populations. Several derivatives of formamidines bind to octopamine receptors, affect monoamine-mediated production of cyclic AMP [19,36] and induce adverse behavioural changes in treated insects. The formamidines bind also to dopamine and 5-hydroxytryptamine receptors in insect nervous tissue [51]

and also inhibit the major enzyme of monoamine degradation in insects, N-acetyltransferase [65], therefore, the insecticidal effects cannot be attributed entirely to interaction of the compound with the octopamine receptor. Nonetheless, it seems probable that at least some of the observed behavioural effects are due to agonism or partial agonism of octopamine-sensitive adenylate cyclase.

Phenyliminoimidazolidines were also identified as agonists of the octopamine receptor (see section on octopamine-sensitive adenylate cyclase) and a series of substituted derivatives of clonidine indicate excellent capacity to elevate cyclic AMP levels in the firefly light organ and disrupt feeding in larvae of the tobacco horn worm [35]. The phenylimidazolines, naphthazoline and tolazoline are also effective agonists of the octopamine receptor and derivatives have been used with some success for acarine control [66]. Several substituted imidazothiozoles are also capable of stimulating adenylate cyclase activity in locus CNS [41] but their effectiveness in controlling insect pests has not been reported.

By contrast, few if any compounds directed specifically against the dopamine or serotonin (5-HT) receptors have been developed. These neuroeffectors also play important roles in many aspects of insect physiology and there is considerable merit in pursuing strategies to perturb dopaminergic or serotonergic function in insecticide development.

The prospects of developing useful insecticides directed against monoamine targets is obviously enhanced if the possibility of effects on non-target species is lessened. The demonstrations that the insect dopamine receptor is pharmacologically distinct from those of vertebrate species and that the octopamine receptors comprise a new pharmacological class of monoamine receptor suggest that the development of insect-specific insecticides directed against these targets may be possible. However, it should be recognized that the monoamine receptor is not the only locus at which to attack the monoaminergic system. Agents that interfere with normal routes of monoamine synthesis or degradation are also likely to disrupt monoaminergic function, and warrant intensive investigation.

References

1 Kebabian, J.W. and Nathanson, J.A. (eds.). (1982) Handbook of Experimental Pharmacology, Vols. I and II. Springer-Verlag, New York.
2 Bodnaryk, R.P. (1982) Biogenic amine-sensitive adenylate cyclases in insects. Insect Biochem. 12, 1–6.
3 Bodnaryk, R.P. Cyclic Nucleotides. (1985) In: Endocrinology of Insects (R.G.H. Downer and H. Laufer, eds.), pp. 567–614. Alan R. Liss, NY.
4 Ross, E.M. and Gilman, A.G. (1980) Biochemical properties of hormone-sensitive adenylate cyclase. Ann. Rev. Biochem. 49, 533–564.
5 Hanoune, J., Henry, D. and Stengel, D. (1985) The adenylate cyclase system. In: Regulatory Peptides in Digestive, Nervous and Endocrine Systems (M.J.M. Lewin and S. Bonfils, eds.), pp. 123–132. Elsevier, Amsterdam.
6 Casperson, G.F. and Bourne, H.R. (1987) Biochemical and molecular genetic analysis of hormone-sensitive adenylyl cyclase. Ann. Rev. Pharmacol. Toxicol. 27, 371–384.
7 Orr, G.L., Gole, J.W. and Downer, R.G.H. (1985) Characterisation of an octopamine-sensitive adenylate cyclase in haemocyte membrane fragments of the American cockroach, Periplaneta americana L. Insect Biochem. 15, 695–701.
8 Gole, J.W.D., Orr, G.L. and Downer, R.G.H. (1987) Forskolin-insensitive adenylate cyclase in cultured cells of Choristoneura fumiferana (Insecta). Biochem. Biophys. Res. Commun. 145, 1192–1197.

9 Stengel, D. and Hanoune, (1981) The catalytic unit of ram sperm adenylate cyclase can be activated through the guanine nucleotide regulatory component and prostaglandin receptors of human erythrocytes. J. Biol. Chem. 256, 5394–5398.

10 Stengel, D., Guenet, L., Desmier, M., Insel, P. and Hanoune, J. (1982) Forskolin requires more than the catalytic unit to activate adenylate cyclase. Mol. Cell. Endocrinol. 28, 681–690.

11 Daly, J.W. (1984) Forskolin, adenylate cyclase and cell physiology: an overview. Adv. Cyc. Nucleotide Protein Phosphor. Res. 17, 81–89.

12 Livingstone, M.S., Sziber, P.P. and Quinn, W.G. (1984) Loss of calcium/calmodulin responsiveness in adenyl cyclase of rutabaga, a *Drosophila* learning mutant. Cell 37, 205–215.

13 Codina, J., Hildebrandt, J., Iyengar, R., Birnbaumer, L., Sekura, R.D. and Manclark, C.R. (1983) Pertussis toxin substrate, the putative N_i component of adenylate cyclases, is an $\alpha\beta$ heterodimer regulated by guanine nucleotide and magnesium. Proc. Natl. Acad. Sci. USA 80, 4276–4280.

14 Orr, G.L., Gole, J.W.D., Gupta, J. and Downer, R.G.H. (1988) Modulation of octopamine-mediated production of cyclic AMP by phorbol ester-sensitive protein kinase C in an insect cell line. Biochim. Biophys. Acta, in press.

15 Hayakawa, Y., Downer, R.G.H. and Bodnaryk, R.P. (1987) Taurine inhibits octopamine-stimulated cAMP production in cockroach haemocytes. Biochim. Biophys. Acta 929, 117–120.

16 Hayakawa, Y., Bodnaryk, R.P. and Downer, R.G.H. (1987) Effect of taurine on excitation-induced changes in brain and hemolymph octopamine levels in *Periplaneta americana*. Arch. Insect Biochem. Physiol. 5, 129–137.

17 Nathanson, J.A. and Greengard, P. (1973) Octopamine-sensitive adenylate cyclase: evidence for a biological role of octopamine in nervous tissue. Science 180, 308–310.

18 Harmar, A.J. and Horn, A.S. (1977) Octopamine-sensitive adenylate cyclase in cockroach brain: effects of agonists, antagonists and guanyl nucleotides. Mol. Pharmacol. 13, 512–520.

19 Gole, J.W.D., Orr, G.L. and Downer, R.G.H. (1983) Interaction of formamidines with octopamine-sensitive adenylate cyclase receptor in the nerve cord of *Periplaneta americana*. Life Sci. 32, 2939–2947.

20 Downer, R.G.H., Gole, J.W.D. and Orr, G.L. (1985) Interaction of formamidines with octopamine-, dopamine- and 5-hydroxytryptamine-sensitive adenylate cyclase in the nerve cord of *Periplaneta americana*. Pestic. Sci. 16, 472–478.

21 Downer, R.G.H., Orr, G.L., Gole, J.W.D. and Orchard, I. (1984) The role octopamine and cyclic AMP in regulating hormone release from corpora cardiaca of the American cockroach. J. Insect Physiol. 30, 457–462.

22 Gole, J.W.D., Orr, G.L. and Downer, R.G.H. (1987) Pharmacology of octopamine-, dopamine- and 5-hydroxytryptamine-stimulated cyclic AMP accumulation in the corpus cardiacum of the American cockroach, *Periplaneta americana* L. Arch. Insect Biochem. Physiol. 5, 119–128.

23 Gole, J.W.D. and Downer, R.G.H. (1979) Elevation of adenosine 3′,5′-monophosphate by octopamine in fat body of the American cockroach, *Periplaneta americana*. Comp. Biochem. Physiol. 64C, 223–226.

24 Gole, J.W.D., Orr, G.L. and Downer, R.G.H. (1987) Octopamine-mediated elevation of cyclic AMP in haemocytes of the American cockroach, *Periplaneta americana*. Can. J. Zool. 65, 1509–1514.

25 David, J.C. and Fuzeau-Braesch, S. (1979) Amines biogenes et AMP cyclique chez *Locusta migratoria*: recherche de récepteur à octopamine. C.R. Acad. Sci. Paris 288, 1207–1210.

26 Orchard, I., Loughton, B.G., Gole, J.W.D. and Downer, R.G.H. (1983) Synaptic transmission elevates adenosine 3′,5′-monophosphate (cyclic AMP) in locust neurosecretory cells. Brain Res. 259, 152–155.

264

27 Orchard, I. and Lange, A. (1986) Pharmacological profile of octopamine receptors on the lateral oviducts of the locust, *Locusta migratoria*. J. Insect Physiol. 32, 741–745.

28 Lafon-Cazal, M. and Bockaert, J. (1985) Pharmacological characterization of octopamine-sensitive adenylate cyclase in the flight muscle of *Locusta migratoria* L. Eur. J. Pharmacol. 119, 53–59.

29 Kilpatrick, A.T., Vaughan, P.F.T. and Donnellan, J.F. (1982) The effect of guanyl nucleotides on the monoamine-sensitive adenylate cyclase of *Schistocerca gregaria* nervous tissue. Insect Biochem. 12, 393–397.

30 Bodnaryk, R.P. (1979) Basal dopamine and octopamine-stimulated adenylate cyclase activity in the brain of the moth. *Mamestra configurata* during its metamorphosis. J. Neurochem. 33, 275–282.

31 Bodnaryk, R.P. (1979) Identification of specific dopamine and octopamine-sensitive adenylate cyclase in the brain of *Mamestra configurata* Wlk. Insect Biochem. 9, 155–162.

32 Bodnaryk, R.P. (1979) Characterization of an octopamine-sensitive adenylate cyclase from insect brain (*Mamestra configurata* Wlk.). Can. J. Biochem. Physiol. 57, 226–232.

33 Gole, J.W.D., Downer, R.G.H. and Sohi, S.S. (1982) Octopamine-sensitive adenylate cyclase in haemocytes of the forest tent caterpillar, *Malacosoma disstria* Hubner (Lepidoptera, Lassiocampidae). Can. J. Zool. 60, 825–829.

34 Nathanson, J.A. (1979) Octopamine receptors: Adenosine $3',5'$-monophosphate and neural control of firefly flashing. Science 203, 65–68.

35 Nathanson, J.A. (1985) Phenyliminoimidazolines: characterization of a class of potent agonists of octopamine-sensitive adenylate cyclase and their use in understanding the pharmacology of octopamine receptors. Mol. Pharmacol. 28, 254–258.

36 Nathanson, J.A. and Hunnicutt, E.J. (1981) N-demethyl-chlordimeform: a potent partial agonist of octopamine-sensitive adenylate cyclase. Mol. Pharmacol. 20, 68–75.

37 Uzzan, A. and Dudai, Y. (1982) Aminergic receptors in *Drosophila melanogaster*: responsiveness of adenylate cyclase to putative neurotransmitters. J. Neurochem. 38, 1542–1550.

38 Evans, P.D. (1981) Multiple receptor types for octopamine in the locust. J. Physiol. (Lond.) 318, 99–122.

39 Evans, P.D. and Gee, J.D. (1980) Action of formamidine pesticides on octopamine receptors. Nature 287, 60–62.

40 Hollingworth, R.M. and Murdock, L.L. (1980) Formamidine pesticides: octopamine-like action in a firefly. Science 208, 74–76.

41 Evans, P.D. and Davenport, A.P. (1986) The action of pesticides on biogenic amine receptors and second messenger systems in insects. In: Neuropharmacology and Pesticide Action (M.G. Ford, G.G. Lunt, R.C. Reay and P.N.R. Usherwood, eds.), pp. 315–341. Ellis Horwood, Chichester, England.

42 Downer, R.G.H. (1988) Octopamine, dopamine and 5-hydroxytryptamine in the cockroach nervous system. In: Cockroaches as Models in Biomedical Research: Neurophysiology (I. Huber, P. Masler, B. Rao, eds.), in press, CRC Press, Boca Raton, FL.

43 Downer, R.G.H., Gole, J.W.D., Martin, R.J. and Orr, G.L. (1988) Pharmacological characteristics of octopamine-sensitive adenylate cyclase and N-acetyl octopamine transferase in insects. In: Trace Amines: Comparative and Clinical Neurobiology (A.A. Boulton, A.V. Juorio, R.G.H. Downer, eds.), In press, Humana Press, Clifton, NJ.

44 Dudai, Y. (1982) High-affinity octopamine receptors revealed in *Drosophila* by binding of [3H]-octopamine. Neurosci. Lett. 28, 163–167.

45 Dudai, Y. and Zvi, S. (1982) Aminergic receptors in *Drosophila melanogaster*: properties of [3H]-dihydroergocryptine binding sites. J. Neurochem. 38, 1551–1558.

46 Hashenzadeh, M., Hollingworth, R.M. and Voliva, A. (1985) Receptors for [3H]-octopamine in the adult firefly light organ. Life Sci. 37, 433–440.

47 Minhas, N., Gole, J.W.D., Orr, G.L. and Downer, R.G.H. (1987) Pharmacology of [3H]-mianserin binding in the nerve cord of the American cockroach, *Periplaneta americana*. Arch. Insect Biochem. Physiol. 6, 191–201.

48 Grigoriadis, D. and Seeman, P. (1985) Complete conversion of brain D_2-dopamine receptors from the high- to low-affinity state for dopamine agonists using sodium ions and guanine nucleotide. J. Neurochem. 44, 1925–1935.

49 Hiripi, L. and Rozsa, K.S. (1973) Fluorometric determination of 5-hydroxytryptamine and catecholamines in the nervous system and heart of Locusta migratoria migratoides. J. Insect Physiol. 19, 1481–1485.

50 Combest, W.L., Sheridan, D. and Gilbert, L.I. (1985) The brain adenylate cyclase system of the tobacco hornworm, Manduca sexta: putative control by biogenic amines. Insect Biochem. 15, 579–588.

51 Downer, R.G.H., Gole, J.W.D., Martin, R.J., Milton, G.W.A., Notman, H.J. and Orr, G.L. (1988) Distribution, pharmacology, and metabolism of dopamine in the system of the American cockroach, Periplaneta americana. Int. Symp. on Catecholamines, Jerusalem; in press.

52 Beard, R.L. (1960) Electrographic recording of foregut activity in larvae of Galleria mellonella. Ann. Entomol. Soc. Amer. 54, 346–350.

53 Freeman, M.A. (1966) The effect of drugs on the alimentary canal of the African migratory locust Locusta migratoria. Comp. Biochem. Physiol. 17, 755–764.

54 Robertson, M.A. (1975) The innervation of the salivary gland of the moth, Manduca sexta: evidence that dopamine is the transmitter. J. Exp. Biol. 63, 413–419.

55 Samaranayaka, M. (1976) Possible involvement of monoamines in the release of adipokinetic hormones in the locust Schistocerca gregaria. J. Exp. Biol. 65, 415–425.

56 Ginsborg, B.L. and House, C.R. (1976) The response to nerve stimulation of the salivary gland of Nauphoeta cinerea Olivier. J. Physiol. 262, 477–487.

57 Finlayson, L.H. and Osborne, M.P. (1977) Effect of cyclic AMP and other compounds on electrical activity of neurohaemal tissue Carausius. J. Insect Physiol. 23, 429–434.

58 House, C.R. and Ginsborg, B.L. (1982) Properties of dopamine receptors at a neuroglandular synapse. In: Neuropharmacology of Insects, Ciba Foundation Symposium 88, pp. 32–47. Pitman, London.

59 Seeman, P. (1980) Brain dopamine receptors. Pharmacol. Rev. 32, 229–313.

60 Orr, G.L., Gole, J.W.D., Notman, H.J. and Downer, R.G.H. (1987) Pharmacological characterisation of the dopamine-sensitive adenylate cyclase in cockroach brain: evidence for a distinct dopamine receptor. Life Sci. 41, 2705–2715.

61 Notman, J.J. and Downer, R.G.H. (1987) Binding of [^{3}H]pifluthixol, a dopamine antagonist, in the brain of the American cockroach, Periplaneta americana. Insect Biochem. 17, 587–590.

62 Orr, G.L., Gole, J.W.D., Notman, H.J. and Downer, R.G.H. (1988) The regulation of basal and dopamine-sensitive adenylate cyclase by salts of monovalent cations in brain of the American cockroach, Periplaneta americana L. Insect Biochem. 18, 79–86.

63 Evans, P.D. Octopamine. In: Comprehensive Insect Physiology, Biochemistry and Pharmacology, Vol. 11 (G.A. Kerkut, L.I. Gilbert, eds.), pp. 499–530. Pergamon Press, Oxford.

64 Brown, C.S. and Nestler, C. (1985) Catecholamines and indolalkylamines. In: Comprehensive Insect Physiology, Biochemistry and Pharmacology, Vol. 11 (G.A. Kerkut, L.I. Gilbert eds.), pp. 435–497. Pergamon Press, Oxford.

65 Downer, R.G.H. and Martin, R.J. (1987) N-acetylation of octopamine: a potential target for insecticide development. In: Sites of Action for Neurotoxic Pesticides (R.M. Hollingworth, M.B. Green, eds.), pp. 202–210. ACS Symposium Series 356. Washington, DC.

66 Hollingworth, R.M., Johnstone, E.M. and Wright, N. (1984) Aspects of the biochemistry and toxicology of octopamine in Arthropods. American Chemical Society Symposium #225, 103–125. ACS, Washington.

Molecular neurobiological approaches to receptors and ion channels

CHAPTER 20

Molecular and cellular approaches to neurotoxicology: past, present and future

Toshio Narahashi

Department of Pharmacology, Northwestern University Medical School,
303 East Chicago Avenue, Chicago, IL 60611, U.S.A.

Introduction

The mechanism of action of toxic substances on the nervous system has been studied for many years, yet it was not until the 1970s and '80s that advanced approaches and techniques were developed to allow us to study the toxic action at the molecular and cellular levels. The present paper is concerned mainly with neurotoxicology of insecticides, and represents some highlights of the studies performed in our laboratories during the past 39 years. Emphasis is placed on the rationale of development of the study rather than mere historical aspects or technical details.

Early studies of DDT and pyrethrins

In an attempt to develop an in vitro method to assay the effect of insecticides, Lowenstein [1] in as early as 1942 discovered massive discharges in the insect nervous system poisoned with pyrethrum extract. As a variety of synthetic insecticides were developed during and shortly after World War II, the toxicology of insecticide became a hot subject of investigations. However, major efforts were focused on the metabolic degradation of insecticides and the inhibition of cholinesterases by organophosphates and carbamates, and only a handful of investigators were studying the mechanism of action of insecticides on the nervous system. In 1946, Roeder and Weiant [2] found that certain sensory neurons of cockroach legs were very sensitive to DDT, generating trains of impulses. Repetitive discharges were also observed by Welsh and Gordon [3] in arthropod nerves poisoned with DDT and other insecticides. When poisoned with DDT or pyrethrins, insect peripheral nerve fibers produced repetitive discharges in response to a single stimulus [4]. However, nothing was known about the mechanism by which DDT and pyrethrins caused repetitive discharges to be produced.

Discovery of depolarizing after-potential in DDT

While studying the effect of DDT on synaptic transmission of cockroach ganglion, we discovered that the postsynaptic response was greatly augmented and that the extracellularly recorded action potentials arising from individual nerve fibers were followed by a large depolarizing (negative) after-potential [5]. The increase in depolarizing after-potential by DDT was later demonstrated unequivocally using intracellular microelectrode recording techniques [6]. It was indeed shown that the increased depolarizing after-potential, upon reaching the threshold level, led to the generation of repetitive after-discharges in cockroach giant axons poisoned with DDT [7] or allethrin [8] (Fig. 1). The next question to be resolved was how the depolarizing after-potential was elevated by these insecticides. Voltage clamp experiments gave the straightforward answer.

Voltage clamp studies

The first voltage clamp study with DDT was performed by Narahashi and Haas [9,10] using lobster giant axons, and a similar study with allethrin was performed by Narahashi and Anderson [11] using squid giant axons. Both insecticides caused a prolonged sodium current to flow (Fig. 2), and this effect accounts for the increase in depolarizing after-potential. More detailed voltage clamp analyses of the action of DDT and pyrethroids were then pursued by us and several other investigators [12–23].

Two types of pyrethroids

Inspection of the records in Fig. 2 reveals that the sodium current is prolonged by allethrin not only during a depolarizing pulse but also after termination of the pulse
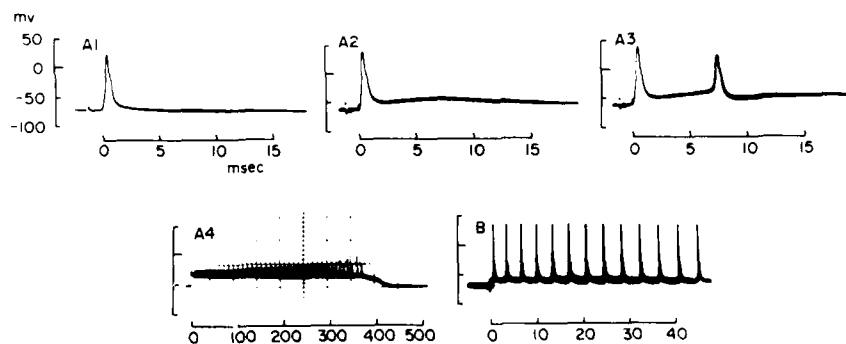

FIG 1 Increase in depolarizing after-potential and generation of repetitive after-discharges in lobster giant axons exposed to 500 μM DDT. A1: control action potential evoked by a single stimulus before DDT application; A2: 36 min in DDT, increase in depolarizing after-potential; A3: 42 min in DDT, after-discharges superimposed on the increased depolarizing after-potential; A4, 78 min in DDT, repetitive after-discharges superimposed on a prolonged, plateau action potential. The initial spike is too faint to be reproduced due to slow sweep. B: another axon, repetitive after-discharges superimposed on an increased depolarizing after-potential, 9 min in DDT (from Narahashi and Haas [10]).
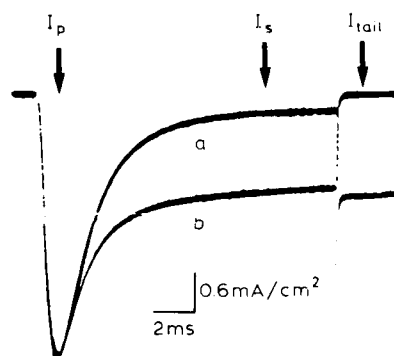
FIG 2   Membrane sodium currents in a squid giant axon before (a) and during (b) internal perfusion with 1 μM (+)-*trans* allethrin. Sodium current associated with a step depolarization from -100 mV to -20 mV was recorded after cesium and tetramethylammonium had been substituted for internal K^+ and external K^+, respectively, to eliminate the potassium current. In the control record (a), the peak sodium current (I_p) is followed by a small slow sodium current (I_s) during a depolarizing pulse, and the tail current (I_{tail}) associated with step repolarization decays quickly. In the presence of allethrin (b), I_p remains unchanged while I_s is greatly increased in amplitude. I_{tail} is also increased in amplitude and decays very slowly (from Narahashi and Lund [76]).

(tail current). Type II pyrethroids which possess a cyano group at the α position also exerted similar effects on the sodium current, but the current prolongation was much greater than that caused by type I pyrethroids which lack the α cyano group. However, the difference between the two types of pyrethroids is by no means clear-cut. In fact all the pyrethroids along with DDT and its derivatives so far examined, could be arranged in a continuous spectrum based on the time constant of the decay of the tail current. DDT with a very short time constant and deltamethrin with a very long time constant [24]. In the presence of a type II pyrethroid, the potential dependence of the sodium channel activation was shifted in the direction of hyperpolarization. This change, together with a prolongation of sodium current, causes depolarization of the membrane. The important point to be stressed here is the fact that both type I and type II pyrethroids interact with the sodium channel. It is of interest to see that DDT and type I pyrethroids have very similar effects despite the drastic difference in their chemical structures.

Single sodium channel studies of pyrethroid action

The prolonged sodium channel current in the axon poisoned with pyrethroids and DDT accounts for the increase in depolarizing after-potential and membrane depolarization. However, the sodium current recorded from an axon is an algebreic sum of currents passing through a large number of sodium channels in the membrane. Thus the next step was to study the activity of individual sodiun channels as affected by the insecticides. Patch clamp single channel recording techniques originally developed by Neher and Sakmann [25] and improved by Hamill et al. [26] were applied to a cultured N1E-115 neuroblastoma cell line.

Tetramethrin, a type I pyrethroid, drastically prolonged the open time of individual sodium channels without changing the single channel conductance [27]. The sodium channel population in the membrane patch exposed to tetramethrin could be divided into two groups, one showing an average open time of 1.8 ms and the other an average open time of 17 ms. The former is very close to that of normal sodium channels (1.7 ms). Therefore, those channels with the short open time are unmodified by tetramethrin and those with the long open time are modified, suggesting that individual sodium channels are modified by tetramethrin in an all-or-none manner. Whereas the normal sodium channels opened more frequently at the beginning of a depolarizing pulse, the tetramethrin modified channels could open at any time during a prolonged depolarizing pulse (see Fig. 3). Such late openings account for the prolonged sodium current recorded from the tetramethrin poisoned cell or axon. The modified channels could also be kept open after termination of a depolarizing pulse. Such openings would generate a large and prolonged tail current.

Type II pyrethroids such as deltamethrin and fenvalerate also prolonged the open time of individual sodium channels [28,29]. With the mean open time of 1.1 s, the prolongation was more marked than that observed in tetramethrin modified chan-
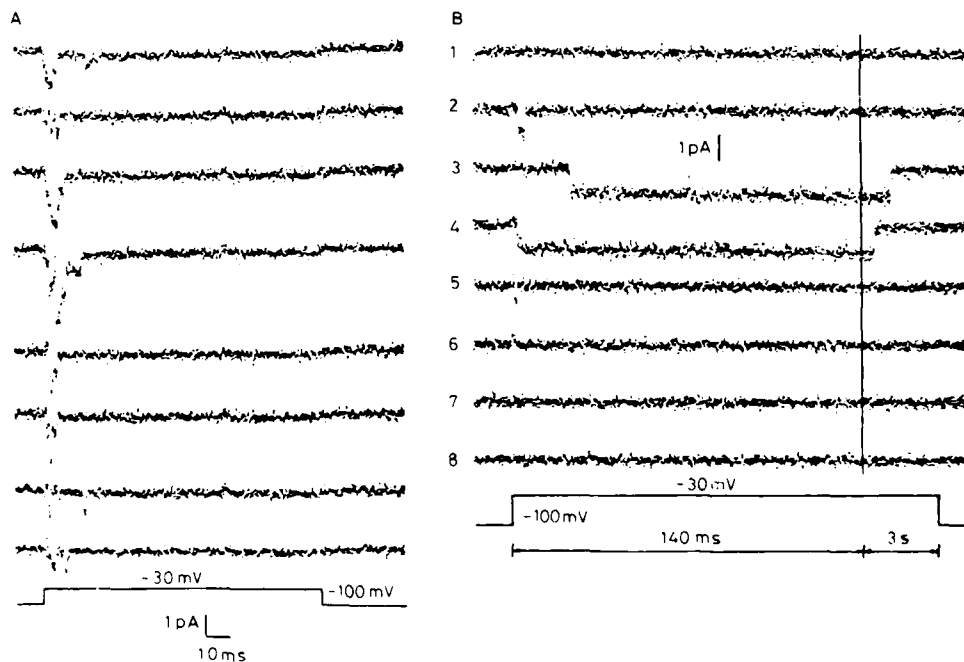

FIG 3   Effects of deltamethrin on single sodium channel currents. A: currents from a cell before drug treatment in response to 140 ms depolarizing steps from a holding potential of -100 to -30 mV with a 3 s interpulse interval. Records were taken at a rate of 100 μs per point. B: currents after exposure to 10 μM deltamethrin. The membrane patch was depolarized for 3140 ms from a holding potential of -100 to 30 mV. The interpulse interval was 3 s. The time scale changes during the voltage step as indicated in the Figure. During the first 140 ms, data records were taken at a rate of 100 μs per point and after the vertical line records were taken at a rate of 10 ms per point (from Chinn and Narahashi [28]).
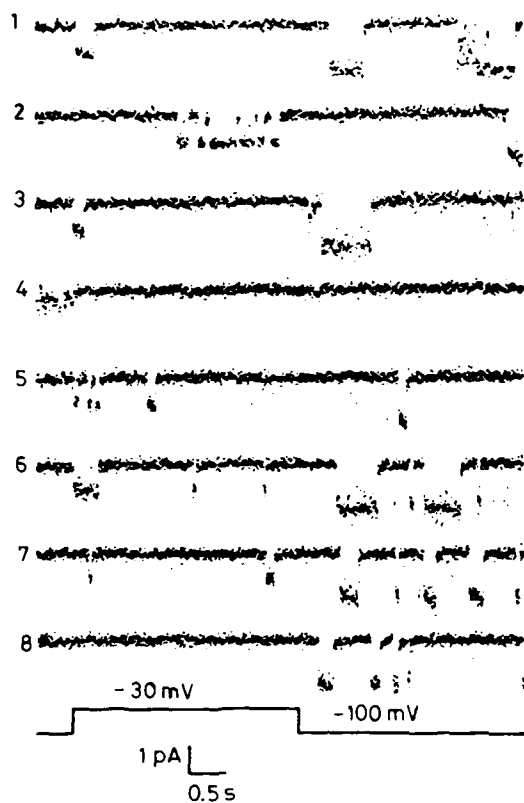
FIG 4 Sodium channel openings after a voltage pulse in the presence of 10 μM deltamethrin. A series of consecutive current traces taken from a membrane patch depolarized from a holding potential of -100 to -30 mV for 3 s and then repolarized for 6 s (only a 3 s period after each voltage step is shown). Data were taken at a rate of 10 ms per point (from Chinn and Narahashi [28]).

nels (Fig. 3). The modified channels that were open during a depolarizing pulse were kept open after termination of the pulse. Channel openings were frequently observed even after termination of a depolarizing pulse (Fig. 4). These openings during and after a depolarizing pulse are responsible for the extremely prolonged sodium current during a pulse and for the sodium tail current after the pulse. Single channel conductance was not affected by type II pyrethroids. These results are interpreted as indicating that type II pyrethroids stabilize a variety of channel states such as closed and open states by reducing the transition rates between them [28].

Affinity of pyrethroids for open and closed sodium channels

In our earlier study with squid giant axons, it was suggested that tetramethrin bound to both open and closed sodium channels [16]. This question was further pursued using squid axons and neuroblastoma cells.
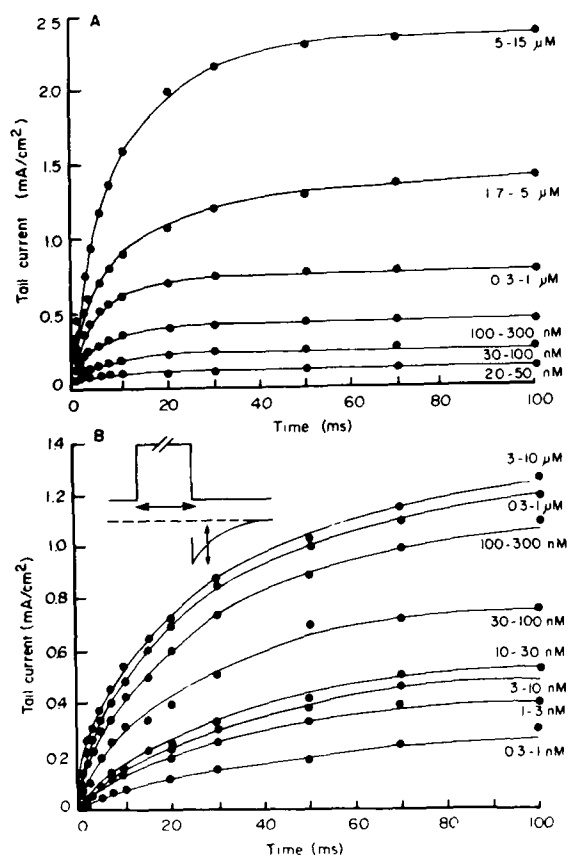
274

FIG 5 The amplitude of the phenothrin (A)- or cyphenothrin (B)-induced sodium tail current as a function of the duration of depolarizing pulse at several concentrations of the pyrethroids in squid giant axons. Inset shows the pulse protocol used and applies to both A and B (from the Weille et al. [30]).

If pyrethroids modified the sodium channel only in its closed configuration, the rate at which the pyrethroid-induced sodium tail current developed during depolarization would represent the kinetics of opening of the modified sodium channel and should be independent of the concentration of pyrethroids. The development of the pyrethroid-induced tail current was measured as a function of the duration of depolarizing pulse in the presence of various concentrations of phenothrin (Fig. 5A) and cyphenothrin (Fig. 5B) [30]. Each curve could be fitted by a single exponential function, and the time constant is plotted against the pyrethroid concentration in double logarithmic scale in Fig. 6. Two examples of each for phenothrin, cyphenothrin and deltamethrin are shown. The time constant is either independent of the pyrethroid concentration (one case of phenothrin and deltamethrin) or only slightly dependent on the concentration with a slope of approximately 0.12. indicating that the process is close to first order. These data clearly show that a large fraction of sodium channels is modified in the closed state and that, in addition, a small fraction of channels is modified in the open state during depolarization.
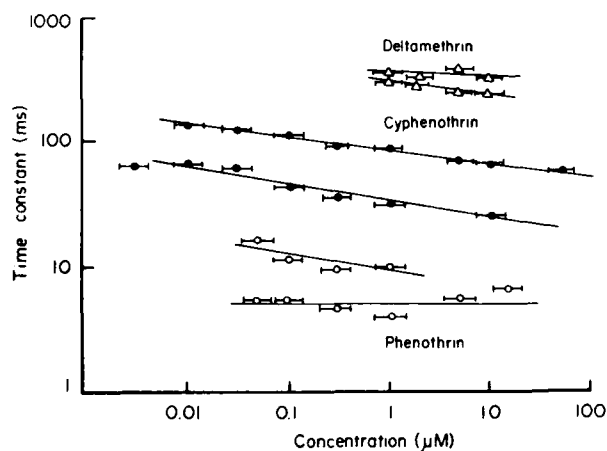
FIG 6 Time constant of the development of tail current amplitude as a function of the duration of depolarizing pulse at several concentrations of phenothrin, cyphenothrin and deltamethrin. Squid giant axons. Double exponential scales (from de Weille et al. [30]).

The open channel modification by pyrethroids may be limited by the process of sodium channel inactivation. In the absence of the inactivation, the degree of open channel modification would be expected to increase. This was shown to be the case in the axon in which the sodium channel inactivation had been removed by internal perfusion of pronase which destroyed the inactivation gate [30]. The time constant of the tail current development during depolarization became more dependent on the pyrethroid concentration after pronase treatment with a slope of 0.25 for both phenothrin and cyphenothrin (Fig. 7). However, the kinetics are still far from second order which calls for a slope of unity in the Hill plot of Fig. 7. Thus, it was
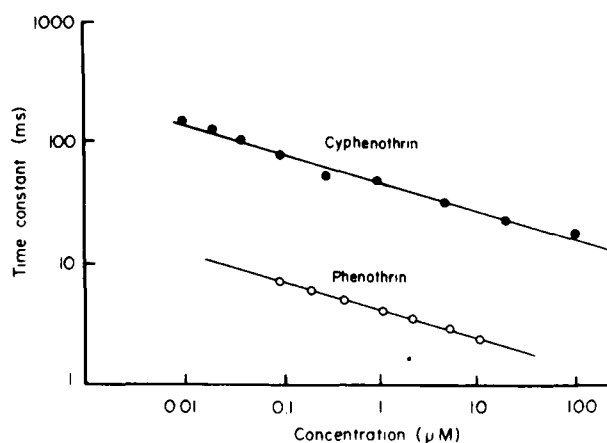

FIG 7 Time constant of development of the phenothrin- and cyphenothrin-induced sodium tail currents as a function of the duration of depolarizing pulse at several concentrations of the pyrethroids after removal of inactivation by pronase treatment. Squid giant axons. Double logarithmic scales (from de Weille et al. [30]).

concluded that pyrethroids modify the sodium channel largely in its closed configuration.

The above conclusion was also supported by single sodium channel experiments with neuroblastoma cells poisoned with fenvalerate [29]. It would be predicted that, if the modification occurred only in the open state, the probability of modification should depend on the open time. A depolarizing pulse lasting only 5 ms was applied to the membrane patch to open the sodium channels. Normal channels opened and closed at various moments during the pulse. Modified channels also opened during the pulse but were kept open for various periods of time after termination of the short pulse. If the channels were modified only in their open state, the probability of their being modified would be low when they opened toward the end of the depolarizing pulse, because they had only a brief time period in which to become modified. However, the channels that opened within 1 ms before the termination of the pulse showed the same probability of modification as those that were kept open for 2 to 4 times longer. Thus this observation also lends support to the notion that fenvalerate modification of the sodium channels occurs largely in their closed state.

Properties of pyrethroid modified open channels

The results described in preceding sections clearly show that the gating mechanism of sodium channel is impaired by both type I and type II pyrethroids. A question arises as to whether the properties of the open modified channel are altered. Two properties of open channels are important and worthy of examination in the presence of pyrethroids. One is ionic selectivity and the other is cation block [31].

Ionic selectivity of sodium channels of squid giant axons was not altered by tetramethrin in any significant manner [32]. Permeability ratios were calculated from the changes in the reversal potential for sodium tail current as the external sodium was replaced by various test cations. The permeability ratios for Na^+, Li^+, NH_4^+, guanidine and formamidine were not affected by tetramethrin at test cation concentrations of either 300 mM or 600 mM (Table 1). Thus it was concluded that this property of the selectivity filter of the sodium channel remains intact after gating modification by tetramethrin.

A variety of cations are known to block the open sodium channel in a manner dependent on the membrane potential [31]. The block was particularly noticeable at large negative potentials, and is illustrated by an upward deflection of the instantaneous current–voltage ($I-V$) curve (Fig. 8A). Various permeant monovalent cations

TABLE 1   Permeability ratios of sodium channels in control and 50 μM tetramethrin-treated squid giant axons

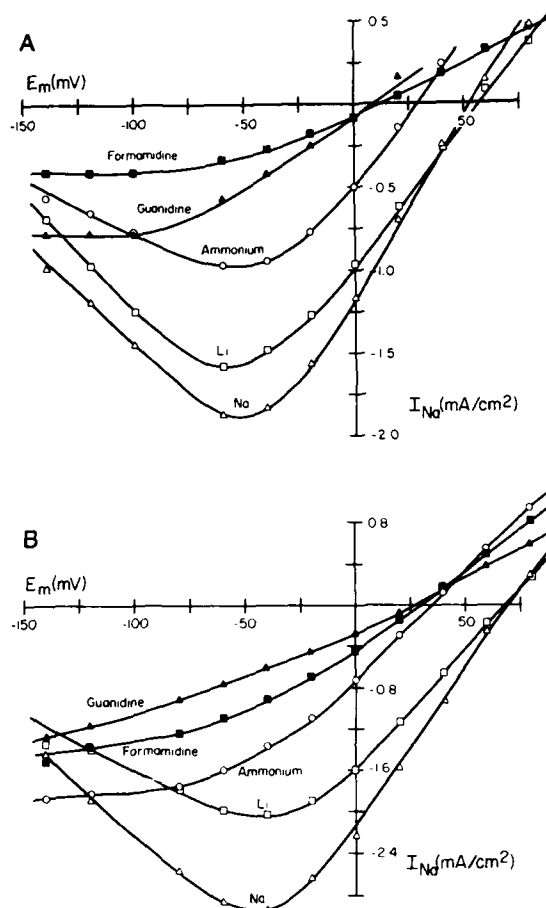|	Test cation concentration (mM)	Permeability ratio				
		P_{Na}	P_{Li}	P_{NH_4}	$P_{Guanidine}$	$P_{Formamidine}$
Control	300	1	1.13	0.27	0.34	0.23
Tetramethrin	300	1	0.93	0.29	0.21	0.21
Control	600	1	1.19	0.21	0.28	0.20
Tetramethrin	600	1	1.18	0.29	0.29	0.25

From Yamamoto et al. [32]

FIG 8 Instantaneous $I-V$ relationships in external solutions containing various permeant cations (300 mM) in a normal squid axon (A) and in an axon internally perfused with 50 μM tetramethrin (B). Permeant cations are Na ($\triangle$), Li ($\square$), NH$_4$ ($\circ$), formamidine ($\blacksquare$) and guanidine ($\blacktriangle$). The amplitude of the instantaneous tail current in the normal axon was measured upon step repolarization of the membrane to various levels following a 1 ms depolarizing pulse to 0 mV. The tail current amplitude in the tetramethrin-treated axon was measured upon step repolarization to various levels following an 80 ms depolarizing pulse to + 20 mV. Different axons were used for each cation in the control, whereas one axon was used for all cations in tetramethrin (from Yamamoto et al. [32]).

blocked the open sodium channel to different extents. Tetramethrin had no significant effect on the $I-V$ curve for each cation (Fig. 8B) [32].

Divalent cations such as Ca^{2+} and Mg^{2+} also block the open sodium channel [31]. Tetramethrin was without any significant effect on the instantaneous $I-V$ curve of the squid axon in the presence of various concentrations of Ca^{2+} in the external perfusate [32]. The $I-V$ curve for single sodium channel currents of neuroblastoma cells also showed open channel block in a manner dependent on external calcium concentration and membrane potential indicating voltage-depen-

dent calcium block [33]. Tetramethrin had no effect on the $I-V$ curve in either squid axons or neuroblastoma cells. Based on Eyring's barrier model, these results indicate that tetramethrin does not alter the barrier nor the wells of the energy profile of the open sodium channel [33].

Site of action of pyrethroids in sodium channels

Having established the alteration by pyrethroids of the gating kinetics without change in ionic permeation properties, the next question is concerned with the site of action in the sodium channel. In order to answer this question, several chemicals known to act on specific sites of the sodium channel were used as tools.

Tetrodotoxin (TTX) is known to block the voltage-activated sodium channel by binding to a site near its external orifice [34,35]. TTX inhibited the pyrethroid-induced sodium tail current in a non-competitive manner [36]. Thus TTX and pyrethroids act on different sites of the sodium channel.

Grayanotoxin (GTX) and batrachotoxin (BTX) remove the inactivation of the sodium channel and shift the activation voltage in the direction of hyperpolarization. The sodium current was prolonged during a depolarizing pulse, and under current clamp conditions a large membrane depolarization ensued [37-41]. Both toxins appear to bind to a site inside the sodium channel and presumably to a local anesthetic site with which the inactivation gate interacts [42]. GTX and tetramethrin have been found to act on the squid axon sodium channel independently [43]. Fig. 9A shows a family of sodium currents recorded from a squid axon exposed to tetramethrin. The inward sodium current was generated at potentials equal to and more positive than -40 mV, and the tail currents were large and decayed slowly. Grayanotoxin I (GTX I) was added to the same preparation poisoned with tetramethrin (Fig. 9B). The activation potential was shifted in the hyperpolarizing direction, and the inward sodium current was generated at potentials equal to and more positive than -100 mV, the change characteristic of GTX I. Fig. 9C shows another example in which GTX I application was followed by tetramethrin application. Record a is the current at -60 mV before application of GTX I. After exposure to GTX I, the inward, non-inactivating sodium current appeared at the same potential (record b). Addition of tetramethrin to this preparation resulted in a large and prolonged sodium tail current (record c). Thus tetramethrin acts on a site other than the GTX binding site which is located inside the sodium channel.

When perfused internally, octylguanidine blocked the sodium channel in a manner similar to that of local anesthetics [44]. Octylguanidine caused a time-dependent block of the sodium channel in which the inactivation gate had been destroyed by exposure to pronase. However, octylguanidine failed to block the sodium channel when the inactivation had been blocked by BTX [42]. Thus, octylguanidine and BTX act on the same intrachannel site. However, when octylguanidine and pyrethroids were combined, they acted on the sodium channel in a manner independent of each other [30]. It was concluded that pyrethroids bind to a site different from the intrachannel site of BTX and octylguanidine.

The results of experiments described above indicate that pyrethroids do not act on the TTX binding site near the external orifice of the sodium channel or on an intrachannel site. Experiments using active and inactive isomers of tetramethrin have shown that there are multiple binding sites in the sodium channel [36].
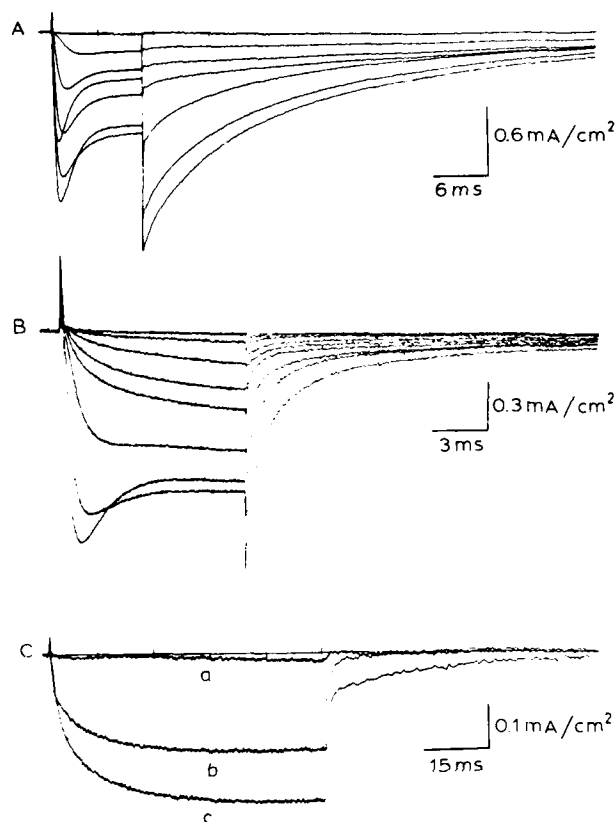
FIG 9 Simultaneous effects of grayanotoxin I (GTX I) and (+)-tetramethrin on sodium current of squid giant axons. A: membrane currents for an axon treated with 10 μM (+)-tetramethrin. Test pulse duration 10 ms; holding potential − 80 mV; test pulses from − 60 mV to 60 mV. Note the prolonged sodium current time course during the depolarizing step and the pronounced sodium tail current following step repolarization. B: same axon following treatment with both (+)-tetramethrin and 50 μM GTX I. The characteristic tetramethrin-induced tail current and the GTX-induced slow sustained sodium current are both present. Test pulse duration 10 ms; holding potential − 140 mV; test pulses from − 120 mV to 20 mV. C: membrane currents from another axon for control 50 ms depolarizations to − 60 mV from a holding potential of − 140 mV (a), and successively following perfusion of 50 μM GTX I (b) and both GTX I and 10 μM (+)-tetramethrin (c) (from Takeda and Narahashi [43]).

Whereas (+)-trans and (+)-cis isomers of tetramethrin were effective in causing a prolonged sodium current, (−)-trans and (−)-cis isomers were without effect. Furthermore (−)-trans and (−)-cis tetramethrin antagonized the action of (+)-trans and (+)-cis tetramethrin in either a competitive or non-competitive manner depending on the combination. Based on these results, three tetramethrin binding sites were identified, a trans site, a cis site, and a negative allosteric site (Fig. 10).

Interactions of the inactive isomer with the active isomer were also observed with deltamethrin [45]. Unlike the active deltamethrin with the 1R, 3R, αS configuration,
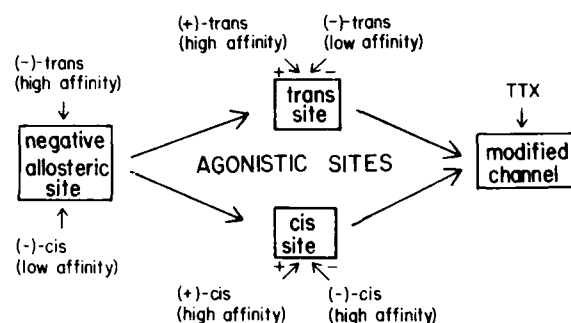
FIG 10 Hypothetical model for the interactions of isomers of tetramethrin with the sodium channel (from Lund and Narahashi [36]).

RU 40767, an inactive isomer of deltamethrin with the 1S, 3S, αR configuration had no effect on the sodium current of neuroblastoma cells even at 50 and 100 μM. However, RU 40767 antagonized the active deltamethrin in an uncompetitive manner, indicating that the inactive isomer binds to a site different from that of the active isomer. The separate binding sites were also implicated by the dose–response curve for the TTX block of sodium current. Whereas the active isomer did not change the TTX dose–response curve with a K_d of 3 nM, the inactive isomer shifted the curve to increase the K_d to 20 nM.

In view of the experimental results summarized above and of the highly hydrophobic nature of pyrethroid molecules, the binding site of the active forms of pyrethroids appears to be located within the membrane on or near the sodium channel macromolecule. The pyrethroid molecule will be dissolved in membrane lipid and get access and bind to the channel structure thereby modifying the gating machinery of both activation and inactivation systems.

Dose–response relationship

A variety of pyrethroids and pyrethrins are known to stimulate nerve preparations at very low concentrations ranging from 5 pM to 10 nM (e.g. Refs. 4, 46–51). However, in voltage clamp and patch clamp experiments, relatively high concentrations of pyrethroids were used ranging from 10 nM to 100 μM. Thus a question arises as to whether the modification of sodium current caused by higher concentrations of pyrethroids is relevant to the toxic action on animals.

This question can be resolved when consideration is given to the concentration of pyrethroids sufficient to increase the depolarizing after-potential to the level of threshold for repetitive discharges. For observing the effects of pyrethroids on the sodium current, very high concentrations were routinely used in order to produce a large change in the channel gating kinetics. However, the fraction of the sodium channel population that needs to be modified to increase the depolarizing after-potential to the threshold level (10 mV depolarization) for repetitive discharges which would cause the animal to develop the symptoms of poisoning is calculated to be less than 0.1% [36]. The concentration of tetramethrin that causes this degree of channel modification is of the order of 1–10 nM, which actually evokes repetitive

discharges in axons. Thus it is concluded that the modification of sodium channel gating kinetics by pyrethroids is enough to account for repetitive discharges observed at low concentrations. It should be pointed out that this 'toxicological amplification' could occur whenever the threshold phenomenon is involved. Thus the same argument is applicable to type II pyrethroids for the membrane depolarizing action. When the depolarization caused by a low concentration of pyrethroids reaches the threshold for an increase in discharge frequency of sensory neurons or in transmitter release from the nerve terminal, the animal develops symptoms of poisoning. Mere comparison of the ED_{50}s between different parameters such as the increase in sodium current and the initiation of repetitive discharges would lead to the wrong interpretation.

Pyrethroids and calcium channels

Based on high sensitivities of certain insect neurons to pyrethroids, it was speculated that calcium channels would be a target site. For instance, neurosecretory cells of stick insect, which are known to generate action potentials by calcium channels [48], were stimulated by permethrin at concentrations as low as 50 pM to generate repetitive discharges [49]. This observation was taken as indicating that pyrethroids could act on calcium channels [50]. However, the result does not necessarily indicate that calcium channels are affected, because both sodium and calcium channels are present depending on the region of the cell. Although the cell body of neurosecretory cell uses calcium channels to generate action potentials, the axon uses sodium channels and the nerve terminal is endowed with both sodium and calcium channels. Therefore, repetitive discharges caused by pyrethroids may originate in sodium channels, calcium channels, or both. This problem remains to be resolved.

However, two observations are at variance with the above calcium channel hypothesis. Ruigt [52] found no effect of pyrethroids on calcium channel currents of neuroblastoma cells. We have observed a progressive block of calcium channels by tetramethrin in neuroblastoma cells [53]. Neuroblastoma cell line N1E-115 is endowed with two types of calcium channels; one generates a transient or inactivating current (type I or T type), while the other generates a long-lasting current (type II or L type) [54]. Tetramethrin (50 μM) blocked type I channel current by 75% and type II channel current by 30%. The block of both channels was time-dependent, being enhanced during a 400 ms depolarizing pulse. The time-dependent component of block was easily reversible after washing with drug-free solution, while the time-independent component persisted after washing, suggesting two separate sites of action of tetramethrin in calcium channels. Deltamethrin and fenvalerate had no effect on either type of calcium channels, and modified sodium channels only. This difference in action between type I and type II pyrethroids may be partially responsible for the different symptoms of poisoning in animals.

Pyrethroids and GABA receptor-channels

GABA receptor-channel complex was proposed to be a target site of type II pyrethroids. The binding of [^{35}S]t-butylbicyclophosphorothionate (TBPS), a ligand for the channel site of GABA receptors, and that of Ro 5-4864, a diazepam analog

and benzodiazepine ligand, were inhibited by type II pyrethroids but not by type I pyrethroids [55–59]. GABA-stimulated chloride uptake by mouse brain vesicles was inhibited by deltamethrin [60]. Type II pyrethroids were also found to antagonize the GABA-induced decrease in input resistance of crayfish muscle fibers [61]. However, in both cases the effective concentrations were high, the apparent K_ds being 10 μM or above. Indirect support for this hypothesis was also obtained by experiments with diazepam which protected the cockroaches from poisoning with type II pyrethroids but not with type I pyrethroids [62].

Experiments conducted in a few other laboratories challenged the validity of the hypothesis. Deltamethrin was much less potent on the GABA system than on the sodium channel, the difference in effective concentrations amounting to as much as 100 times [63]. In the cockroach nerve, deltamethrin, fenvalerate and cypermethrin had little or no effect on the specific binding of [^{3}H]dihydropicrotoxinin, a ligand for the GABA-activated channel [64]. More direct evidence against the GABA hypothesis has recently been obtained by our patch clamp experiments using the primary cultured neurons isolated from the rat dorsal root ganglion [65]. In these neurons, bath application of GABA caused chloride channels to open. The voltage-activated sodium channel currents were also recorded from the same neuron. Application of 10 μM deltamethrin caused no change in the GABA-induced chloride current while increasing and prolonging the sodium current in a manner characteristic of type II pyrethroids. Therefore, the GABA receptor-channel complex plays no role in the toxic action of deltamethrin in the mammalian neurons. The validity of this conclusion in invertebrate animals remains to be seen.

Lindane on acetylcholine and GABA receptor-channels

Lindane is known to stimulate synaptic transmission and to cause repetitive discharges [66–69]. An example of the lindane-induced synaptic facilitation is shown in Fig. 11 [70]. The postsynaptic response in the cockroach last abdominal ganglion in response to a single presynaptic stimulus was composed of initial large spikes followed by after-discharges of small amplitudes (Fig. 11A). After application of 10 μM lindane, the postsynaptic after-discharges were greatly augmented and prolonged (Fig. 11B–D).

Lindane also stimulated neuromuscular transmission of frogs [71]. At a concentration of 100 μM, lindane increased the frequency of spontaneous miniature end-plate potentials and the quantal content of the end-plate potential. It decreased the amplitude of the miniature end-plate potentials through a suppression of end-plate to acetylcholine as demonstrated by experiments with iontophoretic application of acetylcholine. Thus lindane has two effects, one being to suppress the end-plate response to acetylcholine and the other being an effect consistent with a small increase in intracellular free Ca^{2+}. However, the calcium channels of neuroblastoma cells, both transient (type I) and long-lasting (type II), were unaffected by lindane [71].

One of the possible sites of action of lindane is the GABA receptor-channel complex. The symptoms of poisoning resemble those caused by GABA antagonists, and a chronic exposure to a low dose of lindane produced proconvulsant effects in the kindling model of experimental epilepsies [72,73]. Lindane was indeed found to
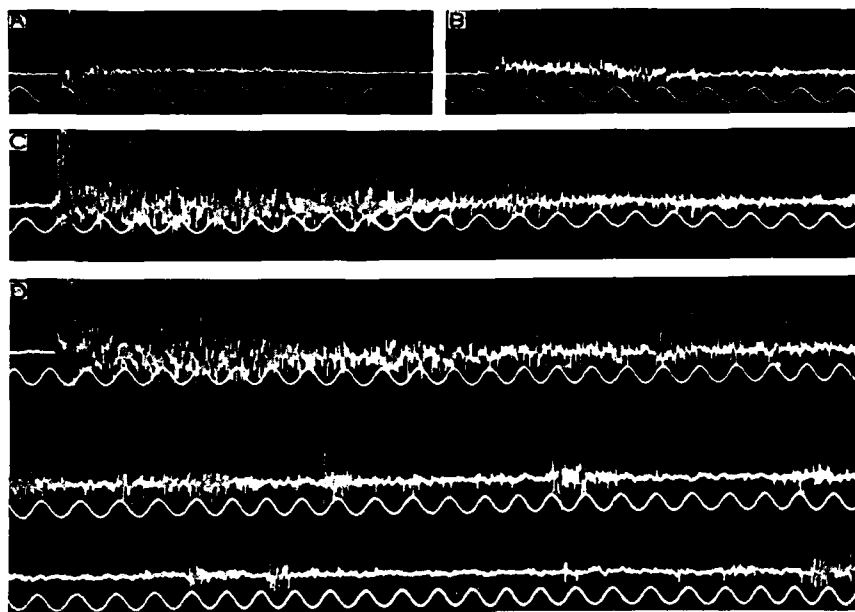
283

FIG 11   After-discharges of the postsynaptic giant fibers induced by a single supramaximal
stimulus to the cercal (presynaptic) nerve of the American cockroach before and after
treatment with 10 μM lindane. 17°C, time marker 50 Hz. A: before treatment; very short
after-discharge (100 ms). B: 1 h and 25 min after treatment; slight after-discharge (380 ms).
C: 4 h and 10 min after treatment; prolonged after-discharge (940 ms). D: 6 h and 10 min
after treatment. The three lines are continuous showing very prolonged after-discharge (2380
ms) (from Yamasaki and Ishii (Narahashi) [70]).

antagonize the action of GABA in stimulating ^{36}Cl uptake by cockroach muscles
[74] and mouse brain vesicles [60], and to inhibit the binding of [^{3}H]α-dihydro-
picrotoxinin and [^{35}S]TBPS to rat brain membrane preparations [75]. The seizures
induced by lindane in rats were reduced by administration of diazepam [69]. These
effects of lindane led us to the hypothesis that it blocks the GABA-activated
receptor-channel complex thereby causing the hyperactive symptoms of poisoning in
animals.

Our recent patch clamp study using the primary cultured neurons isolated from
the rat dorsal root ganglion has clearly demonstrated the validity of the hypothesis
[65]. Bath application of GABA induced two components of inward chloride
current. One was a transient component which was desensitized with time, and the
other was a non-desensitizing component. The desensitizing component of chloride
current was completely blocked by 10 μM lindane, while the non-desensitizing
component remained unaffected. Thus lindane blocks one of the GABA-activated
receptor-channel complexes leading to hyperexcitation. This accounts for synaptic
facilitation observed earlier with the lindane-treated cockroach ganglion and
vertebrate preparations.

284

Future studies

Whereas our current research deals with the mechanism of action of insecticides at the single channel level, the future study of this field will be directed toward the molecular mechanisms. One of such studies will be concerned with the identification of the molecular components of subunits of the target receptor-channel complex with which insecticides interact. This will be followed by characterization of the mechanism involved in insecticide–receptor molecule interaction. Current rapid developments in molecular biology and cell biology should be incorporated into such studies of insecticides.

Conclusions

It has taken a long time to identify and characterize the target sites of various insecticides since the study of insecticide neurotoxicology started flourishing in the 1960s. The progress has been slower than we anticipated. One of the reasons for this delay is the difficulty in adopting modern and powerful approaches and techniques in this field. A key to success in mechanistic studies of insecticides, or of any other drugs and chemicals for that matter, is to utilize such powerful techniques as voltage clamp, patch clamp, receptor isolation, and gene cloning. Thus the progress in insecticide neurotoxicology depends to a great extent on the development of newer and more powerful techniques and on swift adoption of them. Whenever such a technique was utilized effectively, a quantum leap of the progress was made opening up a new avenue through which a large amount of useful knowledge was accumulated. This has clearly been documented in the discovery of the DDT- and pyrethroid-induced depolarizing after-potential by adopting intracellular microelectrode techniques; pyrethroid-induced prolongation of sodium current by voltage clamp techniques; pyrethroid-induced prolongation of single sodium channel open time by patch clamp techniques; and lindane block of GABA receptor choloride channels by patch clamp techniques. Future applications of molecular biology and genetics techniques promise additional quantum jumps in characterizing the molecular aspects of interactions of insecticide molecules with specific components or subunits of receptors and/or channels.

References

1 Lowenstein, O. (1942) A method of physiological assay of pyrethrum extracts. Nature 150, 760–762.
2 Roeder, K.D. and Weiant, E.A. (1946) The site of action of DDT in the cockroach. Science 103, 304–306.

3 Welsh, J.H. and Gordon, H.T. (1947) The mode of action of certain insecticides on the arthropod nerve axon. J. Cell. Comp. Physiol. 30, 147–172.

4 Yamasaki, T. and Ishii (Narahashi), T. (1952) Studies on the mechanism of action of insecticides (IV). The effects of insecticides on the nerve conduction of insect. Oyo-Kontyu (J. Nippon Soc. Appl. Entomol.) 7, 157–164.

5 Yamasaki, T. and Ishii (Narahashi). T. (1952) Studies on the mechanism of action of insecticides (V). The effects of DDT on the synaptic transmission in the cockroach. Oyo-Kontyu (J. Nippon Soc. Appl. Entomol.) 8, 111–118.

6 Yamasaki, T. and Narahashi, T. (1957) Intracellular microelectrode recordings of resting and action potentials from the insect axon and the effects of DDT on the action potential. Studies on the mechanism of action of insecticides (XIV). Botyu-Kagaku 22, 305–313.

7 Narahashi, T. and Yamasaki, T. (1960) Mechanism of increase in negative after-potential by dicophanum (DDT) in the giant axons of the cockroach. J. Physiol. 152, 122–140.

8 Narahashi, T. (1962) Effect of the insecticide allethrin on membrane potentials of cockroach giant axons. J. Cell. Comp. Physiol. 59, 61–65.

9 Narahashi, T. and Haas, H.G. (1967) DDT: Interaction with nerve membrane conductance changes. Science 157, 1438–1440.

10 Narahashi, T. and Haas, H.G. (1968) Interaction of DDT with the components of lobster nerve membrane conductance. J. Gen. Physiol. 51, 177–198.

11 Narahashi, T. and Anderson, N.C. (1967) Mechanism of excitation block by the insecticide allethrin applied externally and internally to squid giant axons. Toxicol. Appl. Pharmacol. 10, 529–547.

12 Brown, L.D. and Narahashi, T. (19870 Activity of tralomethrin to modify the nerve membrane sodium channel. Toxicol. Appl. Pharmacol. 89, 305–313.

13 de Weille, J.R., Vijverberg, H.P.M. and Narahashi, T. (1986) Sodium depletion in the periaxonal space of the squid axon treated with pyrethroids. Brain Res. 386, 169–174.

14 Hille, B. (1968) Pharmacological modification of the sodium channels of frog nerve. J. Gen. Physiol. 51, 199–219.

15 Lund, A.E. and Narahashi, T. (1981) Modification of sodium channel kinetics by the insecticide tetramethrin in crayfish giant axons. Neurotoxicology 2, 213–229.

16 Lund, A.E. and Narahashi, T. (1981) Kinetics of sodium channel modification by the insecticide tetramethrin in squid axon membranes. J. Pharmacol. Exp. Ther. 219, 464–473.

17 Lund, A.E. and Narahashi, T. (1981) Interaction of DDT with sodium channels in squid giant axon membranes. Neuroscience 6, 2253–2258.

18 Murayama, K., Abbott, N.J., Narahashi, T. and Shapiro, B.I. (1972) Effects of allethrin and Condylactis toxin on the kinetics of sodium conductance of crayfish axon membranes. Comp. Gen. Pharmacol. 3, 391–400.

19 Pichon, Y. (1969) Aspects Électriques et Ioniques du Fonctionnement Nerveux chez les Insectes. Cas Particulier de la Chaine Nerveuse Abdominals d'une blatte Periplaneta americana L. Thèse, Univ. Rennes.

20 Vijverberg, H.P.M., van der Zalm, J.M. and van den Bercken, J. (1982) Similar mode of action of pyrethroids and DDT on sodium channel gating in myelinated nerves. Nature 295, 601–603.

21 Vijverberg, H.P.M., van der Zalm, J.M., van Kleef, R.G.D.M. and van den Bercken, J. (1982) Temperature and structure-dependent interaction of pyrethroids with the sodium channels in frog node of Ranvier. Biochim. Biophys. Acta 728, 73–82.

22 Wang, C.M., Narahashi, T. and Scuka, M. (1972) Mechanism of negative temperature coefficient of nerve blocking action of allethrin. J. Pharmacol. Exp. Ther. 182, 442–453.

23 Wu, C.H., Oxford, G.S., Narahashi, T. and Holan, T. (1980) Interaction of a DDT analog with the sodium channel of lobster axon. J. Pharmacol. Exp. Ther. 212, 287–293.

24 Lund, A.E. and Narahashi, T. (1983) Kinetics of sodium channel modification as the basis for the variation in the nerve membrane effects of pyrethroids and DDT analogs. Pestic. Biochem. Physiol. 20, 203–216.

286

25 Neher, E. and Sakmann, B. (1976) Single-channel currents recorded from membrane of denervated frog muscle fibres. Nature 260, 779–802.

26 Hamill, O.P., Marty, A., Neher, E., Sakmann, B. and Sigworth, F.J. (1981) Improved patch-clamp techniques for high-resolution current recording from cells and cell-free membrane patches. Pflügers Arch. 391, 85–100.

27 Yamamoto, D., Quandt, F.N. and Narahashi, T. (1983) Modification of single sodium channels by the insecticide tetramethrin. Brain Res. 274, 344–349.

28 Chinn, K. and Narahashi, T. (1986) Stabilization of sodium channel states by deltamethrin in mouse neuroblastoma cells. J. Physiol. 380, 191–207.

29 Holloway, S.F., Salgado, V.L., Wu, C.H. and Narahashi, T. (1984) Maintained opening of single Na channels by fenvalerate. 14th Ann. Mtg. Soc. Neurosci. Abstr. 10, 864.

30 de Weille, J.R., Vijverberg, H.P.M. and Narahashi, T. (1988) Interactions of pyrethroids and octylguanidine with sodium channels of squid giant axons. Brain Res. in press.

31 Yamamoto, D., Yeh, J.Z. and Narahashi, T. (1985) Interactions of permeant cations with sodium channels of squid axon membranes. Biophys. J. 48, 361–368.

32 Yamamoto, D., Yeh, J.Z. and Narahashi, T. (1986) Ion permeation and selectivity of squid axon sodium channels modified by tetramethrin. Brain Res. 372, 193–197.

33 Yamamoto, D., Yeh, J.Z. and Narahashi, T. (1984) Voltage-dependent calcium block of normal and tetramethrin-modified single sodium channels. Biophys. J. 45, 337–344.

34 Narahashi, T. (1974) Chemicals as tools in the study of excitable membranes. Physiol. Rev. 54, 813–889.

35 Narahashi, T., Moore, J.W. and Scott, W.R. (1964) Tetrodotoxin blockage of sodium conductance increase in lobster giant axons. J. Gen. Physiol. 47, 965–974.

36 Lund, A.E. and Narahashi, T. (1982) Dose-dependent interaction of the pyrethroid isomers with sodium channels of squid axon membranes. Neurotoxicology 3, 11–24.

37 Khodorov, B.I. (1978) Chemicals as tools to study nerve fiber sodium channels: effects of batrachotoxin and some local anesthetics. In: Membrane Transport Processes Vol. 2 (D.C. Tosteson, A.O. Yu, R. Latorre, eds.), pp. 153–174, Raven Press, New York.

38 Khodorov, B.I. (19850 Batrachotoxin as a tool to stu ᵗ voltage-sensitive sodium channels of excitable membranes. Prog. Biophys. Mol. Biol. 45, 7–148.

39 Narahashi, T. and Seyama, I. (1974) Mechanism of nerve membrane depolarization caused by grayanotoxin I. J. Physiol. 242, 471–487.

40 Narahashi, T., Albuquerque, E.X. and Deguchi, T. (1971) Effects of batrachotoxin on membrane potential and conductance of squid giant axons. J. Gen. Physiol. 58, 54–70.

41 Seyama, I. and Narahashi, T. (1981) Modulation of sodium channels of squid nerve membranes by grayanotoxin I. J. Pharmacol. Exp. Ther. 219, 614–624.

42 Tanguy, J., Yeh, J.Z. and Narahashi, T. (1984) Interaction of batrachotoxin with sodium channels in squid axons. Biophys. J. 45, 184a.

43 Takeda, K. and Narahashi, T. (1988) Chemical modification of sodium channel inactivation: separate sites for the action of grayanotoxin and tetramethrin. Brain Res. in press.

44 Kirsch, G.E., Yeh, J.Z., Farley, J.M. and Narahashi, T. (1980) Interaction of n-alkylguanidines with the sodium channels of squid axon membranes. J. Gen. Physiol. 76, 315–335.

45 Brown, L.D. and Narahashi, T. (1988) Stereospecific action of the pyrethroid deltamethrin on sodium channels. Toxicologist 8, 227.

46 Burt, P.E. and Goodchild, R.E. (1971) The site of action of pyrethrin I in the nervous system of the cockroach Periplaneta americana. Entomol. Exp. Appl. 14, 179–189.

47 Nishimura, K. and Narahashi, T. (1978) Structure-activity relationship of pyrethroids based on direct action on nerve. Pesticide Biochem. Physiol. 8, 53–64.

48 Orchard, I. (1980) The effects of pyrethroids on the electrical activity of neurosecretory cells from the brain of Rhodnius prolixus. Pesticide Biochem. Physiol. 13, 220–226.

49 Orchard, I. and Osborne, M.P. (1979) The action of insecticides on neurosecretory neurons in the stick insect, Carausius morosus. Pesticide Biochem. Physiol. 10, 197–202.

50 Osborne, M.P. (1986) Insect neurosecretory cells - structural and physiological effects induced by insecticides and related compounds. In: Neuropharmacology and Pesticide Action (M.G. Ford, G.G. Lunt, R.C. Reay, P.N.R. Usherwood, eds.), pp. 203–243. Ellis Horwood Ltd., Chichester, England.

51 Takeno, K., Nishimura, K., Parmentier, J. and Narahashi, T. (1977) Insecticide screening with isolated nerve preparation for structure-activity relationships. Pestic. Biochem. Physiol. 7, 486–499.

52 Ruigt, G.S.F. (1984) An Electrophysiological Investigation into the Mode of Action of Pyrethroid Insecticides. Ph.D. Thesis, University of Utrecht, 163 pp.

53 Yoshii, M., Tsunoo, A. and Narahashi, T. (1985) Effects of pyrethroids and veratridine on two types of Ca channels in neuroblastoma cells. Soc. Neurosci. Abstr. 11, 518.

54 Narahashi, T., Tsunoo, A. and Yoshii, M. (1987) Characterization of two types of calcium channels in mouse neuroblastoma cells. J. Physiol. 383, 231–249.

55 Crofton, K.M., Reiter, L.W. and Mailman, R.B. (1987) Pyrethroid insecticides and radioligand displacement from the GABA receptor chloride ionophore complex. Toxicol. Lett. 35, 183–190.

56 Gammon, D.W. and Sander, G. (1985) Two mechanisms of pyrethroid action: Electro-physiological and pharmacological evidence. Neurotoxicology 6(2), 63–86.

57 Lawrence, L.J. and Casida, J.E. (1983) Stereospecific action of pyrethroid insecticides on the γ-aminobutyric acid receptor-ionophore complex. Science 221, 1399–1401.

58 Lawrence, L.J., Gee, K.W. and Yamamura, H.I. (1985) Interactions of pyrethroid insecticides with chloride ionophore-associated binding sites. Neurotoxicology 6(2), 87–98.

59 Lummis, S.C.R., Chow, S.C., Holan, G. and Johnston, G.A.R. (1987) γ-Aminobutyric acid receptor ionophore complexes: Differential effects of deltamethrin, dichlorodiphenyl-trichloroethane, and some novel insecticides in a rat brain membrane preparation. J. Neurochem. 48, 689–694.

60 Bloomquist, J.R. and Soderlund, D.M. (1985) Neurotoxic insecticides inhibit GABA-dependent chloride uptake by mouse brain vesicles. Biochem. Biophys. Res. Commun. 133, 37–43.

61 Gammon, D. and Casida, J.E. (1983) Pyrethroids of the most potent class antagonize GABA action at the crayfish neuromuscular junction. Neurosci. Lett. 40, 163–168.

62 Gammon, D.W., Lawrence, L.J. and Caside, J.E. (1982) Pyrethroid toxicology: Protective effects of diazepam and phenobarbital in the mouse and the cockroach. Toxicol. Appl. Pharmacol. 66, 290–296.

63 Chalmers, A.E., Miller, T.A. and Olsen, R.W. (1985) A pharmacological investigation of invertebrate GABA receptors. Neurotox '85. Neuropharmacology and Pesticide Action. Univ. Bath, Abstr. 41–42.

64 Matsumura, F. and Tanaka, K. (1984) Molecular basis of neuroexcitatory actions of cyclodiene-type insecticides. In: Cellular and Molecular Neurotoxicology. (T. Narahashi, ed.), pp. 225–240. Raven Press, New York.

65 Ogata, N., Vogel, S.M. and Narahashi, T. (1987) Lindane but not deltamethrin blocks a component of GABA-activated chloride channels. Soc. Neurosci. Abstr. 13, 65.

66 Joy, R.M. (1982) Mode of action of lindane, dieldrin and related insecticides in the central nervous system. Neurobehav. Toxicol. Teratol. 4, 813–823.

67 Narahashi, T. (1971) Effects of insecticides on excitable tissues. In: Advances in Insect Physiology, Vol. 8 (J.W.L. Beament, J.E. Treherne, V.B. Wigglesworth, eds.), pp. 1–93. Academic Press, London, New York.

68 Uchida, M., Fujita, T., Kurihara, N. and Nakajima, M. (1978) Toxicities of γ-BHC and related compounds. In: Pesticide and Venom Neurotoxicity (D.L. Shankland, R.M. Hollingworth, T. Smyth Jr., eds.), pp. 133–151. Plenum Press, New York.

69 Woolley, D., Zimmer, L., Dodge, D. and Swanson, K. (1985) Effects of lindane-type insecticides in mammals: Unsolved problems. Neurotoxicology 6(2), 165–192.

70 Yamasaki, T. and Ishii (Narahashi), T. (1954) Studies on the mechanism of action of insecticides. X. Nervous activity as a factor of development of γ-BHC symptoms in the

288

cockroach. Botyu-Kagaku (Scientific Insect Control) 19, 106–112. English translation In: Japanese Contributions to the Study of the Insecticide-Resistance Problem. Publ. by Kyoto Univ. for the WHO 1957; pp. 176–183.

71 Joy, R.M., Vogel, S.M. and Narahashi, T. (1987) Effects of lindane upon transmitter release and end-plate responsiveness in the neuromuscular junction of the frog. Neuropharmacology 26, 1223–1229.

72 Joy, R.M., Stark, L.G. and Albertson, T.E. (1983) Proconvulsant actions of lindane: Effects on afterdischarge thresholds and durations during amygdaloid kindling in rats. Neurotoxicology 4, 211–220.

73 Joy, R.M., Stark, L.G. and Albertson, T.E. (1983) Proconvulsant action of lindane compared at two different kindling sites in the rat amygdala and hippocampus. Neurobehav. Toxicol. Teratol. 5, 461–465.

74 Ghiasuddin, S.M. and Matsumura, F. (1982) Inhibition of gamma-aminobutyric acid (GABA)-induced chloride uptake by gamma-BHC and heptachlor epoxide. Comp. Biochem. Physiol. 73C, 141–144.

75 Matsumura, F. and Ghiasuddin, S.M. (1983) Evidence for similarities between cyclodiene type insecticides and picrotoxinin in their action mechanisms. J. Environ. Sci. Health B18, 1–14.

76 Narahashi, T. and Lund, A.E. (1980) Giant axons as models for the study of the mechanism of action of insecticides. In: Insect Neurobiology and Pesticide Action (Neurotox '79), pp. 497–505. Soc. Chem. Industry, London.

289

CHAPTER 21

Specific binding sites for pyrethroids on the voltage-dependent sodium channel

MICHEL LAZDUNSKI, ALAIN LOMBET * AND CHRISTIANE MOURRE

Centre de Biochimie du CNRS, Parc Valrose, 06034 Nice Cedex, France

Introduction

A number of naturally occurring neurotoxins acting at distinct binding sites have been used as tools to characterize various structural and functional aspects of Na^+ channels [2,11,13,17,33].

Pyrethroids are synthetic derivatives of the natural toxins pyrethrins contained in the flowers of the *Chrysanthemum* species. They currently constitute the most interesting class of insecticides [5] but they are also toxic in mammals. These compounds have been found to drastically prolong Na^+ currents in both vertebrate and invertebrate nerve membranes [16,24,35,38]. Their mechanism of action on the Na^+ channel has been studied in considerable detail with the patch-clamp technique both at the single channel [9,30,38] and at the whole cell [9,18,25,34] levels. Pyrethroids have also been found to induce $^{22}Na^+$ influx through tetrodotoxin-sensitive Na^+ channels in neuronal cells in culture [10,12,29]. This approach as well as binding studies [17] with tritiated and iodinated toxins specific for the Na^+ channel has shown that pyrethroids are not acting at the tetrodotoxin/saxitoxin binding site or at the batrachotoxin/veratridine site, neither do they act at specific sites involved in the recognition of polypeptide scorpion and sea anemone toxins. These data have led to the conclusion that pyrethroids have a specific binding site on the Na^+ channel protein which is distinct from binding sites previously identified for other toxins acting on the same channel.

Receptors for several different classes of toxins acting on the Na^+ channel have now been biochemically identified using ^3H-labelled or ^{125}I-labelled toxins. This type of biochemical identification has not yet been possible with [^3H]pyrethroids.

The purpose of this paper is to describe the properties of binding of pyrethroids to the Na^+ channel protein using the allosteric interaction between the pyrethroid binding site and the batrachotoxin binding site that has been identified with [^3H]batrachotoxinin A 20-α-benzoate ([^3H]BTX-B). Allosteric interactions between

---

the pyrethroid binding site, the sea anemone toxin binding site and the brevetoxin binding site are also described. Autoradiographic procedures have been used to determine the distribution of pyrethroid binding sites in rat brains.

Results

A number of Na^+ channel effectors have been previously shown to increase specific [^{3}H]BTX-B binding to Na^+ channels. They include polypeptide toxins such as sea anemone and scorpion toxins [8] and non peptide toxins such as brevetoxins [7].

Fig. 1 confirms that the sea anemone toxin As_2 and PbTx-2 alone increase [^{3}H]BTX-B binding. Enhancement of [^{3}H]BTX-B binding was also observed with
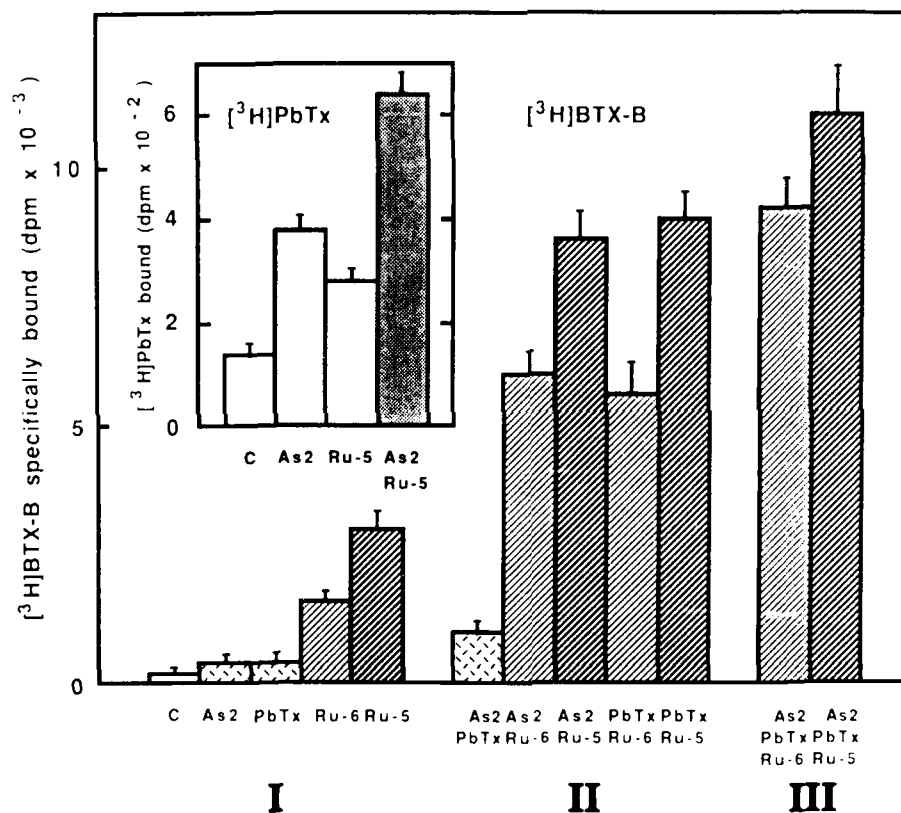

FIG 1 Binding of [^{3}H]BTX-B to rat brain microsomes in the presence of various effectors. Binding of 2 nM [^{3}H]BTX-B was measured at 22°C with 0.35 mg/ml of protein in the absence (controls) or in the presence of 40 μM As_2, 0.3 μM PbTx-2, 1 μM RU 39568 (RU-6), 10 μM RU 39568 (RU-5) or a combination of these toxins at the same concentrations. In all cases, non-specific binding was measured in the presence of 100 μM veratridine and represented 500 dpm. Inset: binding of [^{3}H]PbTx-3 to rat brain microsomes in the presence of various effectors. Binding of [^{3}H]PbTx-3 was measured at 4°C with 0.35 mg/ml of protein in the absence (control) or in the presence of 40 μM As_2, 10 μM RU 39568 (RU-5) or a combination of these toxins. Non-specific binding was measured in the presence of 10 μM unlabelled PbTx-2. In all cases data are given as mean ± S.E.M. ($n = 3$).

the pyrethroid molecule RU 39568 at concentrations of 1 nM (RU-6) and 10 μM (RU-5) (Fig. 1, I). The specific binding of [^{3}H]BTX-B in all these conditions was inhibited by unlabelled batrachotoxin as will be described later in more detail.

Fig. 1 also presents the interesting observation that there is an additive activation not only between As$_2$ and PbTx-2 but also between As$_2$ and pyrethroids and between PbTx-2 and pyrethroids (Fig. 1, II). An increase of specific [^{3}H]BTX-B binding is observed with a mixture of the three different toxins As$_2$, PbTx-2 and the pyrethroid which all appear to work additively (Fig. 1, III). The [^{3}H]PbTx-3 binding site has been recently identified [27]. The sea anemone toxin As$_2$ enhances [^{3}H]PbTx-3 binding and the mixture of As$_2$ and the pyrethroid produces a larger enhancement than that observed with As$_2$ or the pyrethroid alone (Inset, Fig. 1).

The K_d value for the binding of [^{3}H]BTX-B was 460 nM when experiments were carried out in the absence of toxin other than batrachotoxin. The K_d was 200 nM in
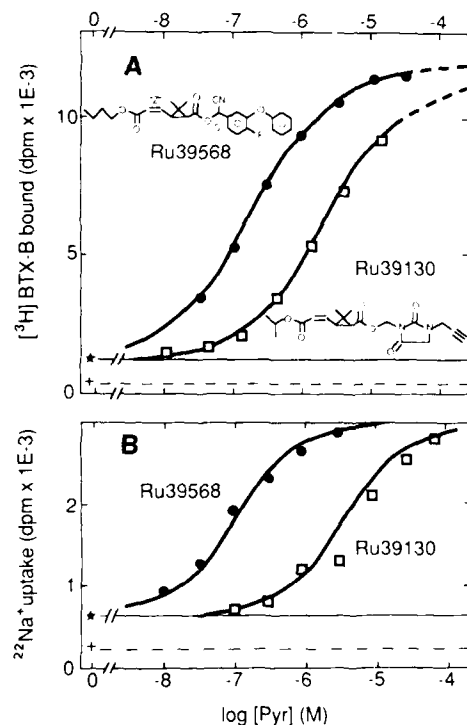

FIG 2 Effects of pyrethroids on [^{3}H]BTX-B binding and ^{22}Na$^+$ influx. A: effect of different pyrethroids on the binding of [^{3}H]BTX-B in the presence of 40 μM As$_2$ and 0.3 μM PbTx-2: The binding of 2 nM [^{3}H]BTX-B was measured in the presence of increasing concentrations of RU 39568 (●) and RU 39130 (□). Levels of total binding in absence of pyrethroid (★) and of the non-specific binding (+) in the presence of 100 μM veratridine are represented in full line and dotted line respectively. B: effect of pyrethroids on ^{22}Na$^+$ influx in N1E 115 neuroblastoma cells in the presence of 100 μM veratridine: ^{22}Na$^+$ influx was measured in the presence of increasing concentration of RU 39568 (●) and RU 39130 (□). Levels of ^{22}Na$^+$ uptake measured in the presence of 100 μM veratridine (★) and in the presence of 100 μM veratridine and 1 μM TTX (+) are represented in full line and dotted line respectively.

the presence of As_2 (40 μM), 40 nM in the presence of 1 μM RU 39568 and 15 nM in the presence of 10 μM RU 39568. The maximum binding capacity (B_{max}) was unchanged by either As_2 or the pyrethroid ($B_{max} = 2.2$ pmol of BTX-B bound (B_{max}) per mg of protein). The K_d value for BTX-B was found to be 70 nM in the presence of the mixture of As_2 and PbTx-2. It decreased to 29 and 12 nM upon addition of 1 and 10 μM of the pyrethroid deltamethrin to this mixture. Addition of 1 and 10 μM of RU 39568 to the mixture instead of deltamethrin shifted the K_d values to 4.8 and 2.9 nM respectively. With all toxin mixtures the B_{max} value remained at 2.2 pmol/mg of microsomal protein.

Enhancement of [^{3}H]BTX-B binding to Na^+ channels in synaptosomal membranes by pyrethroids is concentration-dependent. Dose–response curves for two pyrethroids, RU 39568 and RU 39130 are given in Fig. 2A. Half-maximum activations were seen at $K_{0.5}$ values of 0.2 μM and 2.5 μM respectively. The same type of difference in efficacy between the two pyrethroids ($K_{0.5}$ values of 0.1 μM and 5 μM) is shown in Fig. 2B using the $^{22}Na^+$ influx technique to follow the functional activity of this class of toxins on the Na^+ channel in neuroblastoma cells.

A classical compound belonging to another class of insecticide, DDT, also enhances [^{3}H]BTX-B binding to rat brain membranes in the presence of both As_2 and PbTx-2. The enhancement of the binding is not as large as for pyrethroids (see Fig. 3, inset B). A 1.8-fold increase was found for DDT as compared to a 9-fold increase for RU 39568 in the same type of experiment. The dose–response curve shown in the main panel of Fig. 3 indicates a $K_{0.5}$ value of 15 μM for DDT.
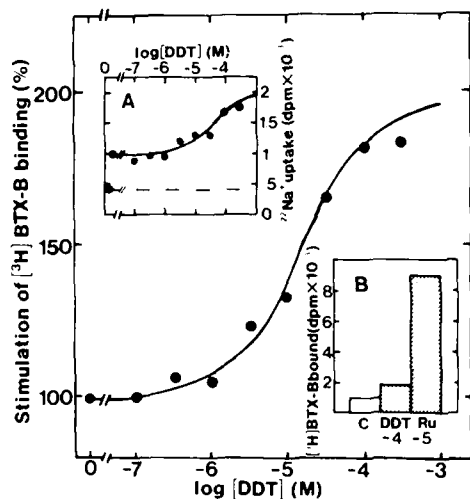

FIG 3 Effect of DDT on [^{3}H]BTX-B binding and Na^+ influx. Main panel: the effect of DDT was measured on the binding of 2 nM [^{3}H]BTX-B, in the presence of 40 μM As_2 and 0.3 μM PbTx-2 (100%). The stimulation obtained with increasing concentrations of DDT (●) was expressed as % of the control (100%). The non-specific binding was obtained in the presence of 100 μM veratridine. A $K_{0.5}$ value of 15 μM was observed for DDT. Inset A: the effect of DDT on $^{22}Na^+$ influx in N1E 115 was measured in the presence of 100 μM veratridine. The half-maximum increase in $^{22}Na^+$ uptake occurred at 40 μM DDT. Basal $^{22}Na^+$ uptake was measured at each concentration of DDT in the presence of 1 μM TTX (dotted line). Inset B: a comparison of the stimulation produced by DDT and RU 39568 on [^{3}H]BTX-B binding in the presence of As_2 and PbTx-2.
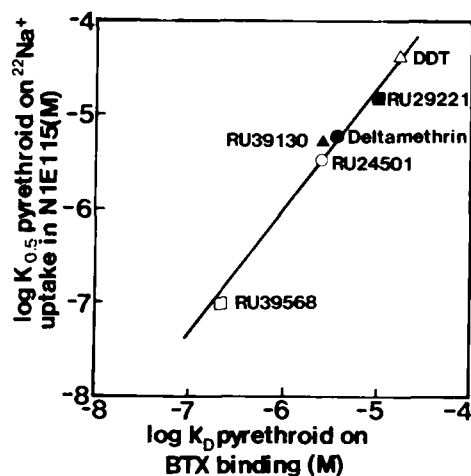
FIG 4 Correlation between efficacies of various pyrethroids (and DDT) in enhancing specific [^{3}H]BTX-B binding to rat brain membranes and activating TTX-sensitive ^{22}Na$^+$ uptake in neuroblastoma N1E 115 cells. K_d (half-stimulation of [^{3}H]BTX-B binding obtained in the presence of As$_2$ and PbTx-2) was plotted vs $K_{0.5}$ (half-stimulation of ^{22}Na$^+$ uptake obtained in the presence of 100 μM veratridine). Correlation was described for RU 39568 (□); RU 24501, cis-cypermethrin (o); RU 39130 (▲); deltamethrin (●), RU 29221 (■) and DDT (△).

DDT stimulates [^{3}H]BTX-B binding to synaptosomal membranes in the same range of concentration over which it activates the tetrodotoxin-sensitive ^{22}Na$^+$ influx through the Na$^+$ channel in neuroblastoma cells ($K_{0.5}$ = 40 μM) (Fig. 3, inset A).

Fig. 4 compares the efficacy of pyrethroids to bind to the pyrethroid receptor and the efficacy of pyrethroids to activate the Na$^+$ channel. This correlation includes the data obtained with DDT. A good correlation has been observed (r = 0.990) between $K_{0.5}$ values corresponding to half-maximum enhancement of [^{3}H]BTX-B binding to brain membranes and $K_{0.5}$ values for activation of the Na$^+$ channel in neuroblastoma cells by the same compounds.

Quantitative autoradiographic measurements were used to analyse the distribution of pyrethroid binding sites in the CNS. Since direct experiments with [^{3}H]pyrethroids were not possible, we analysed pyrethroid-induced [^{3}H]BTX-B-binding. Other authors have recently analysed scorpion venom induced [^{3}H]BTX-B binding [37].

Incubations for brain slices with [^{3}H]BTX-B (1.5 nM) either alone or in the presence of As$_2$ failed to provide a significant specific labeling of the [^{3}H]BTX-B binding site. However differences were seen in the presence of pyrethroids. The binding of [^{3}H]BTX-B (1.5 nM) to brain slices in the presence of the pyrethroid RU 39568 (10 μM) alone or associated to the sea anemone toxin As$_2$ (40 μM) leads to a clear identification of a large enough component of [^{3}H]BTX-B binding which could be prevented by the presence of veratridine (100 μM). These results obtained on brain slices are in agreement with results previously described for brain membranes.

The CNS distribution of [^{3}H]BTX-B binding revealed in the presence of RU 39568 is heterogeneous (Table 1) while the non-specific binding component was

TABLE 1 Distribution of [^{3}H]BTX-B binding sites revealed in the presence of RU 39568 and As$_2$ in rat brain.

Results, expressed in fmol/mg protein, are the mean ± S.E.M. of 6 to 8 separate autoradiographic measurements. Each value is the difference between the total binding and the non-specific binding and is determined with 1.5 nM [^{3}H]BTX-B associated with Ru 39568 (10 μM) and As$_2$ (40 μM).

Autoradiographic procedures. Whole rat brains were quickly removed, frozen and the brain sections (15 μm thickness) were prepared using a previously described procedure [20]. The sections were incubated for 2 h at 4°C in the same standard incubation medium as described for binding experiments described above with [^{3}H]BTX-B (1.5 nM) in presence or absence of As$_2$ (40 μM) plus RU 39568 (10 μM) as indicated. The non-specific binding component was determined by adding veratridine (0.1 mM) 15 min prior to the addition of [^{3}H]BTX-B. At the end of the incubation, the sections were washed twice for 5 s in 100 mM Tris in the presence of 0.1% BSA and twice for 5 s in water. A part of the slices was used to prepare and to quantify autoradiograms as previously described [21]. The other labelled brain sections were removed and counted.

Brain structures	Specific binding	S.E.M.
Neocortex		
Frontoparietal cortex, motor area	97.5 ± 17.4	
Frontoparietal cortex, sensory area	105.5 ± 8.9	
Cingulate cortex	104.0 ± 11.6	
Temporal cortex auditory area	120.5 ± 3.1	
Striate cortex	92.0 ± 1.7	
Entorhinal cortex	72.5 ± 18.4	
Primary olfactory cortex	52.5 ± 2.7	
Hippocampal formation		
Ammon's Horn, strati oriens and radiatum	49.0 ± 1.1	
Ammon's Horn, stratum lacunosum moleculare	41.5 ± 1.7	
Dentate gyrus	63.5 ± 1.6	
Subiculum	74.0 ± 2.2	
Cerebellar cortex		
Molecular layer	34.5 ± 1.3	
Granular layer	30.0 ± 4.5	
White matter	4.5 ± 0.2	
Forebrain		
Accumbens nucleus	28.5 ± 0.2	
Caudate putamen	41.5 ± 3.6	
Lateral septal nucleus	25.0 ± 0.5	
Medial septal nucleus	34.0 ± 5.5	
Nuclei of the diagonal band of broca	27.5 ± 0.9	
Basolateral amygdaloid nucleus	65.5 ± 3.6	
Thalamus		
Anterior thalamic nuclei	92.0 ± 9.8	
Laterodorsal thalamic nucleus	77.5 ± 1.1	
Ventroposterior thalamic nucleus	53.0 ± 3.7	
Centromedian thalamic nucleus	76.0 ± 4.3	
Geniculate nuclei	80.0 ± 3.2	
Habenula	34.5 ± 4.2	
Hypothalamus		
Anterior hypothalamic area	70.0 ± 10.2	
Ventromedian hypothalamic nucleus	66.0 ± 0.8	
Posterior hypothalamic nucleus	73.0 ± 7.2	

TABLE 1 (continued)

Brain structures	Specific binding	S.E.M.
Midbrain		
Mammillary nuclei	53.0 ±	0.7
Ventral tegmental nucleus	40.5 ±	2.0
Substantia nigra	81.0 ±	0.8
Interpeduncular nuclei	68.0 ±	3.6
Central gray	104.0 ±	3.7
Superior colliculus	90.5 ±	3.7
Inferior colliculus	77.5 ±	9.4
Pontine nuclei	54.0 ±	7.1
Median raphe nucleus	53.0 ±	3.5
Deep mesencephalic nuclei	30.0 ±	2.0
Medulla oblongata		
Cochlear nuclei	50.0 ±	7.5
Nucleus of the spinal tract of the trigeminal nerve	25.5 ±	4.3
Vestibular nuclei	28.5 ±	1.2
Reticular pontine nuclei	20.5 ±	2.9
Myelinated fibers tracts		
Corpus callosum	36.0 ±	0.6
Internal capsule	21.5 ±	0.6
Brain average	59.5	

uniformly distributed throughout the CNS ($47\% \pm 7\%$ of the total binding). [^{3}H]BTX-B binding alone is uniformly distributed and is identical to the non-specific binding component of [^{3}H]BTX-B measured in the presence of veratridine (not shown). The same result was observed for [^{3}H]BTX-B binding in the presence of As$_2$ alone. A specific binding component only appeared in the presence of the toxin mixture containing the pyrethroid. Therefore [^{3}H]BTX-B binding sites are only revealed in brain areas where pyrethroid binding sites are present.

Structures that are particularly rich in [^{3}H]BTX-B receptors in the presence of the pyrethroid are the different areas of the neocortex, the central gray and to a lesser extent the anterior thalamic nuclei, and the superior colliculus and substantia nigra (Table 1). Regions with the lowest densities of pyrethroid-induced [^{3}H]BTX-B binding include the caudate putamen and medulla oblongata.

Discussion

Numerous toxins are active on the voltage-sensitive Na$^+$ channel and some of them have been instrumental in revealing new aspects of Na$^+$ channel structure and function [1]. These toxins bind at separate receptor sites [17,19,25,33]. Sites that have been well identified by binding studies using labelled toxins are those for (i) tetrodotoxin and saxitoxin that inhibit Na$^+$ flux through the Na$^+$ channel (site 1), (ii) batrachotoxin and other lipid soluble toxins like veratridine, aconitine or grayanotoxin that cause a persistent activation of Na$^+$ channels at the resting potential by shifting the voltage-dependence of the activation and by blocking

inactivation (site 2), (iii) scorpion toxins from North Africa and North America and sea anemone toxins that slow down Na^+ channel inactivation (site 3), (iv) another class of scorpion toxins that shifts the voltage-dependence of Na^+ channel activation to more negative membrane potentials (site 4), (v) brevetoxins and ciguatoxin that cause repetitive firing and depolarization of excitable membranes by activating the Na^+ channel (site 5).

A good number of [^{3}H]pyrethroids have been assayed in this laboratory to try to characterize pyrethroid binding sites. Unfortunately, it turned out that even with the most active of these insecticides, it was impossible to identify a specific binding component on rat brain synaptosomes or on insect neuronal membranes (D. Pauron and J. Barhanin, unpublished results). The non-specific binding component of [^{3}H]pyrethroids was always too high compared to the specific binding component. Furthermore, it has already been shown previously that pyrethroids are without effect on the binding of ^{3}H-labelled tetrodotoxin (A. Lombet, unpublished results) and ^{125}I-labelled sea anemone toxin [36] and scorpion toxins [3] to their respective receptors.

This paper demonstrates that pyrethroids, similarly to sea anemone toxins and to brevetoxin PbTx-2, enhance [^{3}H]BTX-B binding. Pyrethroids, similarly to sea anemone toxin and brevetoxin, do not change the maximum binding capacity of BTX-B to brain membranes, however they increase the affinity of BTX-B for its specific receptor site. This increase in the affinity for [^{3}H]BTX-B explains the enhancement of [^{3}H]BTX-B binding at non-saturating concentrations (2 nM) of [^{3}H]BTX-B. A new synthetic pyrethroid, RU 39568, increased the affinity of [^{3}H]BTX-B for its binding site by a factor of 30 while As_2 and PbTx-2 only increased the affinity by factors of 2.3 and 4.3 respectively [7,8]. The mixture of As_2 and PbTx-2 at concentrations at which they saturate their binding site produced a 7.5-fold increase in affinity for BTX-B at its binding site. The addition of RU 39568 to these two toxins further increased the affinity of BTX-B which then became 100-fold higher than in the absence of any toxin.

The functional channel protein is known to be constituted by a single polypeptide of about 270 kDa that bears all the identified binding sites for the different toxins [1,17,26]. Depending on the membrane potential and on the time after a step depolarization, the channel can exist in a non-conducting or a conducting form. Batrachotoxin is known to bind preferentially to the conducting form [14,28]. Therefore, toxins like sea anemone toxins or brevetoxins or pyrethroids or mixtures of these toxins that increase the probability of finding the Na^+ channel in the open form [6,17,25] will of course favour the binding of batrachotoxin. Cumulative effects of sea anemone toxins, brevetoxins and pyrethroids on [^{3}H]BTX-B binding imply of course that these three categories of Na^+ channel effectors have different types of receptors and also that these receptors are distinct from the batrachotoxin binding sites.

The stimulation of [^{3}H]PbTx-3 binding by both As_2 and pyrethroids and by the mixture of the two (Fig. 1, inset) confirms that the three types of toxins bind to three different types of receptors.

Conclusions regarding the different types of binding sites and allosteric interactions between the different receptor sites for different toxins coming from [^{3}H]BTX-B binding experiments are perfectly consistent with $^{22}Na^+$ flux studies through the voltage-sensitive Na^+ channel in neuroblastoma cells. Previous studies from this laboratory have shown that batrachotoxin, veratridine, grayanotoxin and sea

anemone toxin and also α-scorpion toxins act synergistically with pyrethroids [12]. For all these reasons, it is now clear that pyrethroids bind to a special category of receptor sites (site 6). The good correlation between binding results on brain membranes and $^{22}Na^+$ flux data (Fig. 4) in neuroblastoma cells clearly indicates that receptor sites for pyrethroids that have been biochemically identified in Fig. 2 are those that are responsible for Na^+ channel activation under the influence of this class of insecticides.

Electrophysiological experiments [18] have suggested that DDT, in spite of its different structure from pyrethroids, acts similarly and at the same binding site as pyrethroids. Moreover, acquisition of pyrethroid resistance in insects is often accompanied by resistance to DDT [23]. Observations made in this paper also show the analogy between DDT and pyrethroids. Data for DDT are well integrated into the correlation presented in Fig. 4.

The direct autoradiographic localization of pyrethroid binding sites with labelled pyrethroids is not possible at present. Therefore, pyrethroid binding sites have been indirectly localized by their capacity to reveal [^{3}H]BTX-B binding to the CNS. The distribution of [^{3}H]BTX-B binding sites which then reveal the distribution of pyrethroid binding sites is similar but not identical to the previously identified distribution of tritiated tetrodotoxin or saxitoxin binding sites [22] that are also known to reside on voltage-dependent Na^+ channels.

Large amounts of tetrodotoxin and saxitoxin binding sites were previously found [22] in hippocampus (region 3 of the Ammon's horn), in substantia nigra and in the molecular layer of the cerebellar cortex. No such property was found for pyrethroid binding sites revealed from [^{3}H]BTX-B binding. The probable interpretation of these results is linked to the existence of sub-types of voltage-sensitive Na^+ channels. Among these sub-types some are sensitive to tetrodotoxin and saxitoxin, others are resistant to the two toxins and require much higher toxin concentrations to be blocked. Labelled tetrodotoxin and saxitoxin probably label selectively the sub-type of Na^+ channels with a high affinity for the toxins. Conversely pyrethroid induced [^{3}H]BTX-B binding will reveal both types of Na^+ channels since pyrethroids have previously been shown to act with the same efficacy on tetrodotoxin-sensitive and tetrodotoxin-resistant Na^+ channels [3].

The assay developed in this work to analyse pyrethroid binding properties to the Na^+ channel in mammalian neuronal membranes can be used with insect neuronal membranes and serves to analyse the structure–function relationships of these important compounds in relation with their insecticide properties and to analyse the mechanism of acquired resistance of insects to insecticides of the pyrethroid family [32].

Summary

Measurement of neurotoxin binding in rat brain membranes and neurotoxin-activated $^{22}Na^+$ influx in neuroblastoma cells were used to define the site and mechanism of action of pyrethroids and DDT on sodium channels. A highly potent pyrethroid, RU 39568, alone enhanced the binding of [^{3}H]batrachotoxinin A 20-α benzoate up to 30-times. This effect was amplified by the action of neurotoxins such as sea anemone toxins and brevetoxin acting at different sites of the sodium channel protein in brain membranes. The ability of various pyrethroids and DDT to

enhance batrachotoxin binding was related to their capacity to activate tetrodoto-xin-sensitive $^{22}Na^+$ uptake. These results point to an allosteric mechanism of pyrethroids and DDT action involving preferential binding to active states of sodium channels which have high affinity for neurotoxins, causing persistent activa-tion of sodium channels. Pyrethroids do not block [^{3}H]tetrodotoxin binding, ^{125}I *Anemonia sulcata* toxin 2 binding, ^{125}I *Tityus serrulatus* toxin γ binding at neuro-toxin receptor sites 1, 3 and 4 respectively. Pyrethroids appear to act at a new neurotoxin receptor site on the sodium channel. The distribution of pyrethroid binding sites in rat brain was determined by quantitative autoradiographic proce-dures using the property of pyrethroids to reveal binding sites for [^{3}H]batrachotoxin A 20-α benzoate.

References

1 Agnew, W.S., Tomiko, S.A., Rosenberg, R.L., Emerick, M.C. and Cooper, E.C. (1986) The structure and function of the voltage-sensitive Na channel. In: Tetrodotoxin, Saxitoxin, and the Molecular Biology of the Sodium Channel, Vol. 479 (C.Y. Kao, S.P. Levinson, eds.), Annals of the New York Academy of Sciences, pp. 238–256.

2 Albuquerque, E.X. and Daly, J.W. (1976) Batrachotoxin, a selective probe for channels modulating sodium conductances in electrogenic membranes. In: The Specificity and Action of Animal, Bacterial and Plant Toxins, Vol. 1 (P. Cuatrecasas, ed.), pp. 297. Chapman Hall, London.

3 Barhanin, J., Giglio, J.R., Léopold, P., Schmid, A., Sampaio, S.V. and Lazdunski, M. (1982) *Tityus serrulatus* venom contains two classes of toxins. J. Biol. Chem. 257, 12553–12558.

4 Brown, G.B. (1986) [^{3}H]Batrachotoxinin-A benzoate binding to voltage-sensitive sodium channels: inhibition by the channel blockers tetrodotoxin and saxitoxin. J. Neurosci. 6, 2064–2070.

5 Casida, J.E., Gammon, D.W., Glickman, A.H. and Lowell, J.L. (1983) Mechanisms of selective action of pyrethroid insecticides. Ann. Rev. Pharmacol. Toxicol. 23, 413–438.

6 Catterall, W.A. (1977) Activation of the action potential Na^+ ionophore by neurotoxins. J. Biol. Chem. 252, 8669–8676.

7 Catterall, W.A. and Gainer, M. (1985) Interaction of brevetoxin A with a new receptor site on the sodium channel. Toxicon 23, 497–504.

8 Catterall, W.A., Morrow, C.S., Daly, J.W. and Brown, G.B. (1981) Binding of batracho-toxinin A 20-α Benzoate to a receptor site associated with sodium channels in synaptic nerve ending particles. J. Biol. Chem. 256, 8922–8927.

9 Chinn, K. and Narahashi, T. (1986) Stabilization of sodium channel states by deltameth-rin in mouse neuroblastoma cells. J. Physiol. (Lond.) 380, 291–307.

10 Holan, G., Frelin, C. and Lazdunski, M. (1985) Selectivity of action between pyrethroids and combined DDT-pyrethroid insecticides on Na⁺ Influx into mammalian neuroblastoma. Experientia 41, 520–522.

11 Honerjäger, P. (1982) Cardioactive substances that prolong the open state of sodium channels. Rev. Physiol. Biochem. Pharmacol. 92, 1–74.

12 Jacques, Y., Romey, G., Cavey, M.T., Kartalowski, B. and Lazdunski, M. (1980) Interaction of pyrethroids with the Na⁺ channel in mammalian neuronal cells in culture. Biochim. Biophys. Acta 600, 882–897.

13 Kao, C.Y. and Levinson, S.R. (eds) (1986) In: Tetrodotoxin, Saxitoxin and the Molecular Biology of the Sodium Channel, Vol. 479. Annals of the New York Academy of Sciences, pp. 1–445.

14 Khodorov, B.I. (1985) Batrachotoxin as a tool to study voltage-sensitive sodium channels of excitable membranes. Prog. Biophys. Mol. Biol. 45, 57–148.

15 Krueger, B.K., Ratzlaff, R.W., Strichartz, G.R. and Blaustein, M.P. (1979) Saxitoxin binding to synaptosomes, membranes, and solubilized binding sites from rat brain. J. Memb. Biol. 50, 287–310.

16 Laufer, J., Pelhate, M. and Sattelle, D.B. (1985) Actions of pyrethroid insecticides on insect axonal sodium channels. Pestic. Sci. 16, 651–661.

17 Lazdunski, M., Frelin, C., Barhanin, J., Lombet, A., Meiri, H., Pauron, D., Romey, G., Schmid, A., Schweitz, H., Vigne, P. and Vijverberg, H.P.M. (1986) Polypeptide toxins as tools to study voltage-sensitive Na⁺ channels. In: Tetrodotoxin, Saxitoxin, and the Molecular Biology of the Sodium Channel, Vol. 479 (C.Y. Kao, S.P. Levinson, eds.), pp. 204–220. Annals of the New York Academy of Sciences.

18 Lund, A.E. and Narahashi, T. (1983) Kinetics of sodium channel modification as the basis for the variation in the nerve membrane effects of pyrethroids and DDT analogs. Pestic. Biochem. Physiol. 20, 203–216.

19 Meves, H., Simard, J.M. and Watt, D.D. (1986) Interactions of scorpion toxin with the sodium channel. In: Tetrodotoxin, Saxitoxin, and the Molecular Biology of the Sodium Channel, Vol. 479 (C.Y. Kao, S.P. Levinson, eds.), pp. 113–132. Annals of the New York Academy of Sciences.

20 Mourre, C., Hugues, M. and Lazdunski, M. (1986) Quantitative autoradiographic mapping in rat brain of the receptor of apamin, a polypeptide toxin specific for one class of Ca²⁺-dependent K⁺ channels. Brain Res. 382, 239–249.

21 Mourre, C., Cervera, P. and Lazdunski, M. (1987) Autoradiographic analysis in rat brain of the postnatal ontogeny of voltage-dependent Na⁺ channels, Ca²⁺-dependent K⁺ channels and slow Ca²⁺ channels identified as receptors for tetrodotoxin, apamin and (−)desmethoxyverapamil. Brain Res. 417, 21–32.

22 Mourre, C., Moll, C., Lombet, A. and Lazdunski, M. (1988) Distribution of voltage-dependent Na⁺ channels identified by high-affinity receptors for tetrodotoxin and saxitoxin in rat and human brains: quantitative autoradiographic analysis. Brain Res. 448, 128–133.

23 Narahashi, T. (1983) Resistance to insecticides due to reduced sensitivity of the nervous systems. In: Pest Resistance to Pesticides: Challenges and Prospects (G.P. Georghiou, T. Saito, eds.), pp. 333. Plenum Press, New York.

24 Narahashi, T. (1985) Nerve membrane ionic channels as the primary target of pyrethroids. Neurotoxicology 6, 3–22.

25 Narahashi, T. (1986) Toxins that modulate the sodium channel gating mechanism. In: Tetrodotoxin, Saxitoxin, and the Molecular Biology of the Sodium Channel, Vol. 479 (C.Y. Kao, S.P. Levinson, eds.), pp. 133–151. Annals of the New York Academy of Sciences.

26 Noda, M., Ikeda, T., Suzuki, H., Takeshima, H., Takahashi, T., Kuno, M. and Numa, S. (1986) Expression of functional sodium channels from cloned cDNA. Nature 322, 826–828.

27 Poli, M.A., Mende, T.J., Baden, D.G. (1986) Brevetoxins, unique activators of voltage-sen-

sitive sodium channels, bind to specific sites in rat brain synaptosomes. Mol. Pharmacol. 30, 129–135.

28 Quandt, F.N. and Narahashi, T. (1982) Modification of single Na^+ channels by batrachotoxin. Proc. Natl. Acad. Sci. U.S.A. 79, 6732–6736.

29 Roche, M., Frelin, C., Bruneau, P. and Meinard, C. (1985) Interaction of thralomethrin, tralocythrin, and related pyrethroids in Na^+ channels of insect and mammalian neuronal cells. Pestic. Biochem. Physiol. 24, 306–316.

30 Ruigt, G.S.F., Neyt, H.C., Van der Zalm, J.P. and Van den Bercken, J. (1987) Increase of the sodium current after pyrethroid insecticides in mouse neuroblastome cells. Brain Res. 437, 309–322.

31 Schweitz, H., Vincent, J.P., Barhanin, J., Frelin, C., Linden, G., Hugues, M. and Lazdunski, M. (1981) Purification and pharmacological properties of eight sea anemone toxins from *Anemonia sulcata, Anthopleura xanthogrammica, Stoichactis giganteus,* and *Actinodendron plumosum.* Biochemistry 20, 5245–5252.

32 Scott, J.G. and Georghiou, G.P. (1986) Mechanism responsible for high levels of permethrin resistance in the house fly. Pestic. Sci. 17, 195–206.

33 Strichartz, G., Rando, T. and Wang, G.K. (1987) An integrated view of the molecular toxicology of sodium channel gating in excitable cells. Ann. Rev. Neurosci. 10, 237–267.

34 Vijverberg, H.P.M., Van der Zalm, J.M. and Van den Bercken, J. (1982) Similar mode of action of pyrethroids and DDT on sodium channel gating in myelinated nerves. Nature 295, 601–603.

35 Vijverberg, H.P.M. and de Weille, J.R. (1985) The interaction of pyrethroids with voltage-dependent Na channels. Neurotoxicology 6, 23–34.

36 Vincent, J.P., Balerna, M., Barhanin, J., Fosset, M. and Lazdunski, M. (1980) Binding of sea anemone toxin to receptor sites associated with the gating system of sodium channel in synaptic nerve endings in vitro (scorpion neurotoxin/synaptosomes). Proc. Natl. Acad. Sci. U.S.A. 77, 1646–1650.

37 Worley, P.F. and Baraban, J.M. (1987) Site of anticonvulsant action on sodium channels: autoradiographic and electrophysiological studies in rat brain. Proc. Natl. Acad. Sci. U.S.A. 84, 3051–3055.

38 Yamamoto, D., Quandt, F.N. and Narahashi, T. (1983) Modification of single sodium channels by the insecticide tetramethrin. Brain Res. 274, 344–349.

CHAPTER 22

Receptors for acetylcholine in the nervous system of insects

H. BREER

Universität Stuttgart-Hohenheim, Institut für Zoophysiologie, 7000 Stuttgart 70, F.R.G.

In the central nervous system of insects, as in other species, nerve cells communicate with their target cells mostly by means of chemical substances. Acetylcholine (ACh) appears to be the predominant excitatory neurotransmitter in the central nervous system of insects [1]. Thus, exploring the molecular elements of cholinergic synapses is of particular importance for understanding molecular functions in the insect nervous system, and may elucidate interesting aspects of insect neuropharmacology.

Cholinergic receptors are perhaps the oldest and certainly the most studied transmitter receptors [2]; they were first classified by Dale based upon responses to nicotine and muscarine [3]. Electrophysiological research and binding studies have revealed that the receptors for ACh in insects as in vertebrates can be classified into nicotinic and muscarinic receptor types. However, a different receptor type predominates in each animal group: in vertebrate brain muscarinic receptors are in a large majority whereas in insect nervous tissue there is a very high concentration of nicotinic receptors [4]. The exploration of the molecular properties and microphysiological functions of the receptors for ACh in the central nervous system of insects are under investigation in several laboratories, using a variety of approaches mostly developed for studying transmitter receptors in vertebrates.

The existence of specific receptors for ACh in insects was first demonstrated by the high sensitivity of certain neurones to applied ACh following the inhibition of endogenous acetylcholinesterase [5,6]. In recent years a wealth of new data on properties and functions of insect acetylcholine receptors (AChR) has been collected using electrophysiological and biochemical approaches [7] and in fact there is still a number of reasons for extensive research on receptors for ACh in the nervous system of insects; e.g. the elucidation of functional and molecular properties of the ACh receptors in arthropods, which are far apart from vertebrates on the evolutionary scale, may allow some interesting comparisons that are of particular interest for understanding the phylogenetic evolution of receptor molecules. Furthermore a combination of data on receptor structure with physiological and pharmacological findings on receptor function from different species, may provide some new insights into molecular mechanisms of receptor molecules.

In contrast to vertebrates, ACh receptors in insects are confined to the central nervous system and correspondingly high concentrations of cholinergic receptors,

predominantly of the nicotinic type, have been detected in the ganglionic tissue. The nervous tissue of insects thus provides a rich source of neuronal nicotinic ACh receptors (nAChR) and it will be of great interest if differences in the cholinergic microphysiology of neuromuscular junctions, electromotor synapses and neuronal synapses are reflected in a different molecular structure of the receptor complex.

In order to devise more selective and specific control agents for insects, it is of particular importance to study and to identify the strategic elements of neuronal function. Since many of today's insecticides poison the cholinergic synapse, the receptor for ACh, the molecular transducer of chemical signals at cholinergic synapses, may be considered as one such key element and characterization of insect ACh receptors may thus enhance our understanding of insecticide action. More detailed information on the receptors for ACh may provide a formula for the production of more potent and safer receptor blockers and thus be a step towards more specific and selective insect control agents. Exploring the molecular structure of the receptor proteins may also provide new insight into the molecular basis of certain types of insecticide resistance.

Functional role of ACh receptors

Electrophysiological studies on the pharmacology of cholinergic synaptic transmission in insects have revealed that receptors for ACh are widely distributed on the synapse-free cell bodies of neurones as well as throughout the complex, synapse-rich neuropil and that cholinergic synaptic transmission is irreversibly blocked by nanomolar concentrations of α-bungarotoxin [8]. Thus both synaptic and extrasynaptic membranes in insect ganglia apparently contain nicotinic cholinergic receptors, which mediate signal transduction by activating specific cation channels [9].

The function of the muscarinic type of ACh receptors, which in insects represents only a small fraction of the cholinergic receptors, is less clear. Pharmacological studies using subcellular fractions have revealed that different muscarinic receptor subtypes can be distinguished on the membranes from perikarya and synaptosomes: predominantly M_1-type on cell bodies, mainly M_2-type on nerve terminals. Microperfusion experiments on locust synaptosomes have revealed that the presence of elevated concentrations of ACh or muscarinic agonists consistently yielded reduced levels of ACh release, suggesting a negative feedback regulation of transmitter release at cholinergic synapses in insects. Studies with cholinergic ligands showed that muscarinic agonists like oxotremorine reduced the rate of ACh release, whereas antagonists, like atropine, increased the release rate [10]. By contrast, nicotinic ligands showed no effect. Thus, it appears that muscarinic receptors are located on cholinergic nerve terminals of insect ganglia and are involved in autoregulation of ACh release. Evidence for a functional role of presynaptic muscarinic receptors has also been reported for several vertebrate synapses [11].

Functional properties of the receptors

Voltage-clamp experiments on insect nerve cell bodies, e.g. on motorneurones, have revealed that nicotinic ACh receptors gate cation channels permeable to sodium,

potassium and possibly calcium [12]. Patch-clamp techniques have been applied to dissociated cells in short term culture, using a cell-attached configuration; the activation of a single class of inward channels by ACh was observed. At resting potential the inward current was about 1.5 pA and the single channel conductance was approximately 40 pS [13,14]. Channels with similar properties have been observed recently in membrane patches from locust nerve cells using the outside-out-configuration (Tareilus and Hanke, in preparation). When purified nicotinic ACh receptors from locust ganglia were reconstituted in planar lipid bilayer membranes, a channel conductance of a somewhat large amplitude (75 pS) was detected. The reconstituted receptor probably derives predominantly from material of synaptic origin, whereas the cell body receptors studied by the patch clamp techniques are not found in synaptic regions. The differences observed for single channel conductance of the cell body receptor and the reconstituted neuronal nicotinic receptor are quite similar to those reported for nicotinic receptors in vertebrate muscle cells when synaptic and extrasynaptic regions are compared [15].

The different muscarinic receptor subtypes in the vertebrate brain have been found to transduce the external signal into different intracellular second messengers systems; the M_1-type is thought to be coupled with the phosphoinositol-system, whereas the M_2-type is concerned with the down-regulation of adenylate cyclase. Accordingly, it has been found that the adenylate cyclase activity in synaptosomal preparations was inhibited by muscarinic M_2-type agonists.

Ligand binding

As an alternative to direct, electrophysiological approaches to study ligand–receptor interaction, binding studies have been performed using radiolabelled ligands in order to quantify specific receptors and to determine kinetic constants as well as the pharmacological profile of the receptor. Based on high affinity, specific and saturable binding, nicotinic receptors have been probed by labelled snake α-neurotoxins, notably α-bungarotoxin. Putative nicotinic receptors were found in the nervous tissue of various insect species at concentrations several orders of magnitude higher than in vertebrate brain tissue (Table 1). The binding constants closely resemble those reported for other species and the pharmacology of toxin binding was clearly nicotinic [7].

Muscarinic receptors were studied using tritiated quinuclidinyl benzylate as a specific probe. The number of putative muscarinic receptors is about an order of magnitude lower than that for toxin binding sites in insect nervous tissue and is also much lower than the concentration of mAChR in vertebrate brain (Table 1).

TABLE 1   Levels of putative nicotinic and muscarinic receptors in the nervous tissue

Species	Tissue	nAChR	mAChR
Locust	ganglia	1775	116
Cockroach	nerve cord	910	138
Drosophila	heads	800	65
Rat	hippocampus	85	502

Values given as fmol/mg protein.

The observation that the relative levels of nicotinic and muscarinic receptors in vertebrate and insect nervous tissue are reversed is a major difference between cholinergic binding sites in arthropods and vertebrates although its functional implications are still unknown.

Recently it has been discovered that perturbation of membrane preparations, e.g. pretreatment with mild detergent, significantly enhanced the binding of α-toxins, suggesting that an endogenous inhibitor of cholinergic ligand binding was eliminated. Further experiments to be reported have shown that this endogenous inhibitor is not ACh itself, or choline, but is a thermostable polypeptide with a molecular weight of approximately 15,000. Since the inhibitor does not act competitively with cholinergic ligands, it may act at the membrane level as an allosteric modulator of cholinergic binding sites; however, the exact mechanism by which α-toxin binding is inhibited remains to be explored in detail.

Biochemical characterization

Biochemical studies including gradient centrifugation, polyacrylamide gel electrophoresis and radiation-inactivation have shown that the putative nicotinic ACh receptor in the nervous tissue of several insect species apparently represents a macromolecular protein complex with a sedimentation coefficient of about 10 S. Size determinations of the native receptor protein gave M_r-values between 236,000 and 300,000 [16,17]. In the presence of SDS, however, the receptor protein obviously dissociated into several subunits; the major protein migrated as a polypeptide band (M_r about 65,000) together with a minor component of about 58,000. The minor band has been considered as proteolysis product, but may in fact represent a different receptor subunit, as a more complex polypeptide pattern has been found of a purified receptor preparation isolated by a different procedure [18], and accordingly a more complicated subunit composition has been suggested. In this context it is of considerable interest to note that results of recent immunological, biochemical and molecular approaches suggest that the nicotinic ACh receptor in vertebrate brain is apparently composed of only two different subunits and is thus quite different from the muscle receptor [19,20].

There have been only a few attempts to identify the muscarinic receptor in insect nervous tissue. In affinity labelling and immunochemical experiments the muscarinic receptor has been identified as an 80,000 Da polypeptide [21]; a similar polypeptide was labelled in experiments using locust membranes [22]. These results are in good agreement with the value of 77,600 found in radiation-inactivation studies on *Periplaneta* membranes [23].

Immunochemistry

In immunological approaches (ELISA, Western blot) it was found that monoclonal antibodies raised against the nicotinic ACh receptor from *Torpedo* significantly cross-react with locust membranes and with purified receptor proteins; these results point to considerable similarities in the molecular structure of the receptors from these two distinct sources [16]. Antisera raised against the purified locust receptor protein were employed in immunohistochemical studies and the specific antibodies

densely stained distinct areas in the neuropile of ganglia from different insect species including regions which are known to contain functional nicotinic receptors [7].

Reconstitution of a nicotinic ACh receptor

The ultimate proof that the purified membrane protein is in fact a functional ACh receptor (i.e. contains both the agonist-binding site and the channel that it regulates) can only be achieved by reconstituting the receptor in artificial lipid membranes. The purified locust receptor protein has recently been incorporated into planar lipid bilayers. It was found that addition of cholinergic agonists induced the activation of cationic channels with a conductance of about 75 pS and an open time of a few ms (Fig. 1), thus demonstrating that the purified toxin binding protein from insect nervous tissue behaves like a functional nicotinic ACh receptor [24]. After more detailed analyses some interesting features of this neuronal ACh receptor channel emerged: the probability of channel being in the open state was 0.1, the mean life time of the open state was 4 ms and of the closed state was 46 ms. Pharmacological experiments revealed that the agonist-activated-membrane conductance was inhibited by the classical antagonist d-tubocurarine, however, only very weak effects were found with hexamethonium, which is known as a good blocker of the peripheral vertebrate receptor. These observations are in good agreement with results from electrophysiological and binding studies, which document a low affinity of hexamethonium for ACh receptors in insects [12] indicating the pharmacological integrity of the purified receptor protein. The neuronal ACh receptor exhibits properties (multiple gating of the channel, burst behaviour, fast flickering, desensitization), similar to those of the reconstituted receptor from electric tissue [25] and to receptors in muscle cells analysed in situ [15], however, very distinct pharmacological and kinetic differences were also observed [26]. These results demonstrate that most if not all of the electrophysiological criteria for ACh-activated cation channels
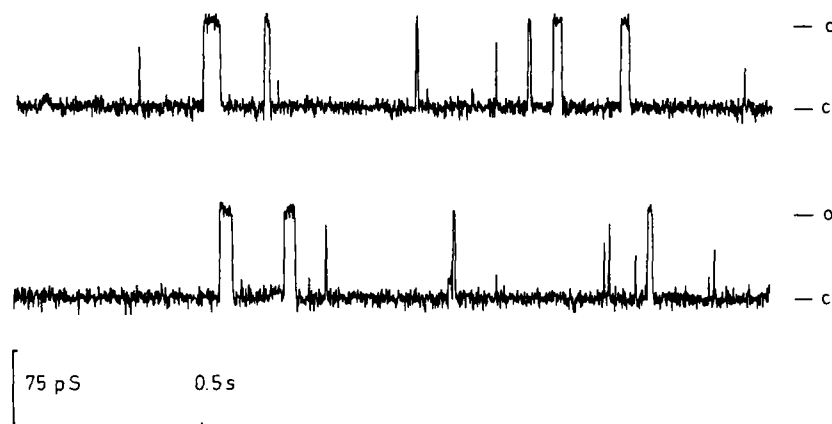

FIG 1 Fluctuation of a purified AChR channel isolated from locust nervous tissue and reconstituted in planar lipid bilayer. The receptor was activated by 0.5 μM carbamylcholine at 90 mV.

are met by the membrane protein purified from locust ganglia. Very recently functional ACh receptors have successfully been reconstituted in planar lipid bilayers after electrophoretic separation of receptor polypeptides on SDS–poly-acrylamide gel, followed by electroelution of the peptide bands and incorporation into artificial membranes. From these results it might be concluded that receptor polypeptides which migrate as a single band on SDS–gel are sufficient to form functional ACh receptors in planar lipid bilayers. This observation does not, however, unequivocally address the issue of the subunit structure of the nicotinic ACh receptor in insect nervous tissue in vivo.

Expression of receptor-specific mRNA

In order to recognize mRNA encoding receptor polypeptides, isolated poly A$^+$ RNA was translated in a cell-free system as well as in *Xenopus* ooytes. RNA isolated from nervous tissue of locusts was translated in a rabbit reticulocyte lysate in the presence of labelled amino acids. Immunoprecipitation experiments followed by electrophoretic analysis indicated that about 0.1% of the polypeptides could be separated, showing that antigenic sites already exist on non-processed polypeptides and that the poly A$^+$-fractions obviously contain receptor-specific mRNA [27]. Isolated RNA was expressed in oocytes in order to estimate if functional receptors could be synthesized in this system. When poly A$^+$ RNA isolated from nervous tissue of young locusts was microinjected into oocytes, after 1 day binding activity for α-bungarotoxin could be detected (Fig. 2). The binding activity showed a linear relationship to the amount of injected RNA over the range of 0–15 ng per oocyte [28]. Immunoprecipitation experiments have revealed that receptor polypeptides synthesized in vivo display the same or a similar size as the native subunits, indicating that all posttranslational modifications of the insect proteins were performed in oocytes and suggesting that probably functional ACh receptors have been produced. This problem was analysed using an ion flux assay; it was found that in
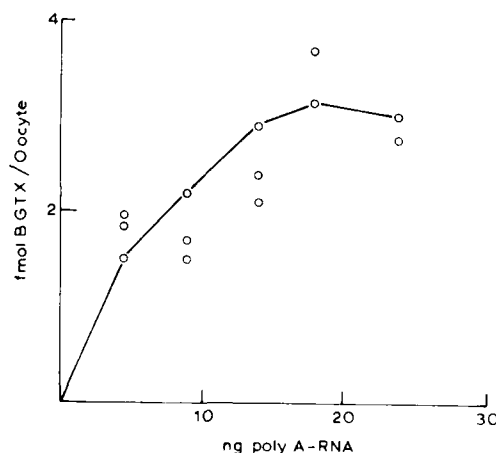

FIG 2 Expression of α-bungarotoxin binding sites in *Xenopus* ooytes after microinjection of poly A$^+$ RNA isolated from nervous tissue of locusts. The appearance of binding sites after 24 h of incubation is up to 20 ng RNA dependent on the amount of RNA injected.

oocytes microinjected with insect mRNA and incubated for 24 h a significant influx of ^{86}Rb could be induced by cholinergic agonists. Thus indicating that receptor-specific mRNA can be isolated from locust nervous tissue and that ACh-activated cation channels are synthesized and assembled in injected oocytes.

The nucleic acid preparation containing receptor-specific RNA was used as a template to produce a cDNA library. The cDNA was cloned into the gt11 expression vector which promotes synthesis of fusion proteins. The library was assayed for receptor-specific clones using receptor-specific antibodies. Several plaques were found to be immunoreactive; two were further plaque purified. Lysogens were made and grown under conditions to induce the synthesis of β-galactosidase fusion protein and the fusion protein was identified on Western blots using anti-receptor antibodies. This clone is now considered to be a promising candidate for evaluating the primary structure of the locust receptor protein.

In recent studies cDNA libraries from *Drosophila* have been screened using DNA-probes corresponding to *Torpedo* receptor α-subunits. A clone which resembles the general structure of a cholinergic subunit has been produced; the mature protein is predicted to consist of 497 aminoacids [21] but does not contain the typical elements characteristic of the α-subunit. However, in a recent report [30] an α-like subunit of a nicotinic AChR from *Drosophila* has also been described but this subunit does not bind α-toxins. In the light of the similarity which has been found between ligand-activated ion channels and the multiplicity of α-subunit-like structures described for neuronal proteins [19], the identification of *Drosophila* clones as genuine acetylcholine receptor components based solely on homology may be premature. Attempts to clone ACh receptors of other insect species are going on in a number of laboratories and new, more detailed, information is expected in the near future.

Conclusion

The results of studies on the nicotinic ACh receptor in insects emphasize the potential of insect nervous tissue for tackling general problems of cellular and molecular neurobiology. Experimental analysis of insect material has provided the first clear evidence for a functional postsynaptic role of an α-bungarotoxin-sensitive nicotinic ACh receptor in synaptic transmission at an identified central cholinergic synapse. Furthermore an affinity purified binding protein isolated from insect nervous tissue was the first neuronal nicotinic ACh receptor functionally reconstituted in planar lipid bilayer. This protein now permits for the first time the comparison of functional properties of receptor activated channels in vivo following reconstitution in membranes of defined lipid composition. Pharmacological evidence has recently accumulated indicating that some insecticide molecules are active at the nicotinic receptor-channel complex in the insect nervous system. Thus we can anticipate that a more detailed knowledge of receptor molecules for ACh in the insect nervous system will offer new approaches to the development of more selective and safer control agents for insects.

References

1 Florey, E. (1963) Acetylcholine in invertebrate nervous system. Can. J. Biochem. Physiol. 41, 2619–2626.

2 Michelson, M.J. (1973) Pharmacology of cholinergic systems in some other phyla. In: Comparative Pharmacology (M.J. Michelson, ed.) pp. 169–190. Pergamon, N.Y.

3 Dale, H.H. (1914) The action of certain esters and ethers of choline, and their relation to muscarine. J. Pharmacol. 6, 147–190.

4 Dudai, Y. (1979) Cholinergic receptors in insects. Trends Biochem. Sci. 4, 40–44.

5 Kerkut, G.A., Pitman, R.M. and Walker, R.J. (1969) Iontophoretic application of acetylcholine and GABA onto insect central neurons. Comp. Biochem. Physiol. 31, 611–633.

6 Sattelle, D.B. (1977) Cholinergic synaptic transmission in invertebrate central nervous systems. Biochem. Soc. Tans. 5, 849–852.

7 Breer, H. and Sattelle, D.B. (1987) Molecular properties and functions in insect acetylcholine receptors. J. Insect Physiol. 33, 771–790.

8 Sattelle, D.B., Harrow, D., Hue, B., Gepner, J. and Hall, L.M. (1983) α-Bungarotoxin blocks excitatory synaptic transmission between cercal sensory neurons and giant interneurone 2 of the cockroach, Periplaneta americana. J. Exp. Biol. 107, 473–489.

9 Sattelle, D.B. and David, J.A. (1983) Voltage-dependent block by histrionicotoxin of the acetylcholine-induced current in a insect motoneurone cell body. Neurosci. Lett. 43, 37–41.

10 Breer, H. and Knipper, M. (1984) Characterization of acetylcholine release from insect synaptosomes. Insect Biochem. 14, 337–344.

11 Bartfai, T., Study, R.E. and Greengard, P. (1977) Muscarinic stimulation and cGMP synthesis in the nervous system. In: Cholinergic Mechanisms and Psychopharmacology (L. Iversen, S. Iversen, S.M. Snyder, eds.), pp. 285–95. Plenum Press, N.Y.

12 David, J.A. and Sattelle, D.B. (1984) Actions of cholinergic pharmacological agents on the cell body membrane of the fast coxal depressor motoneurone of the cockroach (Periplaneta americana). J. Exp. Biol. 108, 119–136.

13 Sattelle, D.B., Sun, Y.A. and Wu, C.F. (1986) Neuronal acetylcholine receptor: patch clamp recording of single channel properties from dissociated insect neurones. IRCS Med. Sci. 14, 65–66.

14 Beadle, D. and Lee, G. (1986) Cell cultures: a new tool in insect neuropharmacology. In: Neuropharmacology and Pesticide Action (N.G. Ford, G.G. Lunt, R.C. Reay, P.N.R. Usherwood, eds.), pp. 370–384. Ellis Horwood, Chichester. 1986.

15 Sakmann, B., Bormann, J. and Hamill, O.P. (1983) Ion transport by single receptor channels. In: Molecular Neurobiology (J.D. Watson, R. McKay, eds.) pp. 247–257. Cold Spring Harbor Symposia on Quantitative Biology XLVII.

16 Breer, H., Kleene, R. and Hinz, G. (1985) Molecular forms and subunit structure of the acetylcholine receptor in the central nervous system of insects. J. Neurosci. 5, 3386–3392.

17 Sattelle, D.B. and Breer, H. (1985) Purification by affinity chromatography of nicotinic acetylcholine receptor from the CNS of the cockroach Periplaneta americana. Comp. Biochem. Physiol. 82C, 349–352.

18 Filbin, M.T., Lunt, G.G. and Donnellan, F.F. (1983) Partial purification and characterisation of an acetylcholine receptor with nicotinic properties from the supraoesophageal ganglion of the locust (Schistocerca gregaria). Eur. J. Biochem. 132, 151–156.

19 Boulter, J., Evans, K., Goldman, D., Martin, G., Treco, D., Heineman, S. and Patrick, J. (1987) Isolation of a cDNA clone coding for a possible neural nicotinic acetylcholine receptor α-subunit. Nature 319, 368–374.

20 Whiting, P.J. and Lindstrom, J.L. (1986) Purification and characterization of a nicotinic ACh-receptor from chick brain. Biochemistry 25, 2082–2093.

21 Venter, J.C., Eddy, B., Hall, L.M. and Fraser, C.M. (1984) Monoclonal antibodies detect the conservation of muscarinic cholinergic receptor structure from Drosophila to human brain and detect possible structural homology with-adrenergic receptors. Proc. Natl. Acad. Sci. U.S.A. 81, 272–276.

22 Knipper, M. and Breer, H. (1988) Subtypes of muscarinic receptors in the nervous system of insects. Comp. Biochem. Physiol. 90C, 275–280

23 Lummis, S.C.R., Sattelle, D.B. and Ellory, J.C. (1984) Molecular weight estimates of insect cholinergic receptors by radiation inactivation. Neurosci. Lett. 44, 7–12.

24 Hanke, W. and Breer, H. (1986) Channel properties of a neuronal acetylcholine receptor protein purified from central nervous system of insect reconstituted in planar lipid bilayers. Nature (Lond.) 321, 171–174.

25 Labarca, P., Lindstrom, J. and Montal, M. (1984) Acetylcholine receptor in planar lipid bilayers: Characterization of the channel properties of the purified nicotinic acetylcholine receptor from Torpedeo californica reconstituted in planar lipid bilayers. J. Gen. Physiol. 83, 473–496.

26 Hanke, W. and Breer, H. (1987) Characterization of the channel properties of a neuronal acetylcholine receptor reconstituted into planar lipid bilayer. J. Gen. Physiol. 90, 855–879.

27 Benke, D. and Breer, H. (1988) In vitro synthesis of neuronal acetylcholine receptor polypeptides. Mol. Cell. Neurobiol. 7, 391–401.

28 Breer, H. and Benke, D. (1986) Messenger RNA from insect nervous tissue induces expression of neuronal acetylcholine receptors in Xenopus oocytes. Mol. Brain Res. 1, 111–117.

29 Hermans-Borgmeyer, I., Zopf, D., Rysek, R-P., Hovemann, B., Betz, H. and Gundelfinger, E.D. (1986) Primary structure of a developmentally regulated nicotinic acetylcholine receptor protein from Drosophila. EMBO J. 5, 1503–1508.

30 Bossy, B., Ballivet, M. and Spierer, P. (1988) Conservation of neural nicotinic acetylcholine receptors from Drosophila to vertebrate central nervous systems. EMBO J. 3, 611–618.

CHAPTER 23

Genetic and pharmacological analyses of potassium channels in *Drosophila*

CHUN-FANG WU [1] AND BARRY GANETZKY [2]

[1] *Department of Biology, University of Iowa, Iowa City, IA 52242*
and [2] *Laboratory of Genetics, University of Wisconsin, Madison, WI 53706, U.S.A.*

Introduction

The rich diversity of neurons and other excitable cells with distinctive signalling capability must reflect cellular differences in the expression of ion channel types, their distribution and their modulation. Much of this diversity is attributable to the existence of a large variety of potassium channels, as suggested by previous physiological and pharmacological studies [1,2]. One approach to dissecting the mechanisms that underlie this biological complexity is to mutate the genes that encode channels or that control other aspects of their function, such as assembly, post-translational modification, membrane localization, regional distribution and modulation.

Drosophila is becoming increasingly important for such studies because it is well-suited for molecular as well as classical genetics analyses. In addition, a variety of electrophysiological techniques, including voltage- and patch-clamp recordings, are now being successfully applied to study ion currents in a growing collection of mutants [3–13]. By utilizing a variety of techniques available in *Drosophila*, therefore, it should be possible to correlate the functional defects in particular mutants with the structural perturbations within ion channel-related proteins as revealed by gene cloning and DNA sequence analysis.

The mutant phenotypes also provide an indication of the range of possible alterations in channel properties and the functional consequences of such alterations in different parts of the nervous system. Functional interrelationships among different channel types can often be revealed by phenotypic interactions in particular double mutants. Furthermore, in combination with toxins and drugs, mutations that affect specific channels are very effective tools for separating various currents present in a particular cell type and for comparing the properties and distribution of channel types in different excitable membranes.

In this article, we provide a brief description of the genetics and pharmacology of potassium channels in *Drosophila*, focusing on the results from muscle membranes and larval neuromuscular junctions.

312

Muscle membrane currents

Membrane currents in *Drosophila* have been best characterized in muscle fibres because their relatively large size permits application of the two-microelectrode voltage-clamp technique. These individually identifiable fibres are rather short and thus approach isopotential conditions for accurate membrane voltage control and current measurements [14,15]. The inward current in these cells is carried by Ca^{2+} but not Na^+. The outward currents consist of both voltage-dependent and Ca^{2+}-dependence potassium currents; each can be further separated into a fast and a slow component with distinct sensitivity to different mutations and pharmacological agents. As shown in Fig. 1A, in Ca^{2+}-free saline the inward calcium currents and Ca^{2+}-dependent potassium currents are eliminated and only voltage-activated potassium currents remain. Depolarizing pulses elicit an early transient component, I_A, which rises rapidly to a peak and then inactivates, and a second, delayed component, I_K, which rises more slowly to a plateau value. When a depolarizing prepulse precedes the test pulse, I_A is inactivated, unmasking I_K (Fig. 1A). Subtraction of the two traces yields the amplitude and time course of the inactivating I_A (Fig. 1B) in physiological isolation from I_K [15,16].
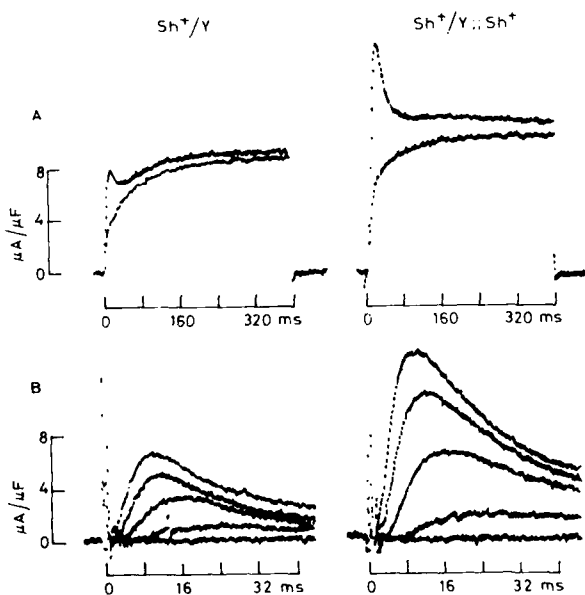
FIG 1 Gene-dosage effect of the *Shaker (Sh)* locus on I_A in *Drosophila* larval muscle. A: physiological separation of I_A and I_K in Ca^{2+}-free saline at 4°C. Two superimposed traces of membrane currents elicited by a voltage-clamp step from a holding potential (V_H) of − 80 mV to + 20 mV with or without a prepulse. The prepulse inactivates I_A, unmasking I_K [15,16,19]. B: superimposed traces of I_A elicited by voltage steps from V_H = 80 mV to − 20, − 20, 0, + 20 and + 40 mV (determined by subtraction of corresponding traces as shown in A). Duplicating the *Sh* locus in aneuploid males (*Sh* /Y; *Sh*⁺) produces an I_A with twice amplitude of that in normal males (*Sh*⁺/Y) without altering I_K. (Adapted from Ref. 16.)

Voltage-activated potassium currents

Mutants affecting potassium currents have been identified among those displaying abnormal leg-shaking behaviour under ether anesthesia. Mutations of the Sh (Shaker) locus reduce, eliminate or otherwise alter I_A without affecting I_K [15] in both adult [8] and larval [15,16] muscles (Fig. 2). A variety of studies, including gene-dosage experiments in larval muscle, suggested that the Sh locus codes for the I_A channel. As shown in Fig. 1, aneuploid males possessing an extra copy of the Sh locus on the third chromosome ($Sh^{\pm}/Y$; $Sh^{\pm}$) produce an I_A with twice amplitude of that in normal males. This results suggests that the Sh locus either codes for the entire structure of the I_A channel or contributes subunits whose quantity limits the assembly of channel components, which may include additional subunits encoded by different genes. Combinations among different Sh mutations in heterozygotes have produced evidence for interactions among dissimilar gene products, suggesting a heteromultimeric assembly of Sh products within the I_A channel [16]. Recent molecular genetic studies demonstrate that the Sh locus contains a complex transcription unit that generates multiple transcripts by alternative exon splicing [17,18]. Certain species of Sh transcripts have been used to express I_A-like currents in *Xenopus* oocytes [18].

In addition to the selective effect of Sh on I_A, the two voltage-activated currents can be distinguished by the differential effects of various pharmacological agents. For example, dendrotoxin (DTX), a convulsant peptide from the mamba snake venom, reduces I_A in a temperature-dependent manner (Fig. 3A) with decreased effectiveness at lower temperatures. However, other potassium currents are not apparently affected by this toxin [19]. In addition, 50 μM 4-aminopyridine (4-AP)
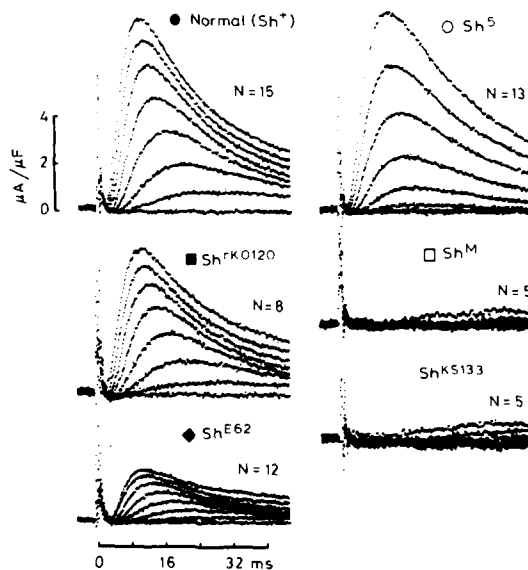
FIG 2   Effects of different mutations of the Sh locus on I_A in larval muscle. Superimposed traces represent I_A evoked by depolarization steps (up to $+40$ mV, in 10 mV steps, from $V_H = -80$). A change in the voltage dependence is evident in Sh^5. I_A is eliminated or reduced in other Sh mutants. (Adapted from Ref. 16.)
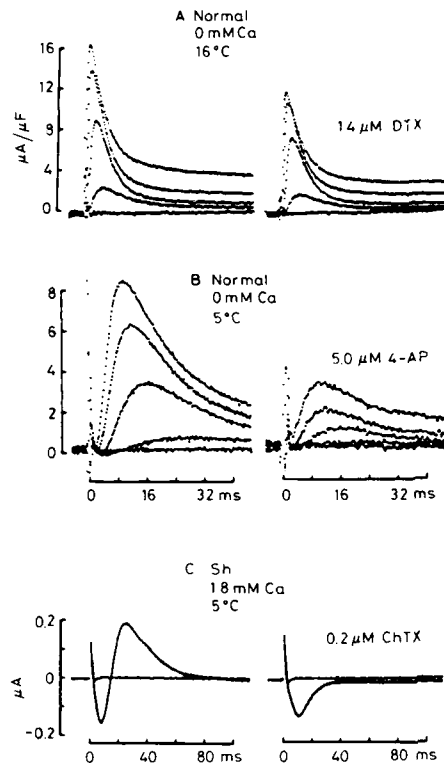
FIG 3   Action of dendrotoxin (DTX), 4-aminopyridine (4-AP), and charybdotoxin (ChTX). A: I_A in normal larval muscle is reduced by 1.4 μM DTX at 16°C. Further increase of the concentration of DTX does not completely block I_A. The effectiveness of DTX is also decreased at low temperature [19]. B: I_A in normal larvae is reduced (50%) by 5 μM 4-AP. Traces in A and B show currents induced by the same pulse protocol described in Fig. 1. C: ChTX removes the early outward current in Sh^{KS133} adult flight muscle evoked by a pulse to -40 mV from $V_H = 80$ mV in normal saline (1.8 mM Ca^{2+}). The outward current in Sh^{KS133} contains no I_A but only I_C, which is blocked by ChTX to reveal the remaining inward calcium current. (A adapted from Ref. 19; C adapted from Ref. 24.)

blocks I_A almost completely but causes only minimal reduction in I_K [20]. In larval muscle fibres, 5 μM 4-AP reduces I_A by 50% (Fig. 3B).

Ca^{2+}-activated potassium currents

In saline containing physiological concentrations of Ca^{2+}, an inward calcium current can be evoked, which subsequently elicits a fast and a slow Ca^{2+}-dependent potassium current [21,23] superimposing on the voltage-activated I_A and I_K (Fig. 4A). The mutation *slo (slowpoke)* demonstrates that the fast outward current has two separate components, a Ca^{2+}-dependent I_C in addition to the voltage-activated I_A. The *slo* mutant displays uncoordinated behaviour at high temperature and, like other mutants with defective potassium currents, shows ether-induced leg shaking.
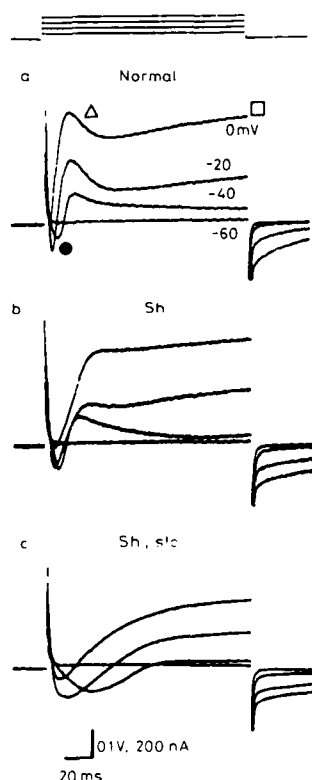
FIG 4   Membrane currents in adult flight muscle fibres. Traces represent currents elicited by voltage steps from $V_H = -80$ mV to the indicated potentials (a). In normal saline, an inward calcium current (filled circle) is followed by an inactivating outward current (open triangle). At -20 and 0 mV, a late current appears that does not inactivate during the voltage pulse (open square). The early inactivating outward current is separable into I_A, which is removed by the Sh^{KS133} mutation (b), and I_C, which is removed by slo. In Sh^{KS133}; slo double mutants, removal of both I_A and I_C reveals the inward calcium current (c). (Adapted from Ref. 24.)

Analysis in both adults [24] and larvae [23] indicates that this mutation greatly reduces I_C but leaves I_A intact. Under voltage-clamp conditions, I_A and I_C can be distinguished in normal flies because I_A but not I_C is blocked by 4-AP whereas I_C but not I_A is eliminated in Ca^{2+}-free saline. In the presence of 4-AP no fast outward current is detectable at all in slo flies [24]. These data indicate that the channels mediating the two components of fast outward current are molecularly distinct, consistent with the observation that Sh mutations elminate I_A but not I_C (Figs. 2 and 4B). The complementary effects of Sh and slo are clearly evident in the muscle of Sh slo double mutants which entirely lack fast outward currents (Fig. 4C).

The pharmacological properties of I_C have been characterized in adult [22,24] and larval [21,23] muscles. I_C, as well as I_A and I_K, were all nearly eliminated by 100 mM tetraethylammonium (TEA). Two other drugs known to block certain Ca^{2+}-dependent potassium channels failed to block I_C in Drosophila muscle. I_C

was unaffected by 1.5×10^{-6} M apamin, or by 1×10^{-3} M quinidine [24]. However, charybdotoxin (ChTX), which is known to block Ca^{2+}-dependent potassium channels in various vertebrate cells, did specifically block I_C channels in adult flight muscles. In the example shown in Fig. 3C, a Sh^{KS133} fly was used to isolate the I_C component of the early outward current which was then eliminated by ChTX. The K_i of ChTX for blocking I_C was estimated to be about 75 nM [24].

The *slo* mutation also enables a distinction between the two Ca^{2+}-activated potassium currents in larval muscle; I_C is eliminated by *slo* but the slow Ca^{2+}-activated potassium current is unaffected [23]. Patch-clamp recording has identified a species of Ca^{2+}-dependent single-channel current that gives rise to the macroscopic I_C in larval muscle membrane. This single-channel activity is present in normal but not in *slo* larvae [25].

So far, no mutation is known to remove completely either the voltage-activated I_K or the Ca^{2+}-activated slow potassium current. However it was possible to make a pharmacological distinction between these two currents by use of quinidine. Quinidine at a concentration of 100 μM nearly eliminated I_K without any apparent effect on the Ca^{2+}-activated slow current or other currents in larval muscle [23]. Thus all four potassium currents in larval muscle fibres can be uniquely distinguished by their sensitivity to different mutations and drugs. Because of this distinction, it is unlikely that the voltage-activated and Ca^{2+}-activated potassium currents, despite their similarity in time course and other properties [22], represent alternative activation mechanisms of the same set of channels but rather identify molecularly distinct species of potassium channels.

In another leg-shaking mutant, *eag (ether á go-go)*, abnormal spontaneous activities occur at the larval neuromuscular junction (see below). Voltage-clamp experiments indicate that I_K in larval muscle of different *eag* alleles is reduced or modified but not eliminated [26]. Some alleles appear to alter I_A to different degrees as well [13,27].

Roles of different potassium currents in the regulation of membrane potential

The above results demonstrate that by appropriate combination of mutations and pharmacological agents, individual potassium currents can be extracted or eliminated, enabling the properties of these currents to be analysed and their roles in the regulation of membrane potential to be determined. For example, the role of individual potassium currents in muscle excitability can be examined under current clamp. Normal larval fibres show only graded potentials (Fig. 5A). When the driving force for current flowing through different potassium channels is reduced by raising the external K^+ concentration, all-or-none calcium action potentials can be evoked (Fig. 5B). The same is true if Ba^{2+} is present in saline (Fig. 5C). It is known that Ba^{2+} is a more efficient charge carrier through calcium channels and blocks the various channels in *Drosophila* muscle to a different extent [21,28]. In Sh^{KS133}, lack of I_A leads to a stronger depolarization, which is still, however, not sufficient to generate an action potential (Fig. 5D). The eag^1 mutation exerts a slightly stronger effect (Fig. 5E). A still more striking membrane potential oscillation can be observed in $eag^2 Sh^{KS133}$ double mutants (Fig. 5F). In *slo* larvae, an all-or-none action potential can be evoked [29]. In these cells, I_C is absent and I_A becomes inactivated soon after the initial membrane depolarization. This combined effect on potassium currents is apparently sufficient to develop regenerative calcium spikes.

A Normal   D Sh

B +K   E eag

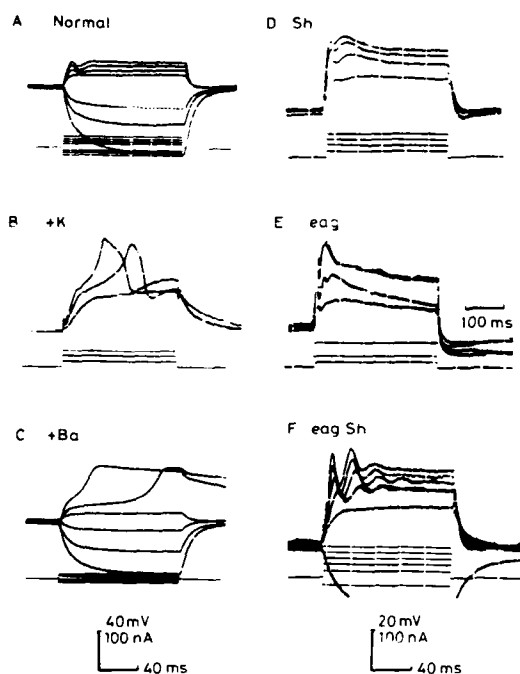C +Ba   F eag Sh

40mV
100 nA
40 ms

20mV
100 nA
40 ms

FIG 5 Voltage responses to constant current injection into larval muscle fibres. In normal larval muscle only graded potentials are present (A). When the K^+ concentration is increased from 2 to 20 mM (B) or when 10 mM Ba^{2+} is added to the normal saline [6], regenerative action potentials can be evoked. In Sh^{KS133} (D), eag^1 (E) and Sh^{KS133} eag^1 (F), stronger membrane depolarization or oscillation can be elicited.

The role of I_C is better demonstrated in adult flight muscle, in which calcium action potentials can be evoked by nerve stimulation or current injection (Fig. 6). The *slo* mutation prolongs the depolarization phase of the spike potentials from the normal 2 ms to 30 ms. However, as shown in Fig. 6, the first response of *slo* flight

normal   slowpoke

20 mV
100 nA
20 ms
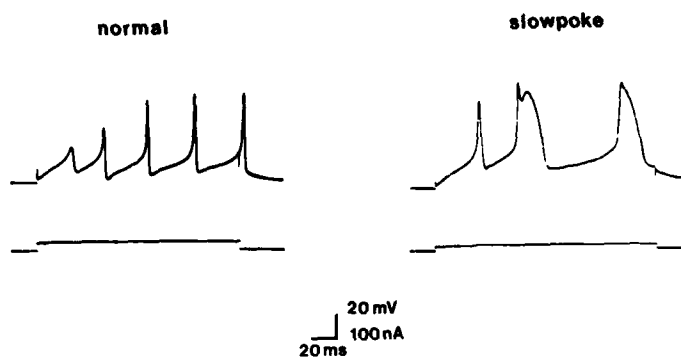
FIG 6 Adult flight muscle fibres under current clamp. Left, normal fly; Right, *slo* fly.

muscles either to current injection or to repetitive nerve stimulation is a spike of much shorter duration than those that follow. Treating *slo* muscles with 5 mM 4-AP causes the first spike to become as prolonged as those that followed. Similar results are observed in Sh^{KS133}; *slo* double mutants [30]. These results indicate that I_A normally is responsible for the fast repolarization of the initial spike but quickly becomes inactivated. Repolarization of subsequent spikes is mediated primarily by I_C.

Neuromuscular transmission

Synaptic transmission in mutants defective in membrane currents has been extensively characterized at the larval neuromuscular junction [5,6,26,31,32]. The larval neuromuscular preparation is readily accessible to physiological recording and pharmacological manipulations. Nerve stimuli elicit excitatory junctional potentials (ejps) in the postsynaptic muscle membrane (Fig. 7).
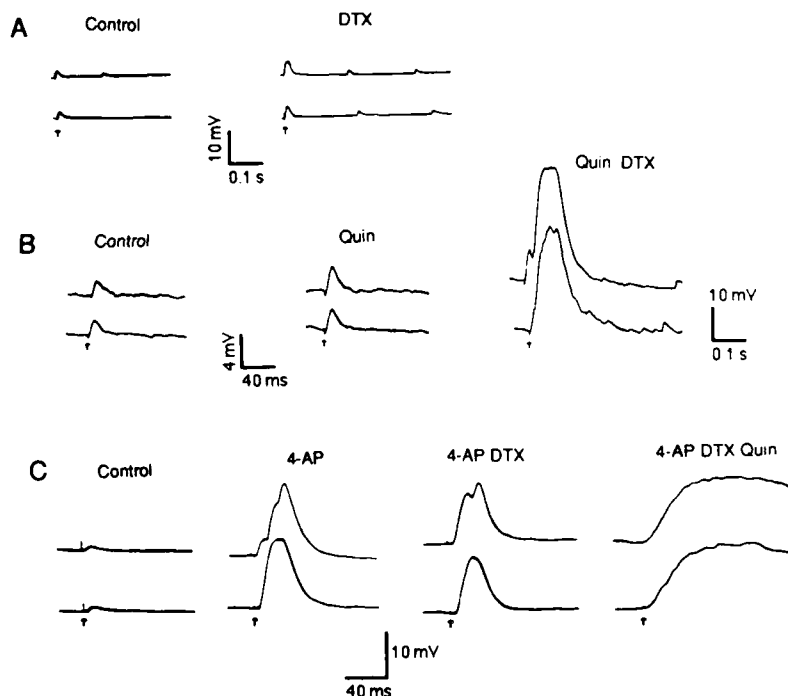
FIG 7 Effects of potassium channel blockers on excitatory junction potentials (ejps) recorded intracellularly from normal larval muscle fibres. A: DTX (4.2 μM) causes a slight increase in the ejp amplitude and, in addition, repetitive discharges of ejps. B: treatment with 50 μM quinidine only mildly enhances transmitter release. Further addition of 4.2 μM DTX results in prolonged giant ejps. (Note difference in time scale.) C: adding 0.1 μM 4-AP transformed small responses into giant ejps. No further enhancement of transmission is produced by addition of DTX (4.2 μM). In contrast, 50 μM quinidine immediately augments the effect of 4-AP, resulting in greatly prolonged ejps. Saline contains 0.1 mM Ca^{2+}, 4 mM Mg^{2+} in A and C and 0.2 mM Ca^{2+}, 4 mM Mg^{2+} in B. (Adapted from Ref. 19.)

In spite of its importance in signal transmission, direct measurements of the various ion currents in presynaptic nerve terminals by voltage-clamp have been hampered by technical difficulties. Therefore, pharmacological agents and mutations known to affect specific ion channels provide a useful means of experimentally manipulating the currents in presynaptic terminals. These experiments allow comparisons of the types and properties of ion channels present in the nerve terminals with those characterized in excitable membranes more accessible to voltage-clamp analysis.

Effects of pharmacological agents

At a low concentration of external Ca^{2+} (0.1–0.2 mM), transmitter release at normal neuromuscular junctions is suppressed and nerve stimuli elicit ejps of small amplitudes (Fig. 7). Elimination of I_A by 4-AP treatment (0.1 mM) greatly facilitates neuromuscular transmission, producing ejps of much greater amplitudes (Fig. 7C). Consistent with voltage-clamp results in muscle (Fig. 3), the effect of DTX at neuromuscular junctions is relatively mild as compared with that of 4-AP (compare Fig. 7A, C). Quinidine, when applied alone, only slightly enhances transmission (Fig. 7B) even though it is fully capable of eliminating I_K in muscle membranes [23]. Surprisingly, quinidine can, nevertheless, drastically augment the effects of DTX and 4-AP, giving rise to prolonged giant ejps (Fig. 7B, C) whereas DTX and 4-AP show little synergistic effect when applied together (Fig. 7C). As predicted from these observations, the large ejps in Sh larvae (Fig. 8b) are not further enhanced by DTX but greatly prolonged by quinidine [19].

Apparently, I_A in nerve terminals is more effective than I_K in membrane repolarization to terminate transmitter release. However, the contribution of I_K to terminal repolarization becomes evident when both I_A and I_K are eliminated (Fig. 7). Even when I_A is only partially removed by DTX, reduction of I_K by quinidine greatly enhances neuromuscular transmission.

Effects of mutations

Mutations that are known to affect potassium currents in muscle also alter synaptic transmission, producing phenotypes analogous to those drug effects described above. Action potentials recorded from the adult cervical giant axon in Sh flies show delayed repolarization [7]. The neuromuscular junction in Sh larvae also fails to repolarize properly and as a result a much greater amount of transmitter is released [5,31,32]. This enhanced response is correlated with anomalous repetitive firing of the motor axon following a nerve stimulus (Fig. 8A, B).

In eag larvae, transmitter release is only slightly enhanced but a high frequency of spontaneous ejps occur in the absence of nerve stimulation. These ejps are correlated with spontaneous firing of motor axons (Fig. 8C). Similar phenomena can sometimes be observed in normal larvae following quinidine treatment [19].

In double mutants, eag and Sh interact synergistically; transmitter release at the neuromuscular junction in eag Sh larvae persists at least ten times longer than in either single mutant, generating prolonged giant ejps [32]. These plateau-shaped ejps occur in response to nerve stimulation or spontaneously and are correlated with a train of repetitive spikes in the motor axon (Fig. 8D).

No Stim.   Stim.

a

Normal

b

Sh

c

eag

$0\ 4\atop 20$ mV

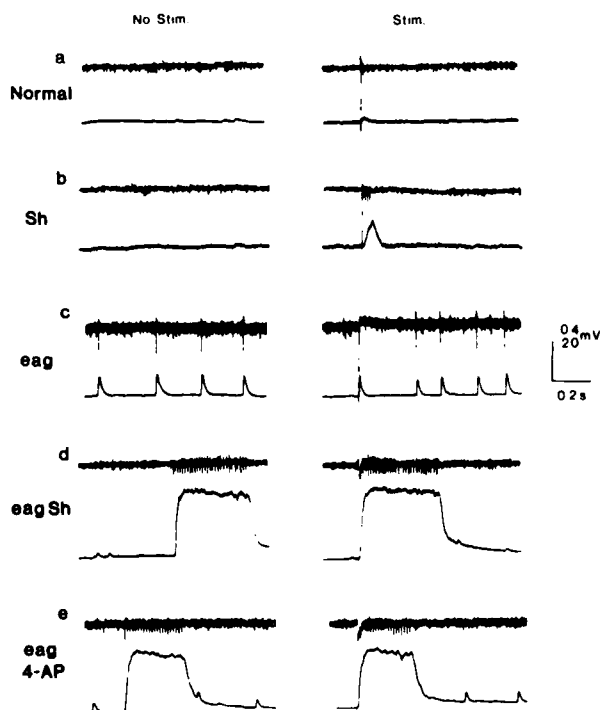$0\ 2$ s

d

eag Sh

e

**eag
4-AP**

FIG 8   Simultaneous nerve and muscle recordings from normal, *Sh*, *eag*, and *eag Sh* larvae. Activities evoked by nerve stimulation (right panels) and occurring spontaneously without stimulation (left panels) are shown. The motor axon spikes are the most prominent units that can be picked up by the suction electrode from the segmental nerve. At low external Ca^{2+} concentrations (0.2 mM for a and c, and 0.1 mM for b, d and e), the nerve stimulation evokes enhanced neuromuscular transmission in mutants (b–e) as compared with normal (a) larvae. In *Sh* a single nerve stimulus causes the motor axon to fire several extra spikes (b). Repetitive firing of motor axons, correlated with ejps, occurs spontaneously in *eag* (c). Combining *eag* and *Sh* in double mutants produces striking synergistic effects, resulting in greatly prolonged ejps correlated with bursts of motor axon spikes (d). This phenotype of the *eag Sh* double mutant is exactly mimicked (e) by treating *eag* larvae with 4-aminopyridine (4-AP). *Sh* refers to Sh^{KS133} allele (Adapted from Ref. 12.)

The size and shape of these giant ejps are similar to those observed in normal larvae treated with quinidine and DTX or quinidine and 4-AP (Fig. 7). The phenotype of the double mutant can also be mimicked by treating normal larvae with TEA, which blocks both I_A and I_K [14,21]. Furthermore, 4-AP when applied to *eag* (Fig. 8C) but not normal larvae [22] can also produce the similar ejps. These results are consistent with the interpretation that *Sh* and *eag* affect currents in nerve terminals corresponding to I_A and I_K in muscle.

Previous extracellular nerve recordings and focal ejp recordings in *Sh* and *eag* larvae and in normal larvae treated with 4-AP or TEA have suggested that the abnormal ejps reflect predominantly presynaptic defects rather than a failure in postsynaptic membrane repolarization [5,31]. Abnormal synaptic transmission may involve defects in repolarization of both axon and nerve terminal. The repetitive
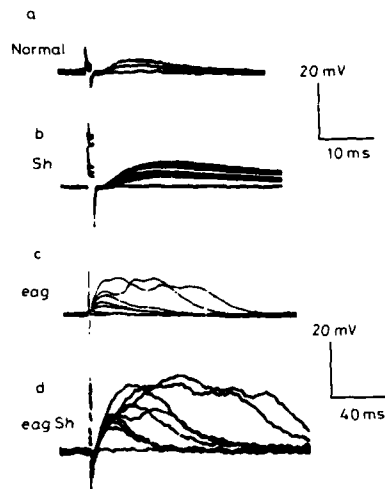
FIG 9 Electrotonically evoked ejps in normal, Sh, eag, and eag Sh larvae at low external Ca^{2+} concentrations (0.2 mM for a, b, and c, and 0.1 mM for d). Nerve action potential is abolished by 300 nM tetrodotoxin and, therefore, the ejp amplitude increases gradually with the stimulus intensity until saturation is reached (a). The Sh^{KS133} terminal shows prolonged transmitter release (b). The eag terminal is capable of sustaining a prolonged release (c). The terminal excitability is further enhanced in the double mutant (d).

firing of the motor axons in Sh, eag or the double mutant larvae reflects activity of sodium action potentials which are blocked by tetrodotoxin (TTX) [31]. Under this condition the nerve terminals can still be stimulated electrotonically to examine the enhanced excitability in the presynaptic membrane and the resulting increase in transmitter release [5,31]. As shown in Fig. 9, the Sh presynaptic terminal generates a greater and longer transmitter release than normal, whereas the eag terminal appears even more excitable, capable of sustaining a prolonged release. This effect is further enhanced in the eag Sh double mutant (Fig. 9D). When the strength of the electrotonic stimulation is gradually increased, plateau-shaped ejps are elicited above a certain threshold. This result suggests that, even when sodium channels are blocked by TTX, calcium channels in the presynaptic terminal can still support regenerative action potentials if potassium currents are reduced.

The above results demonstrate that different potassium currents play essential and interdependent roles in regulating the excitability of the presynaptic terminal. The intricate balance established by the repolarization capability of different potassium currents is evidenced by the wide range of phenotypic effects on synaptic transmission when one or more of the currents is reduced. The comparative study also shows that the I_A and I_K channels in the nerve terminal and muscle membrane are similar in their sensitivities to different mutations, toxins and drugs, suggesting that I_A and I_K channels are identical in the two excitable membranes. However, the possibility cannot be ruled out that corresponding channel types in different excitable membranes represent alternative products encoded by the same gene. Moreover, it is possible that the channels contain additional subunits whose identity may vary with cell types [27]. This is particularly relevant to the distribution of I_A channels because the phenotypic severity of certain Sh alleles is known to vary in a

322

tissue-specific manner [11,15,27,32,33] and because the *Sh* locus has been shown to specify a multiplicity of products [17,34,35].

Conclusions

Toxins and drugs that specifically block ion channels have long provided neurobiologists with essential tools to study membrane excitability and to infer structural and functional features of ion channels. The genetic tractability of *Drosophila* has enabled an extension of this approach with the isolation of mutations affecting ion channels and the analysis of their functional interrelationships in double mutants [12,27]. The combined use of pharmacological agents with mutants thus provides new opportunities to characterize the functional properties of particular channels and the physiological role of the current they mediate. In addition, mutations can provide a basis for further recombinant DNA studies in relating functional alterations with structural perturbations in ion channels. With the full extent of genetic, molecular genetic, pharmacological and physiological techniques available [12,13], it can be expected that very rapid progress will be made in our understanding of channel structure, function and biological control in *Drosophila*.

References

1 Hille, B. (1984) Ionic Channels of Excitable Membranes. Sinauer, Sunderland, MA.
2 Latorre, R. and Miller, C. (1983) Conduction and selectivity in potassium channels. J. Membr. Biol. 71, 11–30.
3 Ikeda, K. and Kaplan, W.D. (1970) Patterned neural activity of a mutant *Drosophila melanogaster*. Proc. Natl. Acad. Sci. U.S.A. 66, 765–772.
4 Sidiqi, O. and Benzer, S. (1976) Neurophysiological defects in temperature-sensitive paralytic mutants of *Drosophila melanogaster*. Proc. Natl. Acad. Sci. U.S.A. 73, 3253–3257.
5 Jan, Y.N., Jan, L.Y. and Dennis, M.J. (1977) Two mutations of synaptic transmission in *Drosophila*. Proc. R. Soc. Lond. Ser. B. 198, 87–108.
6 Wu, C.-F., Ganetzky, B., Jan, L.Y., Jan, Y.-N. and Benzer, S. (1978) A *Drosophila* mutant with a temperature-sensitive block in nerve conduction. Proc. Natl. Acad. Sci. U.S.A. 75, 4047–4051.
7 Tanouye, M.A., Ferrus, A. and Fujita, S.C. (1981) Abnormal action potentials associated with the *Shaker* locus of *Drosophila*. Proc. Natl. Acad. Sci. U.S.A. 78, 6548–6552.
8 Salkoff, L. (1983) Genetic and voltage-clamp analysis of a *Drosophila* potassium channel. Cold Spring Harbor Symp. Quant. Biol. 48, 221–231.
9 Beyerly, L. (1986) Potassium, sodium and calcium currents in embryonic cultures of *Drosophila* neurons. Biophys. J. 49, 574a.
10 Yamamoto, D. and Suzuki, N. (1987) Polymeric structure of a chloride channel unveiled by HEPES buffer blocking. Proc. R. Soc. Lond. Ser. B. 230, 93–100.
11 Solc, D.K., Zagotta, W.N. and Aldrich, R.W. (1987) Single-channel and genetic analyses reveal two distinct A-type potassium channels in *Drosophila*. Science 236, 1094–1098.
12 Ganetzky, B. and Wu, C.-F. (1985) Genes and membrane excitability in *Drosophila*. Trends Neurosci. 8, 322–326.
13 Wu, C.-F. (1988) Neurogenetic studies of *Drosophila* central nervous system neurons in culture. In Cell Culture Approaches to Invertebrate Neurosciences (D. Beadle, G. Lees, S.B. Kater, eds.) Academic Press, London.
14 Salkoff, L. and Wyman, R. (1983) Ion currents in *Drosophila* flight muscles. J. Physiol. 337, 687–708.

15 Wu, C.-F. and Haugland, F.N. (1985) Voltage clamp analysis of membrane currents in larval muscle fibers of Drosophila: Alteration of potassium currents in Shaker mutants. J. Neurosci. 5, 2626–2640.

16 Haugland, N.H. and Wu, C.-F. (1988) A voltage clamp analysis of gene-dosage effects of the Shaker locus on larval muscle potassium currents in Drosophila. J. Neurosci. Submitted.

17 Schwarz, T.L., Tempel, B.L., Papazian, D.M., Jan, Y.N. and Jan, L.Y. (1988) Multiple potassium-channel components are produced by alternative splicing at the Shaker locus in Drosophila. Nature 331, 137–142.

18 Timpe, L.C., Schwarz, T.L., Tempel, B.L., Papazian, D.M., Jan, Y.N. and Jan, L.Y. (1988) Expression of functional potassium channels from Shaker cDNA in Xenopus oocytes. Nature 331, 143–145.

19 Wu, C.-F., Tsai, M.-C., Chen, M.-L., Zhong, Y., Singh, S., and Lee, C.Y. (1988) Actions of dendrotoxin on K^+ channels and its synergistic effects on neuromuscular transmission with K^+ channel-specific drugs and mutations in Drosophila melanogaster. J. Neurophysiol. Submitted.

20 Haugland, F.N. and Wu, C.-F. (1987) Concommitant alteration of potassium channel gating and pharmacology in a Shaker mutant of Drosophila. Abstr. Soc. Neurosci. 13, 350.

21 Gho, M. and Mallart, A. (1986) Two distinct calcium-activated potassium currents in larval muscle fibers of Drosophila melanogaster. Pflügers Arch. 407, 526–533.

22 Wei, A. and Salkoff, L. (1986) Occult Drosophila potassium channels and twinning of calcium- and voltage-activiated potassium channels. Science 233, 780–782.

23 Singh, S. and Wu, C.-F. (1987) Genetic and pharmacological separation of four potassium currents in Drosophila larvae. Soc. Neurosci. Abstr. 13, 579.

24 Elkins, T., Ganetzky, B. and Wu, C.-F. (1986) A Drosophila mutation that eliminates a calcium-dependent potassium current. Proc. Natl. Acad. Sci. U.S.A. 83, 8415–8419.

25 Komatsu, A. and Wu, C.-F. (1987) Single-channel potassium currents in membrane vesicles derived from normal and mutant Drosophila larval muscles. Soc. Neurosci. Abstr. 13, 530.

26 Wu, C.-F., Ganetzky, B., Haugland, F. and Liu, A.-X. (1983) Potassium currents in Drosophila: Different components affected by mutations of two genes. Science 220, 1076–1078.

27 Wu, C.-F. and Ganetzky, B. (1986) Genes and ionic channels in Drosophila. In: Ion Channels in Neural Membranes (J.M. Ritchie, R.D. Keynes and L. Bolis, eds.). Alan R. Liss, Inc., New York.

28 Suzuki, N. and Kano, M. (1977) Development of action potential in larval muscle fibers in Drosophila melanogaster. J. Cell. Physiol. 93, 383–388.

29 Singh, S., Wu, C.-F. and Ganetzky, B. (1986) interactions among different K^+ and Ca^{++} currents in normal and mutant Drosophila larval muscles. Abstr. Soc. Neurosci. 12, 559.

30 Elkins, T. and Ganetzky, B. (1988) The roles of potassium currents in Drosophila flight muscles. J. Neurosci. 8, 428–434.

31 Ganetzky, B. and Wu, C.-F. (1982) Drosophila mutants with opposing effects on nerve excitability: Genetic and spatial interactions in repetitive firing. J. Neurophysiol. 47, 501–514.

32 Ganetzky, B. and Wu, C.-F. (1983) Neurogenetic analysis of potassium currents in Drosophila: Synergistic effects on neuromuscular transmission in double mutants. J. Neurogenet. 1, 17–28.

33 Timpe, L.C. and Jan, L.Y. (1987) Gene dosage and complementation analysis of the Shaker locus in Drosophila. J. Neurosci. 7, 1307–1317.

34 Baumann, A., Krah-Jentgens, I., Müller-Holtkamp, F., Seidel, R., Kecskemethy, N., Casal, J., Ferrus, A. and Pongs, O. (1987) Molecular organization of the maternal effect region of the Shaker complex of Drosophila: characterization of an I_A channel transcript with homology to vertebrate Na^+ channel. EMBO J. 6, 3419–3429.

35 Kamb, A., Tseng-Crank, J. and Tanouye, M.A. (1988) Multiple products of the Drosophila Shaker gene contribute to potassium channel diversity. Neuron 1, 421–430.

CHAPTER 24

Acetylcholine, GABA and glutamate receptor channels in cultured insect neurones

YVES PICHON AND DAVID BEADLE

[1] Département de Biophysique, Laboratoire de Neurobiologie Cellulaire et Moleculaire du C.N.R.S., F-91190 Gif-sur-Yvette, France and [2] School of Biological and Molecular Sciences, Oxford Polytechnic, Headington, Oxford OX3 OBP, U.K.

Introduction

There is good evidence that acetylcholine (ACh) [1–6] is the main excitatory neurotransmitter in the central nervous system (CNS) of insects. γ-Aminobutyric acid (GABA) and L-glutamic acid are the most likely candidates for inhibition and excitation respectively at the neuromuscular junction [2,7–9]. GABA also appears to be involved in inhibitory neurotransmission in the CNS [2,3,5] and there are indications of the possible involvement of glutamic acid as an excitatory neurotransmitter in the ganglia [2].

The recent development of sophisticated biophysical and biochemical techniques has enabled considerable progress to be made in the understanding of the molecular events associated with synaptic transmission in vertebrates. On the one hand, the use of recombinant DNA techniques have enabled the sequencing of nicotinic ACh receptor and $GABA_A$ receptor proteins [10,11]. On the other hand, the development by Neher and Sakmann [12] of the patch-clamp technique which enables the electrophysiological recording of the opening and closing of a single ionic channel has led to a tremendous improvement in our knowledge of the physiology of the gating mechanisms associated with synaptic transmission. The development of new and selective insecticides depends partly on our knowledge of the differences between insect preparations and their vertebrate counterparts.

Although important information can be obtained from cells in ganglia [13], such preparations are not ideally suited for patch-clamp experiments. Cultured neurones offer many experimental advantages for both electrophysiological and biochemical studies. Primary cultures from embryonic neurones can be prepared from embryos of the american cockroach, *Periplaneta americana*. These cultures are uniquely suited to pharmacological studies especially since they can be kept free from glial cell contamination. Under such conditions, (1) it is possible to control exactly the ionic environment, (2) the nerve membrane is directly accessible to putative transmitters or toxins, (3) membrane patches suitable for single channel analysis are easily formed without enzymatic treatment of the culture. These neurones have been shown to be sensitive to ACh [14] to GABA [15] and to glutamate [16]. In a

collaborative work with D.J. Beadle's laboratory, we have recently gathered a significant amount of information concerning the single channel events associated with the application of these three neurotransmitters and some of their agonists on these cultured neurones. Some of the data have already been published [17] or have been submitted for publication [18].

In the present chapter, we shall summarize the main results of these experiments.

Materials and methods

Cultures

The methods used for the cultured neurones were those described earlier [19]. Essentially, brains were isolated from the embryos contained in 21 to 23 days old egg cases from *Periplaneta americana* and mechanically dissociated in a first medium made of 5 parts Schneider's revised *Drosophila* medium and 4 parts Eagles's basal medium and antibiotics. After 7 days, this culture medium was replaced by a new medium consisting of equal parts of Leibovitz's L-15 and Yunker's modified Grace's medium also containing antibiotics. The cells were grown at 29°C in air in Falcon Petri dishes.

Electrophysiology

The saline used for most electrophysiological experiments derived from that of Pichon and Treherne [20] and contained Na^+ 210 mM, K^+ 3.1 mM, Ca^{2+} 10 mM and Cl^- 233 mM and was buffered at pH 7.2 with Hepes.

All experiments were performed using the improved patch-clamp technique as described by Hamill et al. [21]. Electrodes were pulled from 1.5 mm haematocrit tubing on a modified Kopf puller. The electrodes were polished and coated with syllgard. Their resistance was between 2 and 7 MΩ when filled with saline.

To obtain information on the entire population of channels which is responsible for the physiological response of the cell, the whole cell clamp configuration of the technique was used. The patch electrode was filled with a solution containing K^+ 114 mM, Mg^{2+} 1.6 mM, Ca^{2+} 0.2 mM, Cl^- 118 mM, EGTA 5 mM and glucose 100 mM buffered at pH 7.2 with Hepes. The agonists (ACh, CCh, GABA and muscimol) were pressure applied from a micropipette positioned in the vicinity of the neurone under study. The induced current and associated current fluctuations were stored on analogue tape (Ampex PR 500). Information on single channel kinetics and conductances was obtained using the standard technique of fluctuation analysis [22]. This analysis was performed off-line using a spectrum analyser (HP 3582 A) connected to a desk computer (HP 9825 T) and a digital plotter (HP 9872 A). The power spectra of the current fluctuations were determined for bandwidths between 0 and 250 or 500 Hz using a uniform filter. Spectra were averaged 8 to 64 times before being loaded into the computer memory and stored on digital tape. The averaged spectra were fitted with one or two Lorentzian functions characterized by their corner frequencies (f_c) which are related to the time constants of the single channel currents $\tau_m = 1/2\pi f_c$. Single channel conductances were estimated from the mean current, the variance (calculated from the fitted spectra) and the driving force as described by Shimahara et al. [17].

Single channel recordings were made in the cell-attached mode. The patch electrode contained the external solution to which the various agonists were added

at concentrations ranging from 0.1 to 50 μM. Single channel activity was displayed on an oscilloscope and stored on video cassettes connected to a modified digital audio processor. Analysis of the single channel data was performed using 10–120 s steady recordings (mean 40 s). The stored data were filtered using a 5-pole Tchebicheff filter (1–10 kHz), digitized on 12 bits at 10 kHz using a Data Translation DL 2801 A board and stored on a Winchester disc. Most data were then analysed using IPROC, a program developed by F. Sachs and J. Neil and based on the paper of Sachs et al. [23] and lent to us by C.J. Lingle. The output of this program consists of a series of files containing information on the amplitude, the duration of each valid event and on-time and off-time histograms. Curve fitting programs linked to statistical libraries were subsequently used to analyse this information.

Results and discussion

Acetylcholine and carbamylcholine

Fluctuation analysis

Pressure application of ACh and CCh at concentrations ranging from 10 to 50 μM in the vicinity of the neuronal membrane induced an inward current of up to 250 pA accompanied by a large increase in the current fluctuations (Fig. 1). Spectral analysis of this current revealed the existence of two Lorentzian components in the case of ACh and only one component in the case of CCh. At the resting level (i.e. about -65 mV), the corner frequencies of these Lorentzians were of respectively 10 $\pm$ 0.6 Hz and 116.8 $\pm$ 9 Hz for ACh, and 35 $\pm$ 13 Hz for CCh (Fig. 2A,B). Membrane hyperpolarization resulted in a shift of the spectra towards lower frequencies, suggesting an increase in the mean open time of the single channel events (the mean corner frequency with CCh decreased from 35 $\pm$ 13 Hz at rest to 16.5 $\pm$ 2 Hz for an 80 mV hyperpolarization. Increase in the ACh concentration did not appreciably modify the corner frequencies whereas the overall noise increased (together with the response) and the relative contribution to the spectrum of the high frequency component increased.

Single channel analysis

When added to the patch pipette at micromolar concentrations, both ACh and CCh induced small inward unitary currents. At the resting potential (RP), the mean

10^{-5} M ACh

40 pA

20 s
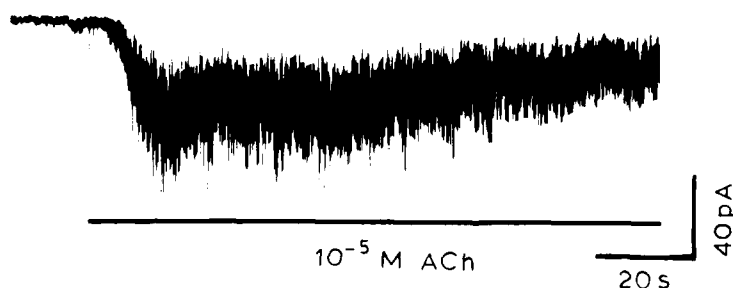
FIG 1   Inward current induced by prolonged application of 10 μM ACh onto the membrane of cultured neurone under whole-cell voltage-clamp. From Ref. 18.

328
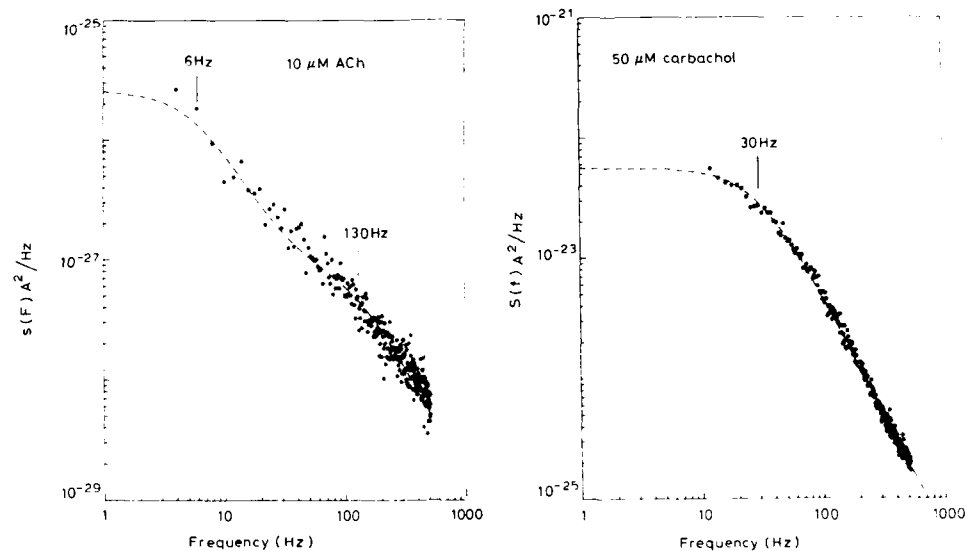
FIG 2   Power spectra of the noise induced by pressure application of ACh (A) and CCh (B) onto cockroach cultured neurones. Note the existence of two Lorentzians in A and only one in B. From Ref. 18.

amplitude and mean durations of these channels were of respectively 2.36 pA and 0.29 ms for ACh and 2.58 pA and 0.4 ms for CCh. Membrane hyperpolarization revealed the existence of two categories of unitary currents (Fig. 3A,B): large events with a mean current of 4.77 pA with ACh and 6.79 pA with CCh and small events with a mean current of 1.92 pA with ACh and 2.3 pA with CCh (for a 60 mV hyperpolarization). These events could be classified into three categories from their time course: long bursts (several tens of ms with several partial or complete closures), short channels with occasional closings or substates (a few ms) and very short triangular events. The bursting behaviour and triangular events were more frequent with ACh than with CCh. The mean open time of the short channels was longer with CCh than with ACh.

There is a reasonable agreement between the results of the spectrum analysis and the single channel data. The two spectral components seen with ACh most certainly correspond to the bursts (low frequency) and the short channels. The very short channels are too short and too few to contribute significantly to the spectrum. Furthermore, their contribution would only be seen at frequencies higher than 1 kHz and hidden by the background noise. The fact that only one spectral component was seen with CCh whereas two populations or channels were present in single channel recordings can be readily explained since (1) the mean duration of the two categories of channels is not significantly different (their time constants were of 0.7 ms and 1.87 ms for a 60 mV hyperpolarization [24]), and (2) because of their relative size the contribution of the small events to the spectrum is much smaller than that of the large events (probably less than 10%). This overall agreement suggests that ACh receptors are homogeneously distributed, at least qualitatively, over the entire cell surface.
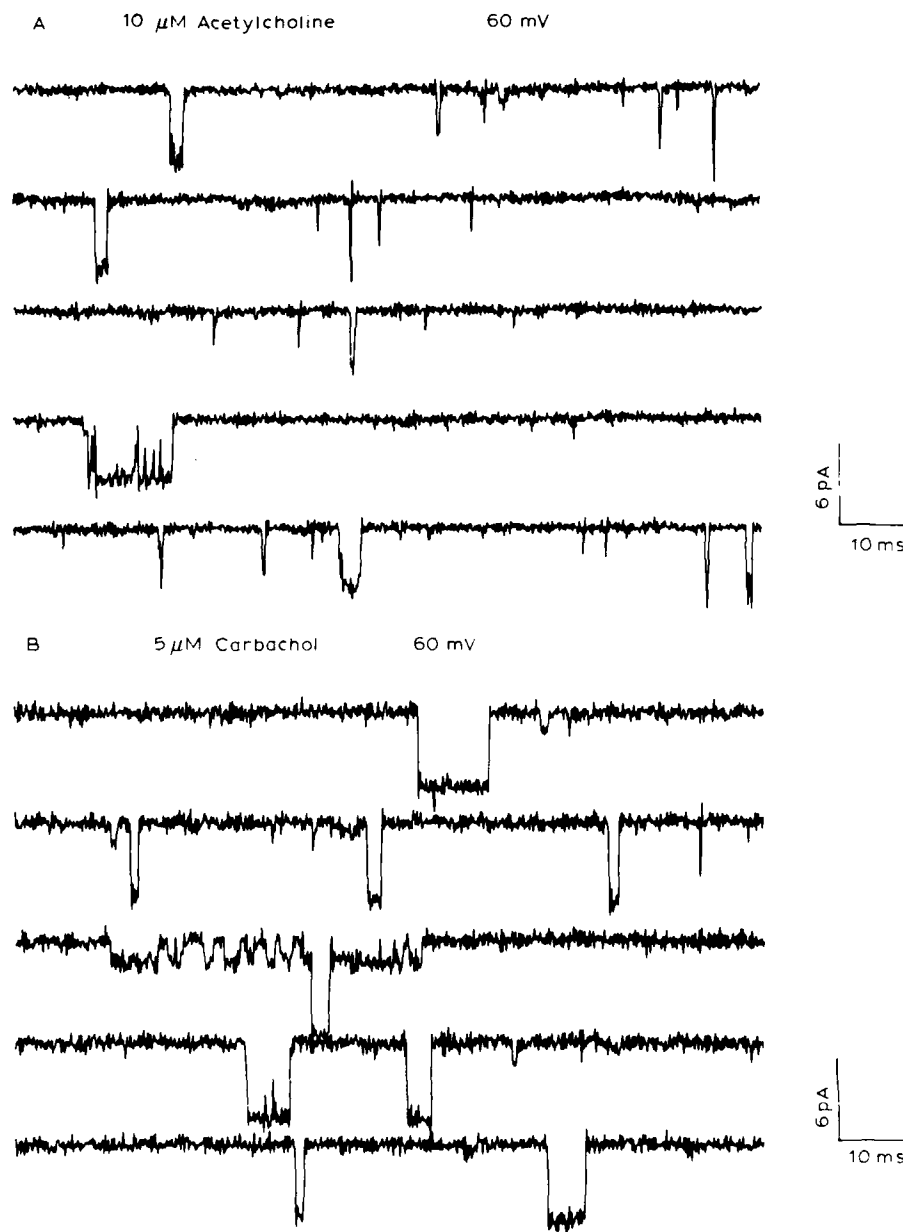
FIG 3 Representative (non consecutive) traces of ACh-sensitive (A) and CCh-sensitive (B) channels in cultured embryonic cockroach neurones. Note the existence of two distinct amplitudes of events. The membrane was hyperpolarized by 60 mV. All records were low-pass filtered at 3 kHz. Calibration bars: 6 pA, 10 ms. Agonist concentrations: A, 10 μM ACh; B, 5 μM CCh. Cell attached configuration. From Ref. 18.

330
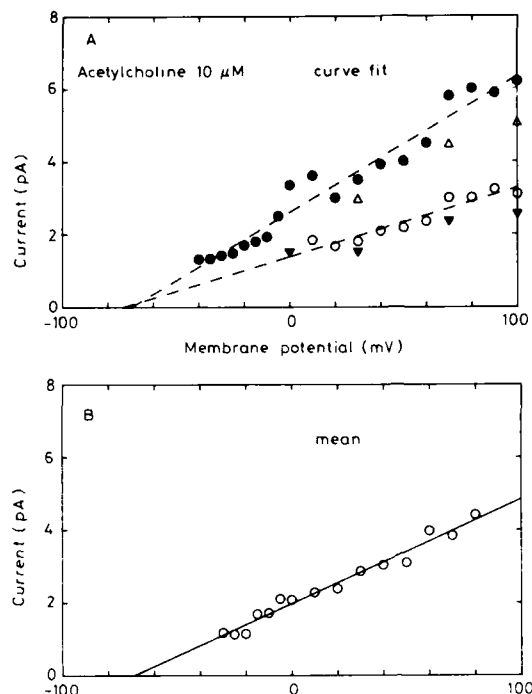
FIG 4 Current–voltage relations for ACh-activated channels. In A, the data were obtained by curve fitting the data with gaussian functions, the filled circles corresponding to the high conductance level and the empty circles to the low conductance level. Triangles refer to the same experiments but were obtained by a different fitting procedure (the open triangles correspond to the large channels, the closed triangles to the small ones). In B, the open circles correspond to the mean current computed by the IPROC. The three sets of data can be fitted with straight lines: the high conductance channel with a conductance of 37 pS, a reversal potential of −70 mV and a correlation coefficient of 0.978 (n = 19); the low conductance channel with a conductance of 19 pS, a reversal potential of −73 mV and a correlation coefficient of 0.952 (n = 9); the mean current with a mean conductance of 29 pS, a reversal potential of −68 mV and a correlation coefficient of 0.986 (n = 15). In this Figure as in the following ones, the X axis indicates the pipette potential (i.e. the relative membrane potential of the cell with respect to resting potential which is taken as 0). From Ref. 18.

Special attention was paid to the effects of membrane potential on single channel events. For both agonists, the single channel current obtained by taking the mean current for several hundreds of channels or by curve fitting the data with two Gaussian functions was found to increase linearly with membrane hyperpolarization. The reversal potential for the two agonists was at around −70 mV, in agreement with the previously measured equilibrium potential for the ACh current in these cultured neurones [14] (Fig. 4). The single channel conductance values were of 19 pS and 37 pS for ACh and of 15 pS and 52 pS for CCh. The large conductance value is in reasonable agreement with the value of 40 pS reported by Sattelle [13] for the D_f neurone. The duration of the single channel events was found to increase with membrane hyperpolarization as expected from the above mentioned shifts in

Acetylcholine 10 μM   2 Experiments

Membrane potential (mV)
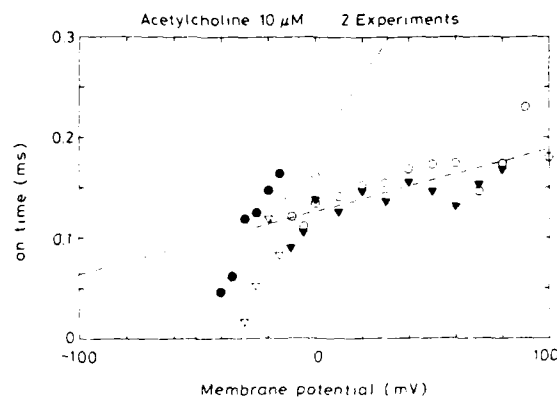
FIG 5 Relationship between the apparent mean open time of ACh-activated channels and membrane potential between − 40 and 100 mV. Two experiments (circles and triangles). The data can be reasonably well fitted with two straight lines, one for the membrane potential more positive than − 20 mV (open circles and filled triangles; slope: 0.62 ms/V, correlation coefficient: 0.745, $n = 24$), one for larger depolarizations (filled circles and empty triangles; slope 3.6 ms/V, correlation coefficient: 0.623, $n = 10$). From Ref. 18.

the spectrum. The frequency of events per unit time was also found to be slightly voltage-dependent and to increase with membrane hyperpolarization, resulting in a slight increase in the open time probability with membrane potential (Fig. 5).

The properties of the ACh receptors of cultured embryonic cockroach neurones are very similar to those of nicotinic receptors in vertebrate preparations.

GABA and muscimol

Pressure injection of 50 μM GABA onto the surface of a cultured neurone under whole-cell-clamp conditions induced an inward current when the patch pipette was filled with KCl and an outward current when it was filled with potassium gluconate. As for ACh, large fluctuations were superimposed on this current. Similar results were obtained with muscimol. Spectral analysis of these current fluctuations revealed only one Lorentzian component (Fig. 6) with a corner frequency of 13.5 ± 2.53 Hz for GABA and 24.5 ± 3.08 Hz for muscimol corresponding to mean channel opening times of 11.8 ms for GABA and 6.5 ms for muscimol. The mean single channel conductances calculated from the variance of the noise and the mean current intensity were 18.6 ± 6.2 pS for GABA and 15.2 ± 5.3 pS for muscimol.

Benzodiazepines such as flunitrazepam potentiate GABA responses in the locust [25]. Addition of flunitrazepam (2 μM) to the solution bathing the cultured cockroach neurones resulted in an increased response to GABA. The spectra and the single channel conductance values remained basically unchanged (mean corner frequency of 11.1 ± 2.46 Hz after flunitrazepam as compared with 13.5 ± 2.53 Hz before drug addition; mean single channel conductance of 18.3 pS as compared to 18.6 ± 6.2 pS before drug addition). This result suggests that, as in mammalian preparations [26], the effects of the benzodiazepines is to increase the frequency of channel openings without altering their properties.

332
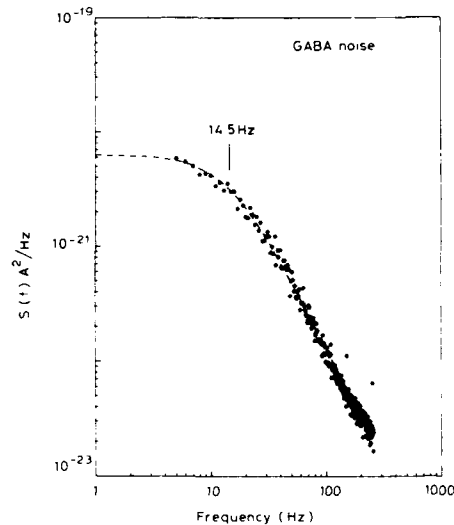
FIG 6 Power spectra of the noise induced by pressure application of GABA onto the membrane of a cultured neurone. Note that the power spectrum can be fitted with one Lorentzian function. From Ref. 17.

In the absence of single channel recordings, it is difficult to draw definite conclusions about the GABA receptors. The fact that, despite a large number of attempts, no characteristic GABA channel has so far been recorded in our neuronal cultures could indicate that, unlike the ACh receptor channels, the GABA receptor channels are not uniformly distributed over the surface of the cell and may be located in clusters inaccessible to the patch pipette.

Whereas the cockroach GABA receptors differ from the vertebrate $GABA_A$ receptors in that they are insensitive to bicuculline [17], the properties of the associated channels are very similar to those observed in other preparations. Thus, chloride channels associated with the GABA receptors in mouse spinal neurones have a conductance of 15.4 pS [27] and of 16 pS in cultured rat cerebellar neurones [28].

Glutamate

When applied to the membrane of embryonic cultured cockroach neurones, L-glutamate produces either a depolarization, or a hyperpolarization [16]. Single channel events underlying the depolarizing responses were analysed. These responses were recorded for L-glutamate concentrations ranging from 0.1 to 10 μM. In most experiments, 1 μM Concanavalin-A (Con-A) was added to the solution to avoid desensitization. In most cases, the single channel activity occurred as long bursts of several seconds separated by variable silent periods. Whereas the duration of the single channels and their mean amplitude was fairly constant from one preparation to another, their frequency and time course varied from one cell to another. Two examples of single channel activity are shown in Figs. 7 and 8. In the first case, the amplitude of the single channel events was fairly homogeneous and
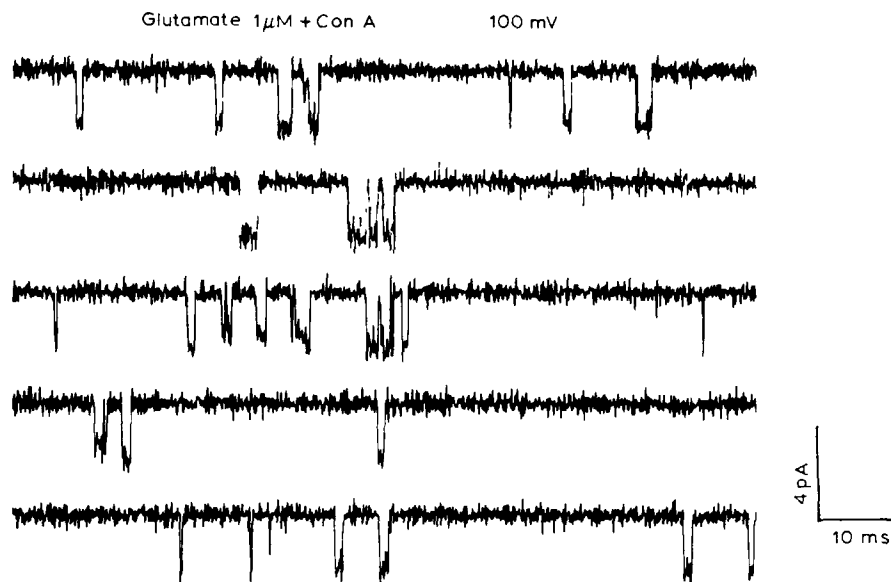
FIG 7 Representative (non-consecutive) traces of glutamate-induced channels in cultured embryonic cockroach neurones. The membrane was hyperpolarized by 100 mV. All records were low-pass filtered at 3 kHz.

the frequency reasonably low. In the second, which was filtered to reduce the background noise, the activity (which was recorded during a burst) was extremely high and the events were complex, being made of a succession of various 'substates' each characterized by a different intensity. In many cases, the current trace obviously jumped from one state to the other. Transitions in both directions were

FIG 8 Representative (consecutive) traces of channels induced by L-glutamate. Note the existence of a large number of substates. The membrane was hyperpolarized by 60 mV. All records were low-pass filtered at 1 kHz.

Glutamate 1 μM + Con A
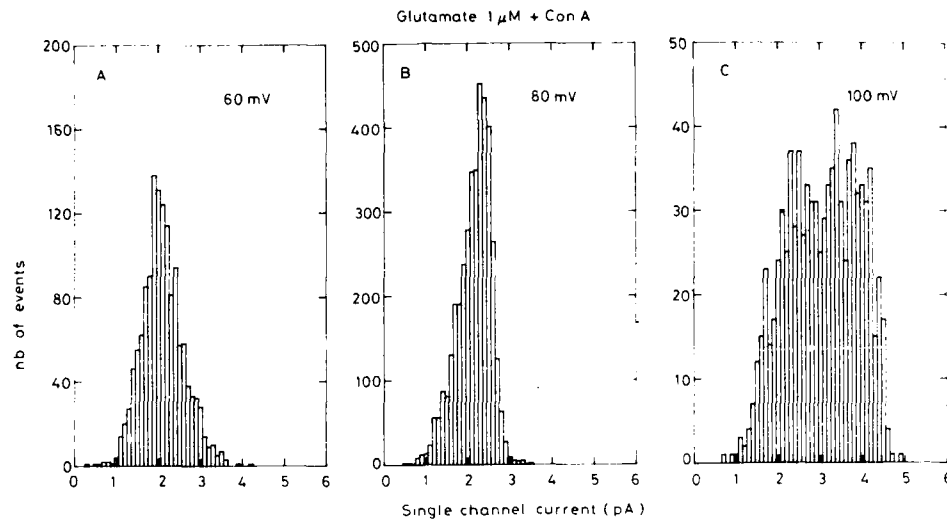
FIG 9 Amplitude histograms for glutamate channels at three potential levels.

found to occur at about the same frequency, in agreement with the interpretation of these events as substates of the same channel. The short durations of each substate made the analysis of this phenomenon quite difficult.

The amplitude of the large events was between 1.6 and 2.1 pA. This amplitude increased with membrane potential as the amplitude histogram became broader and started exhibiting distinct peaks (Fig. 9). In the experiment illustrated in Fig. 10, the number of substates was reduced and the current voltage relationship was linear. The calculated reversal potential of the curve was 73.5 mV and the single channel conductance was 22 pS (correlation coefficient: 0.995, $n = 7$). The value of the reversal potential is in agreement with that of the macroscopic current [16]. The open-time histograms could usually be reasonably well fitted with a single exponential with a voltage independent time constant of about 0.25 ms (Fig. 11). The
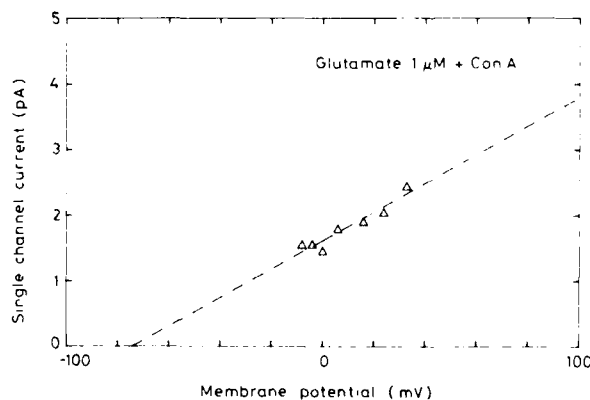
FIG 10 Current–voltage relationship for L-glutamate operated channels. In this experiment, as in that illustrated Fig. 7, the number of substates was small.
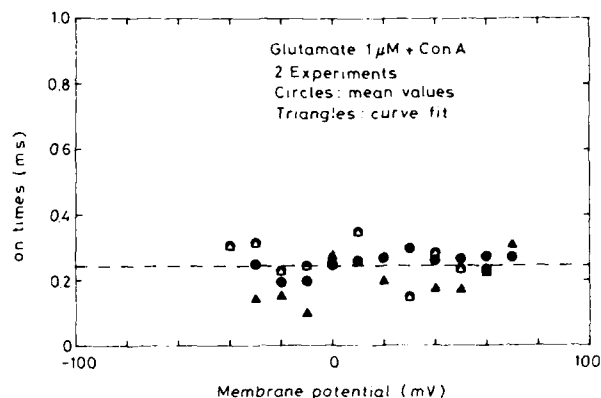
FIG 11 Relationship between membrane potential and mean open time (circles) and once time constants (triangles) for two different patches.

glutamate channels of cockroach cultured neurones have a much lower conductance than the glutamate receptors of the adult locust muscles [29,30] or the glutamate receptors of the embryonic locust muscles [31].

Conclusion

The results presented in this paper illustrate some of the properties of the receptor channels in embryonic cockroach neurones. These properties are reminiscent in most cases of those of vertebrate preparations which have been studied in more detail. This similarity in the biophysical properties was to be expected from the known large degree of conservation of the receptor proteins throughout evolution and the high degree of identity of the various receptors [11].

Many more experiments are obviously needed to fully characterize the receptors biophysically and pharmacologically. The next step in this direction should be a detailed pharmacological study of the properties of the receptor channels in embryonic as well as in adult neurones. Such a study could reveal certain subtypes of receptors (such as those which have been found in vertebrate muscarinic receptors) which might eventually be used as specific targets for insecticides.

References

1 Pitman, R.M. (1970) Transmitter substances in insects: a review. Comp. Gen. Pharmacol. 2, 347–371.

2 Pichon, Y. (1974) The pharmacology of the insect nervous system. In: the Physiology of Insecta (M. Rockstein, ed.), pp. 102–174. Academic Press, New York.

3 Callec, J.J. (1974) Synaptic transmission in the central nervous system of insects. In: Insect Neurobiology (J.E. Treherne, ed.), pp. 119–178. North Holland, Amsterdam.

4 Sattelle, D.B. (1980) Acetylcholine receptors of insects. Adv. Insect. Physiol. 15, 215–315.

5 Callec, J.J. (1985) Synaptic transmission in the central nervous system. In: Comprehensive Insect Physiology, Biochemistry and Pharmacology (G.A. Kerkut, L.I. Gilbert, eds.), Vol. 5, pp. 140–179. Pergamon Press, Oxford.

6 Pichon, Y. and Manaranche, R. (1985) Biochemistry of the nervous system. In: Comprehensive Insect Physiology, Biochemistry and Pharmacology (G.A. Kerkut, L.I. Gilbert, eds.), Vol. 10, pp. 417–450. Pergamon Press, Oxford.

7 Gerschenfeld, H.M. (1973) Chemical transmission in invertebrate central nervous systems and neuromuscular junctions. Physiol. Rev. 53, 1–119.

8 Usherwood, P.N.R. (1978) Aminoacids and synaptic transmission. Adv. Comp. Physiol. Biochem. 7, 227–309.

9 Pichon, Y. and Ashcroft, F.M. (1985) Nerve and muscle: electrical activity. In: Comprehensive Insect Physiology, Biochemistry and Pharmacology (G.A. Kerkut, L.I. Gilbert, eds.), Vol. 5, pp. 85–113, Pergamon Press, Oxford.

10 Numa, S., Noda, M., Takahashi, H., Tanabe, T., Toyosato, M., Furutani, Y. and Kityotani, S. (1983) Molecular structure of the nicotinic acetylcholine receptor. In: Molecular Neurobiology, Cold Spring Harbor Symposia on Quantitative Biology 18, 57–69.

11 Schofield, P.R., Darlison, M.G., Fujita, M., Burt, D.R., Stephenson, F.A., Rodriguez, H., Rhee, L.M., Ramachandran, J., Reale, V., Glencorse, T.A., Seeburg, P.H. and Barnard, E.A. (1987) Sequence and functional expression of the $GABA_A$ receptor shows a ligand-gated receptor super-family. Nature 328, 221–227.

12 Neher, E. and Sakmann, B. (1976) Single channel currents recorded from membrane of denervated from muscle fibres. Nature 260, 799–802.

13 Sattelle, D.B. (1986) Insect acetylcholine receptors — biochemical and physiological approaches. In: Neuropharmacology and Pesticide Action (M.G. Ford, G.G. Lunt, R.C. Reay, P.N.R. Usherwood, eds.) pp. 445–497. Ellis Horwood, Chichester.

14 Lees, G., Beadle, D.J. and Botham, R.P. (1983) Cholinergic receptors on cultured insect neurones from the central nervous system of embryonic cockroaches. Brain Res. 288, 49–59.

15 Neumann, R., Lees, G., Beadle, D.J. and Benson, J.A. (1987) Responses to GABA and other neurotransmitters in insect central neuronal somata in vitro. In: Sites of Action for Neurotoxic Pesticides (R.M. Hollingworth, M.B. Green, eds.), pp. 25–43. ACS Symposium series 356.

16 Horseman, B.G., Seymour, C., Bermudez, I. and Beadle, D.J. (1988) The effects of L-glutamate on cultured insect neurones. Neurosci. Lett. 86, 65–70.

17 Shimahara, T., Pichon, Y., Lees, G., Beadle, C.A. and Beadle, D.J. (1987) γ-Aminobutyric acid receptors on cultured cockroach brain neurones. J. Exp. Biol. 131, 231–244.

18 Beadle, D.J., Horseman, G., Pichon, Y., Amar, M. and Shimahara, T. (1989) Acetylcholine activated ion channels in embryonic cockroach neurones growing in culture. J. Exp. Biol. (in press).

19 Dewhurst, S. and Beadle, D.J. (1985) Culturing nerve cells and tissues from insects in vitro. In: Neurochemical Techniques in Insect Research (H. Breer, T.A. Miller, eds.), pp. 207–222. Springer Verlag, Berlin.

20 Pichon, Y. and Treherne, J.E. (1973) An electrophysiological study of the sodium and potassium permeabilities of insect peripheral nerves. J. Exp. Biol. 59, 447–461.

21 Hamill, O.P., Marty, A., Neher, E., Sakmann, B. and Sigworth, F.J. (1981) Improved patch-clamp techniques for high resolution current recording from cells and cell-free membrane patches. Pflugers Arch. 391, 85–100.

22 Anderson, C.R. and Stevens, C.F. (1973) Voltage clamp analysis of acetylcholine produced end-plate current fluctuations at frog neuromuscular junction. J. Physiol. (Lond.) 235, 665–691.

23 Sachs, F., Neil, J. and Barkakati, N. (1982) The automated analysis of data for single ionic channels. Pflugers Arch. 395, 331–340.

24 Beadle, D.J., Pichon, Y. and Shimara, T. (1986) Patch-clamp and noise analysis studies of transmitter receptors of cultured insect neurones. In: Insect Neurochemistry and Neurophysiology (A.B. Borkovec, D.B. Gelman, eds), pp. 379–382. Humana Press, New Jersey.

25 Lees, G., Beadle, D.J., Neumann, R. and Benson, J.A. (1987) Responses to GABA by isolated insect neuronal somata: pharmacology and modulation by benzodiazepine and a barbiturate. Brain Res. 401, 267–278.

26 Mathers, D.A. (1987) The $GABA_A$ receptor: new insights from single-channel recording. Synapse I, 96–101.

27 Barker, J.L. and Mathers, D.A. (1981) GABA analogues activate channels of different duration on cultured mouse spinal neurones. Science 212, 358–361.

28 Cull-Candy, S.G. and Ogden, D.C. (1985) Ion channels activated by L-glutamate and GABA in cultured cerebellar neurons of the rat. Proc. R. Soc. Ser. B 224, 367–373.

29 Patlak, J.B., Gration, K.A.F. and Usherwood, P.N.R. (1979) Single glutamate activated channels in locust muscle. Nature 278, 643–645.

30 Cull-Candy, S.G., Miledi, R. and Parker, I. (1980) Single glutamate-activated channels recorded from locust muscle fibres with perfused patch-clamp electrodes. J. Physiol. (Lond.) 312, 195–210.

31 Duce, J.A. and Usherwood, P.N.R. (1986) Primary cultures of muscles from embryonic locusts (Locusta migratoria, Schistocerca gregaria): developmental, electrophysiological and patch-clamp studies. J. Exp. Biol. 123, 307–323.

CHAPTER 25

Molecular biology of *Drosophila* choline acetyltransferase

PAUL M. SALVATERRA

Division of Neurosciences, Beckman Research Institute of the City of Hope, 1450 E. Duarte Rd., Duarte, CA 91010, U.S.A.

Introduction

Choline acetyltransferase (ChAT) catalyses the biosynthesis of the important central and peripheral neurotransmitter Acetylcholine (ACh). Very little structural information is available regarding this enzyme from any source due to its extremely low abundance. The enzyme is present in the nervous systems of all animals, with relatively high concentrations in the brains of insects [1]. Even in *Drosophila* nervous system the protein is present in only about 1 part in 30,000. We have previously reported the complete purification of *Drosophila* ChAT from adult fly heads [2]. We have also produced a number of different monoclonal antibodies [3] which can specifically recognize ChAT after separation of *Drosophila* proteins by SDS gel electrophoresis and Western blotting [4] or by staining tissue sections of *Drosophila* by immunocytochemical techniques [5].

Using these monoclonal antibodies as screening reagents we have isolated a cDNA clone which contains the complete coding sequence for *Drosophila* ChAT [6]. A number of lines of evidence support the identification of this cDNA clone as the structural gene for ChAT. The clone maps to the correct position on the polytene chromosomes identified independently as the cytogenetic locus for ChAT in *Drosophila* [7]. The protein produced by the clone is recognized by several different monoclonal anti-*Drosophila* ChAT antibodies and amino acid sequences obtained from Edman degradation of 10 different ChAT tryptic peptides are all present in the clone. Recently, we have also demonstrated that the clone can code for active ChAT enzyme [8].

Results and Discussion

Drosophila ChAT and Torpedo AChE appear to be derived from a common ancestral gene
There is a striking global homology between the amino acid sequence of *Drosophila* ChAT and *Torpedo* AChE [9]. It is possible to identify six polypeptide segments along the length of the two polypeptide chains which contain significant homology. These segments include 274 and 319 amino acid residues and cover 38 and 54% of
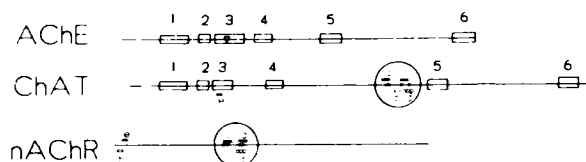
FIG 1 Schematic representation of amino acid homologies between ChAT, AChE, and nAChR. Each sequence is represented by a horizontal line. The relative positions of the homologous peptides are represented as boxes drawn along each sequence and numbered above each box. The active site peptide of AChE is indicated by a triangle inside homologous peptide 3. The relative positions of the analogous peptides identified in ChAT and nAChR are shown as small symbols above and below the lines and are labeled (a-e) with small letters. The large circles indicate the presumed acetylcholine binding domain of nAChR and a clustering of four analogous peptides in ChAT. The positions of the four potentially important cysteine residues are indicated as small circles along each line. Data have been adapted from Ref. 9.

the ChAT and AChE molecules, respectively. The degree of homology ranges from 19 to 39% identical amino acids. The relative positions of the homologous peptides are shown schematically in Fig. 1. This degree of homology ranges from 27 to 55% when homologous amino acid replacements [10] are considered. It should be noted, also, that the homology starts at the N-terminal region and spans almost the entire coding region of each protein.

The significance of such homologous peptides does not necessarily imply a common secondary or tertiary structure for ChAT and AChE [11], it does however act as a guide to predicting a possible evolutionary relationship between these two cholinergic enzymes [12]. For example the active site residues of *Torpedo* AChE (Gly-Glu-Ser-Ala-Gly-Gly; residues 198–203) are completely replaced in *Drosophila* ChAT (Ala-Phe-Pro-Leu-Pro-Ile; residues 172–177). Since the active site for ChAT is not yet known we can not assess the importance of this observed sequence divergence for the catalytic function of the enzyme. It seems likely however, that these two proteins share a common evolutionary origin. It is interesting in this regard that AChE, like ChAT has been shown to catalyse the synthesis of acetylcholine [13].

ChAT and neuronal type nicotinic AChR α-subunit also share several analogous peptides
We have noted five homologous sequences when comparing *Drosophila* ChAT with a rat neuronal nicotinic AChR α-subunit [9,14]. The five regions in AChR are all thought to be in the extracellular portion of this integral membrane protein [15]. Interestingly, three of them (segments a,c and d in Fig. 1) are located in the vicinity of the presumed acetylcholine binding site which forms two loops connected by double disulfide bonds between Cys 192 and Cys 193 and between Cys 128 and Cys 142 [16]. Four of these analogous sequences in ChAT (segments a-d in Fig. 1) cluster in a central region around residues 439–492, where four cysteine residues are present at positions 423, 428, 488 and 510 [6]. If disulfide bonds are formed between Cys 423 and Cys 428 and between Cys 488 and Cys 510, they would bring these four homologous sequences with AChR into close proximity with this region of ChAT. Moreover, segments a, c and d contain negatively charged amino acids which could

possibly function as a binding site for the positively charged choline substrate of ChAT. The related segments of ChAT and neuronal AChR are not always conserved in muscle nicotinic AChR and none of these sequences can be found in AChE. Consequently, the segmental homologies between *Drosophila* ChAT and rat neuronal AChR α-subunit seem to reflect convergent evolution rather than divergent evolution.

There is a striking degree of amino acid homology between Drosophila ChAT and porcine ChAT

The deduced amino acid sequence of porcine brain ChAT has recently been reported [18]. It is clear from a comparison of the amino acid sequences of ChAT from these two species that a large number of amino acids have been conserved over a long evolutionary time. The alignment shown in Fig. 2 corrects several typographical errors present in the *Drosophila* amino acid sequence used by Berrard et al. [18]. By inserting only two short gaps in the *Drosophila* sequence and 5 gaps in the porcine sequence it is possible to match 218 identical and 127 homologous amino acid residues. An especially conserved peptide is present from amino acid 492–567 in the *Drosophila* sequence and residues 402–478 in the porcine sequence. In this peptide there are 50 amino acid identities and 11 conservative substitutions (i.e. 80% homology). Another highly conserved peptide (76% homology) is the sequence near the C-terminus of each protein (residues 658–725 in *Drosophila* ChAT and residues 548–615 in porcine ChAT). Both of these regions are likely candidates for functionally important domains in ChAT and it will now be possible to test structure-function relationships using in vitro mutagenesis.

The Drosophila cDNA clone can produce a functional enzyme

We have tested the ability of our original *Drosophila* ChAT cDNA clone to produce a functional enzyme when translated by several different systems. Injection of cRNA transcribed from this clone into *Xenopus* oocytes results in production of active ChAT [8]. In addition the size of the ChAT protein produced in oocytes appears to be indistinguishable from native *Drosophila* ChAT [8,19]. When *E. coli* are transfected with an expression vector (pKK-223) containing this cDNA insert downstream from a tryptophan-lactose (TAC) promoter sequence the bacteria also produce active ChAT with properties similar to native enzyme (Sugihara and Salvaterra, unpublished results). The enzyme is under control of the TAC promoter since its expression can be induced by IPTG added to the medium. In addition in vitro transcribed RNA from this cDNA clone can also produce active enzyme when translated by rabbit reticulocyte lysates (Table 1). The translation of this cDNA into active ChAT is surprising since this is not a full length cDNA (i.e. the mRNA for *Drosophila* ChAT is approximately 5 kb while the cDNA insert is only 2.4 kb in length) and more importantly the cDNA contains no in frame upstream AUG (methionine) initiation codon before position 330-333. The methionine codon present at this position cannot be used to initiate translation in vivo since it is the 10th internal amino acid in a sequenced tryptic peptide [6].

It was possible that the RNA from the clone was initiating at this first AUG and making a shorter protein than that produced in vivo, which still retained enzyme activity. This seems unlikely however for several reasons. The proteins made by all three translation systems are identical in size to the largest form of native *Drosophila* ChAT. In addition we have constructed a number of in vitro mutants and tested

```
D   1  IPDPKGANVASNEASTSAAGSGPESAALFSKLRSFSIGSGPNSPQRVVSNLRGFLTHRLS   60


D  61  NITPSDTGWKDSILSIPKKWLSTAESVDEFGFPDTLPKVPVPALDETMADYIRALEPITT  120
              |   |  *       *         |***|***|*||*|* *|*||   |  |
P   1                 MPILEKTPPKMAAKSPSSEEEPGLPKLPVPPLQQTLATYLRCMQHLVP   48


D121   PAQLERTKELIRQFSAPQGIGARLHQYLLDKREARITGPITTGSTRGTWIFAFPLPINSN  180
          *  *|   ||  **|** *|*   * *  **||  *                  |**|**
P  49  EEQFRRSQAIVQQFGAPGGLGETLQQKLLERQEQTANWVSEYWLNDMYLNNRLALPVNSS  108


D181   PGIGVPAASLQDRPRRAHFAARLLDGIRSHREMLDSGELPLERALAE-KNQPLCMAQYYRL  240
       *|| |   |   |*      |*** *| *| * | |***  |*|| * ||  ***** *** *
P109   PAVIFARQHFEDTNDQLRFAANLISGVLSYKALLDSHSIPIDCAKGQLSGQPLCMKQYYGL  169


D241   LGSCRRPGVKQDSQFLPSRERLNDEDRHVVVICRNQMYCLVLQASDRGKLSESEIASQIL  300
       |* * ** **|  ||  |  |   *  **|* * **  | * |     * |***||| |*|
P170   FSSYRLPGHTQDT-LVAQKSSVMPEPEHVIVACCNQFFVLDVVINFR-RLSEGDLFTQLR  227


D301   YVLSDAPCLPAKPVPVGLLTAEPRSTWARDREMLQEDERNQRNLELIETSQVVLCLDEPL  360
       ||  *|   |   *|****|||** **  * |*   *   *  *||**    ||*** *
P228   KIVRMASNEDERLPPIGLLTSDGRSEWAEARTVLVKDSTNRDSLDMIERCICLVCLDAPG  329


D361   AGNFNARGFTGATPTVHRAGDRDETNMAHEMIHGGGSEYNSGNRWFDKTMQLIICTDGTW  420
       |                      | |** * |||****  *||***|**||* ||  ***
P288   GM-----------------ELSDTNRALQLLHGGGCSKNGANRWYDKSLQFVVGRDGTC  329


D421   GLCYEHSCSEGIAVVQLLEKIYKKIEEHPD-EDNGLPQHHLPPPERLEWHVGPQLQLAFAQ  480
       *|   ***  |** |** *|| *||   |     | |  **|* ** *| |*||*    *
P330   GVVCEHSPFDGIVLVQCTEHLLKHMVKSSKKMVRADSVSELPAPRRLRWKCSPEIQGLLAS  390


D481   ASKSVDKCIDDLDFYVYRYQSYGKTFIKSCQVSPDVYIQLALQLAHYKLYGRLVATYESA  540
       ||   ||   | |*** **||| *******    *** |**|***** *|* ****|*****
P391   SAEKLQQIVKNLDFTVYKFDDYGKTFIKQQKCSPDAFIQVALQLAFYRLHGRLVPTYESA  450


D541   STRRFLHGRVDCIRAASTEALEWAKAMCQGEGANLPLESDREDEEESRKVKFSIYSKDHL  600
       * ***    ****  **|*||***  |  ***    |*    *      | *
P451   SIRRFHEGRVDNIRSATPEALHFVKAITDHASAMPDSEKLLLLKDAIR-----------  498


D601   RELFRCALARQTEVMVRISWAMASTSRCWPARGQYRGHRRDARAVQRRVLQQCSQCNLLS  660
                 *  **  |  *|         | *   ||   || |    *|   |**
P499   -------AQTQYTVMAITGMAIDNHLLGLRELA--REVCKELPEMFTDETYLMSNRFVLS  549


D661   TSQLACSTDSFMGYGPVTPRGVGCSYNPHPEQIVFCVSAFYSCEDTSASRYAKSLQDSLD  720
       ***|| | | * **** * *** *** ** *|**|* * |* |**|||||**||||*
P550   TSQVPTTMEMFCCYGPVVPNGYGACYNPQPESILFCISSFHGCKETSSTKFAKAVEESFI  600


D721   IMRDLLQN                    728
       *| *
P610   EMKGLCSLSQSGMGKPLATKEKVTRPSQVHQP  641
```

TABLE 1   ChAT activity produced by rabbit reticulocyte lysate translation of pCha-12 and two deletion (frame shift) mutants

Clone	ChAT activity μmol/min 10^{-2}
pCha 12	4.9
Apa 1 Deletion	0.1
Xho 1 Deletion	< 0.0001

their ability to synthesize ChAT in the reticulocyte lysate system. These mutants were constructed by digesting the full length clone by restriction enzymes with unique sites in the 5' region of the clone and digesting away a few bases before religation. The resulting constructs are shorter than the original clone and if translation initiation occurs 5' to the restriction site the resulting protein translation product downstream from the restriction site will be out of frame and result in a non-sense protein being produced. If, however, initiation occurs 3' to the deletion site a normal protein should be produced. When cRNA from the full length clone is translated by the reticulocyte system the major protein has an M_r of 75 kDa and at least 2 minor proteins with smaller molecular sizes are also produced. ChAT activity is easy to detect. When a deletion mutant is prepared by cutting the clone with XhoI and removing bases 371–377 to create a frame shift mutant, only the smallest protein is synthesized and no ChAT activity can be detected. When the clone is restricted with ApaI and bases 118–136 are removed both the two small proteins are synthesized but not the 75 kDa band. When ChAT activity is measured a significant amount is detected but it amounts to only 1/50th of that produced by the full length clone. It thus seems likely that protein translation is initiating primarily upstream from the ApaI site. The results of these experiments are summarized in Table 1. The most likely position for initiation is a GUG codon present at position 33–36. GUG is known to function, although rarely, as an initiation codon for prokaryotic mRNA. This codon is even more likely to be used since it resides in an almost perfect initiation context for Drosophila [20]. Drosophila ChAT thus seems to use a non-AUG codon for translation initiation. This unusual feature has been described for only one other eukaryotic RNA the c-myc gene product [21]. Perhaps this unusual feature may indicate regulatory control of ChAT translation in vivo. In this regard we have also recently observed that an independently isolated Drosophila ChAT cDNA clone with approximately 0.8 kb of additional DNA at the 5' end is much less efficiently translated by reticulocyte lysates than the shorter cDNA clone, perhaps indicating secondary structure in the 5' part of ChAT mRNA.

FIG 2   Proposed alignment of the amino acid sequences of Drosophila and porcine ChAT. The sequences are identified by a D or P preceding the amino acid residue number on the left of the figure. Amino acids are identified by the standard one letter code and identities are indicated by a (*) between the sequences while conservative substitutions are noted with a (|). The dashes represent gaps inserted in each sequence in order to optimize the amino acid homology.

344

TABLE 2 ChAT mRNA and enzyme activity during *Drosophila* development

Developmental stage		mRNA (fg/organism)	Enzyme activity (μmol/min/organism $\times 10^6$)
Embryo	4 h	0	0
	7 h	0.24 ± 0.03	0.17 ± 0.06
	13 h	6.79 ± 0.78	0.25 ± 0.07
Larval	1 day	14.00 ± 1.15	19.80 ± 9.50
	3 days	6.30 ± 0.45	42.70 ± 29.70
Pupal	5 days	7.17 ± 0.89	30.20 ± 3.65
	7 days	12.90 ± 1.15	19.60 ± 4.40
Adult	9 days	307.00 ± 10.70	712.00 ± 106.00
	21 days	481.40 ± 62.80	1790.00 ± 105.00

Drosophila ChAT is expressed in a developmentally regulated fashion

ChAT is expressed exclusively in the nervous system in only a subset of the neurons. It is thus a member of the family of genes expressed in a tissue and cell type specific manner. When a cell expresses the ChAT gene it has selected the cholinergic neurotransmitter phenotype. In addition to this important decision with major functional consequences, the levels of ChAT must be regulated throughout development to maintain the appropriate concentration of enzyme. The steady state levels of ChAT specific mRNA vary considerably during the course of normal fly development.

We have recently investigated some aspects of the developmental expression of ChAT activity and steady state mRNA levels in *Drosophila*. *Drosophila*, a holometabolus insect, has 3 larval stages, a pupal stage and an adult stage. The body plan of the organism changes radically during this development history. Many of the neurons from the original larval nervous system remain throughout metamorphosis and innervate new structures in the adult. In addition the adult nervous system adds new neurons when the sensory imaginal disks differentiate during metamorphosis. We have noted expression of both ChAT mRNA and enzyme activity very early in development (between 6 and 7 hours after oviposition) at a time when very few neurons are present and neurogenesis is still proceeding (see Table 2). The levels of ChAT mRNA increase rapidly reaching an initial peak concentration between the 2nd and 3rd instar larval stages. This increase in mRNA levels is mimicked by enzyme activity with a temporal delay of several hours. During the 3rd instar larval stage the levels of ChAT mRNA decrease dramatically into latter pupal stages while enzyme activity levels stay constant. Near the end of pupation the levels of mRNA begin to rise again and are followed by increasing levels of enzyme activity. The results of these studies are summarized in Table 2. These results are consistent with the hypothesis that developmental expression of ChAT is under transcriptional control. The two phases of rapidly increasing ChAT specific mRNA levels and enzyme activity correlate well with the times when *Drosophila* neurons are making physical contact with each other while the decreasing phase of mRNA expression seen during early pupation correlates with the degeneration of neural processes.

Summary

Choline acetyltransferase (ChAT, EC 2.3.1.6) is the enzyme responsible for the biosynthesis of the important central and peripheral neurotransmitter, acetylcholine (ACh). We have recently obtained detailed structural information about this protein by isolating and sequencing several cDNA clones from *Drosophila melanogaster*. The results of these studies have led us to several interesting structural and functional conclusions regarding *Drosophila* ChAT and its evolutionary relationship to other macromolecules which interact with ACh. A detailed comparison of the amino acid sequence of *Drosophila* ChAT with that of *Torpedo* acetylcholinesterase (AChE) reveals a global homology between these two proteins suggesting that they may have evolved from a common ancestral gene. We have also noted several short amino acid analogous sequences when comparing ChAT with a neuronal nicotinic type ACh receptor sequence (nAChR). The analogous peptides are not extensive enough to propose a common origin for these two genes but may indicate regions of structural and/or functional convergence.

Another interesting structural aspect of ChAT involves the mechanism of protein translation initiation. We have succeeded in obtaining translation of our cDNA clone in several test systems including *Xenopus* oocytes, *E. coli*, and rabbit reticulocyte lysates. These results are unusual since our cDNA clone has no usual AUG initiation codon upstream from the known protein coding region. It seems likely that *Drosophila* ChAT may use a non-AUG codon to initiate protein translation. In an attempt to identify the likely initiation codon we have created several in vitro mutants and tested them for their ability to produce active enzyme of the proper size.

We have also recently completed studies which describe the pattern of ChAT mRNA and enzyme production during *Drosophila* development. The steady state mRNA levels appear to have a biphasic pattern of expression temporally preceding a similar pattern of expression for enzyme activity by several hours. The increasing phases of ChAT mRNA levels seem to correlate with development of cell-cell contacts within the nervous system.

References

1 Salvaterra, P.M. (1987) Molecular biology and neurobiology of choline acetyltransferase. Mol. Neurobiol. 1, 247–280.

2 Slemmon, J.R., Salvaterra, P.M., Crawford, G.D. and Roberts, E. (1982) Purification of choline acetyltransferase from *Drosophila melanogaster*. J. Biol. Chem. 257, 3847–3852.

3 Crawford, G.D., Slemmon, J.R. and Salvaterra, P.M. (1982) Monoclonal antibodies selective for *Drosophila melanogaster* choline acetyltransferase. J. Biol. Chem. 257, 3853–3856.

4 Salvaterra, P.M. and McCaman, R.E. (1985) Choline acetyltransferase and acetylcholine levels in *Drosophila melanogaster*: A study using two temperature-sensitive mutants. J. Neurosci. 5, 903–910.

5 Buchner, E., Buchner, S., Crawford, G., Mason, W.T., Salvaterra, P.M. and Sattelle, D.B. (1986) Choline acetyltransferase-like immunoreactivity in the brain of *Drosophila melanogaster*. Cell Tissue Res. 246, 57–62.

6 Itoh, N., Slemmon, J.R., Hawke, D.H., Williamson, R., Morita, E., Itakura, K., Roberts, E., Shively, J.E., Crawford, G.D. and Salvaterra, P.M. (1986) Cloning of *Drosophila* choline acetyltransferase cDNA. Proc. Natl. Acad. Sci. U.S.A. 83, 4081–4085.

346

7 Greenspan, R.J. (1980) Mutations of choline acetyltransferase and associated neural defects in *Drosophila melanogaster*. J. Comp. Physiol. 137, 83–92.

8 McCaman, R.E., Carbini, L., Maines, V. and Salvaterra, P.M. (1988) Single RNA species injected in *Xenopus* oocyte directs the synthesis of active choline acetyltransferase. Mol. Brain Res. 3, 107–114.

9 Mori, N., Itoh, N. and Salvaterra, P.M. (1987) Evolutionary origin of cholinergic macromolecules and thyroglobulin. Proc. Natl. Acad. Sci. U.S.A. 84, 2813–2817.

10 Dayhoff, M.O., Barker, W.C. and Hunt, L.T. (1983) Establishing homologies in protein sequences. Methods Enzymol. 91, 524–545.

11 Kabsch, W. and Sander, C. (1984) On the use of sequence homologies to predict protein structure: Identical pentapeptides can have completely different confirmation. Proc. Natl. Acad. Sci. U.S.A. 81, 1075–1078.

12 Doolittle, R.F. (1981) Similar amino acid sequences: Chance or common ancestry? Science 214, 149–159.

13 Hestrin, S. (1949) The reaction of acetylcholine and other carboxylic acid derivatives with hydroxylamine and its analytical application. J. Biol. Chem. 180, 879–881.

14 Boulter, J., Evans, K., Goldman, D., Martin, G., Treco, D., Heinemann, S. and Patrick, J. (1986) Nature 319, 368–374.

15 Finer-Moore, J. and Stroud, R.M. (1984) Amphipathic analysis and possible formation of the ion channel in an acetylcholine receptor. Proc. Natl. Acad. Sci. U.S.A. 81, 155–159.

16 Kao, P.N. and Karlin, A. (1986) Acetylcholine receptor binding site contains a disulfide cross-link between adjacent half-cystinyl residues. J. Biol. Chem. 261, 8085–8088.

17 Anderson, D.J. and Blobel, G. (1983) Molecular events in the synthesis and assembly of a nicotinic acetylcholine receptor. Cold Spring Harb. Symp. Quant. Biol. 48, 125–134.

18 Berrard, S., Brice, A., Iottspeich, F., Braun, A., Barde, Y.-A. and Mallet, J. (1987) cDNA cloning and complete sequence of porcine choline acetyltransferase: in vitro translation of the corresponding RNA yields an active protein. Proc. Natl. Acad. Sci. U.S.A. 84, 9280–9284.

19 Muñoz-Maines, V.J., Slemmon, J.R., Panicker, M.M., Neighbor, N. and Salvaterra, P.M. (1987) Production of polyclonal antisera to choline acetyltransferase using a fusion protein produced by a cDNA clone. J. Neurochem. 50, 167–175.

20 Davener, D.R. (1987) Comparison of the consensus sequence flanking translational start sites in *Drosophila* and vertebrates. Nucleic Acids Res. 15, 1353–1361.

21 Hann, S.R., King, M.W., Bentley, D.L., Anderson, C.W. and Eisenman, R.N. (1988) A non-AUG translational initiation in c-myc cxon 1 generates an N-terminally distinct protein whose synthesis is disrupted in Burkitt's lymphomas. Cell 52, 185–195.

Electrophysiological approaches to receptors and ion channels

CHAPTER 26

The role of carbamates and oximes in reversing toxicity of organophosphorus compounds: a perspective into mechanisms

E.X. Albuquerque [1,2], M. Alkondon [1], S.S. Deshpande [1], W.M. Cintra [1,2], Y. Aracava [1,2] and A. Brossi [3]

[1] Department of Pharmacology and Experimental Therapeutics, University of Maryland School of Medicine, 655 W. Baltimore St., Baltimore, MD 21201, U.S.A; [2] Molecular Pharmacology Training Program, Institute of Biophysics "Carlos Chagas Filho", Federal University of Rio de Janeiro, Rio de Janeiro-Ilha do Fundão-CEP 2194, Brazil; and [3] Laboratory of Chemistry, National Institute of Diabetes and Digestive and Kidney Diseases, Bethesda, MD 20892, U.S.A.

Introduction

Carbamates and oximes have been used successfully in conjunction with atropine in the treatment of organophosphorus (OP)-poisoning. The effectiveness of the reversible anticholinesterase (anti-AChE) carbamates has been attributed to protection of the enzyme from irreversible inhibition by OPs [1]. Oximes such as pyridine-2-aldoxime (2-PAM), similarly, have been thought to owe their effectiveness to reactivation of phosphorylated acetylcholinesterase (AChE). However, recent evidence indicates that carbamylation and reaction of AChE are inadequate to explain either the antidotal effect of these compounds against OPs or the morphological and functional alterations produced by carbamates at the neuromuscular junction [2–5]. The major findings regarding the carbamates are as follows:

(1) Despite similarities in chemical structures, (−) and (+) physostigmine, neostigmine, pyridostigmine and edrophonium exhibited large variations in their therapeutic and toxic effects and their antidotal efficacy against OP compounds.

(2) The natural (−)-physostigmine offered superior protection against lethal doses of OP in comparison to neostigmine or pyridostigmine [4].

(3) Inclusion of mecamylamine [6] or amantadine (unpublished results), which have no significant anti-AChE activity, markedly enhanced the efficacy of (−)-physostigmine.

(4) The (+) optical isomer of (−)-physostigmine had much lower AChE inhibitory activity, yet was able to significantly protect animals exposed to lethal doses of OP [5,7].

(5) Carbamates produced neuromuscular damage to different degrees in slow- and fast-contracting muscles and showed a differential pattern of recovery of muscle and nerve terminal morphology [5,8,9].

Regarding oximes, recent studies [10,11] have revealed the following observations that argue for the importance of mechanisms other than reactivation of AChE:

(1) Fully recovered muscle function can be observed in the absence of significant reactivation of AChE with muscles treated with oximes subsequent to exposure to certain OPs.

(2) Marked specificity of HI-6 vs 2-PAM was seen against soman poisoning.

(3) Though HI-6 in general was more potent than 2-PAM in recovering muscle function, 2-PAM but not HI-6 was able to antagonize tabun's toxic effects.

(4) SAD-128 (1,1'-oxybis(methylene)-bis-4-(1,1-dimethyl)pyridinium dichloride), a compound with no oxime moiety and therefore devoid of dephosphorylating effect, produced antagonism in soman poisoning [12].

(5) Our study also revealed a significant degree of chemical interaction of oximes with the natural ligand acetylcholine (ACh) and with AChE at the nicotinic synapse of the frog neuromuscular junction.

In view of these findings, electrophysiological studies, especially those utilizing single channel recordings, have been carried out. The results have disclosed alterations of the postsynaptic AChR activation process by direct interactions of carbamates and oximes, as well as OPs, with the AChR macromolecule. Interactions at agonist recognition sites (agonistic activity) and at the ion channel component of the AChR molecule (which responds to various noncompetitive blockers) were the most frequently found mechanisms. These direct interactions must be taken into account in explaining the antidotal efficacy of carbamates and oximes against OPs.

Materials and methods

Animals

All experiments except single channel studies were conducted at room temperature (21–23°C) either on the sartorius muscle of *Rana pipiens* or on the diaphragm muscle of Wistar rats (190–210 g). The physiological solution for frog muscles had the following composition (in mM): NaCl 116; KCl 2.0; $CaCl_2$ 1.8; Na_2HPO_4 1.3; and NaH_2PO_4 0.7, and was bubbled with O_2. The bathing medium for mammalian muscle had the following composition (in mM): NaCl 135; KCl 5.0; $MgCl_2$ 1.0; $CaCl_2$ 2.0; $NaHCO_3$ 15.0; Na_2HPO_4 1.0, and glucose 11.0, and was continuously aerated with 95% O_2 and 5% CO_2.

Techniques

Twitch recordings Twitch studies were performed on frog sciatic nerve-sartorius muscle preparations and on rat phrenic nerve-diaphragm muscle preparations. Muscles were indirectly stimulated at 0.2 Hz for sartorius and 0.1 Hz for diaphragm preparations with supramaximal square-wave pulses of 0.1 ms duration applied to the nerve via bipolar platinum electrodes. Using frog muscles, after obtaining stable responses, the oximes were added, and the recording continued for at least 30 min. Thirty min of frequent washing were allowed between sequential drug applications. With diaphragm muscles, the responses to single twitch and tetanic (50 Hz) nerve stimulations were obtained in the presence of OP agents and a subsequent exposure to oximes 2-PAM or HI-6.

Macroscopic endplate currents Membrane potentials, endplate potentials (EPPs), and endplate currents (EPCs) were recorded from junctional regions of surface fibres of frog muscles, and the effects of oximes were studied after a 30-min equilibration period. The recording of EPCs was done according to the method described earlier [13].

Single channel recordings Patch clamp studies were performed at 10 °C on single fibres isolated from interosseal and lumbricalis muscles of the longest toe of hind legs from the frog *Rana pipiens*. The procedures for enzymatic dissociation of muscle fibres, patch clamp recording and analysis of single channel data have been described elsewhere [14–18].

Determination of AChE activity The enzyme activity in frog sartorius muscles after exposure to the oximes 2-PAM and HI-6 were determined using Ellman's colorimetric method [19]. Because the oximes hydrolysed acetylthiocholine, appropriate drug-blank tests were made (see details in Ref. 11).

Statistical analysis
The data are expressed as mean ± S.E.M. Wherever applicable, the two-tailed Student's *t* test was used to determine significance between means.

Results and discussion

Reversible cholinesterase inhibitors: molecular targets and interactions

In this study we have attempted to correlate the chemical reactivity of selected anti-AChE compounds with their ability to directly alter the function of the nicotinic AChR and thereby improve the neuromuscular transmission following OP poisoning. Physostigmine is one of the most interesting carbamates for this study because the (+) optical isomer has no significant anti-AChE activity, yet both isomers affect the AChR and demonstrate antidotal efficacy. Neostigmine and pyridostigmine are interesting carbamates because of their structural similarity to ACh, including a positively charged quaternary ammonium group (Fig. 1). Edrophonium is also similar to ACh and possesses a charged head at the nitrogen atom, but is not a carbamate and also is less potent in inhibiting AChE than the other two carbamates [20]. Lack of a carbamyl group is thought to account for weaker anti-AChE activity and faster kinetics as it precludes AChE carbamylation. In agreement with this view, a reduction of three orders of magnitude in anti-AChE potency is seen with (−)-eseroline, a noncarbamate metabolite of (−)-physostigmine [21]. An appropriate interaction of the quaternary amine moiety should be capable of opening channels through interaction with the anionic site of the AChR as seen in the case of alkyl ammonium compounds [22]. However, in general, these agonists have much lower potency than ACh, and they open channels with shorter lifetime as compared to the neurotransmitter [22].

Neostigmine, edrophonium and pyridostigmine

Agonist property Neostigmine as well as pyridostigmine and edrophonium exhibited very weak or no agonist activity at the nicotinic AChR of the adult frog

Edrophonium
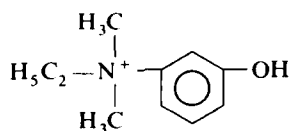
Pyridostigmine
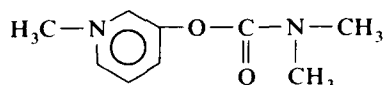
Neostigmine
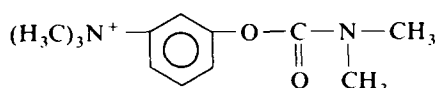
(+) Physostigmine
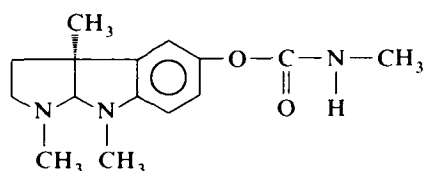
(−) Physostigmine
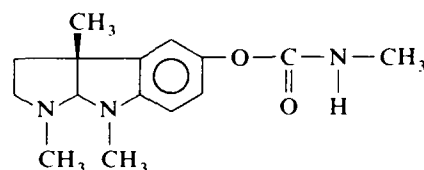
FIG 1   Structural formulae of carbamates and edrophonium.

TABLE 1   AChE inhibitory activity and agonist and antagonist properties of reversible AChE inhibitors at muscle AChR

Drug	AChE inhibition [a] IC_{50} (μM)	Agonist property [b] (μM)	Noncompetitive antagonism [c] (μM)
(−)-Physostigmine [d]	4.8	0.5–1.0	> 20
(+)-Physostigmine	195	> 10	5
Neostigmine	0.7	> 20	2
Pyridostigmine	8	≫ 200	2
Edrophonium	11	> 100	2

[a] AChE was measured from the frog sartorius muscle homogenates using Ellman's modified method. The IC_{50} values were obtained from a log response curve of at least four doses and three determinations were made for each dose.
[b] Concentration necessary to elicit some activation (1–2 openings per second).
[c] Concentration necessary to decrease the channel open times of about 50%.
[d] Data extracted from Shaw et al. [18].

muscle fibre (Table 1). Neostigmine, even at high micromolar concentrations, elicited a low level of activation, and this weak activation could preclude the production of significant membrane depolarization and consequent muscle contraction. At negative holding potentials, neostigmine (20–100 μM) activated inward currents [3] which appeared as bursts of successive fast openings and closures and had a slope conductance of 32 pS, a value similar to that of ACh [14]. Increasing neostigmine concentrations decreased the mean channel open time and increased the number of 'fast' (intraburst) closures. Neostigmine, as well as other AChE inhibitors tested, blocked channels activated by ACh (see below) at a concentration range lower than that necessary to induce agonist activity. This suggested that at the concentrations used to unveil agonist activity, neostigmine may block its own channels in the open conformation. However, as discussed later, the blockade induced by concentrations of neostigmine higher than 100 μM no longer followed the predictions of the model used for analysis since the bursts were decreased in duration.

Pyridostigmine up to 200 μM was practically devoid of any agonist property. Edrophonium, at concentrations higher than 100 μM, produced some openings which appeared noisier than currents activated by ACh. Also, such openings disappeared at hyperpolarized potentials and reappeared after a period of depolarization, suggesting the occurrence of desensitization [3].

Studies in cultured myotubes with neostigmine [23] and in myoballs with pyridostigmine [17] have shown significant agonistic properties for these drugs. Some developmental differences of nicotinic AChRs or a preferential activation of one of the various (at least three) populations or states of AChR with distinct conductance and kinetics reported in cultured cells [24–26] were indicated. Some of the differences in agonist potency also reflected differences in preferred conformation, correct distance and angle between the two main functional groups or dependence on more subtle differences in solvation, charge distribution, hydrophobicity, etc. of the agonist molecule. Indeed, studies of rigid and semirigid analogue have provided evidence for more complex requirements for successful agonist–receptor interaction and activation of nicotinic AChR. Preliminary results on the quaternary analogue of anatoxin-a, N,N-dimethyl anatoxin-a, which is 1000-fold less potent as an agonist than (+)-anatoxin-a [27] demonstrated that the presence of a charged nitrogen group or quaternization are not important for agonist potency.

Blockade of ACh-activated channels

Neostigmine In contrast to ACh (0.4 μM) alone, neostigmine (0.1–50 μM) in combination with ACh in the patch pipette, produced well-defined bursts (Fig. 2). There was no alteration of the single channel conductance by neostigmine, and the open-state currents were interrupted by many brief flickers, suggesting blockade of the channel in its open state.

The data were analysed using the simple sequential model for open channel blockade of the nicotinic AChR shown below:

$$ nA + R \underset{k_{-1}}{\overset{k_1}{\rightleftharpoons}} A_nR \underset{k_{-2}}{\overset{k_2}{\rightleftharpoons}} A_nR^* \underset{D\,k_{-3}}{\overset{D\,k_3}{\rightleftharpoons}} A_nR^*D $$
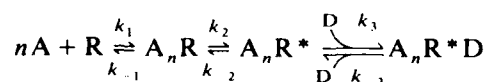
In this series of reactions, n represents the number of molecules, usually two, of A (the agonist) that bind to R (AChR at resting state) to form A_nR (the agonist-bound nonconducting state) which undergoes an conformational change to A_nR^* (the

354
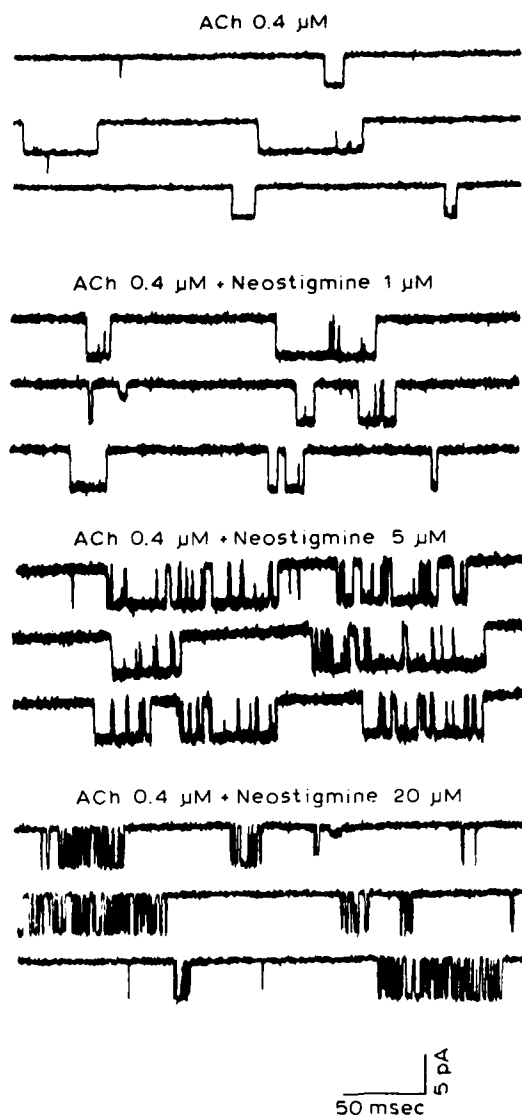
FIG 2 Samples of ACh-activated channel currents in absence and presence of different concentrations of neostigmine in the patch pipette solution.

conducting state). This state is likely to be blocked by D (the blocker) to form A_nR^*D, a state with no conductance. This model states that the final closing of the channel is achieved via opening of the blocked channels [28] and was used to explain the blocking kinetics of many drugs such as QX-222 [28], scopolamine [29] bupivacaine [24] and (−)-physostigmine [18].

Analysis of the open state showed progressive shortening of the duration of the openings within a burst (open times) with increasing concentrations of neostigmine
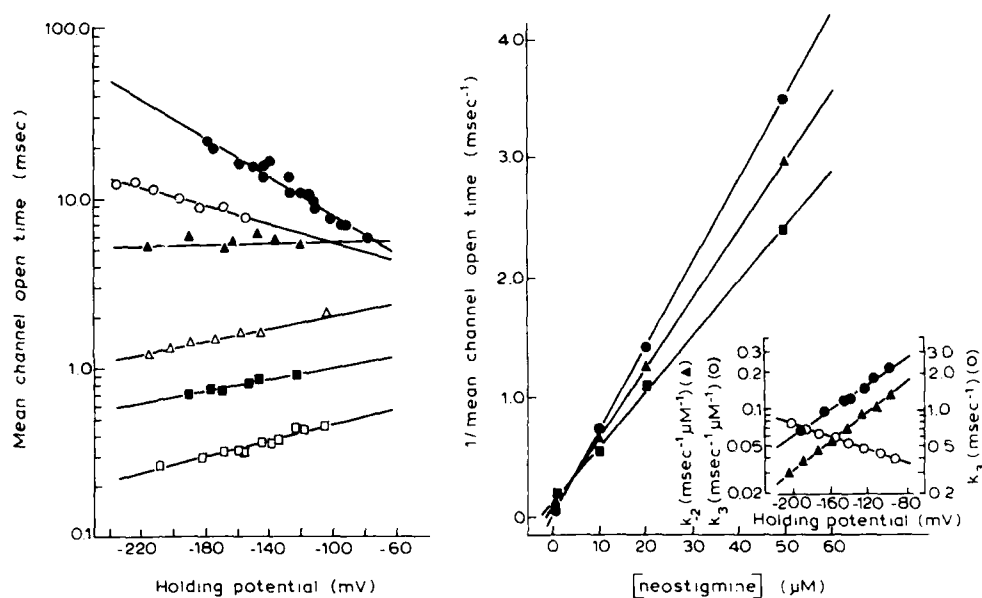
FIG 3 Voltage-dependent changes in mean channel open time under control condition (●), and in presence of 0.1 μM (○), 2 μM (▲), 10 μM (△), 20 μm (■) and 50 μM (□) of neostigmine are shown on the left. The relation between neostigmine concentration and mean channel open time at -125 mV (■), -155 mV (▲) and -185 mV (●) are shown on the right. The inset in B describes the relation between different rate constants and the transmembrane voltage.

(Fig. 3). When the drug concentration was increased, up to 50 μM, mean burst times (τ_b) were prolonged without altering the total open time per burst. The single exponential distribution of open and burst times observed under control conditions was maintained with all of the concentrations tested, indicating the existence of only one open state. At -120 mV holding potential, the mean open times (τ_o) were decreased from 11.5 ms (ACh 0.4 μM) to 1.8 ms (ACh 0.4 μM plus neostigmine 10 μM). The shortening of these intraburst openings was strongly voltage-dependent, such that hyperpolarization produced a greater blockade of the ACh-activated currents.

Linear concentration-dependence on the reciprocal of the mean channel open time is predicted by the sequential model and is expressed in the first order equation $1/\tau_o = k_{-2} + k_3$ [D]. Under control conditions, k_{-2} (see inset of Fig. 3) τ_o, and the mean burst times (τ_b) of ACh-activated channels disclosed a steep dependence on voltage, reflecting the voltage dependence of the closing rate constant. In the presence of D, the voltage-dependence of τ_o depends upon the contribution of k_{-2} and k_3, which have opposing voltage sensitivities, the latter amplified by the concentration of D (neostigmine or other blocker). Accordingly, a gradual loss of the voltage dependence of τ_o observed under control conditions and even a reversal of the sign of the slope were observed as the neostigmine concentration increased (Fig. 3). A linear relationship between $1/\tau_o$ and concentration of the blocking agent at various holding potentials was observed in the presence of neostigmine up to 50

TABLE 2   Blocking kinetics of the reversible AChE inhibitors at the ion channels activated by ACh [a]

Drug	k_3 $(\text{ms}^{-1}\,\mu\text{M}^{-1})$	k_{-3} (ms^{-1})	K_d (μM)
(−)-Physostigmine [b]	0.015	about 4.0	–
(+)-Physostigmine [c]	0.015 (287) [d]	–	–
Neostigmine	0.047 (165)	2.0 (79)	42.5 (50)
Edrophonium	0.056 (190)	2.1 (75)	37.5 (50)
Pyridostigmine	0.172 (92)	2.4 (85)	13.0 (46)

[a] The currents were activated by ACh (0.4 μM) in the presence of carbamates. Data obtained at holding potential of − 125 mV.
[b] From Shaw et al. [18]. k_3 value was determined from EPC data.
[c] (+)-Physostigmine produced very stable blockade, thus preventing the discrimination between the blocked state and other closed states.
[d] Numbers in parentheses are the voltage variation (mV) that produces an e-fold change.

μM (Fig. 3). From the slopes of these linear plots obtained for various holding potentials, the forward blocking rate, k_3, was calculated and its voltage dependence was determined (inset of Fig. 3 and Table 2). Above 50 μM concentration, the linearity was no longer observed and τ_b instead of being increased, became shorter, departing from the predictions of the sequential model.

Bursting-type activity generated total closed time histograms with two distinct populations of shut times, a fast component corresponding to the numerous brief intraburst closures and a slow component representing the duration of the nonconducting states before channel opening (R and A_nR). The intraburst fast closures were interpreted as the duration of the channel blocked state (A_nR^*D). As was pointed out before, according to the sequential model, the AChR escapes from its blocked state only through blocked-open transition described by the rate constant k_{-3}. Values of k_{-3} can be experimentally determined from the reciprocal of the mean blocked times (time constant of the fast component, τ_f). As expected if the binding site for blocking agent is within the electric field of the membrane, k_3 as well as k_{-3} each had exponential but opposite voltage dependencies, k_{-3} values decreasing with membrane hyperpolarization. In contrast to τ_o, no significant change of τ_f values was observed with increased neostigmine concentration, in agreement with the predictions of the model used. The values of k_{-3} determined from the reciprocal of τ_f, and its voltage sensitivity are shown in the inset of Fig. 3 and Table 2.

Edrophonium and pyridostigmine   Both of the drugs produced bursting-type channel activity similar to neostigmine when present along with ACh in the patch pipette (Figs. 4 and 5). Concentration- and voltage-dependent shortening of the intraburst openings followed the predictions of the sequential model up to 25 μM pyridostigmine and up to 50 μM edrophonium (Figs. 4, 5). Determination of k_{-3} from blocked times at various holding potentials showed that compared to neostigmine and edrophonium, the unblocking rate was higher for pyridostigmine. The lower conductance observed with high concentrations of pyridostigmine and edrophonium could be attributed to marked shortening of the intraburst openings which became too brief to be recorded at a filter bandwidth of 3 kHz. For open channel blockade, the presence of a charged head is sufficient for the interaction
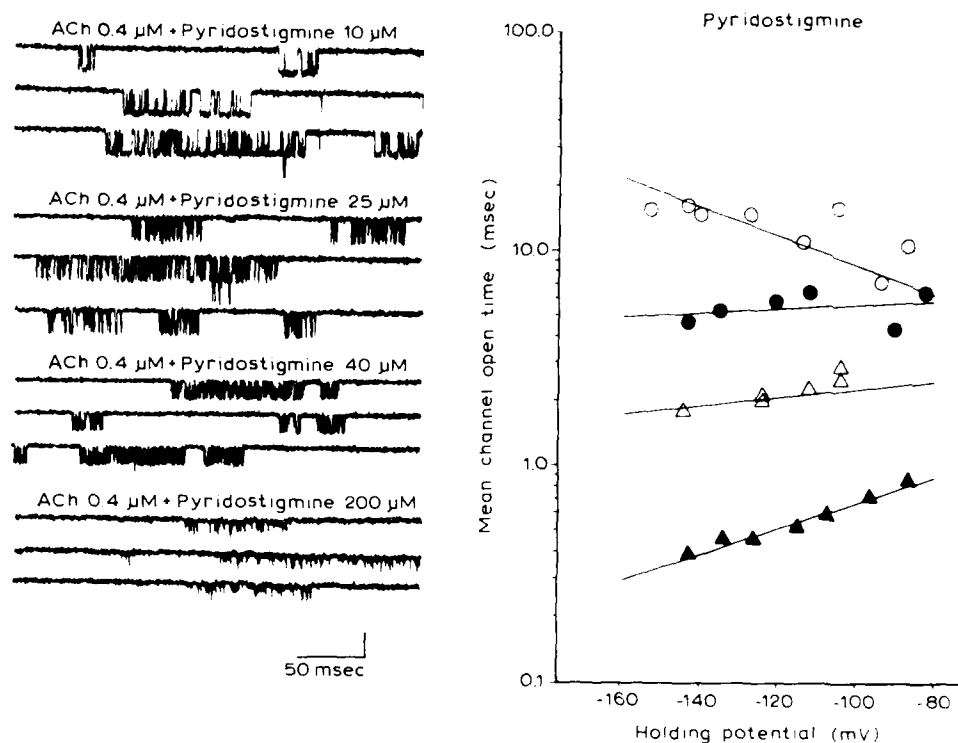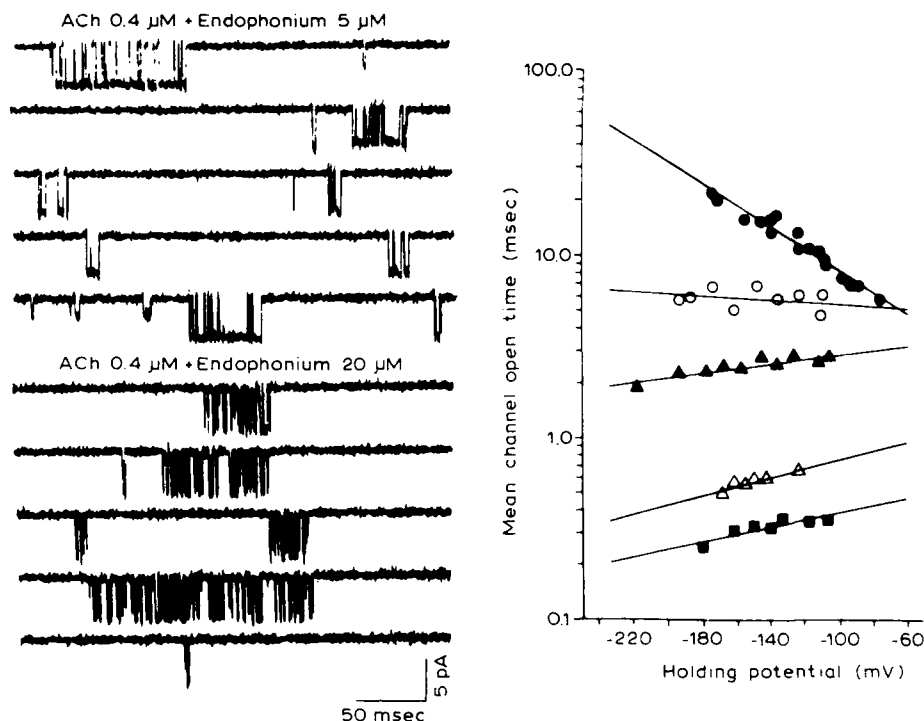
FIG 4 Samples of ACh-activated channel currents in the presence of different concentrations of pyridostigmine are shown on the left. The voltage dependence of mean channel open times under control condition (○), and in presence of 2 μM (●), 10 μM (△) and 25 μM (▲) of pyridostigmine is shown on the right.

with the ion channel site, and the additional presence of a hydrogen bond does not enhance the blocking rate or further stabilize the blocked state. Experimental support was given by edrophonium and neostigmine studies, which provided similar k_3, k_{-3} and K_d values and voltage sensitivity for both compounds (Table 2).

(+)-vs (−)-Physostigmine

Agonist property Both enantiomers of physostigmine activated channel openings, and a moderate degree of stereoselectivity was observed between them for the ACh recognition site of the muscle AChR. The (+) isomer was found to be approximately 10-times less potent than the (−) form of physostigmine for the agonistic property in contrast to a 40-fold potency ratio for inhibition of muscle AChE (Table 1). In contrast to the (−) isomer which produces many fast flickers during the open state [18], (+)-physostigmine-activated currents were square-wave pulses with few flickers similar to those induced by ACh. However, the mean channel open time was much shorter than that of channels activated by ACh. At − 140 mV holding potential, mean channel open time was 5.2 ms for (+)-physostigmine (10 μM) and 13 ms for ACh (0.4 μM)-activated channels. Increasing the concentrations of the

358

ACh 0.4 μM + Endophonium 5 μM

ACh 0.4 μM + Endophonium 20 μM

50 msec

5 pA

Mean channel open time (msec)

100.0

10.0

1.0

0.1

-220   -180   -140   -100   -60

Holding potential (mV)

FIG 5   Samples of ACh-activated channel currents in the presence of different concentrations of edrophonium are shown on the left. The voltage dependence of mean channel open times under control conditions (●), and in presence of 1 μM (○), 5 μM (▲), 20 μM (△) and 50 μM (■) of edrophonium is shown on the right.

(+)-physostigmine yielded shorter and well separated currents indicating that this carbamate produced a stable blockade of the open state of the channels at the same concentrations that caused activation. The analysis of the open times using the sequential model described earlier disclosed a reduction of the open-state duration that was linearly related to drug concentration. A gradual change in the voltage dependence of the mean open times was observed upon increasing drug concentration, thus fulfilling the model's prediction.

Blockade of ACh-activated channel currents   At the macroscopic current level, blockade of the open conformation did not display clear stereospecificity with physostigmine isomers, nor has it with other enantiomeric pairs which have been tested [30,31]. However, at the elementary current level, differences in the kinetics of the blocking reaction could be discerned. (+)-Physostigmine produced stable blockade so that bursts could no longer be distinguished as such. On the other hand, (−)-physostigmine induced bursts composed of very fast flickers that could not be well resolved at the filtering bandwidth of the recording system. (+)-Physostigmine when applied together with ACh (0.4 μM) through the patch micropipette at concentrations ranging from 1 to 50 μM decreased channel open time (Fig. 6). The open time histogram showed a single exponential distribution with τ_0 shorter than

ACh 0.4 µM + (+)Physostigmine 5 µM

ACh 0.4 µM + (+)Physostigmine 20 µM

25 msec $\overline{\qquad}$ 3 pA
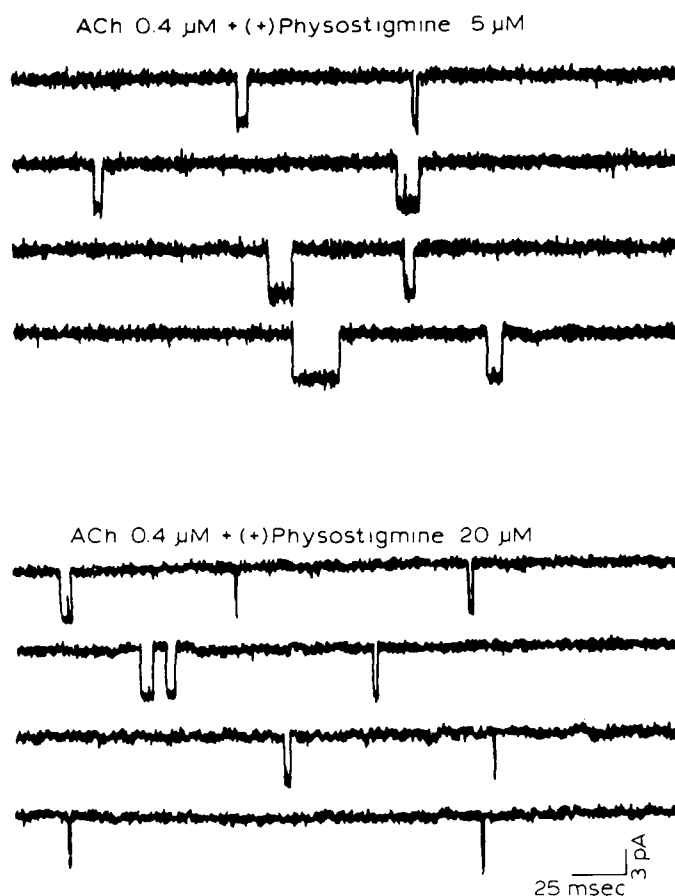
FIG 6   Samples of ACh-activated channel currents in the presence of (+)-physostigmine.

that produced by ACh, as expected for a very slowly reversible open channel blockade. The strong voltage-dependence of τ_0 seen under control conditions was gradually reduced with increasing (+)-physostigmine concentrations. The exponential but opposite dependence of k_3 on membrane potential (Table 2) compared to k_{-3} accounted for the gradual loss of voltage dependence of τ_0 observed as the concentration of the blocker was increased. Indeed, at concentrations higher than 50 µM an inversion in the sign of the voltage dependence in relation to control condition was seen. The slow unblocking reaction in the case of (+)-physostigmine precluded distinction of the blocked state from the other closed states and the calculation of k_{-3} values.

The reversible cholinesterase inhibitors used in this study exhibited a varying degree of agonistic and blocking properties at the AChR without affecting single channel conductance. Among these drugs, (−)-physostigmine showed the greatest agonistic potency, pyridostigmine had the highest blocking rate, and (+)-physostigmine had the lowest unblocking rate (Tables 1 and 2).

Protection against OPS: AChE inhibition vs AChR interactions

In vivo protection afforded by reversible AChE inhibitors
Comparative study of the effectiveness of (+)- and (−)-physostigmine, neostigmine or pyridostigmine treatment prior to a sarin challenge (0.13 mg/kg, a dose producing 100% lethality) showed that (−)-physostigmine was by far the most effective in preventing OP-induced mortality [4]. As seen in Table 3, addition of neostigmine (0.2 mg/kg) to the pretreatment regimen containing atropine (0.5 mg/kg) protected only 12% of the animals. Pyridostigmine, even at a higher dose of 0.8 mg/kg did not protect more than 28% of the rats. On the other hand, (−)-physostigmine at a dose of 0.1 mg/kg protected 100% of the animals against one lethal dose of sarin. (+)-Physostigmine (0.1–0.5 mg/kg), though devoid of significant anti-AChE activity, also afforded significant protection to animals exposed to a lethal dose of sarin as seen in Table 3.

We tested whether the addition of a ganglionic blocker such as mecamylamine and chlorisondamine [6] to the pretreatment regimen with (−)-physostigmine (0.1 mg/kg) and atropine (0.5 mg/kg) would afford extra protection to rats exposed to multiple lethal doses of VX (0.05 mg/kg; $LD_{100} = 0.015$ mg/kg). The ganglionic and muscarinic blockers alone did not protect the animals (data not shown). On the other hand, coadministration of (−)-physostigmine and ganglion blocking agents prior to VX exposure, protected all the animals (Table 4). It should be noted that mecamylamine, at the muscle nicotinic AChR, acts as a noncompetitive drug, blocking the ion channels in the open conformation [32]. Preliminary tests with another open channel blocker with free access to the central nervous system reinforced the findings with mecamylamine. Amantadine, an antiviral agent used clinically to relieve the symptoms of Parkinson's disease, significantly potentiated (−)-physostigmine's actions against OP lethal effects (see Table 4; Deshpande and Albuquerque, unpublished results). Therefore, antagonism at agonist receptor and ion channel sites, yielding a reduction of nicotinic hyperactivation, seems to play an important role in the effectiveness of a prophylactic drug regimen against OPs.

Protection by carbamates against myopathic damage induced by sarin
Exposure of the animals to carbamates alone produces myopathic lesions which differ in features and degree depending on which carbamate is applied. Among the carbamates, (−)-physostigmine and especially its (+) isomer induced the least

TABLE 3 Potency of carbamates in protecting animals exposed to a lethal dose of sarin

Pretreatment regimen [a]	Carbamate dose (mg/kg)	Lethality [b] %
None	−	100
(−)-Physostigmine	0.1	0
(+)-Physostigmine	0.5	13
Neostigmine	0.2	88
Pyridostigmine	0.8	72

[a] The pretreatment regimen contained atropine 0.5 mg/kg and was injected 30 min prior to injection of a lethal dose (0.13 mg/kg) of sarin.
[b] For lethality records, the animals were observed for 24 h.

TABLE 4 Potentiation of the protection in rats afforded by (−)-physostigmine by inclusion of open channel blockers

Pretreatment regimen and dose (mg/kg)		OP [a] (mg/kg)	Lethality [b] (%)
Sarin [c]			
(−)-Physostigmine	0.1	0.13	4
(−)-Physostigmine	0.1	0.65	100
(−)-Physostigmine	0.1		
+ mecamylamine	8.0	0.65	56
VX [c]			
(−)-Physostigmine	0.1	0.05	50
(−)-Physostigmine	0.1		
+ mecamylamine	4.0	0.05	0
(−)-Physostigmine	0.1		
+ chlorisondamine	2.0	0.05	0
Tabun [d]			
(−)-Physostigmine [d]	0.1	0.6	50
Amantadine	20.0	0.6	100
(−)-Physostigmine	0.1		
+ amantadine	20.0	0.6	17

[a] Without any pretreatment, sarin, VX and tabun at all doses shown produced 100% lethality.

[b] The lethality was based on 24-h observation in at least 6 rats per group.

[c] Pretreatment drugs were administered i.m. 30 min prior to subcutaneous injection of OP agents. For Sarin and VX, the pretreatment regimen also included 0.5 mg/kg atropine.

[d] In rats receiving tabun, atropine (5 mg/kg) was injected (i.m.) immediately after the injection of OP agent. This dose of atropine alone did not protect the animals.

damage to the neuromuscular junction. After 1-h exposure of the animals to (+)-physostigmine (0.3 mg/kg), the profiles of most soleus muscle endplates examined looked intact (see Fig. 2 from Ref. 5). (−)-Physostigmine (0.1 mg/kg) induced irregularities of the subjunctional sarcomere band patterns as well as of the junctional contour space in 25% of the endplates examined (see Fig. 3 from Ref. 5).

Neostigmine and pyridostigmine were most toxic and most ineffective in protecting animals against OP poisoning. For example, chronic applications of pyridostigmine induced alterations similar to those produced by a single, large dose of an irreversible anti-AChE agent such as sarin [8]. In vitro experiments showed that, in comparison to (−)-physostigmine, exposure of the muscles to neostigmine with or without nerve stimulation (i.e. spontaneous or evoked ACh release), produced much greater myopathic alterations as disclosed by light and electron microscopic analysis [9].

Whereas a sublethal dose (0.08 mg/kg) of sarin produced a severe and extensive loss of band pattern, vacuolation and supercontracture of the subjunctional area, damage to numerous fibers and infiltration of phagocytes, the muscles from rats pretreated with (−)-physostigmine and injected with a lethal dose (0.13 mg/kg) of sarin showed a dramatic reduction in the severity and the extent of postjunctional damage. Although higher doses of (+)-physostigmine were necessary, the EM and morphometric data showed that the degree of protection afforded by (+)-physostigmine was similar to that observed with (−)-physostigmine.

Correlation of in vivo and in vitro toxicity with mechanisms of interactions with AChR and their relevance to the antidotal efficacy

The following conclusions emerge from the results on whole animal, electron micrographic, and electrophysiological studies.

(1) Reversible AChE inhibition by carbamates and related compounds produced various levels of morphological damage and whole animal toxicity. Morphological alterations by either (+)- or (−)-physostigmine alone were minimal and were not related to AChE inhibition.

(2) The AChE hypothesis is weakened by the findings that neostigmine and pyridostigmine (quaternary amines), which though producing similar AChE inhibition at concentrations used in our protection studies, caused a higher degree of myopathy than (−)-physostigmine. The effect of excessive cholinergic hyperactivation induced by AChE inhibition at nicotinic synapses is most likely counteracted by mechanisms involving blockade of AChR conductance by carbamates.

(3) Carbamates are more effective antidotes when prophylactically applied. Experiments using equipotent AChE-inhibitory doses (IC_{50}) of carbamates exhibited differential antidotal efficacy against OPs, suggesting the involvement of mechanisms other than through AChE system.

(4) Electrophysiological studies showed that all of the reversible AChE inhibitors exhibit direct and multiple interactions with the nicotinic AChR. Comparatively, among carbamates tested in our studies, (−)- as well as (+)-physostigmine were most effective in reducing the endplate conductance, as shown by the drastic reduction of the EPC peak amplitude and shortening of EPC decay time constant. Mechanisms involving various sites on the postsynaptic AChR may also contribute to this reduction. Significant interaction of (−)-physostigmine with the agonist recognition site, as indicated by its ability to act as an agonist combined with its powerful capability to block channels activated by the neurotransmitter are mechanisms responsible for the reduced toxicity and high protection offered against OPs. Furthermore, the additional reduction in endplate conductance can be afforded by AChR desensitization.

(5) Although neostigmine, pyridostigmine, and edrophonium acted as open channel blockers, they did not decrease endplate conductance as disclosed by the lack of change in frequency of openings and total current per opening. These drugs induced longer bursts as concentrations increased.

(6) Assuming that better protection against OPs can be achieved by using effective channel blockers of AChR, one can explain the enhancement of the prophylactic potency when an open channel blocker such as mecamylamine or chlorisondamine was added to the (−)-physostigmine regimen [6]. In addition, these ganglion blockers can pass the blood-brain barrier, ensuring better protection at central nicotinic synapses.

(7) These findings strengthen the hypothesis that AChR mechanisms play a significant role in the antagonism of toxicity of OP agents. A similar hypothesis can be extended to oxime-OP antagonism as shown below.

Oximes: activation and inhibition of AChR

Increase in AChR activation

Oximes, especially 2-PAM, produced an excitatory effect at the macroscopic level revealed by increases in twitch tension and in the peak amplitude and decay time constant of EPCs. Similar facilitatory effects were also suggested by others for 2-PAM and for obidoxime [33,34] based on studies on EPPs and ACh-induced endplate depolarization. Although pre- or postsynaptic mechanisms could underlie facilitation [35,36], presynaptic effects were ruled out because no changes in either MEPP frequency or quantal release were observed. AChE inhibition was not adequate to explain the facilitatory effects, since EPC amplitude and τ_{EPC} were increased at concentrations that had no anti-AChE activity. Single channel studies revealed an alternative mechanism to explain the facilitatory effects of the oximes [11]. One of the most striking effects observed with 2-PAM (10–200 μM) is a distinct concentration-dependent increase in the frequency of bursts activated by ACh (0.4 μM). This effect was more pronounced with 2-PAM than with HI-6. The increase in AChR activation produced by these drugs could have contributed to the facilitation of amplitude of EPC and twitch, since all of the three effects also occurred at a concentration range which had a minimal AChE-inhibitory effect.

To study the nature of the increase in the burst activation produced by the oximes, and determine whether or not it was related to an alteration in the desensitization process, single channel currents were recorded for a long time at a fixed pipette potential after establishing the seals. Under control conditions using
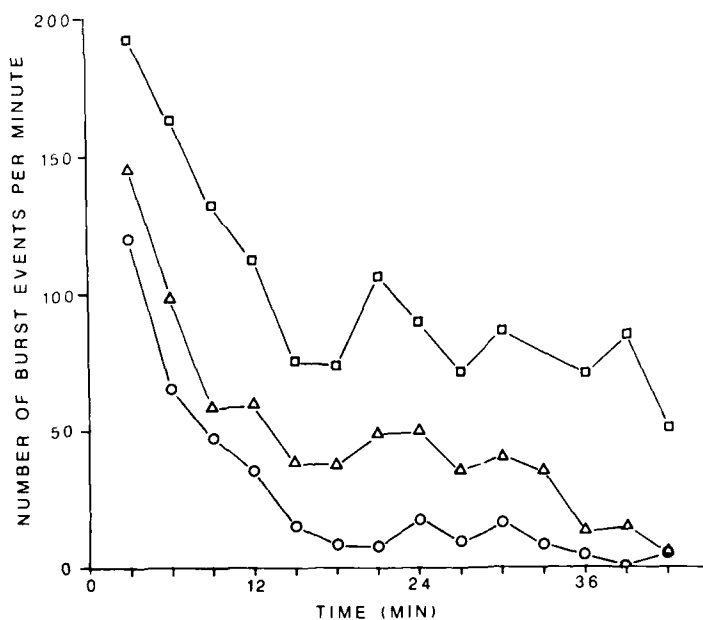
FIG 7 Effect of 2-PAM on the frequency of ACh-activated channel currents. Each point represents the mean number of bursts per min (calculated every 3 min) as recorded from 3 fibres in each case. Control (o) and 1 μm ($\triangle$) and 50 μM ($\square$) of 2-PAM are shown. Holding potentials of all patches included here range from -150 to -160 mV.

0.4 μM ACh in the patch pipette, the frequency of bursts declined during the 40-min observation period (Fig. 7) which indicated the occurrence of a slow desensitization of the AChRs. When 2-PAM was added to the pipette at 1 and 50 μM along with ACh, the frequency curve was shifted to higher values whereas the same slope was maintained (Fig. 7). Since plots of frequency for control and drug were shown to be roughly parallel (Fig. 7), the effects of the drug on frequency appear to be time-independent. The increase in frequency was also observed in patches where a higher ACh concentration (4 μM instead of 400 nM) was tested.

Earlier electrophysiological data have identified the existence of a desensitization process which reportedly occurred on a millisecond time-scale [37]. However, the occurrence of a fast desensitization step would be easily missed in single channel recordings, which usually are done at least 30 s after achieving the gigaohm seal. Therefore, the recordings obtained in the presence of low concentrations of ACh alone may represent the activity of receptors which escaped a fast desensitization action of the agonist. The increased channel activity observed in the presence of the oximes, could therefore be attributed to the ability of these compounds to arrest fast component of desensitization (ms time-scale). On the other hand, the frequency pattern in the presence of 2-PAM showed a slow decline from the initial higher level with a rate similar to that seen under control conditions. This would imply that the 2-PAM was unable to prevent the slow desensitization occurring on a minute time-scale.

Inhibitory actions of oximes

Kinetics of blockade of channels activated by ACh The nature and kinetics of AChR blockade were investigated at the single channel current level. 2-PAM (10 to 200 μM) and HI-6 (1 to 50 μM) when added to ACh solution induced openings in bursts. Typical tracings of currents activated by ACh in the presence of 2-PAM and HI-6 are shown in Fig. 8. Unlike that seen in the control condition, the noise level during the open state appeared broader than during the closed state in the presence of 2-PAM. Flickering of open channels presumably due to very fast blocking and unblocking reactions has contributed to this phenomenon. The inadequate recording and digitization of the very fast events during a burst were also responsible for an apparent decrease in the single channel conductance observed with higher concentrations (> 100 μM) of 2-PAM or HI-6.

The analysis of the channel opening kinetics showed that both oximes caused a concentration- and voltage-dependent reduction of mean open time. At low concentrations, the blocking effects of the oximes were only observed at holding potentials more negative than − 100 mV while at the highest concentration used the effect was seen even at less negative potentials such at − 7 mV. The decrease in mean channel open time was brought about by increased flickering during the open state and was dependent on drug concentration and voltage. However, higher concentrations of the oximes, particularly HI-6 tended to decrease the number of flickers at very negative potentials in association with shortening of the burst duration.

The histograms of the channel open times showed a single exponential distribution in the presence of oximes. The relationship between the concentration of the oximes and the reciprocal of mean open time was found to be linear (Fig. 9). However, at higher concentrations of 2-PAM (200 μM), this linearity was no longer observed.

2-PAM 50 µM +ACh 400 nM   HI-6 50 µM +ACh 400 nM
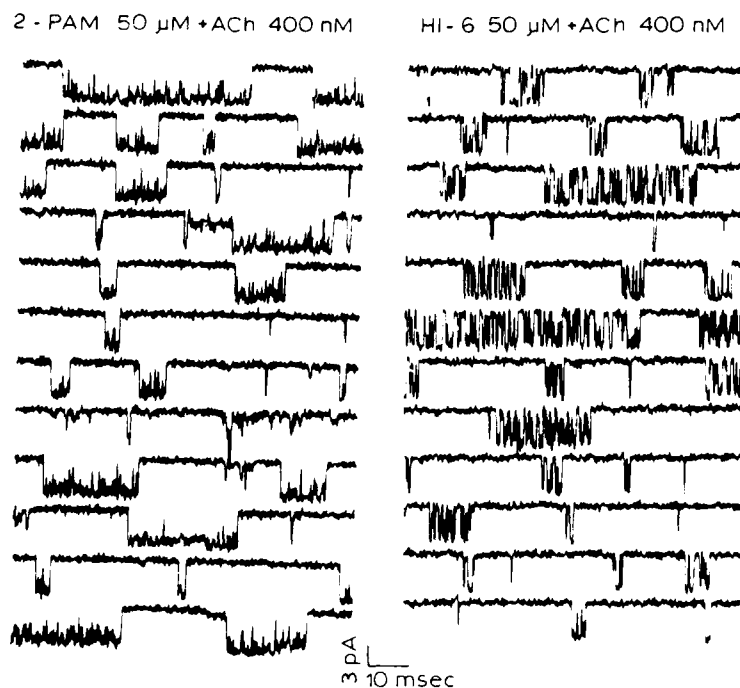
FIG 8   Samples of ACh-activated channel currents in the presence of 2-PAM and HI-6.

The sequential model for open channel blockade described earlier was used to explain the effects of the oximes on the kinetic properties of nicotinic AChR-ion channels during activation. The k_3 (s^{-1} M^{-1}) values were found to be 0.59×10^7 and 2.39×10^7, for 2-PAM and HI-6, respectively, at -140 mV holding potential. These values increased exponentially with hyperpolarization. Unlike $(-)$-physos-
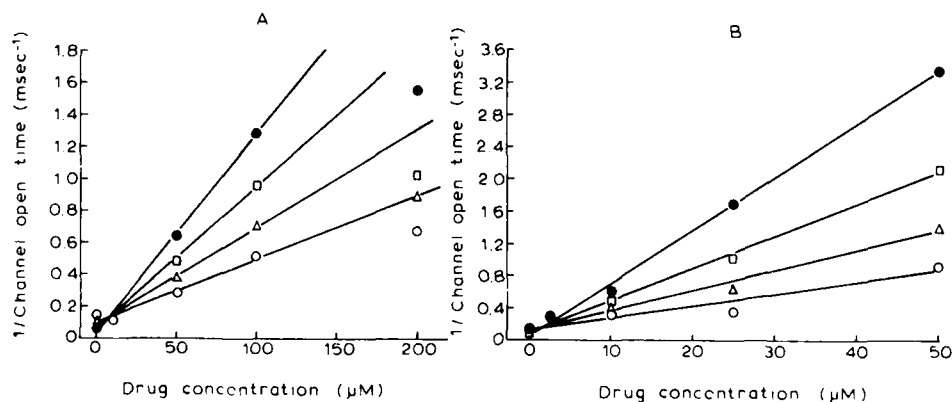
FIG 9   Relation between drug concentration and the reciprocal of mean open time at -120 ($\bigcirc$), -140 ($\triangle$), -160 ($\square$) and -180 ($\bullet$) mV in the presence of 2-PAM (A) and HI-6 (B).
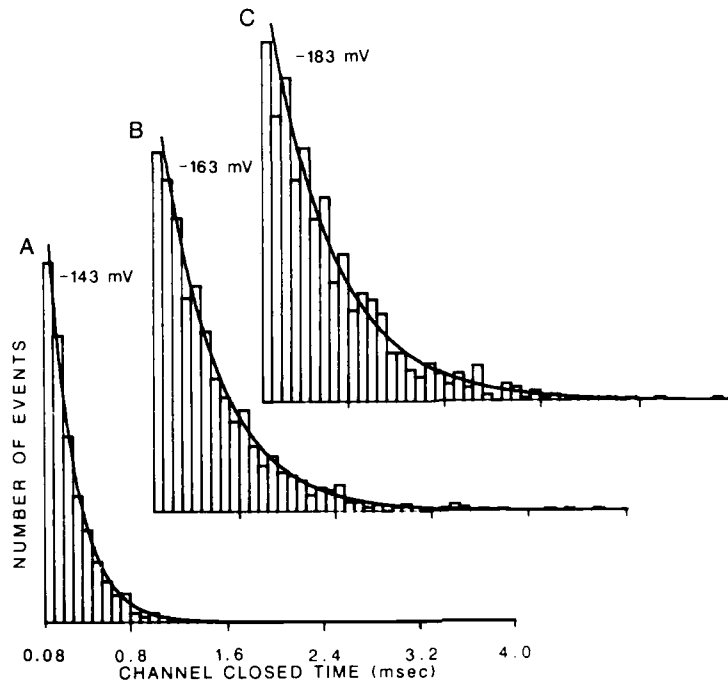
FIG 10 Intraburst closed time histograms of channels activated by ACh in the presence of 50 μM of HI-6 at −143 (A, 1031 events), −163 (B, 1023 events) and −183 (C, 824 events) mV holding potential from a single fibre. The mean channel closed time as determined from the fit of the distribution to a single exponential function (correlation > 0.97) is: 0.221 (A), 0.454 (B) and 0.538 (C) ms.

tigmine [18] and QX-222 [28], the channel open time was reduced with a slightly greater voltage sensitivity so that the k_3 values changed an e-fold per 52 mV and 40 mV for 2-PAM and HI-6, respectively. The voltage sensitivity of k_3 for the oximes was also greater when compared to that seen with other carbamates (see Table 2).

Analysis of the distributions of closed intervals obtained under control condition and in the presence of the two oximes revealed that they were best fitted by the sum of two exponential functions. As illustrated in Fig. 10, the numerous fast closed times showed only a single exponential distribution. The fit to an exponential function provided a mean of about 130 μs in the case of 2-PAM, and it was neither concentration- nor potential-dependent. In the case of HI-6, the mean fast closed intervals increased in duration with hyperpolarization of the patched membrane (Fig. 10) and it was concentration independent at a range of 2.5 to 25 μM. The backward rate constant, k_{-3}, for the blocking reaction of 2-PAM and HI-6 (up to 25 μM) is given in Table 5.

From values and voltage dependence of k_3 and k_{-3}, one can calculate the equilibrium dissociation constant (K_d) and estimate the affinity and the location of the binding site. As shown in Table 5, compared to AChE inhibitors such as neostigmine and edrophonium [3] and the local anesthetic QX-222 [28], high K_d values were obtained for these oximes (millimolar for 2-PAM and hundreds of

TABLE 5 Channel blocking kinetics by oximes

Holding Potential (mV)	2-PAM			HI-6		
	k_3 $(s^{-1} M^{-1}$ $10^6)$	k_{-3} $(s^{-1}$ $10^3)$	K_d (M $10^{-3})$	k_3 $(s^{-1} M^{-1}$ $10^6)$	k_{-3} $(s^{-1}$ $10^3)$	K_d (M $10^{-3})$
−120	4.013 [a]	7.75 [b]	1.987	14.49 [a]	7.14 [b]	0.499
−140	5.910	7.75	1.270	23.97	5.00	0.204
−160	8.705	7.75	0.870	39.63	3.59	0.091
1/slope (mV)	52 [c]	—	52	40	58	24

[a] k_3 values calculated from the slope of linear regression plot of drug concentration vs reciprocal of mean open time.
[b] k_{-3} was calculated from the reciprocal of pooled mean fast closed intervals obtained at all membrane potentials and at all concentrations in the case of 2-PAM. In the HI-6 group, for each potential the data were obtained from the best fit line of semilog plot of membrane potential versus 1/fast closed time up to 25 μM.
[c] Numbers represent voltage variation that produces an e-fold change.

micromolar range for HI-6, at −120 mV) suggesting that they bind to low-affinity sites in the ion channel of the receptor. The K_d of HI-6 changed e-fold for a change of 24 mV. In the case of 2-PAM, 52 mV were necessary for a similar change. Previous work has shown that the voltage dependence of K_d can be described by the Boltzmann distribution [28,29,38] such that the exponent of the above equation should be, $-ze\delta V/kT$ where ze is the charge of the drug, δ is the fraction of the membrane potential sensed by the ion as it reaches its binding site, V is the holding membrane potential, k is the Boltzmann constant and T is the absolute temperature. Values of 0.47 and 0.51 were found for 2-PAM and HI-6, respectively, which indicate that for a constant membrane field, the binding site would be roughly halfway across the membrane. Similar locations were estimated for the neostigmine and edrophonium binding sites [3].

The linear increase in the reciprocal of mean open time with drug concentration in the case of 2-PAM (up to 100 μM) and HI-6 (up to 50 μM) and an increase in the mean intraburst closed time with hyperpolarization in the case of HI-6 are points in favour of the sequential model of channel blockade for these drugs. However, some deviations from the expectations of the sequential model [28] have also been found in the case of oximes. For example, the above model requires that the total time the channel spends in the conducting state should remain constant in the absence and presence of drugs. Though less pronounced than the effects on the individual intraburst open times, the analysis showed that the total open time in a burst (i.e., the total ion conducting period during the burst) (Fig. 11) and also the burst times were decreased by the oximes in a concentration- and voltage-dependent manner. This departure from the sequential model observed with most of the doses of the oximes and potentials tested was not seen with other blocking agents such as QX-222 (up to 40 μM) which induced an increased mean burst duration [28]. Thus it becomes apparent that alternative mechanisms are needed to explain the kinetic reactions of oximes with the AChR.

The following alternative routes could be considered: (i) a new stable conformational state can be reached either directly from the open $(A_n R^*)$ or from the previously existing blocked state $(A_n R^* D)$; (ii) $A_n R^* D$ goes to another closed state
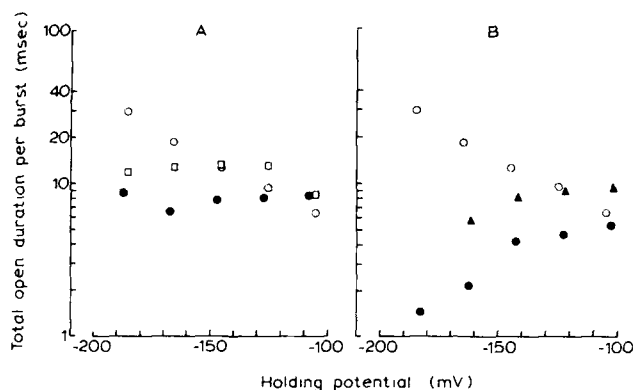
FIG 11   Effect of oximes on the total open time per burst. Control (○ in both A and B), and in the presence of 50 (□), 100 (●) μM of 2-PAM (A) and 25 (▲), 50 (●) μM of HI-6.

($A_n RD$ or $A_n R$ or R), bypassing the open state ($A_n R^*$) or (iii) the oximes alter the rate constants for channel closing (k_{-2}). The first possibility predicts that more than one blocked state should be identified in the distribution of the closed intervals. However our closed time distributions showed two exponentials, one showing the distribution of the short intervals (representing the blocked state) and another showing the long interval (representing the gaps between different channel activation). As seen in Fig. 10, no evidence for a new distribution in the closed time histograms could be found. If a stable blocked state exists it cannot be clearly delineated from the long closed intervals (i.e., the intervals between individual channel activation). The possibility that $A_n R^* D$ goes to a closed state directly, bypassing the open state $A_n R^*$, thereby causing a reduction in the mean burst and mean total open time, cannot be eliminated from any evidence from the current data. Our data may suggest but do not prove that there is a change in the channel closing rate in the presence of oximes. Reduction in the total open time per burst compared to control, as seen with the oximes, could be interpreted as an increase in k_{-2}.

AChE-like and AChE-inhibitory effect of oximes

It is possible that the hydrolytic reaction reported between hydroxylamine and acetylthiocholine can result in an AChE-type activity which can be extended to the oximes 2-PAM and HI-6. At concentrations higher than 10 μM, 2-PAM and HI-6 interfered with the assay of AChE activity by hydrolysing the substrate (acetylthicholine) themselves. In this respect, 2-PAM was 2–2.5-times more potent than HI-6 (Table 6). The AChE-like reaction could occur between the neurotransmitter and the oximes studied here. The implications of this type of reaction on the antidotal efficacy of oximes against OP are discussed below. On the other hand, the oximes exhibited some inhibitory effect on the AChE activity. The values shown in Table 6 indicate that 2-PAM has a greater inhibitory effect on AChE than HI-6. The weak AChE-inhibitory effects of 2-PAM and HI-6 may be of no significance under conditions of OP poisoning, where maximal inhibition of the enzyme is already present.

TABLE 6 Chemical interaction of oximes with acetylthiocholine (ATC) and effect on AChE activity

Concen-tration (μM)	Rate of ATC breakdown (μM/min)		% AChE inhibition [a]	
	2-PAM	HI-6	2-PAM	HI-6
10	–	–	10.7 [b]	7.1
50	1.08	0.41	24.6	–
100	2.02	0.92	30.7	6.2
200	4.78	1.90	60.7	18.0

[a] All the activity of AChE was measured from sartorius muscle extract.
[b] Each number refers to the mean of 2 to 3 determinations from homogenates of 9 different muscles.

Correlation of actions of oximes and their antidotal potency

The present study indicated that reactivation of the phosphorylated AChE by itself is not adequate to explain the effectiveness of oximes against OP poisoning. Many lines of evidence from this study support this hypothesis.

(1) Specificity of oximes against OPs regardless of their AChE reactivation potency (Table 7): against tabun, we have observed that in spite of very weak reactivation of AChE activity (less than 5%), 2-PAM was able to produce complete recovery of muscle function (twitch and tetanic tension). On the other hand, HI-6 (in general a more potent antidote) failed to affect the blockade of tetanic tension after exposure

TABLE 7 Effects of 2-PAM and HI-6 on the recovery of muscle function depressed by lethal doses OP agents [a]

OP agent and dose (μM)	Condition	Twitch tension	Tetanus tension 50 Hz	Tetanus sustaining ability	AChE activity
None	control	100	100	100	100
Soman	15-min exposure	51	13	12	4
(0.2)	3-h wash	108	56	6	7
2-PAM [b]		93	54	0	18
HI-6		108	64	100	21
Tabun	15-min exposure	59	15	0	6
(0.4)	3-h wash	67	42	5	21
2-PAM		92	74	100	6
HI-6		136	53	2	21
VX	15-min exposure	33	8	0	4
(0.2)	3-h wash	44	61	96	29
2-PAM		75	98	99	70
HI-6		63	95	100	100
Sarin	15-min exposure	57	15	3	4
(0.4)	3-h wash	83	106	100	37
2-PAM		81	55	86	50
HI-6		76	96	99	100

[a] Results are expressed as percentage of control values.
[b] Muscles were treated with 2-PAM (0.1 mM) or HI-6 (0.1 mM) for 1 h after 15-min exposure of OP and removal of its excess.

to tabun. Furthermore, in these muscles the level of AChE activity level after HI-6 was higher than that provided by 2-PAM. Sarin- and VX-induced depression in muscle function was fully recovered by both 2-PAM and HI-6. HI-6 could recover 100% of the enzyme activity inhibited by sarin or VX but usually 20% of AChE activity was observed in soman- and tabun-poisoned muscles. The degree of reversibility of both AChE activity and muscle function by oximes is directly related to each OP; however, these two parameters are not necessarily linked.

(2) An AChE-like reaction reported between 2-PAM or HI-6 and acetylthiocholine (Table 6) could also be predicted for the neurotransmitter ACh. Such a reaction although of little significance under normal conditions, could in fact play an important role under conditions of OP-poisoning where it would be beneficial to hydrolyse part of the excess ACh at the synaptic cleft.

(3) Possible role of AChR activation in the antidotal efficacy of oximes: 2-PAM and to a lesser extent HI-6 induced an increase in the AChR-channel opening probability, i.e., an excitatory action at the receptors. The increase in the channel activation in the presence of oximes could be of significant value in reversing the function of OP-poisoned endplates towards normalcy especially in the late stages of the OP poisoning where the desensitizing states of the nicotinic AChR may be prevailing. Desensitization of the AChR in its various phases or types could be caused not only by ACh accumulation, but also by direct effects of OPs on these receptors, or by both [39]. In fact, recent biochemical evidence suggests that diisopropylfluorophosphate could cause desensitization of the AChR through binding to a site at the receptor which is different from the agonist-recognition or high-affinity noncompetitive sites [40]. The channel activation produced by the oximes could therefore counteract the effect of OPs and restore the normal neuromuscular function.

(4) Reversible blockade of AChR-channels vs antidotal efficacy: 2-PAM and HI-6 produce significant blockade of the channels activated by the neurotransmitter. The blockade of the open conformation occurs through reversible reaction. This action, combined with the property of the oximes to increase AChR activation, via mechanisms discussed above, may release significant number of AChRs from the desensitizing states.

(5) Studies on a bispyridinium compound, SAD-128, have further reinforced the AChR vs AChE hypothesis. The more striking feature of this compound is that it does not carry an oxime moiety. SAD-128 has been reported to be effective in protecting animals against soman-poisoning [12]. The electrophysiological studies have shown a marked blockade of the channels activated by ACh. Comparative analysis showed that SAD-128 produced a more stable blocking state than HI-6 and induced long-lasting bursts, consequently a double exponential decay of the EPCs elicited by nerve stimulation [41].

Conclusions

The present study provides new insights into the molecular mechanisms underlying the antidotal efficacy of carbamates and oximes against OP poisoning. The AChR

was found to be significantly affected by these drugs in a manner consistent with their antidotal potency. The effect on AChE appears not to be a primary mechanism in the therapeutic actions of carbamates and oximes in OP poisoning. The AChR-channel blocking property appears to be the pivotal mechanism for the antidotal property since carbamates, oximes and ganglion blocking compounds, despite their chemical diversity exhibited similarity in possessing the above two properties. Moreover, the less powerful channel blockers such as neostigmine and pyridostigmine are indeed weaker antidotal agents against OPs. Other properties like an agonistic effect seen with carbamates may also influence the antidotal efficacy. Oxime 2-PAM and HI-6 in addition had an activating effect at the AChR and an AChE-like activity, properties which are favourable for exerting an antagonistic effect against OPs. Furthermore the effect of these agents at the nicotinic as well as glutamatergic synapses of the central nervous system may also have to be considered in relation to their therapeutic actions.

Acknowledgements

References

1 Gordon, J.J., Leadbeater, L. and Maidment, M.P. (1978) The protection of animals against organophosphate poisoning by pretreatment with a carbamate. Toxicol. Appl. Pharmacol. 43, 207–216.

2 Albuquerque, E.X., Allen, C.N., Aracava, Y., Akaike, A., Shaw, K.P. and Rickett, D.L. (1986) Activation and inhibition of the nicotinic receptor: Actions of physostigmine, pyridostigmine and meproadifen. In: Dynamics of Cholinergic Function (I. Hanin, ed.) pp. 677–695. Plenum Publishing Corp., New York.

3 Aracava, Y., Deshpande, S.S., Rickett, D.L., Brossi, A., Schönenberger, B. and Albuquerque, E.X. (1987) Molecular basis of anticholinesterase actions on nicotinic and glutamatergic synapses. Ann. N.Y. Acad. Sci. 505, 226–255.

4 Deshpande, S.S., Viana, G.B., Kauffman, F.C., Rickett, D.L. and Albuquerque, E.X. (1986) Effectiveness of physostigmine as a pretreatment drug for protection of rats from organophosphate poisoning. Fund. Appl. Toxicol. 6, 566–577.

5 Kawabuchi, M., Boyne, A.F., Deshpande, S.S., Cintra, W., Brossi, A. and Albuquerque, E.X. (1988) Enantiomer (+)Physostigmine prevents organophosphate- induced subjunctional damage at the neuromuscular synapse by a mechanism not related to cholinesterase carbamylation. Synapse 2, 139–147.

6 Albuquerque, E.X., Deshpande, S., Kawabuchi, M., Aracava, Y., Idriss, D.L. and Boyne, A.F. (1985) Multiple actions of anticholinesterase agents on chemosensitive synapses: Molecular basis for prophylaxis and treatment of organophosphate poisoning. Fund Appl. Toxicol. 5, S182 S203.

7 Albuquerque, E.X., Aracava, Y., Idriss, M., Schönenberger, B., Brossi, A. and Deshpande, S.S. (1987) Activation and blockade of the nicotinic and glutamatergic synapses by reversible and irreversible cholinesterase inhibitors. In: Neurobiology of Acetylcholine (N.J. Dun, R.L. Perlman, eds.), pp. 301 328. Plenum Publishing Corp., New York.

372

8 Meshul, C.K., Boyne, A.F., Deshpande, S.S. and Albuquerque, E.X. (1985) Comparison of the ultrastructural myopathy induced by anticholinesterase agents at the end plates of rat soleus and extensor muscles. Exp. Neurol. 89, 96–114.

9 Kawabuchi, M., Boyne, A.F., Deshpande, S.S. and Albuquerque, E.X. (1986) Comparison of the endplate myopathy induced by two different carbamates in rat soleus muscle. Neurosci. Abs. 12, 740.

10 Reddy, V.K. Deshpande, S.S. and Albuquerque, E.X. (1987) Bispyridinium oxime HI-6 reverses organophosphate (OP)-induced neuromuscular depression in rat skeletal muscle. Fed. Proc. 46, 861.

11 Alkondon, M., Rao, K.S. and Albuquerque, E.X. (1988) Acetylcholinesterase reactivators modify the functional properties of the nicotinic acetylcholine receptor ion channel. J. Pharmacol. Exp. Ther. 245, 543–556.

12 Clement, J.G. (1981) Toxicology and pharmacology of bispyridinium oximes-Insight in to the mechanism of action vs soman poisoning in vivo. Fund. Appl. Toxicol. 1, 193–202.

13 Ikeda, S.R., Asonstam, R.S., Daly, J.W., Aracava, Y. and Albuquerque, E.X. (1984) Interactions of bupivacaine with ionic channels of the nicotinic receptor. Electrophysiological and biochemical studies. Mol. Pharmacol. 26, 293–303.

14 Allen, C.N., Akaike, A. and Albuquerque, E.X. (1984) The frog interosseal muscle fiber as a new model for patch clamp studies of chemosensitive- and voltage- sensitive ion channels: actions of acetylcholine and batrachotoxin J. Physiol. (Paris) 79, 338–343.

15 Hamill, O.P., Marty, A., Neher, E., Sakmann, B. and Sigworth, F.J. (1981) Improved patch clamp techniques for high-resolution current recording from cells and cell-free membrane patches. Pflügers Arch. 391, 85–100.

16 Sachs, F., Neil, J. and Barkakati, N. (1982) The automated analysis of data from single ionic channels. Pflügers Arch. 395, 331–340.

17 Akaike, A., Ikeda, S.R., Brookes, N., Aronstam, R.S., Pascuzzo, G.J., Rickett, D.L. and Albuquerque, E.X. (1984) The nature of interactions of pyridostigmine with the nicotinic acetylcholine receptor-ion channel complex II. Patch clamp studies. Mol. Pharmacol. 25, 102–112.

18 Shaw, K.P., Aracava, Y., Akaike, A., Daly, J.W., Rickett, D.L. and Albuquerque, E.X. (1985) The reversible cholinesterase inhibitor physostigmine has channel-blocking and agonist effects on the acetylcholine receptor-ion channel complex. Mol. Pharmacol. 28, 527–538.

19 Ellman, G.L., Courtney, K.D., Andres Jr. V. and Featherstone, R.M. (1961) A new and rapid colorimetric determination of acetylcholinesterase activity. Biochem. Pharmacol. 7. 88–95.

20 Taylor, P. (1985) Anticholinesterase agents, In: Goodman and Gilman's The Pharmacological Basis of Therapeutics (A.G. Gilman, L.S. Goodman, T.W. Rall, F. Murad, eds.). pp. 110–129. Macmillan Publishing Co., New York.

21 Brossi, A., Shonenberger, B., Clark, O.E. and Ray, R. (1986) Inhibition of acetylcholinesterase from electric eel by (−)- and (+)-physostigmine and related compounds. FEBS Lett. 201, 190–192.

22 Auerbach, A., Del Castillo, J., Specht, P.C. and Titmus, M. (1983) Correlation of agonist structure with acetylcholine receptor kinetics: Studies on the frog end-plate and on chick embryo muscle. J. Physiol. (Lond.) 343, 551–568.

23 Merriam, L.A. and Fiekers, J.F. (1986) Single channel analysis of the interaction between antiesterases and cholinergic agonists on ACh receptor activation in rat myotubes. Neurosci. Abstr. 12, 1077.

24 Aracava, Y., Ikeda, S.R., Daily, J.W., Brookes, N. and Albuquerque, E.X. (1984) Interaction of bupivacaine with ionic channels in the nicotinic receptor: analysis of single-channel currents. Mol. Pharmacol. 26, 304–313.

25 Brehm, P., Kidokoro, Y. and Moody-Corbett, F. (1984) Acetylcholine receptor channel properties during development of Xenopus muscle cells in culture. J. Physiol. (Lond.) 357, 203–217.

26 Leonard, R.J., Nakajima, S., Nakajima, Y. and Takahashi, T. (1984) Differential development of two classes of acetylcholine receptors in Xenopus muscle in culture. Science 226, 55-57.

27 Costa, A.C.S., Aracava, Y., Rapoport, H. and Albuquerque, E.X. (1988) N,N-Dimethylanatoxin: An electrophysiological analysis. Neurosci. Abstr. (to be presented).

28 Neher, E. and Steinbach, J.H. (1978) Local anaesthetics transiently block currents through single acetylcholine-receptor channels. J. Physiol. (Lond.) 277, 153-176.

29 Adler, M., Albuquerque, E.X. and Lebeda, F.J. (1978) Kinetic analysis of endplate currents altered by atropine and scopolamine. Mol. Pharmacol. 14, 514-529.

30 Spivak, C.F., Maleque, M.A., Takahashi, K., Brossi, A. and Albuquerque, E.X. (1983) The ionic channel of the nicotinic acetylcholine receptor is unable to differentiate between the optical antipodes of perhydrohistrionicotoxin. FEBS Lett. 163, 189-193.

31 Rozental, R., Aracava, Y., Kapai, N. and Albuquerque, E.X. (1987) Actions of stereoisomers of SKF 10,047 on the ionic channel of nicotinic AChR. Fed. Proc. 46, 861.

32 Varanda, W.A., Aracava, Y., Sherby, S.M., Vanmeter, W.G., Eldefrawi, M.E. and Albuquerque, E.X. (1985) The acetylcholine receptor of the neuromuscular junction recognizes mecamylamine as a noncompetitive antagonist. Mol. Pharmacol. 28, 128-137.

33 Karczmar, A.G., Koketsu, K. and Soeda, S. (1968) Γ⁻ 'ble reactivating and sensitizing action of neuromyally acting agents. Int. J. Neuropharmacol. 7, 241-252.

34 Caratsch, C.G. and Waser, P.G. (1984) Effects of obidoxime chloride on native and sarin-poisoned frog neuromuscular junctions. Pflügers Arch. 401, 84-90.

35 Magleby, K.L. and Stevens, C.F. (1972) The effect of voltage on the time course of end-plate currents. J. Physiol. (Lond.) 223, 151-171.

36 Kordas, M., Brazin, M. and Majcen, Z. (1975) A comparison of the effect of cholinesterase inhibitors on end-plate current and on cholinesterase activity on frog muscle. Neuropharmacology 14, 791-800.

37 Magleby, K.L. and Pallotta, B.S. (1981) A study of desensitization of acetylcholine receptors using nerve-released transmitter in the frog. J. Physiol. (Lond.) 316, 225-250.

38 Woodhull, A.M. (1973) Ionic blockage of sodium channels in nerve. J. Gen. Physiol. 61, 687-708.

39 Karczmar, A.G. and Ohta, Y. (1981) Neuromyopharmacology as related to anticholinesterase action. Fund. Appl. Toxicol. 1, 135-142.

40 Eldefrawi, M.E., Schweizer, G., Bakry, N.M. and Valdes, J.J. (1988) Desensitization of the nicotinic acetylcholine receptor by diisoprophylfluorophosphate. Biochem. Toxicol. (in press).

41 Alkondon, M. and Albuquerque, E.X. (1987) Bispyridinium compounds SAD-128 and HI-6 modulate endplate currents of frog sartorius muscle. Neurosci. Abstr. 13, 709.

CHAPTER 27

Patch-clamp analysis of single chloride channels in primary neuronal cultures of *Drosophila*

DAISUKE YAMAMOTO[1] AND NOBUYUKI SUZUKI[2]

[1] *Laboratory of Neurophysiology, Mitsubishi-Kasei Institute of Life Sciences, 11, Minamiooya, Machida, Tokyo 194 and* [2] *Department of Physiology, Kitasato University Medical School, Sagamihara, Kanagawa 228, Japan*

Introduction

Within the last five years, neuronal chloride channels have aroused the interest of many pesticide scientists, as they have been advanced as potential primary targets for several insecticidal compounds, such as type II pyrethroids [1], avermectins [2], and cyclodienes [3]. In spite of the need for detailed information on insect chloride channels in the field of pesticide science, little is known about the physiology, pharmacology, and biochemistry of these membrane proteins. The recent development of patch-clamp techniques makes it possible to record the unitary current flowing through single ion channels [4]. This enables investigation of the actions of drugs and pesticides on individual channel proteins in membrane patches isolated from the cell under conditions where both sides of the membrane are bathed in artificial solutions of known composition.

Using the gigaohm-seal patch clamp technique, we have identified two types of chloride channels that are spontaneously active in cell body membranes of *Drosophila melanogaster* larval neuronal cultures. One type of chloride channel (the fast channel) has a relatively small unitary conductance of 7 pS, when the chloride concentration is 145 mM in both sides of the membrane. The mean open time is typically 1.2–1.6 ms, and there is no evidence for voltage sensitivity of the open-time distribution. The properties of this channel have been fully described elsewhere [6].

Another type of chloride channel (the slow channel), with a larger conductance (35 pS), was revealed to have an unusual multi-barrelled structure by experiments with open-channel blockers [7]. In the following discussion, attention will be focused on this slow chloride channel.

The slow channel is multi-barrelled

The channel remained predominantly in the open state for tens of minutes with occasional interruptions by short, closing transitions when the internal membrane

376
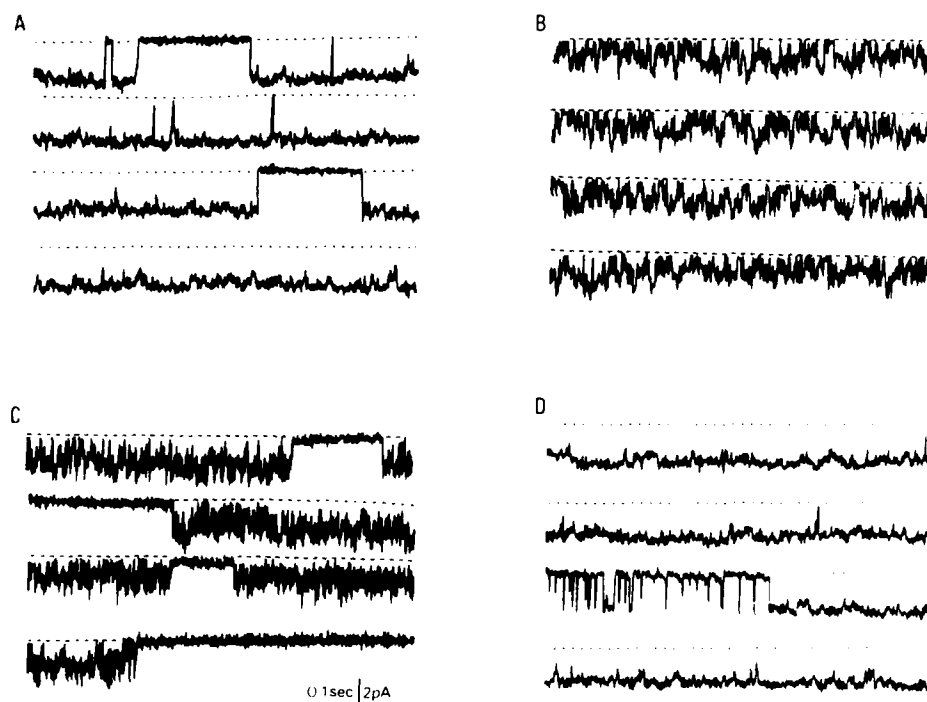
FIG 1 Single chloride channel currents recorded in cell-attached (a) or inside-out (b-d) membrane patches from cultured *Drosophila* neurones. a: inward currents through a chloride channel; the pH of the external solution (both pipette and perfusing solution) was adjusted with 10 mM bis-Tris. Segments with a long-closed state were chosen here to facilitate comparison of various conductance steps. A holding potential of − 70 mV was added to the cell resting potential. b-d: currents from different inside-out membrane patches with their cytoplasmic side exposed to 10 mM Hepes (b), Mops (c), or Tes (d). Membranes were clamped at a holding potential of − 70 mV and a temperature of 12°C. Broken lines represent zero conductance level. In this and later figures, inward currents are displayed as downward deflections. All experiments were done at $10 \pm 1°$ C. The pipette (external) solution contained (in mM): choline Cl 145; $Mg(CH_3COO)_2$ 3; EGTA 2. The bathing (internal) solution contained (in mM): KCl 145; $Mg(CH_3COO)_2$ 1.13; EGTA 1.92. The pH was adjusted to 7.0 with one of the buffering agents shown in Fig. 4, and tetramethylammonium hydroxide or HCl. Dissociated cell cultures from Canton-S wild type strain of the 3rd instar larvae were obtained by the method developed by Wu et al. [5]. From Yamamoto and Suzuki [6].

surface was perfused with buffer-free solutions or solutions buffered with cations such as tris(hydroxymethyl)aminomethane (Tris) and 2,2-bis(hydroxymethyl)-2,2′,2″-nitrilotriethanol (bis-Tris) (Fig. 1). However, this rather simple behaviour of the channel can readily be altered if the cytoplasmic side of the channel is exposed to the anionic buffers N-2-hydroxyethylpiperazine-N′-2-ethanesulfonic acid (Hepes) or 3-(N-morpholino)propanesulfonic acid (Mops) (Fig. 1). In the presence of Hepes or Mops, the open Cl⁻ channel appeared to exhibit several discrete conductance levels, some of which were barely detectable in the absence of these buffers (Fig. 2).

A

20ms(upper)
10ms(lower) | 2pA

B
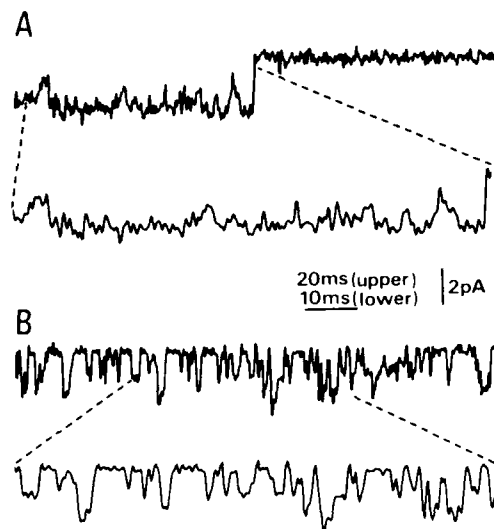
FIG 2 The slow chloride channel exposed to Hepes (B) displays multiple conductance states, many of which are not detectable in solutions buffered with bis-Tris (A). Records were obtained from a single inside-out patch at a holding potential of −90 mV. The buffer concentration was 10 mM. Single traces are shown in two different sweep speeds.

An increase in the buffer concentration increased the frequency of lower conductance channel openings at the expense of unitary events with a higher conductance, whereas the levels of the minimum and maximum step remained unchanged. The channel tended to dwell longer in the high-conductance open states at more depolarized membrane potentials. These results are consistent with the following hypothesis: the single chloride channel is composed of multiple pores that are gated simultaneously, each of which is subject to an independent hit by a blocker (Hepes or Mops) molecule. As a consequence, the conductance of a partly blocked channel decreased in a stepwise fashion as the number of blocked pores increases (Fig. 3).

It contrast to Hepes and Mops, the anionic buffer, 2-[tris(hydroxymethyl)-methylamino]-1-ethanesulfonic acid (Tes), did not affect channel activity (Fig. 1d). An examination of the chemical structures of these compounds suggests that the

closed   open   blocked
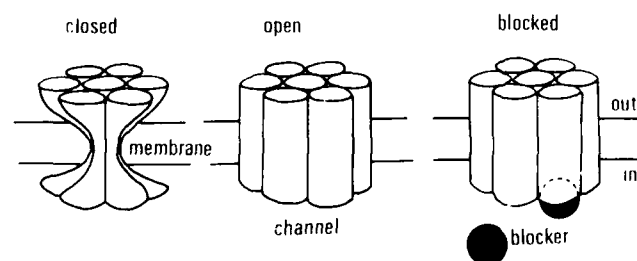
FIG 3 A cartoon illustrating the multi-barrelled structure of the slow chloride channel. The exact number of elementary pores has not been determined.

Hepes $\quad HOCH_2CH_2-N\underset{\underbrace{}}{\overset{\overbrace{}}{}}N-CH_2CH_2SO_3H$

Mops

$CH_2CH_2CH_2SO_3H$

Tes $\qquad (HOCH_2)_3CNHCH_2CH_2SO_4H$

Bis-Tris $\quad (HOCH_2CH_2)_2NC(CH_2OH)_3$

Tris $\qquad (HOCH_2)_3CNH_2$
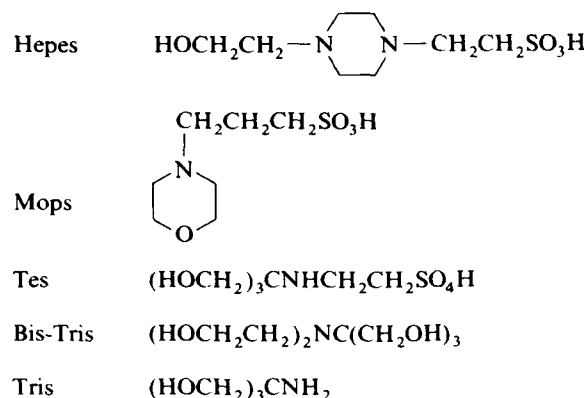
FIG. 4 Chemical structures of buffering compounds tested in this study.

piperadine moiety appears to be important in modulating the Cl^- channel activity (Fig. 4).

The slow channel is selective to anions

To examine ionic selectivity of the channel, the cytoplasmic side of the inside-out patch membrane was exposed to solutions of different ionic composition. The single channel current was unaffected by replacing K^+ with either Cs^+ or Na^+. In contrast, total replacement of chloride with glutamate completely eliminated the inward current at a holding potential of -90 mV. Large inward currents were observed with solutions containing NO_3^-, Br^-, or I^- in place of Cl^-. The channel was also permeable to F^-. The single channel current–voltage relationships were determined under conditions where the anionic composition of the internal (to which the cytoplasmic face of the inside-out membrane patch was exposed) solution was changed, while that of the external solution was fixed (i.e. 145 mM Cl^-). The current reversed its polarity from inward to outward at $+1.7 \pm 1.30$ mV ($n = 5$) when the internal solution contained 145 mM Cl^-. The chord conductance estimated between the reversal potential and -90 mV was 35.2 ± 0.52 pS in this condition. The reversal potentials and the chord conductances for the unitary current through the slow channel were determined with six different anions. The channel had the selectivity sequence: NO_3^- (1.97) > Br^- (1.12) $\approx I^-$ (1.03) $\approx Cl^-$ (1) > F (0.32) $\gg$ glutamate (< 0.02) as estimated by the permeability ratio based on the reversal potential measurement. The conductance ratio gave a slightly different selectivity order: NO_3^- (1.51) > Br^- (1) = Cl^- (1) > I (0.8) $\gg$ F (0.53) $\gg$ glutamate (0).

The slow channel is blocked by SITS but not by avermectin

It is well established that some disulfonic stilbene derivatives, such as 4-acetoamido-4'-isothiocyanostilbene-2,2'-disulfonic acid (SITS) and 4,4'-diisothiocyanostilbene-
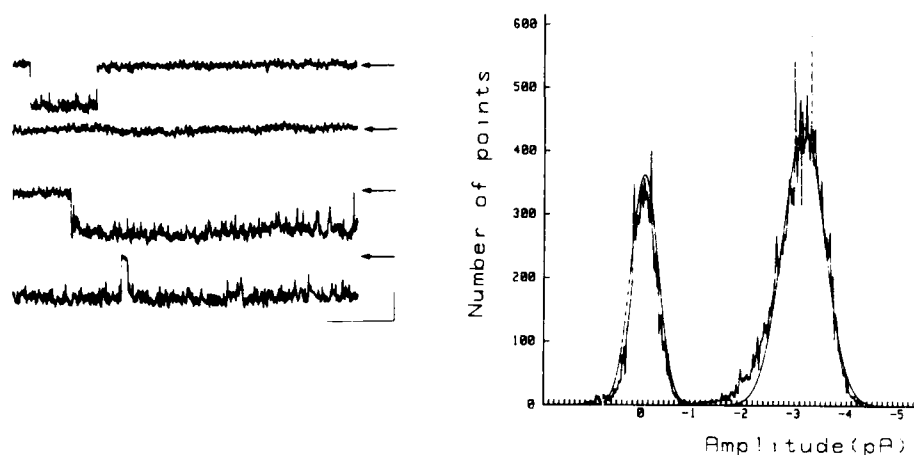
FIG 5   Effects of dihydroavermectin in B_{1a} (AVM) on the slow chloride channel. Examples (left) of chloride currents through the slow channel in an inside-out patch during exposure of the cytoplasmic side of membrane to 0.01 μg/ml AVM at a holding potential of -70 mV. Arrows indicate the closed conductance level. AVM was first dissolved in dimethylsulfoxide, then diluted with the internal solution. The mean amplitude estimated by the histogram analysis (right) was 3.0 pA, indicating that the unitary conductance was unaffected by AVM. The noisy curves represent the experimental distributions and smooth curves represent the Gaussian fits to them. Calibration: 10 ms, 2 pA.

2,2'-disulfonic acid (DIDS), which are aminoreactive reagents, produce a specific and irreversible inhibition of the anion transport of the erythrocyte membrane [8] and of the sarcoplasmic reticulum membrane [9]. SITS applied to the cytoplasmic side of the membrane at concentrations of 10–100 μM completely blocked the inward current through the slow channel. The current did not recover after extensive washing of the membrane.

As avermectin has been reported to enhance a chloride conductance in nerve and muscle cells of arthropods [10–14], we examined its possible effect on the slow channel. Fig. 5 illustrates results of a typical experiment in which the cytoplasmic side of an inside-out membrane patch was exposed to 0.01 μg/ml dihydroavermectin B_{1a}(AVM). AVM appeared not to alter either the kinetics or the conductance of the single slow channel. Addition of AVM (0.04 μg/ml) to the external side of the membrane also failed to produce any effects on the slow channel.

Conclusion

The slow chloride channel in *Drosophila* neurones appears to function as a complex of multiple protochannels. Most of the single channel records of chloride currents from a variety of cell types have revealed the existence of numerous substates [15–19]. These sub-conducting states may result from partial block of the channel, as shown by our experiments, or they may represent unsynchronized opening and closing of elementary pores. This implies that the multi-barrelled structure of a single channel proposed here is not unique to the *Drosophila* slow channel but may

prove to be a common feature of several types of chloride channel. As recently reported, some potassium channels appear to be composed of three elementary pores [20,21]. The assembly of multi-barrelled structures might be a common way to build up both anionic and cationic channels.

The selectivity sequence of the *Drosophila* slow channel is very similar to that of anion-selective channels in the rabbit epithelium [22] and of the Cl^--transporting mechanism in the guinea-pig vas deferens [23]. In addition, the slow channel shares the SITS-sensitivity with many other anion channels [24] and anion transporting mechanisms [8,9].

On the other hand, we failed to detect any effect of avermectin on the slow chloride channel of *Drosophila* neurones. As avermectin increases the chloride conductance of neuronal and muscle cells with no inhibitory GABAergic innervation [12], it has been suggested that avermectin-sensitive chloride channels are not necessarily associated with the GABA receptor.

However, our negative result with the slow channel seems to suggest that avermectin may have rather strict selectivity in acting on chloride channels. The selectivity sequence of anion conductance induced by avermectin in the locust muscle has been reported [25] to be $Cl^- > Br^- > I^-$, which differs from that of the slow channel in *Drosophila* neurones. This fact might indicate that different subtypes of chloride channels could have quite different sensitivities to avermectin.

Acknowledgements

References

1 Lawrence, L.J. and Casida, J.E. (1983) Streospecific action of pyrethroid insecticides on the γ-aminobutyric acid receptor-ionophore complex. Science 221, 1399–1401.
2 Fritz, L.C., Wang, C.C. and Gorio, A. (1974) Avermectin B_{1a} irreversibly blocks postsynaptic potentials at the lobster neuromuscular junction by reducing muscle membrane resistance. Proc. Natl. Acad. Sci. U.S.A. 76, 2062–2066.
3 Matsumura, F. (1985) Involvement of picrotoxinin receptor in the action of cyclodiene insecticides. Neurotoxicology 6, 139–164.
4 Neher, E. and Sakmann, B. (1976) Single channel currents recorded from membrane of denervated frog muscle fibres. Nature 260, 799–802.
5 Wu, C.-F., Suzuki, N. and Poo, M.-M. (1983) Dissociated neurons from normal and mutant *Drosophila* larval central nervous system in cell culture. J. Neurosci. 3, 1888–1899.
6 Yamamoto, D. and Suzuki, N. (1987) Single-channel recordings of chloride currents in primary cultured *Drosophila* neurons. Arch. Insect Biochem. Physiol. 6, 151–158.
7 Yamamoto, D. and Suzuki, N. (1987) Blockage of chloride channels by HEPES buffer. Proc. R. Soc. Lond. Ser. B. 230, 93–100.
8 Cabantchik, Z.I. and Rothstein, A. (1972) The nature of the membrane sites controlling anion permeability of human red blood cells as determined by studies with disulfonic stilbene derivatives. J. Membr. Biol. 10, 311–330.
9 Kasai, M. and Kometani, T. (197^4) Inhibition of anion permeability of sarcoplasmic reticulum vesicles by 4-acetoamido-4'-isothiocyanostilbene-2.2'-disulfonate. Biochim. Biophys. Acta. 557, 243–247.

10 Kass, I.S., Wang, C.C., Walrond, J.P. and Stretton, A.O.W. (1980) Avermectin B_{1a}, a paralyzing anthelmintic that affects interneurons and inhibitory motoneurons in *Ascaris*. Proc. Natl. Acad. Sci. U.S.A. 77, 6211-6215.

11 Mellin, T.N., Bursch, R.D. and Wang, C.C. (1983) Postsynaptic inhibition of invertebrate neuromuscular transmission by avermectin B_{1a}. Neuropharmacology 22, 89-96.

12 Duce, I.R. and Scott, R.H. (1985) Actions of dihydroavermectin B_{1a} on insect muscle. Br. J. Pharmacol. 85, 395-401.

13 Chalmers, A.E., Miller, T.A. and Olsen, R.W. (1986) The actions of avermectin on crayfish nerve and muscle. Eur. J. Pharmacol. 129, 371-374.

14 Lees, G. and Beadle, D.J. (1986) Dihydroavermectin B_1: actions on cultured neurones from the insect central nervous system. Brain Res. 366, 369-372.

15 Geletyuk, V.I. and Kazachenko, V.N. (1985) Single Cl^- channels in molluscan neurones: multiplicity of the conductance states. J. Membr. Biol. 86, 9-15.

16 Krouse, M.E., Schneider, G.T. and Gaze, P.W. (1986) A large anion-selective channel has seven conductance levels. Nature 319, 58-60.

17 Young, G.P.H., Young, J.D.E., Deschpande, A.K., Goldstein, M., Koide, S.S. and Cohen, Z.A. (1984) A Ca^{2+}-activated channel from *Xenopus laevis* oocyte membranes reconstituted into planar bilayers. Proc. Natl. Acad. Sci. U.S.A. 81, 5155-5159.

18 Greger, R., Schlatter, E. and Gogelein, H. (1987) Chloride channels in the luminal membrane of the rectal gland of the dogfish (*Squalus acanthu*). Pflügers Arch. 409, 114-121.

19 Bolotina, V., Borecky, J., Vlachove, V., Baudysova and Vyskovil, F. (1987) Voltage-dependent chloride channels with several substates in excised patches from mouse neuroblastoma cells. Neurosci. Lett. 77, 298-302.

20 Hunter, M. and Giebisch, G. (1987) Multi-barrelled K channels in renal tubules. Nature 327, 522-524.

21 Matsuura, H., Matsuda, H. and Noma, A. (1987) The inward rectifier K channel in cardiac muscle is composed of three pores with identical conductance. Biophysics (Tokyo) 27, 5266 (in Japanese).

22 Hanrahan, J.W., Alles, W.P. and Lewis, S.A. (1985) Single anion-selective channels in basolateral membrane of a mammalian tight epithelium. Proc. Natl. Acad. Sci. U.S.A. 82, 7791-7795.

23 Aickin, C.C. and Brading, A.F. (1985) The effects of bicarbonate and foreign anions on chloride transport in smooth muscle of the guinea-pig vas deferens. J. Physiol. 366, 267-280.

24 Inoue, I. (1985) Voltage-dependent chloride conductance of the squid axon membrane and its blockade by some disulfonic stilbene derivatives. J. Gen. Physiol. 85, 519-537.

25 Scott, R.H. and Duce, I.R. (1986) Anion selectivity of γ-aminobutyric acid (GABA) and 22,23-dihydroavermectin B_{1a} (DHAVM)-induced conductance changes on locust muscle. Neurosci. Lett. 68, 197-201.

CHAPTER 28

Comments on the action of polyamine spider toxins on insects with particular reference to argiotoxin$_{636}$

P.N.R. USHERWOOD

Department of Zoology, University of Nottingham, Nottingham NG7 2RD, U.K.

Introduction

Since the original demonstration in 1984 that venoms of certain orb-web spiders contain toxins with molecular weights less than 1 kDa which block glutamatergic nerve-muscle transmission in locusts [1,2], a number of laboratories have isolated, structurally characterized and synthesized these compounds [3–6]. In some respects these toxins are similar structurally and pharmacologically to a wasp toxin δ-philanthotoxin (PTX-433), first identified by Piek and colleagues [7,8] and subsequently synthesized by his group (Chapter 5) and by Eldefrawi et al. [9]. The reader is referred to Piek's comparative account of spider and wasp toxins which is presented in Chapter 5.

The low molecular weight toxins isolated from venom of *Argiope spp.* spiders comprise two families and are called argiotoxins [10,11]. Members of both families of argiotoxins have a terminal arginine linked via a polyamine to asparagine. which

TABLE 1   Questions which remain unanswered concerning the interaction of argiotoxin$_{636}$ with insect excitable tissues

1. Site of action
Peripheral GluR?
Other peripheral receptors?
Presynaptic and/or postsynaptic?
Voltage-gated channels?
Central nervous receptors?
2. Mode of action
Competitive antagonist of GluR?
Non-competitive antagonist of GluR?
Open channel blocker?
Closed channel blocker?
3. Access to specific binding site(s) on GluR
Direct?
Indirect?

in turn is coupled to a phenol in one family, to which argiotoxin$_{636}$ belongs and to an indol in the other family [6,10,11]. Because it was the first to be discovered [1] and because of its high potency argiotoxin$_{636}$ (or argiopine [3]) is the most studied of these toxins. It has been described as a non-competitive antagonist of excitatory glutamate receptors of locust leg muscle [1,2,10–13] and of blowfly and housefly larval body wall muscle [6,13]. Although the interactions of argiotoxin$_{636}$ with insect excitable tissues have been studied using a variety of approaches, ranging from measurements of its effects on the neurally-evoked twitch contractions of whole nerve-muscle preparations to patch clamp studies of single glutamate receptor channels on locust leg muscle, there remain a number of unanswered questions about its site and mode of action in insects, the subjects of which are central to this chapter. The major questions are listed in Table 1. They deserve serious considera-tion if this and similar spider toxins are to be considered as lead structures for pesticide/pharmaceutical discovery.

Site of action of insects

Very few present-day pesticides act at insect glutamatergic nerve-muscle junctions which, in principle, should be prime target sites for the chemical control of pest insects. Given this and the fact that the postjunctional glutamate receptors (GluR) at these sites have been difficult to study because of the lack of potent antagonists, it is perhaps not surprising that the discovery of spider toxins which block excitatory nerve-muscle in insects by antagonizing GluR should arouse interest amongst both industrial and academic scientists.

There is general agreement that argiotoxin$_{636}$ is an antagonist of excitatory GluR of locust and housefly muscle, but does it also influence presynaptic events at peripheral glutamatergic sites in insects? Piek using locust (Chapter 5) and Mag-azanik et al. using larval blowfly [13] nerve-muscle preparations suggest that it does not, but more evidence is required fully to substantiate this conclusion. The possibility that argiotoxin$_{636}$ interacts with other types of peripheral receptor in insects, of which the γ-aminobutyrate receptors present postjunctionally at inhibi-tory nerve-muscle junctions [14–16] immediately spring to mind, remains to be investigated. I am unaware of any studies of the effects of spider toxins on insect inhibitory nerve-muscle junctions, although Kawai and colleagues [16] have shown that JORO spider toxin does not affect transmission at GABAergic, inhibitory synapses on crayfish leg muscle. Now that it is possible to record the activity of single voltage-gated channels in membrane patches of insect muscle [17–19] and neurone cell body [22,23] it should be a relatively simple matter to determine whether argiotoxin$_{636}$ interacts with this type of membrane protein, but as yet, such studies have not been undertaken.

The crucial question of whether argiotoxin$_{636}$ and other low molecular weight spider toxins gain access to central neurones in vivo when an insect prey is 'bitten' by an orb-web spider is central to many of the issues about site and mode of action which are raised in this Chapter. Piek [7] has shown that the digger wasp *Philanthus triangulum*, which produces PTX-433, injects its venom into the central nervous system of its honeybee prey, so there is reason to assume that PTX-433 acts at central synapses in this insect as well as possibly antagonizing peripheral GluR. However, *Argiope* spiders are more likely to inject their toxin into the haemocoel of

their insect prey, which raises the question of whether the relatively hydrophilic argiotoxins such as argiotoxin$_{636}$ gain access to the central nervous system, i.e. whether they can cross the insect blood-'brain' barrier. Studies with radiolabelled toxin will undoubtedly provide an answer to this question, but in the meantime there is already evidence to suggest that if the argiotoxins do gain access to the insect central synapses from haemocoel then they are not very effective there, at least in vivo. This evidence comes from studies of Usherwood and Duce [24] who injected partially purified *Argiope trifasciata* and *Araneus gemma* venom into the haemocoel of restrained locusts [25]. Activation-induced block of nerve-muscle transmission ensued in these insects which could still be observed 48 h post-injection of the venom. However, the venom seemed to have little effect on sensory reflex activation of the leg muscles of these restrained locusts, which suggests that central nervous function remained relatively unimpaired.

Mode of action

The only target site for argiotoxin$_{636}$ in insects that has been identified unequivocally is the excitatory GluR of skeletal muscle. The rest of this chapter will concentrate on the interaction of argiotoxin$_{636}$ with this peripheral membrane protein.

There have been conflicting views about the mode of interaction of low molecular weight spider toxins with peripheral GluR in arthropods. A number of laboratories agree with the interpretation that in insects these toxins are reversible non-competitive antagonists, possibly channel blockers [1,2,6,10-13]. This contrasts with the view of Kawai and colleagues who have suggested that JSTX and NSTX are non-reversible, competitive antagonists of crustacean muscle GluR [19,26]. These fundamental differences are surprising in view of the many similarities between insect and crustacean muscle GluR [27].

In insects the evidence for reversible, non-competitive antagonism of GluR is derived from a variety of studies involving locust, housefly and blowfly nerve-muscle preparations. The earliest studies, which were undertaken on whole nerve-muscle preparations showed that partially-purified *Argiope sp.* and *Araneus sp.* venom reduced the amplitude of the neurally-evoked twitch contraction of locust leg muscle and that the site and extent of this inhibition were directly dependent upon stimulus frequency [1,2,10,24]. This use-dependent inhibition was confirmed by studying the influence of venom on the postsynaptic potential and current recorded from locust excitatory nerve-muscle junctions and the potential change induced during ionophoretic application of L-glutamate to such sites [2,10]. The toxin-induced reduction in amplitude of the postsynaptic current was enhanced by muscle hyperpolarization, which suggests that the use-dependent postsynaptic block of transmission by argiotoxin$_{636}$ is voltage-sensitive. These studies led to the conclusion that one major action of the low molecular weight toxins, like argiotoxin$_{636}$, in orb-web spider venoms is to block the open channels gated by peripheral excitatory GluR in insects.

The recent availability of purified argiotoxin$_{636}$ has enabled more quantitative studies to be made of its mode of action in insects. Magazanic et al. [13] studied the interaction of this toxin with glutamatergic synapses on blowfly body wall muscle. They concluded that its action at this site was non-competitive and reversible, but

involved both open and closed channel block. Hyperpolarization of the muscle increased open channel block but weakened closed channel block. The K_ds for open channel and closed channel block were similar, i.e. 6.7×10^{-7} M and 4.4×10^{-7} M respectively. Significantly, Magazanic et al. [13] also found that argiotoxin$_{636}$ reversibly blocks the nicotinic acetylcholine receptor (nAChR) channel of frog muscle in its open state, but with a K_d of 2.4×10^{-5} M. It appears to have no effect on the closed nAChR channel.

Single channel studies

Studies by Kerry et al. [12] on the interaction of argiotoxin$_{636}$ with single excitatory GluR (D-receptor) channels in locust extrajunctional membrane of locust leg muscle. which have already been published in detail are summarized below.

The properties of the extrajunctional GluR channel are summarized in Table 2. The experimental protocols employed in the single channel studies of argiotoxin$_{636}$ [32,33] are illustrated in Fig. 1 and the megaohm seal experimental design is illustrated in Fig. 2. The influence of argiotoxin$_{636}$, applied either in patch pipette or muscle bath, on the channel open probability (p_o), channel open event frequency (f), channel mean open time (m_o) and channel mean closed time (m_c) was investigated. The toxin caused time-dependent and concentration-dependent changes in these parameters.

Three types of channel behaviour, which have been designated type I, type II and type III, respectively (Table 3) were identified in the presence of argiotoxin$_{636}$. These have been compared qualitatively and quantitatively with the channel activity recorded with 10^{-4} M L-glutamate in the patch pipette, but in the absence of toxin [32,33,38]. With low concentrations ($10^{-14}-10^{-11}$ M) of toxin in the patch pipette along with 10^{-4} M L-glutamate, the single channel activity was initially similar to that of controls, but this was superceded first by type I, then type II and finally type III behaviour. The rate at which these transitions took place was directly proportional to the concentration of toxin in the patch pipette. With higher concentrations of toxin the effects on GluR were immediate and with concentrations $\geq 10^{-9}$ M,

TABLE 2 Summary of the properties of glutamate D-receptor channels present in extrajunctional membrane of locust leg muscle

1. Quisqualate-sensitive [18,28]
2. Single channel conductance 100-150pS [29]
3. Weak cation selectivity:
   $NH_4^+ < Li^+ < Na^+ < Cs^+ = K^+ < Rb^+$ [30,31]
4. Blocked by high concentrations (> 20 mM) Ca^{2+}.
   Ca^{2+} not required for gating of channel [18,30]
5. Channel kinetics [32,33]
   a. Minimum 3 open, 4 closed states
   b. Non-linear gating mechanism
   c. Rapid desensitization onset with apparent slow recovery
   d. Concanavalin A blocks desensitization
6. Non-competitive antagonists:
   Chlorisondamine [34], trimetaphan [35], δ-PTX (PTX-433) [36].
   (+)-tubocurarine [37].
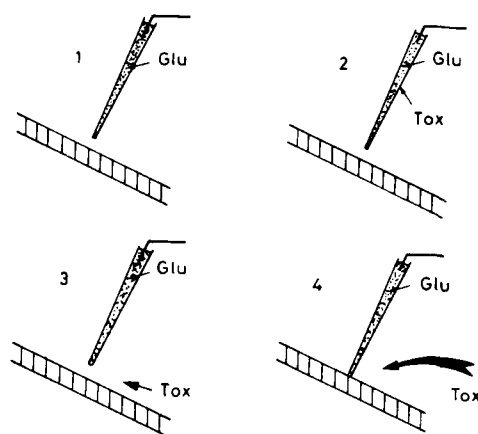
FIG 1 Experimental protocols employed in single channel studies of the interactions of argiotoxin$_{636}$ with extrajunctional GluR of locust leg muscle [12]. 1: control experiment. Patch pipette containing 10^{-4} M L-glutamate [32]. In other studies the glutamate concentration ranged between 10^{-6} M and 10^{-2} M [28,33]. 2: argiotoxin$_{636}$ in patch pipette with L-glutamate. Concentrations of toxin were 10^{-14} M–10^{-9} M. Concentrations of glutamate were 10^{-4} M–10^{-2} M. 3: argiotoxin$_{636}$ in bath (pre-megaohm seal formation). Concentrations of toxin were 10^{-12} M–10^{-9} M. 10^{-4} M L-glutamate in patch pipette. Seals between patch pipette and muscle fibre were made after application of toxin. (From Kerry et al. [12].) 4: argiotoxin$_{636}$ in bath (post-megaohm seal formation). Concentrations of toxin were 10^{-11}–10^{-9} M. 10^{-4} M L-glutamate in patch pipette. Seals between patch pipette and muscle were made *before* application of toxin.

channel openings were never observed (Table 3). Similar data were obtained when the toxin was applied via the muscle bath. A salient point which emerges from these studies with argiotoxin$_{636}$ is the reduction in m_o recorded during type II behaviour, a change which is consistent with open channel block. Autocorrelation and cross-correlation analyses of such data lend further support to this conclusion [12], as does the reduction in the number of channel open states from 3 in controls to 1 during type II behaviour in toxin (Table 3).

If it is assumed that argiotoxin$_{636}$ blocks the glutamate receptor channel by entering the open channel according to the scheme 38:

$$\text{channel closed} \xleftrightarrow{k_c} \text{channel open} \xleftrightarrow{bk_B} \text{channel blocked}$$
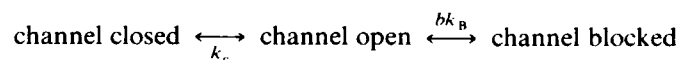
TABLE 3 Effect of argiotoxin$_{636}$ on the extrajunctional GluR channel of locust leg muscle. Kinetic properties associated with different single channel behaviours observed when the toxin was present either in the patch pipette or the muscle bath

Activity	P_o	f	m_c	m_o	No. of channel states	
					open	closed
Control	–	–	–	–	3	4
Type 1	↓	↓	↑	–or ↑	3	4
Type 2	↓↓	↓↓	↑↑	↓	1	4
Type 3	0?	0?	00?	0?	0?	1?

388
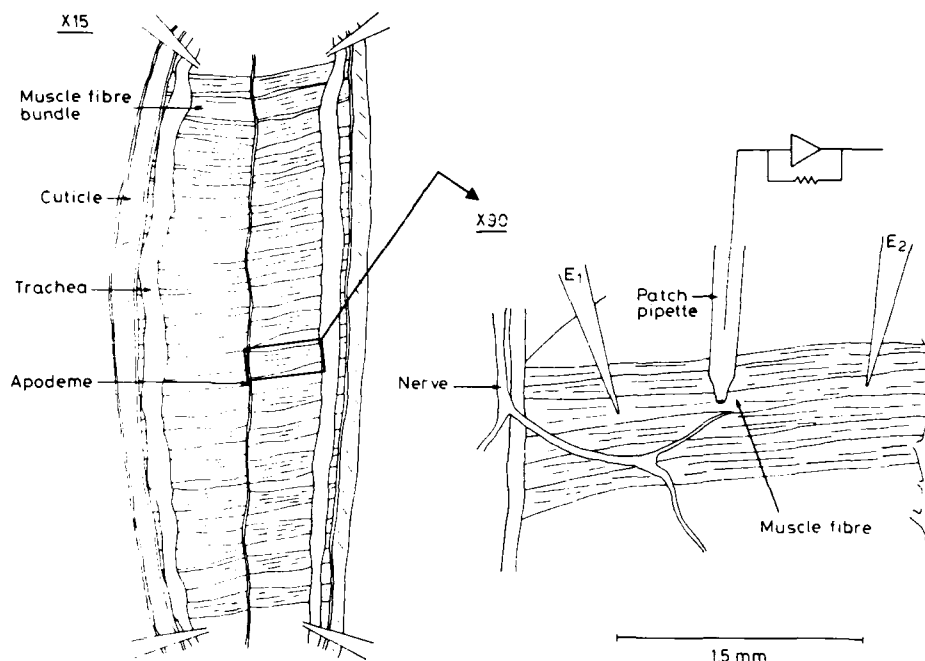
FIG 2 Experimental arrangement for recording from single glutamate D-receptor channels of locust leg muscle using a megaohm seal technique. The metathoracic extensor tibiae nerve-muscle preparation is shown on the left and the muscle fibre (in its bundle of fibres) from which single channels were recorded is located on the right. The patch pipette contained L-glutamate in locust saline in the presence or absence of argiotoxin$_{636}$. The potential difference across the membrane patch isolated by the tip of the patch pipette was controlled by a two-electrode voltage clamp (E_1, E_2). The muscle was pretreated for 30 min with 10^{-6} M concanavalin A before patching commenced. (From C. Kerry, unpublished.)

where the open channel closing rate is $k_c = 1/m_o = 10^3$ s^{-1} for 10^{-4} M L-glutamate [32] then for rapid, diffusion limited block the open channel blocking rate k_B is ca. 10^8 M^{-1} s^{-1}. Since, according to this scheme, $m_o = (k_c + bk_B)^{-1}$ a significant reduction in m_o would only occur when the concentration of argiotoxin$_{636}$ is $\geqslant 10^{-6}$ M. However, it has been found that open channel block, indicated by the reduction in m_o during type II behaviour, occurred with much lower concentrations of toxin than this. It follows, therefore, that either the above scheme is inadequate or that the toxin concentrates in a muscle compartment from which it gains access to the GluR channel [12] (see later).

The results of these single channel studies do not exclude the possibility that argiotoxin$_{636}$ also blocks the closed channel and/or is a competitive antagonist of locust muscle glutamate D-receptors. There was an increase in m_c during type I behaviour without any apparent reduction in m_o. Indeed, m_o sometimes increased at this time. This result might appear, at first sight, to support the contention of closed channel block. However, returning to the channel block scheme:

channel closed $\longleftrightarrow$ channel open $\underset{k_{-B}}{\overset{bk_B}{\longleftrightarrow}}$ channel blocked
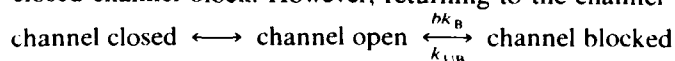
if k_{UB}, the unblocking rate for argiotoxin$_{636}$ is much lower than bk_B (e.g. $K_d = 10^{-10}$ M) then for low concentrations (b) of argiotoxin$_{636}$ one might expect an increase in m_c without a measurable concomitant change in m_o. However, the voltage clamp studies of the effects of partially purified *Argiope sp.* and *Araneus sp.* venom [2,10] and with pure argiotoxin$_{636}$ [13] on postsynaptic currents recorded from locust [2,10] and blowfly [13] excitatory nerve-muscle junctions suggest that the unblocking rate may not be low. Magazanic et al. [13] have determined an unblocking rate for the interaction of argiotoxin$_{636}$ with the open excitatory synaptic channel of blowfly muscle of between 36 s^{-1} and 55 s^{-1}.

The possibility of allosteric interaction between the argiotoxin and L-glutamate binding sites on the postjunctional and extrajunctional GluR of locust leg muscle is raised by the increase in m_o seen, albeit infrequently, during type I behaviour [12].

Access of argiotoxin$_{636}$ to specific binding sites on GluR

Most of the studies undertaken on locust muscle to investigate the pharmacology of argiotoxin have raised questions about its access to binding sites on GluR. For example, how does one account for the increasingly delayed onset of the inhibition of the neurally-evoked twitch which has been observed in locust nerve-muscle preparations as the concentration of argiotoxin$_{636}$ (and other argiotoxins) is lowered? (Fig. 3.) The toxin-induced time-dependent changes in amplitude (and time-course) of postsynaptic events, including ionophoretic glutamate potentials, together with
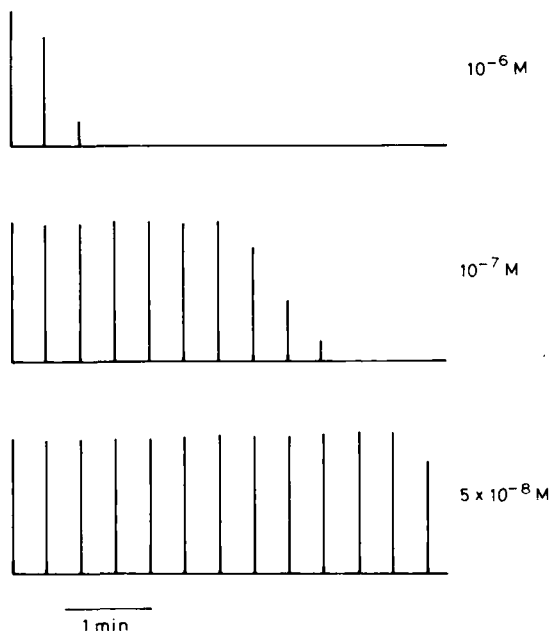
FIG 3 Diagrammatic representation of delay in onset of neurally-evoked twitch depression of locust metathoracic retractor unguis muscle. The delay increases in duration when the concentration of argiotoxin$_{636}$ is reduced.

the time-dependent changes in single GluR channel behaviour also need to be clarified and explained. Finally, how does one account for the very slow and sometimes apparently incomplete recovery from argiotoxin antagonism which occurs, especially after application of high concentrations of toxin?

Given the many hydrophilic groups present on the $argiotoxin_{636}$ molecule it might appear unlikely that this toxin partitions into the membrane lipid of insect muscle. However, if it does then this could account for all of the observations referred to above. Accumulation of the toxin in the membrane lipid could also account for the apparent discrepancy between the (exceptionally low) bath or patch pipette concentrations of $argiotoxin_{636}$ required in single channel studies to cause GluR antagonism and those concentrations required theoretically to block the open glutamate receptor channel (see earlier).

An alternative possibility is that the toxin binds tightly to 'extracellular' components on the muscle membrane surface or to the membrane lipid from which it can gain access to GluR. The experimental protocol in Fig. 1(4) involved making a seal between the tip of a patch pipette, containing 10^{-4} M L-glutamate but no toxin, and the muscle fibre membrane and then introducing $argiotoxin_{636}$ into the bathing medium. Open channel block (and possibly closed channel block and/or competitive antagonism) of the extrajunctional D-receptor isolated by the patch pipette still occurred under these conditions, the rate of onset of antagonism being directly proportional to the concentration of toxin present in the muscle bath. Perhaps the toxin can still gain access to the GluR by crossing the megaohm seal formed between the patch pipette top and the muscle membrane. Current studies made using gigaohm seal techniques should unequivocally test this possibility.

Summary

1. $Argiotoxin_{636}$ is a non-competitive antagonist of insect peripheral GluR.
2. $Argiotoxin_{636}$ possibly interacts allosterically with the glutamate binding sites on GluR.
3. $Argiotoxin_{636}$ possibly gains access to its binding sites indirectly by compartmentalizing, for example into the muscle membrane lipid. Alternatively it may bind very tightly to sites on the muscle surface from which it proceeds to block the open GluR.
4. $Argiotoxin_{636}$ is an open channel blocker of GluR. It may also be a closed channel blocker and/or a competitive antagonist of this receptor membrane protein.

References

1 Boden, P., Duce, I.R. and Usherwood, P.N.R. (1984) Activation-induced postsynaptic block of insect nerve-muscle transmission by a low molecular weight fraction of spider venom. Br. J. Pharmacol. 83, 221P.
2 Usherwood, P.N.R., Duce, I.R. and Boden, P. (1984) Slowly reversible block of glutamate receptor channels by venoms of *Argiope trifasciata* and *Araneus gemma*. J. Physiol. (Paris) 97, 169–171.
3 Volkova, T.M., Grishin, E.V., Alzeniev, A.S., Reshetova, O.S. and Onoprienko, V.V. (1986) Structural characteristics of argiopine-blocker of glutamate channels from the venom of spider, *Argiope lobata*. Proc. 6th ESN meeting Prague, 189P.

4 Aramaki, Y., Yasuhara, T., Higashijima, T., Yoshioka, M., Miwa, A., Kawai, N. and Nakajima, T. (1986) Chemical characterisation of spider toxin JSTX and NSTX. Proc. Jap. Acad. Sci. B. 62, 359–362.

5 Teshima, T., Wakamiya, T., Aramaki, Y., Nakajima, T., Kawai, N. and Shiba, T. (1987) Synthesis of a new neurotoxin NSTX-3 of Papua New Guinean spider. Tetrahedron Lett. 28, 3509–3510.

6 Adams, M.E., Carney, R.L., Enderlin, F.E., Fu, E.T., Jarema, M.A., Li, J.P., Miller, C.A., Schooley, D.A., Shapiro, M.J. and Venema, V.J. (1982) Structures and biological activities of three synaptic antagonists from orb weaver spider venom Biochem. Biophys. Res. Commun. 148, 678–683.

7 Piek, T. (1982) Delta-philanthotoxin, a semi-irreversible blocker of ion channels. Comp. Biochem. Physiol. 72C, 311–315.

8 Piek, T. and Spanjer, W. (1986) Chemistry and pharmacology of solitary wasp venoms. In: Venoms of the Hymenoptera (T. Piek, ed.), pp. 161–307. Academic Press, London.

9 Eldefrawi, A.T., Edlefrawi, M.E., Konno, K., Mansour, A.A., Nakanishi, K., Oltz, E. and Usherwood, P.N.R. (1988) Identification and synthesis of a potent glutamate receptor antagonist in wasp venom. Proc. Natl. Acad. Sci. U.S.A. 85, 4910–4914.

10 Bateman, A., Boden, P., Dell, A., Duce, I.R., Quicke, D.L.J. and Usherwood, P.N.R. (1985) Postsynaptic block of a glutamatergic synapse by low molecular weight fractions of spider venom. Brain Res. 339, 237–244.

11 Budd, T., Clinton, P., Dell, A., Duce, I.R., Johnson, S.J., Quicke, D.L.J., Taylor, G.W. Usherwood, P.N.R. and Usoh, G. (1988) Isolation and characterization of toxins from venoms or orb-web spiders. Brain Res. 448, 30–39.

12 Kerry, C.J., Ramsey, R.L., Sansom, M.S.P. and Usherwood, P.N.R. (1988) Single channel studies of non-competitive antagonism of a quisqualate-sensitive glutamate receptor by argiotoxin$_{636}$—a fraction isolated from orb-web spider venom. Brain Res. (in press).

13 Magazanic, L.G., Antonov, S.M., Fedorova, I.M., Volkova, T.M. and Grishin, E.V. (1986) Effects of the spider *Argiope lobata* crude venom and its low molecular weight component, argiopine, on the postsynaptic membrane. Biol. Membr. 3, 1204–1219.

14 Usherwood, P.N.R. and Grundfest, H. (1984) Inhibitory postsynaptic potentials in grasshopper muscle. Science 143, 817–818.

15 Usherwood, P.N.R. and Grundfest, H. (1965) Peripheral inhibition in skeletal muscle of insects. J. Neurophysiol. 28, 497–518.

16 Usherwood, P.N.R. (1968) A critical study of the evidence for peripheral inhibitory axons in insects. J. Exp. Biol. 49, 201–222.

17 Huddie, P.L. and Usherwood, P.N.R. (1986) Single potassium channels of adult locust (*Schistocerca gregaria*) muscle recorded using the giga-ohm seal patch clamp technique. J. Physiol. 378, 60P.

18 Dudel, J., Franke, Chr., Hatt, H., Ramsey, R.L. and Usherwood, P.N.R. (1988) Rapid activation and desensitization by glutamate of excitatory, cation-selective channels in locust muscle. Neurosci. Lett. 88, 33–38.

19 Dudel, J., Franke, Chr., Hatt, H. and Usherwood, P.N.R. (1988) Chloride channels gated by extrajunctional glutamate receptors (H-receptors) on locust leg muscle. Brain Res. (in press).

20 Duce, J.A., Miller, B.A. and Usherwood, P.N.R. (1988) Patch clamp studies of cultured muscle from locust embryos. In: Cell Culture Approaches to Invertebrate Neuroscience (D. Beadle, ed.). pp. 221–223. Academic Press, London.

21 Huddie, P.L. and Usherwood, P.N.R. (1988) Ryanodine modifies the ion selectivity of potassium channels of locust muscle. In: Proc. 4th Intl. Conf. on Water and Ions in Biological Systems (A. Pullman, N. Vasilescu, eds.). Birkhauser Verlag, Berlin (in press).

22 Christensen, B.N., Larmet, Y., Shimahara, T., Beadle, D. and Pichon, Y. (1988) Ionic currents in neurones cultured from embryonic cockroach (*Periplaneta americana*) brains. J. Exp. Biol. 135, 193–214.

392

23 Christensen, B.N., Shimahara, T., Pichon, Y., Beadle, D. and Larmet, Y. (1985) Potassium currents in developing cockroach neurons. Biophys. J. (Abstr.) 49, 5749.

24 Usherwood, P.N.R. and Duce, I.R. (1985) Antagonism of glutamate receptor channel complexes by spider venom polypeptides. Neurotoxicology 6, 239–250.

25 Runion, H.I. and Usherwood, P.N.R. (1966) A new approach to neuromuscular analysis of the intact free-walking insect preparation. J. Insect Physiol. 12, 1255–1263.

26 Abe, T., Kawai, N. and Miwa, A. (1983) Effects of a spider toxin on the glutamatergic synapse of lobster muscle. J. Physiol. 339, 243–252.

27 Shinozaki, H. (1988) Pharmacology of the glutamate receptor. Progr. Neurobiol. 30, 399–435.

28 Gration, K.A.F. and Usherwood, P.N.R. (1980) Interactions of glutamate with amino acid receptors on locust muscle. Verh. Dtsch. Zool. Ges. 1980, 122–132.

29 Patlak, J.B., Gration, K.A.F. and Usherwood, P.N.R. (1979) Single glutamate-activated channels in locust muscle. Nature (Lond.) 278, 643–645.

30 Kits, K.S. and Usherwood, P.N.R. (1988) Ion selectivity of single glutamate-gated channels in locust skeletal muscle. J. Exp. Biol. (in press).

31 Kitts, K.S. and Usherwood, P.N.R. (1984) Ion selectivity of glutamate gated channels. In: Electropharmacology of the in vitro synapse (G.A. Cottrell, ed.), 140P. St. Andrews University Press 1984.

32 Kerry, C.J., Kitts, K.S., Ramsey, R.L., Sansom, M.S.P. and Usherwood, P.N.R. (1987) Single channel kinetics of a glutamate receptor. Biophys. J. 51, 137–144.

33 Kerry, C.J., Ramsey, R.L., Sansom, M.S.P. and Usherwood, P.N.R. (1988) Glutamate receptor-channel kinetics: the effect of glutamate concentration. Biophys. J. 53, 39–52.

34 Ashford, M.L.J., Boden, P., Ramsey, R.L., Sansom, M.S.P., Shinozaki, H. and Usherwood, P.N.R. (1988) Voltage-dependent block of locust muscle glutamate channels by chlorisondamine. J. Exp. Biol. 134, 131–154.

35 Ashford, M.L.J., Boden, P., Ramsey, R.L., Shinozaki, H. and Usherwood, P.N.R. (1987) Effect of trimetaphan on locust glutamate receptors. J. Exp. Biol. 130, 405–424.

36 Clark, R.B., Donaldson, P.L., Gration, K.A.F., Lambert, J.J., Piek, T., Ramsey, R.L., Spanjer, W. and Usherwood, P.N.R. (1982) Block of locust muscle glutamate receptors by δ-philanthotoxin occurs after receptor activations. Brain Res. 241, 105–114.

37 Kerry, C.J., Ramsey, R.L., Sansom, M.S.P., Usherwood, P.N.R. and Washio, H. (1987) Single-channel studies of the action of (+)-tubocurarine on locust muscle glutamate receptors. J. Exp. Biol. 127, 121–134.

38 Adams, P.R. (1976) Drug blockade of open end-plate channels. J. Physiol. (Lond.) 26. 531–552.

CHAPTER 29

The mammalian neuronal nicotinic receptor and its block by drugs

ALISTAIR MATHIE, STUART G. CULL-CANDY AND DAVID COLQUHOUN

MRC Receptor Mechanisms Research Group, Department of Pharmacology, University College London, Gower St., London WC1E 6BT, U.K.

Introduction

Fast synaptic transmission in mammalian sympathetic ganglia is brought about by acetylcholine (ACh), released from preganglionic fibres, acting on postganglionic nicotinic receptors. In response to ACh binding, these nicotinic receptors undergo a conformational change which allows the flow of cations through a channel that is an integral part of the same protein. It has been known since the work of Paton and Zaimis [1] that the nicotinic receptors in mammalian ganglia differ pharmacologically from those in muscle. More recently it has been found that the structural and functional properties of the neuronal receptors also show many differences from muscle receptors (e.g. Refs. 2–6, see also 7).

Patch-clamp recording methods [8] can be used to characterize the functional properties of these receptor-channels in more detail than was previously possible [9–11]. In this chapter we will describe some of the basic properties (i.e. kinetic properties and conductance) of the neuronal nicotinic receptor-channels in mammalian sympathetic ganglia and in mammalian chromaffin cells. Chromaffin cells share the same embryonic origins as sympathetic neurones and both cells have many features in common. In addition, the actions of κ-bungarotoxin (κ-toxin) and clonidine will be compared. Both of these substances block the neuronal nicotinic receptors. We will therefore consider how they affect the properties of the individual receptors, and the conclusions that can be drawn about the molecular mechanism of action of these drugs.

Functional properties of mammalian neuronal nicotinic receptors

Fig. 1A shows examples of the whole-cell responses of rat sympathetic neurones to 10 μM ACh perfused over the surface of a cell held at three different potentials. ACh produces a fast inward current which shows some desensitization with time. The inward current is accompanied by a large increase in the membrane current noise. This reflects the random opening and closing of the individual channels which make up the whole-cell current induced by ACh. Analysis of the noise produced by

A

-50mV

-70mV

-90mV

200pA

10s

B
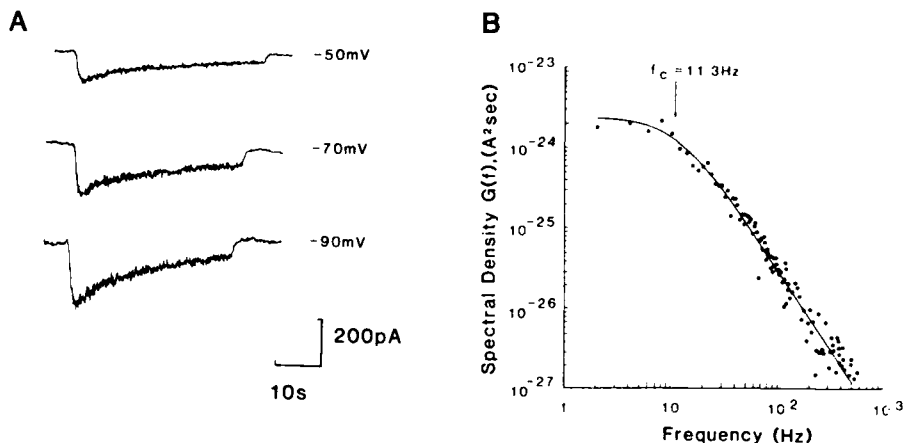
FIG 1 A: membrane current changes produced by 10 μM ACh in a single rat sympathetic neurone clamped at -50 mV, -70 mV and -90 mV. Bandwidth DC $=1$ kHz. B: power spectrum of current noise produced by steady application of 10 μM ACh to a neurone under whole cell clamp. The spectrum was fitted with a single Lorentzian curve (continuous line) with half-power frequency, $f_c = 11.3$ Hz. $V_h = -70$ mV. Band pass-filtered, 0.1 Hz–2 kHz (-3 dB, 8 pole Butterworth filter), temperature $= 22°$ C. From Ref. 9 with permission.

ACh gave spectra which could be fitted by a single Lorentzian component (Fig. 1B), which suggests that the simplest view of the channel is that it oscillates between two kinetically distinct states: closed $\rightleftharpoons$ open. At a holding potential of -70 mV, the time constant obtained from the single Lorentzian fit was 13.1 ± 0.7 ms ($n = 6$). This value is thought to represent the open lifetime [12,13] or burst length [14] of the individual channels underlying the current noise, in response to a single receptor activation. Similar analysis of ACh-noise in bovine chromaffin cells [15] gave a burst length of 11.0 ± 0.9 ms ($n = 7$) at a holding potential of -80 mV (see also Refs. 16, 17).

While whole-cell responses and noise analysis are useful in that they allow certain kinetic parameters to be estimated and allow the study of the average behaviour of a number of channels, a more detailed view of channel properties can be obtained by looking directly at the single channel currents in cell-attached or outside-out patches. Fig. 2A shows single channel currents recorded from a cell-attached patch on a rat sympathetic neurone. The channels were activated by 5 μM ACh contained in the pipette solution [11]. With 150 mM NaCl and 1 mM $CaCl_2$ in the extracellular solution the single channels have a slope conductance of 34.9 ± 1.2 pS ($n = 19$ patches). An individual receptor activation gives rise to a burst of openings separated by brief gaps (see Fig. 2A) similar to those described for muscle ACh-receptors [14,18–20]. Burst-length distributions have been constructed (see Ref. 18); an example is shown in Fig. 2B. The distributions were fitted well by the sum of two exponential components. Mean values for their time constants, in 8 cell-attached patches, were 0.42 ± 0.15 ms and 11.9 ± 1.0 ms (ACh 1–5 μM, at -100 mV and temperature $= 21–23°$ C). Single nicotinic channels in bovine chromaffin cells showed strikingly similar properties: the single channel conductance was 39.0 ± 0.7 pS (in 1 mM $CaCl_2$, $n = 10$ patches) and the burst-length distribu-

A
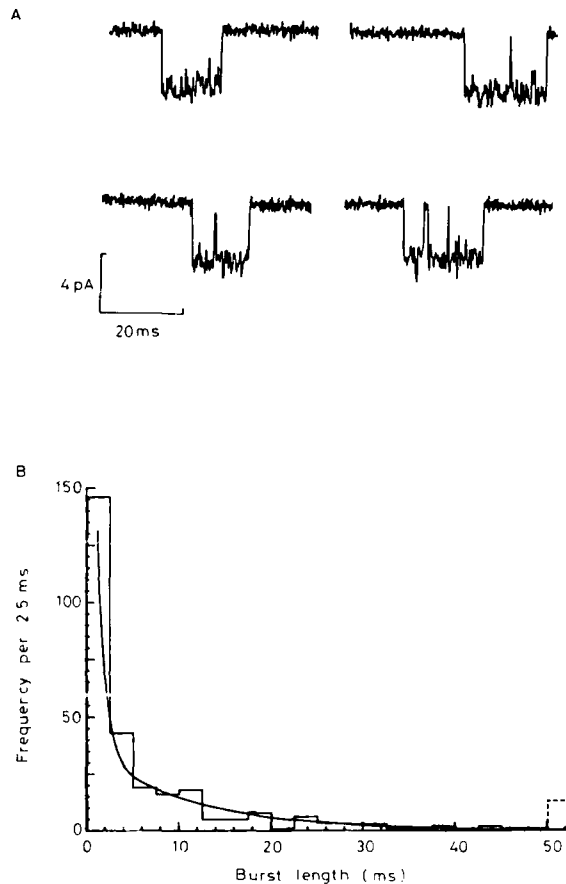
FIG 2   A: single channel currents activated by 5 μM acetylcholine in a cell-attached patch on a rat sympathetic neurone. Membrane potential was $V_m = (V_{rest} - 50)$ mV where V_{rest} is the resting potential of the cell usually about -50 mV. Bandwidth DC $= 2$ kHz, temp. $= 22°$ C. B: distribution of the duration of individual activations ('bursts') of channels evoked by acetylcholine (3 μM): cell-attached patch; $V_m = (V_{rest} - 50)$ mV. Dashed box shows the number of bursts longer than 50 ms. The distribution is fitted with two exponential components (solid line). Time constants were 0.8 ms and 11 ms with areas of 47% and 53% respectively. Modified from Ref. 11 with permission

tion was fitted by two exponential components with time constants of 0.69 ± 0.17 ms and 9.51 ± 0.84 ms ($n = 5$) [15]. For the receptors in both cells the relative areas of the two components that make up the burst distributions are about equal at these ACh concentrations (the concentration dependence is unknown at present). However, the longer burst component will carry most of the charge (about 97%) and may therefore have more relevance for synaptic transmission. It is also clear that the longer component of the burst-length distribution for single channels is very sim:'..r to the burst-length estimated from the time constant of the noise spectra. Furthermore, the burst-length duration is similar to the time constant of decay of the

synaptic current in mammalian sympathetic neurones, after appropriate corrections have been made for temperature and holding potential [5,6].

The blocking actions of κ-toxin and clonidine

Unlike muscle nicotinic receptors, most neuronal nicotinic receptors are insensitive to the blocking action of α-bungarotoxin (e.g. Ref. 21). However κ-toxin, another toxin fraction purified from the venom of the same snake, *Bungarus multicinctus*, blocks neuronal nicotinic receptors [22-24] including those in mammalian sympathetic ganglia [25]. It does not, however, appear to be equally effective in blocking all nicotinic receptors that are insensitive to α-bungarotoxin. Perhaps surprisingly, it has been shown that κ-toxin only weakly antagonizes nicotinic function in bovine adrenal chromaffin cells [26]. Fig. 3A shows the effect of this toxin on ACh-evoked whole cell currents in a rat sympathetic neurone. After 25 min, 100 nM κ-toxin had completely abolished the ACh current. The effect was reversible; the ACh response in this example had recovered after 61 min of wash with toxin-free solution. Sah et al. [25] have suggested that recovery from blockade by κ-toxin may be a biphasic
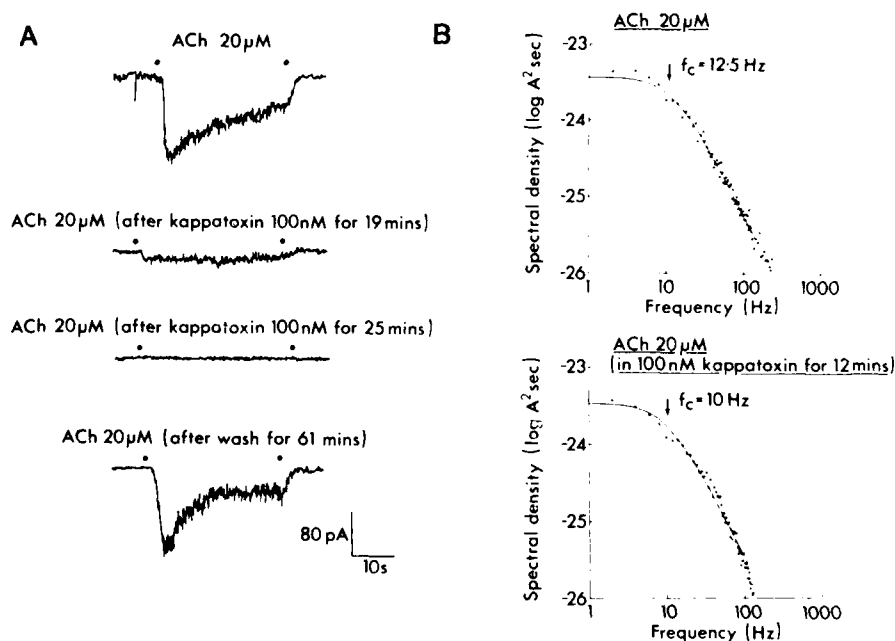
FIG 3 A: inward currents produced by steady application of 20 μM acetylcholine to rat sympathetic neurones in control solution; the presence of 100 nM κ-toxin for 19 min; the presence of 100 nM κ-toxin for 25 min and after wash for 61 min $V_H = -60$ mV, temp. = 23°C. B: (top) spectral density of ACh (20 μM) current-noise recorded in a rat sympathetic neurone under whole-cell clamp. Spectrum is fitted by a single Lorentzian component with $f_c = 12.5$ Hz; hence $\tau = 12.7$ ms ($V_H = -60$ mV). (Bottom) spectral density of ACh (20 μM) current-noise recorded in a rat sympathetic neurone under whole-cell clamp in the presence of 100 nM κ-toxin for 12 min. Spectrum is fitted by a single Lorentzian component with $f_c = 10$ Hz; hence $\tau = 15.9$ ms ($V_H = -60$ mV). Temperature = 23°C.
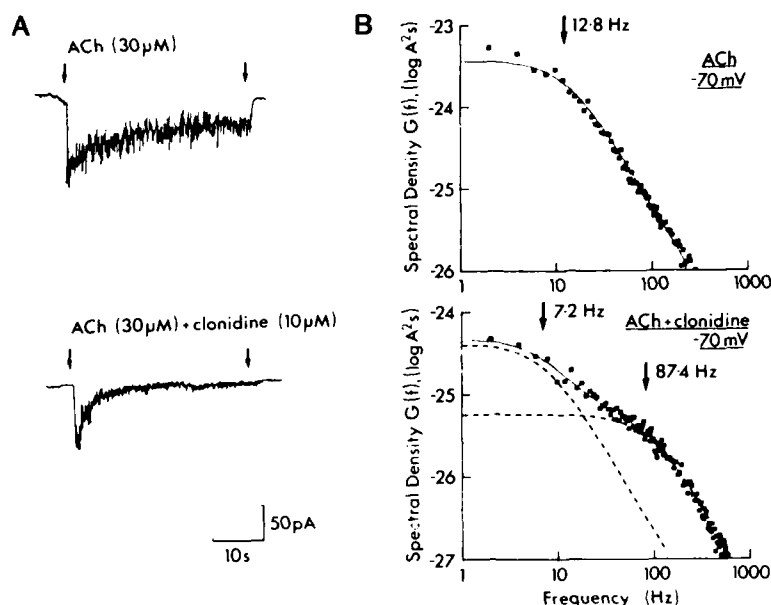
FIG 4   A: inward currents produced by steady application of 30 μM acetylcholine to a chromaffin cell in control solution then in the presence of 10 μM clonidine; V_H = - 90 mV. temp. = 22°C. B: (top) spectral density of ACh (30 μM) current-noise recorded under whole-cell clamp in a bovine chromaffin cell. Spectrum is fitted by a single Lorentzian component with f_c = 12.8 Hz; hence τ = 12.4 ms (V_H = - 70 mV). (Bottom) spectral density of ACh (30 μM) current-noise in the same cell in the presence of 10 μM clonidine. Spectrum is fitted by 2 Lorentzian components with f_{c1} = 7.2 Hz, f_{c2} = 87.4 Hz (τ_s = 22.1 ms, τ_f = 1.82 ms), V_H = - 70 mV. Temperature = 22°C. From Ref. 15 with permission.

process, with the rate of recovery of a population of neurones being dependent on the length of time that they were exposed to κ-toxin. In their experiments [25], if neurones were exposed only briefly to κ-toxin by pressure ejection most cells only took a few minutes to recover. On the other hand if they were exposed to κ-toxin for several minutes by bath perfusion, then most cells took tens of minutes or even hours to recover. Both phases of recovery from κ-toxin block are, however, much faster than recovery from blockade of muscle nicotinic receptors by α-bungarotoxin [27].

Clonidine is an α-adrenoceptor agonist used clinically in the control of hypertension. Initially, the inhibitory effect of clonidine on ACh-evoked secretion of catecholamines from bovine chromaffin cells was thought to be mediated via an α-adrenoceptor. However, it has recently been suggested [28] that clonidine may act on the nicotinic receptor-channel in bovine chromaffin cells. Patch-clamp experiments have demonstrated that clonidine does indeed have a direct action on the nicotinic receptor-channel complex both in chromaffin cells and in rat sympathetic neurones [15]. Fig. 4A shows this effect of clonidine on the ACh-evoked whole cell current of bovine chromaffin cells.

By comparing the reduction of the ACh-current produced by κ-toxin and clonidine in Figs. 3 and 4, it is not possible to get any real idea about their

mechanism of action, or indeed to decide whether they act at the same or different sites in the membrane. To do this it is necessary to look at the kinetic and conductance properties of the individual receptor-channels in the presence of these two substances.

Effect of κ-toxin on ACh noise

κ-Toxin (100 nM) produced a gradual reduction in the size of the whole-cell ACh current, with time, and eventually abolished it completely (Fig. 3A). However the single channel properties derived from analysis of ACh noise obtained 12 min after the application of 100 nM κ-toxin (i.e. when the whole-cell current was considerably reduced) were apparently unaltered (Fig. 3B). So, although less channels were open at any given time in the presence of κ-toxin, those that were opened by ACh showed normal kinetic and conductance properties.

The simplest way to interpret these observations is to suppose that κ-toxin acts to reduce the probability of ACh-binding to the receptor, without influencing events that occur subsequent to the ACh-binding step. This is, of course, not the only interpretation possible. A number of other actions by κ-toxin (including block of the ion channel itself) could occur at rates which produce no detectable influence on the noise spectrum. However this observation should not be taken in isolation. It has been shown that the presence of high concentrations of certain reversible antagonists like tubocurarine [23] and dihydro-β-erythroidine [25] can 'protect' the receptors and prevent κ-toxin binding and blockade. In contrast, other antagonists such as hexamethonium, which act at sites other than the receptive site, do not protect the receptor from blockade by κ-toxin [25]. Such protection experiments must be interpreted with some caution as the localization of the site of action of drugs like tubocurarine is itself complicated. Tubocurarine can act at the ganglionic nicotinic receptor primarily as a competitive antagonist in the frog [29] yet act primarily as a channel blocking drug in the rat [30]. The situation is further complicated by its action at muscle nicotinic receptors where it is both a competitive antagonist and a channel blocking drug [31]. Nevertheless it appears that the most likely site of action of κ-toxin is either at the ACh binding sites on the receptor protein or at a site nearby, which renders the ACh binding sites either unavailable or inaccessible.

Effect of clonidine on ACh noise

Clonidine alters the ACh noise spectra in bovine chromaffin cells so that they are best fitted by two Lorentzian components, rather than one; one component is faster and one slower than the single Lorentzian for the control noise spectra (Fig. 4B). This implies that clonidine alters the gating properties of the channels so that they can now exist in three kinetically distinct states rather than the two described for the control spectra [32,33]. If this third state is a blocked state the mechanism may (in the simplest case) be described by the sequential mechanism: closed ⇌ open ⇌ blocked [34,35]. The simplest, but by no means the only, physical mechanism which can account for such a scheme is to suppose that the blocking molecule enters and plugs the channel when it is open.

One consequence of this sequential scheme is that the channel cannot close directly from being blocked—it must open on becoming unblocked before returning to its original closed state. Because of this, a number of predictions can be made about the behaviour of the two Lorentzian components of the noise when the antagonist concentration is altered. For example, as the antagonist concentration is increased the fast time constant should get faster and the slow time constant slower, and the relative amplitude of the two components should vary in a predictable way (e.g. Ref. 36). Detailed analysis of the noise spectra obtained with varying clonidine concentration has shown that these parameters do not vary in the predicted manner (see Ref. 5 for details) and suggest that a more complex mechanism of block by clonidine must occur.

Single ACh channels in the presence of clonidine

From noise analysis it is clear that clonidine affects the kinetics of the ACh channels, however its mechanism of action seems to be complex, so it is worth considering its effect on single ACh channels to try to obtain further information about its mechanism of action. Inspection of the single channels in Fig. 5 shows that clonidine has no effect on the unitary conductance of the ACh channels. It does, however, appear to alter their kinetics as suggested from noise analysis. Fig. 5B shows that clonidine reduces the length of 'apparent openings'. The corrected mean open time (corrected to account for the many brief closings below the resolution of the recording system [18]) is reduced from 1.57 ms to 0.43 ms by 2 μM clonidine. Clonidine also reduced the length of bursts of openings (Fig. 5C). 2 μM clonidine reduced the fast component of the burst distribution from 0.69 ms to 0.42 ms and the slow component from 9.51 ms to 3.75 ms. Finally, clonidine also reduced the frequency of apparent openings. In one particular experiment the frequency of apparent openings (produced by 5 μM ACh) was reduced by 5 μM clonidine from 4.57 per second to 0.44 per second.

These results, as with the data from noise analysis, are inconsistent with the simple 3-state sequential block scheme described earlier, as well as being inconsistent with purely competitive block. For example, a consequence of the sequential block scheme is that the total length of time the channel stays open during a single activation, a burst, should be independent of the antagonist concentration [37,38]. Thus the mean burst length should increase in the presence of the antagonist due to the increased time spent in the blocked state, while the length of time spent in the open state within a single burst should add up, on average, to the same length of time seen in the open state in the absence of the antagonist. The single channel data for clonidine suggests, rather, that the burst length is reduced in the presence of the antagonist, and that the total length of time the channel spends in the open state is also considerably reduced.

Therefore a simple 3-state sequential model will not suffice and it must be proposed either that clonidine pushes the channel into a blocked state from which it can close directly (i.e. a cyclical model) or that a fourth long-lived blocked state must exist (e.g. Refs. 39, 40). These two possibilities are difficult to distinguish [40], particularly when the blocking effect shows little dependence on the membrane potential as is the case with clonidine [15]. A number of other drugs, (for example, procaine [41,42], benzocaine [43], substance P [17,44], trifluoperazine [45], hexa-
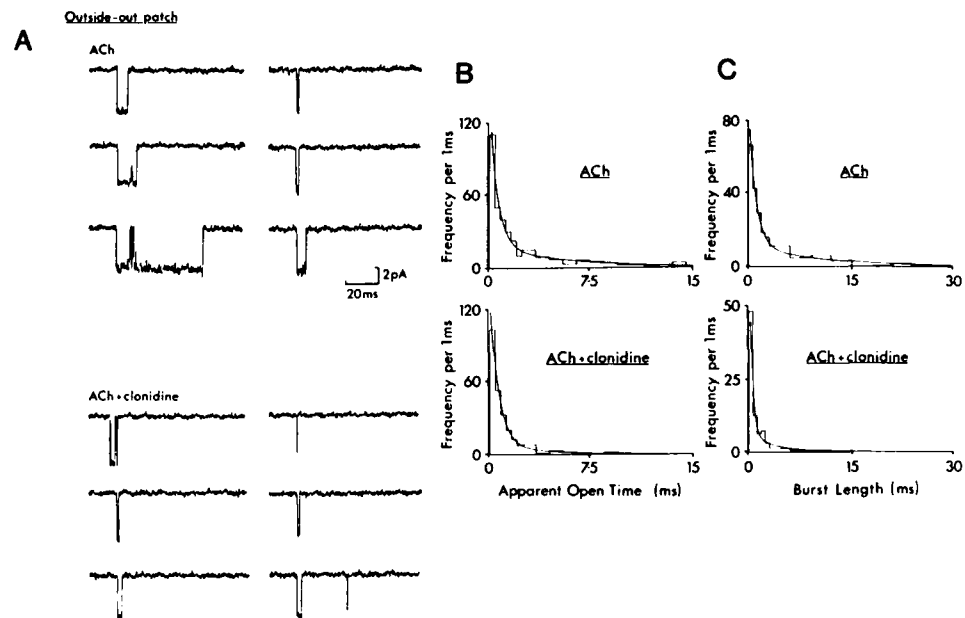
FIG 5 A: single channel currents activated by ACh in an outside-out patch from a chromaffin cell. (top) currents produced by 5 μM ACh ($V_H = -110$ mV). (Bottom) ACh-currents in the same patch in the presence of 2 μM clonidine. Temperature $= 23°$C. B: examples of the distributions of all apparent open-times of ACh channels in outside-out patches. (Top) 5 μM ACh alone, distribution fitted with 2 exponential components, $\tau_f = 0.61$ ms and $\tau_s = 5.49$ ms ($V_H = -90$ mV). (Bottom) 5 μM ACh and 2 μM clonidine fitted with 2 exponentials, $\tau_f = 0.65$ ms and $\tau_s = 3.98$ ms ($V_H = -110$ mV). C: examples of the burst-length distributions for ACh channels in outside-out patches. (Top) 5 μM ACh alone (critical gap length $= 1.05$ ms) fitted with 2 exponentials, $\tau_f = 1.02$ ms and $\tau_s = 10.3$ ms (V_H -90 mV). (Bottom) 5 μM ACh and 2 μM clonidine (critical gap length $= 0.896$ ms) fitted with 2 exponentials, $\tau_f = 0.42$ ms and $\tau_s = 3.75$ ms ($V_H = -110$ mV). For all histograms the resolution was set at 90 μs for open-time and 60 μs for shut-times. From Ref. 15 with permission.

methonium [39] and pentobarbitone [46]) appear to block both muscle and neuronal nicotinic channels in a similarly complex manner.

It is much more difficult to correlate these more complicated kinetic models with a physical view of how the blocking drug acts. As noted above a physical plugging of the ion channel is too simple a model. A number of other possibilities can be proposed, but at present they remain difficult to test. For example, it may be that the blocking drug plugs the channel which can then shut, so that the drug remains trapped within the channel (e.g. Ref. 39). Alternatively, the blocking drug may act with different affinities at more than one site in the channel, or it may act at a site or sites close to the channel and alter its gating by some allosteric mechanism. Finally, the blocking effect could be related to an enhancement of agonist-induced desensitization. This last suggestion would be difficult to substantiate until either the physical mechanism of agonist-induced desensitization is better understood, or a method is found for inhibiting or reducing the agonist-induced desensitization itself.

Conclusions

It is clear that patch-clamp recording techniques and the kinetic analysis of the results obtained provide a useful tool to help to elucidate the site of action of agents which block transmitter-activated ion channels. This is particularly true when trying to discover whether a particular chemical acts principally at the transmitter binding site, or at the ion channel itself (either to reduce the rate of ion conduction through the channel when it is open, or to alter its gating properties). It is equally clear, however, that there are a number of chemicals (such as clonidine) that interfere with channel kinetics, by mechanisms that are too complex to be fully resolved at present.

Acknowledgements

References

1 Paton, W.D.M. and Zaimis, E.J. (1951) Paralysis of autonomic ganglia by methonium salts. Br. J. Pharmacol. 6, 155–168.
2 Boulter, J., Evans, K., Goldman, D., Martin, G., Treco, D., Heinemann, S. and Patrick, J. (1986) Isolation of a cDNA clone coding for a possible neural nicotinic acetylcholine receptor α-subunit. Nature 319, 368–374.
3 Goldman, D., Simmons, D., Swanson, L., Patrick, J. and Heinemann, S. (1986) Mapping brain areas expressing RNA homologous to two different acetylcholine receptor alpha subunit cDNAs. Proc. Natl. Acad. Sci. U.S.A. 83, 4076–4080.
4 Goldman, D., Deneris, E., Luyten, W., Kochhar, A., Patrick, J. and Heinemann, S. (1987) Members of a nicotinic acetylcholine receptor gene family are expressed in different regions of the mammalian central nervous system. Cell 48, 965–973.
5 Derkach, V.A., Selyanko, A.A. and Skok, V.I. (1983) Acetylcholine-induced current fluctuations and fast excitatory post-synaptic currents in rabbit sympathetic neurones. J. Physiol. 336, 511–526.
6 Hirst, G.D.S. and McLachlan, E.M. (1984) Post-natal development of ganglia in the lower lumbar sympathetic chain of the rat. J. Physiol. 349, 119–134.
7 Colquhoun, D., Ogden, D.C. and Mathie, A. (1987) Nicotinic acetylcholine receptors of nerve and muscle: functional aspects. Trends Pharm. Sci. 8, 465–472.
8 Hamill, O.P., Marty, A., Neher, E., Sakmann, B. and Sigworth, F.J. (1981) Improved patch clamp techniques for high-resolution current recording from cells and cell-free membrane patches. Pflügers Arch. 391, 85–100.
9 Cull-Candy, S.G. and Mathie, A. (1986) Ion channels activated by acetylcholine and γ-aminobutyric acid in freshly dissociated sympathetic neurones of rat. Neurosci. Lett. 66, 275–280.
10 Derkach, V.A., North, R.A., Selyanko, A.A. and Skok, V.I. (1987) Single channels activated by acetylcholine in rat superior cervical ganglion. J. Physiol. 388, 141–151.
11 Mathie, A., Cull-Candy, S.G. and Colquhoun, D. (1987) Single-channel and whole-cell currents evoked by acetylcholine in dissociated sympathetic neurones of the rat. Proc. Roy. Soc. Ser. B 232, 239–248.

12 Katz, B. and Miledi, R. (1972) The statistical nature of the acetylcholine potential and its molecular components. J. Physiol. 224, 665–699.

13 Anderson, C.R. and Stevens, C.F. (1973) Voltage clamp analysis of acetylcholine produced end-plate fluctuations at frog neuromuscular junction. J. Physiol. 235, 655–691.

14 Colquhoun, D. and Sakmann, B. (1981) Fluctuations in the microsecond time range of the current through single acetylcholine receptor ion channels. Nature 294, 464–466.

15 Cull-Candy, S.G., Mathie, A. and Powis, D.A. (1988) Acetylcholine receptor-channels and their block by clonidine in cultured bovine chromaffin cells. J. Physiol. 402, 255–278.

16 Fenwick, E.M. Marty, A. and Neher, E. (1982) A patch-clamp study of bovine chromaffin cells and of their sensitivity to acetylcholine. J. Physiol. 331, 577–597.

17 Clapham, D.E. and Neher, E. (1984) Substance P reduces acetylcholine-induced currents in isolated bovine chromaffin cells. J. Physiol. 347, 255–277.

18 Colquhoun, D. and Sakmann, B. (1985) Fast events in single-channel currents activated by acetylcholine and its analogues at the frog muscle end-plate. J. Physiol 369, 501–557.

19 Dionne, V.E. and Leibowitz, M. (1982) Acetylcholine receptor kinetics: a description from single-channel currents at snake neuromuscular junctions. Biophys. J. 39, 253–261.

20 Sine, S.M. and Steinbach, J.H. (1984) Activation of a nicotinic acetylcholine receptor. Biophys. J. 45, 175–185.

21 Brown, D.A. and Fumagalli, L. (1977) Dissociation of α-bungarotoxin binding and receptor block in the rat superior cervical ganglion. Brain Res. 129, 165–168.

22 Ravdin, P.M. and Berg, D.K. (1979) Inhibition of neuronal acetylcholine sensitivity by α-toxins from Bungarus multicinctus venom. Proc. Natl. Acad. Sci. U.S.A. 76, 2072–2076.

23 Chiappinelli, V.A. (1983) Kappa-bungarotoxin: a probe for the neuronal nicotinic receptor in avian ciliary ganglion. Brain. Res. 277, 9–22.

24 Loring, R.H., Chiappinelli, V.A. Zigmond, R.E. and Cohen, J.B. (1984) Characterization of a snake venom neurotoxin which blocks nicotinic transmission in the avian ciliary ganglion. Neuroscience 11, 989–999.

25 Sah, D.W.Y., Loring, R.H. and Zigmond, R.E. (1987) Long-term blockade by toxin F of nicotinic synaptic potentials in cultured sympathetic neurones. Neuroscience 20, 867–874.

26 Higgins, L.S. and Berg, D.K. (1987) Immunological identification of a nicotinic acetylcholine receptor on bovine chromaffin cells. J. Neurosci. 7, 1792–1798.

27 Blanchard, S.G., Quast, U., Reed, K., Lee, T., Schimerlik, M.I. Vandlen, R., Claudio, T., Strader, C.D., Moore, H.-P.H. and Raftery, M.A. (1978) Interaction of $[^{125}I]$ α-bungarotoxin with the acetylcholine receptor from Torpedo californica. Biochemistry 18, 1875–1883.

28 Powis, D.A. and Baker, P.F. (1986) α_2-Adrenoceptors do not regulate catecholamine secretion by bovine adrenal medullary cells: a study with clonidine. Mol. Pharmacol. 29, 134–141.

29 Lipscombe, D. and Rang, H.P. (1988) Nicotinic receptors of frog ganglia resemble pharmacologically those of skeletal muscle. J. Neurosci., in press.

30 Rang, H.P. (1982) The action of ganglionic blocking drugs on the synaptic responses of rat submandibular ganglion cells. Br. J. Pharmacol. 75, 151–168.

31 Colquhoun, D. (1986) On the principles of postsynaptic action of neuromuscular blocking agents. In: Handbook of Experimental Pharmacology. (D.A. Kharkevich, ed.), Vol. 79 pp. 59–113. Springer-Verlag.

32 Colquhoun, D. and Hawkes, A.G. (1977) Relaxations and fluctuations of membrane currents that flow through drug-operated ion channels. Proc. R. Soc. Ser. B 199, 231–262.

33 Neher, E. and Stevens, C.F. (1977) Conductance fluctuations and ionic pores in membranes. Ann. Rev. Biophys. Bioeng. 6, 345–381.

34 Armstrong, C.M. (1971) Interaction of tetraethylammonium ion derivatives with the potassium channels of giant axons. J. Gen. Physiol. 58, 413–437.

35 Adams, P.R. (1976) Drug blockade of open end-plate channels. J. Physiol. 260, 531–552.

36 Colquhoun, D. and Sheridan, R.E. (1981) The modes of action of gallamine. Proc. Roy. Soc. Ser. B 211, 181–203.

37 Neher, E. and Steinbach, J.H. (1978) Local anaesthetics transiently block currents through single acetylcholine receptor channels. J. Physiol. 277, 153–176.

38 Colquhoun, D. and Hawkes, A.G. (1982) On the stochastic properties of bursts of single ion channel openings and of clusters of bursts. Phil. Trans. Roy. Soc. Ser. B. 300, 1–59.

39 Gurney, A.M. and Rang, H.P. (1984) The channel blocking action of methonium compounds on rat submandibular ganglion cells. Br. J. Pharmacol. 82, 623–642.

40 Ogden, D.C. and Colquhoun, D. (1985) Ion channel block by acetylcholine, carbachol and suberyldicholine at the frog neuromuscular junction. Proc. Roy. Soc. Ser. B. 225, 329–355.

41 Katz, B. and Miledi, R. (1975) The effect of procaine on the action of acetylcholine at the neuromuscular junction. J. Physiol. 249, 269–284.

42 Adams, P.R. (1977) Voltage jump analysis of procaine action at frog end-plate. J. Physiol. 268, 291–318.

43 Ogden, D.C., Siegelbaum, S.A. and Colquhoun, D. (1981) Block of ACh-activated ion channels by an uncharged local anaesthetic. Nature 289, 596–598.

44 Role, L.W. (1984) Substance P modulation of acetylcholine-induced currents in embryonic chicken sympathetic and ciliary ganglion neurons. Proc. Natl. Acad. Sci. U.S.A. 81, 2924–2928.

45 Clapham, D.E. and Neher, E. (1984) Trifluoperazine reduces inward ionic currents and secretion by separate mechanisms in bovine chromaffin cells. J. Physiol. 353, 541–564.

46 Gage, P.W. and McKinnon, D. (1985) Effects of pentobarbitone on acetylcholine-activated channels in mammalian muscle. Br. J. Pharmacol. 85, 229–235.

CHAPTER 30

Glutamate activated membrane channels in crustacean muscle fibres

J. Dudel, Ch. Franke and H. Hatt

Physiologisches Institut der Technischen Universität München, Biedersteiner Straße 29, 8000 München 40, F.R.G.

Two kinds of membrane channels can be activated by L-glutamate in the membrane of muscles of crayfish and rock lobster [1-3]. Previously published information on these channels will be briefly reviewed and some new, recent findings will be treated in greater detail.

The first kind of channel is excitatory with about 100 pS conductance (Fig. 1). Cations pass through this channel with permeabilities similar to those of the channels of the vertebrate endplate [4,5]. The channels have been recorded in cell-attached and excised patches [1,6]. The single channel openings have an average duration of 0.15 ms. Openings are grouped in bursts with intermittent gaps of on average < 0.1 ms duration. The mean burst length depends on the glutamate concentration, increasing from 0.2 ms at 0.1 mM to about 2 ms at 20 mM glutamate (Fig. 1) [7]. The kinetics of this channel can be described by a reaction scheme in which consecutive binding of two glutamate molecules leads to a channel configuration which is still closed but from which the channel molecule can change its conformation to an unstable open state, oscillating between the open and the closed conformation until dissociation of one of the bound glutamate molecules ends the 'burst' [1,7]. These kinetics and the respective rate constants are very similar to those proposed for the nicotinic cholinergic channels of the vertebrate by Colquhoun and Sakmann [8].

The excitatory channels of crayfish muscle show a curious dependence on extracellular calcium concentration. Reduction of the extracellular calcium concentration from the 'physiological' level of 13.5 mM to e.g. 1 mM does not affect the channel current amplitude appreciably, but reduces the rate of channel openings by orders of magnitude and shortens the bursts to single openings. In the absence of extracellular Ca^{2+} no channel openings can be observed [9]. Addition of inorganic 'Ca channel blockers' like La^{3+}, Cd^{2+}, Co^{2+} and Ni^{2+} to physiological saline depresses the rate of channel openings exactly like a low Ca^{2+} concentration. On the other hand, Ba^{2+} or relatively high concentrations of Mg^{2+} can replace Ca^{2+} in permitting channel openings [9]. It was concluded that the excitatory glutamate receptor/channel contains one or two binding site(s) for Ca^{2+}, occupation of which by Ca^{2+}, Ba^{2+} or Mg^{2+} permits gating of the channel by glutamate. The inorganic Ca-channel blockers are supposed to inhibit the occupation of the binding site(s) by

406

0.1 mM GLUTAMATE

10 pA

5 mM GLUTAMATE

5 ms
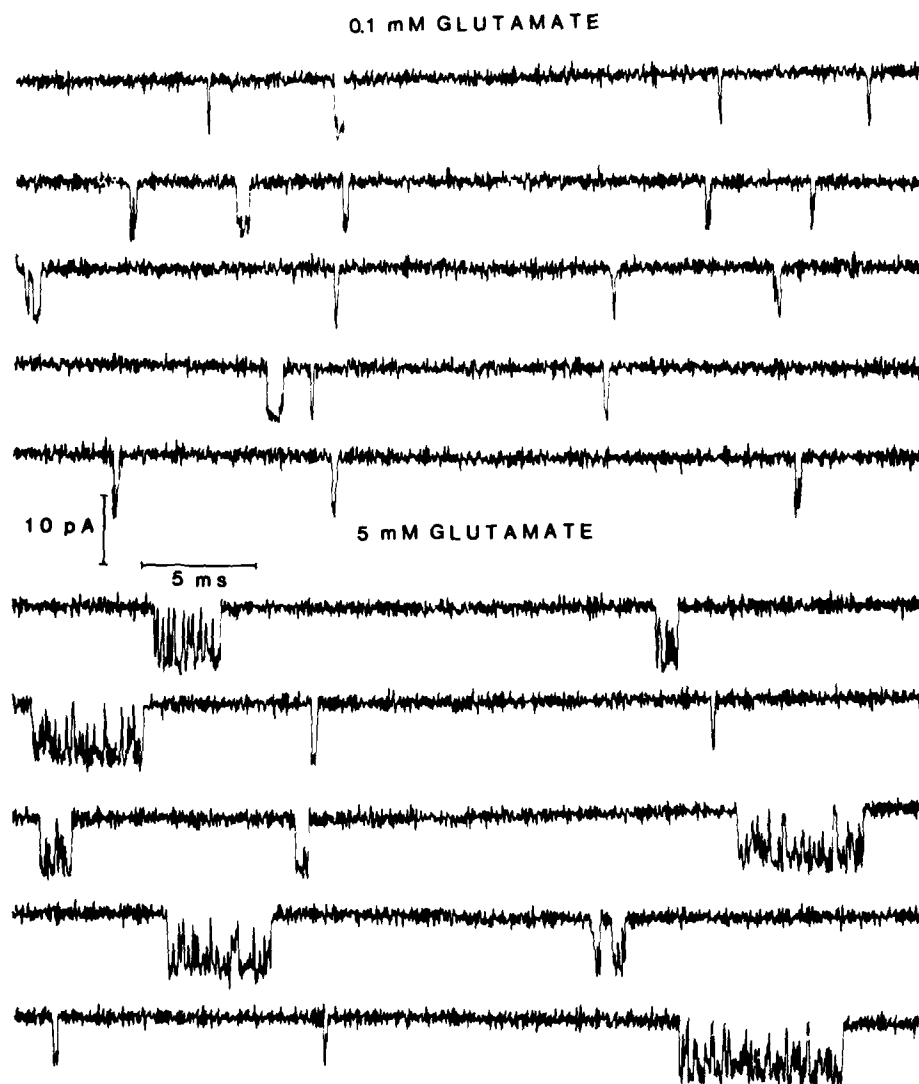
FIG 1 Samples of single channel recordings with a low (0.1 mM) and a high (5 mM) concentration of glutamate. Bandwidth 10 kHz, calibration same for all samples. Excitatory. cation channel. Reprinted from Ref. 7.

Ca^{2+}. Also synaptic quantal currents recorded at low extracellular Ca concentrations or on addition of Cd^{2+} are greatly reduced in amplitude and shortened [9]. The reduction of the amplitude of excitatory currents in crayfish muscle has already been reported by Florey and Woodcock [10] and especially by Nickell and Boyarski [11].

While glutamate seems to be the natural transmitter at the neuromuscular junctions of crayfish [12], the excitatory channels are activated more potently by
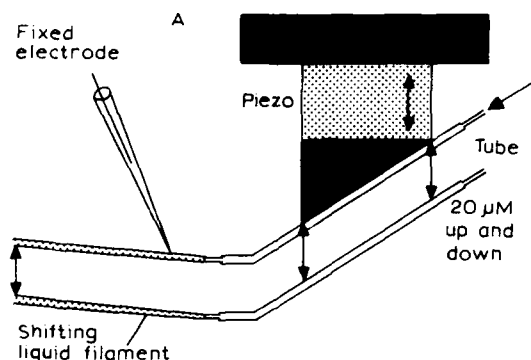
FIG 2   Liquid-filament switch for the application of pulses of agonists to an outside-out patch at the tip of an electrode. A: scheme of the apparatus, description in text. B: displacement of the tube on application of 1000 V to the piezo.

quisqualate [13] with kinetics very similar to those of activation by glutamate [1]. In contrast, the glutamate agonists kainate and N-methyl-D-aspartate did not trigger channel openings, even if applied in mM concentrations [1]. In the accepted classification of glutamate channels [14], the excitatory channels of crustacean muscle thus belong to the quisqualate type.

It is known from macroscopic measurements in crayfish muscle that membrane current elicited by glutamate pulses exhibits strong desensitization with time constants of decay < 1 s [15,16]. The recordings of channel currents discussed so far were all done in the continuous presence of the agonist, and it seemed necessary to study channel currents after rapid application of glutamate to the excised patch. A liquid-filament switch was developed [17], in which a thin filament of glutamate containing solution was ejected from a tube with about 30 μm inner diameter into the saline superfusing the patch (Fig. 2A). The filament remained confined to a small diameter for the length of the chamber. The tube from which the filament was ejected was fixed to a piezo crystal, which on application of a high voltage could move the tube upward by 20 μm. The movement was complete within 200 μs (Fig. 2B). The filament was arranged to pass a small distance below the outside-out patch when the piezo was extended, and to be shifted onto the patch when the piezo was contracted (Fig. 2A). Very rapid glutamate pulses could be applied in this fashion. and large numbers of pulses could be used at one patch to obtain sufficient data to evaluate non-steady-state channel kinetics.

In the experiments in which glutamate was applied continuously, about half of the outside-out patches showed no activity of the excitatory channel. When glutamate was applied with the rapid switch, excitatory channel activity was evoked in most patches. However, a considerable proportion of patches contained channels which desensitized completely in presence of glutamate. In the patch of Fig. 3 [18], no channels opened in some glutamate applications (second trace in left hand column). If channel activity appeared, it was evoked within the first few ms of application,with no further channel opening 30 ms after glutamate application. The trace at the bottom of the left hand column in Fig. 3 is an average of 50 single recordings. It shows that channel opening declined to zero with a time constant of about 5 ms. In the right hand column of Fig. 3 recordings from another patch of

outside-out patch,opener muscle

-75 mV | 1mM glutamate

I2 pA

10 pA   singles

2ms   singles

1pA   50 averaged

02 nA   EPSC
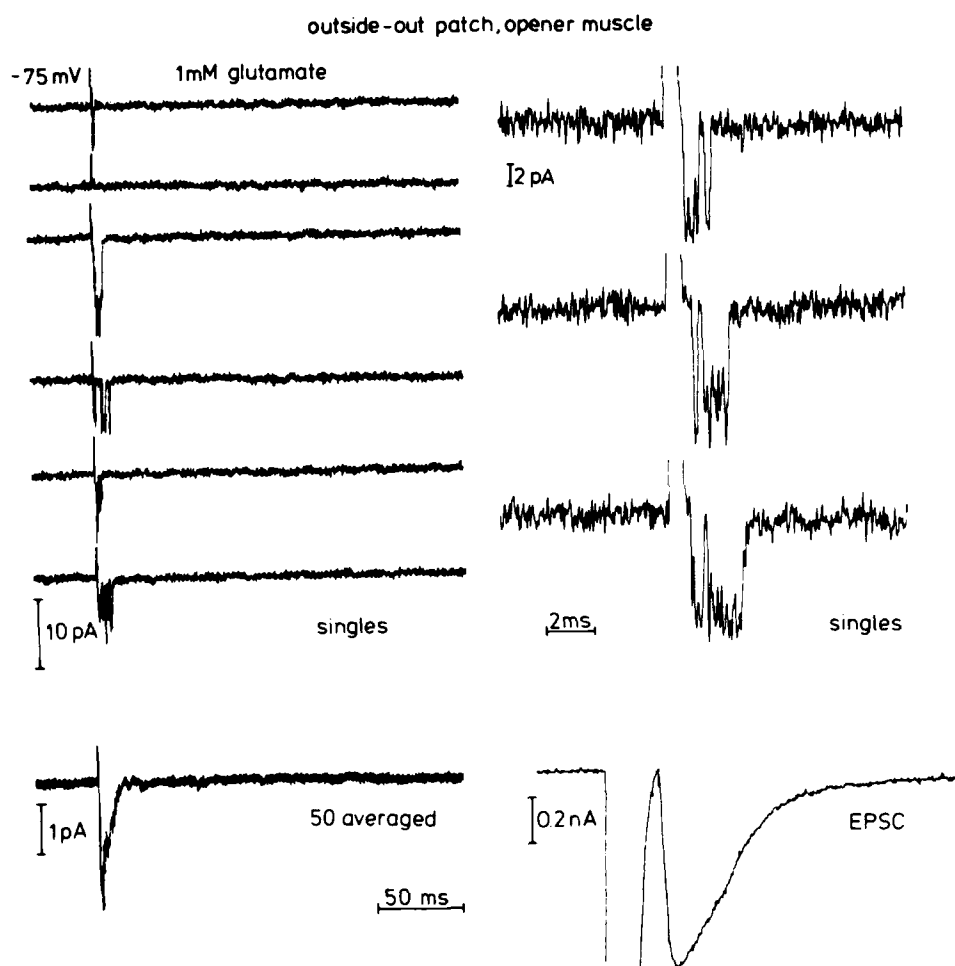
50 ms

FIG 3 Left hand column: openings of excitatory channels elicited by a step of 10^{-3} M glutamate starting at the switching artefact and lasting more than 250 ms (end not shown). The upper six traces are single recordings, the lowest trace an average of 50 such recordings. Right hand column: 3 traces from other patch shown at higher time resolution, same glutamate pulses as in left column. Bottom: quantal postsynaptic current recorded with macro-patch clamp. Same time resolution as above, for comparison of time courses.

this type are presented with a better time resolution. Bursts of channel openings are seen to be triggered within 0.2 to 0.5 ms after application of glutamate. Maximally one burst was evoked after each stimulus, the channels obviously being desensitized before there is a chance of generation of another burst. The bottom trace on the right of Fig. 3 is an extracellular recording of a quantal current by means of the macro-patch technique [19]. This quantal current was arranged to have the same time resolution as the channel openings presented above. It seems possible that the decay of the quantal current could have been generated by the average of the single
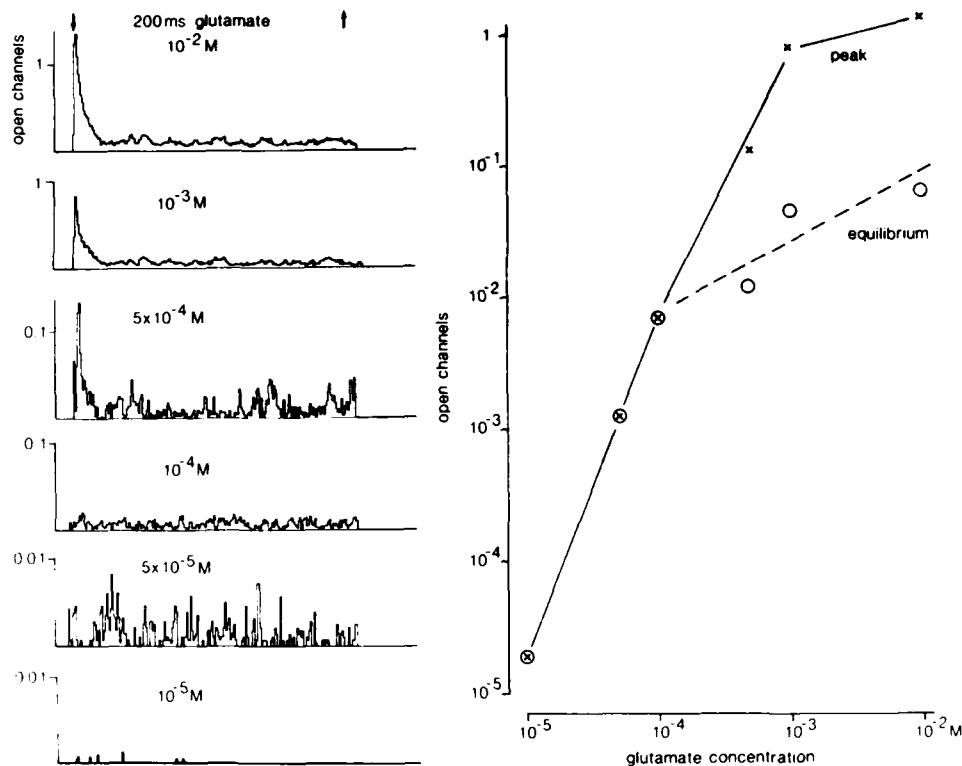
FIG 4 Openings of excitatory channels elicited by a 200 ms pulse of 10^{-5} to 10^{-2} M glutamate. Left hand column: evaluation of average number of open channels during 0.1 ms time intervals after the start of the glutamate pulse. Two excitatory channels present in patch. Note different calibrations of ordinates for different glutamate concentration. Graph: peak number of open channels and equilibrium level of channel opening (from the averages to the left), plotted against the applied glutamate concentration. Logarithmic scales.

bursts above, i.e. that the decay of the quantal current might reflect desensitization after a glutamate pulse lasting more than a few ms.

The excitatory channels do not desensitize completely in all patches in the presence of glutamate. An example of this type of channel is shown in Ref. 17, Fig. 2, and Fig. 4 presents average probabilities of the open state for another patch for glutamate concentrations from 10^{-5} to 10^{-2} M. Two excitatory channels were present in this patch, and if the ordinate values are divided by two they represent the average probability for one channel to be open. On application of 10 mM glutamate, a peak probability to be open of 0.7 is reached within 0.3 ms, and then desensitization takes over with an apparent time constant of about 5 ms. Finally, desensitization reaches a steady state of about 0.05 peak amplitude. Activations at 1 mM and 0.5 mM glutamate had a similar time course, but the time-to-peak lengthened to 0.5 ms at 0.5 mM glutamate. At 10^{-4} M glutamate and lower concentrations, no desensitization was observed. The dependence on glutamate concentration of the peak values of 'open channels', and of the respective equi-

librium levels are plotted also in Fig. 4. Up to 1 mM glutamate the double-logarithmic slope of this relation for the 'peaks' is 2.5, showing a highly cooperative dependence on glutamate concentration. For concentrations higher than 1 mM, the peak values approach a saturation level, and the same applies to the equilibrium levels for glutamate concentrations above 0.1 mM.

The apparent time constant of desensitization was about 5 ms in the experiments of Figs. 3 and 4, with no obvious dependence on glutamate concentration. We call this time constant 'apparent', because it may not reflect solely the desensitization process. At high glutamate concentrations, the average duration of bursts is several ms (Fig. 1, see also Fig. 5), and the decay of the open probability should contain a negative exponential caused by burst duration in addition to the decay in the probability of new bursts due to desensitization. The 'apparent time constant of desensitization' of 5 ms thus is an upper limit for the 'true' time constant of desensitization. The present data are not conclusive regarding the mechanism of desensitization. The evidence seems to be compatible with different classes of mechanisms: desensitization from the open state by a conformation change as suggested originally by Katz and Thesleff [20] or by binding or unbinding of agonist, or desensitization from a closed state by binding of agonist. Nevertheless, desensitization in these glutamate activated channels is much more rapid and effective than imagined.

In their classical description of the time course of the quantal endplate current, Magleby and Stevens [21] gave evidence that the transmitter opened the channels almost simultaneously and only once, so that the time constant of decay of the endplate current was about the same as the average duration of the single channel opening. With better resolution, this average duration was identified as the duration of bursts of openings (e.g. Ref. 8). This concept implied that the transmitter was present at the receptors for less than the average burst length, since reopenings of channels should be rare. To mimic the proposed synaptic conditions, we applied glutamate in short pulses. Fig. 5 shows results of control pulses of 20 ms duration, as well as those of 0.4 ms pulses. The average duration of bursts of channel openings after the 20 ms pulses was 4 ms. The average current rose to its peak rapidly and decayed with the usual time constant of desensitization of 5 ms. The 0.4 ms pulse elicited the same number of bursts as the longer pulse, as evidenced by the same average peak current amplitudes for both pulse lengths. Also the rise times were identical at 0.3 ms. However, after the 0.4 ms pulses the bursts were clipped short, and the average current decayed with a time constant < 1 ms. The 0.4 ms glutamate pulse thus generated an average current which rose more rapidly and decayed more rapidly than a natural quantal current (compare Fig. 3). These results indicate that activation of receptors occurs with more temporal dispersion in the synapse as compared with the pulse in the patch, and that a high concentration of glutamate is present at the synaptic receptors for more than 0.4 ms, and probably for several ms. It seems probable, therefore, that desensitization contributes to the decay of quantal currents in the neuromuscular junction of crayfish.

The excitatory, glutamate-activated channels in crayfish seem to be close relatives of the D-receptor/channels of locusts (see Chapter 28). Also the rapid activation and desensitization properties are similar for the excitatory channels of locusts and crayfish, as shown in a preliminary publication together with Ramsey and Usherwood [18].

To our great surprise, L-glutamate applied to outside-out patches activated also a
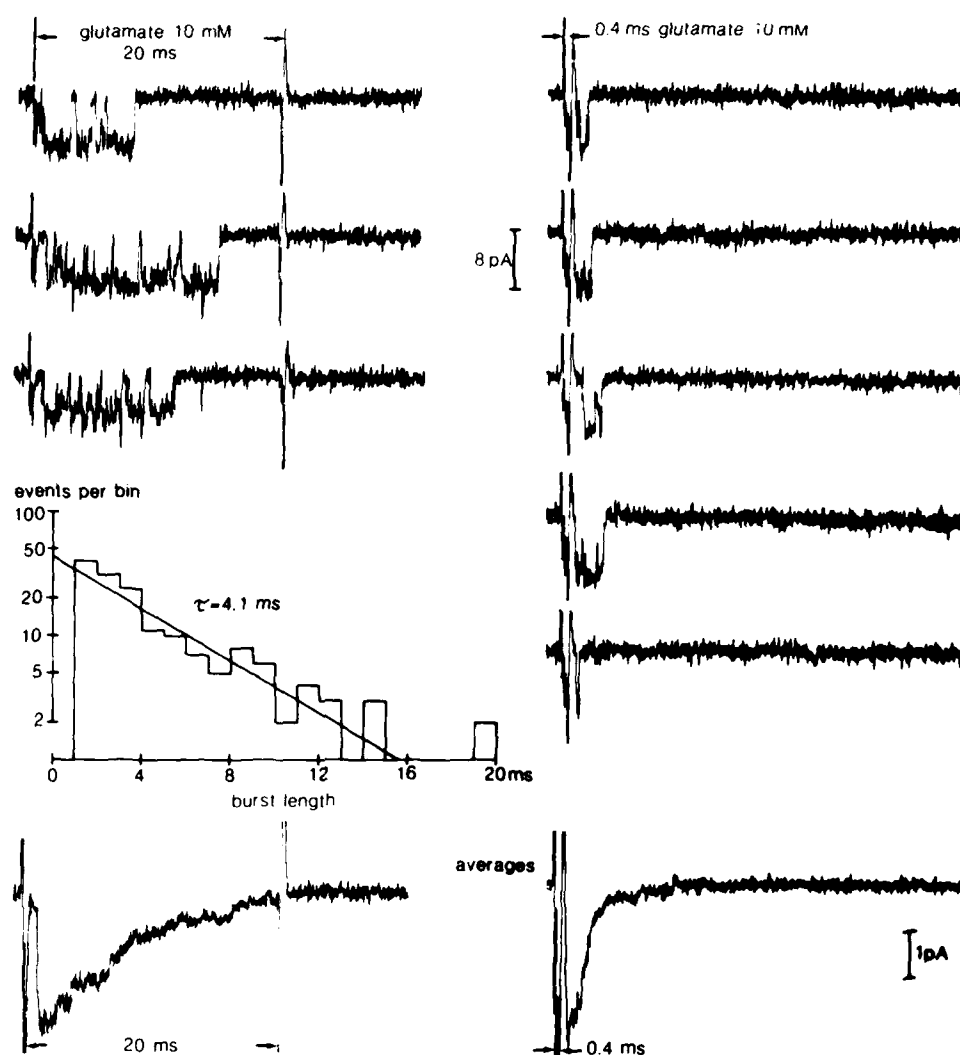
FIG 5 Results of application of 10 mM glutamate in pulses of 20 ms (left hand column) or
0.4 ms duration (right hand column) in one patch. For the 20 ms pulses, 3 sample traces of
excitatory channel openings are shown. Below is a distribution of the burst durations
measured under these conditions. In the bottom, the average current is presented. For the 0.4
ms pulse, 5 sample traces are shown, and below an average. Note that after both pulses the
average currents reached the same peak amplitude, but that the brief pulse shortened burst
duration.

chloride channel [2]. The left hand row of traces of Fig. 6 shows an example: 1 μM
glutamate elicited many, relatively long channel openings. These openings have a
basic amplitude of 22 pS, but in addition to this basic state 1, openings occurred to
a state 2 of 44 pS and rarely to state 3 of 66 pS. These higher 'states' are not

412

Opener, leg, outside-out patch, -100 mV

Glu 1 μM

GABA 10 μM

5 pA

100 ms
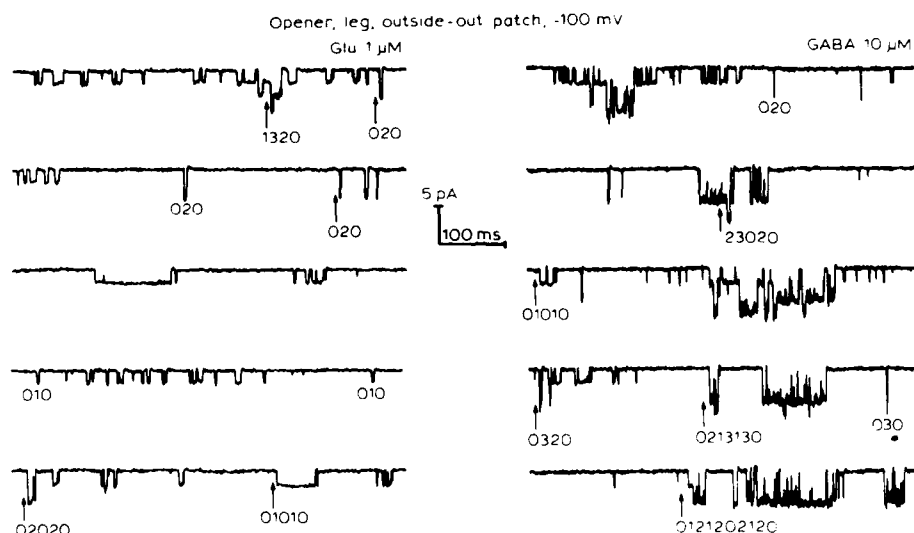
FIG 6   Recordings from one outside-out patch polarized to −100 mV, Cl⁻-channel openings being elicited by 1 μM glutamate (left hand panel) and 10 μM GABA (right hand panel). The channel opens to 3 substates I_1, I_2, I_3, with amplitudes of about −2, −4 and −6 pA. Some sequences of substates are marked by 0, 1, 2, 3 which refer to the closed state, and open state I_1, I_2, I_3, respectively. If necessary, the starting points of the respective sequences are marked by arrows. Patch from opener muscle of the first walking leg. Bandwidth 0–1 kHz. Reprinted from Ref. 2.

superimpositions of openings of several channels, but openings of single channels as seen at higher time resolution. The occurrence of the states I_1, I_2 and I_3 is demonstrated also in the channel amplitude distribution of Fig. 7A. In the right hand column of Fig. 6, in the same patch, similar channel activity was elicited by 10 μM GABA. With GABA, state 2 was predominant, and state 3 less rare than in activations by glutamate (compare also Fig. 7C). Both activation by glutamate and by GABA can be suppressed by picrotoxin (Fig. 7), the typical blocker of inhibitory currents [22,23]. Comparison of the effects of glutamate or GABA alone with those of simultaneous applications of both show that these substances really activate the same channels [1]. Quisqualate acts like glutamate, and β-guanidino-propionic acid or muscimol act like GABA.

Average open times were determined for the different states of channels. They are characteristic for the state but apparently largely independent of the agonist used. The burst lengths contained components of about 3 and about 35 ms for activations both by glutamate and by GABA [1].

Further experiments with F. Zufall [24] had the unexpected result that nicotinic agonists also opened the chloride channels. Fig. 8 shows, for one patch, activation of the same channel type by carbachol, glutamate and GABA. Carbachol, like glutamate, elicited channel openings predominantly into state 1. The activation of chloride channels by GABA and nicotinic agonists depends very much on the extracellular Ca^{2+} concentration. In the experiment of Fig. 9 relatively high concentrations of agonists were applied by means of the liquid-filament switch. The
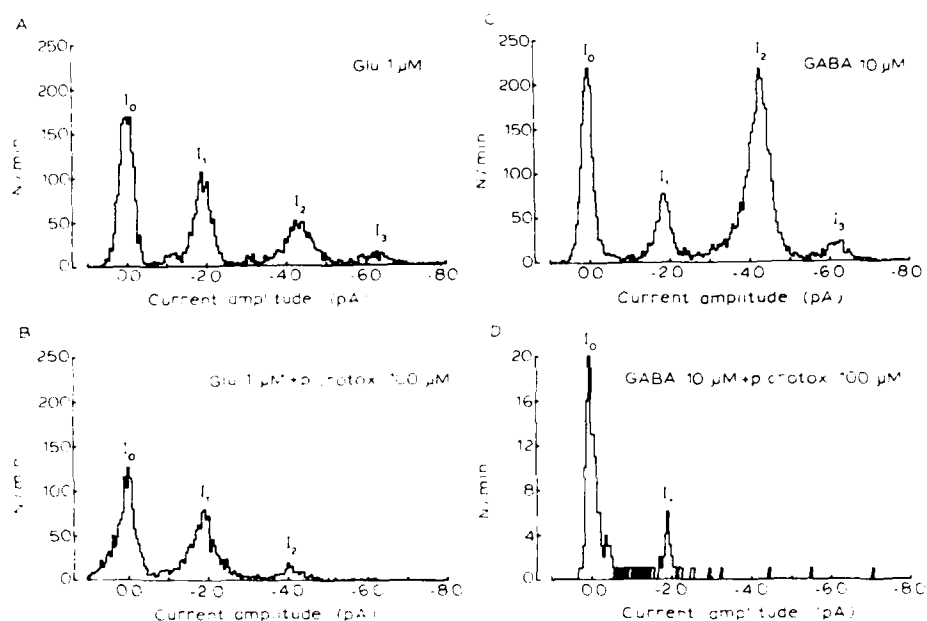
FIG 7 Amplitude distributions for single chloride channel currents from the same patch that yielded the results in Fig. 6. A: channels opened by 1 μM glutamate. B: channels opened by 1 μM glutamate in presence of 100 μM picrotoxin. C: channels opened by 10 μM GABA. D: channels opened by 10 μM GABA in presence of 100 μM picrotoxin. Polarization -100 mV. Reprinted from Ref. 2.

maximum currents elicited reached -700 pA with GABA, indicating simultaneous activation of several hundred channels. Such large numbers of chloride channels, compared to a few glutamate activated cationic channels in the same patch, were a general finding. Fig. 9 shows that the effect of glutamate was little affected by lowering of the extracellular Ca^{2+} concentration. Glutamate produced a strong desensitization with a time constant of several hundred ms. In contrast, 10^{-5} M GABA opened relatively few channels at the normal Ca^{2+} concentration of 13.5 mM, but its effectivity increased more than 50-fold in 0.1 mM Ca^{2+}. 10^{-4} M carbachol activated very few channel openings at 13.5 mM Ca^{2+}, but had a several hundred-fold stronger effect at 0.1 mM Ca^{2+}. This Ca^{2+}-dependence of the effects of GABA and of nicotinic agonists is in the opposite direction compared to the Ca^{2+}-dependence of the excitatory channels [9]. It should be noted that the rise and the decay of the channel activity at the onset and the end of an agonist pulse were much slower than for the excitatory channels recorded under the same conditions. Further, only activation by glutamate (or quisqualate) caused a relatively rapid desensitization of the chloride receptors/channels. Activation by GABA led to desensitization with time constants of minutes.

The fact that in normal Ca^{2+} carbachol has a very low activity in opening chloride channels can be used to demonstrate competition of the different agonists for the same receptor. In the experiment of Fig. 10, the agonists glutamate or GABA were applied to the same patch with the rapid switch either alone or in

414

Outside-out patch, -85 mV, opener muscle
Carbachol 10 nM

Glutamate 0.1 µM   100 ms

GABA 10 µM
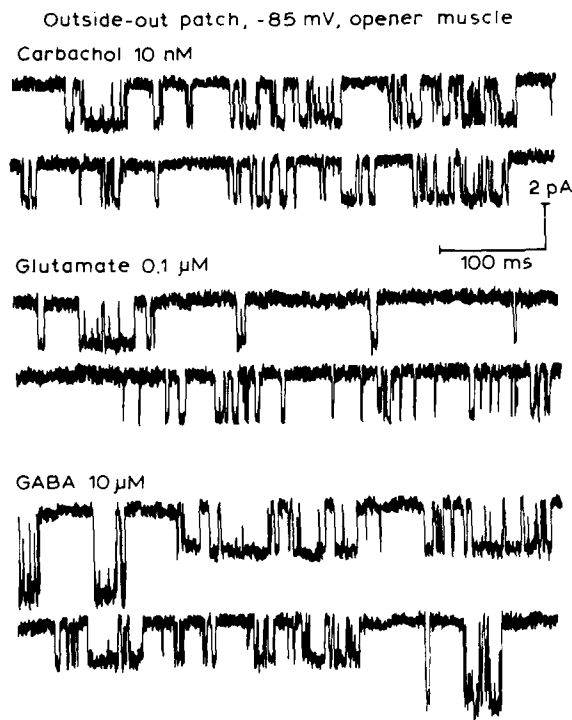
FIG 8 Single-channel chloride currents recorded in one patch in presence of 10 nM carbachol (upper two traces), 0.1 µM glutamate (middle traces) and 10 µM GABA (bottom traces). While carbachol and glutamate activate only state 1 (see Fig. 6). GABA also activates state 2. Reprinted from Ref. 24.

presence of carbachol. In the left hand column, 100 µM glutamate elicited a large current. When glutamate was added to 10 µM carbachol, channel opening was suppressed. When glutamate alone was applied again, the same large number of channel openings was evoked as in the control before. The analogous experiment is shown for GABA and carbachol in the right-hand column. Evidently carbachol, in the presence of glutamate or GABA, could occupy most of the receptors and prevent the action of the other agonist. These results show that carbachol, glutamate and GABA activate the same population of channels, and further, that in high Ca^{2+} carbachol reacts with the receptors, but does not open most channels.

The unusual reactivity of the chloride receptor/channels to three classes of transmitters raises the suspicion that the opening of chloride channels is mediated through different receptors on the cell surface, which act on second intracellular messengers via G-proteins. However, openings of chloride channels could also be triggered in inside-out patches which were superfused rapidly. Variation of the intracellular Ca^{2+} concentration did not affect channel opening, neither did addition of adenosine triphosphate, cyclic adenosine monophosphate or guanosine triphosphate (GTP). Also, addition of GTP-β-S or of pertussis toxin had no effect on the gating of chloride channels. It seems very improbable, therefore, that a

Stomach muscle, outside-out patch, -75 mV

v.H. 13.5 mM Ca⁺⁺   0.1 mM Ca⁺⁺

Glutamate 10⁻⁴ mol/l

200 pA

GABA 10⁻⁵ mol/l

20 pA   200 pA

Carbachol 10⁻⁴ mol/l

20 pA   200 pA

1 s
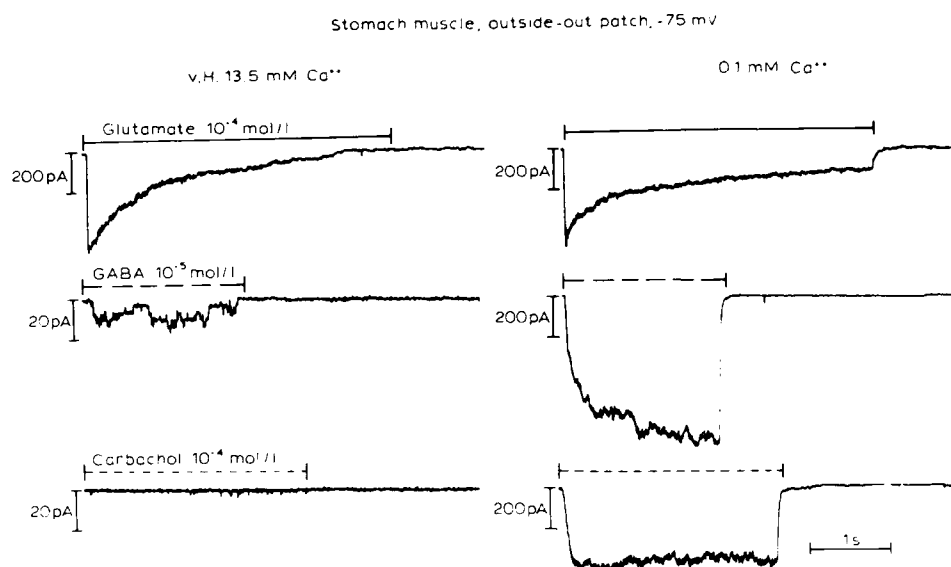
FIG 9   Chloride currents elicited at one patch by one pulse each of glutamate, GABA and carbachol, as marked. Pulses applied by liquid filament switch. In the recordings in the left hand column the Ca^{2+} concentration in the background superfusion of the patch, as well as in the liquid filament was 13.5 mM. In the right hand column, the background perfusion contained again 13.5 mM Ca^{2+}, but in the liquid filament which contained the agonists the Ca^{2+} concentration was 0.1 mM. Note the different amplitude calibrations. Isolated single channel openings at about −2 pA are only visible in carbachol 10^{-4} M, Ca^{2+} 13.5 M; the other recordings are superimpositions of up to several hundred channels.

second messenger system is involved in the opening of the chloride channels on crayfish muscle by agonists of glutamate, GABA and nicotine. Biochemical studies have shown that at least nicotinic, GABA- and glycine receptor-channel complexes are closely related proteins [25], and probably the channel molecules activated by glutamate, GABA and acetylcholine form a closely related family. We suggest, therefore, that the chloride channels found on crayfish muscle are 'primitive' or non-selective members of this family which accept different classes of transmitters to achieve binding to and/or opening of the channel, but which are quite selective in allowing only anions to pass the channel. Other examples of this class of channel have been seen [26].

In most muscles of crayfish and of other crustaceans, excitation is mediated synaptically by glutamate and inhibition by GABA. The excitatory channels activated by glutamate should be the synaptic channels [7]. However, it is difficult to see how the chloride channels studied here could be the synaptic ones. The chloride channels were found on the opener muscle which has rich inhibitory innervation, but also on intrinsic stomach muscles (Figs. 9, 10) which have no inhibitory innervation. At least some of the chloride channels therefore are 'extrasynaptic'. In the opener muscle, synaptic inhibitory currents were measured by voltage clamping muscle fibres and stimulating the inhibitory axon as in Ref. 27. The inhibitory postsynaptic currents (IPSCs) were not depressed by applied carbachol or glutamate, as expected for the chloride channels studied here. How-

416
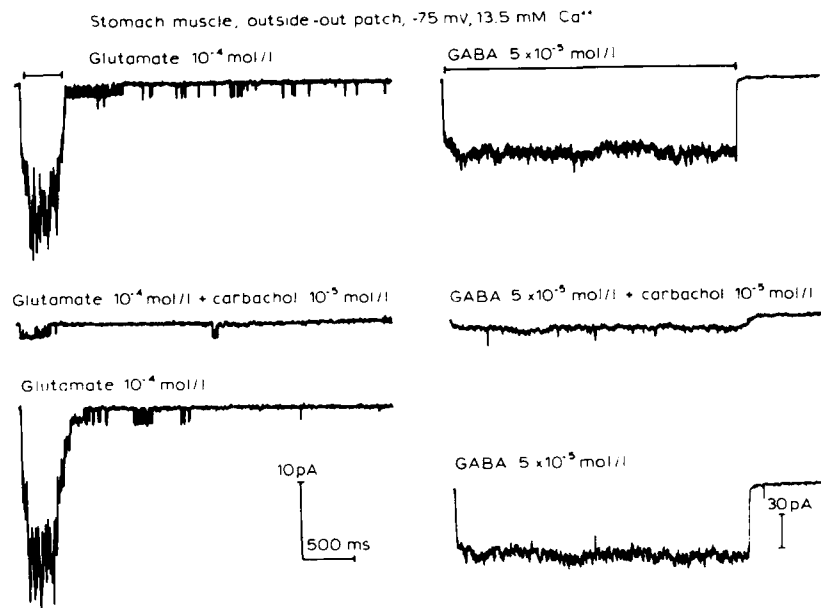
FIG 10   Chloride currents elicited in one patch, like in Fig. 9. The top and the bottom traces are controls before and after the recording in the middle trace. In the latter, the background perfusion of the patch as well as the liquid filament contained 10^{-5} M carbachol, and the agonists glutamate or GABA were added to the filament. Note the different amplitude calibrations in the left hand and the right hand columns.

ever, the IPSCs were blocked rapidly and reversibly by picrotoxin, and the inhibitory synapses thus were readily accessible to superfused drugs. On the other hand, low glutamate concentrations and also carbachol in low Ca^{2+} elicited a small current with the same equilibrium potential as the IPSCs. Chloride channels with the same characteristics as the ones observed in patches thus seem to be present in the intact muscle. We assume, tentatively, that treatment with collagenase and isolation in a patch either directly affect the GABAergic synaptic or extrasynaptic channel molecules, or may modify the membrane microenvironment of the receptors, to make these channels less selective towards the agonists than they are in synaptic complexes.

Acknowledgement

References

1 Franke, Ch., Hatt, H. and Dudel, J. (1986) The excitatory glutamate-activated channel recorded in cell-attached and excised patches from the membranes of tail, leg and stomach muscles of crayfish. J. Comp. Physiol. A 159, 579–589.

2 Franke, Ch., Hatt, H. and Dudel, J. (1986) The inhibitory chloride channel activated by glutamate as well as γ-amino-butyric acid (GABA). Single channel recordings from crayfish muscle. J. Comp. Physiol. A 159, 591–609.

3 Parnas, I., Dudel, J., Cohen, I. and Franke, C. (1984) Strengthening of synaptic contacts of one axon on elimination of an agonistic second one. J. Neurosci. 4, 1912–1932.

4 Hatt, H., Franke, Ch. and Dudel, J. (1988) Ionic permeabilities of L-glutamate activated, excitatory synaptic channel in crayfish muscle. Pflügers Arch. 411, 8–16.

5 Hille, B. (1984) Ionic channels of excitable membranes. Sinauer Associates Inc., Sunderland MA.

6 Franke, Ch. and Dudel, J. (1987) Single glutamate-gated synaptic channels at the crayfish neuromuscular junction. I. The effect of enzyme treatment. Pflügers Arch. 408, 300–306.

7 Dudel, J. and Franke, Ch. (1987) Single glutamate-gated synaptic channels at the crayfish neuromuscular junction. II. Dependence of channel open time on glutamate concentration. Pflügers Arch. 408, 307–314.

8 Colquhoun, D.C. and Sakmann, B. (1985) Fast events in single-channel currents activated by acetylcholine and its analogues at the frog muscle end-plate. J. Physiol. (Lond.) 369, 501–557.

9 Hatt, H., Franke, Ch. and Dudel, J. (1988) Calcium dependent gating of L-glutamate activated, excitatory synaptic channel on crayfish muscle. Pflügers Arch. 411, 17–26.

10 Florey, E. and Woodcock, B. (1968) Presynaptic excitatory action of glutamate applied to crab nerve-muscle preparations. Comp. Biochem. Physiol. 26, 651–661.

11 Nickell, W.T. and Boyarski, L.L. (1980) The effects of calcium at the crayfish neuromuscular junction. Comp. Biochem. Physiol. 66, 259–264.

12 Kawagoe, R., Onodera, K. and Takeuchi, A. (1984) The uptake and release of glutamate at the crayfish neuromuscular junction. J. Physiol. (Lond.) 354, 69–78.

13 Stettmeier, H. and Finger, W. (1983) Excitatory postsynaptic channels operated by quisqualate in crayfish muscle. Pflügers Arch. 397, 237–242.

14 Watkins, J.C. and Evans, R.H. (1981) Excitatory amino acid transmitters. Ann. Rev. Pharmacol. Toxicol. 21, 165–204.

15 Takeuchi, A. and Takeuchi, N. (1964) The effect on crayfish muscle of iontophoretically applied glutamate. J. Physiol. (Lond.) 170, 296–314.

16 Dudel, J. (1977) Dose-response curve of glutamate applied by superfusion to crayfish muscle synapses. Pflügers Arch. 368, 49–54.

17 Franke, Ch., Hatt, H. and Dudel, J. (1987) Liquid filament switch for ultrafast exchanges of solutions at excised patches of synaptic membrane of crayfish muscle. Neurosci. Lett. 77, 199–204.

18 Dudel, J., Franke, Ch., Hatt, H., Ramsey, R.L. and Usherwood, P.N.R. (1988) Rapid activation and desensitization by glutamate or excitatory, cation-selective channels in locust muscle. Neurosci. Lett. 88, 33–38.

19 Dudel, J. (1983) Graded or all-or-nothing release of transmitter quanta by local depolarization of nerve terminals on crayfish muscle. Pflügers Arch. 398, 155–164.

20 Katz, B. and Thesleff, S. (1957) A study of the 'desensitization' produced by acetylcholine at the motor end-plate. J. Physiol. (Lond.) 138, 63–80.

21 Magleby, K.L. and Stevens, C.F. (1972) A quantitative description of end-plate currents. J. Physiol. (Lond.) 223, 173–197.

22 Takeuchi, A. and Takeuchi, N. (1969) A study of the action of picrotoxin on the inhibitory neuromuscular junction of the crayfish. J. Physiol. (Lond.) 205, 377–391.

23 Smart, T.G. and Constanti, A. (1986) Studies on the mechanism of action of picrotoxin and other convulsants at the crustacean muscle GABA receptor. Proc. R. Soc. Ser. B 227, 191–216.

24 Zufall, F., Franke, Ch. and Hatt, H. (1988) Acetylcholine activates a chloride channel as well as glutamate and GABA. Single channel recordings from crayfish stomach and opener muscles. J. Comp. Physiol. in press.

418

25 Barnard, E.A., Darlison, M.G. and Seeburg,P. (1987) Molecular biology of the $GABA_A$ receptor: the receptor/channel superfamily. Trends Neurosci. 10, 502–509.

26 King, W. and Carpenter, D.O. (1987) Distinct GABA and glutamate receptors may share a common channel in Aplysia neurons. Neurosci. Lett. 82, 343–348.

27 Dudel, J. (1977) Voltage dependence of amplitude and time course of inhibitory synaptic current in crayfish muscle. Pflügers Arch. 371, 167–174.

CHAPTER 31

Ion channels in artificial lipid bilayers

MARK S.P. SANSOM AND IAN R. MELLOR

Department of Zoology, Nottingham University, University Park, Nottingham, NG7 2RD, U.K.

Introduction

Single channel recording from planar lipid bilayers is widely employed for investigating the biochemistry and biophysics of ion channels [1]. There are several rationales behind the adoption of this approach. Firstly, it allows investigation of the properties of model ion channels formed by relatively simple peptides. From such studies one should be able to establish rules governing the structure–function relationships of receptor-channel proteins. This is of particular importance given the wealth of sequence information becoming available for the latter class of molecules [2]. A second reason for adopting the bilayer approach is that it enables one to transplant ion channel molecules away from their native cellular membranes [3], and hence to probe the influences of lipid microenvironment [4], and cytoskeletal structures on their biophysical properties. Finally, reconstitution [5] in lipid bilayers may be used to characterize the conductance and gating properties of purified receptor-channel proteins.

In this chapter, examples of the first two applications of bilayer studies will be considered. Ion channels formed by peptides are discussed in the context of channel formation by δ-toxin from *Staphylococcus aureus*, and by mastoparan from wasp venom. Transplantation experiments are represented by an investigation of ion channels present in locust muscle membrane, with particular emphasis on the glutamate receptor [6].

'Pipette dipping'

There are two main experimental configurations for recording from planar bilayers —black lipid membranes (BLMs) [7], and bilayers formed at the tips of patch electrodes ('pipette dipping') [8]. We have employed the latter technique because (a) it uses smaller amounts of channel forming material; and (b) it provides a higher signal to noise ratio and better temporal resolution [9]. The latter is readily understood if one considers the small area of the bilayer formed at the tip of a patch pipette (ca. 1 μm^2) relative to that formed in a BLM experiment (ca. 10 000 μm^2). For experimental details of the method of bilayer formation, the reader is referred to Refs. 8 and 10.

Channel-forming peptides

Much of the existing work on model ion channels focuses on the antibiotic gramicidin [11]. Whilst this has provided important concepts concerning the nature of ion channels, the β-helical structure adopted by the alternating D,L-amino acid sequence of gramicidin is not present in protein molecules. More recently, interest has turned to the formation of ion channels by clusters of peptide molecules in the α-helical conformation, particularly since the structural work of Fox and Richards on alamethicin [12]. Such helix clusters have been widely discussed in the context of models for the ionophoric region of the nicotinic acetylcholine receptor [13] and of other channel proteins.

Alamethicin, and related peptides [14], are all extremely hydrophobic, containing the α,α-dimethylated amino acid α-amino isobutyrate. We have chosen instead to concentrate on peptides containing only those amino acids commonly found in proteins. These would seem to be more likely to provide realistic models of the pore forming regions of receptor-channel proteins. To date, we have looked in detail at two such peptides—δ-toxin from *Staphylococcus aureus*, and mastoparan from the venom of the wasp *Vespa lewisii*.

δ-Toxin

δ-Toxin is an extracellular cytolytic peptide which has been demonstrated to have surface-active effects on a variety of biological membranes [15]. It is a 26-residue peptide, molecular weight 2977, which forms tetrameric and higher aggregates in aqueous solution [16]. The amino acid sequence is:

M-A-Q-D-I-I-S-T-I-G-D-L-V-K-W-I-I-D-T-V-N-K-F-T-K-K

with the N-terminal methionine being formylated. NMR studies [17] have shown the peptide to adopt an α-helical structure in the presence of lipid micelles. Preliminary crystallographic studies of δ-toxin have been reported [18], and more recent results are consistent with an helical structure (D. Rice, personal communication).

As can be seen from Fig. 1a, the δ-toxin helix is amphipathic i.e. the amino acid sidechains are arranged such that one face of the helix is hydrophobic, the other hydrophilic. As suggested by Freer and Birkbeck [19], a cluster of δ-toxin helices would be capable of forming a transmembrane pore. In such a cluster, the hydrophobic faces of the helices point outwards, facing the lipid acyl chains, and the hydrophilic faces are directed inwards, forming a potential ion channel (Fig. 1b). Note that a 26-residue peptide such as δ-toxin forms an α-helix 3.9 nm long. This is sufficient to traverse a lipid bilayer, of thickness ca. 4 nm. Thus one might expect a cluster of δ-toxin helices to form a relatively stable transmembrane pore.

Using the 'pipette dipping' approach to form bilayers of diphytanoyl phosphatidylcholine on the tips of patch electrodes, it was possible to demonstrate that ion channels were formed when δ-toxin was present inside the electrode. The inside of the electrode is therefore defined as the *cis* face of the bilayer. The electrolyte used was 0.5 M KCl. It was only possible to observe channel activity within a rather narrow window of δ-toxin concentrations—between 0.05 and 2.0 μM. Channel formation was optimal at 0.3 μM δ-toxin. Concentrations in excess of 2 μM generally resulted in loss of the electrical seal between the bilayer and the patch electrode.
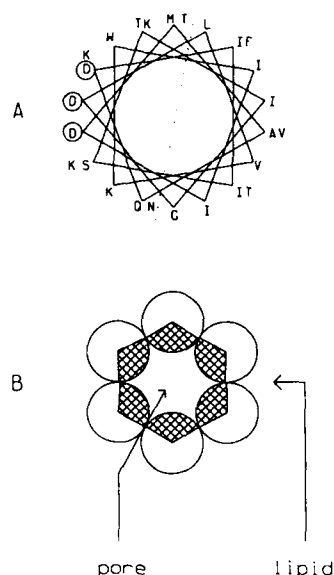
FIG 1 A: the δ-toxin sequence is shown in a helical wheel projection. Amino acids, represented by their one letter codes, are shown in their positions as viewed down the helix axis. The residues to the left of the broken line are predominantly hydrophilic, and those to the right predominantly hydrophobic. The three aspartate residues are ringed. B: cartoon of formation of an ion channel by a cluster of α-helices, seen in cross section. The hatched regions represent the hydrophilic faces of the helices.

In the presence of 0.34 μM δ-toxin, channels were seen at both positive and negative potentials (where the sign of the potential refers to the *cis* face of the membrane). Channel behaviour was stationary for up to 15 min, brief channel openings of ca. 100 pS conductance being seen. At higher δ-toxin concentrations (0.94 μM), a greater degree of channel activity was seen. This appeared to be non-stationary, although no loss of electrical seal was observed for up to 20 min. Multiple conductance levels were seen, presumably resulting from the simultaneous presence of several channels within the bilayer.

Stationary single channel recordings obtained in the presence of 0.34 μM δ-toxin were analysed in terms of the amplitudes of the channel openings. Two major conductance classes were observed—'small' channels of ca. 100 pS, and 'large' channels of ca. 450 pS. The 'small' channels were much more frequent at 0.34 μM δ-toxin. More detailed examination revealed that the 'small' channels were made up of 70 pS and 100 pS openings. There were also openings of 20–30 pS, but these were brief (< 0.5 ms), and consequently difficult to resolve unambiguously. The 'large' channels were split into 420 pS and 470 pS subconductance levels. Examples of both 'small' and 'large' channels, in the same recording, are shown in Fig. 2. 'Large' channels occurred more often at higher δ-toxin concentrations. Multiple 'large' channel openings frequently preceded breakdown of the electrical seal.

Current–voltage relationships for bilayers containing δ-toxin channels were determined by applying a sawtooth voltage ramp, from −200 to +200 mV, to the membrane, at a frequency of 0.1 s^{-1}. The membrane currents were averaged to give
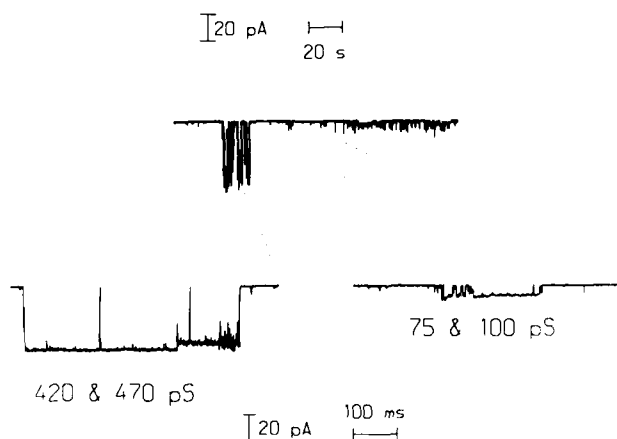
FIG 2 Single channel currents recorded from a diphytanoyl phosphatidylcholine bilayer exposed to 0.34 μM δ-toxin. The membrane potential was -100 mV and the electrolyte 0.5 M KCl. The lower traces are expanded views of the indicated sections of the upper trace, showing 'large' (LHS) and 'small' (RHS) δ-toxin channels.

an overall current–voltage relationship. This was approximately symmetrical above 0 mV, and deviated from linearity at potentials in excess of 60 mV. Inspection of individual current–voltage curves suggested that this non-linearity reflected a voltage dependent component of δ-toxin channel gating, with an increased probability of channel opening at higher potentials. This was investigated further by construction of three-dimensional current–voltage diagrams. In these, the voltage is plotted on the horizontal axis, and the current on the vertical axis. The surface height at a voltage–current point, represented in Fig. 3 by contours, is the frequency of occurrence of that voltage-current pair. So, if a section of the surface was taken at a constant voltage, a standard current amplitude histogram would be obtained. Thus, a single ohmic conductance would be seen as a ridge of contours, the angle of which to the horizontal is determined by the value of the conductance. Such an analysis for a bilayer formed in the presence of 0.94 μM δ-toxin (Fig. 3) revealed only the 'small' channel to have been active during the experiment. Three ridges of contours, plus a near horizontal ridge corresponding to the closed channel (bilayer leakage), were seen, with conductances of 28 pS, 72 pS and 110 pS. Note that these three values are very close to those determined in the constant potential experiments, and confirm the existence of a 'small' channel sub-conductance at ca. 30 pS. The heights of the 100pS and 72 pS ridges increase, relative to those for 28 pS and the closed channel, as the membrane potential is increased. This demonstrates that there is a voltage-dependent component to δ-toxin channel gating, with the probability of the channel being open increasing with increasing membrane potential.

Average current–voltage relationships were used to determine the concentration dependence of δ-toxin channel formation. Plotting the log of the conductance at 0 mV against the log of peptide concentration yielded a line of slope ca. 7. This is in reasonable agreement with the predicted slope of 6 for the hexameric cluster model for the δ-toxin channel [19].

Reversal potentials measured in the presence of a 5-fold cis /trans KCl concentration gradient was used to estimate the ion selectivity of the δ-toxin channels.
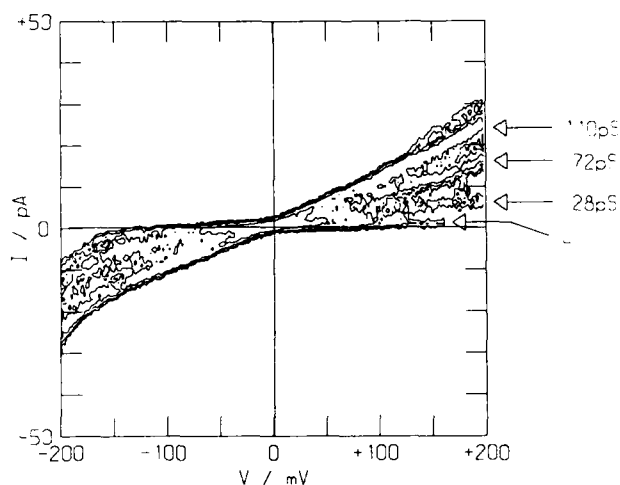
FIG 3 Three-dimensional current–voltage diagram obtained in the presence of 0.94 μM δ-toxin, with 0.5 M KCl as the electrolyte. The three conductance levels of the 'small' channel, plus the membrane leakage (L), are indicated by arrows.

The 'small' channels had a permeability ratio of $P_K/P_{Cl} = 9$, the 'large' channels a ratio of $P_K/P_{Cl} \approx 3$. Thus the 'small' channels seem to be more selective for cations over anions. These results may be interpreted in terms of the hexameric cluster model of the channel (Fig. 4). This diagram represents the first stage of more extensive attempts to model possible helix clusters for δ-toxin. More recent studies, employing interactive molecular graphics modelling, lend support to the overall conclusions (D. Rice, personal communication). The peptide sequence was projected down the helix axis, i.e. as a helical wheel projection (Fig. 1a). Six helix projections were placed with the projected axes at the apices of a regular hexagon. The distance between neighbouring axes were set such that the helices would be in stereochemical close contact. The individual helices were oriented such that the hydrophilic sidechains were directed towards the central pore. The putative ion channel in the model can be seen to be lined by aspartate residues. At neutral pH, these sidechains would be negatively charged, and therefore may form the structural basis of the
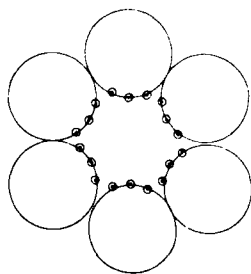
FIG 4 Schematic diagram of the hexameric cluster model of the δ-toxin channel. The large circles represent the α-helices in cross section. The small circles indicate the positions of the aspartate residues lining the central pore.

cation selectivity of δ-toxin channels. Further studies will investigate this hypothesis in more detail.

Mastoparan

Mastoparan is also surface active [20], and is 14 amino acids long with the sequence:

I-N-L-K-A-L-A-A-L-A-K-K-I-L

the C-terminus being amidated. In a helical conformation it is amphipathic, though less so than δ-toxin. The helix formed by mastoparan is only 2.1 nm long, i.e. half of the bilayer thickness. It is therefore of interest to see if such a peptide is capable of forming ion channels.

Mastoparan has been shown to form ion channels in diphytanoyl phosphatidylcholine bilayers. Again, channel formation was observed over a relatively narrow concentration range—ca. 0.2 to 2.0 μM. Channel formation was optimal at ca. 0.7 μM mastoparan, at which concentration stationary recordings with numerous brief openings of the order of 100 pS conductance were seen at cis + 100 mV. Interestingly, if a cis negative potential was imposed, little channel activity was observed. Channel openings observed with mastoparan were extremely brief when 0.5 M KCl was employed as the electrolyte. Current amplitude histogram analysis yielded a broad envelope, with no discrete conductance peaks. This is consistent with bandwidth limitation of brief (< 0.1 ms) openings by the frequency response of the amplifier. At a higher ionic strength (3.0 M KCl), longer duration channel openings were visible, with conductances of ca. 50, 100 and 200 pS. A similar effect of increased ionic strength on channel duration has been reported for the bee venom peptide melittin [22].

Mastoparan channel current–voltage relationships were determined using the three-dimensional current–voltage diagram procedure described above (Fig. 5). This clearly showed that at negative potentials only the leakage (closed channel) current
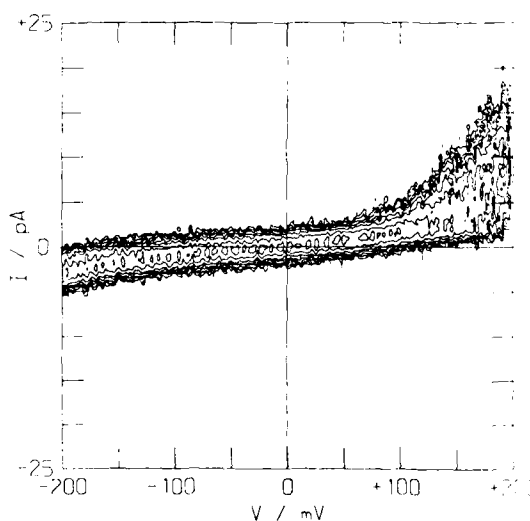
FIG 5 Three-dimensional current–voltage diagram obtained in the presence of 0.7 μM mastoparan, with 0.5 M KCl as the electrolyte. Note that channel activity is only seen at cis positive potentials.

was present. At positive potentials, a non-linear increase in mean current was seen in response to increasing potential, but discrete conductance ridges could not be resolved. As these measurements were made with 0.5 M KCl as the electrolyte, this presumably reflects brief, bandwidth limited channel openings, as seen in constant potential experiments under similar conditions.

Summary

The bilayer approach has been used to characterize the properties of ion channels formed by two naturally occurring peptide toxins. The longer peptide (δ-toxin), capable of spanning the lipid bilayer in the α-helical conformation, forms voltage-activated ion channels at either positive or negative potentials. These channels have multiple conductance levels and are of sufficient duration for discrete channel openings to be resolved. The shorter peptide (mastoparan), only capable of spanning half the bilayer in the helical conformation, forms channels predominantly at cis positive potentials. The channel openings are so brief-lived that they may only be resolved at high ionic strength. We are now investigating the channel forming properties of synthetic analogues of these peptides in an attempt to more tightly define the relationship between peptide structure and channel activity.

Ion channels from locust muscle membranes

Transplantation of ion channels to planar lipid bilayers has been carried out with a view to characterizing the properties of the locust muscle glutamate receptor [6] in a novel membrane environment. These studies parallel those of Vodyanoy et al. [23] on NMDA receptors from rat brain, and of Taskmukhamedov et al. [24] on glutamate receptors from rat brain and from crayfish muscle.

The strategy adopted was to purify locust muscle membrane fractions, and to detergent solubilize the proteins contained therein. The biochemical details of the methodology are contained in Ref. 25. The solubilized protein was added to the solution within the patch electrode, and a planar bilayer formed at the electrode tip. A transbilayer potential was imposed, and glutamate dependent channel openings searched for.

Initial experiments employed a constant concentration of glutamate in the bath. Both electrode and bath contained standard locust saline [6] as electrolyte. In the presence of 0.1 mM glutamate, occasional bursts of channel openings were seen, separated by long silent periods of several seconds duration. Inspection of the bursts revealed them to be made up of brief (ca. 1 ms) channel openings, and to have a chord conductance of 80–100 pS. The long silent periods may represent receptor-channel desensitization, as concanavalin A, used to block desensitization when recording from intact muscle membranes, was not present.

The effect of addition of glutamate some time after formation of the bilayer was investigated. In these experiments, a membrane protein preparation which had been partially purified via concanavalin A affinity chromatography was employed (Usoh, personal communication). The bilayer was formed in the absence of glutamate and a potential of +50 mV was imposed. No channel activity was seen for several minutes (Fig. 6). Upon addition of glutamate to a final concentration of 0.1 mM, channel activity was induced. This lasted for several seconds, and then disappeared, presumably again reflecting a desensitization phenomenon. Detailed inspection of the

426
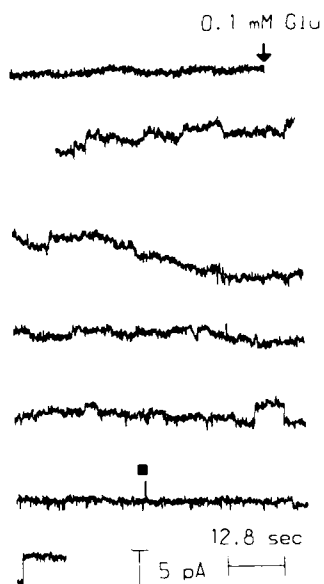
FIG 6 Recording from a bilayer formed in the presence of a solubilized locust muscle membrane fraction, at a potential of +50 mV. At the time indicated by the arrow, glutamate was added to a final concentration of 0.1 mM. This appeared to induce channel activity. Inspection of e.g. the region indicated by the square on an expanded timescale revealed clusters of channel openings.

channel openings showed them to be clustered, and revealed that multiple conductance levels of ca. 50–100 pS were present.

These results suggest that glutamate sensitive ion channels may be transplanted from locust muscle membranes to planar lipid bilayers. Work is under way to more fully characterize the properties of these channels and to explore the effects of bilayer lipid composition upon them.

Conclusions

The pipette dipping approach seems to be a relatively straightforward and reproducible procedure for single channel recording from planar lipid bilayers. It has permitted detailed biophysical characterization of model ion channels formed by simple peptides. Initial explorations of the potential of the method for transplantation of ion channels from locust membranes have yielded promising results.

References

1 Miller, C. (ed.) (1986) Ion Channel Reconstitution. Plenum Press, New York.
2 Barnard, E.A., Darlison, M.G. and Seeburg, P. (1987) Molecular biology of the GABA$_A$ receptor: the receptor/channel superfamily. Trends Neurosci. 10, 502–509.
3 Krueger, B.K., Worley, J.F. and French, R.J. (1983) Single sodium channels from rat brain incorporated into planar lipid bilayers. Nature 303, 172–175.
4 Bell, J. (1986) The sarcoplasmic reticulum potassium channel. In: Ion Channel Reconstitution (C. Miller, ed.), pp. 469–482. Plenum Press, New York.
5 Montal, M. (1987) Reconstitution of channel proteins from excitable cells in planar lipid bilayer membranes. J. Membr. Biol. 98, 101–115.
6 Patlak, J.B., Gration, K.A.F. and Usherwood, P.N.R. (1979) Single glutamate-activated channels in locust muscle. Nature 278, 643–645.
7 Montal, M. and Mueller, P. (1972) Formation of bimolecular membranes from lipid monolayers and a study of the electrical properties. Proc. Natl. Acad. Sci. U.S.A. 69, 3561–3566.
8 Coronado, R. and Latorre, R. (1983) Phospholipid bilayers made from monolayers on patch-clamp pipettes. Biophys. J. 43, 231–236.
9 Montal, M., Anholt, R. and Labarca, P. (1986) The reconstituted acetylcholine receptor. In: Ion Channel Reconstitution (C. Miller, ed.). pp. 157–204. Plenum Press, New York.
10 Mellor, I.R., Thomas, D.H. and Sansom, M.S.P. (1988) Properties of ion channels formed by Staphylococcus aureus δ-toxin. Biochim. Biophys. Acta 942, 280–294.
11 Andersen, O.S. (1984) Gramicidin channels. Ann. Rev. Physiol. 46, 531–548.
12 Fox, R.O. and Richards, F.M. (1982) A voltage-gated ion channel model inferred from the crystal structure of alamethicin at 1.5 A resolution. Nature 300, 325–330.
13 Guy, H.R. and Hucho, F. (1987) The ion channel of the nicotinic acetylcholine receptor. Trends Neurosci. 10, 318–321.
14 Menestrina, G., Voges, K.-P., Jung, G. and Boheim, G. (1986) Voltage-dependent channel formation by rods of helical peptides. J. Membr. Biol. 93, 111–132.
15 Freer, J.H., Birkbeck, T.H. and Bhakoo, M. (1984) Interaction of staphylococcal δ-lysin with phospholipid monolayers and bilayers—a short review. In: Bacterial Protein Toxins (J.E. Alouf, F.J. Fehrenbach, J.H. Freer, J. Jeljaszewicz, eds.), pp. 179–189. Academic Press, London.
16 Fitton, J.E. (1981) Physicochemical studies on delta haemolysin, a staphylococcal cytolytic polypeptide. FEBS Lett. 130, 257–260.
17 Lee, K.H., Fitton, J.E. and Wuthrich, K. (1987) Nuclear magnetic resonance investigation of the conformation of δ-haemolysin bound to dodecylphosphocholine micelles. Biochim. Biophys. Acta 911, 144–153.
18 Thomas, D.H., Rice, D.W. and Fitton, J.E. (1986) Crystallisation of the delta toxin of Staphylococcus aureus. J. Mol. Biol. 192, 675–676.
19 Freer, J.H. and Birkbeck, T.H. (1982) Possible conformation of delta-lysin, a membrane damaging peptide of Staphylococcus aureus. J. Theor. Biol. 94, 535–540.
20 Okumura, K., Inui, K.-I., Hirai, Y. and Nakajima, T. (1981) The effect of mastoparan on ion movement in black lipid membrane. Biomed. Res. 2, 450–452.
21 Chothia, C. (1984) Principles that determine the structure of proteins. Annu. Rev. Biochem. 53, 537–572.
22 Hanke, W., Methfessel, C., Wilmsen, H.-U., Katz, E., Jung, G. and Boheim, G. (1983) Melittin and a chemically-modified trichotoxin form alamethicin-type multi-state pores. Biochim. Biophys. Acta 727, 108–114.

23 Vodyanoy, V., Muller, D., Kramer, K., Lynch, G. and Baudry, M. (1987) Functional reconstitution of N-methyl-D-aspartate receptors in artificial lipid bilayers. Neurosci. Lett. 81, 133–138.

24 Tashmukhamedov, B.A., Makhmudova, E.M., Kazakov, I., Khafizov, A.G. and Lim, T.M. (1987) Reconstitution of glutamate receptors into planar bilayers. In: Receptors and Ion Channels (Y.A. Ovchinnikov, F. Hucho, eds.) pp. 117–125. de Gruyter, Berlin.

25 Usoh, G., Duce, I.R. and Usherwood, P.N.R. (1988) ^{3}H-Glutamate binding to locust CNS membranes. (in preparation.)

Structure–activity relationships

CHAPTER 32

Molecular recognition, structural dissimilarity and future developments in QSAR

P.M. DEAN

Department of Pharmacology, University of Cambridge, Hills Road, Cambridge CB2 2QD, U.K.

Introduction

Quantitative structure–activity relationships have been of great value in the development of putative ligand compounds into useful drug molecules or better pesticides. There can be no doubt about the utility of the methods; they have been the technique of choice in industry for decades. However, despite their usefulness, the scientific basis for QSAR is not well founded and its credibility is frequently called into question; the methods can be criticized on a number of counts. 1. The methods are largely retrospective. A good lead compound is needed at the beginning of the study. A set of modifications are made to the parent structure. Biological activity in the series is tested for, and from the differences in activity it is possible to identify various parameters correlated with activity. Once these 'determinant' parameters are known, the chemist can refine the parent structure by adding or subtracting suitable moieties in accordance with their tabulated parameter values in a database. 2. Many of the parameters used in QSAR are dimensionless and have little direct physical meaning. The parameters reflect a scale of empirically fitted values. The parameters rarely give an indication of what might be taking place at molecular levels in drug–receptor interaction. 3. It is often acknowledged that improvements in potency are really quite cosmetic and have more to do with improving the pharmacokinetics of in vivo dosage rather than describing a relationship between structure and affinity/efficacy in the environment of the ligand binding site. 4. QSAR methods encounter major problems where molecules of dissimilar 3-D structure are being evaluated. Despite the descriptive adjective 'quantitative' used in QSAR, the methods are only quantitative in the sense of describing a trend in multivariate analysis; each structural change is treated as a separate object and not directly as a variable, or set of variables, changing in 3-space.

It is possible that commercial pressures, in forcing the pace of evolving methods of QSAR, are responsible for the development of empirical correlations that unfortunately have little to do with sound molecular theory of drug–receptor interaction. In this paper I would like to focus attention on the problem of structural dissimilarity and QSAR. The discussion will be restricted to rigid mole-

cules, and will illustrate the useful role of molecular recognition in providing a firm theoretical basis for QSAR.

Incorporation of structure into QSAR

Three-dimensional structural information is represented by the spatial disposition of atoms. The expression of structure as a list of atomic Cartesian coordinates is the most basic representation. Adjacency matrices can then be used to define chemical bonds. If a molecule is composed of n atoms, there are $3n$ coordinates and $(n^2 - n)/2$ possible connections of which $n - 1$ will be chemical bonds. Thus, any representation of a chemical group by a single or a few parameters would involve a gross reduction of structural information and would be hopelessly inappropriate for comparing molecules with a significant degree of dissimilarity. In certain strictly defined cases Taft's or Charton's steric parameters may be of some value but their use cannot be generalized. Similar criticisms apply to attempts to describe groups by their gross dimensions. Sterimol parameters reduce the description to 5 parameters, consisting of the principal axis and 4 axes orthogonal to it.

Structural differences may be taken into account by attempting to overlay molecules to give the best fit. This can be simply achieved by distance matrix methods [1]. The distance matrix is an $n \times n$ matrix, DM, composed of the interatomic distances, d_{ij}, between atoms i and j

$$d_{ij} = \left[(x_i - x_j)^2 + (y_i - y_j)^2 + (z_i - z_j)^2 \right]^{1/2} \tag{1}$$

The matrix is symmetric with diagonal elements of zero; conventionally only the lower half of the matrix is used. If two molecules are to be compared, the corresponding elements in the two matrices, DM1 and DM2, are subtracted to give the difference distance matrix

$$DDM_{ij} = \left| DM1_{ij} - DM2_{ij} \right| \tag{2}$$

The statistical difference between the two matrices, s, is given by [2]

$$s = \frac{1}{n} \left\{ \sum_i^n \sum_j^n DDM_{ij}^2 \right\}^{1/2} \tag{3}$$

Distance matrix methods for comparing molecules work well if the ordering of atoms is well defined. If the two molecules are very dissimilar, then the atomic order is not clear and the elements in the distance matrix DM2 have to be re-ordered combinatorially; the number of orderings is n! The amount of computer time needed to solve the problem to give the best match becomes unreasonable for $n > 13$. However, if matching between functional groups is sought, such as matching between hydrogen-bonding donors or acceptors, the search can be limited to the functional atoms only. This method of searching can be optimized by a branch-and-bound strategy [3]. The disadvantage of searching for functional atoms only, is that 'non-functional' atoms are ignored and overall poor steric correspondences are likely to be generated.

Distance matrix methods operate solely on the Cartesian coordinates; bonding information is neglected. Maximal common subgraphs (MCS) take atoms to be

vertices of the molecular graph with the bonds representing the edges of the graph. MCS searching locates the portions of molecular structure that are common to both molecules [4,5]. The MCS methods are very useful in searching for pharmacophores which can be represented by a common subgraph. However the procedures are almost entirely based on similarity in chemical structure. The method is not appropriate if structural dissimilarity is a strong feature in molecular comparisons.

Molecular recognition

An alternative approach to studying similarity in structurally dissimilar molecules is to turn to the chemical theory of molecular interactions. We ask the question: what molecular properties in the ligand lead to a significantly attractive interaction energy? The process of molecular recognition may be defined as a mutual association of two molecules through the interaction of their respective force-fields. Thus in order to understand the recognition process, and why molecules differ from each other in their affinity for the receptor, we have to study each of the component forces. Our understanding of QSAR needs to be re-examined in the light of this new information.

The energy of interaction of two neutral atoms A and B, infinitely separated, can be described as the sum of the energy associated with each atom.

$$E_{tot} = E_A + E_B \tag{4}$$

If both atoms are now brought to a separation, r, the energy is

$$E_{tot} = E_A + E_B + U(r) \tag{5}$$

where $U(r)$ is the inter-atomic pair-potential. Similarly if A and B are molecules, then $U(r)$ is dependent on the separation of the centres of mass R_{AB} and the relative orientations ωA and ωB.

The potential U is composed of the component forces: electrostatic, induction, dispersion and repulsion.

$$U = U_{el} + U_{ind} + U_{disp} + U_{rep} \tag{6}$$

This equation can be approximated by the well known intermolecular pair-potential method which has been exploited extensively by Clementi [6]. Thus the energy of interaction between two molecules in vacuo is given by

$$E = \sum_i \sum_{j \neq i} \left(-A_{ij}^{ab}/r_{ij}^6 + B_{ij}^{ab}/r_{ij}^{12} + C_{ij}^{ab} q_i q_j / r_{ij} \right) \tag{7}$$

This equation has similarities with a Lennard-Jones type of potential plus a coulombic component. The total energy is expressed as the sum of all atom pairs between the two molecules, taking atom i in one and atom j in the other molecule. Subscripts a and b refer to the type of atom and its class (belonging to a chemical group); r_{ij} is the interatomic distance between i and j; q_i and q_j are atomic charges on atoms i and j. The constants A, B and C are determined by extensive quantum chemistry calculations and fitted for each atom type and class by regression analysis. The method works well in practice and has been used successfully in Monte Carlo simulations of hydration at protein surfaces.

Three important deductions for QSAR can be drawn from Eqn. 7. 1. The bonding topologies of both molecules are not incorporated into the equation. 2. Only atoms at the interface between the two molecules will affect the first and second terms due to the 6 and 12 inverse power relationship. 3. The electrostatic term operates over large distances. These conclusions lead to a very important corollary for two ligands binding to the same site: both ligands may possess very similar patterns of molecular fields at the surface but have different bonding topologies. Stated another way, we may infer that the recognition properties of two ligands may be nearly identical even though they are structurally dissimilar. One route through the impasse of accounting for structural dissimilarity in QSAR may be achieved by reconsidering the implications of Eqn. 7

Matching molecular surfaces

Eqn. 7 suggests that there are two factors of over-riding importance in molecular recognition: the disposition of atoms at the ligand binding face and the electrostatic potential, generated by all atoms in the ligand, that emanates from the binding face. Ligands which bind to the same site region should have similar surface binding motifs. A motif is defined as the pattern in 3-dimensions generated by atoms at the accessible surface of a ligand and/or the pattern of electrostatic potential projected onto the accessible surface generated by all the ligand atoms. Progress in QSAR might be made if methods can be developed for matching surfaces and electrostatic potentials. Two questions then arise and should be tackled. 1. If the binding motif on molecule A is known, can we search for a matched surface motif on molecule B? 2. If the binding motif on A is known, can we use that surface to form a mould in which a molecule of dissimilar structure might be designed with the same binding motif as A? In other words, can we create a new class of molecules and thus release current QSAR methods from retrospective modifications to a congeneric series? This latter possibility, if it can be achieved, should have significant commercial implications.

In Eqn. 7, where recognition occurs through non-covalent interactions, the smallest value for r_{ij} between an atom in the receptor and an atom in the ligand will coincide with the accessible surface of the ligand. Therefore, it makes sense to use the ligand accessible surface as the one on which comparisons between ligands are to be made. This accessible surface is constructed by rolling a spherical probe (1.7 Å radius) over the ligand surface. The match between any two specified surfaces is then related to the difference between them when the surfaces are superimposed.

A statistical expression for the match can be obtained from Spearman's rank correlation coefficient [7]

$$R_{\text{rank}} = \left\{ (n^3 - n) - 6 \sum_{k=1}^{n} d_k^2 - (T_A^* + T_B^*)2 \right\}$$

$$/\left\{ \left[(n^3 - n) - T_A^* \right]\left[(n^3 - n) - T_B^* \right] \right\}^{1/2} \tag{8}$$

where d_k is the difference in ranks between corresponding points on the surfaces. n is the number of point pairs to be compared, and

$$T_A^* = \sum (t_A^3 - t_A)$$

where t_A is the number of ties (similarly for T_B^*). If the two surfaces are related by a linear regression, and V_A and V_B are actual surface values at corresponding positions k, then

$$V_{Ak} = \alpha V_{Bk} + \beta$$

where α is the regression coefficient and β is the regression constant. Pearson's product-moment correlation coefficient, r, is given by

$$r = \left\{ \sum_{k=1}^{n} (V_{Bk} - \overline{V}_B)(V_{Ak} - \overline{V}_A) \right\} \Big/ \left\{ \sum_{k=1}^{n} (V_{Bk} - \overline{V}_B)^2 \sum_{k=1}^{n} (V_{Ak} - \overline{V}_A)^2 \right\}^{1/2} \qquad (9)$$

These statistical expressions are particularly useful measures of a pattern match if there is a difference in magnitude between surface values, for example, where one molecule is singly charged and the other is doubly charged. The pattern of potential may be very similar although the differences in surface values, in this case, would differ by a factor of two.

Searching for a motif by minimization

Consider the case where the binding motif of molecule A is known. The problem is to find a similar motif on a dissimilar molecule B. In principle, all that has to be done is to rotate B until a match occurs where the difference in motifs is a minimum. This procedure can be expressed formally

$$\text{minimize } F(x_1, x_2, \cdots x_n); \; x_j \in \mathbb{R}^n$$

where the variables x_j are the Euler angles for the rotation of B. The function F must be continuous and differentiable; this excludes the use of R_{rank} as the objective function since it is discontinuous. Let the feature of the surface motif be P computed at points i on A and B, then the residual, e_i, is

$$e_i = P_{iA} - P_{iB}$$

$$F(x_1, x_2, \cdots x_n) = \sum_{i=1}^{k} e_i^2 \qquad (10)$$

for k point pairs. In this example, where only B is rotated, n is 3, i.e. the three Euler angles for B. The function can be minimized by a Quasi-Newton algorithm.

The distribution of points, i, on the surfaces of A and B has to be as even as possible to avoid statistical distortion in sampling the surfaces. Gnomonic tessellation of an icosahedron provides the best semi-regular distribution [8]. Points i at the surface are then obtained by calculating the pierce-point of a ray from the centroid to a tessellation point passing through the accessible surface. The feature value P is calculated at each point i. If only the accessible surfaces are to be matched, then P_i is the length of the ray from the centroid to the pierce-point at position i. Similarly, if the electrostatic potential is to be matched, P_i is the value of the potential at the pierce-point position i. A convenient number of points for matching a hemispherical projection is 90.

Minimization algorithms stop at the first minimum encountered. If we wish to find the global minimum, or an orientation corresponding to a minimum near to the

global minimum, the algorithm needs to start from a number of randomly distributed orientations. Unless the searching technique can itself be optimized these procedures become too costly for routine use. Very significant gains in optimization can be derived from the fact that the Quasi-Newton algorithms converge fast in early iterations. Therefore if we have a large number of starting orientations, these points in rotational 3-space move into clusters after a short minimization. Each cluster can then be used as a new starting orientation for further extensive minimization. A 50-fold optimization can be gained by splitting the search into two levels [9,10]. The steps for each level are:

Level 1:
(1) start with 1000 random orientations of B;
(2) minimize for 40 function calls;
(3) end points fall into clusters which are fuzzy;
(4) make the fuzzy clusters discrete by filtering off the largest residuals;
(5) apply cluster analysis to the remaining points with low residuals;
(6) select 20 clusters with the lowest residuals.

Level 2:
(1) minimize again using the 20 cluster optimum positions as new starting points;
(2) allow full optimization.

Example of searching for a matched motif

The two neurotoxins, tetrodotoxin and saxitoxin (structures shown in Fig. 1) will be used as an example of searching for a motif. Molecule A (tetrodotoxin) is kept fixed in a defined orientation. The accessible surface is computed on a hemispherical projection. Molecule B (saxitoxin) is rotated around its centre of mass and the accessible surface calculated. Both gnomonically projected faces are compared by computing the residuals. A uniformly distributed set of random starting angles is used to provide the initial orientations; these are illustrated in Fig. 2a. The distribution of orientations at step 3 of level 1 is shown in Fig. 2b after minimization for 40 function calls. It can be seen that the orientations have clustered into regions along the trajectories in 3-space; these are fuzzy clusters. Our objective is to find orientations of B with low residuals. Therefore we can reject high residuals; a cut-off point R_p in the frequency distribution of residuals is taken at a point
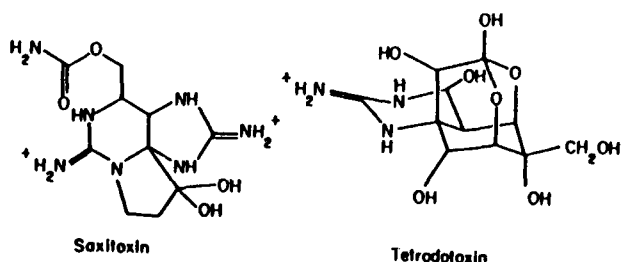
FIG 1   Molecular structures of tetrodotoxin and saxitoxin.

Initial starting positions

Level 1 Fuzzy clusters

a   b
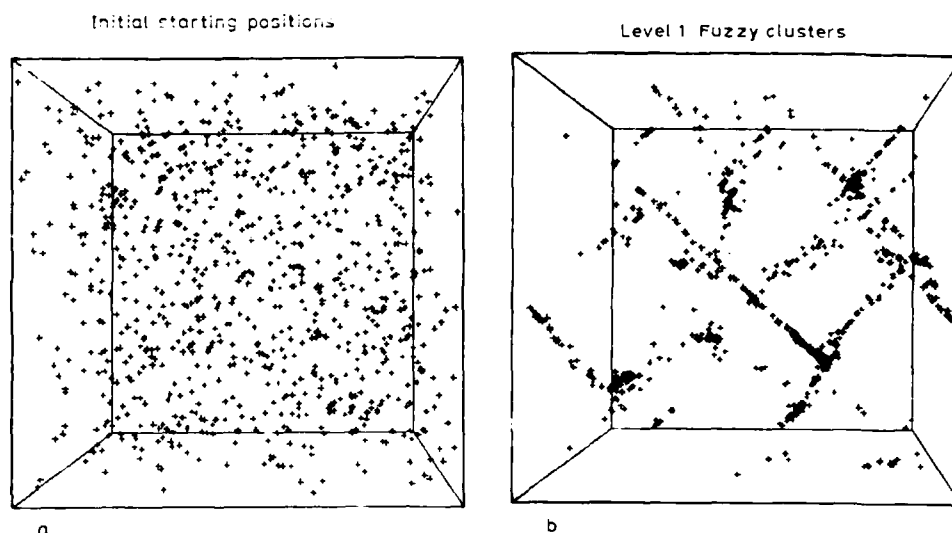
FIG 2   a: random distribution of orientation positions for saxitoxin. The axes of the block represent the Euler angles x_1, x_2, x_3 and the dimensions of the block are 2π for x_1 and x_2 in the plane of the paper, and π for x_3 normal to this plane. b: distribution of points after step 3 of level 1 optimization.

corresponding to the maximum frequency. Only values lower than R_p are retained for cluster analysis. The distribution of points after filtration is shown in Fig. 3a; this distribution is more discrete   detailed examination of the structure of the clusters by principal components analysis reveals that there are two principal

Level 1 Clusters after filtration

Level 2 Final positions

a   b
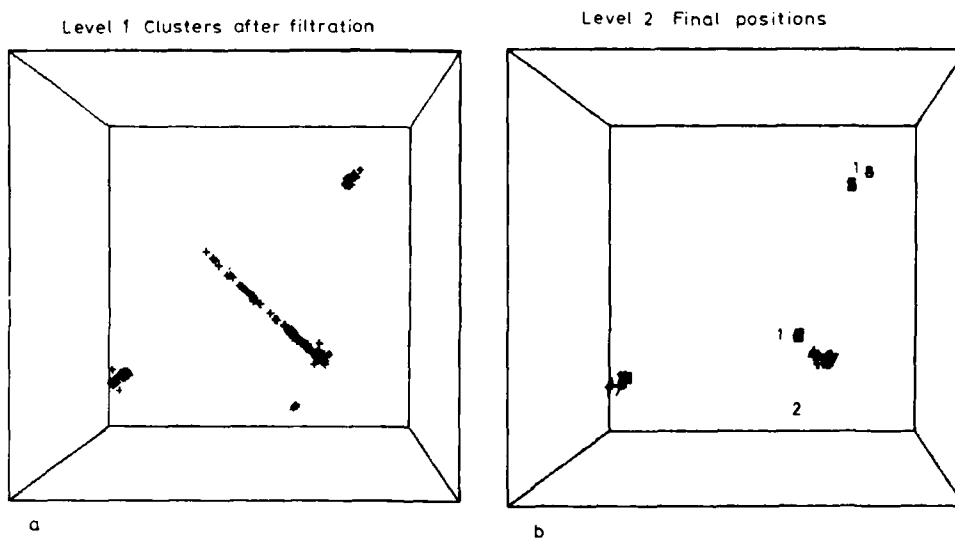
FIG 3   a: the data from Fig. 2b after removal of points with residuals $R_p > 47$ Å^2. b: final positions of local minima after full optimization at level 2.
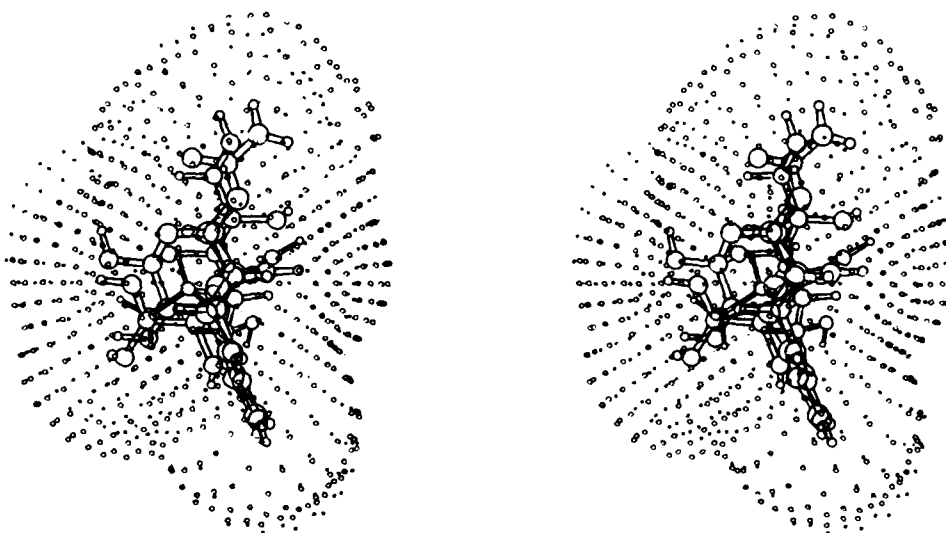
FIG 4   The accessible surface match for tetrodotoxin (+) and saxitoxin (o) superimposed.

components in 3-space; this indicates that the distribution of points is not spherical but planar. Since the structure of the clusters determines which clustering technique may be used in the analysis, we rejected spherical clustering methods and used an agglomerative single-linkage hierarchical method on the data from Fig. 3a. The desired number of clusters has been set to 20. In each of the 20 clusters, the position associated with the lowest residual in the cluster is chosen at step 6 and used for step 1 in level 2. After a full minimization the final orientation positions are shown in Fig. 3b. Six orientations with low residuals are found. A match between two accessible surface motifs is shown in Fig. 4. Not only is there a good fit at the periphery of the two surfaces, stereoscopic drawings show that the projected faces also fit remarkably well [9,10].

Blind-searching for undefined motifs

It is frequently found in practice that the binding face of ligands to be compared is not known. If both ligands bind at the same site, then we may assume from Eqn. 7 that they possess a binding motif in common. Blind-searching is a technique to identify common motifs. The method does not guarantee that the best common motif is the binding motif, but it does provide a number of possible motifs to consider.

The principles of blind-searching are closely related to those of searching for a matched motif [11]. In blind-searching, so named because the target motif and orientation are not specified, we find a number of matches with low residuals and high rank correlation coefficients. Both molecules are rotated simultaneously, the only fixed reference frame is the size and shape of the window through which the molecules are to be compared. The problem is to minimize the residuals in rotational 6-space; 6-D cluster analysis is used to identify the best discrete matched
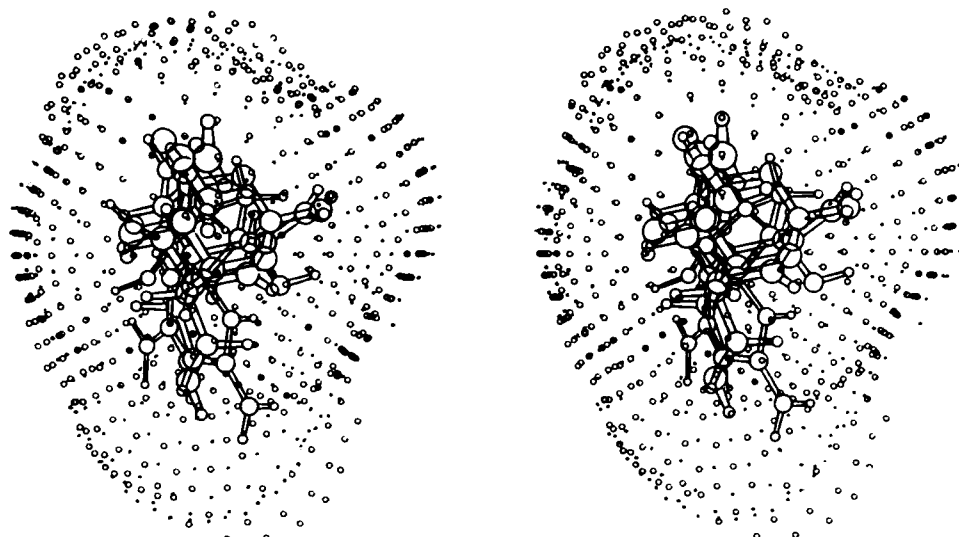
FIG 5 The best match in the accessible surface of tetrodotoxin and saxitoxin revealed by blind-searching.

orientations. Searching can be optimized in exactly the same way as before; the only differences are that at step 1 of level 1 we use 1000 random orientations for each of the 6 Euler angles.

Blind-searching has been tested on tetrodotoxin and saxitoxin. A number of well matched orientations can be found for the accessible surfaces. The best matched hemispherical projection is shown in Fig. 5; the surfaces show an rms separation of 0.45 Å.

Window shapes for searching

In the foregoing illustrations, the window used has been a hemispherical projection. This was used to simulate a receptor cleft into which the ligand might bind. Different window shapes may be more appropriate in other circumstances. For example, if the ligand is believed to bridge between two macromolecular chains, or subunits, it would be better to use a spherical projection that only includes bipolar patches. However, if a molecule is approximately planar and the ligand points are distributed at the edges, it would be appropriate to incorporate a spherically projected band as the window. Where the window shape can be determined, the particular spherical projection can be easily incorporated into the searching routines.

Motifs containing multiple features

The methods outlined for matching and searching for motifs have considered a single feature only. However, it can be seen from Eqn. 7 that both the steric surface and the electrostatic potential contribute to the interaction energy between the

440

ligand and its site. It would be advantageous to match and search simultaneously for both features in a motif. The difficulty here is that in matching surfaces and potentials together, the units and scales are different. In principle this difficulty could be overcome by autoscaling the features. Consider the general problem where we have Q features. Each feature on A and B needs to be sampled statistically. For k points in the sample (i.e. spherically tessellated points in the window), the mean value of the feature, P_m, is

$$P_m = k^{-1} \sum_{i=1}^{k} P_i \tag{11}$$

and the variance is

$$s = k^{-1} \sum_{i=1}^{k} (P_i - P_m)^2 \tag{12}$$

Thus the autoscaled feature at point i is

$$P_i = (P_i - P_m)/s \tag{13}$$

This distribution has a mean of 0 and a variance of 1 and so has removed potential difficulties with different units and scales. Now minimize the residuals, e_i,

$$e_i = P'_{iA} - P'_{iB}$$
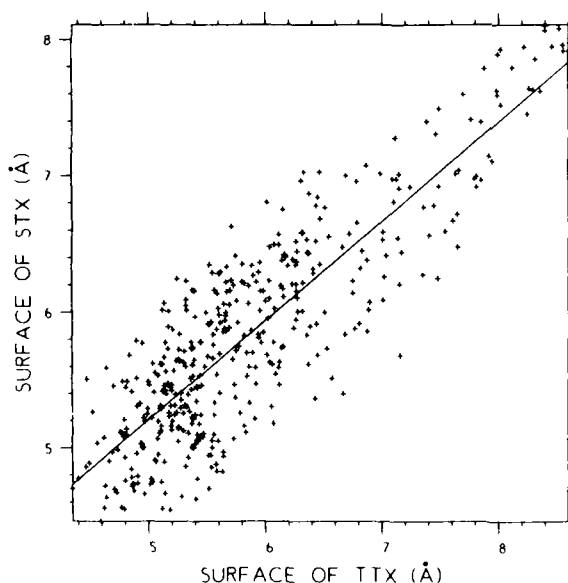
FIG 6 The regression line for the accessible surface match between tetrodotoxin and saxitoxin. The data is taken from the blind-search with the final orientations illustrated in Fig. 5.

Therefore, for Q features each with an associated weight, w, the function to be minimized is

$$F(x_1, x_2, \cdots x_n) = \sum_{i=1}^{k} w_1 e_{1i}^2 + w_2 e_{2i}^2 + \cdots w_Q e_{Qi}^2 \qquad (14)$$

Appropriate weighting of individual features has yet to be examined.

Future directions in QSAR

Linking motif matching to QSAR studies

Inspection of the regression line of Fig. 6, for the surface values of STX plotted against those of TTX, shows that the spread of points about the line varies; $R_{rank} = 0.83$ and $r = 0.86$. If the points composing the window were to be ordered systematically into defined regions, such as an icosahedral face, then it ought to be possible to study the differences in regression associated with the distribution on
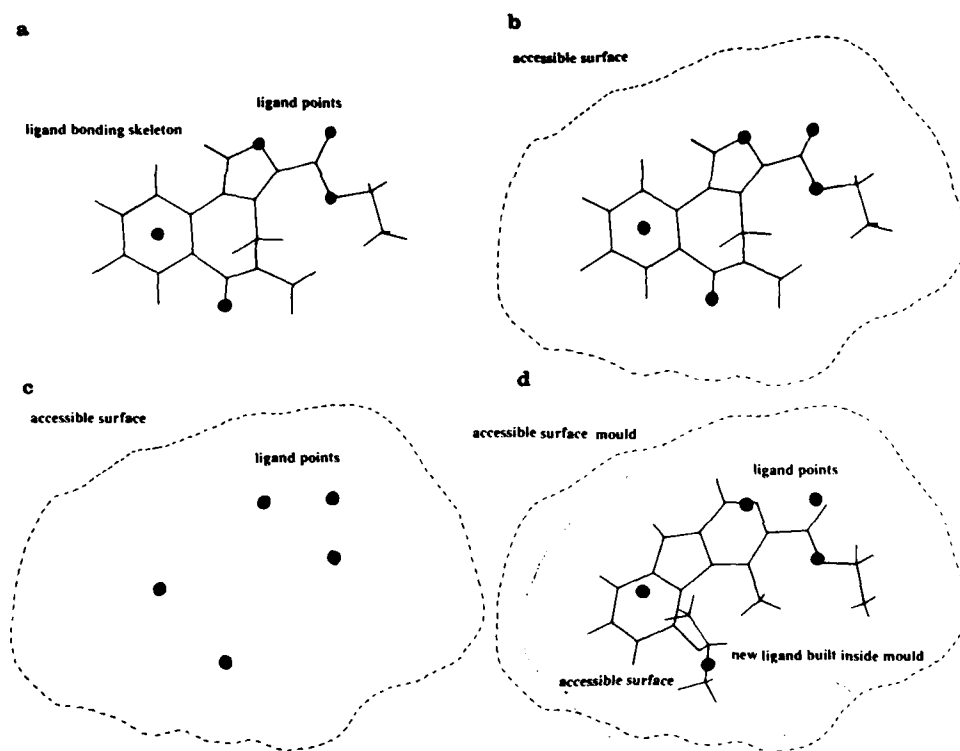
FIG 7 A scheme for generating new classes of compounds from the accessible surface of a known bioactive ligand. a: a molecule with ligand points defined (●). b: accessible surface constructed round the ligand. c: ligand removed from the accessible surface. d: a molecular graph incorporating the ligand points at appropriate positions.

each regional face. Multivariate analysis on a group of ligands could be used to identify regional differences in features composing the motif; these might be related to biological affinity or activity. This analysis should provide an approach to QSAR based solely on the principles of molecular recognition; it would fully incorporate structural dissimilarity as an integral part of a general methodology.

Generation of new classes of bioactive compounds

One of the most persistent criticisms of QSAR is that the methods are, strictly speaking, unable to suggest new classes of molecular structure that have a reasonable chance of behaving as bioactive ligands at specified binding sites. The fact that it is now possible to match motifs on dissimilar structures raises the question: how many other dissimilar structures could present a similar matched motif? It has been observed earlier that the disposition of surface atoms largely determines the outcome of Eqn. 7; the bonding topology is not a feature of the equation. What may therefore be of great interest would be to determine how many dissimilar bonding topologies may be used to incorporate atoms that define the motif. There could be some leeway in atom positions if the site can accommodate slight differences in motifs.

The following scheme outlined in Fig. 7 can be proposed to investigate this fascinating question. Take a molecule with a known binding face and motif. Identify the ligand points in the structure (Fig. 7a). Construct the accessible surface round the ligand (Fig. 7b). This surface then functions as a mould. Remove the ligand (Fig. 7c). What remains is a possible impression of the shape of the site with the key ligand points left in the mould. All that has to be done is to establish a set of networks of standard bonds and bond angles that incorporate the key ligand points as vertices at feasible positions on the evolving molecular graphs (Fig. 7d). Finally, the vertices of the graph have to be replaced with atoms which are appropriate for a correct valence bond description and which match the same ligand points or electrostatic potential. With the benefit of hindsight, one could have taken a benzodiazepine derivative (Ro 151788) (Fig. 7a) and derived a β-carboline (ZK93426) (Fig. 7d) which has matching accessible surface and electrostatic motifs. How many other compounds could be constructed in a similar way?

Discussion

Molecular recognition provides a fresh perspective for re-examining the scientific basis of QSAR. This paper has drawn attention to two aspects of recognition and the impact they may have on new QSAR studies. These key aspects are: (1) the surface shape and (2) the electrostatic potential at the binding face; their importance has been inferred from the equation for intermolecular pair-potentials. This equation is strictly applicable only for the in vacuo state. Further intermolecular effects, not included in the equation, come into play when solvent is included [1]. Thus we should also consider hydrogen bonding and regions of surface hydrophobicity as further features to be incorporated in a comprehensive molecular theory of QSAR. Adequate methods need to be developed for mapping these features onto the ligand accessible surface.

The intermolecular atom-pair-potential equation, so important in our understanding of molecular recognition, draws attention to those molecular factors that

determine affinity between the ligand and its receptor. The equation says nothing about efficacy, that is the ability of the molecule to be an agonist, a partial agonist, an inverse agonist or a competitive antagonist. Strictly speaking, we should limit any statistical study, based on molecular recognition, to correlations between structure and affinity in the first instance; if the relationship between efficacy and affinity is straightforward, then we may, with confidence, extend molecular recognition theory to developing a description of activity.

Pattern matching and pattern searching techniques have been outlined which enable the chemist to measure similarity between faces on dissimilar molecules. The simple fact that similar motifs can be found on molecules of diverse chemical structures, suggests that a new approach to de novo drug design might be possible; the accessible surface binding motif of a known ligand could be used as a mould from which we might be able to construct novel classes of molecules.

Summary

Key forces in molecular recognition are identified from a consideration of inter-molecular pair-potentials. The shape of the molecule at the binding face and the electrostatic potential form the principal determinants of molecular recognition. These features on molecules can be characterized and patterns between ligand faces can be matched. Patterns may also be searched for, either by comparison with a fixed face or blind-searched where no pattern has been identified explicity. Dissimilar molecular structures can have similar binding motifs These motifs could be used to generate new classes of bioactive compounds designed for activity at specified structural sites.

Acknowledgements

References

1 Dean, P.M. (1987) Molecular Foundations of Drug-Receptor Interaction. Cambridge University Press.
2 Padlan, E.A. and Davies, D.R. (1975) Variability of three dimensional structure in immunoglobulin Proc. Natl. Acad. Sci. U.S.A. 72, 819–823.
3 Danziger, D.J. and Dean, P.M. (1985) The search for functional correspondences in molecular structure between dissimilar molecules. J. Theor. Biol. 116, 215–224.
4 Golender, V.E. and Rosenblit, A.B. (1983) Logical and Combinatorial Algorithms for Drug Design. Research Studies Press, Chichester; John Wiley & Sons.
5 Brint, A.T. and Willett, P. (1987) Pharmacophoric pattern matching in files of 3D chemical structures: comparison of geometric searching algorithms. J. Mol. Graph. 5, 49–56.
6 Clementi, E. (1980) Computational aspects of large chemical systems. In: Lecture Notes in Chemistry, Vol. 19. Springer Verlag, Berlin.

7 Namasivayam, S. and Dean, P.M. (1986) Statistical method for surface pattern matching between dissimilar molecules: electrostatic potentials and accessible surfaces. J. Mol. Graph. 4, 46–50.

8 Chau, P.-L. and Dean, P.M. (1987) Molecular recognition: 3D surface structure comparison by gnomonic projection. J. Mol. Graph. 5, 97–100.

9 Dean, P.M. and Chau, P.-L. (1987) Molecular recognition: optimised searching through rotational 3-space for pattern matches on molecular surfaces. J. Mol. Graph. 5, 152–158.

10 Dean, P.M. and Callow, P. (1987) Molecular recognition: identification of local minima for matching in rotational 3-space by cluster analysis. J. Mol. Graph. 5, 159–164.

11 Dean, P.M., Callow, P. and Chau, P.-L. (1988) Molecular recognition: blind-searching for regions of strong structural match on the surfaces of two dissimilar molecules. J. Mol. Graph. (in press).

CHAPTER 33

Structure–activity studies on mammalian glutamate receptors

J.C. WATKINS

Department of Pharmacology, The Medical School, Bristol BS8 1TD, U.K.

Introduction

In the mammalian central nervous system, excitatory amino acid (EAA) receptors can be easily differentiated into two main types — those activated preferentially by the synthetic amino acid, N-methyl-D-aspartate (NMDA) * (Fig. 1) and blocked selectively by a range of competitive antagonists, and those activated preferentially by the potent naturally occurring amino acid excitants kainate and quisqualate (Fig. 1), and not blocked by selective NMDA antagonists [1]. For convenience, the terms NMDA receptors and non-NMDA receptors are used for these two main types [2]. Ion channels opened by NMDA receptor activation are subject to blockade by Mg^{2+} in a voltage-dependent manner [3] and also by a range of non-competitive NMDA antagonists [4,5]. Responses induced in mammalian central neurones by kainate and quisqualate can be differentially depressed by several antagonists and this has been interpreted as indicative of two separate subtypes of non-NMDA receptors, the so-called kainate and quisqualate subtypes, which are considered to co-exist on mammalian central neurones together with NMDA receptors [1–3,6].

This interpretation is supported by the high differential in kainate and quisqualate potency observed in some tissues, suggesting the probable existence in those tissues of relatively pure populations of one or the other subtype. Thus, receptors at crustacean neuromuscular junctions seem to be mainly of the quisqualate type [7], while those on mammalian C fibres are mainly of the kainate type [8].

Most of the simple acidic amino acids occurring in brain, including L-glutamate and L-aspartate (Fig. 1), as well as certain sulphur-containing amino acids, are considered to have 'mixed' actions, mediated by more than one type of receptor [1,3,6,9]. The receptors involved may include additional types beyond the NMDA, kainate and quisqualate classes. Of these, the most discrete type appears to be that at which the phosphono analogue of L-glutamate, L-2-amino-4-phosphonobutyrate (L-AP4, Fig. 1) acts in depressing certain excitatory synaptic pathways in the brain

---

* The older nomenclature D and L (instead of R and S) is used throughout this article for stereochemical designation of simple and/or well-known α-amino acids in order to avoid confusion, especially where an enantiomeric letter is included in well-accepted abbreviations (e.g. NMDA, γDGG).
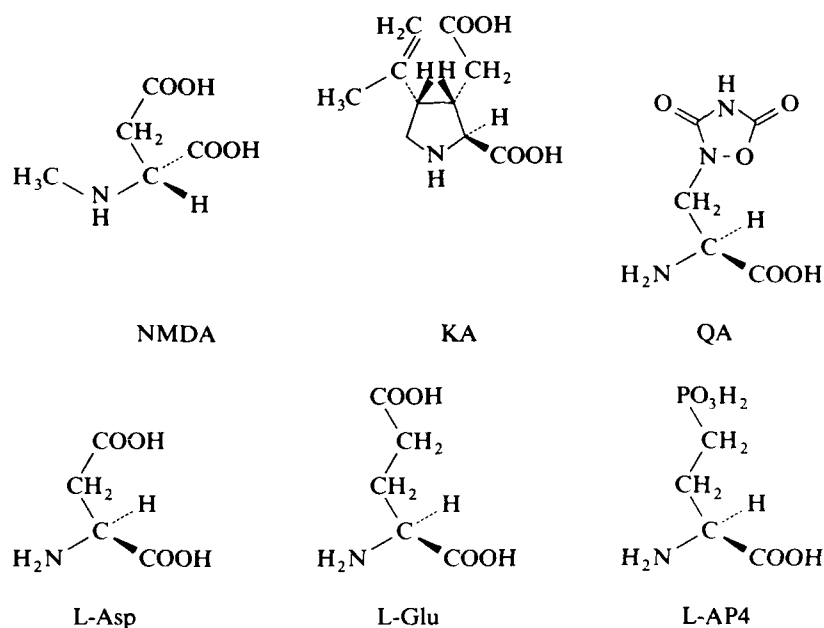
FIG 1 Structures of *N*-methyl-D-aspartic acid (NMDA), kainic acid (KA), quisqualic acid (QA), L-aspartic acid (L-Asp), L-glutamic acid (L-Glu) and L-2-amino-4-phosphonobutyric acid (L-AP4).

[10,11] and spinal cord [12] and which may or may not be the same type of receptor with which this substance interacts in mimicking the hyperpolarizing action of L-glutamate on ON bipolar cells in retina [13].

This chapter will attempt to bring together pharmacological and binding data which elucidate the molecular structural requirements for competitive agonist and antagonist interaction with the recognition site of the various EAA receptors outlined above, with particular emphasis on NMDA receptors. Non-competitive antagonists will not be discussed; for these topics the reader is referred to recent reviews [4,5,14].

NMDA receptors

Detailed structure–activity data have long been available from electrophysiological experiments in relation to the molecular features favouring potency and/or selectivity of NMDA antagonists [1,15,16]. No such data have been available for NMDA receptor agonists due to the 'mixed' nature of this action in many cases (simultaneous activation of more than one type of receptor) and the absence of sufficiently specific antagonists for non-NMDA receptors. Differences in rates of uptake of excitants is a further difficulty in the interpretation of agonist potencies. However, recent binding data have now allowed assessment of affinities of both agonists and antagonists for the NMDA receptor [17–19].

Affinities of agonists and antagonists for the NMDA receptor are reflected in their K_i values (Table 1) for inhibition of the binding of D-[^{3}H]-2-amino-5-phosphonopentanoate (D-[^{3}H]AP5) and/or [3-^{3}H](($\pm$)-2-carboxypiperazin-4-yl)-propyl-1-phosphonate ([^{3}H]CPP) to brain membranes [18,19]. Structure–activity relations are discussed below.

Inter-acidic group separation

Agonists Optimally, two or three carbon (or other) atoms separate the two acidic groups.

Antagonists The optimal separation is four to six atoms.

Enantiomeric preference

Agonists Often both D and L forms are active, with greater activity shown by different enantiomers in different pairs (e.g., by L-glutamate and D-homocysteine sulphinate).

Antagonists The D form is usually far more active than the L form.

Terminal acidic group

Agonists The optimal ω-terminal acidic group varies according to chain length and configuration at the α-carbon atom. The COOH and SO_2H groups are always effective as ω-terminals, and (usually) also the SO_3H group; however, the PO_3H_2 group is relatively ineffective.

Antagonists In contrast, for the PO_3H_2 group is the most effective terminal, with COOH also very effective, while SO_3H is much less effective.

Chain substituents

Agonists Substituents in the chain are generally detrimental to activity, with the C4 position in the glutamate molecule being the least vulnerable position. Dual (ring-forming) substituents such as in *cis*-ACDP, homoquinolinic acid and *trans*-2,3-piperidine dicarboxylic acid are exceptions, these compounds all having high agonist activity.

Antagonists The effects of substituents in the chain have not yet been investigated systematically, but ring-forming dual substituents, as present in the molecule of CPP and CPP analogues, are obviously well tolerated.

α-N-Alkylation
Generally this structural change is highly detrimental in *agonists*, an exception being NMDA. This compound has the same affinity for the receptor as D-aspartic acid (but the latter appears to be a much weaker excitant because of its rapid uptake). The effect of simple α-N-alkylation in the case of open chain *antagonists* has not been investigated, though compounds with ring-forming substituents involv-

TABLE 1 K_i values for inhibition of binding of [D-³H]2-amino-5-phosphonopentanoate (³H-D-AP5) and/or [3-³H]((±)-2-carboxypiperazin-4-yl) propyl-1-phosphonate (³H-CPP) to rat cerebral cortex membranes [18,19].

Agonists   *General formula:*

$$R^1HN \diagdown CH \diagup A - X$$
$$HOOC \diagup \quad R^2$$

	A	R^1	R^2	X	K_i (μM) [a] L	D	DL
Aspartic acid	-CH₂-	H	–	COOH	11	10	
Glutamic acid	-(CH₂)₂-	H	–	COOH	0.9	49	
Cysteine sulphinic acid	-CH₂-	H	–	SO₂H	13	23	
Homocysteine sulphinic acid	-(CH₂)₂-	H	–	SO₂H	10	6.3	
Cysteic acid	-CH₂-	H	–	SO₃H	120	170	
Homocysteic acid	-(CH₂)₂-	H	–	SO₃H	3.9	11	
2-Amino-3-phosphono-propionic acid	-CH₂-	H	–	PO₃H₂			560
2-Amino-4-phosphono-butyric acid	-(CH₂)₂-	H	–	PO₃H₂	510	250	
N-Methyl-aspartic acid	-CH₂-	CH₃	–	CO₂H	160	11	
N-Methyl-glutamic acid	-(CH₂)₂-	CH₃	–	CO₂H	210	800	
N-Ethyl-aspartic acid	-CH₂-	CH₃-CH₂-	–	CO₂H	710	100	
N-Ethyl-glutamic acid	-(CH₂)₂-	CH₃-CH₂-	–	CO₂H	250	>1000	
N-n-Propyl-aspartic acid	-CH₂-	CH₃-(CH₂)₂-	–	CO₂H	560	180	
2-Methyl glutamic acid	-(CH₂)₂-	H	2-CH₃	CO₂H			>1000
3-Methyl-glutamic acid	-CH(R²)-CH₂-	H	3-CH₃	CO₂H			810
3-Hydroxy-glutamic acid	-CH(R²)-CH₂-	H	3-OH	CO₂H			50
4-Methylene glutamic acid	-CH₂-C(=R²)-	H	4-CH₂=	CO₂H	2.8		4.7
4-Methyl-glutamic acid	-CH₂-CH(R²)-	H	4-CH₃	CO₂H			7.9
4-Fluoro-glutamic acid	-CH₂-CH(R²)-	H	4-F	CO₂H			3.2
4-Hydroxy glutamic acid	-CH₂-CH(R²)-	H	4-OH	CO₂H			8.5
4-Amino-glutamic acid	-CH₂-CH(R²)-	H	4-NH₂	CO₂H			31

Other agonists
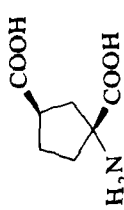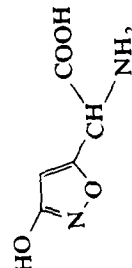
Compound	Structure			
cis-1-Aminocyclopentane-1,3-dicarboxylic acid	H₂N–[cyclopentane]–COOH, COOH			13
Piperidine-2,3-dicarboxylic acid	see Fig 3	cis	>1000	21	46
		trans			30
Homoquinolic acid	CH₂—COOH, COOH (pyridine)		7.1 [b]	
Ibotenic acid	HO–[isoxazole]–CH(NH₂)COOH		16	
α-Amino-3-hydroxy-5-methyl isoxazole-4-propionic acid (AMPA)	see Fig. 2			1000
5-Bromowillardiine	see Fig. 2			>1000
β-N-Oxalyl-α,β-diamino-propionic acid	HOOC-CO-NH-CH₂-CH-COOH, NH₂		130	41 [c]
Kainic acid	see Fig. 1		810	
Quisqualic acid	see Fig. 1		170	

TABLE 1 (continued)

General formula:

H_2N

$HOOC$

$\overset{*}{C}H\text{-}(CH_2)_2\text{-}A\text{-}X$

Antagonists	A–X	K_i (μm) [a]		
		L	D	DL
2-Aminoadipic acid	$CH_2\text{-}COOH$	89	13	
2-Aminosuberic acid	$(CH_2)_3\text{-}COOH$	80	25	
2-Amino-5-phosphono-pentanoic acid	$CH_2PO_3H_2$	40	0.62	
2-Amino-7-phosphono-heptanoic acid	$(CH_2)_3\text{-}PO_3H_2$	28	1.7	
2-Amino-5-sulphopentanoic acid	$CH_2\text{-}SO_3H$			140
2-Amino-7-sulphoheptanoic acid	$(CH_2)_3\text{-}SO_3H$			520
γ-Glutamylglycine	$CO\text{-}NH\text{-}CH_2\text{-}COOH$	75	41	
γ-Glutamylaminomethyl phosphonic acid	$CO\text{-}NH\text{-}CH_2\text{-}PO_3H_2$		25	
γ-Glutamylaminomethyl sulphonic acid	$CO\text{-}NH\text{-}CH_2\text{-}SO_3H$	620	710	

CPP and Analogues   *General formula:*
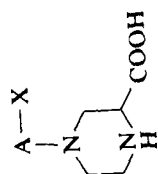
3-(2-Carboxypiperazin-4-yl)-propionic acid	$(CH_2)_3$-COOH	(1.9)
3-(2-Carboxypiperazin-4-yl)-propyl-1-phosphonic acid (CPP)	$(CH_2)_3$-PO_3H_2	0.48 (0.35)
3-(2-Carboxypiperazin-4-yl)-propane-1-sulphonic acid	$(CH_2)_3$-SO_3H	(42)

[a] Determined mainly using ^{3}H-D-AP5; ^{3}H-CPP values given in parentheses.
[b] Only one form.
[c] Antagonist.

ing the α-nitrogen atom (such as in CPP and its analogues) are among the most potent antagonists known.

Differences between NMDA agonists and antagonists

In summary, there are at least three striking differences between the optimal structural features for NMDA agonists and those shown by competitive antagonists.

(1) Most antagonists have a chain length one to three atoms longer than agonists.

(2) D forms of antagonists are invariably more active than the corresponding L forms, whereas both D and L forms of agonists often have high activity.

(3) For antagonists, the phosphonate group is much more effective as the ω-terminal than is the sulphonate group; the reverse activity is shown in agonists.

These differences have given rise to the idea that the ω-acidic group of agonists and antagonists interact with different positively charged sites in the receptor [16,18-20].

Agonists and antagonists at other EAA receptors

Structure–activity studies for agonists and antagonists at non-NMDA receptors have been more limited, and definitive conclusions are difficult to draw because of the lack of specific antagonists for the various individual receptor subtypes that exist. Also, because of the greater molecular complexity of kainic and quisqualic acids relative to NMDA and competitive NMDA antagonists, structural modifications have necessarily been more difficult and the availability of configuration isomers more restricted. Nevertheless, both electrophysiological and binding studies have yielded valuable information, some of which is summarized below.

Kainate agonists

NMDA [21] and AMPA, a quisqualate-like excitant [22], do not inhibit the binding of [^{3}H]kainate to brain membranes, and this method of comparison of kainate analogues probably gives the best indication of specific structural requirements for interaction with the kainate receptor. High affinity for the [^{3}H]kainate binding site has quite strict requirements and only domoic acid (Fig. 2) has an affinity for this site which is as high as or higher than that of kainate [23]. Both the stereochemistry of the pyrrolidine 4-substituent and its unsaturation are important to activity, and, of a range of analogues tested, only the keto analogue (in which the 4-isopropenyl group is replaced by an acetyl group (Fig. 2)) retained moderate activity [21]. The kainate receptors in mammalian C fibres appear to be a relatively pure population [8] which should also give definitive structure–activity data. However, the number of excitants tested in this system is, as yet, relatively low and, apart from domoate, which is exceptionally potent, only 5-bromowillardiine (Fig. 2) has activity similar to or higher than that of kainate. Quisqualate has only weak activity in this system, its potency relative to that of kainate being similar to the ratio of the K_i values of these substances as inhibitors of [^{3}H]kainate binding to brain membranes [28].

Substances which act like kainate in stimulating cGMP accumulation in rat cerebellar slices [24] include several compounds in which one or both of the acidic

α-Keto-KA X = O   5 BW   (S)-AMPA

DA X = CH—CH=CH—CH—COOH with CH₃ branch

7-HPCA   4-AHCP   trans-APPC
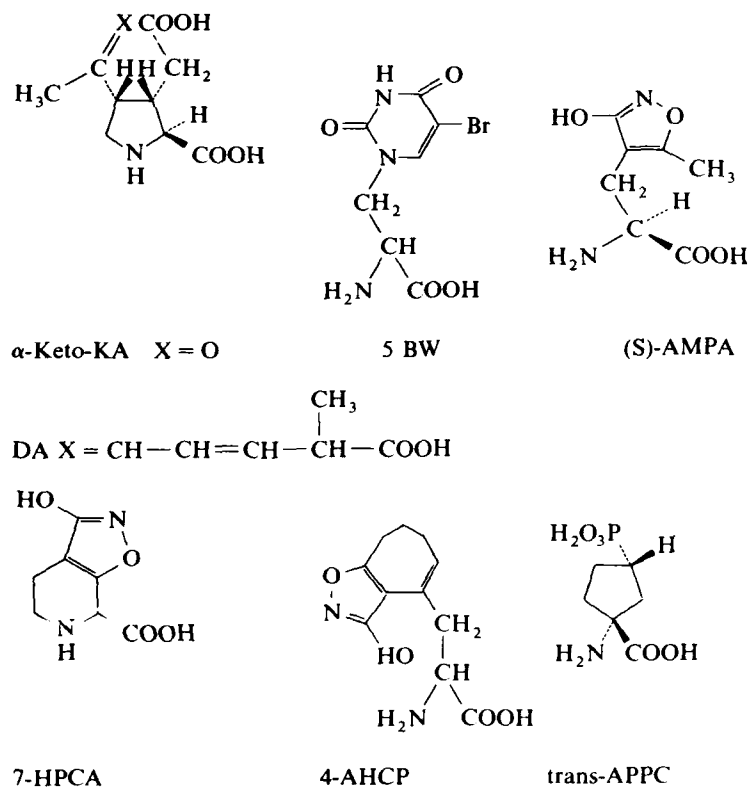
FIG 2 Structures of α-keto-kainic acid (α-keto-KA), domoic acid (DA), 5-bromowillardi-ine, S-α-amino-3-hydroxy-5-methyl-isoxazole-4-propionic acid (S-AMPA), (RS)-3-hydroxy-4,5,6,7-tetrahydroisoxazole [5,4,c]-pyridine-7-carboxylic acid (7-HPCA), α-amino-3-hydroxy-7,8-dihydro-6H-cyclohept[1,2-d]isoxazole-4-propionic acid (4-AHCP), and trans-1 (RS)-amino-3(RS)phosphocyclopentane carboxylic acid (trans-APPC).

groups are absent or modified so that they do not retain their acidic character. Since such groups are considered essential for glutamate-like excitatory activity [25], the relationship between these metabolic actions and electrophysiological responses produced by kainate and like compounds [7] remains to be determined. It is interesting that the 2D form of kainate (β-kainate) has anticonvulsant activity [26], but appears to have agonist rather than antagonist activity [27].

Quisqualate agonists
Structure–activity conclusions in this case are complicated by the possibility that quisqualate interacts with more than one site [28]. However, AMPA (Fig. 2) may be more specific for a particular quisqualate-type receptor. Thus, quisqualate inhibits binding of L-[³H]glutamate and [³H]kainate [29] while AMPA does not inhibit binding of either of these ligands [22]. On the other hand quisqualate and L-glutamate are potent inhibitors of [³H]AMPA binding [30] while kainate is less active.

Krogsgaard-Larsen and his colleagues have synthesized a number of AMPA analogues which are also potent excitants, inhibit [³H]kainate binding weakly or not at all, and are insensitive to blockade by NMDA receptor antagonists [31–34]. It is therefore likely that all these substances act in a similar way to AMPA; two of the most potent substances, 7-HPCA and 4-AHCP, are shown in Fig. 2.

The structures of these compounds suggest that for actions at the quisqualate (AMPA)-type receptors the length of the inter-acidic group chain may be 'glutamate-length', or, in the case of 4-AHCP, one carbon atom longer than this. It is noteworthy that β-N-oxalyl-α,β-diaminopropionic acid (ODAP, Table 1) is another potent excitant with this greater chain length [35]. Its resistance to specific NMDA antagonists [36] and weak action at kainate C fibre receptors [8] probably classify it also as a quisqualate-like excitant. The more active form of AMPA [37], as also of ODAP [38] and quisqualate itself [39], is the L isomer. Methylation of the α-amino group [32], or of the carboxyl or ring-attached hydroxyl group [34] reduces or abolishes activity. The pharmacologically-active conformations of isoxazole excitants have been discussed [33,34].

Kainate and quisqualate receptor antagonists
Several substances are known to depress both kainate- and quisqualate-induced responses in addition to NMDA-induced responses (Fig. 3). Among these, the first to prove useful for characterizing synaptic receptors were γ-D-glutamylglycine (γDGG) and cis-2,3-piperidine dicarboxylic acid (PDA) (Fig. 3) [1]. These were superseded by the more potent non-NMDA receptor antagonists kynurenic acid [40] and the 1-p-chloro and 1-p-bromo derivatives of piperazine-2,3-dicarboxylic acid [41]. Until recently (see below) the most selective non-NMDA receptor antagonists known were γ-D-glutamylaminomethyl sulphonate (GAMS) and γ-D-gluta-myltaurine (Fig. 3) [42] which are, however, less potent at kainate and quisqualate receptors than are kynurenate or the piperazine derivatives.

Certain kainic acid-derived lactones (in which the 3-carboxymethyl and 4-isopropenyl substituents of kainic acid are involved in ring formation) are more effective in depressing kainate-induced ion fluxes in striatal slices than similar fluxes produced by other agonists [43]. However, the low solubility and instability of these substances coupled with their relatively low potency, limit their usefulness as selective kainate antagonists.

Despite its well-known limitations, L-glutamic diethyl acid ester (GDEE) has been the substance of choice over the last ten years for use in ionophoretic experiments in vivo to distinguish those (GDEE-sensitive) responses mediated by quisqualate receptors from those (GDEE-insensitive) responses mediated by kainate or NMDA receptors [44,45]. AMPA and structural analogues [31] also produce GDEE-sensitive responses. However, GDEE is not an effective inhibitor of [³H]AMPA binding [30] and its antagonist action is poorly understood. The substance has not proved a useful glutamate antagonist in vitro [46].

It is possible that barbiturates may act similarly to GDEE in depressing quisqualate-induced responses more effectively than excitation produced by other selective agonists [47,48]. The actions of these substances have been discussed [14].

All the above substances have proved sub-optimal for antagonism of non-NMDA receptors due to their non-specificity and/or low potency. This problem has recently been largely overcome by the disclosure of the FG series of compounds including FG 9065 (CNQX) and FG 9041 (DNQX) (Fig. 3) [49]. These quinoxaline

K/Q ANTAGONISTS

NMDA > K/Q

K/Q ≥ NMDA

$$HOOC-CH_2-NH-CO-CH_2-CH_2-{}^*CH\begin{smallmatrix}NH_2\\\\COOH\end{smallmatrix}$$

γDGG
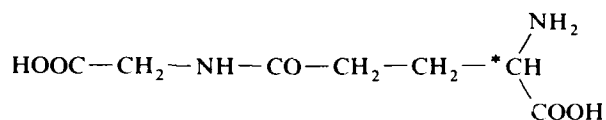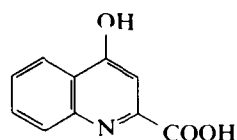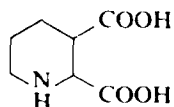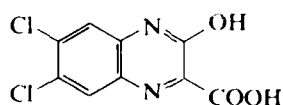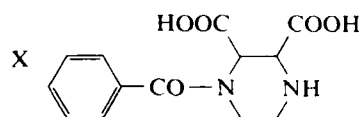
(halo)benzoyl-piperazine dicarboxylic acids

NMDA ≥ K/Q

$(X = H; o-, m-$ or p-Cl; or p-Br)

kynurenic acid

K/Q > NMDA

$$HO_3S-(CH_2)_n-NH-CO-CH_2-CH_2-{}^*CH\begin{smallmatrix}NH_2\\\\COOH\end{smallmatrix}$$

PDA

n = 1 GAMS
n = 2 GLU-TAU

HDC-QXCA
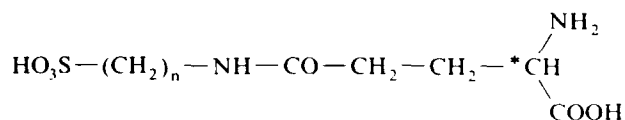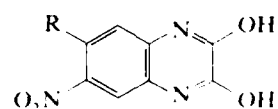
CNQX R CN
DNQX R NO₂

FIG 3 Structures of some kainate and quisqualate receptor antagonists which also have NMDA antagonist activity in varying degree as indicated above each structure. The most potent and selective antagonists for non-NMDA receptors are CNQX and DNQX. Abbreviations: γDGG, γ-D-glutamylglycine; PDA, cis-piperidine-2,3-dicarboxylic acid; HDC-QXCA, 3-hydroxy-6,7-dichloroquinoxaline-2-carboxylic acid; GAMS, γ-D-glutamylaminomethylsulphonic acid; GLU-TAU, γ-D-glutamyl-taurine; CNQX, 6-cyano-7-nitro-2,3-dihydroxyquinoxaline; DNQX, 6,7-dinitro-2,3-dihydroxyquinoxaline.

derivatives are not only relatively specific for non-NMDA receptors, but are considerably more potent at these receptors than those described above. In addition, they have a greater affinity for [^{3}H]AMPA binding sites than for [^{3}H]kainate binding sites, which may be an added advantage in the characterization of synaptic receptor sites. Another quinoxaline derivative (3-hydroxy 6,7-dichloroquinoxaline-2-carboxylic acid, Fig. 3) is also a very potent antagonist at non-NMDA receptors, though less specific than the FG compounds [50], having high potency also at NMDA receptors.

2L-AP4-Like substances

It is not known with certainty if L-AP4 (Fig. 1) acts as an agonist or antagonist at its receptors in depressing spinal cord [12] or hippocampal [10,11] synaptic responses. In these regions its most probable action is as an agonist at presynaptic glutamate autoreceptors exercising feedback reduction of synaptic glutamate release [11,12]. There appear to be strict structural requirements for this action, at least with respect to depression of lateral perforant path synaptic responses in the hippocampus [51-53]. Thus, methylation within the chain or of the amino group or phos phonate group (as phosphonate ester- or methyl phosphinate-type compounds), reduces activity in all cases. Elegant structure–activity studies with geometric isomers of cyclic analogues of AP4 have indicated that the active conformation of L-AP4 may be similar to that of *trans*-1-amino-3-phosphono-cyclopentane carboxylic acid (Fig. 2) [53]. Close correlation has not been found between the activities of these substances as depressants of lateral perforant path synaptic activity and their activities as inhibitors of [^{3}H]AP4 binding to brain membranes, making it unlikely that the binding sites for this substance are the same as those mediating the L-AP4 depressant effects [54]. Other evidence suggests the AP4 binding site may be a glutamate-uptake site [56].

In the retina, L-AP4 produces a hyperpolarizing response in ON bipolar cells similar to that produced by L-glutamate, and (like L-glutamate) also abolishes the light-induced responses of these cells [13]. To the extent that they have been investigated, structure-activity relations for L-AP4 in the retina [56] are similar to those observed in the hippocampus.

References

1 Watkins, J.C. and Evans, R.H. (1981) Excitatory amino acid transmitters. Annu. Rev. Pharmacol. Toxicol. 21, 165-204.
2 Watkins, J.C. (1978) Excitatory amino acids, In: Kainic Acid as a Tool in Neurobiology (E.G. McGeer, J.W. Olney, P.L. McGeer, eds.), pp. 37-69. Raven Press, New York.
3 Mayer, M.L. and Westbrook, G.L. (1987) The physiology of excitatory amino acids in the vertebrate CNS. Progr. Neurobiol. 28, 197-296.
4 Lodge, D., Aram, J.A., Church, J., Davies, S.N., Martin D., O'Shaughnessy, C.T. and Zeman, S. (1987) Excitatory amino acids and phencyclidine like drugs. In: Excitatory Amino Acid Transmission (T.P. Hicks, D. Lodge, H. McLennan, eds.), pp. 83 90. Alan R. Liss, New York.
5 Kemp, J.A., Foster, A.C. and Wong, E.H.F. (1987) Non-competitive antagonists of excitatory amino acid receptors. Trends Neurosci. 10, 294 298.
6 McLennan, H. (1983) Receptors for the excitatory amino acids in the mammalian central nervous system. Progr. Neurobiol. 20, 251-271.

7 Shinozaki, H. (1978) Discovery of novel actions of kainic acid and related compounds. In: Kainic Acid as a Tool in Neurobiology (E.G. McGeer, J.W. Olney and P.L. McGeer, eds.), pp. 17–35. Raven Press, New York.

8 Agrawal, S.G. and Evans, R.H. (1986) The primary afferent depolarizing action of kainate in the rat. Br. J. Pharmacol. 87, 343–355.

9 Mewett, K.N., Oakes, D.J., Olverman, H.J., Smith, D.A.S. and Watkins, J.C. (1983) Pharmacology of the excitatory actions of sulphonic and sulphinic amino acids, In: CNS Receptors: From Molecular Pharmacology to Behaviour (P. Mandel and F.V. DeFeudis, eds.), pp. 163–174. Raven Press, New York.

10 Koerner, J.F. and Cotman, C.W. (1981) Micromolar L-2-amino-4-phosphonobutyric acid selectively inhibits perforant path synapses from lateral entorhinal cortex. Brain Res. 216, 192–198.

11 Cotman, C.W., Flatman, J.A., Ganong, A.H. and Perkins, M.N. (1986) Effects of excitatory amino acid antagonists on evoked and spontaneous excitatory potentials in guinea pig hippocampus. J. Physiol. (Lond.) 378, 403–415.

12 Davies, J. and Watkins, J.C. (1982) Actions of D and L forms of 2-amino-5-phosphono-valerate and 2-amino-4-phosphonobutyrate in the cat spinal cord. Brain Res. 235, 378–386.

13 Miller, R.F. and Slaughter, M.M. (1986) Excitatory amino acid receptors in the retina: diversity of subtypes and conductance mechanisms. Trends Neurosci. 9, 211–218.

14 Simmonds, M.A. and Horne, A.L. (1987) Antagonism of excitatory amino acids by barbiturates. In: Excitatory Amino Acid Transmission (T.P. Hicks, D. Lodge, H. McLennan, eds.) pp. 99–105. Alan R. Liss, New York.

15 Watkins, J.C. (1981) Pharmacology of excitatory amino acid receptors. In: Glutamate: Transmitter in the Central Nervous System. (P.J. Roberts, J. Storm-Mathisen, G.A.R. Johnston, eds.) pp. 124. John Wiley & Sons, Chichester.

16 Watkins, J.C. (1987) Excitatory amino acid receptors in the mammalian central nervous system. Bull. Tokyo Metropol. Inst. Neurosci. 15, 13–39.

17 Olverman, H.J., Jones, A.W. and Watkins, J.C. (1984) L-Glutamate has higher affinity than other amino acids for [^{3}H]-D-AP5 binding sites in rat brain membranes. Nature (Lond.) 307, 460–462.

18 Watkins, J.C. and Olverman, H.J. (1987) Agonists and antagonists for excitatory amino acid receptors. Trends Neurosci. 10, 265–272.

19 Olverman, H.J., Jones, A.W., Mewett, K.N. and Watkins, J.C. (1988) Structure/activity relations of NMDA receptor ligands as studied by their inhibition of ^{3}H-D-AP5 binding in rat brain membranes. Neuroscience (in press).

20 Watkins, J.C. and Olverman, H.J. (1988) Structural requirements for activation of blockade of EAA receptors. In: Excitatory Amino Acids in Health and Disease. (D. Lodge, ed.) pp. 13–45. John Wiley & Sons, Chichester.

21 London, E.D. and Coyle, J.T. (1979) Specific binding of [^{3}H] kainic acid to receptor sites in rat brain. Mol. Pharmacol. 15, 492–505.

22 Krogsgaard-Larsen, P., Honoré, T. Hansen, J.J., Curtis, D.R. and Lodge, D. (1980) New class of glutamate agonists structurally related to ibotenic acid. Nature (Lond.) 284, 64–66.

23 Slevin, J.T., Collins, J.F. and Coyle, J.T. (1983) Analogue interactions with the brain receptor labelled by [^{3}H]kainic acid. Brain Res. 265, 169–172.

24 Anand, H., Roberts, P.J., Badman, G., Dixon, A.G. and Collins, J.F. (1986) Novel kainic acid analogues — Effects on cyclic GMP content of adult rat cerebellar slices. Biochem. Pharmacol. 35, 409–415.

25 Curtis, D.R. and Watkins, J.C. (1960) The excitation and depression of spinal neurones by structurally related amino acids. J. Neurochem. 6 117–141.

26 Collins, J.F., Dixon, A.J., Badman, G., De Sarro, G., Chapman, A.G., Hart, G.P. and Meldrum, B.S. (1984) Kainic acid derivatives with anticonvulsant activities. Neurosci. Lett. 51, 371–376.

458

27 Stone, T.W. and Collins, J.F. (1986) Activity of β-kainic acid on neocortical neurons in vivo and hippocampal neurons in vitro. Neuroscience 17, 629–633.

28 Fagg, G.E., Foster, A.C. and Ganong, A.H. (1986) Excitatory amino acid synaptic mechanisms and neurological function. Trends Pharmacol. Sci. 7, 357–363.

29 Foster, A.C. and Fagg, G.E. (1984) Acidic amino acid binding sites in mammalian neuronal membranes: their characteristics and relationship to synaptic receptors. Brain Res. Rev. 7, 103–164.

30 Honoré, T. Lauridsen, J. and Krogsgaard-Larsen, P. (1982) The binding of [^{3}H]AMPA, a structural analogue of glutamic acid, to rat brain membranes. J. Neurochem. 38, 173–178.

31 Krogsgaard-Larsen, P. and Honoreé, T. (1983) Glutamate receptors and new glutamate agonists. Trends Pharmacol. Sci. 4, 31–33.

32 Krogsgaard-Larsen, P., Nielsen, E.O. and Curtis, D.R. (1984) Ibotenic acid analogues. Synthesis and biological and in vitro activity of conformationally restricted agonists at central excitatory amino acid receptors. J. Med. Chem. 27, 585–591.

33 Lauridsen, J., Honoré, T. and Krogsgaard-Larsen, P. (1985) Ibotenic acid analogues. Synthesis, molecular flexibility, and in vitro activity of agonists and antagonists at central glutamic acid receptors. J. Med. Chem. 28, 668–672.

34 Krogsgaard-Larsen, P., Brehm, L., Johansen, J.D., Vinzents, P., Lauridsen, J. and Curtis, D.R. (1985) Synthesis and structure-activity studies of excitatory amino acids structurally related to ibotenic acid. J. Med. Chem. 28, 673–679.

35 Watkins, J.C., Curtis, D.R. and Biscoe, T.J. (1966) Central effects of β-N-oxalyl-α,β-diaminopropionic acid and other lathyrus factors. Nature (Lond.) 211, 637.

36 Pearson, S. and Nunn, P.B. (1981) The neurolathyrogen, β-N-oxalyl-L-α-β-diaminopropionic acid, is a potent agonist at 'glutamate-preferring' receptors in the frog spinal cord. Brain Res. 206, 178–182.

37 Krogsgaard-Larsen, P., Hansen, J.J., Lauridsen, J., Peet, M.J., Leah, J.D. and Curtis, D.R. (1982) Glutamic acid agonists. Stereochemical and conformational studies of DL-α-amino-3-hydroxy-5-methyl-4-isoxazolepropionic acid (AMPA) and related compounds. Neurosci. Lett. 31, 313–317.

38 Evans, R.H., Nunn, P.B. and Pearson, S. (1982) β-N-oxalyl-L-α,β-diaminobutyrate (β-L-ODAB) a naturally occurring NMDA antagonist. J. Physiol. 327, 81P.

39 Boden, P., Bycroft, B.W., Chhabra, S.R., Chiplin, J., Crowley, P.J., Grout, R.J., King, T.J., McDonald, E., Rafferty, P. and Usherwood, P.N.R. (1986) The action of natural and synthetic isomers of quisqualic acid at a well-defined glutamatergic synapse. Brain Res. 385, 205–211.

40 Perkins, M.N. and Stone, T.W. (1982) An iontophoretic investigation of the actions of convulsant kynurenines and their interaction with the endogenous excitant quinolinic acid. Brain Res. 247, 184–187.

41 Davies, J., Jones, A.W., Sheardown, M.J., Smith, D.A.S. and Watkins, J.C. (1984) Phosphonodipeptides and piperazine derivatives as antagonists of amino acid-induced and synaptic excitation in mammalian and amphibian spinal cord. Neurosci. Lett. 52, 79–84.

42 Jones, A.W., Smith, D.A.S. and Watkins, J.C. (1984) Structure-activity relations of dipeptide antagonists of excitatory amino acids. Neuroscience 13, 573–581.

43 Goldberg, O., Luini, A. and Teichberg, V.I. (1983) Bicyclic lactones derived from kainic acid as novel selective antagonists of neuro excitatory amino acids. J. Med. Chem. 26, 39–42.

44 McLennan, H. and Lodge, D. (1979) The antagonism of amino acid-induced excitation of spinal neurones in the cat. Brain Res. 169, 83–90.

45 Davies, J. and Watkins, J.C. (1979) Selective antagonism of amino acid-induced and synaptic excitation in the cat spinal cord. J. Physiol. (Lond.) 297, 621–636.

46 Davies, J., Evans, R.H., Francis, A.A. and Watkins, J.C. (1979) Excitatory amino acid receptors and synaptic excitation in the mammalian central nervous system. J. Physiol. (Paris) 75, 641–645.

47 Evans, R.H., Francis, A.A. and Watkins, J.C. (1977) Differential antagonism by chlorpromazine and diazepam of frog motoneurone depolarization induced by glutamate-related amino acids. Eur. J. Pharmacol. 44, 325–330.

48 Teichberg, V.I., Tal, N. Goldberg, O. and Luini, A. (1984) Barbiturates, alcohols and the CNS excitatory neurotransmitters: specific effects on the kainate and quisqualate receptors. Brain Res. 291, 285–292.

49 Honore, T., Davies, S.N., Drejer, J., Fletcher, E.J., Jacobsen, P., Lodge, D. and Nielsen, F.E. (1987) Potent and competitive antagonism at non-NMDA receptors by FG 9041 and FG 9065. Soc Neurosci. Abstr. p. 383.

50 Frey, P., Berney, D., Mueller, W., Herrling, P. and Urwyler, S. (1987) Kynurenic acid and quinoxalic acid derivatives as antagonists of excitatory amino acid receptors. Proc.of the IUPHAR Satellite Symposium on Amino Acid Transmitters, Canberra. p. 12.

51 Freund, R.K. Crooks, S.L., Koerner, J.F. and Johnson, R.L. (1984) Antagonist activity of phosphorus-containing glutamate analogues in the perforant path. Brain Res. 291, 150–153.

52 Crooks, S.L., Freund, R.K., Halsrud, D.A., Koerner, J.F. and Johnson, R.L. (1985) Antagonist activity of methyl-substituted analogues of 2-amino-4-phosphonobutanoic acid in the hippocampal slice. Brain Res. 329, 346–349.

53 Crooks, S.L., Robinson, M.B., Koerner, J.F. and Johnson, R.L. (1985) Cyclic analogues of 2-amino-4-phosphonobutanoic acid (APB) and their inhibition of hippocampal excitatory transmissions and displacement of [^{3}H]APB binding. J. Med. Chem. 29, 1988–1995.

54 Robinson, M.B., Crooks, S.L., Johnson, R.L. and Koerner, J.F. (1985) Displacement of DL-[^{3}H]-2-amino-4-phosphonobutanoic acid ([^{3}H]APB) binding with methyl substituted APB analogues and glutamate agonists. Biochemistry 24, 2401–2405.

55 Pin, J.P., Bockaert, J. and Recasens, M. (1984) The Ca^2/Cl^--dependent L-[^{3}H]glutamate binding: a new receptor or a particular transport process? Febs. Lett. 175, 31–36.

56 Slaughter, M.M. and Miller, R.F. (1985) Characterization of an extended glutamate receptor of the ON bipolar neuron in the vertebrate retina. J. Neurosci. 5, 224–233.

CHAPTER 34

The putative binding conformation of glutamate at a well-defined invertebrate glutamatergic synapse

B.W. BYCROFT AND D.E. JACKSON

Department of Pharmaceutical Sciences, University of Nottingham, Nottingham NG7 2RD, U.K.

There is now a substantial body of evidence to support the general view that L-glutamate is an important excitatory neurotransmitter in both vertebrate and invertebrate systems and a growing consensus that at least three principal types of receptor exist; namely quisqualate (Q), N-methyl-D-aspartate (NMDA) and kainate (K) responsive sites [1–3].

The quisqualate-sensitive site is probably the main transmitter receptor at glutamatergic synapses in both vertebrates and invertebrates and at many sites L-quisqualic acid is more potent than L-glutamic acid. One of the initial objectives of our studies relating to glutamate analogues was to shed further light on the molecular basis underlying this apparent potency difference and to employ such data in the design of further potential agonists and antagonists. To this end it was essential to employ a readily accessible system which would give relatively unequivocal results. The quisqualate-sensitive glutamatergic receptors of the well characterized nerve-muscle system of locust leg, the details of which have been described elsewhere [4], met these criteria and was employed throughout the programme.

Recently we reported a convenient synthesis of quisqualic acid and a range of its analogues (1–3) along with their relative activities [4,5]. Surprisingly the carbon (2) and nitrogen (3) analogues were inactive within the test system. Synthetic L-quisqualic acid exhibited, as expected, identical potency to its natural counterpart. Whereas the D-isomer was considerably more active than expected from the known stereoselectivity of this particular receptor sub-type towards L- and D-glutamic acid, respectively.

A possible molecular explanation for these observations stemmed from the examination of the X-ray crystallographic analyses of both racemic quisqualic acid (1) and the carbon analogue (2) [6]. Figs. 1 and 2 show the computer generated drawings for the crystal lattice structures. These clearly reveal a striking difference in the geometries of the nitrogen atoms joining the heterocyclic system to the amino acid side-chain. In the hydantoin (2) the nitrogen is almost planar, as expected for an amide group, whereas in quisqualic acid it is clearly pyramidal. Although X-ray crystallographic analysis of naturally occurring L-quisqualic acid had been reported
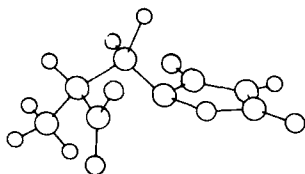
FIG 1 Crystal structure of DL-quisqualic acid (1) clearly showing pyramidal geometry for the sidechain substituted ring nitrogen.

previously, the unusual geometry at this nitrogen centre had not been noted [7]. It is well established that substituted pyramidal nitrogens of this type can interconvert in the manner indicated (Scheme 1) and that the energy barrier to inversion is usually only a few kcal/mol. Consequently at ambient temperatures the frequency of inversion is high and the potential enantiomeric forms are therefore inseparable in solution and the gas phase. However in the crystal lattice such forms can be locked by intermolecular forces and it is particularly noteworthy that our data on racemic quisqualic acid revealed the presence of both enantiomeric forms (invertomers) at the substituted ring nitrogen. Furthermore the L-isomer in the crystal lattice of racemic quisqualic acid possessed the opposite configuration at the ring nitrogen to that observed in the crystal of natural L-quisqualic acid.

The generality of these findings has been supported by theoretical semi-empirical molecular orbital (MO) calculations on simple model systems (4–6) [6]. The resulting energy profiles are shown in Fig. 3a–c. For N-methyl dioxo-oxazolidine (4) two energy minima are observed at $\pm 140\,^\circ$C. These values accord with two inverted pyramidal nitrogen configurations and are in excellent agreement with the corresponding torsion angles observed in the crystal lattice for quisqualic acid. Fig. 3a shows the two invertomers as energy wells with a theoretical inversion barrier of ca. 3–5 kcal/mol. This accords with experimentally determined values for simple pyramidal nitrogen systems and supports the view that the two forms are rapidly equilibrating in solution. Attempts to determine experimentally the energy barrier for (4) as well as quisqualic acid are currently in hand.

Fig. 3b shows the corresponding energy profile for the model hydantoin (5). The calculations predict extremely shallow energy wells close to 180 °C according with almost planar geometry and similar to that observed in the crystal lattice of the carbon analogue of quisqualic acid (2). For the dioxotriazolidine (6), the energy profiles are much more complex and can provisionally be interpreted in terms of pyramidal configurations at both nitrogen centres. Nevertheless the above evidence would support the conclusion that for quisqualic acid both pyramidal configurations at the ring junction nitrogen are of comparable stability and are rapidly interconverting in solution at ambient temperatures (Scheme 1).
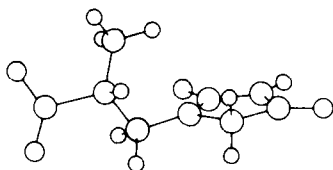
FIG 2 Crystal structure of 3-(2,4-dioxoimidazolidin-1-yl)-alanine (2).

(1) X = O
(2) X = CH$_2$
(3) X = NH

(4) X = O
(5) X = CH$_2$
(6) X = NH
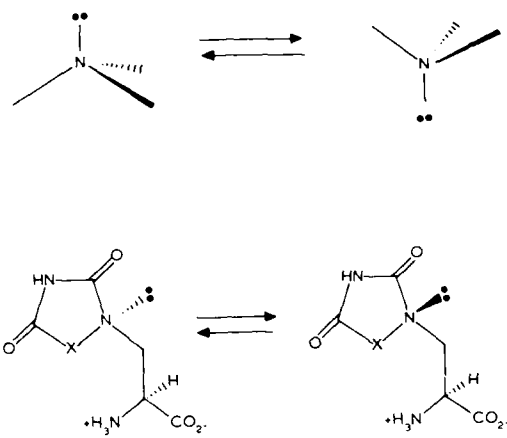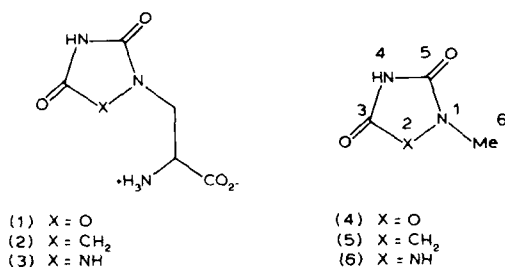
Scheme 1

Concurrent with these studies we were also investigating the action of 4-alkyl substituted glutamates in our test system and had observed that of the four chiral 4-methyl-glutamic acids only the 2S,4R isomer was active (Table 1). This was a particularly interesting and important observation since it not only confirmed the importance of the L(S)-configuration at the α-amino acid centre for glutamate analogues (other than quisqualic) but also established a configurational constraint with respect to the 4-position, i.e. analogous to the pyramidal ring joining nitrogen in quisqualic acid.

At this stage we considered it reasonable to assume that the functional groups of all glutamate analogues with agonist activity within our defined system bind to the receptor in a consistent spatial disposition to one another.

There is ample evidence to support the contention that within glutamate analogues the presence of both acid functions or their equivalent together with an α-amino group is essential for activity. In this respect we had already established that the heterocyclic system of quisqualic acid possesses a pK_a close to that of the γ-carboxylic acid group of glutamate and that the corresponding anion is distributed over the two adjacent carbonyls. The recognition of this latter point coupled with the potential for the inversion of the ring joining nitrogen proved crucial in

464
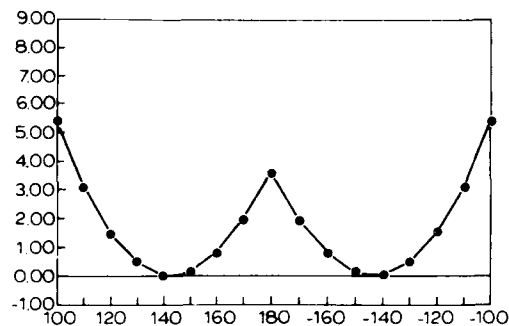
(a) Oxygen analogue (4)
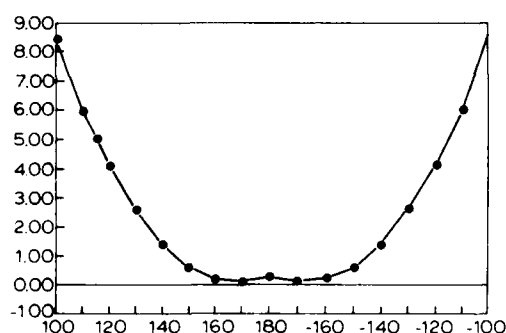
(b) Carbon analogue (5)
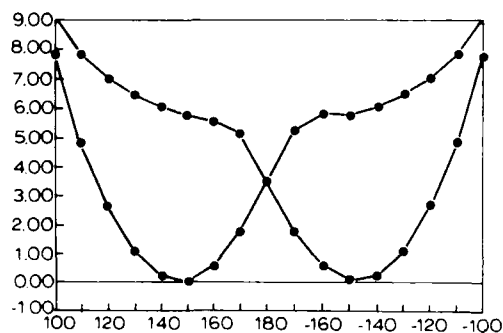
(c) Nitrogen analogue (6)

FIG 3   Relative energy profiles (kcal mol^{-1}) for model systems (4)-(6) with respect to defined torsion angle 3-2-1-6.

proferring an explanation for the substantial activity associated with D-quisqualic acid relative to the D-isomers of glutamate and 4-methyl-glutamate (Table 1). Fig. 4 shows conformations for L- and D-quisqualic acid computer generated to overlap the three functional groups. The D-isomer can only achieve appropriate overlap by flipping the heterocyclic ring through an inversion of the configuration at the ring

TABLE 1 Relative potency of glutamic acid analogues at functional glutamate receptors of locust muscle (retractor unguis) (P.N.R. Usherwood, unpublished results)

L(S)-glutamic acid	1
D(R)-glutamic acid	0
L(S)-quisqualic acid	3
D(R)-quisqualic acid	1
(2S,4R)-4methylglutamic acid	1.5
(2S,4S)-4-methylglutamic acid	0
(2R,4R)-4-methylglutamic acid	0
(2R,4S)-4-methylglutamic acid	0

nitrogen, i.e. the L- and D-isomer are diastereomeric at the pyramidal nitrogen centre. A process which we have established is feasible and within an energy range comparable with bond rotation. Fig. 5 shows the L- and D-isomers of glutamate superimposed on these quisqualate conformations. It is immediately apparent that although the α-amino and α-carboxylic acid groups can readily overlap the γ-carboxylic groups cannot by any conformational adjustment be superimposed. The configurational assignments for the pyramidal nitrogen in the binding conformation of L-quisqualate follows from the previously described observation that only the 2S,4R isomer of 4-methylglutamic acid is active. The agonist activity of D-quisqu-

L - quisqualate   D - quisqualate
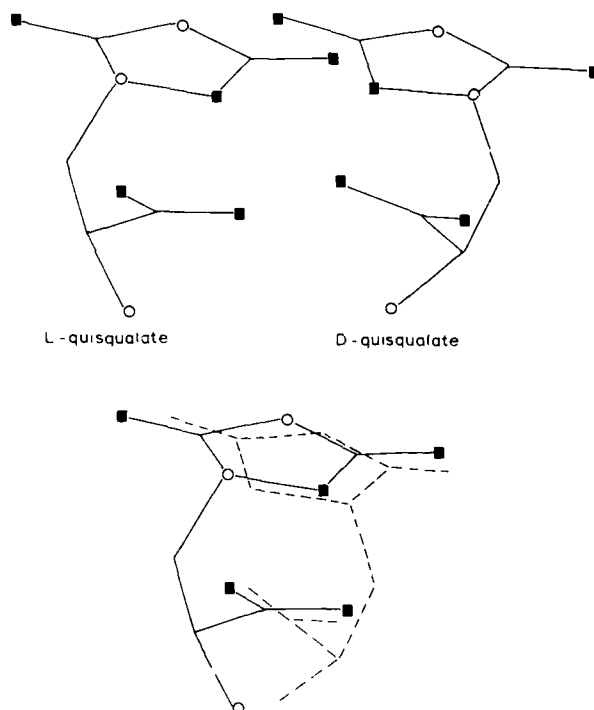
FIG 4 Conformations of L- and D-quisqualic computer generated to overlap function groups; note the inverted configuration at the pyramidal nitrogen in the D-isomer. ■, oxygen; o, nitrogen.

466

L-glutamate   D-glutamate
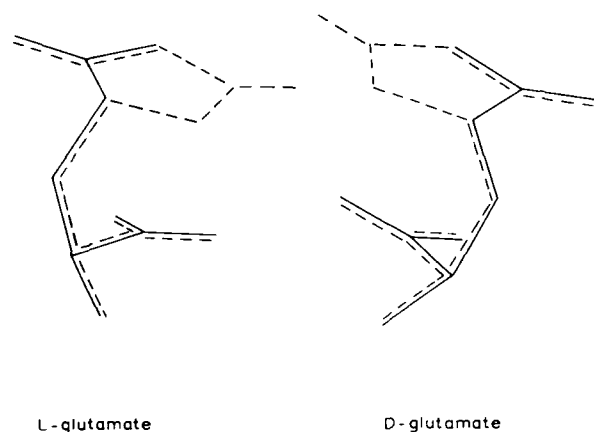
FIG 5   Binding conformation of L-glutamate superimposed on the active conformation of
L-quisqualate (dotted image). D-glutamate superimposed on D-quisqualate demonstrating that
the γ-carboxylic acid function cannot be superimposed on that part of the extended anion of
D-quisqualate which is involved with binding.

alic acid can therefore be ascribed to the ability of the molecule to undergo a
configurational inversion and to employ the full extent of the delocalized anion of
the heterocyclic system to assist binding.

We have now modelled on to this system all our active and inactive glutamate
analogues which are too numerous to be described here. However they do now
provide data for a unique model which not only appears to define the binding
conformation of L-glutamate at this specific receptor but also begins to map space
around the receptor binding site where structural changes may be permitted. How
relevant these studies are to other quisqualic acid-sensitive receptors must await
further investigations. The details of these studies together with a full description of
the pharmacological and physiological data will be reported elsewhere.

References

1 Nistri, A. and Constanti, A. (1979) Pharmacological characterisation of different types of
   GABA and glutamate receptors in vetebrates and invertebrates. Prog. Neurobiol. 13,
   117–235.
2 Usherwood, P.N.R. (1978) Glutamate receptors in eucaryotes. Adv. Pharmacol. Therapeut.
   1, 107–116.
3 Watkins, J.C. and Evans, R.H. (1981) Excitatory amino acid receptors. Annu. Rev.
   Pharmacol. 21, 165–204.
4 Boden, P., Bycroft, B.W., Chhabra, S.R., Chiplin, J., Crowley, P.J., Grout, R.J., King, T.J.,
   McDonald, E., Rafferty, P. and Usherwood, P.N.R. (1986) acid at a well-defined glutama-
   tergic synapse. Brain Res. 385, 205–211.
5 Bycroft, B.W., Chhabra, S.R., Grout, R.J. and Crowley, P. (1984) Convenient synthesis of
   the neuroexcitatory amino acid quisqualic acid and its analogues. J. Chem. Soc. Chem.
   Commun. 1156.

6 Bycroft, B.W., Jackson, D.E. and King, T.J. (1988) Crystallographic studies and semi-empirical MNDO calculations on quisqualic acid and its analogues; systems containing unusual pyramidal heterocyclic ring nitrogens. J. Mol. Graph., in press.

7 Flippen, J.L. and Gilardi, R.D. (1976) Quisqualic acid. Acta Crystallogr. Ser.B. 32, 951–953.

CHAPTER 35

The use of multivariate analysis in toxicological studies

DAVID W. SALT [1] AND MARTYN G. FORD [2]

[1] *Department of Mathematics and Statistics and* [2] *School of Biological Sciences, Portsmouth Polytechnic, Portsmouth, Hampshire, U.K.*

Introduction

Relating biological activity to molecular properties requires appropriate methods which can identify the relationships between sets of variables. Estimates of biological activity might comprise:

(1) a set (A) of variables describing in vivo toxicity e.g. KD_{50} and LD_{50};

(2) a set (B) of pharmacokinetic variables describing uptake, distribution and elimination of materials in a test organism e.g. rate constants for penetration, elimination and distribution; these variables determine the exposure of the site of action to drug or toxicant;

(3) a set (C) of pharmacodynamic variables describing the neurotoxicity of the compounds, estimated using isolated in vitro preparations, e.g. estimates of the threshold concentrations necessary to elicit neurotoxic responses including frequency and height of action potentials, frequency and duration of repetitive bursts of action potentials, nerve block, and changes in resting potential.

This latter set of variables will be the most familiar to neurobiologists; the first two sets will be more familiar to toxicologists. The problem is further complicated by the set (D) of variables which describe molecular properties. A complete appreciation of the action of drugs or agrochemicals will only be possible if attention is paid to all four sets. Moreover, the relationship between the sets must be investigated in a manner which throws light on the mode of action of the compounds under study. This paper will describe a number of multivariate statistical methods which are useful for identifying and explaining associations between variable sets.

Variables are sources of information. The information contained in sets of variables can be considered as being made up from two separate sources: (i) information that is unique to one particular variable, and (ii) information that is common to or shared by a number of variables. Information can be shared by variables found within the same set (intraset association) or occupying different sets (interset association). One of the aims of multivariate techniques is to estimate the unique information and separate it out from the shared or common (communal) information. A second objective is to summarize this information in a concise and clear manner.

Data matrices

Multivariate data consist of observations on several different variables for a number of objects (a term used to refer to the entities on which the measurements are recorded). Unfortunately, although much scientific data is multivariate, details of multivariate methods are rarely found outside specialist texts. Consequently, many scientists continue to apply univariate and bivariate methods to their multivariate data sets and fail to utilize the information content efficiently.

Data sets will usually consist of measurements on n objects for $p > 1$ variables collected at a fixed point in time. If the notation x_{rj} is used to indicate the observation on the rth object on the jth variable, then the n readings on p variables can be displayed in a rectangular array or matrix (X) with n rows and p columns. Thus

$$X = \begin{bmatrix} x_{11} & x_{12} & \cdots & x_{1j} & \cdots & x_{1p} \\ x_{21} & x_{22} & \cdots & x_{2j} & \cdots & x_{2p} \\ \cdot & & \cdot & & & \\ x_{r1} & x_{r2} & \cdots & x_{rj} & \cdots & x_{rp} \\ \cdot & & \cdot & & & \cdot \\ x_{n1} & x_{n2} & \cdot & x_{nj} & \cdots & x_{np} \end{bmatrix} \tag{1}$$

This is the standard form of data matrices familiar to all scientists.

Data sets with a large number of variables are common in many areas of research, particularly in the early stages of a research programme when little is known about the processes of interest. Under these circumstances the scientist may wish to measure many quantities in case they should prove useful at some later stage of the research programme. Many questions can be asked about such data sets. The most common questions, however, relate to the possibility of identifying some underlying structure linking the variables. This is particularly true when a number of the variables are classed as predictor variables and others are response variables (eg LD_{50}, KD_{50}) and interest centres on being able to predict the response(s) based on information contained in the predictors.

Multivariate methods

Multivariate analyses can be loosely defined as the application of techniques that handle situations where a reasonably large number of simultaneous measurements comprising different variables have been made on each object. The important point in this definition is that multivariate analyses handle simultaneous relationships between variables. Attention is directed away from the usual analysis of the mean and variance of a single variable, or the pairwise relationship between two variables. Emphasis is placed instead on the analysis of covariance or correlation which characterize the strength of relationship between three or more variables.

A wide variety of multivariate techniques is available [1]. The choice of the most appropriate method depends not only on the aims and objectives of the particular study, but also on the type of problem and the kind of data generated. One of the main aims of much multivariate analysis is to summarize a large body of data in terms of relatively few parameters and to facilitate their interpretation in terms of a few derived variates.

Constraints on the length of this paper allow only four multivariate techniques (principal component analysis, factor analysis, multiple regression analysis and canonical correlation analysis) to be considered.

(1) Principal component analysis (PCA)

In order to examine the relationship between a set of p correlated variables, X_1, $X_2, \ldots, X_p$, it may be useful to transform the original set of variables to a new set of uncorrelated variables, $PC_1, PC_2, \ldots, PC_p$, called principal components (PC). These new variables or factors are linear combinations of the original variables and are constructed to account for as much of the original total variation as possible. The lack of correlation is a useful property because it means that these indices, the PCs, are measuring different 'dimensions' in the data. The PCs thus represent a new frame of reference axes within which each axis reproduces a maximum amount of the available information. If only two or three PCs are required to describe the largest part (say 80%) of the total information, then it is advantageous, for reasons of economy of description, to project the data upon these components.

The reason that a large number of variables can be reduced to a smaller number of independent factors is that the variables are frequently intercorrelated. The intercorrelations cause redundancy in the multivariate description of the objects, and the PC factorization takes advantage of them in order to reduce the dimensionality of the data. If, however, all the original variables are nearly uncorrelated, then little or no data reduction will be possible. The components identified by the analysis will then be close to the original variables, but ranked in decreasing order of variance. It is important to realize that a PC is nothing more than a particular orientation in the data space and that the data are projected vertically upon this orientation. Thought of in this way, it can be seen that PCA is a technique for finding vantage points based on a new set of coordinate axes from which to view the data in multidimensional space.

The factorization technique is such that the components are derived in decreasing order of importance so that, for example, the first PC, PC_1, accounts for as much as possible of the variation in the original data, PC_2 accounts for the second largest amount of variation, and so on. That is $\text{var}(PC_1) > \text{var}(PC_2) > \ldots > \text{var}(PC_p)$, where $\text{var}(PC_1)$ denotes the variance of the ith PC.

Procedure for principal component analysis

PCA takes as its starting point an $n \times p$ data matrix as given by matrix (1), that is n observations on p variables. The first principal component, PC_1, is the linear combination of the Xs

$$PC_1 = a_{11}X_1 + a_{12}X_2 + \ldots + a_{1p}X_p \tag{2}$$

whose variability is as large as possible subject to the constraint that the the constant coefficients $\{a_{1j}\}$, $j = 1, 2, \ldots, p$ are chosen so that

$$a_{11}^2 + a_{12}^2 + \ldots + a_{1p}^2 = 1 \tag{3}$$

This constraint on the a's ensures that the overall transformation is orthogonal i.e. the distances between the objects in p dimensional space will be the same after the transformation as they were before. The second PC, PC_2, is given by

$$PC_2 = a_{21}X_1 + a_{22}X_2 + \ldots + a_{2p}X_p \tag{4}$$

and is such that the variance of PC_2 is as large as possible subject to the conditions that

$$a_{21}^2 + a_{22}^2 + \ldots + a_{2p}^2 = 1 \qquad (5)$$

and that PC_1 and PC_2 are uncorrelated. PC_3, the third PC, has the same linear structure and constraint on its coefficients and is uncorrelated with PC_1 and PC_2. $PC_4, \ldots, PC_p$ are defined by continuing in the same way.

In order to use the output of a PCA it is not necessary to know how to perform the matrix algebra from which the PC equations are derived. Suffice to say that a PCA involves finding what are termed the eigenvalues and eigenvectors [1] of the sample covariance matrix C_v. C_v will, in general, have p eigenvalues (some of which may be zero) which can be denoted $L_1, L_2, \ldots, L_p$ and, assuming that they are all distinct, we have $L_1 > L_2 > \ldots > L_p$. It can be shown that

$$\text{var}(PC_1) = \text{var}(a_{11}X_1 + a_{12}X_2 + \ldots + a_{1p}X_p) = L_1 \qquad (6)$$

i.e. the variance of the ith PC is L_1 and the constant coefficients $a_{11}, a_{12}, \ldots, a_{1p}$ are the elements of the corresponding eigenvector.

An important property of the eigenvalues is that they sum to the same total as the sum of the sample variances of the original variables i.e. $\Sigma_{i=1}^p L_i = \Sigma_{i=1}^p \text{var}(X_i)$. Consequently, $L_1/\Sigma_{i=1}^p L_i$ is the proportion of the total variation in the original data accounted for by the ith PC, and that $\Sigma_{i=1}^p L_i/\Sigma_{j=1}^m L_j$ is the proportion of the variation accounted for by the first m ($<p$) PCs.

It is quite common to find PCs being found for a set of variables that have been standardized to zero mean and unit variance. This means that we are effectively finding PCs from the correlation matrix C_r rather than the covariance matrix C_v (n.b. $C_v = C_r$ for standardized data). In this case the sum of the variance (standardized) and the sum of the eigenvalues, is equal to p, the number of variables, and hence the proportion of the total variation accounted for by the jth component is simply L_j/p. PCA is sometimes performed on the correlation matrix to prevent one or more variables with large variances having an undue influence on the PCs, as variables with large variances will tend to dominate the structure of the first few PCs.

After calculating the eigenvalues and principal components (eigenvectors) of a correlation (or covariance matrix), it is necessary to decide which eigenvalues are 'large' and which are 'small', so that PCs corresponding to the latter may be disregarded. Unfortunately, there is no objective way of deciding how many components to retain, but as a rule of thumb, eigenvalues of a correlation matrix that are less than unity may be disregarded. The rationale behind this simple rule is that if a PC has a variance less than unity ($\text{var}(PC_1) = L_1$) then it contains less information than one of the original standardized variables alone. Although this rule is useful it may be better to look at the pattern of eigenvalues and see if there is a natural breakpoint.

(2) Factor analysis (FA)

FA like PCA is a data reduction technique and is appropriate when the variables belong to a single grouping i.e. no separation into response variables and descriptor variables. The idea is to derive new variables called factors which will hopefully give

a better understanding of the data. In contrast to PCA, with FA interest centres on only that part of the total variation that a particular variable shares with the other variables in the set. Whereas PCA produces an orthogonal transformation (essentially a geometric rotation of the original axes) of the variables which does not depend on an underlying model, FA is based on a proper statistical model and is more concerned with explaining the covariance structure of the variables than with explaining the variances. Any variance which is unexplained by the common factors can be described by residual error terms in the model.

The FA model assumes that there are m underlying factors where $m < p$ the number of variables in the data set. The m uncorrelated common factors, each with mean zero and unit variance, are denoted $f_1, f_2, \ldots, f_m$, and each observed standardized (zero mean, unit variance) variable X_j, is a linear combination of these factors together with a residual variate. This gives the general FA model

$$X_j = a_{j1}f_1 + a_{j2}f_2 + \ldots + a_{jm}f_m + \epsilon_j, \quad j = 1, 2, \ldots, p \tag{7}$$

where $a_{j1}, a_{j2}, \ldots, a_{jm}$ are called factor loadings for the jth variable and the factor ϵ_j has zero mean and is specific to the jth variable and is uncorrelated with any of the common factors. As the variance of X_j is unity it can be seen that

$$\mathrm{var}(X_j) = 1 = \mathrm{var}(a_{j1}f_1 + a_{j2}f_2 + \ldots + a_{jm}f_m + \epsilon_j)$$

$$= a_{j1}^2 \, \mathrm{var}(f_1) + a_{j2}^2 \, \mathrm{var}(f_2) + \ldots + a_{jm}^2 \, \mathrm{var}(f_m) + \mathrm{var}(\epsilon_j)$$

$$= a_{j1}^2 + a_{j2}^2 + \ldots + a_{jm}^2 + \mathrm{var}(\epsilon_j)$$

$$= \sum_{i=1}^{m} a_{j1}^2 + \mathrm{var}(\epsilon_j) \tag{8}$$

$\sum_{i=1}^{m} a_{j1}^2$ is the part of the variance of X_j that is related to the common factors and is called the communality of X_j, whereas $\mathrm{var}(\epsilon_j)$ is the part of the variance of X_j that is unrelated to the common factors and is referred to as the specificity of X_j. As the communality of a variable cannot exceed one, $-1 < a_{jk} < 1$. One further result of considerable interest is that the correlation between X_j and X_k is

$$r_{jk} = a_{j1}a_{k1} + a_{j2}a_{k2} + \ldots + a_{jm}a_{km} \tag{9}$$

which means that two variables can only be highly correlated if they have high loadings on the same underlying common factor.

Procedure for factor analysis

FA, like PCA, takes as its starting point an $n \times p$ data matrix, and consists of three main steps. In step one provisional factor loadings a_{ij} are determined; the two main methods of doing this are the principal factor method and the maximum likelihood method [1]. Whichever method is used, it can be shown that the factor loadings obtained are not unique. If the provisional factors found are denoted $f_1, f_2, \ldots, f_m$, then the factors $F_1, F_2, \ldots, F_m$ where

$$F_1 = g_{11}f_1 + g_{12}f_2 + \ldots + g_{1m}f_m$$

$$F_2 = g_{21}f_1 + g_{22}f_2 + \ldots + g_{2m}f_m \tag{(}$$

$$\ldots \ldots \ldots \ldots \ldots \ldots \ldots \ldots$$

$$F_m = g_{m1}f_1 + g_{m2}f_2 + \ldots + g_{mm}f_m.$$

which are also uncorrelated, will 'explain' the data as well. Consequently, there is an infinite number of alternative solutions for the FA model, and this leads to the next step in the analysis, which is factor rotation. Factor rotation requires values for the g_{ij} in Eqn. 10 to be found so that the provisional factors can be transformed into new factors, the F_i, that are easier to interpret. The final step in the analysis is the calculation of the factor scores, which are the values of the factors for each of the n objects in the data matrix. Essentially these scores are the coordinates of the n objects in m dimensional factor space.

As with PCA, the 'full benefit' of FA can usually be achieved only if each of the new variables (factors) can be given a meaningful interpretation. Factor interpretation becomes unclear when the original variables 'load' on to more than one factor. In FA this situation can be improved upon by allowing the factors to rotate. Factor rotation can be of two different types — orthogonal or oblique. With orthogonal rotation new uncorrelated factors are formed by essentially rotating the old uncorrelated factors whilst maintaining the orthogonality of the factor axes. The rotation of the factors is such that the factor loadings for the new factors should be either very small or very large (positive or negative). If a factor loading a_{jk} is close to zero then this means that the associated variable X_j is not strongly related to the factor F_k. A value of a_{jk} very different from zero implies that X_j is strongly associated to the factor F_k and may be determined by this factor to a large extent. If the factor pattern, that is, the values of a_{jk}, are such that each variable is strongly associated to some factors, but not at all to others, then identification of the factors becomes easier. The relationship between the original variables and factors can be further simplified if the orthogonality constraint is relaxed, and oblique rotation performed. The resulting factors, however, will no longer be uncorrelated.

(3) Multiple regression

Perhaps the most commonly used (misused) technique, multiple regression analysis (MRA) is concerned with the association of one variable, the dependent or response variable with a set of predictor variables. The aim of this technique is to predict the mean value of the dependent variable based on the known values of the predictor variables.

The $p + 1$ variable linear regression model involving the dependent variable Y and the p independent (predictor) variables $X_1, X_2, \ldots, X_p$ can be written as

$$Y_i = \beta_0 + \beta_1 X_{1i} + \beta_2 X_{2i} + \ldots + \beta_p X_{pi} + \epsilon_i, \quad i = 1, 2, \ldots, n \tag{11}$$

where β_0 denotes the intercept, $\beta_1, \beta_2, \ldots, \beta_p$ are the p partial regression coefficients and ϵ_i is the unobservable residual error associated with the ith observation on Y. The regression coefficients are referred to as 'partial' because the kth coefficient β_k measures the change in the mean value of Y per unit change in X_k, holding all other independent variables constant.

Procedure for multiple regression analysis

The most popular method of estimating the unknown regression coefficients is ordinary least squares (OLS). The OLS estimation of the β_i is obtained by minimizing the sum of squares of the deviations of the observed response variable Y_i from the assumed model (Eqn. 11). The estimated linear model may be written

$$\hat{Y}_i = \hat{\beta}_0 + \hat{\beta}_1 X_{1i} + \hat{\beta}_2 X_{2i} + \ldots + \hat{\beta}_p X_{pi}, \quad i = 1, 2, \ldots, n \tag{12}$$

where $\hat{\beta}_0$, $\hat{\beta}_1, \ldots,$ $\hat{\beta}_p$ are the OLS estimates of the β_i, $i = 0, 1, \ldots, p$, and where $\hat{Y}_i$ is the predicted response.

Multicollinearity

Exact linear dependence of the predictor variables exists if it is possible to find constants $a_1, a_2, \ldots, a_p$, not all zero, such that

$$a_1 X_1 + a_2 X_2 + \ldots + a_p X_p = 0 \tag{13}$$

and 'near' linear dependency exists if

$$a_1 X_1 = a_2 X_2 + \ldots + a_p X_p \approx 0 \tag{14}$$

This dependency is a consequence of the duplication of information that is contained in these variables. When exact linear dependencies occur, the effects of some of the predictor variables are not distinguishable, and the matrix algebra necessary to find the estimators of the β_i is not possible. Of $\therefore$ creasing concern is the tendency for data bases to have near linear dependencies among the predictor variables. As these dependencies are inexact they can remain undetected. This is a common problem in regression analysis and can lead to unjustified inference about the role of the β parameters in the regression model [2]. Multicollinearity is not a condition that either exists or does not exist, it is more a question of degree. The closer the linear combination in Eqn. 14 is to zero, the stronger is the multicollinearity.

There are generally two main effects of multicollinearity: (i) the values of the estimated regression coefficients may become unstable as additional collinear variables are introduced into the model, (ii) the standard errors of the estimates may be considerably increased when collinear variables are present in the model. Unfortunately, no firm rules have been established for assessing the seriousness of such errors. Yet the instability of the estimates may be so serious as to even cause a change in the sign of the parameter estimates as the degree of collinearity increases.

Pairwise multicollinearities can be identified by scrutinizing the off-diagonal elements of the correlation matrix C_r. Just how large the pairwise correlations have to be before one should become concerned about multicollinearities is somewhat subjective. Multicollinearities consisting of three or more predictor variables are unlikely to be detected from an examination of the pairwise correlations. In fact, multivariable multicollinearity can occur without any of the pairwise correlations being very large. One method of detecting multivariate multicollinearities and identifying the variables which are collinear can be found via PCA. If PCA is performed on the correlation matrix so that all variables are on equal footing, the resulting PC$_1$ will have mean zero and variances equal to the eigenvalues L_j. Therefore, a PC$_1$ with a variance (L_1) close to zero implies that the value of the PC$_1$ is also close to zero i.e.

$$PC_1 = a_{11} X_1 + a_{12} X_2 + \ldots + a_{1p} X_p \approx 0, \tag{15}$$

which has the same form as Eqn. 14. Consequently, variables with large coefficients on a PC with a small eigenvalue contribute most to the multicollinearity.

A number of methods have been suggested for dealing with the problem of multicollinearity but there is insufficient space in this paper to give a full account of all the available methods. The interested reader is directed to the work of Mont-

gomery and Peck [2], who give a readable account of the various alternatives. However, one approach worthy of note here is that based on PCA. This method involves performing a PCA on the p descriptor variables to find a transformed set of p variables (the principal components) which are by definition uncorrelated. A MRA on the PCs (BMDP4R, Dixon [4]) then is free of the multicollinearities which existed in the original variable set. The resulting estimated regression model will relate the predicted response to the PCs and through these back to the original variables.

(4) Canonical correlation analysis (CCA)

Many experiments result in several response variables being measured together with the usual set of predictor variables. An obvious question to be considered is what relationships, if any, exist between the response variables and the predictor variables. One way of investigating this is through a CCA. CCA is a technique which finds that linear combination of the response variables that is maximally correlated with a linear combination of the predictor variables. Unlike multiple regression, where the responses are analysed independently (cf. Eqns. 19 and 20) and with one model for each ignoring any correlation structure amongst the responses, CCA utilizes this shared information and affords an analysis of all response variables simultaneously.

Denote the variables in the response group $Y_1, Y_2, \ldots, Y_q$ and the variables in the descriptor group $X_1, X_2, \ldots, X_p$. The principle of the method is to calculate a linear combination of the q response variables:

$$W_1 = a_{11}Y_1 + a_{12}Y_2 + \ldots + a_{1q}Y_q \tag{16}$$

and a linear combination of the p response variables:

$$Z_1 = b_{11}X_1 + b_{12}X_2 + \ldots + b_{1p}X_p, \tag{17}$$

where the coefficients $a_{11}, a_1, \ldots, a_{1q}$ and $b_{11}, b_{12}, \ldots, b_{1p}$ are estimated from the data. These coefficients are chosen so that the pairwise correlation between W_1 and Z_1 will be as large as possible. The idea is that if this maximum correlation, R_{c1}, is significantly large, then there is evidence of an association between the two sets of variables. Y_1 and Z_1 given by Eqns. 16 and 17 are referred to as canonical variates (CV) and the (maximum) correlation between them (R_{c1}) is referred to as the canonical correlation. These CVs are essentially equivalent to the PCs produced in PCA, with the exception that the criterion for their selection has altered. Whereas both techniques produce linear combinations of the original variables, CCA does so not with the object of accounting for as much variance as possible within one set of variables, but with the aim of accounting for a maximum amount of the relationship between two sets of variables.

The techniques of CCA and PCA are analogous in several other respects. Just as PCA selects a first PC to account for a maximum amount of variance in a given set of variables and then computes a second PC accounting for as much as possible of the variance left unaccounted for by the first PC, and so forth, CCA follows a similar procedure. The first pair of CVs, W_1 and Z_1 (Eqns. 16 and 17), are selected so as to have the highest intercorrelation possible, given the particular variables involved. A second pair of CVs, (W_2, Z_2) is then selected to account for a maximum

amount of the relationship between the two sets of variables left unaccounted for by the first pair of CVs, and so forth. In practice, the number of pairs of CVs (W_1, Z_1) extracted by the analysis will be equal to the smaller of p and q. That is to say, linear relationships

$$W_1 = a_{11}Y_1 + a_{12}Y_2 + \ldots + a_{1q}Y_q \qquad Z_1 = b_{11}X_1 + b_{12}X_2 + \ldots + b_{1p}X_p$$

$$W_2 = a_{21}Y_1 + a_{22}Y_2 + \ldots + a_{2q}Y_q \quad \text{and} \quad Z_2 = b_{21}X_1 + b_{22}X_2 + \ldots + b_{2p}X_p \qquad (18)$$

$$W_t = a_{t1}Y_1 + a_{t2}Y_2 + \ldots + a_{tq}Y_q \qquad Z_t = b_{t1}X_1 + b_{t2}X_2 + \ldots + b_{tp}X_p$$

can be found, where t is the smaller of q and p. The pairs of canonical variates are derived in decreasing order of importance so that the (canonical) correlation R_{c1} between the first pair of CVs (W_1, Z_1) is a maximum: The correlation R_{c2} between the second pair (W_2, Z_2) is a maximum subject to these variables being uncorrelated with (W_1, Z_1) and $R_{c2} < R_{c1}$; the correlation R_{c3} between W_3 and Z_3 is a maximum, subject to (W_3, Z_3) being uncorrelated with W_1, Z_1, W_2 and Z_2, and $R_{c3} < R_{c2}$; and so forth.

Procedure for canonical correlation analysis

CCA takes as its basic input two groups of variables (standardized to zero mean and unit variance), each of which can be given theoretical meaning as a group. These two groups will generally comprise a set of response variables $(Y_i, i = 1, 2, \ldots, q)$ and a set of predictor variables $(X_i, i = 1, 2, \ldots, p)$. The method of extracting the successive pairs of CVs involves an eigenvalue-eigenvector [1] problem which has some similarity with that for obtaining the PCs in PCA. The eigenvalues and associated eigenvectors constructed by the CCA are based on the combined $(p + q) \times (p + q)$ correlation matrix, C_{xy}, between the descriptor variables and the response variables. The eigenvalues of C_{xy} are the squares of the canonical correlations between the pairs of CVs i.e. $R_{c1} = \sqrt{L_1}$, and represents the amount of variance in the CV W_1 (the array of response variables) that is accounted for by the other CV Z_1 (the array of predictor variables). The corresponding eigenvectors allow the canonical variate coefficients (a_{1i} and b_{1i} in Eqn. 18) to be calculated.

Interpretation of the CVs is necessary if a picture of the association between the two variables sets is to be formulated. Canonical weights and canonical loadings have been used to assess the relationship between the original variables and the CVs. Canonical weights, a_{1i} and b_{1i} in Eqn. 18, are analogous to the β coefficients in multiple regression analysis (MRA) and indicate the contribution of each variable to the variance of the respective CV. However, as in MRA, the canonical weights may be highly unstable due to multicollinearity [1]. Thus some variable may have a small or negative weight because it is strongly correlated to some other variable(s) in the model. Canonical loadings are thought by many to be more useful in identifying the structure of the canonical relationships. Canonical loadings give the simple correlation of the original variable and its respective CV and reflects the degree to which the variable is represented by a CV.

Case study

The structure–activity relationships described in this case study are based on associations between sets of variables describing chemical structure and toxicity.

The toxicities are those resulting from the topical application to adult mustard beetles (*Phaedeon cochleariae* Fab.) of a congeneric series of 16 pyrethroid insecticides reported by Szydlo [3]. The data matrix for this study comprises LD_{50} at 240 h and KD_{50} at 4 min as measures of toxicity. and a set of standard independent (predictor) variables used routinely in QSAR studies to describe the physicochemical properties of compounds.

The first stage in the analysis of this structure activity data was to calculate the correlation matrix, identify the pairwise correlation structure and assess the extent of multicollinearity. When multicollinearity is present, the same information can be contained in several variables and interpretation of results is then more difficult. One sixth of the observed inter-predictor set correlations in the correlation matrix were significant ($r > 0.497$; 14 df; $P < 0.05$). Most of the collinearity is associated with the sterimol parameters and arises from the related values of L, B1 and B4. These are of equal size for substituents such as halogens which comprise a significant proportion of the ring substituents in this particular set of materials. The size and shape of these substituents can be adequately described by any one of the three variables. Increasing the variety of substituent shapes should help to reduce this source of collinearity. If the correlations between the sterimol parameters are excluded, only 6% of the remaining correlations are significant showing that the data set has been well chosen to minimize the effects of paired associations, and the compounds are therefore spread throughout the multidimensional hyperspace.

Szydlo [3] separately regressed $\log(KD_{50})$ and $\log(LD_{50})$ on the predictor variable set using stepwise multiple regression analysis (MRA) (BMDP2R, Dixon [4]). The regressions selected by this procedure are presented below.

$$\log(KD_{50}) = -23.602 - 0.797*3B4 + 0.641*5B4 - 1.458*6L + 3.366*Kappa$$
$$(\pm0.094) \quad (\pm0.184) \quad (\pm0.169) \quad (\pm0.348)$$
$$-0.703*R - 1.496*S4 + 11.149*Log(MW)$$
$$(\pm0.323) \quad (\pm0.197) \quad (\pm2.400)$$

$(R^2 = 0.911; \ F = 57.78: 7.32 \ df)$ (19)

$$\log(LD_{50}) = 55.55 + 2.681*3B1 + 2.078*4L - 7.403*4B1 - 5.827*5B1$$
$$(\pm0.187) \quad (\pm0.219) \quad (\pm1.185) \quad (\pm0.950)$$
$$+4.191*5B4 - 1.894*Kappa + 0.551*PI + 0.230*F$$
$$(\pm0.458) \quad (\pm0.292) \quad (\pm0.128) \quad (\pm0.055)$$
$$--21.987*Log(MW)$$
$$(\pm1.635)$$

$(R^2 = 0.950: \ F = 83.54: 9.30 \ df)$ (20)

The predictor variables give Eqns. 19, 20 which account for a large proportion of the variation in the dependent variables, but at the expense of the inclusion of a large number of independent variables. The model is said to be overdefined. The stepwise procedure took as its starting point a data matrix with a large number of variables (columns) relative to the number of observations (rows), and the chance of fortuitous correlations is high (Topliss and Edwards [5]). Furthermore, significant correlations between the selected predictor variables (e.g. Kappa : R = 0.707,

5B1 : 5B4 = 0.949) are present and will lead to unstable regression coefficients. Note the change of sign of the partial regression coefficient for Kappa in Eqns. 19 and 20. Thus the relevant information is confounded and, at best, inference becomes speculative.

The separate regressions of the response variables upon the predictor variables treat the response variables as though they were independent of each other, whereas in fact they exhibit a significant association ($r = 0.672$). A more appropriate analysis would be one in which both parameters are considered simultaneously. This would take into account the covariance of the response variables, enabling more constraints to be imposed by the biological data than is possible in separate regressions which treat the two responses independently. This constraint could increase the possibility of reducing the size of the predictor set during the optimization procedure, and lead to self-consistent correlation equations. Canonical correlation was therefore undertaken (BMDP6M, Dixon [4]).

The number of pairs in CVs produced corresponds to the number of variables in the smaller set. Thus, analyses involving the set of two toxicological variables (log LD_{50} and log KD_{50}) will result in two pairs of CVs. The inter-set associations are summarized by the canonical correlation coefficient (R_c), which quantifies the degree of association between the two sets which can be explained by a particular CV. The technique has the considerable advantage that the equations describing the variates each include both response parameters.

An initial analysis to find the 'best' set of predictor variables describing the toxicity of the compounds was undertaken using the set of twenty-two physicochemical variables introduced earlier [3]. These variables are characterized by substantial multicollinearity and so have been reduced to eleven variables prior to analysis without loss of information. The association of the reduced set of eleven variables with the set of two toxicity variables (log LD_{50} and log KD_{50}) was then investigated using CCA. As multicollinearities still characterized the remaining eleven variables, indicating the presence of redundant information, a procedure analogous to backward stepping in stepwise multiple regression analysis, was employed (Szydlo [3]). This procedure resulted in a 'best' set of six predictor variables (Table 1), where the multicollinearities detected within the starting set of eleven variables have been substantially reduced for the smaller set of six predictors with minimal reduction in the size of the canonical correlation coefficients R_{c1} and R_{c2}.

Both pairs of canonical variates ((W_1, Z_1) and (W_2, Z_2)) associating the toxicological variable set with the physicochemical set were highly significant. The two variates are uncorrelated, and describe the variation in response variables (W) as a function of the predictor variables (Z). 88% of the variation in the response set is accounted for by the six predictor variables. The standardized coefficients for the response variables (Table 1), show that the first variate (W_1) is structured from the sum of the weighted log LD_{50} and the weighted log KD_{50}. An increase in this variate can be associated with a simultaneous decrease in both lethal and knockdown activity. 99.6% of the variation in log LD_{50} is explained by this variate compared with 50.5% of the variation in log KD_{50}. The second variate (W_2) is based on the difference between weighted log LD_{50} and log KD_{50} and an increase in this variate can be associated with a decrease in knockdown activity but with an increase in lethal activity. 0.4% of the variation in log LD_{50} is explained by this variate and 49.6% of the variation in log KD_{50} (Fig. 1).

TABLE 1   Summary of results of the CCA using the six variable set of predictors

Variable	Correlations (loadings) of the original variables with the canonical variates		Standardized coefficients for the canonical variates	
	W_1	W_2	W_1	W_2
log LD_{50}	0.998	−0.055	0.949	−0.960
log KD_{50}	0.711	0.703	0.074	1.348
	Z_1	Z_2	Z_1	Z_2
3B4	−0.347	0.117	−0.744	−0.045
4L	−0.134	0.389	0.414	−0.416
4B1	−0.332	0.492	−0.759	1.086
6L	−0.318	−0.062	−0.331	−0.355
Kappa	0.263	0.704	0.517	0.862
S4	−0.582	0.077	−0.552	0.087

Significance test (Bartlett [6]) for the canonical variates: 1st pair of canonical variates (W_1, Z_1): eigenvalue = 0.934, R_{c1} = 0.97, Chi-square = 139.48 (12 df), $P < 0.001$. 2nd pair of canonical variates (W_2, Z_2): eigenvalue = 0.733, R_{c2} = 0.86, Chi-square = 45.52 (5 df), $P < 0.001$.

Szydlo [3] has identified a significant association between the first canonical variate and neurotoxicological potency, measured by the molar threshold concentration (MTC) required to elicit a pyethroid induced response in isolated nerve preparations. The second variate is associated with the pharmacokinetic properties of the insecticides (Szydlo et al. [7]).

Plots of the canonical variate W_2 against the original response variables (Fig. 1) produced four clusters of the sixteen compounds which can be case identified. The spatial arrangement of these clusters is altered by replacing log KD_{50} as the abscissa with log LD_{50} suggesting that W_2 describes processes which contrast the two toxicological responses, knockdown and mortality. Examination of the predictor variable loading (Table 1), indicates that an increase in the size of W_2 is associated
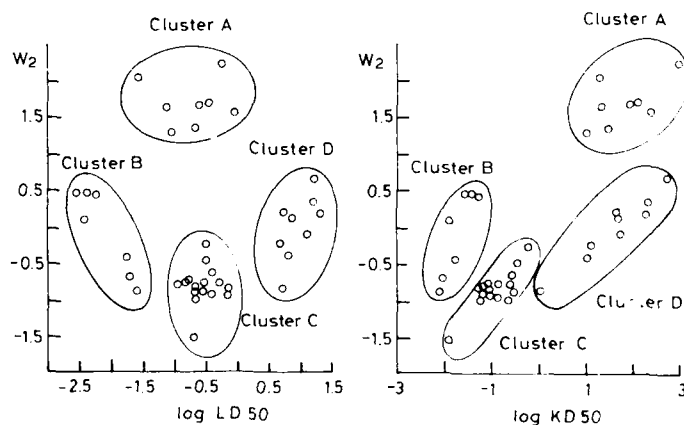
FIG 1   The relationship between the toxicological canonical variate W_2 and the original response variables (log LD_{50} and log KD_{50}).
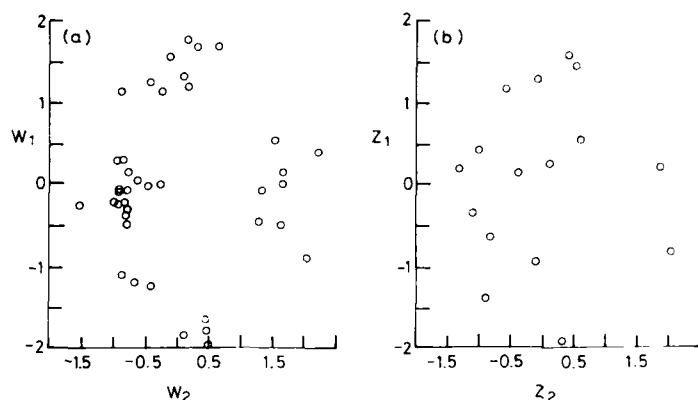
FIG 2 Bivariate maps of (a) the pyrethroid toxicological hyperspace, and (b) the pyrethroid physicochemical hyperspace.

with an increase in the transfer of charge by electron donation from the benzyl ring and an increase in size of the minimum breadth of substituents at the para position.

Cluster A contains compounds which are moderately good killing agents but poor knockdown compounds. Cluster B contains compounds with high insecticidal and knockdown activity; however, an increase in W_2 within this cluster results in increased insecticidal activity but reduced knockdown activity, indicating that substituents with the ability to donate electrons and which have a small minimum width tend to be associated with knockdown compounds. Cluster C comprises compounds of moderate insecticidal activity and relatively high knockdown activity; an increase in the value of W_2 for this group reduces knockdown activity but has little effect on insecticidal activity. The fourth cluster (D) is formed of compounds of weak insecticidal and knockdown activity; increasing W_2 results in a marked reduction in knockdown activity and a smaller reduction in insecticidal activity.

Two-dimensional representations (maps) of the original multidimensional hyperspace (LD_{50}, KD_{50}, 3B4, 4L, 4B1, 6L, Kappa and S4) summarized by the two pairs of CVs are presented in Fig. 2. The observed responses for the different compounds have coordinates (W_1, W_2) (Fig. 2a) positioned in well-defined regions throughout the bivariate map, and are well predicted by descriptor variables (Fig. 2b). Several regions of the hyperspace remain unmapped, however, including two with low values of W_1, which should therefore be associated with compounds of high biological activity.

References

1 Dillon, W.R. and Goldstein, M. (1984) Multivariate Analysis. Methods and Applications. Wiley, N.Y.

2 Montgomery, D.C. and Peck, E.A. (1982) Introduction to Linear Regression Analysis. Wiley, N.Y.

3 Szydlo, R.M. (1987) An investigation of the pharmacokinetics of pyrethroid insecticides in the adult mustard beetle (Phaedon cochlearia Fab.). Ph.D. Thesis, C.N.A.A.

4 Dixon, W.R. (1985) Biomedical Computer Programs P-series. University of California Press, Los Angeles.

482

5 Topliss, J.G. and Edwards, R.P. (1979) Chance factors in studies of quantitative structure-activity relationships. J. Med. Chem., 22, 1238–1244.
6 Bartlett, M.S. (1947) Multivariate analysis. J. Roy. Statist. Soc. B 9, 176–197.
7 Szydlo, R.M., Ford, M.G., Greenwood, R. and Salt, D.W. (1984) The use of multivariate data sets in the study of the structure-activity relationships of synthetic pyrethroid insecticides: Part II. The relationship between pharmacokinetics and toxicity. In: QSAR and Strategies in Design of Bioactive Compounds—Proceedings of the 5th European Symposium on Quantitative Structure Activity Relationships, pp 229–237. Bad Segeberg.

CHAPTER 36

A multivariate QSAR study of pyrethroid neurotoxicity based upon molecular parameters derived by computer chemistry

D.J. Livingstone[1], M.G. Ford[2] and D.S. Buckley[2]

[1] Department of Physical Sciences, Wellcome Research Laboratories, Langley Court, Beckenham, Kent BR3 3BS and [2] School of Biological Sciences, Portsmouth Polytechnic, Portsmouth, Hampshire PO2 2DY, U.K.

Introduction

Synthetic pyrethroids are neurotoxicants with insecticidal properties [1]. Although the structure–activity relationships of pyrethroid insecticides have been examined in some detail, most studies have emphasized the role of stereochemistry in the determination of biological activity. These investigations have resulted in a number of highly potent pyrethroids [1]. Many of the structural requirements for kill are understood, but those required for knockdown are less clear [2]. Relatively low log P values (ca. 5) are considered necessary for knockdown action, but other factors must also be involved and a role for electronic properties has been suggested by recent QSAR studies based on in vitro neurotoxicological assays [3] and in vivo bioassays [4,5]. This paper reports the relationships between these biological responses for a set of pyrethroid insecticides tested against adult houseflies. *Musca domestica*, and isolated housefly haltere nerve preparations [6].

The success of this analysis, as with most QSAR studies, will depend to a large extent on the initial choice of the set of compounds used to investigate the biological systems. The criteria used for this study were that compounds were required possessing a wide range both of biological and molecular properties. The selection of suitable compounds, either for synthesis and testing or for the analysis of previously obtained biological data, was dictated by the physicochemical properties of the compounds involved [7]. The number of biological responses, ten in all, measured for these compounds necessitated the use of multivariate methods for their analysis. Mutlivariate methods were also required to deal with the physicochemical description of the molecules generated using the techniques of computational chemistry, i.e. molecular mechanics and quantum mechanics [8].

This paper illustrates the investigation of the neurotoxicological properties of synthetic pyrethroids starting from the selection of compounds for synthesis and progressing through the generation of molecular descriptors reduction of this descriptor set, multivariate analysis of biological response data and the combined

484

multivariate analysis of response and descriptor data. A major objective of this study was the identification of those neurotoxicological responses which correlate with whole animal insecticide potency. A further objective was to relate these responses to molecular physicochemical properties.

Selection of compounds

In order to investigate the effects of compounds upon any biological system in the most efficient manner, it is necessary to choose molecules which have a wide range of uncorrelated physicochemical properties.

Compound choice will therefore determine the information content of the data set. The substituent series methyl, ethyl, propyl, butyl, 'futile' is often quoted in this context since bulk and hydrophobicity are strongly correlated ($r = 0.999$) with little variation in electronic effects. Thus, this series contains little useful information with which to identify structure–activity relationships.

It was decided to synthesize a series of selected pyrethroids with wide variation in three fundamental physicochemical features: hydrophobic, steric and electronic properties described by the substituent constants π, MR and, for electronic effects, the two descriptors F and R [9]. This selection process was carried out using an in-house computer routine, SELECT [7], written in the programming language RPL of a general data handling package RS/1 (see Appendix). This procedure calculates the inter-parameter correlations and the degree of 'spread' of parameter values for each chosen property. A set of 12 QSAR compounds plus permethrin were chosen by this technique (Table 1); the inter-parameter correlation matrix is given in Table 2. Several studies in our laboratories have shown that the selection of compounds based on these four parameters lead to generally well distributed sets. The next

TABLE 1   Chemical structures of the pyrethroid insecticides used in this study
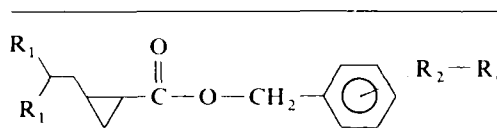
	R_1	R_2	R_3	R_4	R_5	R_6
QSAR1	Me	F	F	F	F	F
2	Cl	F	F	F	F	F
3/4	ME/Cl	Me	Me	Me	Me	Me
5/6	Me/Cl		I			
11/12	Me/Cl		NO2		NO2	
13/14	Me/Cl	Cl	NO2			Cl
17/18	Me/Cl		NO2			
Permethrin	Cl		OPh			

TABLE 2   Inter-parameter correlation matrix for the compounds in Table 1

	π	F	R
F	0.09		
R	−0.02	−0.18	
MR	0.56	−0.13	0.18

stage in this analysis involves the generation of physicochemical descriptors by the methods of computational chemistry.

Generation of molecular descriptors

The pyrethroids are flexible molecules and attempts to calculate their conformation by molecular mechanics may lead to erroneous results. It was decided to fix the conformation of the molecules under study to an experimentally determined conformation, i.e. a structure obtained by X-ray crystallography. The crystal structure of the most active isomer of cypermethrin (α-s (1R, 3R *cis*)) published by Owen [10], was used as the basis for the modelling calculations following removal of the cyano group and conversion of the 3 position of the cyclopropane ring to the S (*trans*) isomer. This configuration is expected to correspond to the active form of the QSAR compounds. Substituents were added to the phenyl ring and the new bonds minimised using the molecular mechanics force-field. Electron distributions were then calculated using the MOPAC package [11] and the resulting structure files transferred to an in-house modelling package WMM. Molecular descriptors were calculated from the WMM structure files using an in-house computer package PROFILES and the MEDCHEM software CLOGP and CMR [12]. In all, 70 parameters were calculated for each of the compounds in the set including log P, steric descriptors, atom charges, reactivity indices and vectors of the dipole moment. Although this descriptor set contained considerable redundancy, the intention was to generate as varied a description of the physicochemical properties of the molecules as possible. The next section describes the reduction of this data set in order to remove redundancy.

Reduction of physicochemical parameter set

One means by which the redundancy in the descriptor set may be described is by calculation of the pair-wise inter-parameter correlation matrix. Although the resultant correlation matrix contains the required information, it is difficult to visualize since there are $N(N - 1)/2$ entries in a correlation matrix of N parameters. In the case of this descriptor set of 70 variables, there are 2415 values. A commonly used method for the display of such associations is cluster analysis [13] but even with a simplified dendrogram it is difficult to adequately portray 70 variables. Non-linear mapping [14] provides an alternative display technique for points in an N-dimensional space. The routine preserves inter-point distances from the N-dimensional space and displays them as a 2-dimensional plot. Because the correlation coefficient (r) is large for strongly associated parameters it was necessary to use the coefficient of non-determination, $(1 - r^2)$, as the distance measure. Variables with high association will be plotted on this map in close proximity. Fig. 1 shows such a map for the starting set of 70 variables; there are several closely associated groups of variables, some of the same 'type' e.g. atom charges, and some different.

An in-house routine called CORCHOP [15] was used to sort the interparameter correlations and to remove descriptors so as to reduce the redundancy of the descriptor set. A flow diagram for this RS/1 procedure is shown in Fig. 2. Variables

486
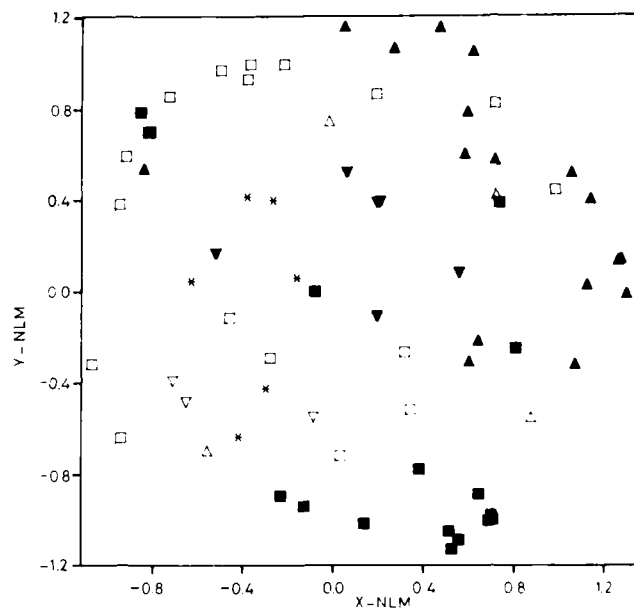
FIG 1 Non-linear map of inter-parameter associations for 70 starting variables. ⊏. atom charges; ∆. dipole moment and vectors; ▽. MOPAC energies; ■. ESDLs; ▲. NSDLs; ▼. shape and log P; *. Moments of inertia and ellipsoid axes.

input parameter data table
|
check distributions and optionally delete
poorly spread (kurtosed) parameters
|
calculate correlation matrix
|
locate and delete one of each pair of very highly
correlated parameters, e.g., r > 0.99
|
user chooses maximum allowed correlation, e.g., r = 0.75
|
- - - - - - - - - - - - count no. of correlations > maxcor for each parameter - - - - - - - - -
|
look at all parameters having the maximum number of correlations
resolve 'ties' by sorting parameters by decreasing maximum r
in each column, then by decreasing kurtosis
|
delete one of these parameters? - yes
|
|no
|
locate the pair of parameters having the highest inter-correlation
|
- - - - - - yes - delete parameter with higher kurtosis - no - delete other parameter - - - - - - -
|
quit or decrease maxcor

FIG 2 Flow diagram for correlation reduction procedure.
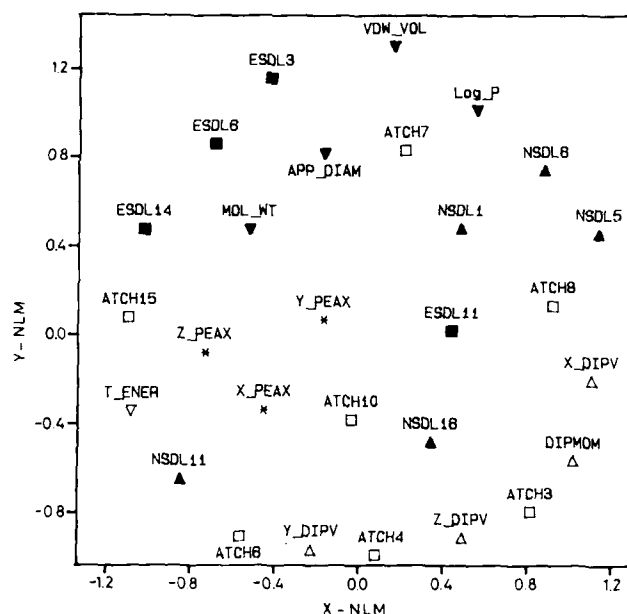
FIG 3 Non-linear map of parameter correlations for the reduced set. ■, atom charges; △, dipole moment and vectors; ▽, MOPAC energy; ■, ESDLs; ▲, NSDLs; ▼, shape and log P; *, ellipsoid axis.

are deleted on the basis of the number and size of their inter-parameter correlations and on their statistical distribution. The intention is to produce a parameter set in which individual variables have been 'nominated' from each cluster of associated variables, thus representing the information content of those clusters. The result of running CORCHOP on this data set was to produce a reduced set of 28 physicochemical descriptors shown in Fig. 3. There is now a much more even distribution of parameters and much of the clustering seen in Fig. 1 has been removed. There is still likely to be some redundancy in this data set but at this stage further data reduction was supervised by the biological data.

Analysis of biological data

The in vitro and in vivo biological effects of the pyrethroid analogues were determined using appropriate bioassays. Eight in vitro neurophysiological responses were measured by extracellular recording of isolated housefly haltere nerve preparations following continuous perfusion of the test compound dissolved at a fixed concentration (10 μm) in insect saline [6]. In vivo insecticidal potencies based on a median effective dose were expressed as the killing activity (KA) observed 48 h and the knockdown activity (KDA) observed 10 min following topical application of a cellosolve solution of the compound [6].

The in vitro and in vivo data will contain common information which can be identified using an appropriate multivariate statistical procedure such as factor analysis. Factor analysis is an analytical technique based on a formal statistical

TABLE 3   Rotated factor loadings for ten biological response variables

	KA	Time onset	Time max. freq.	MTC	Max. freq. of AP	Time to block	Slope	Intcpt.	Max. burst freq.	KDA
F1	−0.93	0.84	0.88	0.71	0.74	0.79	−0.16	0.21	0.06	−0.50
F2	0.28	−0.10	−0.29	−0.57	0.39	0.04	0.23	−0.18	0.90	0.72
F3	0.01	0.15	−0.10	0.00	−0.31	0.10	0.93	0.94	−0.04	0.16

model (the normal multivariate probability density function) (see Chapter 35). It is assumed that a data set contains both common or communal information (shared between the variables) and unique information. The information unique to a variable may be thought of as error, wheras the common information represents that part of the data which is 'useful' for identifying correlation structure. In factor analysis, the unique information is identified and removed to create a reduced correlation matrix containing information relating solely to interpretable associations.

Three significant factors were identified by this analysis, two of which were significantly associated with the in vivo responses. The factor loadings, i.e. correlation of each biological parameter with the individual factors, are shown in Table 3. Factor 1 is associated with both killing and knockdown activity (loadings of −0.93 and −0.5 respectively) and several neurotoxicological responses, whilst factor 2 is mainly associated with knockdown. Factor scores, i.e. the coordinates of the compounds in factor space, are shown in Fig. 4 for some of the compounds along with a summary of the relationship between the scores and biological activity. Factor 3 appears not to have neurotoxicological significance.

FACTOR SCORES

	Factor 1	Factor 2
QSAR 1	−0.496	1.058
2	−1.336	0.936
3	0.597	−0.526
.	.	.
permethrin	−1.880	0.768

low values are potent compounds with short times to maximum frequency of a.p.'s and low values of mtc

high values correspond to good knockdown and large burst frequency

killing and knockdown discriminated   killing and knockdown discriminated
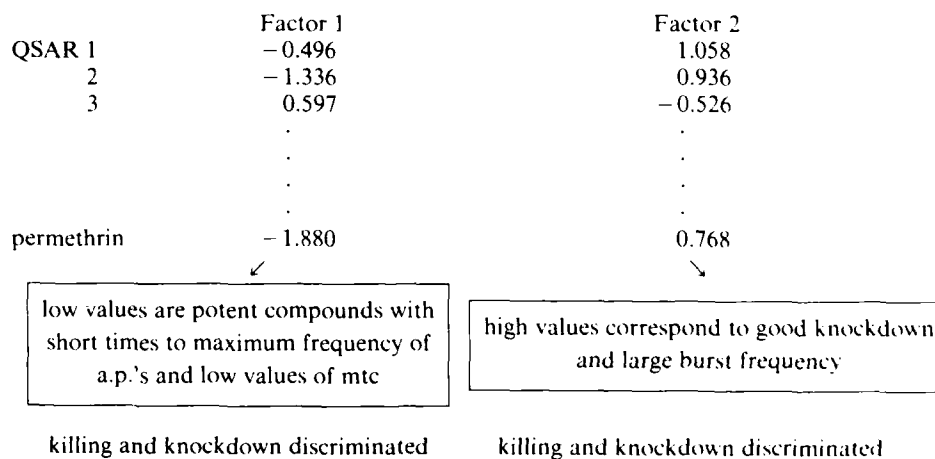
FIG 4   Factor scores and associations of responses.

Combined analysis of biological and physicochemical data

A first stage in the analysis of the combined biological and physicochemical data is to attempt to identify those molecular descriptors which are most strongly associated with the biological data. There are several strategies which may be employed to achieve this aim; the approach described here is only one such method, a later report of this work will compare several variable selection techniques.

Three neurotoxicological responses with high association with in vivo toxicity may be identified by factor analysis. The assocations of these variables are described by two orthogonal, and hence uncorrelated, factors. The logarithm of the time to maximum frequency of action potentials (LTMF) has a high loading with factor 1 (0.88) whilst the logarithm of the maximum burst frequency (LBF) has a high loading with factor 2 (0.90). The logarithm of the minimum threshold concentration (MTC) is the only response to load on to both factor 1 (0.71) and factor 2 (-0.57). This result suggests that the mechanism which underlies pyrethroid induced firing of single action potentials and nerve block is independent from that producing repetitive bursting. Three other responses, the logarithm of time to onset, the logarithm of time to block and the logarithm of the maximum frequency of action potentials, also have high loadings with factor 1 and the inclusion of these parameters may prove useful in a later stage of the analysis. Although two in vivo activities relating to knockdown and kill have high loadings with the first two factors, the activities were excluded at this point since the objective was to relate in vivo to in vitro data and thence to molecular property data. Having identified these significant neurotoxicological responses, the physicochemical data was analysed by the ARTHUR routine SELECT [16] which ranks variables in terms of their correlation with a particular response. The results of this analysis are shown in Table 4 where 24 of the physicochemical variables are listed along with the order in which they were chosen by SELECT.

The individual correlations between each molecular descriptor and a linear combination of the three biological responses MTC, LTMF and LBF were used to

TABLE 4 Molecular parameters calculated by computational chemistry and selected on the basis of their association with MTC, LTMF and LBF

Parameter	MTC	LBF	LTMF	Parameter	MTC	LBF	LTMF
ATCH-3	1		1	ESDL-11			5
ATCH-4		11		ESDl-14	6		10
ATCH-6		6		NSDL-1	7	10	11
ATCH-8		4		NSDL-5		7	3
ATCH-10			6	NSDL-11	5	8	
DIPV-X	8			NSDL-16			9
DIPV-Y			7	APP-DIAM	3	5	
DIPV-Z			8	PEAX-X		13	
DIPMOM	11			PEAX-Y			2
ENERGY	10	1		PEAX-Z		12	
ESDL-3	4			MOL WT	2	3	
ESDL-6	9	2		LOG P			4

The cell numbers indicate the selection order of the molecular descriptors for each biological response; blank entries indicate no significant association.

effect further data reduction. Examination of the correlations of the descriptors with the response set identified six molecular physicochemical parameters with tail probabilities less than 10%. Using this level of probability there is a likelihood of selecting one or two parameters from the set of 24 purely by chance. Interestingly, one of the descriptors chosen by this procedure, ellipsoid axis Z, was not high on the list of parameters chosen by SELECT (Table 4). This serves to emphasize the difference between univariate and multivariate techniques. The routine SELECT operates on only one biological response at a time, whereas selection of variables by the procedure outlined above is multivariate since all three biological responses are considered simultaneously.

This reduced set of 6 descriptor variables and 3 response variables were next analysed by a multivariate method, canonical correlation analysis (CCA), which is multivariate with respect to both variable sets [17]. CCA creates a set of new variables (canonical variates) from linear combinations of the response and descriptor variables. The general form of these linear transformations is given by the expression:

$$\sum_{i=1,N} a_{1,i} R_i = \sum_{j=1,M} b_{1,j} D_j$$

where there are N response variables R, in this case 3, and M descriptor variables D, in this case 6.

The weighting coefficients, a and b, are chosen so as to maximize the correlation between the two sets of variables. Furthermore, this correlation is at a maximum for the first pair of variates and decreases with subsequent pairs. Successive canonical variates are orthogonal (uncorrelated) to one another.

Application of CCA to the reduced data set yielded two pairs of significant canonical variates relating the three neurotoxicological responses (MTC, LBF and LTMF) to six physicochemical descriptors: the atom charges on the *meta* carbon and the ether oxygen, log P, the total molecular energy (MOPAC), the ellipsoid axis Z and the nucleophilic superdelocalizability (NSDL) on carbon 1 of the cyclopropane ring. The canonical correlations between response and descriptor sets were 0.91 and 0.88 for the first and second sets of variates, respectively. However, examination of the multiple correlations between the descriptor variables (Table 5) showed that there was multicollinearity in this set (Set 1).

Backward stepping variable deletion diminished the multicollinearity without loss of information. Removal of the parameter describing total energy (Set 2), for example, caused little change to the canonical correlation coefficients, 0.91 and 0.85, but lowered the multiple correlations considerably.

TABLE 5   The influence of variable deletion on the squared multiple correlations (R^2) of each descriptor with all other molecular descriptors in the variable set

	Set 1	Set 2
Carbon charge	0.981	0.336
Oxygen charge	0.957	0.410
Energy	0.993	Deleted
NSDL	0.962	0.703
PAZ	0.657	0.498
Log P	0.909	0.624
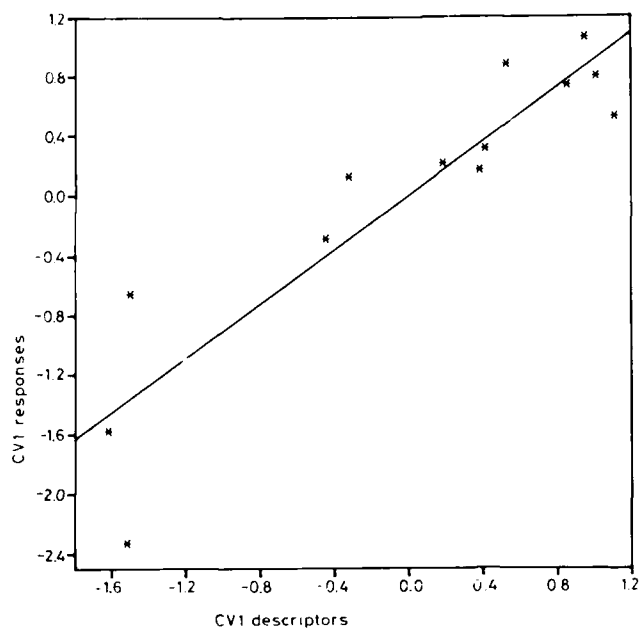
FIG 5   Plot of the first canonical correlation.

The first canonical correlation is shown in Fig. 5 where the canonical variate scores of the first set (responses) are plotted against the scores of the second set (descriptors). A descriptor score may be calculated for a new compound and the
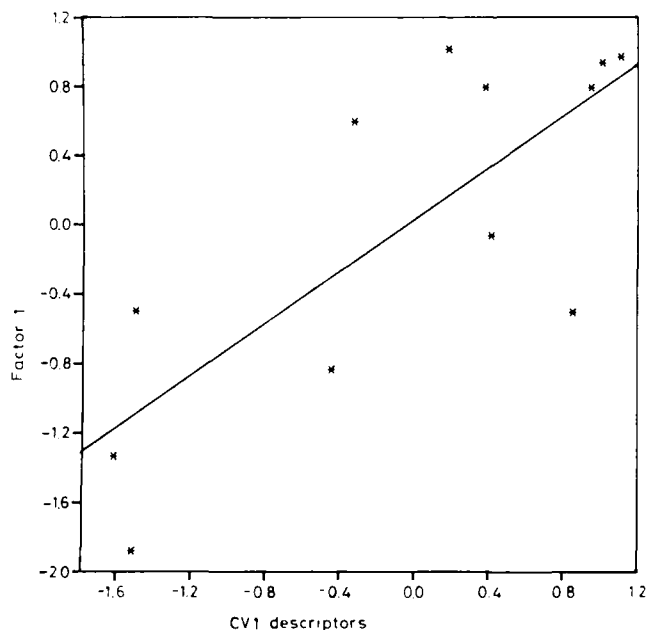
FIG 6   Relationship between the first factor and the first canonical variate scores.

corresponding response score estimated from the fit. This response score, of course, is a combination of neurotoxicological responses and the individual responses cannot readily be estimated. However, the response score may give some indication of the insecticidal potential of candidate compounds [18]. The first canonical variate has a high association with neurotoxicological potency (MTC) whereas the second has a significant association with the ability of a compound to produce repetitive bursts of action potentials (LBF).

The results of CCA may be compared with the results of the factor analysis carried out on the biological data alone (Fig. 6). There is a significant association between canonical variate 1 and factor 1.

Discussion

By the selection of compounds intended to exemplify good variation in physicochemical properties, a 'training' set has been identified in which there is wide variation in neurotoxicological responses. The application of the multivariate statistical method, factor analysis, has not only uncovered some interesting relationships between in vitro and in vivo experimental data, but has also revealed the presence of two factors in the biological responses of this set of pyrethroid analogues. In addition to the multivariate analysis of the biological responses, the compounds have been characterized in physicochemical terms by use of molecular modelling packages and associated software. These modelling studies, based on an X-ray structure determination, led to the generation of a very large chemical descriptor set of 70 parameters. The question may, of course, be raised about how relevant is an X-ray structure compared with the solution conformation of a molecule or the receptor-bound conformation. Little has been published on attempts to determine solution structure and there are no experimental data available for the receptor-bound structure. An X-ray determination at least provides some experimental basis for the modelling studies and, within a closely related series such as this, it might be expected that relative differences in physicochemical properties would be well predicted. Moreover, some of the molecular properties (e.g. dipole vectors) will vary with conformation whilst others (e.g. partial atomic charges) will be relatively insensitive to such changes.

Having produced this large descriptor set, the application of multivariate methods has identified a number of molecular features which are of importance in the description of biological responses. There is, at this stage of the analysis, no implication of causality in the identification of these relationships, nor is any particular significance attached to the identification of individual variables. In the process of removing redundancy from the starting descriptor set, a number of variables have been 'nominated' to represent the information content of different groups or clusters of variables. A relationship between a particular response, or group of responses, and an individual variable may be due to an underlying relationship with another parameter or set of parameters from the same subgroup of molecular descriptors. These nominated descriptor variables represent sets of molecular features which describe particular steric, partition and electronic properties. Thus, the neurotoxicity of a pyrethroid and hence its insecticidal potency and type of action is related to a combination of these molecular properties.

With these points in mind, it is possible to identify a number of features in the relationships between insecticidal potency, neurotoxicity and the molecular properties of pyrethroid insecticides.

The potency of a compound will depend upon the binding energy of its interaction with a receptor and this, in turn, will determine the threshold concentration required to elicit a biological response. The results of the factor analysis (Table 3) confirm that low molar threshold concentrations are required for both high knockdown and killing activities. Pyrethroid insecticides produce a variety of neurotoxicological responses. In previous studies it has proved difficult to identify which of these responses are associated with knockdown or mortality. The use of factor analysis has clearly identified a strong association between the ability of a compound to produce repetitive bursts of action potentials (LBF) and knockdown activity (KDA). Although the other neurotoxicological responses associate to varying extent with killing activity (KA), LBF is uncorrelated to this property. These results suggest that a good knockdown compound not only requires a low value of MTC but also the ability to induce bursting behaviour.

Our investigations of the relationships between molecular properties and the in vitro responses, and hence in vivo potencies, have demonstrated that a number of different molecular properties are required (Table 5). A detailed account of these relationships will be reported in a subsequent publication. However, certain features are already apparent. The identification of two significant canonical variates implies that some of the molecular properties required for bursting, and hence knockdown, are different to those necessary for an increased rate of onset of symptoms (AP frequency and nerve block) and maximum frequency of firing of action potentials, all of which are associated with kill (Table 3). These are the molecular features which have significant loadings on only one of the canonical variates. Furthermore, the loadings of the original descriptor variables suggest that some properties are associated with both of the canonical variates. Thus, the particular combination of molecular properties identified by the canonical correlation analysis should determine the combination of neurotoxicological responses observed for a particular compound. The set of neurotoxicological responses will, in turn, determine the combination of knockdown and killing activities of that compound. Not only does this provide a means for the prediction of biological activity but also can be used as the basis for classifying compounds according to their neurotoxicological behaviour. Such a classification would be quantitative but would be related to the qualitative scheme (Type I, II) proposed by Gammon, Brown and Casida [19] and would have the advantage of being based on both biological response and chemical structure.

Finally, it should be recognized that the combination of neurotoxicological responses associated with knockdown or kill may be obtained for compounds with either high or low potency. As already noted, potency is associated with the molar threshold concentration, MTC. This threshold is determined by several molecular features, the most important of which is the partial atomic charge on a *meta* carbon. A possible interpretation of this observation is that these features are important in determining the binding energy of the ligand with its receptor.

Appendix

Compound selection, molecular modelling, parameter generation, parameter reduction, data display and non-linear mapping calculations were all performed on a

494

DEC VAX 11/750 computer. The software used were the Wellcome in-house routines SELECT [7], CORCHOP [15], WMM [20] and PROFILES [20] and the proprietary software SYBYL [21], RS/1 [22] and ARTHUR [23].

Factor analysis and canonical correlation analysis was carried out on an ICL 2960 computer using the BMDP statistical package [24].

References

1 Leahey, J.P. (1985) The Pyrethroid Insecticides, 440 pp. Taylor & Francis, Ltd, London and Philadelphia.
2 Briggs, G.G., Elliott, M., Farnham, A.W. and Janes, N.F. (1974) Structural aspects of the knockdown of pyrethroids. Pestic. Sci. 5, 643–650.
3 Ford, M.C., Greenwood, R., Leake, L.D., Szydlo, R.M. and Turner, C.H. (1985) The relationship between the physicochemical properties of pyrethroid insecticides and their speed of neurotixic action. Pestic. Sci. 16, 673–683.
4 Ford, M.C. (1979) Quantitative Structure Activity Relationships of Pyrethroid Insecticides, Pestic. Sci. 10, 39–49.
5 Nishimura, K., Ueno, A., Nakagawa, S., Fujita, T. and Nakajima, M. (1982) Quantitiative structure activity studies of substituted benzyl chrysanthemates 3. physicochemical effects and the spontaneous neuroexcitatory activity on the crayfish abdominal nerve cords. Pestic. Biochem. Physiol. 17, 271–279.
6 Buckley, S., Ford, M.G., Leake, L.D., Salt, D.W., Burt, P.E., Moss, M.D.V., Brealey, C.J. and Livingstone, D.J. (1987) A neurotoxicological investigation of the action of synthetic pyrethroid insecticides against adult houseflies *Musca domestica*. In: QSAR in Drug Design and Toxicology (D. Hadzi and B. Jerman-Blazic, eds.), pp. 336–339. Pharmacochemistry Library Vol. 10. Elsevier.
7 Hyde, R.M., Livingstone, D.J. and Rahr, E. (1988) in Preparation.
8 Hyde, R.M. and Livingstone, D.J. (1988) Perspectives in QSAR-Computer Chemistry and Pattern Recognition., J. Comp. Aid. Mol. Design 2(2), 145–147.
9 Norrington, F.E., Hyde, R.M., Williams, S.G. and Wootton, R. (1975) Physicochemical-activity relations in practice. 1. A rational and self-consistent data bank. J. Med. Chem. 18, 604–607.
10 Owen, J.D. (1975) Absolute configuration of the most potent isomer of the pyrethroid insecticide α-cyano-3-phenoxybenzyl *cis*-3-(2,2-dibromovinyl)-2,2-dimethylcyclopropanecarboxylate by crystal structure analysis. J.C.S. Perkin I, 1865–1868.
11 MOPAC, Program No. 455, Quantum Chemistry Program Exchange (QCPE), Bloomington, Indiana.
12 CLOGP and CMR, MEDCHEM Software Version 3.52, Pomona College Medicinal Chemistry Project, Claremont, California (1987).
13 Wolff, D.D. and Parsons, M.L., Pattern Recognition Approach to Data Interpretation, pp. 65–79. Plenum Press, New York & London.
14 Kowalski, B.R. and Bender, C.F. (1972) Pattern recognition. A powerful approach to interpreting chemical data. J. Am. Chem Soc. 94, 5632–5639.
15 Livingstone, D.J. and Rahr, E. (1988) CORCHOP:—an interactive routine for the dimension reduction of large QSAR data sets. Quant. Struct. Act. Relat. (submitted).
16 Kowalski, B.R. and Bender, C.F. (19760 An orthogonal feature selection method. Pattern Recogn. 8, 1–14.
17 Chatfield, C. and Collins, A.J. (1980) Introduction to Multivariate Analysis, pp. 169–173. Chapman & Hall, London & New York.
18 Szydlo, R.M., Ford, M.G., Greenwood, R. and Salt, D.W. (1984) The use of multivariate techniques for the prediction of biological activity. In: QSAR in Design of Bioactive Compounds pp. 301–320. J.R. Prous Barcelona.

19 Gammon, D.W., Brown, M.A. and Casida, J.E. (1981) Two classes of pyrethroid action in the cockroach. Pestic. Biochem. Physiol. 15, 181–191.

20 Glen, R.C. and Rose, V.S. (1987) Computer program suite for the calculation, storage and manipulation of molecular property and activity descriptors. J. Mol. Graph. 5(2), 79–86.

21 SYBYL, Molecular Modelling Package, Tripos Associates, St. Louis, Missouri, USA.

22 RS/1, Data Handling Software, BBN Software Products UK Ltd., Staines, Middlesex, UK.

23 ARTHUR, Version 4.1, 1986; Infometrix Inc., Seattle, Washington, USA.

24 Dixon, W.J. and Brown, M.B. (Eds), Biomedical Programs, P-Series, Los Angeles, California.

CHAPTER 37

Qualitative and quantitative modelling of drugs and pesticides

FLEMMING S. JØRGENSEN [1], JETTE R. BYBERG [1], POVL KROGSGAARD-LARSEN [1]
AND JAMES P. SNYDER [2]

[1] Department of Chemistry BC, Royal Danish School of Pharmacy, Universitetsparken 2, DK-2100 Copenhagen, Denmark; and [2] Drug Design Section, G.D. Searle Research and Development, 4901 Searle Parkway, Skokie, Illinois 60077, U.S.A.

Molecular modelling and computer graphics

Structure–activity relationships are extremely important for gaining a better under-standing of the mechanisms associated with the activity of drugs and pesticides. In the last two decades molecular modelling and computer graphics techniques have made it possible to study the three-dimensional aspects of drug–receptor interactions in a very efficient way. Simultaneously, the application of quantitative structure–activity relationships (QSAR) based on the Hansch approach has matured considerably. Today, the combination of these two approaches is a very powerful tool for the design and development of new biologically active compounds [1].

To illustrate some of the possibilities as well as some of the problems associated with these methods two cases of molecular modelling studies are presented. The first example describes a molecular modelling analysis (pharmacophore mapping) of a series of very flexible pyrethroid esters. The second example describes the construction of a quantitative three-dimensional model for glutamic acid agonists.

Pyrethroid esters

The pyrethroids are very important insecticides due to their low mammalian toxicity combined with a high insecticidal activity. Pyrethrin I (cf. Fig. 1) is an example of one of the naturally occurring pyrethrins, which are esters of either chrysanthemic or pyrethric acid [2]. The molecular framework of the natural products has been extensively modified and some of today's pyrethroids may possess only a marginal resemblance to compounds like Pyrethrin I. During the last decade more detailed studies concerning the mode of action of the pyrethroids have been performed, and at present it is generally accepted that the pyrethroids interact with a sodium channel in the nerve membrane. This interaction is highly stereospecific indicating a receptor-mediated mechanism of action. The pyrethroids are classified into two groups, type I and type II pyrethroids, according to their electrophysiological characteristics [3].

498
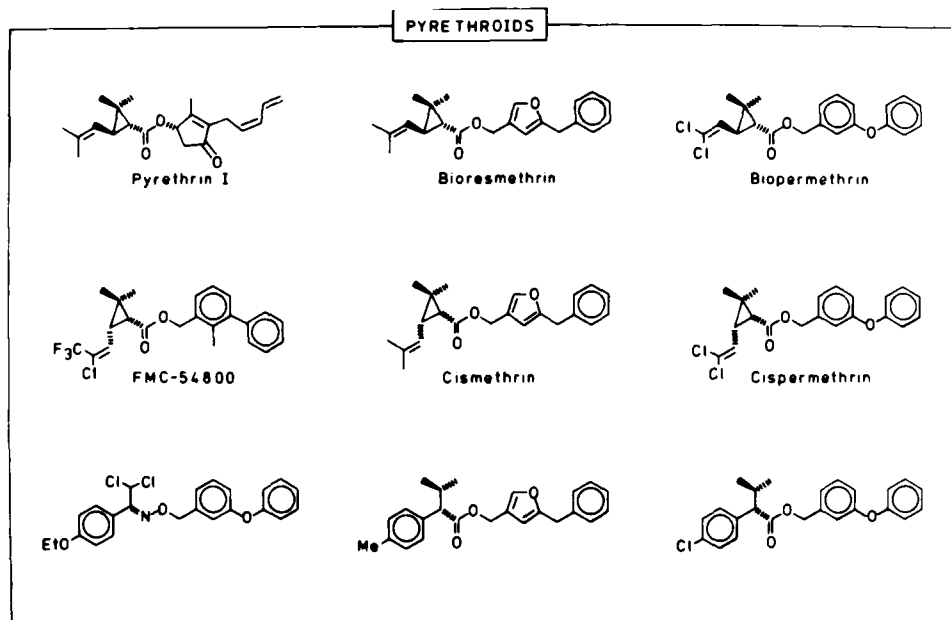
FIG 1 Pyrethroids discussed in the text.

A considerable amount of information about the correlation between molecular structure and biological activity is available from traditional QSAR analyses for certain classes of compounds and for certain parts of the pyrethroid framework [4]. However, only a limited number of studies considering the shape and flexibility of the whole pyrethroid moiety has been reported [5].

In order to determine the active conformation associated with pyrethroid activity. we have selected seven structurally different type I pyrethroid esters (cf. Fig. 1). The compounds were selected to reflect the presence of different acid moieties as well as different alcohol moieties. Furthermore, an oxime O-ether, which can be viewed as a conformationally constrained pyrethroid analogue, and the original Pyrethrin I were included in the modelling analysis.

Based on available structure–activity data it is possible to deduce the groups, which are essential for the insecticidal activity. In Fig. 2 the essential groups are shown schematically. The oxygen atom has been included in order to study the acid and alcohol moieties separately, and subsequently combine the two parts to the original pyrethroid esters.

It was not possible to superimpose these groups in the nine pyrethroids directly. The unsaturated parts of the molecules especially yielded very poor alignments. In
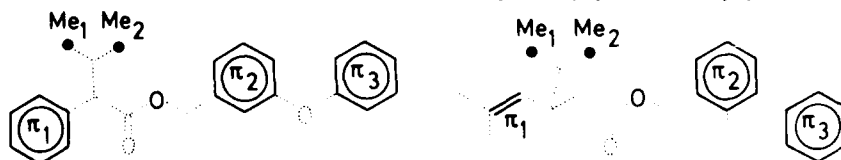
FIG 2 Common groups present in the pyrethroid esters.
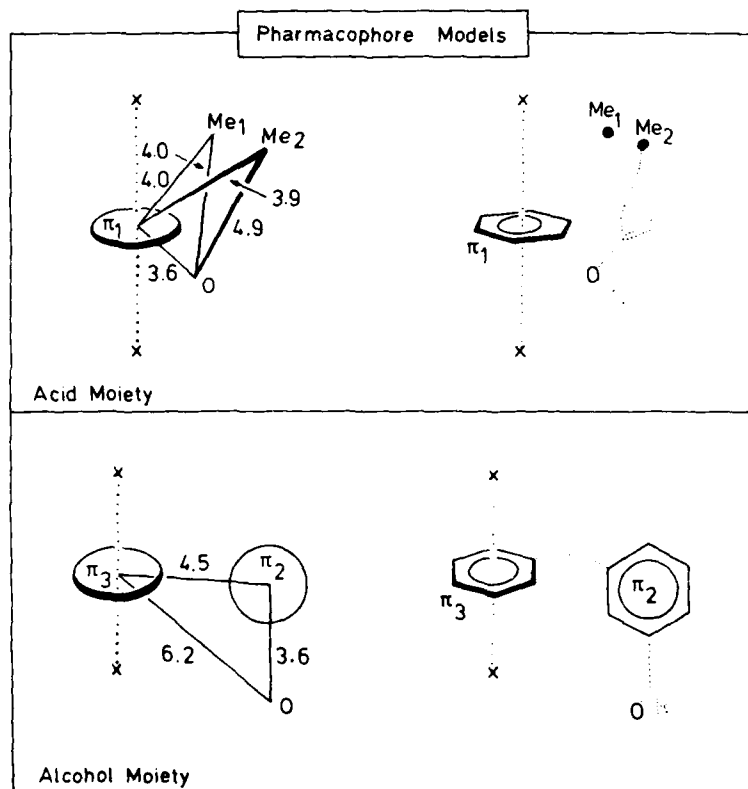
FIG 3 Pharmacophore models for the acid and alcohol moieties of the pyrethroid esters.

order to overcome this problem the three unsaturated moieties were represented by a vector orthogonal to the plane of each π-system. The length of the vectors was fixed at 3.5 Å on each side of the π-systems. This value was chosen to reflect the thickness of π-system, and thus represent a reasonable location for a hydrophobic part of the receptor. Furthermore, this description allows a direct comparison of the different types of π-systems present in the cyclopropane-derivatives and the 2-phenyl butanoates (cf. Fig. 1). Subsequent superimposition of the different acid moieties and the different alcohol moieties, respectively, yielded the pharmacophore models shown on Fig. 3.

The acid pharmacophore model illustrates the stereospecificity of the pyrethroids by having the two methyl groups placed asymmetrically relative to the π_1-system. From the alcohol pharmacophore model the similarity between the 3-phenoxy-benzyl alcohol moiety and the 3-O-phenyl-benzyl alcohol moiety is obvious. The pharmacophore mapping of the acid and alcohol moieties, respectively, have been described in detail elsewhere [6].

In order to establish a pharmacophore model for the complete pyrethroid system the ether oxygen atoms in the two pharmacophore models were superimposed. However, the relative orientation of the two parts remained to be determined. Therefore, each of the nine pyrethroids was analysed separately by scanning the

500
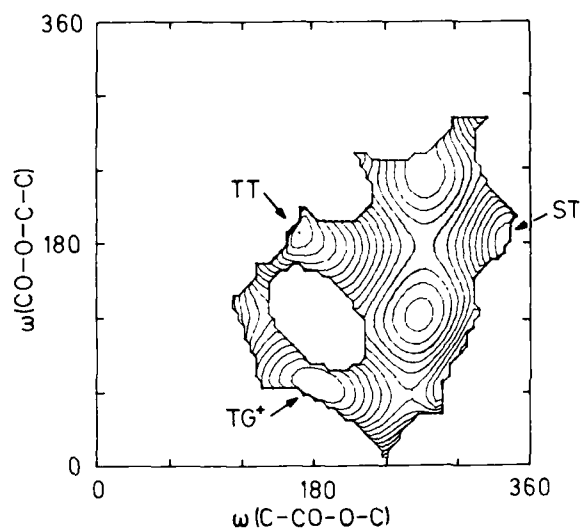
FIG 4   Potential energy surface for rotation around the two central bonds in the methyl-analogue of Cispermethrin.
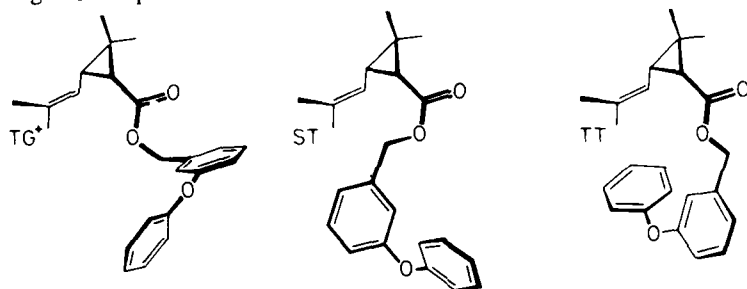
FIG 5   The three conformations obtained for the methyl-analogue of Cispermethrin by the conformational analysis.
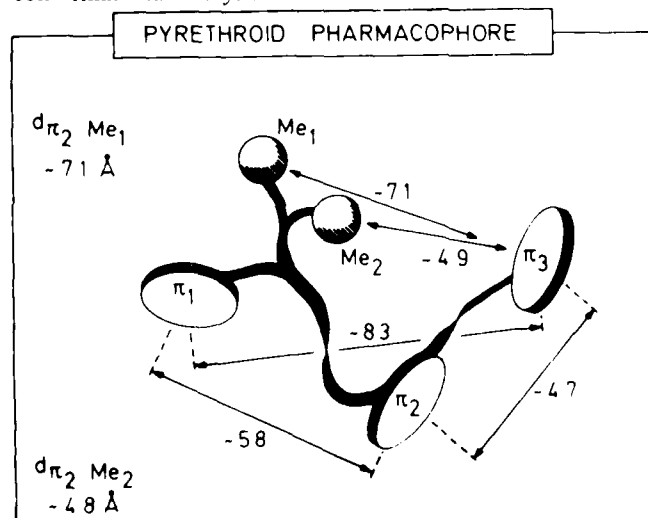
FIG 6   Schematic illustration of one of the obtained pyrethroid pharmacophores.

conformational hyperspace around the two flexible bonds (C–CO– –O–C and CO–O– –C–C). For each of the nine pyrethroids this leads to three minima on the potential energy surface corresponding to three low-energy conformations. The potential energy surface and the three low-energy conformations of the methyl-analogue of Cispermethrin are shown on Figs. 4 and 5, respectively.

Superposition of the relevant low-energy conformations for each of the nine pyrethroids leads to three different and equally reasonable pharmacophores. One of these is shown schematically on Fig. 6. The relative locations of the essential groups are very different for the three models (see also Fig. 5).

At present, work is in progress to evaluate the three pharmacophores. A complete description of the structural characteristics necessary for pyrethroid activity is important for the construction of a quantitative receptor model and for the understanding of the mechanisms associated with pyrethroid activity.

Glutamic acid agonists

(S)-Glutamic acid is a major excitatory neurotransmitter in the central nervous system. The glutamic acid receptor system can be subdivided into at least three receptor subtypes (cf. Fig. 7) for which N-methyl-D-aspartic acid (NMDA), kainic acid and quisqualic acid/AMPA (QUIS/AMPA) are agonists [7,8]. In the following we will focus on structure–activity relationships of agonists for the QUIS/AMPA receptor subtype.

Glutamic acid is a very flexible compound, which may adopt a large number of different low-energy conformations. The structure–activity relationships observed for a variety of conformationally constrained glutamic acid agonists makes it reasonable to assume that different conformations of glutamic acid are responsible for the activation of the different subtypes of receptors. By consideration of the pK_a values for glutamic acid it is most likely that a completely charged form is the preferred one at physiological pH. Thus, all calculations mentioned below have been performed on the fully charged form of the compounds.

In order to determine the receptor-active conformation of glutamic acid for activation of the QUIS/AMPA receptor we have studied a series of conformationally constrained glutamic acid analogues (cf. Fig. 7) by molecular modelling and computer graphics. All of the compounds selected for the analysis contain a 3-hydroxy substituted isoxazole ring. The 3-isoxazolol moiety has in several cases proven to be a bioisosteric group for the carboxyl group. Ibotenic acid is an example of a naturally occurring amino acid containing the 3-isoxazolol moiety [9].

Incorporation of this heterocyclic isoxazole system into glutamic acid leads to compounds with considerably reduced flexibility. Ibotenic acid and AMPA [10] are examples of such compounds with the glutamic acid backbone constrained in different conformations. Whereas ibotenic acid activates all three subtypes of glutamic acid receptors, mainly the NMDA subtype, AMPA is a potent and selective QUIS/AMPA agonist [11].

The compounds 5-HPCA and 7-HPCA represent glutamic acid analogues, which are further constrained [12,13]. Since both 5-HPCA and 7-HPCA are potent and selective QUIS/AMPA agonists, it is reasonable to assume that the conformation of the glutamic acid backbone in these compounds is close to the receptor-active conformation.
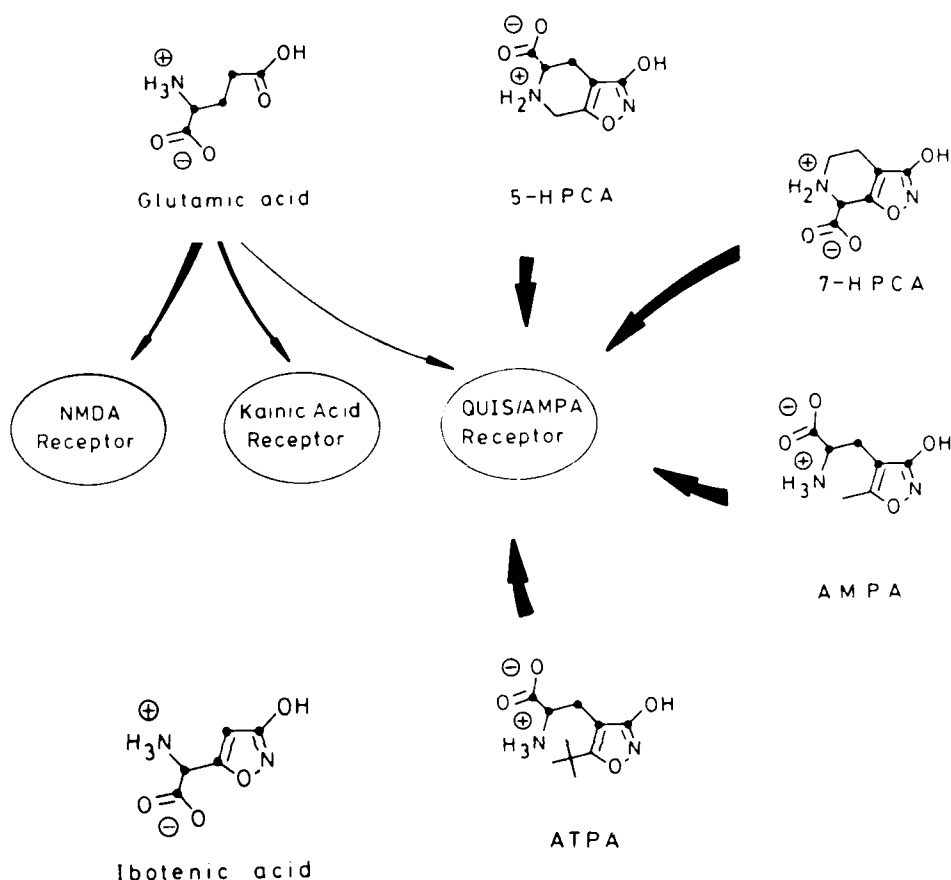
FIG 7   Schematic illustration of the glutamic acid receptor subtypes and the sites of action of the compounds discussed in the text.

It has previously been suggested that these two isomeric compounds actually have conspicuous structural similarities, which can be demonstrated by an inverted alignment of the 3-isoxazolol moieties [13]. By a simple atom-to-atom superposition of certain selected atoms in 5-HPCA and 7-HPCA, respectively, the two compounds can be shown to have similar size and shape (Fig. 8).

The monocyclic QUIS/AMPA agonists AMPA and ATPA [12] cannot easily assume the same conformation of the glutamic acid backbone as the one expressed by 5-HPCA, since it would impose serious steric repulsion between the amino group and the methyl and tert-butyl groups in AMPA and ATPA, respectively. In order to place the functional groups of these two flexible compounds in a relative arrangement identical to the functional groups of 5-HPCA and 7-HPCA, it is necessary for AMPA and ATPA to assume a bent conformation (Fig. 9).

The potent QUIS/AMPA agonist AMPA has been resolved and the activity of the individual enantiomers determined. The (S)-isomer is the most potent enantiomer [14], and accordingly, all the above comparisons have been carried out on this enantiomer. Alignment of the less potent (R)-enantiomer of AMPA in a similar
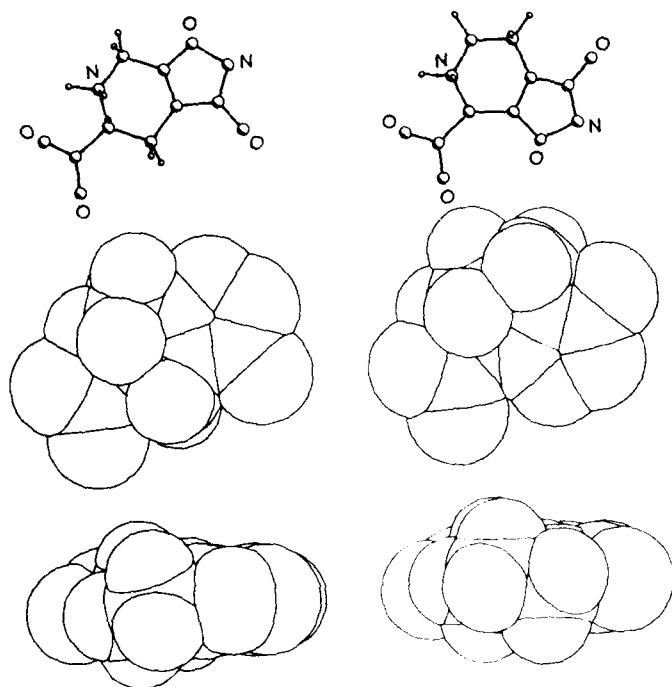
FIG 8 Three-dimensional representations of 5-HPCA (left) and 7-HPCA (right) after superposition. Both compounds are displayed as ball-and-stick (top) and space-filling (middle and bottom; top and side views, respectively) representations.
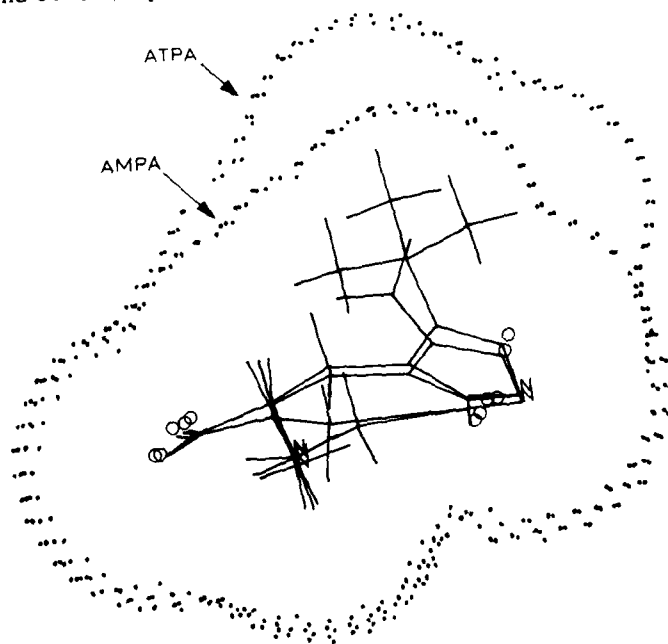
FIG 9 Comparison of AMPA and ATPA with 5-HPCA. The size of the compounds are illustrated by their solvent accessible surfaces.
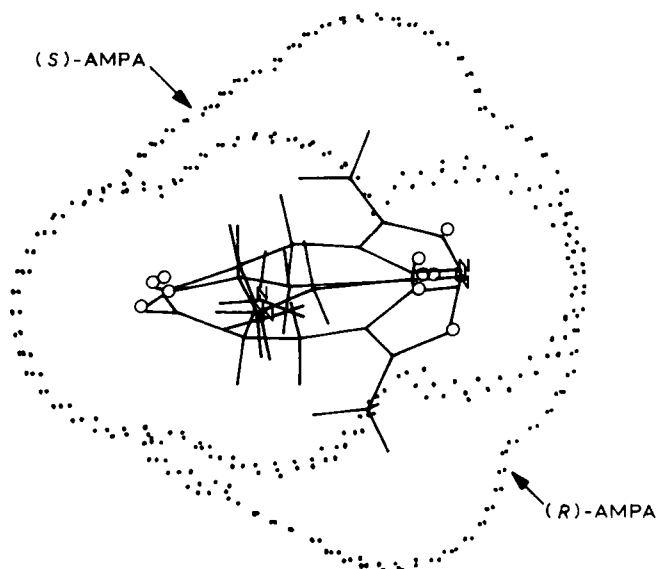
FIG 10 Receptor active conformations of (S)-AMPA and (R)-AMPA obtained by superposition to 5-HPCA. The sizes of the compounds are illustrated by their solvent accessible surfaces.

fashion clearly shows that the two enantiomers occupy different regions in space relative to the 5-HPCA and 7-HPCA compounds (Fig. 10).

Other compounds ranging from potent agonists to compounds devoid of any activity for the QUIS/AMPA receptor system have been superpositioned to 5-HPCA and 7-HPCA in an analogous manner. From these comparisons it seems clear that certain areas in space may be more feasible for substitution ('allowed' regions) than other areas ('forbidden' regions). Thus, a qualitative model of the structural requirements for activation of the QUIS/AMPA receptor has been established.

A quantitative model for QUIS/AMPA agonists has been constructed by surrounding 5-HPCA with three hypothetical receptor groups: one acetate ion and two
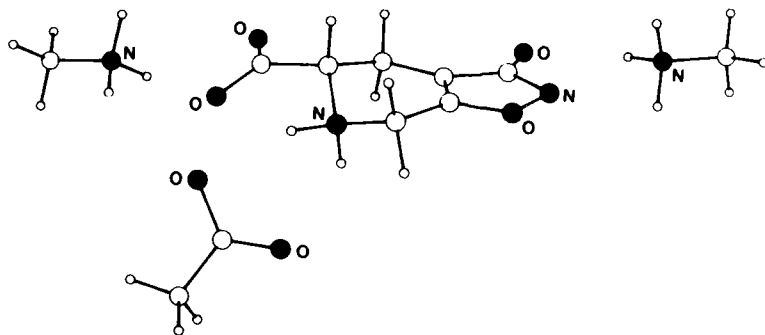
FIG 11 Schematic representation of the QUIS/AMPA receptor model discussed in the text.
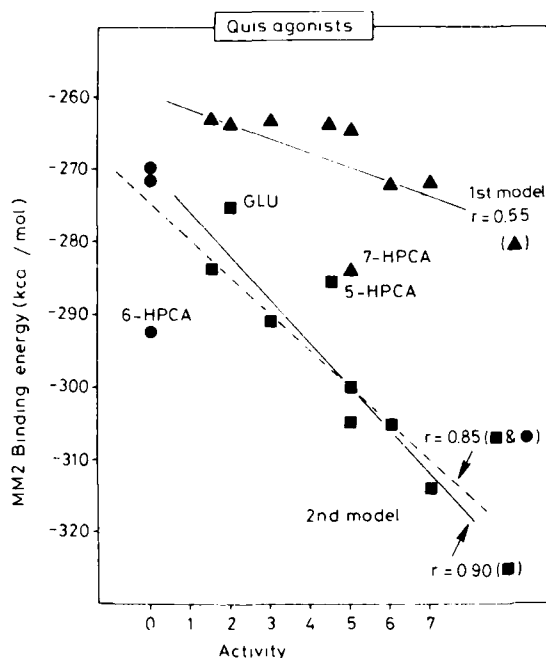
FIG 12 Relationship between calculated binding energies and biological activities for a series of QUIS/AMPA agonists.

methyl ammonium ions (Fig. 11). Although these groups may not have any resemblance with the actual receptor groups, they can be used as anchoring points for the agonists.

The energy of the three receptor groups, complementary to the agonist functionalities, were calculated (E_R) as well as the energy of the individual agonists (E_A). Each agonist was then placed between the receptor groups and the structure of the agonist minimized, whereas the receptor points were kept fixed. The energy for the complex between the agonist and the receptor-groups is called E_{RA} and by subtraction of this value from $E_R + E_A$ we have calculated a ΔE corresponding to an artificial binding energy.

The results for this simple model (1st Model on Fig. 12) were promising, and we have been able to further modify the model and improve the quantitative structure–activity relationship for the QUIS/AMPA agonists (2nd Model on Fig. 12).

Although the models described here are artificial and are based on several assumptions, they have proved useful as a working hypothesis. Further work is necessary in order to establish a quantitative model, which will take into account all the structural (steric and electronic) variations observed for glutamic acid agonists.

Acknowledgements

References

1 Burgen, A.S.V., Roberts, G.C.K. and Tute, M.S. (eds.) (1986) Molecular Graphics and Drug Design, Topics in Molecular Pharmacology, Vol 3, Elsevier, Amsterdam, and references therein.

2 Elliott, M. (1983) In: Natural Products for Innovative Pest Management (D.L. Whitehead, W.S. Bowers, eds.), Pergamon Press.

3 Ford, M.G., Lunt, G.G., Reay, R.C. and Usherwood, P.N.R. (eds.) (1986) Neuropharmacology and Pesticide Action. Ellis-Horwood, Chichester.

4 Doherty, J.D., Nishimura, K., Kurihara, N. and Fujita, T. (1986) Pest. Biochem. Physiol. 25, 295–305, and references therein.

5 Holan, G., Johnson, W.M.P., O'Keefe, D.F., Quint, G.L., Rihs, K., Spurling, T.H., Walser, R., Virgona, C.T. (1985) In: Recent Advances in the Chemistry of Insect Control (N.F. Janes, ed.) pp. 114–132. Royal Society of Chemistry,London.

6 Byberg, J.R., Jørgensen, F.S. and Klemmensen, P.D. (1987) Towards an identification of the pyrethroid pharmacophore. A molecular modelling study of some pyrethroid esters. J. Comp.-Aided Mol. Des. 1, 181–195.

7 Roberts, P.J., Storm-Mathisen, J. and Bradford, H.F. (eds) (1986) Excitatory Amino Acids. MacMillan, London.

8 Hicks, T.P., Lodge, D. and McLennan, H. (eds.) (1987) Excitatory Amino Acid Transmission. Alan R. Liss, New York.

9 Eugster, C.H. (1969) In: Fortschritte der Chemie Organischer Naturstoffe XXVII. (L. Zechmeister, ed.), p. 261. Springer-Verlag, Berlin.

10 Honoré, T. and Lauridsen, J. (1980) Structural analogues of ibotenic acid. Synthesis of 4-methyl-homoibotenic acid and AMPA, including the crystal structure of AMPA, monohydrate. Acta Chem. Scand. B34, 235–240.

11 Krogsgaard-Larsen, P., Honoré, T., Hansen, J.J., Curtis, D.R. and Lodge, D. (1980) New class of glutamate agonist structurally related to ibotenic acid. Nature (London) 284, 64.

12 Krogsgaard-Larsen, P., Honoré, T., Nielsen, E.Ø. and Curtis, D.R. (1984) Ibotenic acid analogues. Synthesis, biological and in vitro activity of conformationally restricted agonists at central excitatory amino acid receptors. J. Med. Chem. 27, 585–591.

13 Krogsgaard-Larsen, P., Brehm, L., Johansen, J.S., Vinzents, P., Lauridsen, J. and Curtis, D.R. (1985) Synthesis and structure-activity studies on excitatory amino acids structurally related to ibotenic acid. J. Med. Chem. 28, 673–679.

14 Lauridsen, J., Honoré, T. and Krogsgaard-Larsen, P. (1985) Ibotenic acid analogues. Synthesis, molecular flexibility, and in vitro activity of agonists and antagonists at central glutamic acid receptors. J. Med. Chem. 28, 668–672.

Selectivity and resistance

CHAPTER 38

The dynamic basis of selective toxicity

MARTYN G. FORD

*School of Biological Sciences, Portsmouth Polytechnic, Portsmouth,
Hampshire PO1 2DY, U.K.*

Introduction

Quite small modifications to the molecular properties of drugs and pesticides can result in substantial variations in biological activity. Compounds of similar chemical class, for example, acting at the same site of action can show relative toxicities in excess of 100,000 [1], and the susceptibility of different strains [2] and species [3,4] to the same toxicant can vary by factors in excess of 500. Selectivity can be beneficial. The control of target pests at commercial doses too low to threaten non-target organisms is a useful agrochemical property; and a large therapeutic ratio is necessary for the safe use of clinical pharmaceuticals. Selective toxicity can, however, sometimes lead to serious problems in the use of drugs and pesticides. The development of strains of organisms resistant to biologically active compounds, for example, can result in their premature withdrawal from commercial use [5].

A number of processes can give rise to selectivity. These may be broadly classified as pharmacokinetic processes, which act by modifying the exposure of the site of action to a drug or pesticide, and pharmacodynamic processes, which determine the strength and mode of binding of the ligand to the receptor. Pharmacodynamics also includes any secondary responses, such as stimulation of second messenger systems, which may result from receptor occupation [6]. This paper will review insecticide pharmacokinetics and pharmacodynamics in a quantitative manner and attempt to evaluate the influence of these processes on selective toxicity.

Pharmacokinetics

Contact of an insecticide deposit by an insect sets in motion a series of dynamic processes which result in exposure of sites of action within the insect to the poison. These processes, which include penetration of the insect integument, distribution throughout the insect body, binding to tissue components, detoxification (or toxification), and elimination of insecticide, proceed simultaneously as poisoning develops [7]. Penetration and distribution are transport processes associated with the delivery of toxicant to the site(s) of action; binding, detoxification, and elimination are loss processes which act to reduce the concentration of insecticide within the organism as time passes.

510

Elapsed time
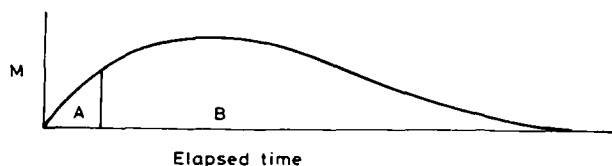
FIG 1   The pharmacokinetic profile describing the change in the internal level of toxicant with time following topical application of a finite dose.

Fig. 1 represents the gross changes of internal insecticide (M_2) with time following topical application of a finite dose. Initially, the rates of the delivery processes outstrip those of loss and there is net accumulation of insecticide within the insect. The finite supply of insecticide at the insect surface becomes depleted with time, however, and the overall rate of delivery is progressively diminished. In contrast, the rates of loss increase during this period as the concentration of internal insecticide increases, until, at some time, t_{max}, the overall rate of loss is equal to that of delivery. At this time, the derivative of the function describing the change in the internal level of insecticide with respect to time (dM_2/dt) will equal zero and the maximum internal concentration will have been achieved. Thereafter, there will be a net reduction in the level of poison since there now remains insufficient insecticide at the cuticle surface to maintain the internal concentration. Eventually, at some long time, t_{inf}, all of the insecticide will have been eliminated from the insect body and no further intoxication will then be possible.

It is not immediately clear how representative this picture is of the level of toxicant within an individual tissue [8], particularly the nervous system which contains the receptor sites of neurotoxicants. There have been very few published studies which allow us to gain a clear impression of the relationship between the total amount of internal insecticide recovered from treated insects following an external solvent wash to remove superficial material, and the amounts recovered from individual tissues. Such information as is available suggests that the changes in tissue levels at least match the form of the gross changes described in Fig. 1. The pharmacokinetic profiles obtained by Soderlund [9,10] following topical application of NRDC 157 or its inactive enantiomer to the adult american cockroach (*Periplaneta americana*) suggest, for example, that the applied compound accumulates at similar rates in the nerve cord and haemolymph, and reaches steady state levels in both tissues at roughly the same time. Thereafter the tissue levels diminish, but at an extremely slow rate. By 24 h, for example, a substantial quantity of material still remained in both tissues. Similar results have been obtained in our laboratories following topical application of cypermethrin to larvae of the Egyptian cotton leafworm, *Spodoptera littoralis*, Fab. (Fig. 2).

These findings are entirely reasonable. The levels of insecticide in a tissue will depend on the rates of uptake and elimination [8]. The larger the uptake rate compared with the elimination rate, the greater will be the tissue level. However, the nervous system, in which the critical lesion of neurotoxins occurs, is an organ of very small mass compared with the gross insect body weight. In larvae of *Spodoptera littoralis* Fab., for example, the isolated nerve cord represents only 0.7% of the total body weight (Table 1). Any change in the insecticide level within the nervous system will be compensated or damped by insecticide movement to or from the surrounding tissue, which acts as a large capacity reservoir for insecticide. Under conditions
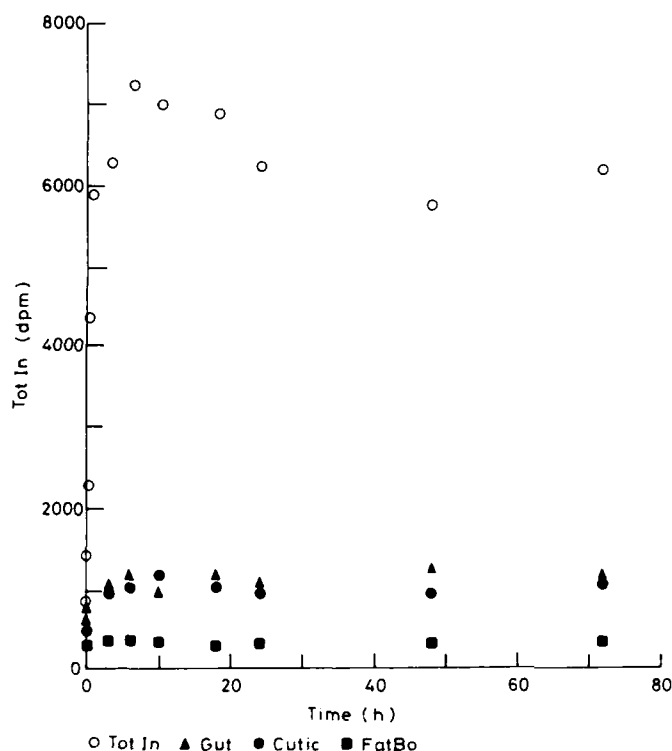
FIG 2   Tissue levels of cypermethrin topically applied in Sirius M180 oil (0.25 µl) to larvae (200 mg) of *Spodoptera littoralis* Boisd. o, total; ▲, gut; ●, cuticle; ■, fatbody.

where buffering of insecticide levels occurs, changes in insecticide tissue levels are likely to reflect the changes observed for whole body extracts [11]. Experimental confirmation of this hypothesis is provided by the positive associations observed between the gross internal recovery of cypermethrin following soxhlet extraction, and the tissue levels in the gut, the cuticle and the fat body (Fig. 3).

The exposure of receptors within the central nervous system will therefore be related to the overall internal exposure to insecticide. However, it is not immediately obvious how internal exposure should be evaluated. Is exposure directly related to the tissue level at the time of observation, or more accurately expressed as the cumulative effect of internal toxicant perfusing the receptor, measured from the time of initial contact with the insecticide deposit? Furthermore, is there a threshold concentration which must be exceeded before a neurotoxicological response is observed? The problem has been discussed in an informative review by Hollingworth [4], who points out that cumulative internal exposure can be expressed as the definite integral, with respect to time, of the pharmacokinetic profile for internal insecticide. This integral is a measure of the area which lies under the curve described in Fig. 1.

Critical integrals

The question of how best to express internal exposure has been investigated for pyrethroid insecticides applied to insects [7,11,12]. The results of these studies have

512
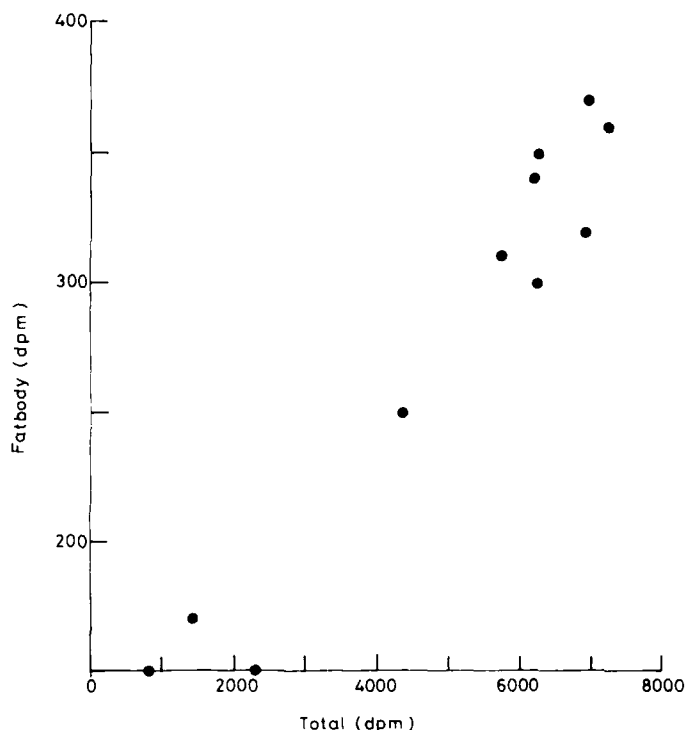
FIG 3 The relationship between the gross internal level of cypermethrin and that observed in the fatbody.

demonstrated that in order to achieve a standard in vivo response (e.g. 50% knockdown or 50% mortality), the median number of insects in the test population must receive a critical cumulative exposure of their target receptors to internal insecticide.

Consider the pharmacokinetic profile of internal mass M_2 shown in the Fig. 1. The total exposure of the target system is described by the sum of the areas A and B under the M_2 curve. Assuming that the threshold mass or concentration for poisoning is extremely small, as is the case for many insecticides, e.g. pyrethroids, where limiting concentrations to induce a neurotoxic response can be as low as 10^{-18} M [13], then the necessary exposure to produce knockdown will be given by the definite integral, area A, and for death at end point by areas A + B. These are critical integrals for knockdown and mortality, respectively, and both will have units of the product of mass and time. A critical exposure may result from a large internal concentration of toxicant bathing the receptor for a short time, or from a smaller internal concentration maintained for a more prolonged period. Critical integrals are inverse measures of the relative pharmacodynamic activities of insecticides.

Evidence in support of this hypothesis has been obtained for knockdown of *Spodoptera littoralis* Boisd. larvae by topically applied permethrin [12] where the observed combinations of time to knockdown and applied dose (measured over a wide range of applied doses) are those required to give a constant definite integral

(area A) of approximately 0.67 microgram hours. It is important to note that this result is only obtained if a limiting time of 3 min is subtracted from all of the observed knockdown times. This limit probably corresponds to the time for insecticide to reach the low but critical concentrations necessary to produce neurotoxic effects at target sites within the cuticle. A critical exposure necessary for death (areas A + B), following application of a range of methyl benzyl chrysanthemates to mustard beetles, is suggested by the linear relationship between the molar relative toxicity (MRT) as endpoint and resistance to elimination, $1/k_e$ [11].

Penetration of the insect integument

The insect integument is the first organ encountered by a contact insecticide. The integument comprises a set of polymeric lamellae of contrasting chemical composition, transversed by microscopic pores. These different structures provide a series of alternative routes for insecticide entry, and material will diffuse down concentration gradients or flow through pores at rates determined by the conductivities of each route. The polymeric material which forms the integument provides a large number of potential sites for insecticide adsorption, and much of the penetrating material will be retained within the integument, at least temporarily. In fact, the pyrethroid insecticide cypermethrin applied to leafworms accumulates rapidly in the cuticle during the early stages of poisoning (Fig. 2). Twenty-five years ago, Matsumura [14] demonstrated adsorption of the organophosphate insecticide, malathion, to proteinaceous cuticular components. Even earlier, Lord [15] had demonstrated a strong binding affinity between chitin, the polymeric carbohydrate which for.ns a substantial part of the arthropod integument, and the insecticide DDT. The cuticle of some species represents a large proportion of their dry body matter: a substantial proportion of the applied insecticide may therefore be bound to the integument, reducing the amount which can penetrate to receptors within the CNS. Receptors within the cuticle may also be protected by cuticular binding, but will remain in very close proximity to the bound insecticide.

Penetration through the integument has usually been investigated by studying the disappearance with time of insecticide from the insect surface. The classic work of R.D.O'Brien in the early 1960's [16,17] demonstrated that, depending on the size or species of insect, the physicochemical nature of the insecticide and carrier solvent, and the period during which penetration was followed, different forms of penetration curves could be obtained. Semi-log plots, for example, suggested that the loss of insecticide from the cuticle surface did not always follow the kinetics expected of a simple first-order process. Furthermore, penetration data were always characterized by a large error component. As a result, small changes with time in the amount of insecticide recovered in surface washes could not always be identified, and the exact nature of the penetration kinetics was often obscure.

To explain the variety of observed penetration curves, the penetration process can be modelled in terms of two compartments [7] representing the cuticle surface (C_1) and underlying tissues (C_2). A study of the penetration of pyrethroid insecticides into adult mustard beetles, Phaedon cochleariae Fab., had suggested that the rate of the penetration process was determined partly by the rate of distribution of insecticide throughout the insect, and partly by the rate of elimination of penetrated material from the insect body [18]. In modelling the process, the following assumptions were made.

(a) Penetration is first-order with respect to the mass of material at the insect surface, and is characterized by a rate constant, k_p, which represents the insecticide conductance of the integument.

(b) Elimination is first-order with respect to the mass of penetrated material, and is characterized by a rate constant, k_e; $1/k_e$ represents the resistance to elimination of insecticide.

(c) Distribution of material between the compartments tends to an equilibrium constant, λ.

(d) The effective mass at the insect surface is related to the thermodynamic potential for movement (λ $M_1 - M_2$) between the two compartments. The parameter λ is estimated by regression analysis.

The model was derived so that net movement of insecticide in the forward direction, i.e. compartment 1 to compartment 2 to the infinitely large sink, could be measured. On integration, the rate equations produce two coupled double exponential expressions which describe the amounts of material on the outside and inside of the insect as a function of elapsed time [7]. When these equations are expressed as semi-log plots, a so-called diphasic penetration curve is obtained.

Although the assumption of first-order penetration is consistent with many sets of results [11,16,18], two other related forms of penetration curve may sometimes be observed, viz. constant rate of penetration, combined with first-order elimination (case 1); delayed penetration, followed by a constant rate of loss from the insect surface (case 2). If the initial penetration rate is zero-order with respect to time (case 1), then the accumulation of material within the insect describes a different pharmacokinetic profile to that obtained for the model of Ford et al. [7]. Although the profile for M_1 describes a linear decay of surface material, that for internal mass rises to approach exponentially a limiting proportion ($k_1 k_p/k_e$) of the applied dose (M_0); the term $k_1 k_p$ is the product of the insecticide conductivity (k_p) of the integument and the proportion (k_1) of the applied dose M_0 which is available for penetration until time $1/(k_1/k_p)$. The proportion k_1 will be related to the surface area of the cuticle which is in contact with the deposit. When the elapsed time equals $1/(k_1 k_p)$, all of the insecticide will have penetrated and the rate equation for M_2 will then contain only one term, ($-k_e M_2$), on the right-hand-side. The level of internal mass at this time will then equal $k_1 k_p M_0/k_e(1 - \exp(-k_e/k_1 k_p))$. This model will only be realistic for situations where the penetration gradient is approximately $k_1 M_0$.

The second departure from the form of penetration curve described by Ford et al. [7] in which a lag phase lasting several minutes precedes a period of penetration at constant rate (case 2) is sometimes observed. This form of curve is characteristic of diffusion through a polymer film [19]. Because the insect integument forms a septum composed of layers of polymeric material (a composite of polymeric films), cuticular diffusion may tend to follow similar kinetics. Once steady state is established, this case may behave thereafter in a manner consistent with the kinetics described in case 1, i.e. a constant rate of penetration combined with first-order elimination. Of course, a constant penetration rate can be maintained only while the concentration gradient across the integument remains constant. As the concentration of internal material starts to approach that at the surface (this means, in practice, that the internal concentration reaches a few percent of the surface concentration), then the concentration gradient and hence the penetration rate will decrease progressively with time. Models assuming constant penetration rates are

valid only where the external insecticide saturates the surface of the cuticle so that external material will tend to stack molecule on molecule and at any fixed time only a proportion of the applied dose will be available for penetration. Once the condition is no longer fulfilled, penetration will become first-order and the kinetics of the original two compartment model will then be observed.

Discontinuities to the penetration curve are sometimes observed, particularly when the applied dose is large and results in intense symptoms of poisoning [18,20]. The discontinuity may be associated with a change in the internal capacity of the insect for insecticide as a result of a reduction in the volume of haemolymph as poisoning proceeds [8,9,20,21]. Discontinuities are absent when sub-lethal doses of insecticides, which do not result in water loss, are applied.

Distribution

A contact insecticide which has diffused across the insect integument is available for transport by the haemolymph, a mobile tissue with a high capacity for insecticides, including both polar and non-polar materials. Non-polar materials with high octanol/water partition coefficients bind to haemolymph transport proteins or partition into suspended lipids and are delivered to tissues throughout the insect body by haemolymph circulation. Insect circulation times are short, typically a few minutes [22], and hence this phase of distribution is rapid. The organs and tissues bathed by the haemolymph comprise separate, identifiable compartments within the insect into which insecticide can move from the haemolymph. The size of these compartments can be measured by their weight. Averaged compartment weights for 200 mg larvae of S. littoralis are presented in Table 1.

The nerve cord forms a minor compartment (0.7%) in which the level of insecticide should be buffered by the circulating haemolymph, which forms a major compartment (31%) in lepidopterous larvae.

The relationship between the applied dose, uptake by the CNS, and biological response
The relationship between the applied dose and the uptake of insecticide by the nervous system is of crucial importance in establishing the role of pharmacokinetics in the action of neurotoxicants. This relationship has been investigated for pyrethroids applied topically to a variety of insect species [10,20]. In one study undertaken in this laboratory, leafworms (200 mg) were treated with cypermethrin at doses corresponding to an LD_{10}, an LD_{50}, and an LD_{90}. After 24 h, when tissue levels should have equilibrated, larvae were washed twice in hexane to remove superficial insecticide and killed. The nerve cords were quickly removed by dissection, placed in acetone (60 μl) and extracted by partition of insecticide into the organic solvent. The recoveries of cypermethrin from the nerve cord are presented in Table 2.

TABLE 1 Mean weights of tissues and organs dissected from 200 mg larvae of *Spodoptera littoralis*

	Gut content	Gut wall	Cuticle	Fat-body	Haemo-lymph	Nerve cord
Weight (mg)	56	16	33	30	62	1.4
Fraction	0.28	0.08	0.17	0.15	0.31	0.007

TABLE 2   Mean recoveries ($n = 2$) of cypermethrin from the nerve cord of larvae (200 mg) of *Spodoptera littoralis* 24 h after topical application of an LD_{90}, an LD_{50}, and an LD_{10} to the dorsal thorax in Sirius M180 mineral oil

	Applied dose (ng/larva)		
	LD_{90} 605	LD_{50} 146	LD_{10} 39.5
Mean recovery (ng/cord)	5.2	0.98	0.15
Nerve cord weight (mg)	1.4	1.4	1.4
Tissue conc. (μM)	8.7	1.6	0.25

For an approximately fifteen-fold change in applied dose (the ratio LD_{90}/LD_{10}), a 34-fold difference in the level of insecticide in the nerve cord was observed. At the higher dose, corresponding to an LD_{90}, 0.86% of the applied dose was recovered, in rough proportion to the ratio of nerve cord weight to insect body weight (0.70%). As the dose was lowered, the proportion of the applied dose recovered in the nerve cord fell to 0.38% for application of an LD_{10}. This reduced efficiency of delivery is not unexpected, since fewer sites of loss should be saturated at the lower dose. On average, the nerve cord of 200 mg larvae weighs 1.4 mg. Thus, the average molar concentration of cypermethrin (mol. wt. 427) in the nerve cord following application of an LD_{50} can be estimated as $0.98 \times 10^3/(1.4 \times 427) = 1.6$ μM. This is a surprisingly high concentration for such a potent neurotoxin. Of course, cypermethrin is unlikely to be distributed evenly throughout the nerve cord, but will decrease in concentration towards its centre so that the threshold for neurotoxic action which results in a median lethal response at end point is probably lower than this estimate.

Penetration to the target receptor
The rapid action of pyrethroids is facilitated by their delivery to the target tissue as a result of mass flow of haemolymph. The final delivery of toxicant to the receptor presumably occurs by diffusion from the haemolymph. Some years ago, we investigated the role of diffusion in the delivery of insecticide to target receptors within the CNS of the leech, *Hirudo medicinalis* [23]. We assumed as a first approximation that movement of pyrethroid into the ganglion to reach the nerve cell bodies from which neurotoxicological recordings were made can be modelled as diffusion into an infinite plane sheet [24]. Numerical methods were used to determine whether this model was appropriate for the description of the time–dose–response relationship observed for perfusion of deltamethrin applied to isolated leech ganglia. Combinations of bath concentrations and elapsed time which produce a fixed concentration of pyrethroid at a fixed distance into the ganglion were calculated for a wide range of bath concentrations of deltamethrin. The times at which pesticide was predicted to reach a threshold concentration at the site of neurotoxic action were in close agreement with times at which the onset of neurotoxin activity was observed [23]. This result demonstrates that diffusion can account for the uptake of insecticide by the target tissue and furthermore, that the concentration will fall with distance into the tissue. The results also suggest that before the onset of pyrethroid-induced depolarizations can occur, a deltamethrin concentration of approximately 4.2×10^{-11} M must be reached at a site 75 μm into the ganglion. This site corresponds to the boundary between the nerve cell bodies and the neuropile, where the cell bodies

attenuate to produce axons of much smaller diameter. The axonal membrane in this region is characterized by a high density of cation channels; it represents the most likely site for the generation of action potentials, and is claimed to be particularly sensitive to pyrethroid action [25].

Binding

The role of binding to the insect cuticle has already been discussed in relation to the availability of insecticide for transport to the receptor. Other tissues may bind insecticide, further reducing the probability of arrival at receptors within the target tissue, usually the nervous system. Binding studies, carried out at Portsmouth and based on exhaustive soxhlet extraction of cypermethrin from treated armyworms sampled at various times after dosing, suggest two phases of binding (Fig. 4); an initial phase occurring immediately the insect has contacted the insecticide, and a slower phase which can reach a maximum many hours after dosing [26]. The initial phase of binding can be very rapid, reaching a maximum within seconds of topical application of insecticide [1,18], and must therefore involve binding to components of the cuticle. The second, slower phase occurs after material has penetrated the integument to become distributed throughout the insect body. During this slow phase, binding occurs at a constant rate (Fig. 4), consistent with the steady internal concentration indicated by the pharmacokinetic profiles shown earlier (Fig. 2). Binding is slow, but over a prolonged period can account for a significant proportion of the applied insecticide.
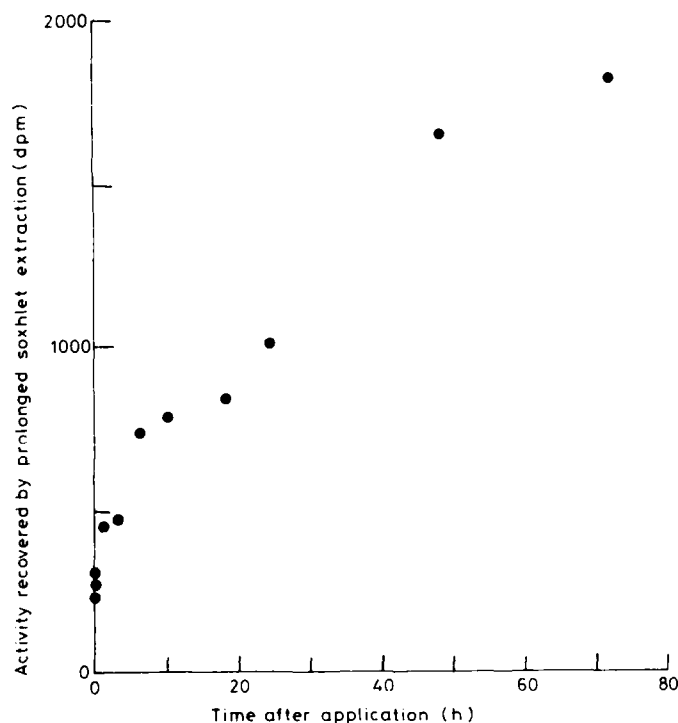
FIG 4   The bound fraction of cypermethrin removed by exhaustive soxhlet extraction of *Spodoptera littoralis* Boisd. larval solids.

518
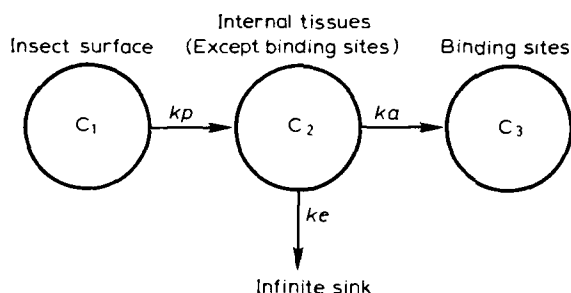
FIG 5 A three-compartment pharmacokinetic model to describe the changes of insecticide levels in insects with time. M_1, M_2 and M_3 are the masses of insecticide in C_1, C_2 and C_3 respectively; $\lambda_1 = M_2/M_1$, and $\lambda_2 = M_3/M_2$ when $k_e = 0$ and t. Equations:
(1) $dM_1/dt = -kp(\lambda_1 M_1 - M_2)$
(2) $dM_2/dt = kp(\lambda_1 M_1 - M_2) - keM_2 - k_a(\lambda_2 M_2 - M_3)$
(3) $dM_3/dt = ka(\lambda_2 M_2 - M_3)$

Binding can modify the form of the pharmacokinetic profiles which describe the exposure of internal tissues to insecticide, with potentially important consequences for selective toxicity. In a recent study of the pharmacokinetics of substituted benzyl ($^3R,1RS$)-cyclopropane-1-carboxylates, we observed that the two compartment model [7] was inappropriate for the data for some compounds, particularly when long elapsed times (up to 240 h) were investigated. These inappropriate profiles were characterized by movement of material from the external surface without an equivalent accumulation in the internal extract. The form of the profiles, however, were inconsistent with rapid elimination, since significant levels of insecticide could be recovered in the internal extracts at these long times after application [1]. Binding of toxicant to the cuticle and other tissues might have been responsible. Provisional results already reported [1,26] suggest that a fairly tight, but reversible binding of material to insect tissues was indeed occurring. It was decided to simulate this process using a three compartment model (Fig. 5). This required the introduction of two new parameters: (1) k_a, the first order rate constant for binding, (2) λ, a distribution coefficient relating the capacities of the compartments C_2 (containing the free pool of insecticide) and C_3 (the sites of binding). On integration with respect to time, the rate equations give rise to three equations based on the sum of three exponential terms. The constants which define the sizes of the compartments and the exponents describing transfer between, accumulation in, and decay from the compartments, are complex functions of the five parameters, k_p, k_e, k_a, λ_1 and λ_2. A much wider range of pharmacokinetic profiles can be obtained from this model than from the earlier two compartment model. Some of these profiles are consistent with observed data for the penetration and accumulation of pyrethroid insecticides in insects, observed over long periods of time [1]. The form of the gross internal pharmacokinetic profile (TotIn) for cypermethrin applied to leafworms (Fig. 2), for example, is predicted by the three compartment model.

Metabolism

Metabolic detoxification is well established as a process by which insecticide is lost from an organism following administration. Most studies involving metabolic degradation of insecticide have been carried out under standard in vitro conditions

whereby insecticide is incubated with enzyme extracts prepared following homogenization of living organisms or tissue. Such studies are often required by registration bodies who wish to identify potential metabolic products prior to the commercial release of a compound. The relevance of such studies to explain insecticide metabolism under in vivo conditions has proved difficult to establish, however, and in spite of fairly extensive studies, it is probably fair to conclude that our understanding of the role of in vivo detoxification of insecticides by insect species as a source of loss is extremely patchy. In spite of the difficulties, however, some progress has been made.

The assumption of first-order elimination of penetrated material is consistent with much of the published data describing in vivo metabolism of drugs and pesticides [27–29]. First order implies that during in vivo metabolism the enzymes involved in the various pathways of degradation must each encounter the same effective concentration of insecticide;

$$\mathrm{d} M_2 / \mathrm{d} t = -k_{e1} M_2 - k_{e2} M_2 - \cdots - k_{ez} M_2$$

$$= M_2 - (k_{e1} + k_{e2} + \cdots k_{ez})$$

First order also implies that the mechanism of detoxification remains unaffected by the poisoning process, and this may not always be so. If the various first order elimination processes operate on different concentrations of insecticide (e.g. they may be located within the insect in different compartments, each with different affinities for the insecticide), more complex pharmacokinetic profiles based upon the sum of several exponential processes will be observed.

Summed exponential degradation will also be observed if different enzymes, acting on the same substrate, are present at different times. An interesting example of this phenomena has been reported by Devonshire [30]. In a study of acetylcholinesterase present in organophosphate resistant (strain arD) and susceptible (strain 608) houseflies, two enzyme extracts were prepared from R and S strains and assayed separately and as a mixture (arD : 608 in an approximate 1 : 2 ratio). In the mixture, the enzymes behaved independently and two phases of inhibition were observed, with rate constants consistent with those of the individual enzymes assayed independently. Moreover, the constants representing the intercept for each cholinesterase hydrolysis matched the 2 : 1 ratio of enzyme titre used in the mixed assay.

Our understanding of the molecular features associated with rapid degradation of xenobiotics by organisms is poor, and the establishment of overall principles has proved difficult. A recently published study of xenobiotic degradation by microorganisms present in sewage sludge, however, has suggested that the rate of biodegradation is closely related to the modulus of the atomic charge across one specific bond in a given class of compound [31]. Moreover, the results obtained for different classes of compound, based on different chemical bonds, can be combined in a single regression equation, suggesting that charge difference across a bond is a fundamental property controlling xenobiotic biodegradation. In any particular species or class of molecule, the critical bond whose fission determines the rate of degradation may prove to be that with the largest charge difference. A similar approach was taken by Briggs [32] who proposed a method for the prediction of soil persistence based in part on the lability of the most unstable bond in a pesticide. in his paper, susceptibility to microbiological degradation was classified for different

substituents and functional groups in terms of their chemical reactivities. The general approach adopted by these two groups of workers is interesting, and should lead to progress in our understanding of how chemical structure influences the degradability of organic materials exposed to living systems. However, a word of caution is necessary. Detoxification of drugs and pesticides can occur as a result of both chemical and enzymatic modes of degradation and the activation energies which determine the rates of degradation will differ, depending whether the attack on the substrate is catalytic or non-catalytic; the class of chemical bond most susceptible to a particular mode may also vary. A comprehensive theory must allow for such considerations.

Elimination

Unchanged insecticide and metabolites may be removed from the insect body by excretion. In insects, excretory products are eliminated from the haemolymph into the urine, passing from the Malpighian tubules, into the hind gut and out of the body with the frass via the anus. In many insect species, including adult Diptera and Lepidopterous larvae, insecticide accumulates in the gut contents where it is degraded and eliminated from the anterior region of the gut in regurgitated fluid. Studies with 200 mg caterpillars of *Spodoptera littoralis* Boisd. treated topically with ^{14}C-labelled cypermethrin regurgitate their gut contents soon after symptoms of incoordination appear. The regurgitant contains high levels of unidentified label, which is not cypermethrin but presumably metabolites, since very little of the
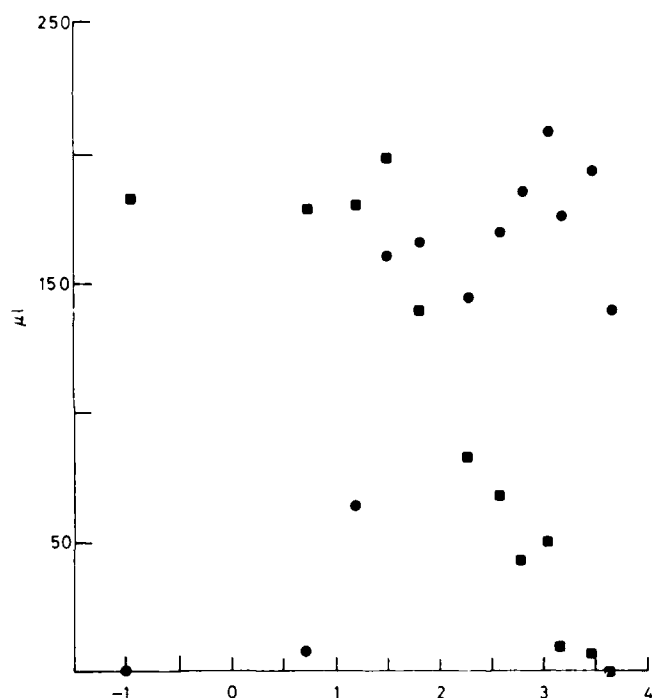
FIG 6   Changes in the volumes of regurgitated gut content (●) and haemolymph (■) following topical application of cypermethrin (LD_{50}/larva) to *Spodoptera littoralis* Boisd.

material co-chromatographs with authentic standard. Regurgitation (Fig. 6) continues until all the gut fluid has been emitted. Once regurgitation is complete, the volume of haemolymph, which until then has remained unchanged, decreases until no further lymph can be harvested from the haemocoel.

In a second experiment using unlabelled cypermethrin, the distribution and fate of the insecticide throughout a variety of tissues and extracts was investigated at different elapsed times. Cypermethrin accumulates rapidly in internal tissues, but to low levels which were maintained thereafter. In contrast, insecticide accumulated steadily in the gut contents to reach a peak after 6 h. At this time, the average mass of insecticide recovered from the gut contents was twice as high as that recovered from the gut wall. Cypermethrin was subsequently lost as the net rate of elimination outstripped the rate of uptake in the gut lumen. It is not clear whether this loss is a result of detoxification, binding to solids in the lumen, or elimination in frass. Similar tissue levels were observed in equivalent experiments with labelled and unlabelled cypermethrin, demonstrating quite clearly that very little cypermethrin was being metabolized in vivo. These important results suggests that, in leafworms at least, penetrated cypermethrin is eliminated primarily from the gut contents, with no significant in vivo loss of insecticide from the tissues.

Pharmacodynamics

Once insecticide has accumulated at critical sites within the target tissue, it will bind to the receptor. Receptor binding is usually expressed by plotting the bound fraction as a function of the concentration of drug or insecticide perfusing the receptor or target tissue (plot 1, Fig. 7). Pharmacologists frequently employ an analogous function relating the intensity of biological response to insecticide concentration (plot 2, Fig. 7). Many examples of these plots may be found in accompanying papers in this volume. The strength of ligand binding to a receptor, i.e. the affinity of the ligand, may be expressed as the reciprocal of the molar concentration
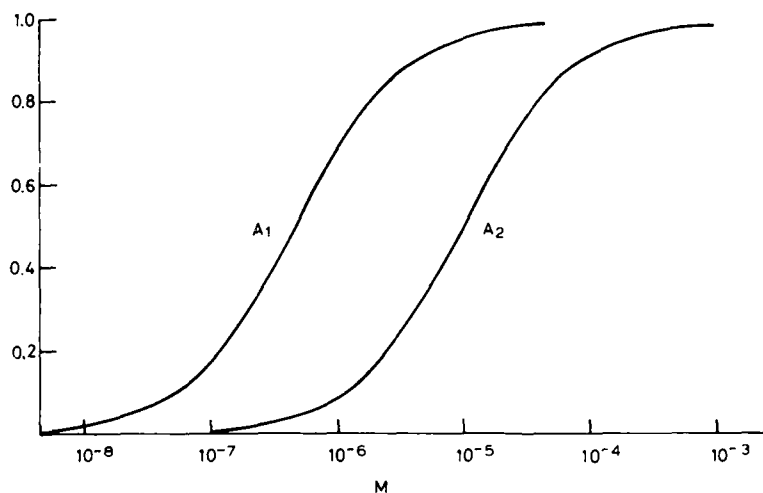
FIG 7 Binding/response curves describing pharmacodynamic affinity/potency. Plot 1 ordinate is fraction bound; plot 2 ordinate is proportion of maximal response.

required for either 50% occupation (plot 1) or 50% response (plot 2). The kinetics of drug binding have been extensively reviewed [33,34], and the reader is referred to the cited texts for further details. The strength of binding will depend on both the number and strength of the atom pair interactions which take place between the insecticide ligand and the receptor. Ligand/receptor interactions usually involve weak bonds with energies of the order of two to thirty kJ per mol. The distances over which these atom pair interactions operate will depend on the bond type, but the closer the ligand approaches the receptor, the stronger any interaction will become. The change in interaction energy depends on some power of the distance between the pairs of molecular features which contribute to binding. Binding strength is increased in proportion to the number of interactions [34].

In contrast to the relatively weak, non-specific binding involved in the retention of insecticide by non-target tissues, binding to target receptors is specific and can occur at very low concentrations of ligand. Irving [13], for example, observed pyrethroid induced miniature excitatory postsynaptic potentials (mepps) in dissected longitudinal muscle fibres of Diabrotica balteata at insecticide bath concentrations as low as 10^{-18} M. This result implies structural complementarity of the insecticide and receptor molecules, such that a very close approach of the ligand to the receptor is possible, accompanied by an increase in the binding forces operating between the two molecular species. Large differences in the affinity for a receptor can occur between insecticides of the same class, and apparently for the same compound tested against different strains [35,36] or species [3] of insect. Such differences may depend not only on the properties of the receptor, but also on the nature of the membrane environment in which the receptor is located [37,38]. Factors which decrease the strength of receptor binding will result in a matching increase in the critical exposure necessary to elicit a biological response.

The relationship between the strength of binding and the intensity of the biological response will be an important determinant of the toxicity of an insecticide. During the docking process, the strength of the local electrostatic field will be modified and the distribution of electrons associated with the ligand and receptor will be perturbed. Furthermore, the energy levels of the frontier electron orbitals (HOMO and LUMO) will change as they become distorted in response to the modified electrostatic field [34]. These changes will control not only events such as gating of ion channels [39], but are likely to modify the final binding strength between the ligand and the receptor. In a recent study, the strength of ligand binding to a calcium channel was found to change by approximately 100-fold as the channel switched between open and closed states [40].

Binding to a receptor will only result in a biological response if the receptor perturbation which accompanies binding can signal a cellular response. This important topic has been reviewed earlier in this volume [6]. Modified cation channel conductance is a very common cellular response to both drugs and insecticides. Synthetic pyrethroids, lipid amides and DDT analogues are all known to change the kinetics of sodium conductance in insect nerve membranes. Characteristic burst discharges of action potentials are produced in nerve preparations exposed to these groups of insecticide. It has been suggested that this repetitive activity is due to the slow decay of the sodium tail current observed in treated neurones. Pyrethroid induced bursting behaviour, however, is now known to be uncorrelated to responses such as the time to nerve block which are characteristic of changes in the properties of the sodium channel [41].

It is difficult to understand how the variety of patterns of repeated bursting observed following exposure of neurones to pyrethroids [42] can arise from the Hodgkin Huxley (H-H) equations without invoking a second cation, calcium, to act as a pacemaker. In their original form the H-H equations will not simulate the type of bursting induced by insecticides, where repeated volleys of spikes appear on the crest of a slower depolarizing wave. Work undertaken by Plant and his colleagues in the United States [43], and Honerkamp and his colleagues in Germany [44] have proposed and developed a general mechanism for cell bursting. The mechanism can be modelled by six coupled differential equations derived from the H-H model. This model gives rise to bursting as a result of interaction between a fast oscillator involving conductance of sodium and potassium ions across the membrane (the action potential) and a slow oscillator, involving calcium conductance. The frequency and size of the simulated slow depolarizations which give rise to bursts of APs, and the frequency and number of action potentials in a burst, are determined by the sodium, potassium and calcium conductances. Any neurotoxic compound which can modify the balance between these cation conductances in an appropriate manner will induce abnormal bursting behaviour.

The simulated bursts of action potential show striking resemblance to the repetitive discharges observed with DDT and type I pyrethroids. Recent reports from our laboratory [45], and those of Osborne [46], Mansour [47] and Narahashi [48,49], suggest that, in addition to effects on sodium conductance, the actions of pyrethroid insecticides also involve modification of calcium conductance. Patch clamp studies have suggested that pyrethroids which induce type I response, e.g. tetramethrin, diminish the conductance of the Ca^{2+} channel in a time dependent manner which eventually leads to channel block; pyrethroids, e.g. deltamethrin and fenvalerate, which induce type II response had no effect on Ca^{2+} conductance during 30 min exposure [49]. A BASIC computer program has been developed at Portsmouth to simulate the model of Honerkamp et al. [44]. We are evaluating the model so that we become familiar with its properties prior to investigating its use as a tool to study pyrethroid and DDT action on nervous systems. Our provisional results suggest that only by changing the conductance of nerve membranes to both sodium and calcium ions, can the wide range of burst discharges produced by type I pyrethroids be simulated. We are intrigued to know whether type II activity, which does not include the pyrethroid bursting response, can also be reproduced.

Conclusions

This review has attempted to identify some of the pharmacokinetic and pharmacodynamic factors which modify the potency of insecticides and which may, as a result, lead to differences in the susceptibility to insecticides of individuals, strains and species. Gross changes in the susceptibility of strains and species result, respectively, in the development of resistance to insecticides and in selective toxicity. A change in the strength of binding at the site of action is probably the major cause of the large differences in insecticidal potency observed both within and between species. In one study [13], the variation in the in vivo toxicity of highly potent pyrethroid insecticides can be explained almost entirely in terms of differences in neurotoxicological potency (Fig. 8). In this example, 94% of the $logLD_{50}$
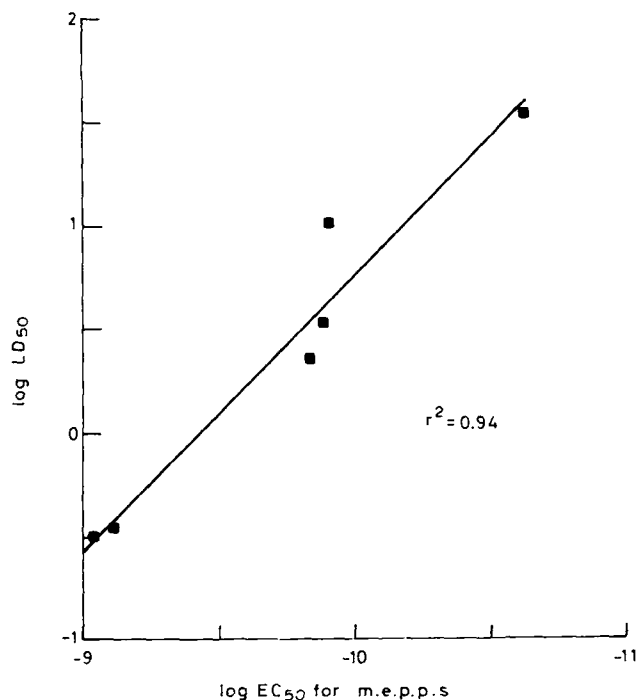
FIG 8 Relationship between the in vivo toxicity and neurotoxicity of six pyrethroid insecticides applied to larvae of *Heliothis virescens* (Irving, 1984).

is explained by the $logEC_{50}$ for pyrethroid induced miniature excitatory potentials. Furthermore, the neurotoxicological potency of the compounds to four insect species varied by a factor of nearly 10^6.

Changes in the strength of receptor binding will modify the critical integrals necessary for a standard biological response, and hence modify the applied dose of insecticide necessary to achieve a critical exposure of receptor to insecticide. However, variation in pharmacokinetic processes can also lead to significant changes in susceptibility to insecticides. The processes of insecticide delivery and loss will vary with compound, individual, strain and species, as indicated by our studies of pyrethroid action, to result in changes in the internal exposure of the receptor to the insecticide. In the study of the weakly toxic methylbenzyl chrysanthemates topically applied to adult mustard beetles [11], 84% of the variation in relative molar toxicity could be explained by changes in the resistance to elimination $(1/k_e)$. Thus, the relative importance of pharmacodynamics and pharmacokinetics in determining selective toxicity will vary from case to case.

In the search for novel insecticides of even greater potency, no amount of structural optimization aimed solely at improving the pharmacokinetics of a candidate material with only weak pharmacodynamic activity will be worthwhile. Research aimed at improving the delivery to the target of a candidate insecticide with high pharmacodynamic activity, but inappropriate pharmacokinetic properties, however, is a more sensible strategy to adopt.

Acknowledgements

References

1 Szydlo, R.M. (1987) An investigation of the pharmacokinetics of pyrethroid insecticides in the adult mustard beetle *Phaedon cochleariae* Fab., PhD Thesis, CNAA.

2 Sawicki, R.M. (1987) Definition, detection and documentation of insecticide resistance. In: Combating Resistance to Xenobiotics (M.G. Ford, D.W. Hollomon, B.P.S. Khambay, R.M. Sawicki, eds.) pp. 105–117. Ellis Horwood Series in Biomedicine, Verlag Chemie.

3 Hill, I.R. (1985) Effects on non-target organisms in terrestrial and aquatic environments. In: The Pyrethroid Insecticides (J.P. Leahey, ed). pp. 151–262.

4 Hollingworth, R.M. (1976) The biochemical and physiological basis of selective toxicity. In: Insecticide Biochemistry and Physiology, (C.F. Wilkinson, ed.) pp. 431–506. Heyden.

5 Ruscoe, C.N.E. (1987) The attitude and role of the agrochemical industry towards pesticide research. In: Combating Resistance to Xenobiotics, (M.G. Ford, D.W. Hollomon, B.P.S. Khambay, R.M. Sawicki, eds.) pp. 26–37. Ellis Horwood Series in Biomedicine, Verlag Chemie.

6 Evans, P.D., Swales, L.S. and Whim, M.D. (1988) Second messenger systems in insects: an introduction. Neurotox '88, Molecular Basis of Drug and Pesticide Action (Lunt, G.G., ed.) pp. 225–234, this volume.

7 Ford, M.G., Greenwood, R. and Thomas, P.J. (1981) The kinetics of insecticide action. Part 1: the properties of a mathematical model describing insect pharmacokinetics. Pestic. Sci. 12, 175–198.

8 Soderlund, D.M., Hessney, C.W. and Helmuth, D.W. (1983) Pharmacokinetics of *cis* and *trans*-substituted pyrethroids in the american cockroach. Pestic. Biochem. Physiol. 20, 161–168.

9 Soderlund, D.M. (1980) Pharmacokinetic modifications of intrinsic insecticide activity. In: Insect Neurobiology and Pesticide Action (Neurotox '79). pp. 449–456. Society of Chemical Industry.

10 Soderlund, D.M. (1979) Pharmacokinetics behaviour of enantiomeric pyrethroid esters in the cockroach, *Periplaneta americana* L. Pestic. Biochem. Physiol. 12, 38–48.

11 Ford, M.G., Greenwood, R. and Thomas, P.J. (1981) The kinetics of insecticide action. Part 2. The relationship between the pharmacokinetics of substituted benzyl (1RS)-*cis-trans*-chrysanthemates and their relative toxicities to mustard beetles (*Phaedon cochleariae* Fab.) Pestic. Sci. 12, 265–284.

12 Salt, D.W. and Ford, M.G. (1982) The kinetics of insecticide action. Part 3. The use of stochastic modelling to investigate the pickup of insecticides from ULV treated surfaces by larvae of *Spodoptera littoralis* Boisd. Pestic. Sci. 15, 382–410.

13 Irving, S. (1984) in vitro activity of pyrethroids. British Crop Protection Conference: Pests and Diseases 3, 859–864.

14 Matsumura, F. (1963) The permeability of the cuticle of *Periplaneta americana* (L) to malathion. J. Insect Physiol. 9, 207–221.

526

15 Lord, K.A. (1948) The sorption of DDT and its analogues by chitin. Biochem. J. 43, 72–78.

16 Olsen, W.P. and O'Brien, R.D. (1963) The relation between physical properties and penetration of solutes into the cockroach cuticle. J. Insect Physiol. 9, 777–786.

17 O'Brien, R.D. (1967) Insecticides—Action and Metabolism. Academic Press.

18 Elliott, M., Ford, M.G. and Janes, N.F. (1970) Insecticidal activity of the pyrethrins and related compounds. III. penetration of pyrethroid insecticides into mustard beetles (Phaedon cochleariae). Pestic. Sci. 1, 220–223.

19 Cussler, E.L. (1984) Diffusion: Mass Transfer in Fluid Systems. pp. 525. Cambridge University Press.

20 Ford, M.G. (1972) Insecticidal Activity and Penetration into Insect of Pyrethroids. PhD Thesis, University of London.

21 Brealey, C.J. (1988) Pharmacokinetics of insecticides in insects. In: Neurotox '88, Molecular Basis of Drug and Pesticide Action (Lunt, G.G., ed.). pp. 529–541, this volume.

22 Gerolt, P. (1975) Role of haemolymph in translocation of insecticides. Pestic. Sci. 6, 233–238.

23 Leake, L.D., Buckley, D.S., Ford, M.G. and Salt, D.W. (1985) Comparative Effects of Pyrethroids on Neurones of Target and Non-target Organisms. Neurotoxicology 6, (2), 99–16.

24 Crank, J. (1975) The Mathematics of Diffusion. Clarendon Press.

25 Chalmers, A.E. (1983) An investigation into the mode of action of pyrethroid insecticides on the arthropod nervous system. Ph.D. Thesis, University of Birmingham.

26 Peace, E.A., Ford, M.G., Greenwood, R. and Salt, D.W. (1987) Binding Properties and Pharmacokinetics of Pyrethroids in Adult Mustard Beetles. In: QSAR in Drug Design and Toxicology, pp. 331–335. Proceedings of the 6th European Symposium on Quantitative Structure-Activity Relationships, Portorose, Yugoslavia.

27 Notari, R.E. (1971) Biopharmaceutics and Pharmacokinetics. Marcel Dekker, Inc. New York.

28 Gibaldi, M. and Perrier, D. (1975) Pharmacokinetics. In: Drugs and the Pharmaceutical Sciences (J. Swarbrick, ed.) p. 329. Marcel Dekker.

29 Rowland, M. and Tozer, T.N. (1980) Clinical Pharmacokinetics: Concepts and Applications. pp. 331. Lea and Febiger, Philadelphia.

30 Devonshire, A.L. (1975) Studies of the acetylcholinesterase from houseflies (Musca domestica L.) resistant and susceptible to organophosphorus insecticides. Biochem. J. 149, 463–469.

31 Dearden, J. and Nicholson, R.A. (1987) QSAR study of the biodegradability of environmental pollutants. In: QSAR in Drug Design and Toxicology (D. Hadzi, B. Jerman-Blazic, eds.), pp. 307–312. Elsevier.

32 Briggs, G.G. (1976) Degradation in Soils. Proceedings of the British Crop Protection Council meeting entitled Persistence of Insecticides and Herbicides.

33 van Rossum, J.M. (ed.) (1977) Kinetics of drug action. Handb. Exp. Pharm. 47, pp. 436. Springer-Verlag.

34 Dean, P.M. (1987) Molecular Foundations of Drug-Receptor Interaction. Cambridge University Press.

35 Sawicki, R.M. (1985) Resistance to pyrethroid insecticides in arthropods. In: Insecticides Vol. 5 (D.H. Hutson, T.R. Roberts, eds.) pp. 143–192.

36 Herve, J.J. (1982) Mode of action of pyrethroids and resistance to these compounds. In: Deltamethrin Monograph, pp. 67–108. Roussel Uclaf.

37 Chialiang, C. and Devonshire, A.L. (1982) Changes in membrane phospholipids, identified by Arrhenius plots of acetylcholinesterase and associated with pyrethroid resistance (kdr) in houseflies (Musca domestica). Pestic. Sci. 13, 156–160.

38 Lunt, G.G. (1985) The biochemistry of neuronal membranes. In: Neuropharmacology and Pesticide Action (M.G. Ford, G.G. Lunt, R.C. Reay, P.N.R. Usherwood, eds.), pp. 12–19. Ellis Horwood Series in Biomedicine, VG Publishers. 1985.

39 Edmonds, D.T. (1988) Electrostatic models of ion channels and pumps. Paper presented at a Society of Chemical Industry Symposium entitled Ion channels as drug targets, Royal College of Physicians, Regents Park, London, 27th April.

40 Triggle, D.J. (1988) Ligand interactions at the Ca^{2+} channel: a dual perspective. Paper presented at a Society of Chemical Industry Symposium entitled Ion channels as drug targets, Royal College of Physicians, Regents Park, London, 27th April.

41 Livingstone, D.J., Buckley, D.S. and Ford, M.G. (1988) A multivariate QSAR study of pyrethroid neurotoxicity based upon molecular parameters derived by computer chemistry. In: Neurotox '88, Molecular Basis of Drug and Pesticide Action (G.G. Lunt, ed.). pp. 483–495, this volume.

42 Leake, L.D. (1988) Patterns of pyrethroid-induced activity in an identified neurone. Pestic. Sci. in press.

43 Plant, R.E. and Kim, M. (1976) Mathematical description of a bursting pacemaker neurone by a modification of the Hodgkin-Huxley equations. Biophys. J. 16, 227–244.

44 Honerkamp, J., Mutschler, G. and Seitz, R. (1985) Coupling of a slow and a fast oscillator can generate bursting. Bull. Math. Biol. 47, 1–21.

45 Leake, L.D., Dean, J.A. and Ford, M.G. (1986) Pyrethroid action and cellular activity in invertebrate neurons. In: Neuropharmacology and Pesticide Action (M.G. Ford, G.G. Lunt, R.C. Reay, P.N.R. Usherwood, eds.), pp. 244–266. Ellis Horwood Series in Biomedicine, VG Publishers.

46 Osborne, M.P. (1980) Action of pyrethroids upon neurosecretory tissues in the stick insect *Carausius morosus*. In: Pyrethroid Insecticides: Chemistry and Action (J. Mathieu, ed.), pp. 18–21. Tables Ronde Roussel Uclaf. No. 37.

47 Mansour, N.A., Annau, Z., Valdes, J.J. and Shamoo, A.E. (1986) Reconstituted acetylcholine-receptor ionic channel complex in lipid bilayer as a target for toxic agents. Abstr. 6th Int. Congr. Pestic. Chem. IUPAC, 8B–06.

48 Narahashi, T. (1986) Mechanisms of action of pyrethroids on sodium and calcium channel gating. In: Neuropharmacology and Pesticide Action (M.G. Ford, G.G. Lunt, R.C. Reay, P.N.R. Usherwood, eds.). pp. 36–60. Ellis Horwood Series in Biomedicine, VG Publishers.

49 Narahashi, T. (1987) Neuronal target sites of insecticides. In: Sites of Action for Neurotoxin Pesticides (R.M. Hollingworth, M.B. Green, eds.), pp. 226–250. ACS Symposium Series 356.

CHAPTER 39

Pharmacokinetics of insecticides in insects

CLIVE J. BREALEY

Wellcome Research Laboratories, Ravens Lane, Berkhamsted, Herts. HP4 2DY, U.K.

Introduction

Pharmacokinetics in insects can be considered to include all the processes which occur between deposition of an insecticide on the surface of the cuticle (most commonly as a droplet) or in the gut (for a stomach poison) and its arrival at the target site macromolecule. For an insecticide this overall process is governed by considerations of spreading over and penetrating through the cuticle; distribution between internal tissues (dependent on solubility, binding and partition of the insecticide), and metabolism and excretion.

Pharmacokinetic studies are undertaken on insecticides to answer questions about resistance mechanisms, to assist in the design of new insecticides by determining the preferred physicochemical characteristics for activity in a particular species, or to investigate inter-species selectivity. In addition the insects form a large and diverse group of animals readily susceptible to genetic and chemical manipulation. Studies on genetics, growth and development and neurobiology have often been centred on insect systems; an understanding of the physiology and biochemistry of their responses to xenobiotics (e.g. the diversity of insect cytochrome *P*-450s) may contribute in a similar way.

Inferences about the penetration and metabolism of an insecticide are often made on the basis of experiments using different dosing routes, formulations and synergists. However quantitative measurements on the rates of penetration, routes of metabolism and concentrations at the target site or target tissue allow more detailed comparisons between strains, compounds and species. Examples of the different approaches to the use of pharmacokinetics in insects are discussed here; cuticle structure, penetration and distribution [1–3] and insecticide metabolism in insects [4,5] have been reviewed in detail elsewhere.

Pharmacokinetics of resistance mechanisms

The relative importance of pharmacokinetic and target site factors in determining an observed resistance phenotype can often be determined from simple comparisons between strains for external and internal amounts of parent insecticide. Resistance mechanisms in mosquitoes are difficult to examine in detail due to the small size of the insect, although neurophysiological studies have been done suggesting the
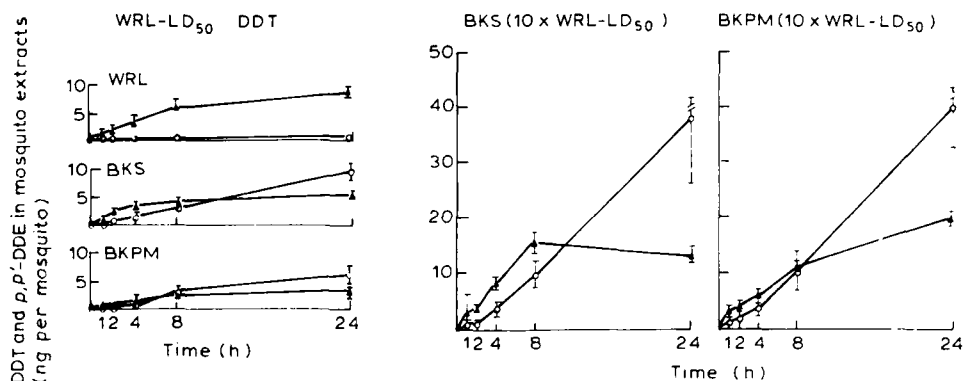
FIG 1   Comparison of internal amounts (mean ± S.D., *n* = 3 groups of 5) of DDT (△) and DDE (○) in whole mosquitoes previously washed in acetone: 1, 2 and 3 WRL, BKS and BKPM respectively at 15 ng DDT per mosquito, 4 and 5 BKS and BKPM respectively at 146 ng per mosquito.

presence of knockdown resistance (kdr) [6]. However the contribution of penetration and metabolism in the resistance to DDT and permethrin observed in the yellow fever mosquito (*Aedes aegypti*) has been examined following topical application to adults of measured doses of the two insecticides [7]. Factors of resistance were > 10 for DDT and > 100 for permethrin in the BKS (a DDT selected strain) and BKPM (a strain selected with permethrin from BKS). Measurement of penetration in all strains at the LD_{50} for the susceptible strain showed that penetration was first-order and there were no significant differences between strains. When the dose was increased penetration was not first-order suggesting saturation of the penetration process in some way. In the case of DDT metabolism at a low dose the susceptible strain produced very low levels of the dechlorinated metabolite DDE whereas both the resistant strains produced this as the major metabolite and were able to more than halve the internal concentration of DDT at 24 hours. Both these strains were almost completely resistant to DDT and when the dose was increased 10-fold the amounts of DDE produced rose dramatically so that the DDT level internally was maintained at a relatively low level compared to the increase in dose (Fig. 1). However this was still above the lethal internal level in the susceptible strain, strongly suggesting the presence of a target site insensitivity. This was confirmed by measurement of internal amounts of permethrin in the three strains. Again there was no marked difference in penetration and the internal amount of permethrin lethal to the susceptible strain was measured. The same dose in the susceptible strain gave rise to similar internal levels of permethrin indicating an absence of a substantial metabolic (oxidative) resistance factor. This again suggested a target site insensitivity and when the dose was increased 100-fold over the susceptible LD_{50}, internal levels rose by 17- and 34-times respectively for BKS and BKPM. Even these large rises in internal permethrin failed to kill all the mosquitoes.

This pharmacokinetic study demonstrated that DDT resistance was due to a combination of DDT-dehydrochlorinase and another factor, probably target site insensitivity, whereas permethrin resistance was entirely due to the latter. Moreover it highlighted the very high metabolic capacity of the dehydrochlorinase

system—greater than that of the oxidative mechanisms even at very high internal substrate concentrations, and the capability of a modification of target site sensitivity to confer large factors of resistance.

Pharmacokinetics in insecticide design

Pharmacokinetic studies can contribute to the design of new insecticides. Insecticidal lipid amides are found as natural products of the black pepper plant (*Piper nigrum*). Synthetic analogues of the natural products show promise as novel control agents against public health pests, having the properties of knock-down and activity against *kdr* resistant strains. Two analogues of these natural products (I and II, Fig. 2) were found to penetrate rapidly into flies, consistent with their knockdown properties [8]. The penetration curves were similar for both compounds, but I achieved a 3-fold greater peak internal concentration than II. Analysis by HPLC of extracts of the acetone-washed whole flies (at 2 h) showed a more complex pattern of metabolites for II than I. The routes of metabolism of these insecticides were described in part by co-chromatography of primary metabolites in the insect with those produced by oxidation in rat liver microsomes and identified using thermal
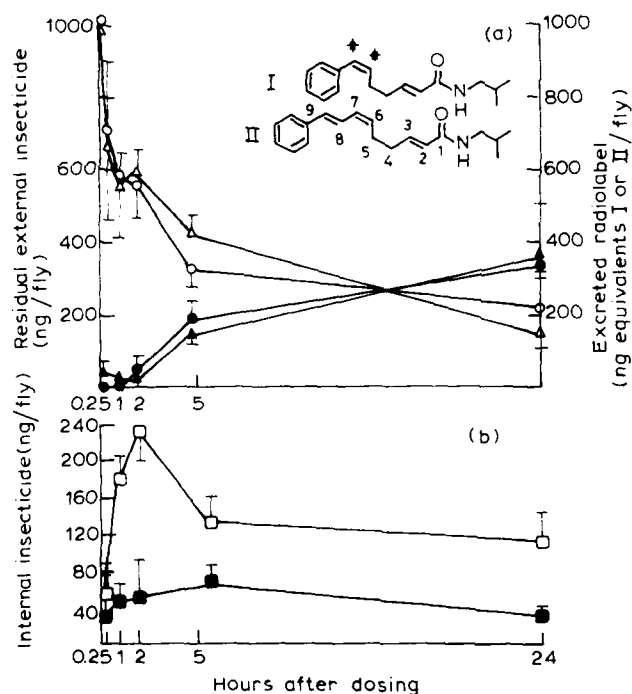
FIG 2 Penetration and excretion (a), and internal amounts (b) of insecticide in houseflies following dosing with ^{3}H-I and ^{3}H-II at 1 μg/fly. Penetration curves show amounts of parent insecticide analysed by HPLC (I○, II△) as do curves for internal insecticide (I●, II▲). Excretion was determined as total radiolabel in storage vials corrected for parent insecticide rubbed off flies at 15 min (I□, II■). All values are mean ± S.E. of three groups of five flies. The position of radiolabelling is indicated by * (redrawn from Ref. 8).

532
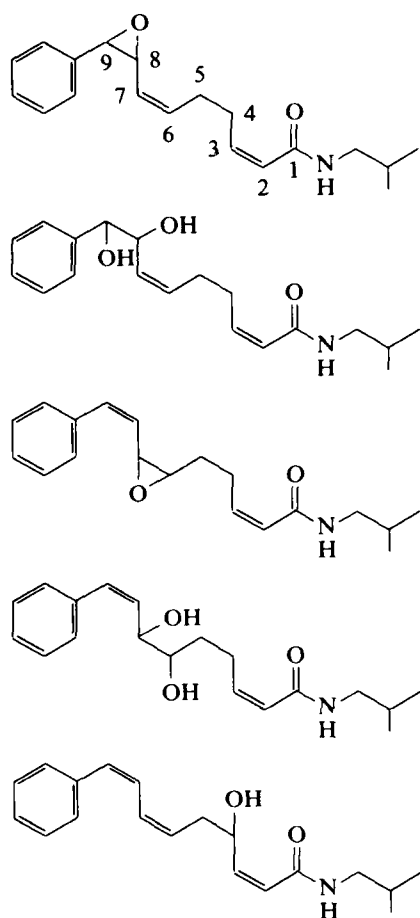
FIG 3   Metabolites of the lipid amide (II) produced by oxidation in rat liver microsomes in vitro, identified by mass spectrometry and NMR.

desorption chemical ionization mass spectrometry and 360 MZ H-NMR. In rat liver microsomes major metabolites were produced by epoxidation of either the 6,7- or 8,9-double bonds of II, hydration of these epoxides to diols and also aliphatic hydroxylation, principally at C4 (Fig. 3). There was no evidence for 2,3-epoxidation or N-dealkylation. The patterns of metabolites for I and II in houseflies (with corresponding metabolites for II indicated) are shown in Fig. 4. The introduction of extra unsaturation (not conjugated with the amide) clearly leads to substantially greater metabolism via epoxidation and at aliphatic carbon centres. In fact, although II achieves a much lower internal whole body concentration than I, it is more toxic to the housefly showing that high target site potency can more than compensate for a pharmacokinetic deficiency. Later developments of the lipid amides have replaced the labile phenyl-diene system with benzyloxy [9] and phenoxy [10] residues to confer enhanced metabolic stability and retain (or enhance) target site potency.
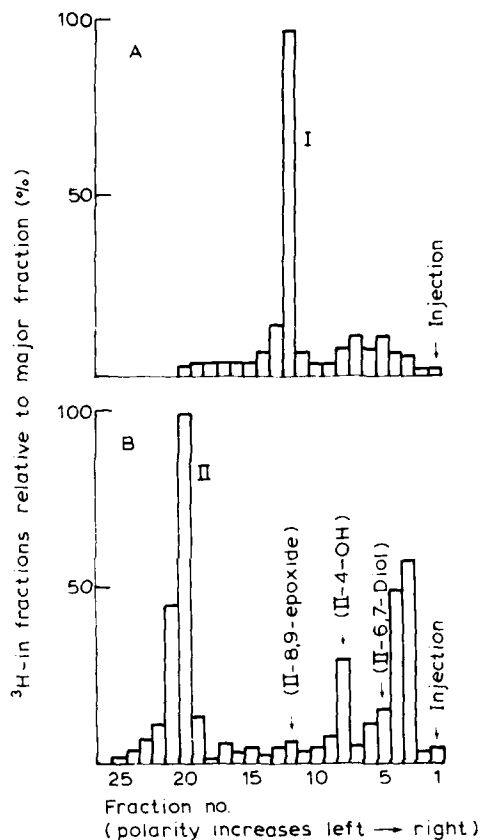
FIG 4 HPLC of ^{3}H-I (A) or ^{3}H-II (B) and labelled metabolites in whole extracts of washed flies. Compounds were separated by HPLC on 10 cm × 4.5 mm i.d. ODS-Hypersol 1 ml/min, 50% (v/v) acetonitrile/water. 3.7 nCi ^{3}H was applied in each case and column recoveries were > 95%.

Direct comparisons such as the above of a limited number of strains or compounds are useful. However when a large range of chemical structures is to be investigated, as in the optimization of insecticidal activity of a chemical series, a simpler approach to insecticide pharmacokinetics is desirable. Measurements of penetration rates from simple 'wash-off' experiments have been criticized [11] as often being susceptible to poor controls and oversimplifying the penetration process. However when supported by other measurements, particularly of haemolymph concentrations, insights may be gained into factors affecting pesticide action. Following dosing by topical application insects are readily rinsed in an organic solvent and the solvent analysed. A standard procedure of washing in 2 ml acetone for 30 s is used in all the studies reported here.

Fig. 5 shows typical data for exterior insecticide washed off houseflies under the standard conditions listed above. A lipid amide (III) penetrated very rapidly with the penetration rate approximating closely to first-order over a 24-h period during which time almost the whole dose was lost from the surface. This compound

534

Time (h)
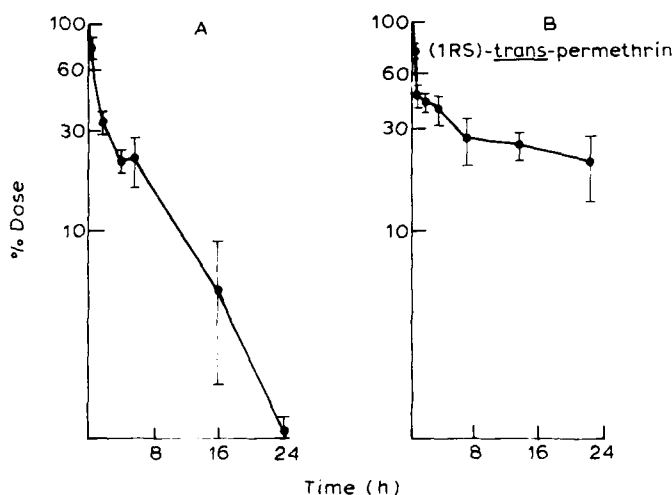
FIG 5 Insecticide washed off the exterior of flies by immersion in 2 ml acetone for 30 s
following a topical sublethal dose of (A) 0.1 μg of a lipid amide (III) and (B) 0.04 μg l(RS)
trans-permethrin applied in 0.4 μl 2-ethoxyethanol. The surface losses measured are attributable to penetration since there was no significant rubbing off of compound in the holding vial
or loss by evaporation in these experiments.

displays knockdown action and acts at the sodium channel in the insect nervous
system at low concentrations. In contrast permethrin, which is a relatively poor
knockdown insecticide, displays non-first-order kinetics over 24 h typical of many
pyrethroids [12]: the penetration process in this case can be represented by two
first-order processes with different rate constants at early and late times. While the
different knockdown characteristics of certain pyrethroids have been attributed to
differences in their neurotoxic properties [13] pharmacokinetics may have an
influence. This is not readily apparent from wash-off data however: for the
compounds in Fig. 5 there is little difference between the amounts penetrated at
early times when knockdown is manifested. These losses from the acetone-washable
phase of the cuticle may represent penetration into deeper, more hydrophilic regions
of the cuticle rather than into the haemolymph and other tissues. This would suggest
that only compounds with properties conferring rapid distribution are able to
achieve knockdown. Difficulties encountered in proving the link between rapid
haemolymph transport and knockdown have been discussed previously by Burt and
co-workers [14].

Mathematical models in pharmacokinetics—the implications of toxic effects

Computer models based on the distribution with time of a given mass of insecticide
between two compartments have been developed by Ford et al. [15]. In these models
the first compartment corresponds to the mass of insecticide washable from the
surface by a given organic solvent: the nature of this compartment will vary
depending on the polarity of the washing solvent and vigour of the washing
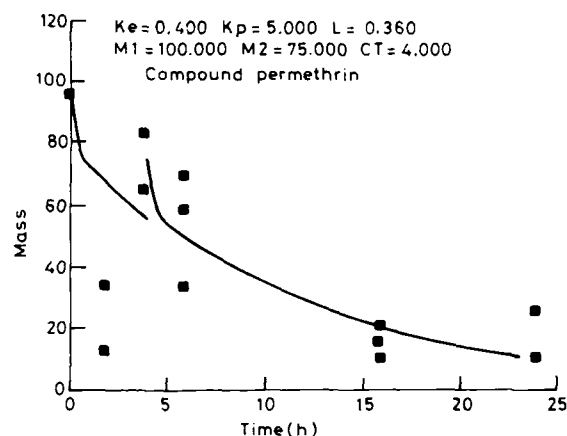
FIG 6 A typical discontinuous loss of insecticide from the surface of an insect. Third instar *Spodoptera littoralis* larvae were dosed topically with 0.1 μg (1*RS*) *trans*-permethrin and washed in acetone. Washed whole bodies were extracted in acetonitrile. All samples were transferred to *n*-hexane for GC-ECD analysis.

procedure. The second compartment is represented by the remaining whole body after washing. Again simple models have been criticized [5,11] on the grounds that they take no account of specific tissue interactions and reverse movements through the cuticle. Nevertheless they do generate curves which fit data well and can be tested rigorously by statistical methods. One failing is that few models take account of the toxic action of an insecticide on the insect.

Inspection of the penetration curves in Figs. 2 and 5 shows a transient decrease in the rate of insecticide penetration or even an increase in the external material for a short period. These discontinuities in an otherwise smooth penetration process, albeit one of changing rate, are often associated with the onset of the severe toxic symptoms of a compound, and necessitate a modification to a simple 2-compartment model.

Fig. 6 shows a marked discontinuity in the external amount of permethrin in 3rd instar larvae of Egyptian cotton-leafworm (*Spodoptera littoralis*) dosed topically with 0.1 μg (1*RS*)-*trans* permethrin and washed in acetone at times up to 24 h. At the time at which there is a sharp rise in the external permethrin level all the larvae were severely affected showing uncoordinated writhing movements. Observation of housefly adults and larvae of the cotton-leafworm during this phase of poisoning shows them to exude copious amounts of fluid almost exclusively by regurgitation of gut contents via the mouth parts. This confirms an earlier observation by Holden [16] that accurate measurement of cuticular penetration of permethrin and cyper-methrin in the Egyptian cotton-leafworm proved extremely difficult because of the effect of the pyrethroids in stimulating loss of water from the surface, together with the regurgitation of the gut contents, which were subsequently transferred to the body surface. In the case of flies this regurgitant is a clear fluid, but in the lepidopteran larva it contains partially digested diet. The storage pots of such insects often appear wetted by these fluids. It is well known that the toxicity of insecticides causes fluid loss and in some insects this is by diuresis e.g. in the bug

Rhodnius [17] and the cockroach [18]. An alternative means of fluid loss by regurgitation from the crop has been reported for the locust (*Schistocerca gregaria*) [19].

This redistribution to the exterior of insecticide which has penetrated into the insect might be explained by two mechanisms which are not mutually exclusive. Firstly loss of dilute fluid from the gut may be followed by increased flow of water into the gut from haemolymph causing the almost complete removal of freely removable haemolymph commonly observed in poisoned insects. This may lead to concentration of insecticides in the haemolymph, reversal of the concentration gradient across the cuticle and back-diffusion of insecticide. Secondly, insecticide may simply be passed to the outside dissolved in the regurgitant.

The latter mechanism was tested by collecting the regurgitated fluid from the mouth parts of 5th instar *Spodoptera littoralis* larvae after poisoning of the insects with 50 μg [^{3}H](1RS)-*trans* permethrin (= 0.64 μCi) applied topically. The larvae were restrained by being fixed with cyanoacrylate adhesive to a glass rod so that the mouthparts were prevented from contacting the dosing site on the posterior dorsal surface of the abdomen. About 10 min after dosing, larvae typically regurgitated approximately 50 μl of fluid which was collected in a glass capillary. Scintillation counting of fractions from reverse phase HPLC analysis of this fluid (following precipitation of protein with an equal volume of acetonitrile) showed it to contain parent insecticide (about 85%) and 15% polar materials, presumed to be metabolites. A separate experiment showed permethrin was stable for 3 h when incubated in vitro at pH 8.5 with gut contents, including the peritrophic membrane. The total radioactivity measured in the regurgitated fluid represented about 1% of the dose, or 0.5 μg permethrin. This is more than sufficient to account for the redistribution of about half the dose (i.e. 0.05 μg permethrin) observed in Fig. 6. While the experiments as performed here cannot exclude rapid movement via the cuticle of insecticide from the dosing site to contaminate the mouthparts and hence the regurgitant, they provide initial evidence that the discontinuities in penetration curves can be explained by the regurgitation mechanism. In addition they show that insecticide rapidly reaches the gut and permeates into the gut contents. Metabolites are also rapidly produced and regurgitated. Fig. 6 shows curves generated by a modified 2-compartment model in which the external mass of insecticide is reset at a specified time to account for this redistribution.

Metabolism and induction

It was seen earlier that metabolism studies play an important part in understanding the pharmacokinetics of insecticides in insects. In addition to measurements of the importance of routes of metabolism in vivo, measurements in vitro are invaluable for characterizing the enzymes present in different insects and comparing the rates of metabolism between substrates differing structurally or isomerically. Synergism studies are often used to infer the importance of metabolism but as discussed by Soderlund et al. (Ref. 5, p. 427) the existence of multiple enzymes, particularly in the case of esterases, and the differing susceptibility to inhibition of these different enzymes complicates the interpretation of synergism data.

A large amount of information on the rates of metabolic conversions of insecticides and other foreign compounds or endogenous substrates has been assembled by

TABLE 1 Specific activities for insect and mammalian enzymic conversions in vitro of insecticides, natural products and other substrates

Species/tissue/enzyme	Substrate	Specific activity (pmol/min/mg protein)	Comment/Reaction	Ref.
Esterase				
Southern army worm/gut	t-permethrin	2628	V_{max}	20
Southern army worm/fat body	t-permethrin	2875	V_{max}	20
Southern army worm/integument	t-permethrin	3622	V_{max}	20
Southern army worm/haemolymph	t-permethrin	n.d.	V_{max}	20
Milkweed bug	(±)-t-resmethrin	66	V_{max}	20
Cockroach	(±)-t-resmethrin	58	V_{max}	21
Housefly	(±)-t-resmethrin	30	V_{max}	21
Cabbage looper	(±)-t-resmethrin	60	V_{max}	21
Mouse/liver	(±)-t-resmethrin	2083	V_{max}	21
Oxidase (cytochrome P-450) — uninduced				
Southern army worm/midgut	p-chloro N-methyl aniline	2038	N-deMe[n]	22
Southern army worm/midgut	Aldrin	1378	epox[n]	22
Southern army worm/midgut	Methoxyresorufin	3.8	O-deMe[n]	22
Cotton leafworm/midgut	t-permethrin	60	All oxid[n] reactions	This author
Fall army worm/midgut	l-menthone	5540	All oxid[n] reactions	23
Housefly/abdomen	Benzphetamine	560	N-deMe[n]	24— recalculated V_{max}
Housefly/abdomen	Lauric acid	570	11-OH	
Housefly/abdomen	Lauric acid	1420	12-OH	
Glutathione S-transferase				
Fall army worm/midgut	t-cinnamaldehyde	10000		
Fall army worm/midgut	t-4-phenyl3-buten-2-one	4150		25
Rat/liver	t-4-phenyl3-buten-2-one	11400		26

many workers. While differences in the methods of measurement and expression of results blur comparisons, some general trends stand out in the relative activities of different enzyme conversions. Table 1 lists specific activities (expressed as pmol/min/mg protein) for a wide range of specific primary metabolic conversions or overall rates of metabolism by a collection of oxidative routes. Conjugation reactions are limited to those with glutathione. It is well known that hydrolysis of the carboxyester bond in pyrethroids, as in the organophosphate malathion, contributes greatly to the low mammalian toxicity of these compounds, but in insects (if the isomer configuration is favourable) extremely rapid enzymic conversions occur as shown for *trans*-permethrin in the Southern army worm. There is marked tissue and species differentiation of this activity.

Although pyrethroids are extensively oxidized the rates of metabolism are relatively slight. Certain oxidations however do approach, or in the case of some natural products present in the diet of phytophagous species, exceed those for ester hydrolysis [23]. Some reactions catalysed by specific multiple forms of cytochrome P-450 which are important in mammals are very weak in insects, e.g. oxidative O-demethylation, but the glutathione S-transferase may more than compensate for this deficiency.

The data in Table 1 are for constitutive rates of metabolism. There is ample evidence that insect detoxifying enzymes show rapid, extensive and specific changes following ingestion of many different inducing agents. For example phenobarbital (PB) and pentamethyl benzene (PMB) induce changes in cytochrome P-450 levels in midgut and fat body of the noctuid larva *Spodoptera frugiperda* [22]. The peak absorbances of the carbon-monoxide bound forms of the induced enzymes indicate the specificity of the process: as expected pB does not alter the wavelength of maximum absorbance (λ_{max}) but PMB induces an enzyme with λ_{max} at 449 nm. Furthermore the λ_{max} of the fat body constitutive enzyme is 451 nm. Table 2 shows the specific induction by clofibrate of a cytochrome P-450 catalysing lauric acid 12-hydroxylation in the housefly. This inducing agent has been shown to induce this activity in the rat when the enzyme displays $\lambda_{max} = 452$ nm [27]. The V_{max} of this enzyme after 5.3-fold induction is 7100 pmol/min/mg protein, in excess of rates for ester hydrolysis shown in Table 1.

Yu [23] and Yu and Wadleigh [25] have shown the rapid induction by natural products of both oxidase and glutathione S-transferase activity in noctuid larvae. It seems likely that these induction effects may alter the pharmacokinetics of insecticides applied to phytophagous larvae or other insects feeding the wild: measure-

TABLE 2   The effect of phenobarbital and clofibrate on the Michaelis-Menten parameter V_{max} (apparent) in housefly microsomes [24]

Determination was from three separate measurements (mean ± S.D.).

Treatment	Cytochrome P-450 specific content (nmol·mg^{-1})	V_{max} (nmol min^{-1} nmol P-450^{-1})		
		Benzphetamine N-demethylation	Lauric acid hydroxylation	
			11-OH	12-OH
Control	0.10 ± 0.02	5.6 ± 1.1	5.7 ± 1.8	14.2 ± 3.7
Phenobarital	0.24 ± 0.04	36.3 ± 8.9	7.2 ± 2.2	14.0 ± 4.2
Clofibrate	0.11 ± 0.01	5.8 ± 2.0	7.3 ± 3.0	75.5 ± 10.6

TABLE 3 Concentrations of pyrethroids in central nervous systems of insects

Insect CNS	Compound	Dose	Peak concentration (at time)		
			μg/g wet weight	μM [a]	Ref.
American	NRDC 157	$2 \times LD_{50}$	0.07 (12-h)	0.15	5
cockroach (adult)	NRDC 163	$2 \times LD_{50}$	0.03 (12-h)	0.07	5
Blowfly (adult)	(1RS)-trans-	Sub-	0.45 (4-h)	1.2	29
(larva)	permethrin	lethal	0.25 (4-h)	0.64	29
Cotton-leafworm	(1RS)-trans-	LD_{50}	0.74 (4-h) [b]	1.9	This
(larva)	permethrin		1.3 (24-h) [b]	3.3	author

[a] Calculated from wet weights assuming density of 1 g/ml for tissues.
[b] Total radioactivity.

ments of metabolic activity and insecticide toxicity for insects reared on artificial diets may be misleading.

Concentrations of insecticides at the target site

Although insect tissues are small, studies on the distribution of insecticides within the insect are possible, especially when insecticides are radiolabelled at high specific activities (typically 1–10 Ci/mmol for ^{3}H-labelling). As an example Table 3 compares concentrations of three pyrethroids in nervous tissue from different insects and life stages. Molar concentrations have been estimated from the peak concentrations expressed in μg insecticide/g wet weight nervous tissue assuming a density of 1 g/ml for wet tissue. In the case of the Egyptian cotton-leafworm larval central nervous system the weight of the intact tissue after dry dissection was 0.42 $\pm$ 0.23 mg (n = 21), equal to 0.42 μl volume. Measurement (using a microscope graticule) of the length and diameter of an isolated cord assumed to be a cylinder of uniform diameter gave a value of 0.2 μl, suggesting the micromolar concentrations in Table 3 are at least of the correct order. The values span a 20-fold range but in all cases are comfortably in excess of concentrations of pyrethroids known to cause substantial disturbances in insect nervous systems studied in neurophysiological assays [14].

References

1 Noble-Nesbitt, J. (1970) Structural aspects of penetration through insect cuticles. Pestic. Sci. 1, 204–208.
2 Hartley, G.S. and Graham-Bryce, I.J. (1980) Penetration of pesticides into insects and fungi; in Physical Principles of Pesticide Behaviour 2, 658–686.

540

3 Brooks, G.T. (1976) Penetration and Distribution of Insecticdes. In: Insecticide Biochemistry and Physiology (C.F. Wilkinson, ed.) pp. 3–58. Plenum Press.

4 Dauterman, W.C. (1976) Extramicrosomal metabolism of insecticides. In: Insecticide Biochemistry and Physiology (C.F. Wilkinson, ed.) pp. 149–176. Plenum Press.

5 Soderlund, D.M. Sanborn, J.R. and Lee, P.W. (1983) Metabolism of pyrethrins and pyrethroids in insects. In: Progress in Pesticide Biochemistry and Toxicology, Vol. 3 (D.H. Hutson, and T.R. Roberts, eds.) pp. 401–436.

6 Omer, S.M., Georghiou, G.P. and Irving, S.N. (1980) DDT-Pyrethroid resistance interrelationships in Anopheles Stephensi. Mosq. News 40, 200–209.

7 Brealey, C.J., Crampton, P.L., Chadwick, P.R. and Rickett, F.E. (1984) Resistance mechanisms to DDT and Transpermethrin in Aedes aegypti. Pestic. Sci. 15, 121–132.

8 Brealey, C.J. (1987) Pharmacokinetics of lipid amides in the housefly. Biochem. Soc. Trans. 15, 1102–1103.

9 Black, M.H., Blade, R.J., Moss, M.D.V. and Nicholson, R.A. (1986) Sixth Int. Congr. Pestic. Chem., IUPAC, Ottawa, 1B–21.

10 Miyakado, M., Nakayama, I., Inoue, A., Hatakoshi, M. and Ohno, N. (1985) Insecticidal activities of phenoxy analogues of dihydropipercide. J. Pestic. Sci. 10, 25–30.

11 Welling, W. (1979) Toxicodynamics of insecticidal action: an introduction. Pestic. Sci. 10, 540–546.

12 Ford, M.G., Greenwood, R. and Thomas, P.J. (1981) The kinetics of insecticide action. Part II: the relationship between the pharmacokinetics of substituted (1RS)-cis,trans-chrysanthemates and their relative toxicities to mustard beetles (Phaedon cochleariae Fab.) Pestic. Sci. 12, 265–284.

13 Buckley, S., Brealey, C.J., Ford, M.G. and Leake, L.D. (1987) Dose-related neurophysiological effects and penetration studies of a congeneric series of synthetic pyrethroids. Pestic. Sci. Biotechnol., Proc. Int. Congr. Pestic. Chem., 205–208.

14 Burt, P.E., Lord, K.A., Forrest, J.M. and Goodchild, R.E. (1971) The spread of topically-applied pyrethrin I from the cuticle to the central nervous system of the cockroach Periplaneta americana. Ent. Exp. Appl. 14, 255–269.

15 Ford, M.G., Greenwood, R. and Thomas, P.J. (1981) The kinetics of insecticide action. Part I: the properties of a mathematical model describing insect pharmacokinetics. Pestic. Sci. 12, 175–198.

16 Holden, J.S. (1987) Absorption and metabolism of permethrin and cypermethrin in the cockroach and cotton-leafworm larvae. Pestic. Sci. 10, 295–307.

17 Casida, J.E. and Maddrell, S.H.P. (1970) Diuretic hormone release on poisoning Rhodnius with insecticide chemicals. Pestic. Biochem. Physiol. 1, 71–83.

18 Flattum, R.F., Watkinson, I.A. and Crowder, L.A. (1973) The effect of insect "autoneurotoxin" on Periplaneta americana (L.) and Schistocerca gregaria (Forksal) Malpighian tubules.Pestic. Biochem. Physiol. 3, 237–242.

19 Samaranayaka, M. (1977) The effect of insecticides on osmotic and ionic balance in the locust Schistocerca gregaria. Pestic. Biochem. Physiol. 7, 510–516.

20 Abdel-Aal, Y.A.I. and Soderlund, D.M. (1980) Pyrethroid-hydrolyzing esterases in Southern army worm larvae: tissue distribution, kinetic properties, and selective inhibition. Pestic. Biochem. Physiol. 14, 282–289.

21 Jao, L.T. and Casida, J.E. (1974) Insect pyrethroid-hydrolyzing esterases. Pestic. Biochem. Physiol. 4, 465–472.

22 Brattsten, L.B., Price, S.L. and Gunderson, C.A. (1980) Microsomal oxidases in midgut and fatbody tissues of a broadly herbivorous insect larva, Spodoptera eridania Cramer (Noctuidae). Comp. Biochem. Physiol. 66C, 231–237.

23 Yu, S.J. (1987) Microsomal oxidation of allelochemicals in generalist (Spodoptera frugiperda) and semispecialist (Anticarsia gemmatalis) insect. J. Chem. Entomol. 13, 423–436.

24 Clarke, S.E., Brealey, C.J. and Gibson, G.G. (1987) The effect of two inducing agents on the cytochrome P-450-dependent metabolism in housefly microsomes. Biochem. Soc. Trans. 15, 1101–1102.

25 Wadleigh, R.W. and Yu, S.J. (1987) Glutathione transferase activity of fall armyworm larvae toward α,β-unsaturated carbonyl allelochemicals and its induction by allelochemicals. Insect Biochem. 17, 759–764.
26 Habig, W.H., Pabst, M.J. and Jakoby, W.B. (1974) Glutathione S-transferases. The first enzymatic step in mercapturic acid formation. J. Biol. Chem. 249 (22), 7130–7139.
27 Gibson, G.G., Orton, T.T. and Tamburini, P.P. (1982) Cytochrome P-450 induction of clofibrate. Purification and properties of a hepatic cytochrome P-450 relatively specific for the 12-hydroxylation and 11-hydroxylation of dodecanoic acid (lauric acid). Biochem. J. 203, 161–168.
28 Nicholson, R.A., Botham, R.P. and Collins, C. (1983) The use of [3H]permethrin to investigate the mechanisms underlying its differential toxicity to adult and larval stages of the sheep blowfly *Lucilia sericata*. Pestic. Sci. 14, 57–63.

CHAPTER 40

Neurophysiological assays for the characterization and monitoring of pyrethroid resistance

J.R. BLOOMQUIST *

Department of Entomology, New York State Agricultural Experiment Station, Cornell University, Geneva, NY 14456, U.S.A.

Introduction

Resistance to pyrethroids in insect pest species continues to be a major problem with respect to their continued use as insecticides. Although metabolic mechanisms are responsible for many cases of resistance to pyrethroids, another type of resistance is due to reduced sensitivity of the insect nervous system. This type of resistance is referred to as knockdown resistance or *kdr*. Knockdown resistance was originally described and is best characterized in the housefly [1], but evidence for this type of resistance has also been found in mosquitoes [2,3], the German cockroach [4], two species of lepidopterous pest [5,6], the cattle tick [7], and most recently the vinegar fly, *Drosophila melanogaster* [8].

Insect strains possessing knockdown resistance can be recognized both by their reduced sensitivity to the rapid paralytic (knockdown) activity of pyrethroids and by their unique spectrum of cross resistance. Busvine [1] showed that an Italian strain of housefly was unaffected by a 20 min exposure to a DDT-treated surface that caused 35% knockdown of susceptible females. Similarly, Nicholson et al. [9] observed that the *kdr* and super-*kdr* strains of the housefly were only transiently affected by an injected dose of *trans*-permethrin that caused immediate and prolonged knockdown in the susceptible Cooper strain. In mortality bioassays, knockdown resistant strains of the housefly display reduced sensitivity to all pyrethroids tested to date, DDT, and DDT analogues [8]. In contrast, they show no cross resistance to cyclodienes, carbamates, or organophosphorus insecticides [10,11]. Exceptions to these rules do exist, however. Knockdown resistant houseflies are about as sensitive as susceptible strains to the action of miticidal carbinol derivatives of DDT [11]. In addition, Gammon and Holden [12] have described a strain of Egyptian cotton leafworm (*Spodoptera littoralis*) that is 4-fold resistant to permethrin, but not cypermethrin, and appears to possess a *kdr*-like factor.

---

* Present address: Rhône-Poulenc AgCo., 2 T.W. Alexander Dr., Research Triangle Park, NC 27709, U.S.A.

Knockdown resistance is due to intrinsic insensitivity of the nervous system and cannot be attributed to enhanced metabolism or reduced penetration of the pyrethroid. At the whole animal level, Busvine [1] has shown that a strain of housefly possessing DDT-dehydrochlorinase as a resistance factor was as sensitive to the knockdown action of DDT as a susceptible strain, even though its mortality at 24 h was greatly reduced. In more detailed studies, Nicholson et al. [9] have shown that metabolism and penetration rates of [^{14}C]permethrin in the susceptible Cooper strain are nearly identical to those in the resistant housefly strains *kdr* and super-*kdr*. Similar studies have failed to demonstrate an increased degradative capacity in knockdown resistant strains of the cattle tick [7] and German cockroach [4]. The lack of involvement of metabolism or penetration as the basis for knockdown resistance has led to the use of synergists as a way of identifying this resistance mechanism in toxicity studies. Resistance that cannot be overcome by addition of piperonyl butoxide (a mixed function oxidase inhibitor [8]) or *S,S,S*-tributyl phosphorotrithioate (DEF, an esterase inhibitor [8]) is considered evidence of a site insensitivity or *kdr* factor. However, Payne [13] has shown that mixed function oxidases present in pyrethroid-resistant *Heliothis virescens* were not sensitive to inhibition by piperonyl butoxide, but were inhibited by propynyl ether synergists. Likewise, the multiplicity and varied inhibitor sensitivities of insect esterases would make lack of synergism by DEF ambiguous, since this result could be due to the presence of knockdown resistance or to the presence of a DEF-resistant esterase. Thus, establishing the presence of knockdown resistance requires the demonstration of reduced neuronal sensitivity with neurophysiological assays.

Neurophysiological assays for *kdr*

Peripheral motor nerve recordings

An excellent neuromuscular preparation for detecting and characterizing knockdown resistance was developed by Salgado et al. [14]. Housefly or mosquito larvae were eviscerated to expose the abdominal nerves and muscles. Single muscle fibres were impaled with a recording microelectrode and at high gain they were able to observe miniature excitatory postsynaptic potentials (mEPSPs). These small (≤ 1 mV) voltage fluctuations represent quanta of neurotransmitter (probably glutamate) released by the presynaptic nerve terminal that activate receptor-linked ion channels on the postsynaptic muscle membrane [15]. The release of neurotransmitter is enhanced by depolarization of the nerve terminal, which is reflected by an increase in the mEPSP amplitude and rate measured in the muscle. Irrigating these preparations with saline containing pyrethroids resulted in increased mEPSP rate and amplitude, which Salgado et al. [14] attributed to depolarization of the nerve terminal via interaction of the pyrethroid with voltage-sensitive sodium channels. Preparations from susceptible housefly larvae displayed these effects at nanomolar concentrations of pyrethroid (Table 1). Equivalent preparations were analysed from the 538 ge strain isolated by Farnham [10]. This strain carries the phenotypic markers *bwb* (brown body) and *ge* (green eye) and possesses a homozygous recessive *kdr* factor that bestows broad cross resistance to pyrethroids. Preparations from 538 ge larvae required 100-fold higher concentrations of pyrethroid to elevate mEPSP frequency. Similar experiments with neuromuscular preparations of mosquito larvae and *Heliothis virescens* larvae established reduced sensitivity to

TABLE 1 Comparison of toxicity and nerve terminal depolarization

Insect	Pyrethroid	Mortality	R/S (ratio)	EC [a] (M)	R/S (ratio)
Musca					
susceptible	deltamethrin	0.5 [b]	(14)	1×10^{-9}	(100)
resistant		7.0		1×10^{-7}	
Culex					
susceptible	permethrin	0.0021 [c]	(4143)	5×10^{-10}	(2000)
resistant		8.7		1×10^{-6}	
Anopheles					
susceptible	permethrin	0.0035 [d]	(23)	5×10^{-11}	(20)
resistant		0.082		1×10^{-9}	
Heliothis					
susceptible	fenvalerate	0.6 [e]	(25)	1×10^{-10}	(50)
resistant		15.0		5×10^{-9}	

[a] Effective concentration—lowest concentration of pyrethroid effective in increasing mEPSP rate.
[b] Adult LD_{50} in ng/fly [11].
[c] Larval LC_{50} in ppm [3].
[d] Larval LC_{50} in ppm [2].
[e] Larval LD_{50} in $\mu g/g$ [5].

pyrethroids in the nervous system of the resistant strains. Moreover, there was a good correlation between resistance ratios measured in this neurophysiological assay and resistance ratios calculated from mortality bioassays (Table 1).

Peripheral motor nerve recordings have also been used to define and quantify pyrethroid resistance in the adult housefly nervous system. Adams and Miller [16] have described a unique preparation based on the particular neurocytology and accessibility of the housefly dorsolongitudinal flight muscles (Fig. 1). They placed
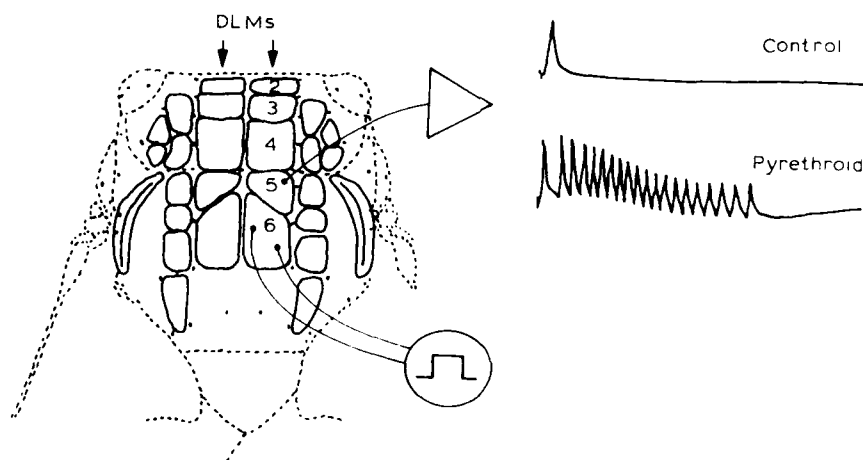
FIG 1 Adams and Miller [16] preparation for recording effects of pyrethroids on nerve terminals of the dorsolongitudinal muscles (DLMs). Electrodes are placed into dorsal thoracic insertions of the muscles using setal landmarks. Control: single EPSP initiated in fibre 5 by a single stimulus applied to fibre 6. Pyrethroid: burst of EPSPs elicited by a single stimulus after topical application of 0.1 μg of fenfluthrin.

TABLE 2   Neural sensitivity to permethrin in four strains of the housefly [a]

Strain	Threshold dose (ng/fly) [b]	Threshold ratio (R/S)	Mortality ratio (R/S)
NAIDM	40	1	1
kdr	320	8	5.3 [c]
Super-*kdr*	1 280	32	28.6
Learn-Pyr	> 1 280	> 32	32 [d]

[a] Modified from Scott and Georghiou [18].
[b] Minimum dose required to cause burst discharges.
[c] Data from Scott and Georghiou [19].
[d] Mortality ratio obtained using pretreatment with piperonyl butoxide.

two stimulating wire electrodes into the dorsal thoracic insertion of muscle fibre 6 by punching holes in the overlying cuticle with a sharpened tungsten probe. A corresponding recording electrode was placed in muscle fibre 5. Since both muscle fibres are innervated by a single excitatory motor neuron [17], stimuli applied to muscle fibre 6 evoke action potentials in the nerve endings that propagate anti-dromically and elicit EPSPs in muscle fibre 5. After treatment with non-cyano pyrethroids, DDT, or DDT analogues, a single electrical stimulus evokes a burst of action potentials (Fig. 1). Adams and Miller [16] demonstrated that these pyrethroid-dependent bursts were initiated at the peripheral motor nerve endings using *en passant* recordings with grease electrodes. Scott and Georghiou [18] used this preparation to characterize reduced nerve sensitivity in the 538 ge, super-*kdr*, and Learn-PyR strains of the housefly. They showed that the 538 ge strain required 8-fold greater doses of permethrin to initiate bursting compared to the susceptible NAIDM strain (Table 2). Super-*kdr*, a strain with even greater resistance, required 32-times as much insecticide to initiate the same physiological response. Both of these threshold ratios are similar to the resistance ratios for these strains measured in toxicity bioassays. In equivalent preparations of Learn-PyR flies, they observed over 32-fold resistance to the bursting action of permethrin, since no bursting occurred even at high doses for 45 min after treatment. However, this finding is complicated by the presence of penetration and mixed function oxidase resistance mechanisms that are also expressed by the Learn-PyR strain, even though the flies were pretreated with piperonyl butoxide.

Peripheral sensory nerve recordings

Peripheral sensory nerves also display reduced sensitivity to the actions of pyrethroids. A simple housefly larval sensory nerve preparation has been developed and exploited by Osborne and Smallcombe [20] for the study of resistance. Third instar larvae are opened sagittally and the abdominal nerves exposed by dissection. One of the nerves is severed close to the CNS and connected to a recording suction electrode. Preparations of this type display a fairly regular background of ascending sensory activity that is extremely sensitive to pyrethroids. Fifty percent of susceptible larvae are induced to fire bursts of action potentials when exposed to permethrin (10^{-12} M) or DDT (10^{-10} M). In the knockdown resistant strain 538 ge, this activity is not observed until the concentrations of permethrin and DDT are increased to 10^{-7} M and 10^{-6} M, respectively. Moreover, the strain super-*kdr* does not respond to permethrin at concentrations below 10^{-6} M [9]. These measurements

provide resistance ratios for permethrin at the level of the nerve of 10^5-fold (538 ge) and 10^6-fold (super-*kdr*). Thus, extremely large differences in pyrethroid sensitivity exist between sensory preparations of susceptible and resistant strains. The resistance ratios calculated from sensory nerve activity are much greater than the toxicity ratios calculated from adult toxicity bioassays and do not show the close correlation observed between pyrethroid action on motor systems and toxicity. However, it is possible that the correlation between resistance in the sensory nerve assay and mortality would be improved by using larval LD_{50} values.

CNS recordings

The central nervous system, like peripheral motor and sensory pathways, has proven itself less sensitive to pyrethroids in neurophysiological assays of resistant insects. Gammon [6] has developed a preparation for analysing the responses of isolated nerve cords of Egyptian cotton leafworm (*Spodoptera littoralis*) larvae that displayed 4-fold resistance to permethrin, but were completely susceptible to cypermethrin. By attaching stimulating and recording suction electrodes to the posterior and anterior connectives of the excised abdominal nerve cord, he was able to measure levels of spontaneous activity and responses to stimulation. Permethrin at 10^{-7} M elevated levels of spontaneous activity and caused the appearance of prolonged after-discharges following a single stimulus. In susceptible individuals, these discharges appeared after 9.1 ± 0.9 min of exposure to 10^{-7} M permethrin, whereas in the resistant strain the latency of this effect was 22.1 ± 2.3 min [6]. Since no repetitive firing was initiated by 10^{-7} M cypermethrin to either susceptible or resistant larvae, time to conduction blockage was used as a measure of CNS poisoning by cypermethrin. No difference in time to blockage was observed between the susceptible and resistant strains, which is consistent with the toxicity profile of this compound. However, there was no correlation between resistance and conduction blockage by permethrin, thereby raising doubts about the appropriateness of this parameter for demonstrating reduced sensitivity of the nervous system. Clearly, more work is required to characterize the mechanism responsible for the interesting toxicity profile of permethrin and cypermethrin in this strain of *Spodoptera littoralis*.

A CNS preparation utilizing patterned motor activity has been applied to the study of knockdown resistance by Miller and his collaborators [21]. In this preparation, adult female houseflies were immobilized in wax and the thoracic ganglion was exposed by dissection. Recording electrodes were placed in two fibres of the dorsolongitudinal muscles. This electrode arrangement displayed signals from one fibre as a positive (upward) displacement from baseline and the other a negative (downward) displacement from baseline. Patterned activity in the fibres of the dorsolongitudinal muscles was monitored while bathing the thoracic ganglion in insect saline containing pyrethroid. Normal, patterned flight muscle activity is shown in Fig. 2A, whereas pyrethroid-dependent disruption of the pattern is evident from the spikes absent in trace B. This effect has been termed 'uncoupling' and is thought to arise from disruption of central nervous pathways involved in the initiation and maintenance of the motor pattern [21]. However, this hypothesis has not been confirmed by direct microelectrode recordings of central neurons. Miller et al. [21] exposed preparations from susceptible (NAIDM) and resistant (538 ge) strains to increasing concentrations of a variety of pyrethroids and DDT analogues and found that 538 ge preparations required longer exposure times and higher concentrations of insecticide to observe uncoupling. Representative data are shown

200 msec
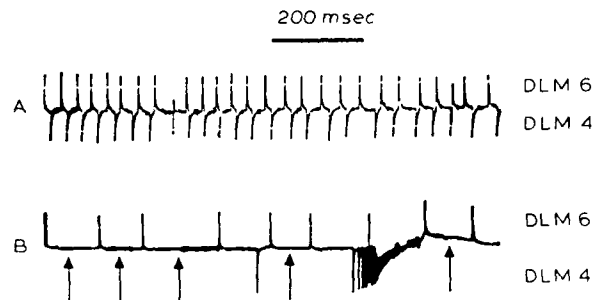
FIG 2 Typical uncoupling effect of pyrethroids on the flight motor pattern of adult houseflies. A: normal, one-to-one asynchronous pattern of DLM activity before insecticide treatment; B: uncoupling of the pattern during poisoning by permethrin. Arrows indicate the missing action potentials in DLM4. Traces modified from Bloomquist and Miller [22].

for tetramethrin (Fig. 3), where the delay to the appearance of uncoupling in the 538 ge strain was over 60 min at 10^{-6} M, whereas the susceptible NAIDM strain showed this effect in about 6 min.

Characteristics of *kdr* observed in physiological studies

Several salient features of knockdown resistance are evident from the results of these neurophysiological studies. Measuring an increased latency to abnormal nerve function in resistant strains provides evidence for the reduced sensitivity of the nervous system that underlies knockdown resistance. Alternatively, reduced sensitivity of the nervous system has been documented by showing that preparations from resistant insects require higher insecticide concentrations to produce equivalent effects seen in preparations from susceptible individuals. Using these criteria, it has been shown that reduced sensitivity to pyrethroids is broadly distributed within the nervous system and that sensory, motor, and possibly central nervous elements are affected. The presence of resistance throughout the nervous system is consistent with the proposal that the voltage-sensitive sodium channel and not the GABA
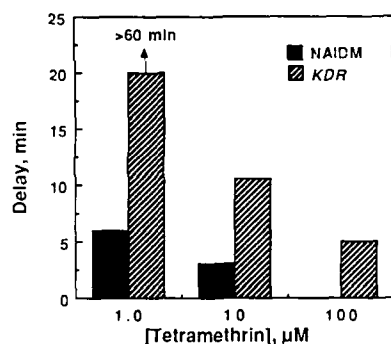
FIG 3 Concentration and time dependence of uncoupling in susceptible (NAIDM) and resistant (*kdr*) strains of the housefly. Delay to the appearance of uncoupling is uniformly longer in the resistant *kdr* strain. NAIDM preparations were not tested at 10^{-4} M. Data taken from Miller et al. [21].

receptor/chloride ionophore complex is the primary target site of pyrethroids, since GABAergic neurons are absent in three different nerve preparations used to characterize *kdr* in the housefly [14,16,20]. Physiological assays also demonstrated that the resistance is expressed in both the larval and adult stages of the housefly and mosquitoes. Reduced neuronal sensitivity has also been implicated as a resistance mechanism in larvae of *Spodoptera littoralis* [6] and *Heliothis virescens* [5]. Additional studies are needed to confirm whether the adults of these strains are resistant as well. When compared to the housefly, the unique resistance spectrum observed in *Spodoptera* larvae suggests that not all types of *kdr* mechanisms are identical. Thus, reliance on the housefly system as a model for all knockdown resistance phenomena may hinder the discovery and characterization of the unique properties of *kdr* in other species.

Monitoring for *kdr* with neurophysiological methods

Monitoring for knockdown resistance in field populations of insects with neurophysiological techniques has distinct advantages and disadvantages compared to other screening methods. In many cases, neurophysiological assays represent available technology and they can detect reduced sensitivity in the nervous system whatever its biochemical basis. Since the precise mechanism(s) underlying knockdown resistance are unknown, there are no biochemical probes available to identify individuals carrying a *kdr* trait. Although they can document reduced sensitivity of the nervous system in any of its possible forms, physiological techniques provide no information on the biochemical mechanisms underlying the observed resistance. Certain neurophysiological assays have the added advantage of being nondestructive, thereby preserving resistant individuals for starting colonies that could be used in further studies. For example, Miller and Adams [23] have described procedures for treating and recording from single detached housefly legs. Resistant individuals identified by this method might be mated in an effort to preserve and propagate the resistant trait. This application of neurophysiological techniques stands in contrast to available biochemical methods, where individual mosquitoes, for instance, are crushed [24] or homogenized [25] prior to analysis of esterase activity. Unlike biochemical methods, however, neurophysiological assays cannot process large numbers of samples because they are time consuming and labour intensive. Because of these limitations, they are not able to detect resistant alleles present at low frequency in field populations, which is an important aspect of resistance monitoring [26]. Finally, neurophysiological techniques are not applicable to very small arthropods such as white flies or phytophagous mites. In the future, neurophysiological studies of these minute species may be approached by cell culture or by expression of the appropriate receptors/ion channels in *Xenopus* oocytes.

References

1 Busvine, J.R. (1951) Mechanism of resistance to insecticide in houseflies. Nature 168, 193–195.
2 Omer, S.M., Georghiou, G.P. and Irving, S.N. (1980) DDT/pyrethroid resistance inter-relationships in *Anopheles stephensi*. Mosquito News 40, 200–209.

3 Priester, T.M. and Georghiou, G.P. (1978) Induction of high resistance to permethrin in *Culex pipiens quinquefasciatus*. J. Econ. Entomol. 71, 197–200.

4 Scott, J.G. and Matsumura, F. (1981) Characteristics of a DDT-induced case of cross-resistance to permethrin in *Blatella germanica*. Pestic. Biochem. Physiol. 16, 21–27.

5 Nicholson, R.A. and Miller, T.A. (1985) Multifactorial resistance to transpermethrin in field-collected strains of the tobacco budworm *Heliothis virescens* F. Pestic. Sci. 16, 561–570.

6 Gammon, D.W. (1980) Pyrethroid resistance in a strain of *Spodoptera littoralis* is correlated with decreased sensitivity of the CNS in vitro. Pestic. Biochem. Physiol. 13, 53–62.

7 Nicholson, R.A., Chalmers, A.E., Hart, R.J. and Wilson, R.G. (1980) Pyrethroid action and degradation in the cattle tick (*Boophilis microplus*). In: Insect Neurobiology and Pesticide Action (Neurotox '79). Soc. Chem. Ind., 481–488.

8 Soderlund, D.M. and Bloomquist, J.R. (1988) Molecular mechanisms of insecticide resistance. In: Pesticide Resistance in Arthropods (R. Roush, B. Tabashnik, eds.). CRC Press (in press).

9 Nicholson, R.A., Hart, R.J. and Osborne, M.P. (1980) Mechanisms involved in the development of resistance to pyrethroids with particular reference to knockdown resistance in houseflies. In: Insect Neurobiology and Pesticide Action (Neurotox '79). Soc. Chem. Ind., 465–471.

10 Farnham, A.W. (1977) genetics of resistance of houseflies (*Musca domestica* L.) to pyrethroids. I. Knockdown resistance. Pestic. Sci. 8, 631–636.

11 Sawicki, R.M. (1978) Unusual response of DDT-resistant houseflies to carbinol analogues of DDT. Nature 275, 443–444.

12 Gammon, D.W. and Holden. J.S. (1980) A neural basis for pyrethroid resistance in larvae of *Spodoptera littoralis*. In: Insect Neurobiology and Pesticide Action (Neurotox '79). Soc. Chem. Ind., 481–488.

13 Payne, G.T. (1987) Inheritance and mechanisms of resistance to permethrin in the tobacco budworm, *Heliothis virescens* (Lepidoptera: Noctuidae). Ph.D. Dissertation. Clemson University, U.S.A.

14 Salgado, V.L., Irving, S.N. and Miller, T.A. (1983) The importance of nerve terminal depolarization in pyrethroid poisoning in insects. Pestic. Biochem. Physiol. 20, 169–182.

15 Usherwood, P.N.R. (1961) Spontaneous miniature potentials from insect muscle fibers. Nature 191, 814–815.

16 Adams, M.E. and Miller, T.A. (1974) Site of action of pyrethroids: repetitive "backfiring" in flight motor units of house fly. Pestic. Biochem. Physiol. 11, 218–231.

17 King, D.G. and Valentino, K.L. (1983) On neuronal homology: A comparison of similar axons in *Musca, Sarcophaga*, and *Drosophila* (Diptera: Schizophora). J. Comp. Neurol. 219, 1–9.

18 Scott, J.G. and Georghiou, G.P. (1986) Mechanisms responsible for high levels of permethrin resistance in the house fly. Pestic. Sci. 17, 195–206.

19 Scott, J.G. and Georghiou, G.P. (1984) Influence of temperature on knockdown, toxicity, and resistance in the house fly, *Musca domestica*. Pestic. Biochem. Physiol. 21, 53–62.

20 Osborne, M.P. and Smallcombe, A. (1983) Site of action of pyrethroid insecticides in neuronal membranes as revealed by the kdr resistance factor. In: IUPAC Pesticide Chemistry, Human Welfare and the Environment (J. Miyamoto, ed.), pp. 103–107. Pergamon Press.

21 Miller, T.A., Kennedy, J.M. and Collins, C. (1979) CNS insensitivity to pyrethroids in the resistant kdr strain of house flies. Pestic. Biochem. Physiol. 12, 224–230.

22 Bloomquist, J.R. and Miller, T.A. (1986) Neural correlates of flight activation and escape behavior in houseflies recovering from pyrethroid poisoning. Arch. Insect. Biochem. Physiol. 3, 551–559.

23 Miller, T.A. and Adams, M.E. (1977) Central vs. peripheral action of pyrethroids on the housefly nervous system. ACS Symp. Ser. 42, 98–115.

24 Pasteur, N. and Georghiou, G.P. (1981) Filter paper test for rapid determination of phenotypes with high esterase activity in organophosphate resistant mosquitoes. Mosquito News 41, 181–183.

25 Brogdon, W.G. and Dickinson, C.M. (1983) A microassay system for measuring esterase activity and protein concentration in small samples and in high-pressure liquid chromatography eluate fractions. Anal. Biochem. 131, 499–503.

26 Roush, R.T. and Miller, G.L. (1986) Considerations for design of insecticide resistance monitoring programs. J. Econ. Entomol. 79, 293–298.

CHAPTER 41

Neuropharmacology and molecular genetics of nerve insensitivity resistance to pyrethroids

DAVID M. SODERLUND AND DOUGLAS C. KNIPPLE

Department of Entomology, New York State Agricultural Experiment Station, Cornell University, Geneva, NY 14456, U.S.A.

Introduction

Resistance to pyrethroids conferred by reduced sensitivity of the nervous system has been detected in several insect species and has been documented in considerable detail in the housefly [1]. In this species, the *kdr* and super-*kdr* traits represent allelic variants at a single locus that confer broad cross resistance to DDT, DDT analogues, and pyrethroids. Because of the central role of the voltage-sensitive sodium channel in the actions of pyrethroids on nerves [2], mechanisms of reduced neuronal sensitivity are likely to involve changes in the number, environment, or properties of this site. Three mechanisms have been proposed to account for reduced neuronal sensitivity in the housefly: reduced number or density of the insecticide target site [3,4]; alterations in the lipid composition of neuronal membranes [5]; and alterations in the insecticide-binding domain of the target macromolecule [6]. In this paper, we review recent studies in our laboratories directed at defining further the pharmacological properties of sodium channels in susceptible and *kdr* houseflies. We also discuss the potential applications of recent progress in sodium channel molecular biology to the identification of the *kdr* mechanism.

Neuropharmacology of housefly sodium channels

The kinetics and sodium conductance of voltage-sensitive sodium channels are modified by a variety of neurotoxins that act at one of six binding domains [7]. Rapid paralysis bioassays with housefly larvae [8] demonstrated that the *kdr* mechanism conferred resistance not only to DDT and pyrethroids but also to aconitine, an alkaloid that activates sodium channels by interacting with a binding domain distinct from the insecticide recognition site. However, no resistance was observed to tetrodotoxin, the α-polypeptide toxin of scorpion (*Leiurus quinquestriatus*) venom, or the local anesthetic procaine, suggesting that the *kdr* mechanism selectively modifies only some of the neurotoxin recognition properties of housefly sodium channels.

554
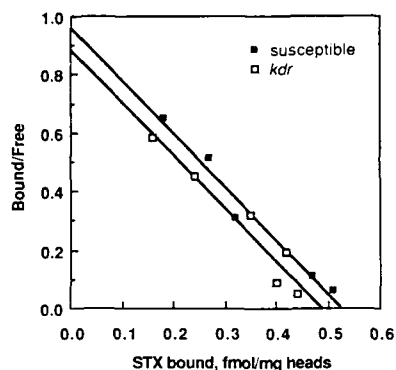
FIG 1   Scatchard plots of the specific binding of [^{3}H]STX to neuronal membrane preparations from susceptible and *kdr* houseflies [9].

The density of sodium channels in neuronal membrane preparations can be estimated by the specific binding capacity of these preparations for [^{3}H]saxitoxin (STX). Reductions in sodium channel density are correlated with a *kdr*-like resistance mechanism involving reduced neuronal sensitivity to DDT and pyrethroids in a temperature-sensitive paralytic mutant strain of *Drosophila melanogaster* [1] and have been implicated in *kdr* houseflies [3,4]. We have determined the specific binding of [^{3}H]STX using a subcellular preparation from housefly heads enriched in neuronal membranes [9]. [^{3}H]STX bound to a single class of saturable, high affinity sites in membranes from insecticide-susceptible (NAIDM strain) flies with an equilibrium dissociation constant (K_d) of 0.55 nM and a capacity at saturation (B_{max}) of 0.53 fmol/mg head equivalents of membranes (Fig. 1). The properties of the [^{3}H]STX site in knockdown-resistant flies (538 ge strain, homozygous for the *kdr* trait and visible genetic markers on autosome 3) were virtually identical to those measured in preparations from susceptible insects ($K_d = 0.56$ nM; $B_{max} = 0.49$ fmol/mg head equivalents) (Fig. 1). In both strains, binding at near-saturating concentrations increased slightly with increases in assay temperature from 4°C to 37°C. These findings tend to rule out reduced target site number as a mechanism underlying the *kdr* trait in the housefly.

The measurement of binding interactions at the alkaloid activator recognition site is also of interest in view of the resistance of *kdr* houseflies to aconitine [8]. The ability of DDT and pyrethroids to modify allosterically both activator-stimulated sodium flux [10,11] and the binding of [^{3}H]batrachotoxinin A-20-α-benzoate (BTX-B) to the activator site [12,13] in mammalian brain preparations suggests that the development of a similar assay in insects might provide insight into the *kdr* mechanism. We have recently completed a preliminary study of the binding of [^{3}H]BTX-B binding to membranes prepared from the heads of insecticide-susceptible houseflies [14]. Specific binding of [^{3}H]BTX-B in these preparations is measured by a rapid filtration assay essentially the same as that described for mammalian brain synaptosomes [15] and is defined as that portion of total binding that can be blocked by coincubation with 1 mM veratridine. In the absence of other modifiers, this membrane preparation bound [^{3}H]BTX-B with a K_d of 133 nM and a B_{max} of 2.2 fmol/mg equivalents of heads (Fig. 2). In the presence of 25 μg of *Leiurus*
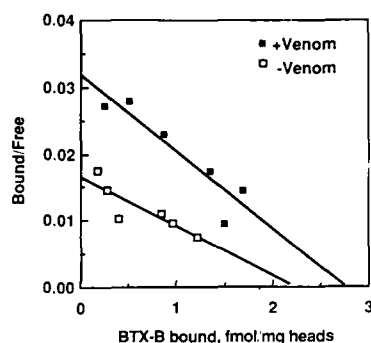
FIG 2 Scatchard plots of the specific binding of [³H]BTX-B to neuronal membrane preparations from susceptible houseflies measured in the absence and presence of a saturating concentration of *Leiurus quinquestriatus* venom [14].

quinquestriatus venom, the K_d was decreased to 86 nM but B_{max} was virtually unchanged (Fig. 1). This result illustrates an allosteric enhancement of [³H]BTX-B binding by the α-polypeptide toxin in the venom that is analogous to the effect observed in rat brain preparations [15]. The affinity for [³H]BTX-B measured in the presence of venom is similar to that found under similar conditions with mammalian brain synaptosomes [15], but the affinity in the absence of venom is much higher than has been reported previously in studies with sodium channels from vertebrate species [15,16]. Sodium channel density in fly head preparations is substantially lower than in mammalian synaptosomes, so that the nonspecific binding of this lipophilic ligand to nonspecific hydrophobic sites in fly preparations constitutes 65–75% of total binding at ligand concentrations equal to the K_d, rather than the 20–30% typically encountered in mammalian brain preparations [13,15].

The enhancement of [³H]BTX-B binding to fly membranes by *Leiurus* venom and the inhibition of binding by veratridine and aconitine are consistent with the pharmacology of sodium channels as defined in mammalian systems, but other properties of the [³H]BTX-B site of housefly head preparations diverge substantially from the mammalian paradigm [14]. For example, the anesthetic dibucaine and the anticonvulsants carbamazepine and diphenylhydantoin, which inhibit the specific binding of [³H]BTX-B to mammalian sodium channels, were only marginally effective in assays with fly head preparations. Even more problematic from the perspective of defining resistance mechanisms is the complete failure of deltamethrin to modify the binding of [³H]BTX-B in fly head membrane preparations, thus precluding the use of this ligand as an allosteric probe of the insecticide recognition site. Attempts to extend this assay to equivalent preparations from *kdr* houseflies suggested that the affinity for [³H]BTX-B was decreased in this strain so that a reproducible saturation isotherm could not be determined (P.M. Adams and D.M. Soderlund, unpublished observations). Taken together, these findings suggest that assays of [³H]BTX-B binding to head membranes from susceptible houseflies may identify a sodium channel site, but that t...s ligand may be of limited value in defining pharmacological properties related to the *kdr* resistance mechanism.

556

Molecular biology of insect sodium channels

To gain further insight into mechanisms of reduced neuronal sensitivity, it is necessary to separate the effects of membrane environment from those involving structural changes in one or more binding domains of the sodium channel. Mammalian sodium channels can be purified and reconstituted into artificial membranes [17], but these methods have not been successful to date with insect sodium channels. However, novel approaches based on the molecular biology of vertebrate sodium channels offer alternatives to purification and reconstitution. Knowledge of the primary structure of the sodium channel has been advanced by the successful cloning and sequencing of genes encoding the α subunit of sodium channels from electric eel [18], rat brain [19], and a structurally homologous gene from *Drosophila melanogaster* [20]. These genes provide potential points of entry for the isolation of sodium channel genes from susceptible and resistant houseflies.

Due to the unavailability of cDNA clones for sodium channels from vertebrate species, our approach to the isolation of the sodium channel gene from the housefly was based on the use of synthetic oligonucleotides as probes. At the time that this effort was initiated, the nucleotide sequences of sodium channel cDNAs from two vertebrate systems had been published [18,19] and a short stretch of amino acid sequence data inferred from the sequencing of genomic DNA fragments of a putative *Drosophila* sodium channel gene had been presented as a meeting abstract [21]. Consideration of the phylogenetic distances between flies and vertebrates and the degeneracy of the genetic code led us to design a synthetic oligonucleotide probe based on the partial *Drosophila* amino acid sequence (Fig. 3) rather than on the vertebrate cDNA sequences. In the construction of this probe, the base inosine (I), which is capable of base pairing with adenosine (A), thymine (T) or cytosine (C) [22], was used in six positions, and all four bases (N) were used in one position; thus, one of the four oligonucleotides in the mixture was capable of complementary base pairing to the coding strand of the *Drosophila* gene.

Using this oligonucleotide as an initial probe, we attempted to isolate a portion of the *Drosophila* sodium channel gene for use as a more suitable heterologous

RAT	1764	Phe	Leu	Val	Val	Val	Asn	Met	Tyr	Ile	Ala
EEL	1558	Phe	Leu	Val	Val	Val	Asn	Met	Tyr	Ile	Ala
FLY	1547	Tyr	Met	Ile	Val	Ile	Asn	Met	Tyr	Ile	Ala

mRNAs	5'- UAU	AUG	AUU	GUU	AUU	AAU	AUG	UAU	AUU	GC-3'
	C		C	C	C	C		C	C	
			A	A	A				A	
				G						

| PROBE | 3'- ATI | TAC | TAI | CAN | TAI | TTI | TAC | ATI | TAI | CG-5' |
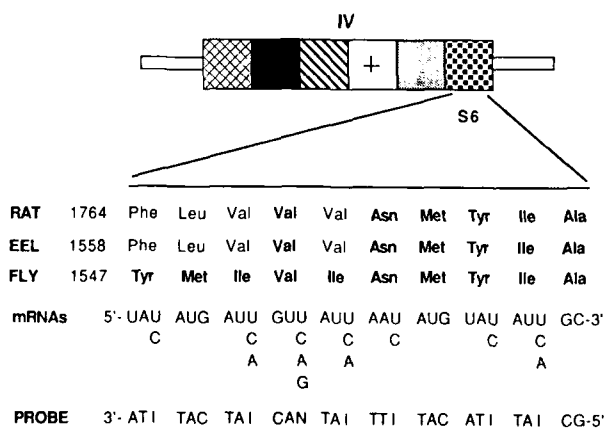
FIG 3   Design of an antisense oligonucleotide probe to region S6 of repeated homology unit IV of the *Drosophila* putative sodium channel gene. Inferred amino acid sequence data were taken from Refs. 18, 19, and 21.

probe in our efforts to isolate the *Musca* sodium channel gene. The oligonucleotide was end-labeled and hybridized under low stringency to Southern blots of Sal I-digested *Drosophila* genomic DNA. Blots were subsequently washed with tetramethylammonium chloride at temperatures significantly below those deemed appropriate for a probe of this length [23] and a band of hybridization in the 4 kb region was detected following autoradiography. A mini-library was prepared from 3.8–4.2 kb Sal I genomic DNA fragments and a clone designated p4A3, which hybridized strongly with the oligonucleotide probe, was isolated and purified.

Analysis of clone p4A3 was aided by the publication of the inferred amino acid sequence of the four internal homology units of the putative *Drosophila* sodium channel gene together with a restriction map and cytogenetic localization [20]. By comparison with these data, clone p4A3 was determined to be different from the putative sodium channel gene on two grounds. First, the restriction map of p4A3 has no similarity to that of the putative sodium channel gene. Second, the putative sodium channel gene was located by in situ hybridization to region 60DE on the right arm of chromosome 2, whereas in situ hybridization of biotinylated probes prepared from p4A3 labelled region 18CD and the chromocenter. Since these sites of hybridization represent neither known ion channel genes having possible homology to the sodium channel nor mutations in which altered sodium channel function is implicated, the in situ hybridization results provide no clues as to the functional roles, if any, of the locus (or loci) from which p4A3 is derived.

In subsequent studies, Salkoff and coworkers [24] identified a second gene at the putative sodium channel locus having unusual properties. This 'minigene' is contained within the first intron of the putative sodium channel gene and is transcribed from the opposite strand to produce a 0.5 kb polyadenylated RNA. Comparisons of this transcription unit in *D. melanogaster* and *D. virilis* showed that it was conserved in position relative to putative sodium channel sequences and exhibited greater nucleotide sequence identity than regions of the putative sodium channel gene sequence that coded for identical amino acid sequences in these two species. If this gene is highly conserved in both sequence and position relative to sodium channel-like genes in other species, it might prove to be extremely valuable in isolating genes homologous to the putative sodium channel locus of *Drosophila*. With this in mind, we initiated studies using the minigene as a probe to identify homologous mRNAs in other species. A single-stranded RNA probe complementary to the *Drosophila* minigene mRNA labelled mRNAs of similar size on Northern blots of *Drosophila melanogaster*, *Drosophila virilis*, housefly, apple maggot, and neonatal rat brain poly-A$^+$ RNAs, thereby providing further evidence for the conservation and ubiquity of this gene. Somewhat surprisingly, the same probe hybridized strongly to clone p4A3 under high stringency conditions. The significance of this finding is not clear at present, but at a minimum it suggests that sequence elements complementary to a portion of the highly-conserved minigene sequence are present at other sites in the *Drosophila* gene. A detailed sequence analysis of p4A3 should provide insight into the relationship of this cloned DNA to both the minigene and conserved sequences coding for transmembrane regions of other ion channel genes.

A fundamental problem in the application of molecular probes from *Drosophila* to the isolation of sodium channel genes from the housefly or any other insect species continues to be the lack of information regarding the functional role of the gene described by Salkoff and colleagues. This locus clearly represents a transcribed

gene and has been designated as a putative sodium channel gene by structural analogy to sodium channel genes of vertebrates. However, the internal repeated homology structure of this gene is not unique to sodium channels, but is also represented in a recently-characterized muscle calcium channel gene [25]. Consequently, structural organization and homology alone are insufficient to define the function of this locus, and direct demonstration of its functional role is needed to establish its value as a source of heterologous probes for sodium channel isolation in other species. A second problem in this area is the potential existence of multiple sodium channels in *Drosophila*, as has been found in rat brain [19]. Although clone p4A3 exhibits homology to sequences contained in both the 3' end of the coding region of the putative sodium channel gene and the highly conserved minigene, it is premature to suggest that it contains sequences from a functional gene encoding a sodium channel or any other kind of ion channel. More significant evidence for multiple genes comes from efforts to characterize the *para*[*ts*] locus, which confers temperature-sensitive paralysis and causes alterations in sodium channel function. Preliminary results from the sequencing of this locus [26], which maps to cytogenetic region 14C-F, suggests that the *para*[*ts*] gene is also homologous to previously-described sodium channel genes. Thus, if the putative sodium channel gene mapping to cytogenetic region 60DE in fact encodes a sodium channel protein it may not be the only gene that does so, and other sodium channel genes and their products could be more relevant as targets of insecticide action.

Heterologous expression of sodium channels in *Xenopus* oocytes

Questions regarding the functional role of putative sodium channel genes in *Drosophila* must be answered using gene expression assays that permit measurement of transient voltage-sensitive sodium currents. For such assays, the oocyte of the clawed frog, *Xenopus laevis*, is the system of choice [27]. *Xenopus* oocytes lack voltage-activated 'fast' sodium channels and have a very low endogenous rate of transcription. When injected with foreign mRNAs for neurotransmitter receptors and ion channels, oocytes efficiently translate these messages and insert functional macromolecules into the cell membrane, where they can be detected using electrophysiological techniques. Oocytes injected with either synthetic sodium channel mRNA, prepared by in vitro transcription from cloned full-length cDNA [28], or hybrid-selected native mRNA [29] expressed sodium channels with properties in voltage clamp assays comparable to those measured for sodium channels of peripheral nerve and skeletal muscle. These methods remain to be applied to mRNA corresponding to the putative sodium channel gene of *Drosophila*. A number of technical problems hinder the direct application of this approach to *Drosophila* sodium channel mRNA, all of which relate to the difficulty of obtaining significant amounts of the mRNA corresponding to the putative sodium channel gene. In particular, mRNA isolated from *Drosophila* pupae is predominantly non-neuronal in origin, so that the native abundance of the putative sodium channel message is much lower than that encountered in brain-specific mRNA extracts from vertebrates. Moreover, no full-length cDNA is available for this gene, thus precluding the in vitro synthesis of mRNA for expression studies. These considerations suggest that large scale mRNA isolation followed by hybrid selection with available cloned cDNA presents the best opportunity to obtain sufficient mRNA for expression assays.

The successful extension of the oocyte expression assay to insect sodium channel mRNA not only will confirm the identity of putative sodium channel genes in *Drosophila* but also may permit the functional characterization of sodium channels from other species in the absence of isolated sodium channel genes. For example, in the absence of homologous cDNA for hybrid selection, the abundance of sodium channel messages in insect mRNA extracts might be enriched by size fractionation, which takes advantage of the unusually large size of sodium channel messages. Application of this strategy to housefly sodium channel mRNA could permit the expression of sodium channels in oocytes, where the properties and insecticide sensitivities of channels from susceptible and *kdr* insects could be compared in the same membrane environment.

Conclusions

Despite the efforts of several laboratories and the use of a variety of approaches, the mechanism underlying the *kdr* factor in houseflies remains elusive. Binding studies with sodium channel-directed radioligands have ruled out a reduction in target site density as a mechanism in the housefly, but these approaches are unable to distinguish between changes in sodium channel structure or in its membrane environment as the primary cause of reduced sensitivity. Recent advances in the molecular biology of sodium channels provide new approaches to this problem. In particular, the isolation of sodium channel genes in *Drosophila* will greatly aid the characterization of homologous genes in the housefly and in other insect species of economic importance. However, the application of molecular probes from *Drosophila* to other insect species is premature, because the number and functional properties of putative sodium channel genes in *Drosophila* are not yet established. The solution of the technical problems that currently limit the expression of insect sodium channel messages in *Xenopus* oocytes not only will contribute to the identification of sodium channel-encoding genes in *Drosophila* but also will create new opportunities to explore the role of altered sodium channel structure as a mechanism of pyrethroid resistance in the housefly and in other insects.

References

1 Soderlund, D.M. and Bloomquist, J.R. (1988) Molecular mechanisms of insecticide resistance. In: Pest Resistance in Arthropods (R. Roush, B. Tabashnik, eds.). CRC Press, Cleveland (in press).

560

2 Narahashi, T. (1984) Nerve membrane sodium channels as the target of pyrethroids. In: Cellular and Molecular Neurotoxicology (T. Narahashi, ed.). pp. 85–108. Raven Press, New York.

3 Chang, C.P. and Plapp, F.W. Jr. (1983) DDT and pyrethroids: receptor binding in relation to knockdown resistance (kdr) in the house fly. Pestic. Biochem. Physiol. 20, 86–91.

4 Rossignol, D.P. and Pipenberg, P.K. (1986) Molecular basis of target site resistance to neurotoxic insecticides. Soc. Neurosci. Abstr. 12, 1075.

5 Chiang, C. and Devonshire, A.L. (1982) Changes in membrane phospholipids, identified by Arrhenius plots of acetylcholinesterase and associated with pyrethroid resistance (kdr) in houseflies (Musca domestica). Pestic. Sci. 13, 156–160.

6 Salgado, V.L., Irving, S.N. and Miller, T.A. (1983) Depolarization of motor nerve terminals by pyrethroids in susceptible and kdr-resistant house flies. Pestic. Biochem. Physiol. 20, 100–114.

7 Lombet, A., Bidard, J.-N. and Lazdunski, M. (1987) Ciguatoxin and brevetoxins share a common receptor site on the neuronal voltage-dependent Na^+ channel. FEBS Lett. 219, 350–359.

8 Bloomquist, J.R. and Miller, T.A. (1986) Sodium channel neurotoxins as probes of the knockdown resistance mechanism. Neurotoxicology 7, 217–224.

9 Grubs, R.E., Adams, P.M. and Soderlund, D.M. (1988) Binding of [^{3}H]saxitoxin to head membrane preparations from susceptible and knockdown-resistant houseflies. Pestic. Biochem. Physiol. (submitted).

10 Ghiasuddin, S.M. and Soderlund, D.M. (1985) Pyrethroid insecticides: potent, stereo-specific enhancers of mouse brain sodium channel activation. Pestic. Biochem. Physiol. 24, 200–206.

11 Bloomquist, J.R. and Soderlund, D.M. (1988) Pyrethroid insecticides and DDT modify alkaloid-dependent sodium channel activation and its enhancement by sea anemone toxin. Mol. Pharmacol. (in press).

12 Brown, G.B. and Olsen, R.W. (1984) Batrachotoxin-benzoate binding as an index of pyrethroid interaction at Na^+ channels. Soc. Neurosci. Abst. 10, 865.

13 Payne, G.T. and Soderlund, D.M., unpublished results.

14 Soderlund, D.M., Adams, P.M. and Grubs, R.E. (1988) in preparation.

15 Catterall, W.A., Morrow, C.S., Daly, J.W. and Brown, G.B. (1981) Binding of batracho-toxinin A 20-α-benzoate to a receptor site associated with sodium channels in synaptic nerve ending particles. J. Biol. Chem. 256, 8922–8927.

16 McNeal, E.T. and Daly, J.W. (1986) The sodium channel in membranes of electroplax. Binding of batrachotoxinin-A [^{3}H]benzoate to particulate preparations from electric eel (Electrophorus). Neurochem. Int. 9, 487–492.

17 Catterall, W.A. (1986) Molecular properties of voltage-sensitive sodium channels. Annu. Rev. Biochem. 55, 953–985.

18 Noda, M., Shimizu, S., Tanabe, T., Takai, T., Kayano, T., Ikeda, T., Takahashi, H., Nakayama, H., Kanaoka, Y., Minamino, N., Kangawa, K., Matsuo, H., Raftery, M.A., Hirose, T., Inayama, S., Hayashida, H., Miyata, T. and Numa, S. (1984) Primary structure of Electrophorus electricus sodium channel deduced from cDNA sequence. Nature 312, 121–127.

19 Noda, M., Ikeda, T., Kayano, T., Suzuki, H., Takeshima, H., Kurasaki, M., Takahashi, H and Numa, S. (1986) Existence of distinct sodium channel messenger RNAs in rat brain. Nature 320, 188–192.

20 Salkoff, L., Butler, A., Wei, A., Scavarda, N., Giffen, K., Ifune, C., Goodman, R. and Mandel, G. (1987) Genomic organization and deduced amino acid sequence of a putative sodium channel gene in Drosophila. Science 37, 744–749.

21 Salkoff, L., Butler, A., Hiken, M., Wei, A., Giffen, K., Ifune, C. and Mandel, G.A. (1986) Drosophila gene with homology to the vertebrate Na^+ channel. Soc. Neurosci. Abstr. 12, 1512.

22 Ohtsuka, E., Matsuki, S., Ikehara, M., Takahashi, Y. and Matsubara, K. (1985) An alternative approach to deoxyoligonucleotides as hybridization probes by insertion of deoxyinosine at ambiguous codon positions. J. Biol. Chem. 260, 2605–2608.

23 Wood, W.I., Gitschier, J., Lasky, L.A. and Lawn, R.M. (1985) Base composition-independent hybridization in tetramethylammonium chloride: A method for oligonucleotide screening of highly complex gene libraries. Proc. Natl. Acad. Sci. U.S.A. 82, 1585–1588.

24 Smith, C. and Salkoff, L. (1987) Interspecies comparison of the promoter region of the putative *Drosophila* sodium channel. Soc. Neurosci. Abstr. 13, 36.

25 Tanabe, T., Takeshima, H., Mikami, A., Flockerzi, V., Takahashi, H., Kangawa, K., Kojima, M., Matsuo, H., Hirose, T. and Numa, S. (1987) Primary structure of the receptor for calcium channel blockers from skeletal muscle. Nature 328, 313–318.

26 Loughney, K. and Ganetzky, B., personal communication.

27 Barnard, E.A. and Bilbe, G. (1987) Functional expression in the *Xenopus* oocyte of mRNAs for receptors and ion channels. In: Neurochemistry - A Practical Approach (A.J. Turner, H.S. Bachelard, eds.), pp. 243–270. IRL Press, Oxford.

28 Noda, M., Ikeda, T., Suzuki, H., Takeshima, H., Takahashi, T., Kuno, M. and Numa, S. (1986) Expression of functional sodium channels from cloned cDNA. Nature 322, 826–828.

29 Goldin, A.L., Snutch, T., Luebbert, H., Dowsett, A., Marshall, J., Auld, V., Downey, W., Fritz, L.C., Lester, H.A., Dunn, R., Catterall, W.A. and Davidson, N. (1986) Messenger RNA coding for only the α subunit of the rat brain Na channel is sufficient for expression of functional channels in *Xenopus* oocytes. Proc. Natl. Acad. Sci. U.S.A. 83, 7503–7507.

CHAPTER 42

Ion channel properties of insects susceptible and resistant to insecticides

D.B. Sattelle [1], C.A. Leech [1], S.C.R. Lummis [1], B.J. Harrison [1],
H.P.C. Robinson [1], G.D. Moores [2] and A.L. Devonshire [2]

Institute of Arable Crops Research: [1] Unit of Insect Neurophysiology and
Pharmacology, Department of Zoology, University of Cambridge, Downing Street,
Cambridge, CB2 3EJ, and [2] Rothamsted Experimental Station, Harpenden,
Herts AL5 2JQ, U.K.

Introduction

Several aspects of insect biology have proved directly susceptible to the actions of insecticides. These include respiration, cuticle formation and hormone action, but for the majority of insecticidally-active molecules synthesized to date the target organ is the insect nervous system [1]. For many years the enzymes for neurotransmitter synthesis and breakdown provided the major molecular targets. Recently, voltage-operated ion channels (VOCs), ligand-operated channels (LOCs) and membrane transport processes have emerged as candidate targets for the present generation of insecticides, together with many compounds currently under development. Fig. 1 summarizes the candidate ion channel targets of several classes of insecticidally-active molecules. In all cases there is a body of evidence pointing to a particular channel as the major site of action, but multiple sites of action have been reported. It is essential to distinguish between actions at the primary molecular target, and secondary effects consequent upon the primary insecticide–target interaction. In addition, the insecticide may interact with additional targets, but with lower affinity than that observed in the case of the primary site. Though it is possible to conceive of an insecticide with truly multiple sites of action, each of identical affinity, no case has yet been documented. Thus the concept of a primary target molecule has proved instructive in interpreting insecticide mode of action studies.

Resistance poses a long-term threat to the usefulness of insecticides, and includes any tolerance to a compound greater than that of the most sensitive reference (= susceptible) strain. It can develop under field conditions, due to excessive and continued application. Laboratory selection and cross-resistance studies can also result in the onset of resistance. The underlying mechanisms which give rise to resistance are diverse and sometimes extremely complex. They may involve changes in access and metabolism of the insecticide, but there are a number of cases for which some evidence has been provided of a possible change in the target site molecule itself. The present study reviews such evidence with reference to cyclodiene

564

RECEPTORS AND ION CHANNELS AS TARGETS FOR INSECTICIDES

Cockroach

Housefly

Nicotinic acetylcholine receptor	$Na^+K^+Ca^+$	Cartap(NTX)
		Nitromethylenes
GABA receptor	Cl^-	Cyclodienes
		Cyclohexanes
		Avermectins
Sodium channel	Na^+	Pyrethroids
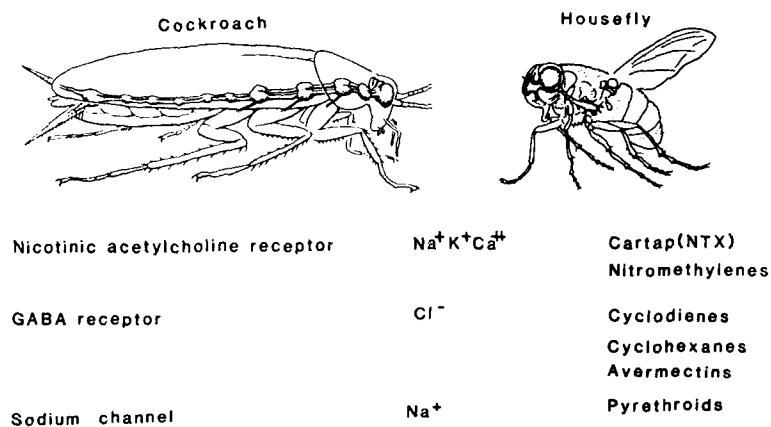
FIG 1 Putative ion channel targets of several classes of insecticides active on the insect nervous system.

Susceptible   Resistant

A

B

C

D

E
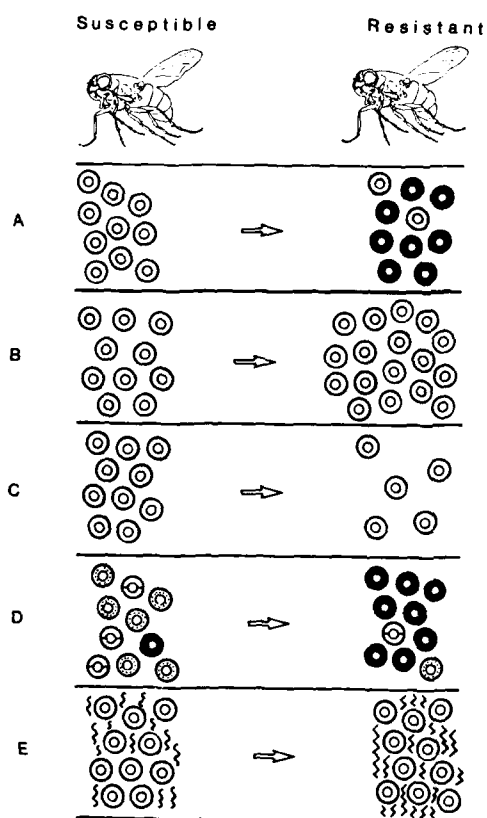
FIG 2 Schema*ic representation of some of the possible changes in ion channels and their membrane environment that could conceivably result in resistance. A: modification of some or all of the target channel. B, C: change in density of the target channel. D: change in the relative proportions of subpopulations of a particular class of channel—for example the increase in proportion of an inherently resistant subtype. E: a change in the membrane environment resulting in reduced sensitivity of the target molecule to its insecticide.

resistance in the cockroach *Blatella germanica*, and nicotine resistance in both the fruitfly *Drosophila melanogaster* and the tobacco horn worm moth *Manduca sexta*. In addition we discuss experimental approaches and preliminary results of our recently initiated investigation of pyrethroid and DDT knockdown resistance (kdr) in the housefly *Musca domestica*.

Prior to detailed consideration of the experimental evidence, some of the possible changes that could lead to resistance will be considered (Fig. 2). If metabolism and access can be eliminated and a single population of channels is envisaged, then changes in channel density, alterations in the channel structure or its lipid environment could conceivably result in resistance. However, if channel subclasses are present, then other possible explanations can be invoked. For example, inherent differences in sensitivity to insecticides may exist between channel subclasses. Hence, even with no change in overall channel density an alteration in the ratio of susceptible to resistant subclasses would be expected to modify the sensitivity of the nervous system to insecticides. If the insecticide is an agonist at its molecular target, then a reduced density of that particular class (or subclass) of sites will result in reduced sensitivity to the compound. By contrast, an insecticidal blocking action would be more effective if the target site density was reduced. No studies to date have tested all these possibilities for a particular ion channel target, but in three cases limited evidence has been accumulated.

GABA-activated chloride channels

γ-Aminobutyric acid (GABA) is a major inhibitory neurotransmitter in vertebrates and invertebrates [2–5]. A great deal of the interest in insect nervous system GABA receptors has stemmed from the finding that insecticidally-active molecules including α-cyano-containing pyrethroids [6] appear to be effective at this membrane site in the mammalian central nervous system (CNS). Recently, evidence has emerged for pharmacological differences between insect and vertebrate CNS $GABA_A$ receptors. The vertebrate $GABA_A$ receptor is linked directly to a chloride channel [7]. Bicuculline is a specific antagonist of vertebrate $GABA_A$ receptors, and binds to the same site as the natural ligand [8]. The $GABA_B$ receptor is less well understood, but baclofen is a specific agonist [9], and there is evidence for a quite separate mechanism of activation.

A saturable specific component of binding has been demonstrated for [³H]GABA and [³H]muscimol in nervous system extracts of several insect species. These sites in the cockroach [10,11], the locust [12,13], and the honeybee [14] differ from the GABA binding sites characterized in vertebrates, as they are inhibited neither by bicuculline nor by baclofen. Specific [³H]GABA binding sites are located in the neuropile of insect ganglia, consistent with a synaptic role for this putative receptor [10]. The recent discovery that a GABA-activated $^{36}Cl^-$ uptake into microsacs prepared from cockroach (*Periplaneta americana*) CNS is bicuculline-insensitive [15], and the finding that a GABA response of an identified neurone from the same tissue is not blocked by bicuculline [16], confirms a functional role in insects for a bicuculline-insensitive GABA-activated Cl^- channel.

The mammalian CNS GABA receptor/chloride channel molecule contains binding sites for benzodiazepines such as [³H]flunitrazepam [17], bicyclophosphates such as [³⁵S]*t*-butylbicyclophosphorothionate (TBPS) [18,19] and [³H]dihydropicro-

566
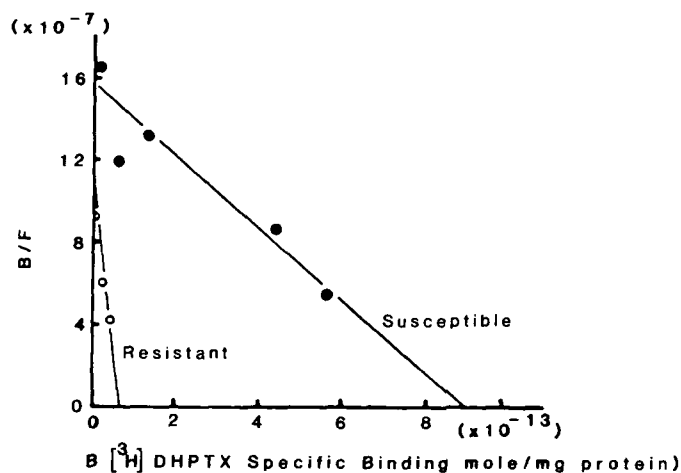
FIG 3   Dihydropicrotoxinin binding sites in susceptible and cyclodiene-resistant cockroaches. Scatchard analysis of [³H]dihydropicrotoxinin binding to CNS membrane preparations from two strains of the cockroach *Blatella germanica*: dieldrin-susceptible CSMA (●), and dieldrin-resistant Lpp (○) strain. Differences in K_d and B_{max} are evident. (From Ref. 24.)

toxinin [20]. Similar sites have been identified in insect CNS, though the results from several laboratories indicate that both the benzodiazepine site [11,21] and the TBPS site [22] differ in their pharmacology from the corresponding sites in vertebrate CNS. A [³H]dihydropicrotoxinin receptor has been identified in the insect nervous system [23,24]. These authors initiated detailed studies of the interactions of cyclodiene insecticides with GABA receptors.

Both mammalian and insect GABA-activated Cl⁻ channels appear to be sensitive to cyclodiene insecticides based on the results of radioligand binding experiments [23]. Recently, cyclodienes have been shown to block functional GABA-activated chloride channels on an identified cockroach motor neurone (Wafford and Sattelle, unpublished observations). The binding sites for [³H]dihydropicrotoxinin in cockroach and vertebrate central nervous tissue are blocked by a variety of cyclodienes [23].

Of particular interest has been the finding that when the dissociation constant (K_d) and the saturation level (B_{max}) of the picrotoxinin binding site are compared for the susceptible CSMA strain and the cyclodiene-resistant (Lpp) strain of *Blatella germanica*, striking differences are detected. The data indicate that the binding site in the nervous system of the resistant strain has only one tenth the affinity of the corresponding site in the susceptible insects. Also, the number of receptors appears to be reduced in CNS membranes prepared from the resistant strain (see Ref. 24).

These findings are illustrated in Fig. 3, and the hypothesis derived from binding studies that a modified GABA receptor/chloride channel complex is present in cyclodiene-resistant cockroaches should now prove testable using a range of experimental techniques. These will include radioligand binding methods employing a range of receptor/channel ligands. This approach may help to pinpoint an altered region of the receptor/channel molecule, and/or any change in receptor density. Physiological experiments will enable a test of whether or not there are functional

differences in GABA receptor molecules from susceptible and resistant strains of a particular species.

Nicotinic acetylcholine receptor-activated cation channel

The well-characterized vertebrate peripheral nicotinic acetylcholine receptor is a multimeric protein with 4 subunits in the molar ratio $\alpha_2\beta\gamma\delta$ [25,26]. The complete amino acid sequence of all four *Torpedo* subunits has been deduced from their complementary DNAs [27–30]. α-Bungarotoxin has proved to be a selective probe for muscle and muscle-derived nicotinic receptors. This snake toxin will bind to certain neuronal nicotinic receptors such as those of the chick optic tectum [31], but there exist neuronal nicotinic receptors that are insensitive to this toxin [32,33]. K-Bungarotoxin blocks all neuronal nicotinic receptors tested to date, but is relatively ineffective on muscle-derived nicotinic receptors [34]. Whiting and Lindstrom [33] have recently immune affinity-purified neuronal receptors from chicken and rat that are clearly distinct from brain α-bungarotoxin binding sites. The receptor purified from chick brain using monoclonal antibody (mAb) 270 contained two subunits and possible structures are $\alpha_2\beta_2$ or $\alpha_3\beta_2$. Although distinct from muscle receptors, those neuronal nicotinic receptors sampled so far at the DNA level are homologous, though the level of homology between brain and muscle receptors of the same animal is considerably less than that observed between nicotinic receptor genes expressed in the electric organ of *Torpedo* and those expressed in mammalian or avian muscle [31].

An insect neuronal nicotinic receptor has been characterized using a range of physiological, biochemical and immunological methods [35]. Insect central nervous tissue provides a rich source of neuronal nicotinic receptors for which a postsynaptic role has been identified [36]. This is the only neuronal nicotinic receptor discovered to date that is sensitive to both α-bungarotoxin and K-bungarotoxin [36–39]. It is a multimeric protein with a sedimentation coefficient of 9–10 S. Though the subunit composition has not been established, a M_r 65,000 subunit is present in the affinity-purified receptor from the CNS of *Periplaneta americana* and *Locusta migratoria* [12,35]. It is the first neuronal nicotinic receptor for which the α-bungarotoxin-binding site has been shown to be a constituent of a functional postsynaptic receptor [36], and the first to be reconstituted into a planar bilayer [40].

Recently, molecular cloning techniques have provided evidence for nicotinic acetylcholine receptor genes in the locust *Schistocerca gregaria* [41,42]. Poly(A)$^+$ RNA was purified from locust embyros. This mRNA was used to construct a λgt10 cDNA library. Screening the library under low stringency, using a 400-basepair fragment, yielded cDNA clones with sequence homology to a *Drosophila* putative neuronal nicotinic receptor. Expression studies using the *Xenopus* oocyte system have yielded clearly defined electrophysiological responses to bath-applied nicotine in cells injected with purified insect mRNA [42].

Nicotine was one of the earliest commercial insecticides [43], and, though it has been superceded, a number of insecticides appear to exert their primary action at insect neuronal nicotinic acetylcholine receptors. These include cartap, which is converted in the insect to the active compound nereistoxin [44], and nicotinoids [43]. With recent advances resulting from the application of molecular biology to the
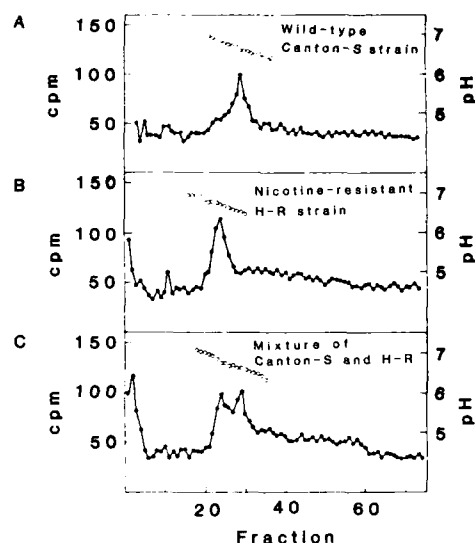
FIG 4 Densitometric traces showing isoelectric focusing of the acetylcholine receptor-α-bungarotoxin complex from wild-type Canton-S and nicotine-resistant HR strains of *Drosophila*. Extracts were prepared and run on isoelectric focusing gels: (A) Canton-S strain alone; (B) nicotine-resistant H-R strain alone; (C) mixture of extracts of Canton-S and HR strains. (From Ref. 46.)

insect nicotinic receptor, it seems likely that in the near future the complete amino acid sequence of the first insecticide ion channel target site will be known.

Resistance to nicotine has been demonstrated in insects. Though the existence of a nicotine-resistant mutant of *Drosophila melanogaster* was first reported by Lindsley and Grell [45], the most detailed study of nicotinic acetylcholine receptors in nicotine-resistant insects was performed by Hall et al. [46]. These authors exposed Canton-S wild type *Drosophila* to a concentration (3.0 mM) of nicotine in the culture medium that killed 96% of the Canton-S strain. One of the eight resistant strains that Hall et al. identified was designated HR (isolated from Hikone-R wild type stock) and 50% of this resistant strain survived when exposed to 3.0 mM nicotine.

In order to identify resistant strains with modified receptors, Hall and co-workers subjected a solubilized receptor-[125I]α-bungarotoxin complex to isoelectric focusing. As shown in Fig. 4, whereas the receptor-toxin complex in extracts from the Canton-S strain focused as a single peak with an isoelectric point of 6.60, the receptor-toxin complex from a nicotine-resistant HR strain focused as a single peak at pH 6.69. In this way a hereditary alteration in the structure of the acetylcholine receptor was identified.

As the authors pointed out, not all nicotine-resistant strains would be expected to affect the structure of the nicotinic acetylcholine receptor. Alterations in components involved in nicotine metabolism, permeability and membrane environment of the receptor/channel molecule could also conceivably produce nicotine resistance. Of the eight nicotine-res'tant strains tested, three (including the resistant HR strain), reveal shifts in iso-lectric point relative to Canton-S. The isoelectric focusing

variants represent either mutations in structural genes coding for the polypeptide subunits of the receptor or mutations in genes coding for enzymes which modify the receptor complex.

Reciprocal crosses between strains indicated that the gene controlling the isoelectric point shift segregates with the X-chromosome (cf. Ref 47). The major nicotine-resistance factor in the resistant stock was also X-linked, indicating that gene(s) on the X-chromosome affect receptor structure. Mapping isoelectric focusing point variants will enable determination of both the number and gene location of loci affecting receptor structure. Insects that feed on the tobacco plant *Nicotiana tobaccum* protect the nervous system from the adverse effects of nicotine ingestion. In the tobacco horn worm *Manduca sexta*, Morris [48] has described excretion and detoxification mechanisms, but the possibility cannot yet be ruled out that the neuronal nicotinic acetylcholine receptor of nicotine-resistant insects is less sensitive to nicotine than the corresponding receptor/channel molecules of susceptible species.

Recently, Trimmer and Weeks [49] have shown, for an identifiable motor neurone in the CNS of larval *Manduca sexta*, that nicotine is less effective than it is on an identified adult cockroach motor neurone [37]. More physiological data are needed to establish how widespread is this nicotine insensitivity among neuronal nicotinic receptors of *Manduca sexta*. It will be of considerable interest to probe the cDNA library of a nicotine-resistant insect with *Drosophila* and locust receptor probes, provided it can be established that resistance involves a reduced sensitivity at the receptor level.

Voltage-activated sodium channels

The voltage-sensitive sodium channel was the first ion channel to be purified and consists of a glycoprotein with an apparent molecular weight of 260,000 (the α subunit) and one or two additional glycoprotein subunits with apparent M_r 33,000–38,000, designated the β-subunits [50]. Several toxins act at distinct sites on this membrane molecule. Saxitoxin and tetrodotoxin bind to neurotoxin receptor site 1 and block sodium ion translocation. Batrachotoxin, veratridine and other lipid soluble toxins bind at neurotoxin receptor site 2, resulting in prolonged activation of the channel. Certain α scorpion toxins and sea anemone toxins bind at neurotoxin receptor site 3 and suppress channel inactivation. By contrast β scorpion toxins are active at a separate site (neurotoxin receptor site 4) and alter sodium channel activation. Toxins from the dinoflagellate *Ptychodiscus brevis* are active at neurotoxin receptor site 5 producing repetitive action potentials.

Full length cDNA clones have been identified for this channel in *Electrophorus* electric tissue. The inferred sequence consists of 1829 residues with a total M_r of 208,321 [80]. Cloning the rat brain sodium channel was pursued by Auld et al. [51] who used antibodies to identify cDNA clones in rat brain expression libraries in the bacteriophage vector λgt11. The amino-acid sequence specified by the clones was highly homologous to the sequence of the electroplax sodium channel. Sequence data reveal four internally homologous domains which suggests gene duplication. The structural motif proposed for the transmembrane channel of the voltage-gated sodium channel is analogous to that proposed for multi-subunit, receptor-activated channels—a quasisymmetric array of homologous subunits lining a central pore.

Vertebrate sodium channels appear to be polymorphic. At least three similar genes are expressed in rat brain tissue [79]. Also, subclasses of sodium channels can be identified by their sensitivity or resistance to neurotoxins [52,53]. Using neuroblastoma cells, cell lines with missing or altered channels can be identified. Cell lines resistant to the toxic actions of veratridine and scorpion toxin are either sodium channel deficient or, as in the case of scorpion-toxin resistant cells, they are functionally indistinguishable from susceptible cells, but nevertheless exhibit reduced affinity for the toxin. These cell lines offer experimental approaches to mutational analysis of sodium channel function.

Another recent advance, with potential for molecular genetic approaches to relating channel structure to function is the sequencing of a putative *Drosophila* sodium channel by Salkoff et al. [54]. This shows considerable homology with the vertebrate sodium channels already described. It too contains four homologous domains. At least two similar genes are expressed in *Drosophila* nervous system [55]. Electrophysiological studies on another insect (*Periplaneta americana*) reveal the presence of two classes of sodium channel in the axonal membrane based on their sensitivity to tetrodotoxin [56].

A number of *Drosophila* genes whose mutation confers a behavioural phenotype of temperature-sensitive paralysis have been suggested as candidates for the sodium channel structural gene. These include no action potential (nap^{ts}), paralysis (para^{ts}), temperature-induced paralysis (tip-E^{ts}), and seizure (sei^{ts}) [28]. Mutations at tip-E^{ts} and sei^{ts} reduce neuronal sodium current density by 40–60% [57]. The *Drosophila* sodium channel gene maps to the right arm of the second chromosome at a position (60 D–E) that is not coincident with any known behavioural mutation reported to date [55].

In our own studies of insect sodium channels we have begun by examining an insect tissue well-suited to both electrophysiological and radioligand binding experimental approaches. The nerve cord of the cockroach *Periplaneta americana* contains uniquely identifiable giant interneurones which can be isolated, voltage-clamped and employed in pharmacological experiments [58]. In this way the sensitivity of cockroach sodium channels to saxitoxin has been demonstrated [59]. Complete block by saxitoxin of inward sodium current in the cockroach giant axon is illustrated in Fig. 5. Thus, saxitoxin binds to functional sodium channels in insect nervous tissue, and one molecule of toxin is required to block a single sodium channel [59].

Membrane extracts prepared from *Periplaneta* nervous system contain a saturable component of specific [^{3}H]saxitoxin binding. Scatchard analyses of the binding data yield a K_d of 2.2 nM, a value similar to that estimated in physiological studies. The specific binding component is blocked by saxitoxin and tetrodotoxin, but not by either veratridine or deltamethrin (Fig. 6). Radioligands for other sites on the sodium channel need to be tested on this preparation, but it is already evident that a multidisciplinary experimental approach to the investigation of insect sodium channels is feasible.

There is now considerable evidence that insect sodium channels are the primary molecular target of pyrethroid insecticides [60]. Cockroach giant axons have been used to assess the actions of a range of pyrethroids on voltage-dependent sodium channels [61,62]. Pyrethroids lacking an α-cyano-3-phenoxybenzyl moiety induce long lasting afterpotentials that follow the axonal action potential. No major, long-term depolarization of the axon is detected. By contrast α-cyano-containing
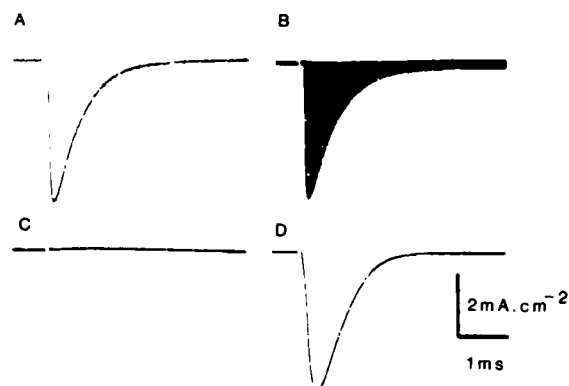
FIG 5 Complete block of sodium current by saxitoxin in the giant axon of the cockroach *Periplaneta americana*. A: sodium current in normal saline (in the presence of 5.0×10^{-4} M 4-aminopyridine. B: progressive abolition of sodium current during 5 min exposure to saxitoxin. Sodium current traces are superimposed. C: complete block of all membrane currents in the presence of saxitoxin and 4-aminopyridine. D: sodium current after 20 min wash in saline containing 4-aminopyridine. Holding potential = -60 mV.

Pharmacology of *Periplaneta* nerve cord [^{3}H]-STX binding site
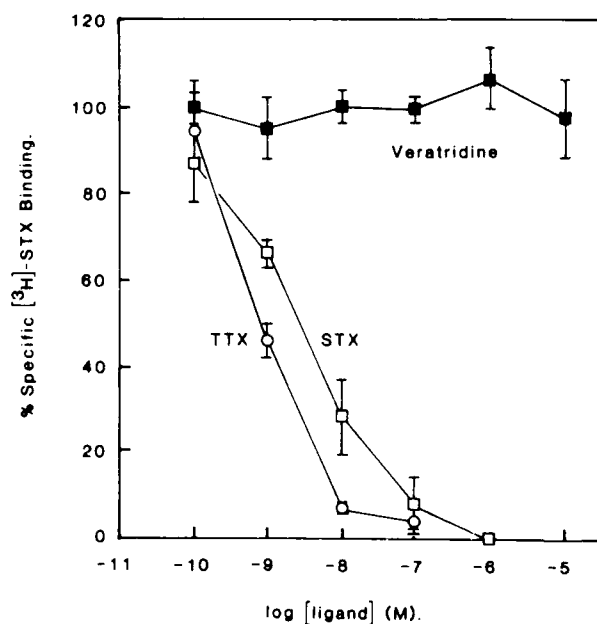
FIG 6 Pharmacology of *Periplaneta* nerve cord [^{3}H]saxitoxin binding site. Inhibition by various test ligands of the specific component of [^{3}H]saxitoxin binding to *Periplaneta* nerve cord extracts. TTX, tetrodotoxin; STX, saxitoxin.

572

(A) Control   (B) 12 min   (C) 20 min   (D) 30 min

0·2μA|
2 ms

(E)   (F)

5nA| 5nA|
5s   1 Hz   30 s

10 Hz
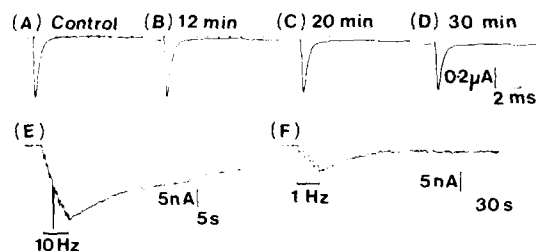
FIG 7   Effects of deltamethrin on voltage-activated sodium channels in the isolated axon of the cockroach *Periplaneta americana*. A: control in normal saline shows the sodium current recorded at a holding potential (E_h) of -60 mV (dotted line indicates zero current) and the peak inward sodium current associated with a 5-ms voltage-clamp pulse to $E_m = -10$ mV. B–D: after application of deltamethrin for, 12, 20 and 30 min, respectively, a reduction in the amplitude of the peak inward sodium current is observed, together with the progressive appearance of a maintained inward sodium current. In D, this current is 80 nA, corresponding to 12.5% of the peak inward current recorded in control experiments. E, F: slower sweep speed, higher gain recordings of sodium currents. The currents are recorded after bursts of voltage pulses (5 ms duration, to $E_m = -10$ mV) at the frequencies indicated. Dashed lines correspond to inward sodium currents of 50 nA in E, and 58 nA in F. Recordings are obtained 18 min (E) and 24 min (F) after application of 2.0×10^{-6} M deltamethrin. The slow (and incomplete) decline of these burst-induced inward sodium currents can be seen. Holding potential (E_h) = -60 mV.

pyrethroids, such as deltamethrin, progressively depolarize the axon leading to conduction block. In voltage-clamp experiments both classes of compound give rise to a maintained inward sodium current (Fig. 7) that is blocked by saxitoxin.

The simplest interpretation of these findings is that all pyrethroids modify the sodium channel but with different kinetics. Support for this view comes from the finding of Lund and Narahashi [63] that intermediate states of the channel can be detected under the influence of pyrethroids. Although other actions of pyrethroids have been reported on GABA receptors, nicotinic acetylcholine receptors, calcium channels and Ca^{2+}-ATPases, much higher concentrations are required compared to those needed to modify sodium channels [60]. The main action of pyrethroids appears to result from the stabilization of an open state of sodium channels. Recent patch clamp studies on NE115 neuroblastoma cells provide a direct demonstration of increased duration of channel opening in the presence of pyrethroids [64].

A well-characterized example of insecticide resistance is knockdown resistance (kdr) to DDT and pyrethroids in the housefly *Musca domestica*. Milani [65] and Farnham [66] isolated the kdr factor genetically and showed it to be controlled by a recessive gene on autosome 3. Alterations in metabolism do not appear to account for the differential sensitivity to pyrethroids of susceptible and resistant strains (see Ref. 67). Chang and Plapp [68,69] proposed, based on radiolabelled insecticide binding studies, that a reduced sodium channel density could account for insensitivity to pyrethroids in kdr houseflies. In this context, it is of interest to note that Kasbekar and Hall [70] found that the nap^{ts} mutation, in which sodium channels are reduced in density, confers pyrethroid insensitivity on sodium channels of *Drosophila melanogaster* [70].

We have therefore examined sodium channel properties in Cooper [71], a susceptible reference strain of *Musca domestica* and 530 [72], a strain homozygous

for the super kdr gene, extensively backcrossed into the Cooper background. Heads were prepared by freezing the flies with solid CO_2, and shaking through a 10 mesh brass sieve which allows the passage of heads, male abdomens, legs and wings [73]. A second 16 mesh sieve retains a head-enriched fraction that consists of approximately 50% head/debris (w/w). Final sorting of the heads is then achieved manually over solid CO_2, and, though time-consuming, this provides an uncontaminated preparation, which is essential if sodium channel densities are to be compared between strains.

Membranes are prepared from housefly heads by homogenization in buffer (HEPES, 20 mM, 0.25 M sucrose) containing the protease inhibitors EDTA and PMSF. The homogenate is then subjected to differential centrifugation and washing in assay buffer (NaCl 126 mM, KCl 2 mM, $CaCl_2$ 0.2 mM, sucrose 36 mM and HEPES 5 mM, pH 7.0). For determination of total [^{3}H]saxitoxin binding, extracts (in triplicate) containing a known amount of protein (of the order of 0.2 mg/ml) are incubated with [^{3}H]saxitoxin (0.3–20 nM) in a final volume of 100 μl assay buffer.

A   Susceptible

B   Resistant
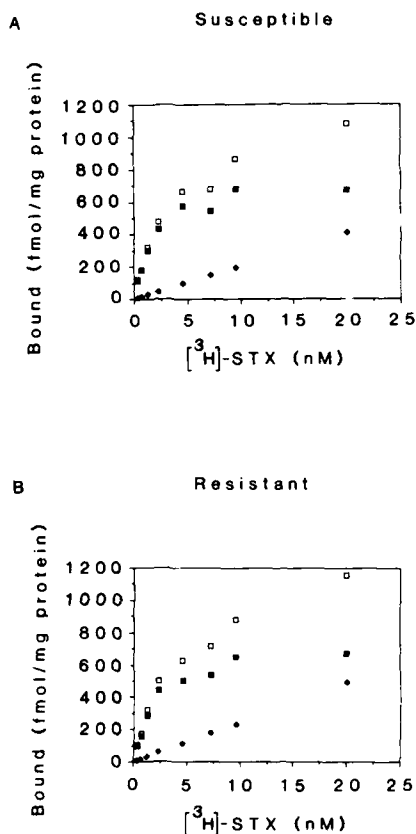
FIG 8   [^{3}H]Saxitoxin binding to membranes prepared from heads of houseflies (*Musca domestica*). Binding of [^{3}H]saxitoxin plotted as a function of the concentration of radioligand. Data show total (□), specific (■) and non-specific (◇) components of [^{3}H]saxitoxin binding. Data are compared for the susceptible (Cooper) strain (A) and a super kdr (530) resistant strain (B).

	EC50	KD (nM)	Bmax (fmol/mg protein)
Musca domestica (heads) Cooper	–	1.2 ± 0.2	337 ± 25
Musca domestica (heads) kdr 530	–	1.0 ± 0.1	313 ± 21
Periplaneta americana	3.0	2.2 ± 0.5	1290 ± 140
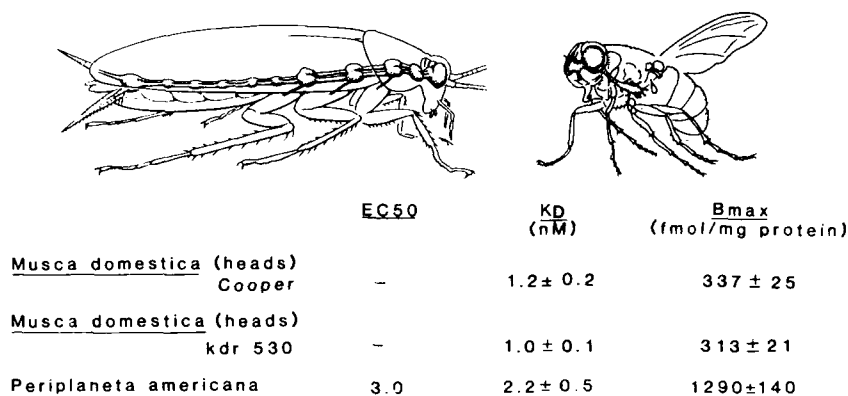
FIG 9 Summary of K_d and B_{max} values obtained in [^{3}H]saxitoxin binding experiments on housefly (*Musca domestica*) head membranes and cockroach (*Periplaneta americana*) nerve cord membranes. An EC_{50} value estimated from electrophysiological studies on cockroach giant axons is included. Data for *Musca* is averaged from 5 independent experiments. Data for *Periplaneta* is averaged from 3 independent experiments. No significant difference in the binding is detected between the two housefly strains when [^{3}H]saxitoxin binding is compared in this way.

To determine non-specific binding, parallel samples are incubated in an identical solution containing in addition 10 μM unlabelled saxitoxin or tetrodotoxin. Following a 60-min incubation at 0°C, the samples are filtered on a Brandel Cell Harvester through prewetted GF/B filter. After three washes with ice-cold assay buffer (2 ml), the ^{3}H on the filters is determined by scintillation counting in Liquiscint scintillation fluid.

Fig. 8 shows the results for one such assay and the results from 5 independent experiments are summarized in Fig. 9. There is no significant difference in the affinity (K_d) or the number of binding sites (B_{max}) between the super kdr (530) and susceptible (Cooper) strain of houseflies. This is in contrast to a report by Rossignol and Pipenberg [74] who suggest there are a 40% fewer [^{3}H]saxitoxin binding sites in kdr flies compared to susceptibles, but in agreement with the findings of D.M. Soderland and colleagues (this volume), who also find no change in either K_d or B_{max} when comparing sodium channels of susceptible houseflies and a resistant 538ge strain homozygous for the kdr trait. It is therefore necessary to examine other properties of sodium channels in order to account for this type of resistance.

To study this further, intracellular recordings have been attempted from giant fibres in the cervical connective of the Cooper strain (Fig. 10). The preparation is slightly modified from that described by Bacon and Strausfeld [75] so that the entire cervical connective and part of the thoracic ganglion is exposed. This more extensive dissection disrupts the tracheal supply to the central nervous system, but preparations remain viable for several hours. The connective is supported either on a chlorided silver plate or on a mound of grease injected into the thoracic cavity. The nerve cord is perfused with a fly saline (based on that of O'Shea and Adams [76]) and impaled with electrodes filled with 1.0 M KCl buffered to pH 7.4 with 5 mM TES. Under these conditions, resting potentials of up to −70 mV are obtained. Action potentials can be recorded both from neurones which are spontaneously
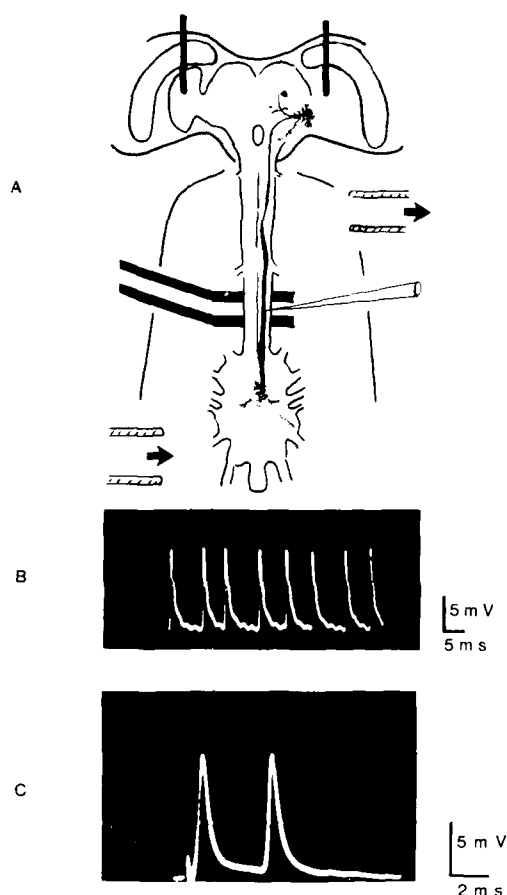
FIG 10 A: schematic representation of the preparation used for intracellular recording from *Musca domestica*. The thoracic wall is removed to reveal the cervical connective and part of the thoracic ganglion. The connective is supported on chlorided silver hooks which also serve as a ground electrode. The thoracic cavity can be perfused with saline or test solution. Two fine pins located in the brain permit electrical stimulation. B: spontaneous action potentials recorded from an axon in the cervical connective are shown. Resting potentials of up to −60 mV can be obtained, though most are lower than this. C: action potentials evoked by electrical stimulation across the brain. Such low amplitude action potentials can be blocked by tetrodotoxin (data not shown).

active and from axons which fire in response to electrical stimulation. Bacon and Strausfeld [75] report that the giant fibres in *Musca* are not spontaneously active. These impalements exhibit poor stability and normally cannot be maintained for long periods, but on one occasion a cell with spontaneous activity was monitored for 30 min and the action potentials were blocked (block was not reversible) by tetrodotoxin suggesting that the spike is sodium dependent in at least some axons of the fly connective. Technical difficulties of maintaining such recordings do not permit routine pharmacological experiments.
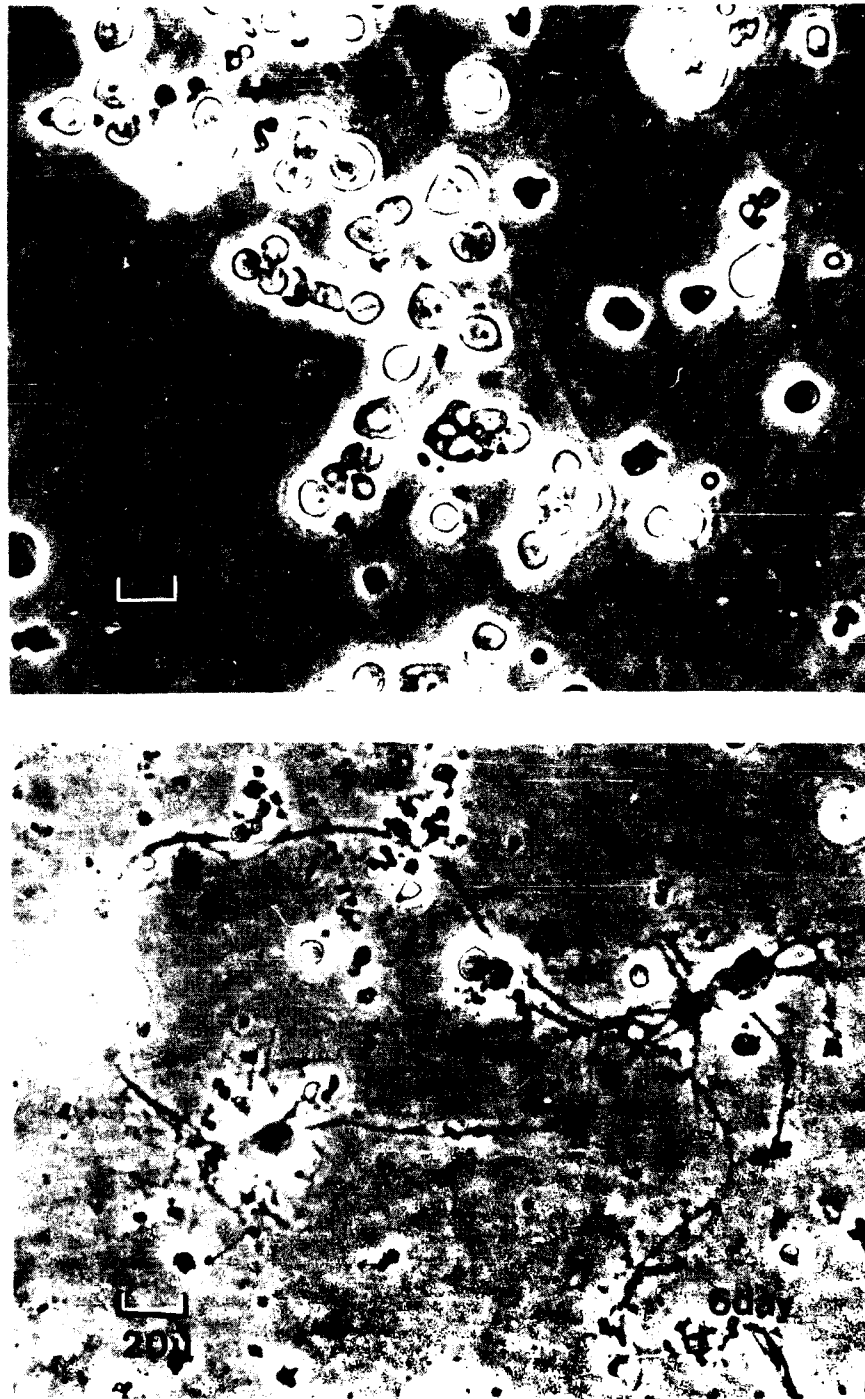
FIG 11 Primary culture of dissociated embryonic tissue from *Musca domestica* (Cooper strain). Upper photomicrograph shows cells 2 h after dissociation. Even at this stage, some signs of cytoplasmic extension are evident. Lower photomicrograph shows 6-day-old neurones with extensive branching of processes. Scale bars equal 20 μm.

A

$E_{rest}{}^{+40}$ mV

$E_{rest}{}^{-30}$ mV

1pA

20ms

Rat SG neurone

B

$E_{rest}{}^{+40}$ mV

$E_{rest}{}^{-30}$ mV

1pA

20ms
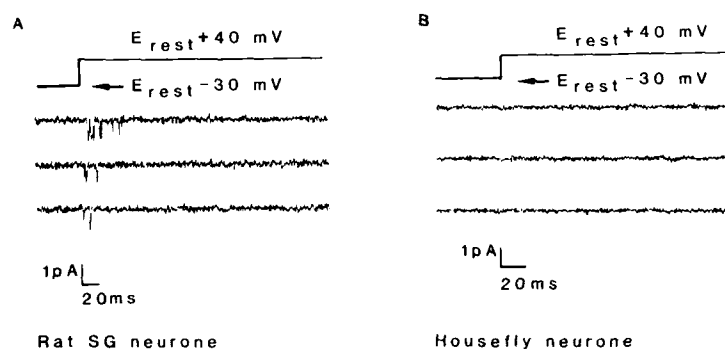
Housefly neurone

FIG 12   The patch-clamp recording technique has been deployed in an attempt to record single sodium channels in cultured rat sympathetic ganglion (SG) neurones (A) and housefly neurones (B). Though sodium channels can be recorded readily ..om the vertebrate neurones tested, to date it has proved more difficult to detect sodium channels on housefly neurones.

Using the patch-clamp technique attempts have been made to record single channel currents in freshly dissociated neurones and primary cultures from *Musca* neuronal tissue. These experiments have been performed on neuronal cell bodies. So far, no evidence has been obtained for the presence of potential-dependent Na-channels (Fig. 12). This result is perhaps not too surprising, at least for freshly dissociated cells, as many insect neuronal cell bodies are not normally excitable. However, some cells which are normally inexcitable in vivo, for example, the cell body of the squid giant neurone, develop an axon-like sodium current over a few days in primary culture [77]. Our experiments on primary cultures of *Musca* neurones, maintained for up to two weeks, have so far failed to detect potential-dependent Na$^+$-channels. It has recently been shown that cell bodies of *Drosophila* neurones can be induced to express Na$^+$-channels by adding insulin to the culture medium and experiments are in progress to see whether this also applies to neurones from *Musca*. A second possibility is that Na$^+$-channels are present in the cell body but that activation of the channels is not voltage-dependent, as in glial cells [78]. These channels can be opened by combinations of neurotoxins and resulting changes in membrane potential and/or ion fluxes can be measured. These approaches will also be attempted on cultures of *Musca* neurones.

Conclusions

At present we have few clues as to the underlying molecular changes that account for the nerve insensitivity accompanying resistance to certain insecticides; recent advances in cellular and molecular neurobiology offer experimental approaches to this problem. Electrophysiological techniques, such as patch-clamp, permit detailed analysis of ion channel properties such as unitary conductance, and duration of channel opening and closing. In combination with radioligand binding and ion flux measurements such methods will enhance our present understanding of ion channel-insecticide interactions.

Elucidation of the complete nucleotide sequence and hence amino acid sequence for insect ion channels will provide insecticide chemists with a better-defined

578
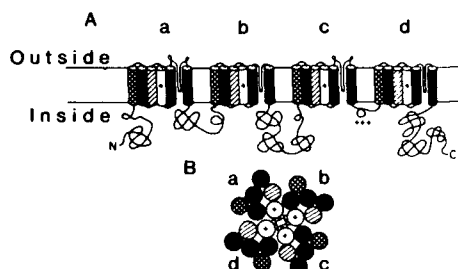
FIG 13   Sodium channel transmembrane topology. A: four homology domains spanning the membrane are displayed linearly. Membrane spanning segments (S1 and S6) are represented as cylinders. The arrangement of transmembrane segments is viewed in the direction perpendicular to the membranes. The central pore is shown lined by negative charges. Based on Refs. 80 and 54.

'target' molecule (Fig. 13) and may therefore accelerate rational design of novel compounds. Analysis of mutants offers experimental approaches to molecular dissection of structure–function relations within the ion channel molecule. This should prove especially useful in the case of mutations responsible for insecticide resistance.

Acknowledgements

References

1 Baillie, A.C. (1985) The Biochemical mode of action of pesticides. In: Recent Advances in the Chemistry of Insect Control (N.F. Janes, ed.) pp. 1–25. Royal Society of Chemistry, London.

2 Kuffler, S.W. and Edwards, C. (1965) Mechanisms of Gamma aminobutyric acid (GABA) action and its relation to synaptic inhibition. J. Neurophysiol. 21, 589–610.

3 Usherwood, P.N.R. and Grundfest, H. (1965) Peripheral inhibition in skeletal muscle of insects. J. Neurophysiol. 28, 497–518.

4 Otsuka, M., Iversen, L.L., Hall, Z.W. and Kravitz, E.A. (1966) Release of gamma-aminobutyric acid from inhibitory nerves of lobster. Proc. Natl. Acad. Sci. U.S.A. 56, 1110–1115.

5 Roberts, E., Krause, D.N., Wong, E. and Mori, E. (1976) Different efficacies of d and l amino hydroxybutyric acids in GABA receptor and transport test systems J. Neurosci. 1, 132–140.

6 Lawrence, L.J. and Casida, J.E. (1984) Interactions of lindane, toxaphene and cyclodienes with the brain specific t-butylbicyclophosphorothionate receptor. Life Sci. 35, 171–178.

7 Enna, S.J. and Gallagher, J.P. (1983) Biochemical and electrophysiological characteristics of mammalian GABA receptors. Int. Rev. Neurobiol. 24, 181–212.

8 Olsen, R.W. (1981) GABA-benzodiazepine receptor interactions. J. Neurochem. 37, 1–13.

9 Simmonds, M.A. (1983) Multiple GABA receptors and associated regulatory sites. Trends Neurosci. 6, 279–281.

10 Lummis, S.C.R. and Sattelle, D.B. (1985) Insect central nervous system γ-aminobutyric acid receptors. Neurosci. Lett. 60, 13–18.

11 Lummis, S.C.R. and Sattelle, D.B. (1986) Binding sites for [^{3}H]GABA, [^{3}H]flunitrazepam and [^{35}S]TBPS in insect CNS. Neurochem. Int. 9, 287–293.

12 Breer, H. and Heilgenberg, H. (1985) Neurochemistry of GABAergic activities in the central nervous system of Locusta migratoria. J. Comp. Physiol. A 157, 343–354.

13 Lunt, G.G., Robinson, T.N., Knowles, W.P. and Olsen, R.W. (1985) The identification of GABA receptor binding sites in insect ganglia. Neurochem. Int. 7, 751–754.

14 Abalis, I.M. and Eldefrawi, A.T. (1986) [^{3}H] Muscimol binding to a putative GABA receptor in honeybee brain and its interaction with avermectin B_1a. Pestic. Biochem. Physiol. 25, 279–287.

15 Wafford, K.A., Sattelle, D.B., Abalis, I., Eldefrawi, A.T. and Eldefrawi, M.E. (1987) γ-Aminobutyric acid-activated $^{36}Cl^-$ influx: a functional in vitro assay for CNS γ-aminobutyric acid receptors of insects. J. Neurochem. 48, 177–180.

16 Sattelle, D.B., Pinnock, R.D., Wafford, K.A. and David, J.A. (1987) GABA receptors on the cell body membrane of an identified insect motor neurone Proc. R. Soc. Lond. Ser. B. 232, 443–456.

17 Braestrup, C. and Squires, R.F. (1977) Specific benzodiazepine receptors in rat brain characterized by high-affinity [^{3}H] diazepam binding Proc. Natl. Acad. Sci. U.S.A. 74, 3805–3809.

18 Squires, R.F., Casida, J.E., Richardson, M. and Saederup, E. (1983) [^{35}S]t-Butylbi-cyclophosphorothionate binds with high affinity to brain specific sites coupled to γ-aminobutyric acid A and ion recognition sites. Mol. Pharmacol. 23, 326–336.

19 Supavilai, P. and Karobath, M. (1984) [^{35}S]t-Butylcyclophosphoro-thionate binding sites are constituents of the γ-amino- butyric acid and benzodiazepine receptor complex. J. Neurosci. 4, 1193–1200.

20 Leeb-Lundberg, F. and Olsen, R.W. (1980) Picrotoxin binding as a probe of the GABA postsynaptic membrane receptor-ionophore complex. In: Psychopharmacology and Biochemistry of Neurotransmitter Receptors (H.I. Yamamura, R.W. Olsen, E. Usdin, eds.) pp. 593–606. Elsevier/North Holland, New York.

21 Robinson, T., MacAllan D., Lunt, G.G. and Battersby, M. (1987) γ-Aminobutyric acid receptor complex of insect CNS: characterization of a benzodiazepine binding site. J. Neurochem. 47, 1955–1962.

22 Cohen, E. and Casida, J.E. (1986) Effects of insecticides and GABAergic agents on a housefly [^{35}S]t-butylbicyclophosphorothionate binding site. Pestic Biochem. Physiol. 25, 63–72.

23 Matsumura, F. and Ghiasuddin, S.M. (1983) Evidence for similarities between cyclodiene type insecticides and picrotoxinin in their action mechanisms. J. Environm. Sci. Health B18, 1–14.

24 Matsumura, F., Tanaka, K. and Ozoe, Y. (1987) GABA-related systems as targets for insecticides. In: Sites of Action of Neurotoxic Pesticides, ACS Symposium Series 356 (R.M. Hollingworth, M.B. Green, eds.) pp. 44–70. American Chemical Society, Washington DC.

25 Conti-Tronconi, B.M. and Raftery, M.A. (1982) The nicotinic cholinergic receptor: correlation of molecular structure with functional properties. Ann. Rev. Biochem. 51, 491–530.

26 Takai, T., Noda, M., Mishina, M., Shimizu, S., Furutani, Y., Kayano, T., Ikeda, T., Kubo, T., Takashima, H., Takahashi, T., Kuno, M. and Numa, S. (1985) Cloning, sequencing and expression of cDNA for a novel subunit of acetylcholine receptor from calf muscle. Nature (Lond.) 315, 761–764.

27 Noda, M., Takahashi, T., Tanabe, T., Toyosato, M., Furutani, Y., Hirose, T., Asai, M., Inayama, S., Miyata, T. and Numa, S. (1982) Primary structure of subunit precursors of Torpedo californica acetylcholine receptor deduced from cDNA sequence. Nature (Lond.) 299, 793–797.

28 Noda, M., Takahashi, H., Tanabe, T., Toyosato, M., KiKyotani, S., Hirose, T., Asai, M., Takashima, H., Inayama, S., Miyata, T. and Numa, S. (1983) Primary structure of β- and δ-subunit precursors of *Torpedo californica* acetylcholine receptor deduced from cDNA sequences. Nature (Lond.) 301, 251–255.

29 Noda, M., Furutani, Y., Takahashi, H., Toyosato, M., Tanabe, T., Shimizu, S., Kikyotani, S., Kayano, T., Hirose, T., Inayama, S. and Numa, S. (1983) Cloning and sequence analysis of calf cDNA and human genomic DNA encoding α-subunit precursor of muscle acetylcholine receptor. Nature (Lond.) 305, 818–823.

30 Claudio, T., Ballivet, M., Patrick, J. and Heinemann, S. (1983) Nucleotide and deduced amino acid sequences of *Torpedo californica* acetylcholine receptor γ-subunit. Proc. Natl. Acad. Sci. U.S.A. 80, 1111–1115.

31 Barnard, E.A., Beeson, D.M.W., Cockroft, V.B., Darlison, M.G., Hicks, A.A., Lai, F.A., Moss, S.J. and Squire, M.D. (1987) Molecular biology of nicotinic acetylcholine receptors from chicken muscle and brain. In: Nicotinic Acetylcholine Receptor Structure and Function, (A. Maelicke, ed.), pp. 389–415. NATO ASI Series H: Cell Biology, Vol. 3 Springer-Verlag, Berlin.

32 Patrick, J. and Stallcup, W.B. (1977) Immunological distinction between acetylcholine receptor and the α-bungarotoxin binding component on sympathetic neurons. Proc. Natl. Acad. Sci. U.S.A. 74, 4689–4692.

33 Whiting, P. and Lindstrom, J. (1987) Purification and characterization of a nicotinic acetylcholine receptor from rat brain. Proc. Natl. Acad. Sci. U.S.A. 84, 595–599.

34 Chiappinelli, V.A. (1987) Toxins affecting cholinergic neurons. In: Neuromethods Vol. 12, Drugs as Tools in Neurotransmitter Research (A.A. Boulton, ed.), pp. 111–133. Humana Press, Clifton, New Jersey.

35 Breer, H. and Sattelle, D.B. (1987) Molecular properties and functions of insect acetylcholine receptors. J. Insect Physiol. 33, 771–790.

36 Sattelle, D.B., Harrow, I.D., Hue, B., Pelhate, M., Gepner, J.I. and Hall, L.M. (1983) α-Bungarotoxin blocks excitatory synaptic transmission between cercal sensory neurons and giant interneurone 2 of the cockroach *Periplaneta americana*. J. Exp. Biol. 107, 473–489.

37 David, J.A. and Sattelle, D.B. (1984) Actions of cholinergic pharmacological agents on the cell body membrane of the fast coxal depressor motoneurone of the cockroach (*Periplaneta americana*). J. Exp. Biol. 108, 119–136.

38 Pinnock, R.D., Lummis, S.C.R., Chiappinelli, V.A. and Sattelle, D.B. (1988) κ-Bungarotoxin blocks an α-bungarotoxin-sensitive nicotinic receptor in the insect central nervous system. Brain Res. 458, 45–52.

39 Chiappinelli, V.A., Hue, B., Mony, L. and Sattelle, D.B. (1989) K-Bungarotoxin blocks nicotinic transmission at an identified invertebrate central synapse. J. Exp. Biol (in press).

40 Hanke, W. and Breer, H. (1986) Channel properties of an insect neuronal acetylcholine receptor protein reconstituted in planar lipid bilayers. Nature (Lond.) 321, 171–174.

41 Marshall, J., Darlison, M.G., Lunt, G.G. and Barnard, E.A. (1988) Cloning of putative nicotinic acetylcholine receptor genes from locust. Biochem. Soc. Trans. (in press).

42 Marshall, J.M., David, J.A., Darlison, M.G., Barnard, E.A. and Sattelle, D.B. (1988) Pharmacology, cloning and expression of insect nicotinic acetylcholine receptors. In: Nicotinic Acetylcholine Receptors in the Nervous System, NATO Advanced Study Institute (F. Clementi, E. Sher, eds.) pp. 257–281. Springer-Verlag, Berlin.

43 Corbett, J.R., Wright, K. and Baillie, A.C. (1984) The Biochemical Mode of Action of Pesticides, pp. 1–382. Academic Press, London.

44 Lindsley, D.L. and Grell, E.H. (1968) Genetic variations of *Drosophila melanogaster*. Publication no. 627. Carnegie Institution, Washington DC.

45 Sattelle, D.B., Harrow, I.D., David, J.A., Pelhate, M., Callec, J.J. Gepner, J.I. and Hall, L.M. (1985) Nereistoxin: actions on a CNS acetylcholine receptor/ion channel in the cockroach *Periplaneta americana*. J. Exp. Biol. 118, 37 52.

46 Hall, L.M., von Borstel, R.W., Osmond, B.C., Hoeltzli, S.D. and Hudson, T.H. (1978) Genetic variations in an acetylcholine receptor from *Drosophila melanogaster*. FEBS Lett. 95, 243–246.

47 Hall, L.M. (1980) Biochemical and genetic analysis of an α-bungarotoxin-binding receptor from *Drosophila melanogaster*. In: Receptors for Neurotransmitters, Hormones and Pheromones in Insects (D.B. Sattelle, L.M. Hall, J.G. Hildebrand, eds.), pp. 111–124. Elsevier Biomedical Press, Amsterdam.

48 Morris, C.F. (1984) Electrophysiological effects of cholinergic agents on the CNS of a nicotine-resistant insect, the tobacco hornworm (*Manduca sexta*). J. Exp. Zool. 229, 361–371.

49 Trimmer, B.A. and Weeks, J.C. (1988) Pharmacological studies on an identified motoneuron and its cholinergic afferent inputs in the nicotine-resistant insect *Manduca sexta*. In: Nicotinic Acetylcholine Receptors in the Nervous System, NATO ASI (F. Clementi, E. Sher, eds.). Springer-Verlag, Berlin, (in press).

50 Catterall, W.A. (1986) Molecular properties of voltage-sensitive sodium channels. Ann. Rev. Biochem. 5, 963–985.

51 Auld, V., Marshall, J., Goldin, A., Dowsett, A. and Catterall, W.A. (1985) Cloning and characterisation of the gene for α subunit of the mammalian voltage-gated sodium channel J. Gen. Physiol. 86, 10a–11a.

52 Frelin, C., Vigne, P. and Lazdunski, M. (1983) Na⁺ channels with high and low affinity tetrodotoxin binding sites in the mammalian skeletal muscle cell Difference in functional properties and sequential appearance during rat skeletal myogenesis. J. Biol. Chem. 258, 7256–7259.

53 Weiss, R.E. and Horn, R. (1986) Functional differences between two classes of sodium channels in developing rat skeletal muscle. Science 233, 361–364.

54 Salkoff, L., Butler, A., Wei, A., Scavarda, N., Baker, K., Pauron, D. and Smith, C. (1987) Molecular biology of the voltage-gated sodium channel. Trends Neurosci. 10, 522–527.

55 Salkoff, L., Butler, A., Wei, A., Scavarda, N., Griffen, K., Ifune, C., Goodman, R. and Mandel, G. (1986) Genomic organization and deduced amino acid sequence of a putative sodium channel gene in *Drosophila*. Science 237, 744–749.

56 Yawo, H., Kojima, H. and Kuno, M. (1985) Low-threshold inactivating Na⁺ potentials in the cockroach giant axon. J. Neurophysiol. 54, 1087–1100.

57 O'Dowd, K. and Aldrich, R.W. (1988) Voltage-clamp analysis of sodium channels in wildtype and mutant *Drosophila* neurons. J. Neurosci. (in press).

58 Pelhate, M. and Sattelle, D.B. (1982) Pharmacological properties of insect axons: a review. J. Insect Physiol. 28, 889–903.

59 Sattelle, D.B., Pelhate, M. and Hue, B. (1979) Pharmacological properties of axonal sodium channels in the cockroach *Periplaneta americana*. I Selective block by synthetic saxitoxin. J. Exp. Biol. 83, 41–48.

60 Sattelle, D.B. and Yamamoto, D. (1988) Molecular targets of pyrethroid insecticides. Adv. Insect Physiol. 20, 147–213.

61 Laufer, J., Pelhate, M. and Sattelle, D.B. (1985) Actions of pyrethroid insecticides on insect axonal sodium channels. Pestic. Sci. 16, 651–661.

62 Laufer, J., Roche, M., Pelhate, M., Elliott, M., James, N.F. and Sattelle, D.B. (1984) Pyrethroid insecticides: actions of deltamethrin and related compounds on insect axonal sodium channels. J. Insect Physiol. 30, 341–349.

63 Lund, A.E. and Narahashi, T. (1981) Kinetics of sodium channel modification by the insecticide tetramethrin in squid axon membranes. J. Pharmacol. Exp. Ther. 219, 464–473.

64 Yamamoto, D., Quandt, F.N. and Narahashi, T. (1983) Modification of single sodium channels by the insecticide tetramethrin. Brain Res. 274, 344–349.

65 Milani, R. (1954). Comportamento mendeliano della restenza alla azione abbattente del DDT: correlazione tra abbattimento e mortalita in *Musca domestica* L. Riv. Parassit. 15, 513–542.

582

66 Farnham, A.W. (1977) Genetics of resistance of houseflies (*Musca domestica* L.) to pyrethroids. I. Knockdown resistance. Pestic. Sci. 8, 631–636.

67 Sawicki, R.N. (1985). Resistance to pyrethroid insecticides in arthropods. In: Insecticides (D.H. Hutson, D.R. Roberts, eds.), pp. 143–191. John Wiley, New York.

68 Chang, C.P. and Plapp, F.W. Jr. (1983) DDT and pyrethroids: receptor binding and mode of action in the housefly *Musca domestica*. Pestic Biochem. Physiol. 20, 76–85.

69 Chang, C.P. and Plapp, F.W. Jr. (1983) DDT and pyrethroids: receptor binding in relation to knockdown resistance (Kdr) in the housefly *Musca domestica*. Pestic. Sci. Biochem. Physiol. 20, 86–91.

70 Kasbekar, D.P. and Hall, L.M. (1988) A *Drosophila* mutation that reduces sodium channel number confers resistance to pyrethroid insecticides. Pestic. Biochem. Physiol. (in press).

71 Farnham, A.W. (1973) Genetics of resistance of pyrethroid selected houseflies *Musca domestica* L. Pestic. Sci. 4, 513–520.

72 Farnham, A.W., Murray, A.W.A., Sawicki, R.M., Denholm, I. and White, J.T. (1987) Characterization of the structure-activity relationship of Kdr and two variants of siper-Kdr to pyrethroids in the housefly (*Musca domestica* L.). Pestic. Sci. 19, 209–220.

73 Moorefield, H.H. (1957) Improved method of harvesting housefly heads for use in cholinesterase studies. Contributions of the Boyce-Thompson Institute 18, 463.

74 Rossignol, D.P. and Pipenberg, P.K. (1986) Molecular basis of target site resistance to neurotoxic insecticides. Soc. Neurosci. Abstr. 12, 1075.

75 Bacon, J.P. and Strausfeld, N.J. (1986). The dipteran 'giant fibre' pathway: neurons and signals. J. Comp. Physiol. A 158, 529–548.

76 O'Shea, M. and Adams, M. (1981) Pentapeptide (Proctolin: Arg-Tyr-Leu-Pro-Thr) associated with an identified neuron. Science 213, 567–564.

77 Brismar, T. and Gilly, W.F. (1987). Synthesis of sodium channels in the cell bodies of squid giant axons. Proc. Natl. Acad. Sci. U.S.A. 84, 1459–1463.

78 Villegas, J., Seville, C., Barnola, F.V. and Villegas, R. (1976) Grayanotoxin, veratrine, and tetrodotoxin-sensitive sodium pathways in the Schwann cell membrane of squid nerve fibres. J. Gen. Physiol. 67, 369–380.

79 Noda, M., Ikeda, T., Kayano, T., Suzuki, H., Takeshima, H., Kurasaki, M., Takahashi, H. and Numa, S. (1986) Existence of distinct sodium channel messenger RNAs in rat brain. Nature (Lond.) 320, 188–192.

80 Noda, M., Shimizu, S., Tanaka, T., Takai, T., Kayano, T., Ikeda, T., Takahashi, H., Nakayama, H., Kanaoka, Y., Minamino, N., Kangawa, K., Matsuo, H., Raftery, M.A., Hirose, T., Inayama, S., Hayashida, H., Miyata, T. and Numa, S. (1984) Primary structure of *Electrophorus electricus* sodium channel deduced from cDNA sequence. Nature (Lond.) 312, 121–127.

CHAPTER 43: EPILOGUE

Summing up and looking ahead—insect neurobiology and the future of pest control

JOHN G. HILDEBRAND

Professor and Director, Arizona Research Laboratories Division of Neurobiology, University of Arizona, 611 Gould-Simpson Building, Tucson, AZ 85721, U.S.A.

It is an honour—and a real challenge—to have the last word in a meeting as wide-ranging and successful as Neurotox '88. The Organizing Committee, under the able leadership of its chairman Professor Peter N.R. Usherwood, put together a stimulating programme addressing several of the timely issues and recent advances in fundamental and applied aspects of insect neurobiology and molecular aspects of pesticide action. Remarks as cursory and brief as these cannot do justice to the many high points of the proceedings. It may be useful however, as we bring Neurotox '88 to its conclusion, to look back to the origins of this conference, review some of the progress made since the first meeting, and contemplate a few of the problems and opportunities that lie ahead of us.

The beginnings of Neurotox

These meetings began in York in September 1979 with Neurotox '79, an enlightening and memorable conference on insect neurobiology and pesticide action motivated by the belief that insect neurobiologists and pest-control scientists would benefit mutually from increased and improved interaction and communication with one another.

In his inspiring opening address [1], Dr. C. Potter began by assuring the participants that there was "no intention of attempting to lure workers on pure aspects to take up applied work" and that "the need for a detailed pure background in insect physiology and biochemistry in which to carry out applied work is clear and urgent." Potter's brief review of the history of modern insecticides reminded us that, by the 1970s, traditional random screening as well as some structure-activity studies had provided numerous effective insecticides, the vast majority of which are neuroactive poisons. These chemicals came to be used wherever insects were pests because they were predators or vectors of disease. But with the striking success of this armamentarium of insecticides came troubles: pollution of the environment by persistent toxic chemicals, action on unintended victims in addition to the intended target species, and the steadily increasing problem of insect resistance to the pesticides. Potter concluded that "only a united effort on fundamental work,

designed to find out more about the mode of action of currently used chemicals and the resistance factors that have developed against them and to find fresh points of attack in the insects' physiological and biochemical systems so that totally new insecticides can be rationally developed, offers any real hope of eventually coping with this problem [of resistance]."

Neurotox '79 succeeded in its primary mission of fostering a closer association—and hence better communication and understanding—between basic and applied scientists. As Dr. Potter predicted, the benefits of the improved relations have been mutual and not one-sided. Neurotox '79 revealed how little the basic and applied scientists knew about each other's concerns. At least some were encouraged to try to interact with and help their counterparts across the apparent gulf. Neurotox '79 also laid bare our ignorance about the insect nervous system and emphasized the great need and opportunity for research on the basic and comparative neurobiology and behaviour of insects as harmful pests and also as biomedical models and beneficial 'partners in agriculture and biotechnology'.

Progress since 1979

At Neurotox '85 in Bath and now especially here at Neurotox '88, we have learned about technical and substantive progress in insect neurobiology, neuropharmacology, and toxicology. The research efforts responsible for this progress undoubtedly have been encouraged and stimulated by these international conferences. Among the advances that have been evident at Neurotox '88 are:

- The widespread adoption and successful use of the patch-clamp technique for recording ionic currents through single ion channels in cell membranes.
- Consequent, significantly increased understanding of ion channels and the receptors that gate some of them.
- Improvement and successful use of methods for in vitro studies of insect neurons.
- Application of powerful contemporary techniques for molecular cloning, sequencing, and expression to obtain, characterize, and probe the production and functions of important functional macromolecules such as ion-channel and receptor proteins, enzymes, and propeptides.
- Progress in understanding the nature and physiological roles of chemical messengers in the insect nervous system, such as neuropeptides and the growing array of second messengers that mediate the effects of neurotransmitters, neuropeptides, hormones, and drugs on cells.

Launching Neurotox '88

This third and largest conference in the Neurotox series began with Dr. Neil McFarlane's thought-provoking Prologue. As I listened, a locker-room metaphor occurred to me: if Dr. Potter's opening address at Neurotox '79 was a 'pre-game pep talk' to urge us to work together and solve urgent and difficult problems of insect neurobiology and pesticide action and resistance, then Dr. McFarlane's talk was a sort of 'half-time analysis of how the game is going.' Dr. McFarlane considered some of the economic and political factors in, and constraints on, the contemporary research enterprise—especially in our own fields. He cautiously urged

us forward, not only to search for new chemicals and new targets associated with the insect nervous system to build our ability to manage harmful insects, but also to contribute to progress in basic science. I was particularly interested and pleased that he called for contributions by insect neuroscientists to the modelling of neural systems and the development of a comprehensive cognitive neuroscience and to progress in robotics and artificial intelligence. Dr. McFarlane urged younger scientists to "step forward from the centre of gravity of today's fields to a new position comfortably allied with molecular biology, psychobiology, and computing". Most importantly, Dr. McFarlane seemed to emphasize basic understanding of, and comparative insights about, principles of organization and function of neural *systems* instead of our traditional preoccupation with often-indiscriminate poisoning of arthropods. He looked ahead to a subsequent conference that might be called 'Neurophenomena 2000.'

Themes of Neurotox '88

Looking back through the proceedings, I detect several clear themes running throughout Neurotox '88. Four of these stand out:

1. *Insect control.* We have a cause: 'kill bugs, not people'. We seek means to poison, manipulate, or otherwise control harmful insects. Increasingly this endeavour calls upon newer, 'higher' technologies such as those of molecular biology and biophysics for help in discovering new targets, agents, and effects. Happily I note a trend, albeit subtle, toward species-specific intoxication and interference with or modification of behaviour instead of broad-spectrum poisoning of insects.

2. *Search for new targets and new agents.* Continuing a theme common to all of the Neurotox meetings, Neurotox '88 has presented numerous examples of the quest for new targets associated with the insect nervous system and new agonists and antagonists to act at those and other targets. While much research continues to explore passive, voltage-sensitive, and receptor-gated ion channels in excitable membranes, cholinergic mechanisms, and monoaminergic mechanisms mediated by intracellular second messengers, newer thrusts have been evident in this meeting. For example, increasing interest and effort focus upon receptors for amino-acid neurotransmitters such as GABA and glutamate, novel amino-acid ligands for such receptors, peptidergic mechanisms, endogenous inhibitors of receptors and enzymes, and the neurotransmitter-releasing machinery of presynaptic neuronal elements. This search for new targets and agents for novel insect-control strategies represents, in fact, a general invigoration of the field of insect neurobiology that has taken place since Neurotox '79.

3. *Naturally occurring neuroactive agents.* As a logical consequence of the growing effort to find new targets and agents in the insect nervous system, there has been a dramatic increase of interest in 'Nature's own insecticides' such as neuroactive natural products in plants, fungi, and microorganisms, and especially toxins in arthropod venoms. For example, whereas only a couple of papers at Neurotox '79 and Neurotox '85 considered venom toxins, at least twenty presentations at this meeting have dealt with toxins from spider, scorpion, and hymenopteran venoms.

These specific agents, products of the slow but powerful 'R & D process' of evolution, are proving to be useful both as selective probes of physiologically important targets such as ion channels and receptors and as candidates or models for new pesticides.

4. *Question of differences.* Finally, a theme recurring in many sessions at Neurotox '88 is what might be called the 'question of differences'. Over and over again, participants have asked about the existence and significance of differences between components (such as receptors, ion channels, and transmitters) of the nervous system of insects and those of other phylogenetic groups or of various insect taxa. For example, in their presentations Drs. Benson, Casida, and Lunt all warned about differences of action of GABA-receptor ligands in vertebrates and insects. Specifically, ligand-binding studies in several laboratories have usually failed to demonstrate sensitivity of putative GABA receptors in insect nervous tissue to bicuculline, a potent inhibitor of GABA binding to $GABA_A$ receptors in vertebrates.

Another related problem, which has been mentioned in this meeting and should be addressed decisively in the future, is the question of possible differences between synaptic and extrasynaptic functional proteins (such as receptors and ion channels) in insect neurons. For example, Professor H. Breer reviewed evidence that acetylcholine receptors on neuronal somata are different from those in synaptic neuropil of insect ganglia: the open-channel conductances of nicotinic acetylcholine receptors of somata and neuropil membranes are different, and the muscarinic acetylcholine receptors of neuronal somata and presynaptic membranes are pharmacologically distinct.

These two related issues arise in the interpretation of experiments from my laboratory to which several speakers have referred. Drs. B. Waldrop, T. Christensen, and I have studied the pharmacology of *synaptic* receptors that mediate an apparently GABAergic inhibitory synaptic interaction between well characterized interneurons in the deutocerebrum of the sphinx moth *Manduca sexta* [2]. This inhibitory interaction is clearly due to a chemical synaptic mechanism that has a reversal potential below the apparent resting potential of the postsynaptic interneuron (and near the likely level of E_{Cl}), is reversibly inhibited by bath-applied 10^{-4} M picrotoxin, and is strongly influenced by changes in extracellular or intracellular Cl concentration. Bath-applied 10^{-4} M bicuculline methiodide also reversibly blocks this GABAergic synaptic interaction. Thus, although we have heard reports at this conference that bicuculline does not significantly inhibit binding of GABA to membranes from insect CNS tissue or block the responses of insect neuronal somata to applied GABA, our experiments on an actual GABAergic inhibitory synaptic mechanism in an insect brain have yielded conflicting results. Our interpretation of these findings is that bicuculline blocks the GABA receptors (presumably similar to vertebrate $GABA_A$ receptors) at GABAergic inhibitory synapses but not the GABA receptors (presumably different from those at synapses) found on neuronal somata and at other extrasynaptic sites. Consistent with this view is our preliminary finding that the potent hyperpolarizing response of the same *Manduca* neurons to pulses of 100 mM GABA pressure-injected into the deutocerebrum [2] is not significantly blocked by bath-applied 10^{-4} M bicuculline methiodide (unpublished). In this case we suspect, but have not yet carefully demonstrated, that the bicuculline-insensitive effect of applied GABA is mediated by a distinct type of GABA receptor associated with the membrane of the neuronal cell body and other extrasynaptic membranes of

the cell in the neuropil. Alternatively it is also possible, of course, that the concentration of bicuculline reaching the sites of action of the applied GABA simply cannot block the effect of such a high concentration of pressure-injected GABA.

Where do we go from here?

It has been said that nothing is as difficult to predict as the future; faced with the challenge of looking ahead, I strongly feel the truth of that bit of wisdom. Nevertheless I wish to venture some notions of what lies before us.

While we will continue to need 'traditional' neuroactive chemical insecticides where effective, it is also clear to me that alternative approaches to insect control surely will become increasingly important over the next two decades. The relatively indiscriminate poisoning and killing of insects and other arthropods through the use of insecticides such as DDT and organophosphates must give way to more selective, less environmentally harmful, and more biologically acceptable strategies. Moreover the development of resistance to such insecticides as well as to the pyrethroids can equip harmful insect pests to go about their business unscathed.

Among alternative strategies for insect control already being pursued and showing promise in at least some applications are the following:

- Inhibition or modification of insect development and/or maturation by means of synthetic hormone analogues (e.g. juvenoids) or antihormones (e.g. Precocenes).
- Interference with essential physiological processes such as digestive-tract function (e.g. with cytotoxin systems such as the *Bacillus thuringensis* toxins), water balance and mobilization and utilization of metabolites (e.g. by means of manipulation of chemical-messenger systems such as neuropeptides), etc.
- Disruption or modification of behaviours, including those underlying:
  - mating (e.g. through manipulation of pheromonal systems);
  - selection, acceptance, and ingestion of food (e.g. using feeding stimulants and deterrents, antifeedants, insectistatics, etc.); and
  - oviposition (e.g. exploiting oviposition stimulants and deterrents).

Whenever a new insect-control strategy is pursued, whether based upon a chemical insecticide or the other kinds of agents outlined above, familiar requirements and problems will continue to loom and require solution. Among these are: effectiveness, environmental acceptability, specificity, resistance, delivery and access to targets, practicality, and cost and marketability. New kinds of challenges will arise as we seek to use genetically engineered plants, viruses, and bacteria to produce and/or deliver insect-control agents. Not the least of the difficulties will be political, sociological, and economic; indeed, advances in science promise to outpace progress in dealing with the societal and business obstacles to introduction of new insect-control measures. In spite of these various problems, however, I predict that industry will soon begin to benefit appreciably from the accelerated research in pure and applied insect neurobiology that has been stimulated and aided by forums such as these Neurotox meetings.

In closing I wish to join Dr. McFarlane in encouraging our younger colleagues—students and postdoctoral fellows—to proceed with vigour and imagin-

ation on a multidisciplinary effort to build our understanding of insect neurobiology and behaviour. I would add that the goal should be not only to control the species of insects that are harmful and economically important agricultural, medical, and veterinary pests, but also to unravel the physiological and behavioural mysteries, mechanisms, and functions of the earth's most numerous, diverse, and biologically successful species of animals.

References

1 Potter, C. (1980) Opening address. In: Insect Neurobiology and Pesticide Action (Neurotox '79), pp. 1–4. Society of Chemical Industry, London.
2 Waldrop, B., Christensen, T.A. and Hildebrand, J.G. (1987) GABA-mediated synaptic inhibition of projection neurons in the antennal lobes of the sphinx moth, *Manduca sexta*. J. Comp. Physiol. A 161, 23–32.

Author Index

Subject Index

594